

FINAL REPORT

Evaluation of Resuspension from Propeller Wash in DoD Harbors

ESTCP Project ER-201031

SEPTEMBER 2016

Pei-Fang Wang
Ignacio Rivera-Duarte
Ken Richter
SSC Pacific

Qian Liao
Department of Civil Engineering and Mechanics

Kevin Farley
**Manhattan College Department of Civil
and Environmental Engineering**

Hamn-Chin Chen
**Texas A& M University Department
of Civil Engineering**

Joe Germano
Germano and Associates

Kimberly Markillie
Naval Facilities Engineering Command Hawaii

Joe Gailani
**U.S. Army Corps of Engineers Engineering Research
and Development Center**

Distribution Statement A
This document has been cleared for public release



Page Intentionally Left Blank

This report was prepared under contract to the Department of Defense Environmental Security Technology Certification Program (ESTCP). The publication of this report does not indicate endorsement by the Department of Defense, nor should the contents be construed as reflecting the official policy or position of the Department of Defense. Reference herein to any specific commercial product, process, or service by trade name, trademark, manufacturer, or otherwise, does not necessarily constitute or imply its endorsement, recommendation, or favoring by the Department of Defense.

Page Intentionally Left Blank

SSC Pacific
San Diego, California 92152-5001

K. J. Rothenhaus, CAPT, USN
Commanding Officer

C. A. Keeney
Executive Director

ADMINISTRATIVE INFORMATION

The work described in this report was performed for the State Environmental Review Processes (SERP) and Energy System Technology Evaluation Program (ESTEP) Office by the Environmental Sciences Branch (Code 71750) and the Energy and Environmental Sustainability Branch (Code 71760) of the Advanced Systems & Applied Sciences Division, Space and Naval Warfare Systems Center Pacific (SSC Pacific), San Diego, CA. Further SSC Pacific support was provided by the Command & Control Technology & Experimentation Division (Code 53603). Partner support was provided by the Department of Civil and Environmental Engineering, University of Wisconsin-Milwaukee, Milwaukee, WI; Manhattan College Department of Civil and Environmental Engineering, Riverdale, NY; Texas A&M University Department of Civil Engineering, College Station, TX; Germano and Associates, Bellevue, WA; Naval Facilities Engineering Command-Hawaii, Pearl Harbor-Hickam, HI; and U.S. Army Corps of Engineers Engineering Research and Development Center, Vicksburg, MS.

Released by
P. Earley, Head
Environmental Sciences Branch

Under authority of
A. D. Ramirez, Head
Advanced Systems &
Applied Sciences Division

ACKNOWLEDGMENTS

Contributions from a team of dedicated experts are acknowledged. First and foremost, the authors would like to thank the Energy System Technology Evaluation Program (**ESTEP**) Office (manager: Dr. Andrea Leeson) and the technical committee (Mr. Tim Thompson) for funding and technical guidance during the study. Field study in San Diego Bay would not have been possible without the strong support of the Commander, Navy Region Southwest (CNRSW), including Mr. Brian Gordon (manager), Mr. Paul Patricio (Port Ops Waterfront Project Manager and Portmaster) and the crew of C-Tractor 14 tug-boat. Equal appreciation goes to Ms. Kimberly Markillie (manager of Naval Facilities Engineering Command Hawaii [NAVFAC-HI]), who provided the logistic support for the field study in Pearl Harbor. On-site support for the sediment trap study in Pier 7 of Sinclair Inlet, WA, from Dr. Bob Johnston (SSC Pacific) and the Puget Sound Naval Shipyard is appreciated.

This is a work of the United States Government and therefore is not copyrighted. This work may be copied and disseminated without restriction.

The citation of trade names and names of manufacturers in this publication is not to be construed as official government endorsement or approval of commercial products or services referenced herein.

Adobe® Photoshop® is a registered trademark of Adobe Systems Incorporated.
Kodak® is a registered trademark of the Eastman Kodak Company.
MATLAB® is a registered trademark of The MathWorks, Inc.
Microsoft® and Excel® are registered trademarks of Microsoft Corporation.
Nikon® and D700® are registered trademarks of Nikon Corporation.
Plexiglas® is a registered trademark of ATOFINA Chemicals, Inc.
Surfer™ is a trademark of Golden Software, Inc.

Page Intentionally Left Blank

EXECUTIVE SUMMARY

Predictions of the mass, fate and transport of resuspended sediments and their associated contaminant load are lacking for Navy harbors. This study provides examples how Maynard's model, predicting tug-boat sediment resuspension, can be linked with CH3D, a curvilinear hydrodynamic three dimensional model to predict transport and fate of resuspended sediments and associated metals in the three harbors studied here: San Diego Bay, CA; Pearl Harbor, HI, and Sinclair Inlet, WA. Field data are necessary to first calibrate, and then validate model predictions to various degrees.

Example One: In San Diego Bay tug wash velocity data is first used to calibrate Maynard's model for the flow field by the tug wash. Total suspended load from the tug wash is used to validate resuspension estimated by Maynard's model. Then model output along with bed sediment particle size and associated metal load is fed into CH3D whose transport predictions are validated by water column pump samples of sediments and metals. Model results of resuspended load and grain size distribution were very similar to pump measurements. The output of CH3D was further coupled to a simplified metal partitioning model, TICKET, predicting the particulate-bound and dissolved fractions of copper. These predictions too matched pump measurements.

Example Two: At two sites in Pearl Harbor sediment was resuspended by a tug different from (smaller than) the one used to calibrate Maynard's model in San Diego. Consequently, pump samples from tug resuspension events at Bravo and Oscar Piers were used as input to CH3D which then predicted dispersal of resuspended sediment. Predicted resuspended sediment concentrations were similar to those measured from acoustic backscatter.

Example Three: In Sinclair Inlet output from Maynard's model simulating a tug resuspension event identical to that modeled and measured in San Diego was fed into CH3D, along with bed sediment particle size and associated metal load, to predict resuspension and dispersal from two tug assists. One assist involved moving a decommissioned submarine into dry dock; the other involved escorting a nuclear carrier out of dry dock. CH3D output was compared to sediment trap results. The comparison suggested that sediment and contaminant loads falling into the traps could not have come solely from such tug scenarios but was probably coming from other resuspension sources as well. The results of this study can be used not only to predict where resuspended sediments will go, but also how susceptible sediments are to resuspension in the first place. Both predictions are relevant to in-place sediment remediation projects.

An incidental observation during this study and reported here was acoustic detection of resuspended sediment under the bow of a deep draft missile destroyer in Pearl Harbor. This observation confirms predictions of the FANS model, shown as graphic output. Hydrodynamic output from CH3D has been calibrated and validated in past studies for these three harbors. Separate user's manuals for Maynard's model and FANS model have already been published and are available on the ESTCP tech transfer product website: [https://www.serdp-estcp.org/Program-Areas/Environmental-Restoration/Contaminated-Sediments/ER-201031/ER-201031/\(language\)/eng-US](https://www.serdp-estcp.org/Program-Areas/Environmental-Restoration/Contaminated-Sediments/ER-201031/ER-201031/(language)/eng-US).

Page Intentionally Left Blank

ACRONYMS

2-D	Two-Dimensional
ADV	Acoustic Doppler Velocimeter
ADCP	Acoustic Doppler Current Profiler
Ag	Silver
CCC	Criterion Continuous Concentration
CERCLA	Comprehensive Environmental Response, Compensation, and Liability Act
CH3D	Curvilinear Hydrodynamics in 3D
CMC	Criterion Maximum Concentration
CoC	Contaminants of Concern
COV	Covariance
CW	Continuous Wave
DoD	Department of Defense
ERDC	Environmental Research and Development Center
FANS	Finite Analytical Navier-Stokes Solver
FOV	Field of View
ICP-MS	Inductively Coupled Plasma with Detection by Mass Spectrometry
LISST	Laser Particle Size Analyzer
MDL	Method Detection Limit
NAVFAC	Naval Facilities Engineering Command
NOAA	National Oceanic and Atmospheric Administration
OBS	Optical Backscatter Sensor
PCBs	Polychlorinated Biphenyls
PHNSY&IMF	Pearl Harbor Naval Ship Yard and Intermediate Maintenance Facility
PIV	Particle Imaging Velocimeter
QA/QC	Quality Assurance/Quality Control
RMS	Root Mean Square
RPM	Revolutions per Minute
SPI	Sediment Profiling Imagery
SRM	Standard Reference Material
TICKET	Tableau Input Coupled Kinetic Equilibrium Transport
TKE	Turbulent Kinetic Energy
TMDL	Total Maximum Daily Load
TSSL	Total Suspended Sediment Load
USEPA	United States Environmental Protection Agency
UWMPIV	Under Water Miniature PIV
WASP	Water Quality Analysis Simulation Program

Page Intentionally Left Blank

CONTENTS

EXECUTIVE SUMMARY	iii
1. INTRODUCTION.....	1
1.1 BACKGROUND	3
1.2 OBJECTIVES OF THE DEMONSTRATION.....	4
1.3 REGULATORY DRIVERS.....	5
2. TECHNOLOGY	6
2.1 TECHNOLOGY DESCRIPTION.....	6
2.2 TECHNOLOGY/METHODOLOGY DEVELOPMENT.....	8
2.3 ADVANTAGES AND LIMITATIONS OF THE TECHNOLOGY/METHODOLOGY.....	9
3. PERFORMANCE OBJECTIVES.....	10
4. SITE DESCRIPTION.....	12
4.1 SITE LOCATION AND HISTORY.....	12
4.2 SITE CHARACTERISTICS.....	13
5. TEST DESIGN (METHODS)	14
5.1 FIELD AND LABORATORY PROCEDURES	14
5.1.1 Tug Propeller Wash Velocities in San Diego Bay	14
5.1.2 Bottom Velocity and Shear in San Diego Bay.....	16
5.1.3 Resuspension Studies	19
5.2 MODEL PROCEDURES	38
5.2.1 Maynard's Resuspension Model	38
5.2.2 FANS Resuspension Model.....	45
5.2.3 CH3D Fate and Transport Model	45
6. PERFORMANCE ASSESSMENT.....	48
6.1 TUG PROPELLER WASH VELOCITIES IN SAN DIEGO BAY.....	51
6.2 IMPLEMENTATION OF MAYNORD'S MODEL FOR SAN DIEGO BAY.....	55
6.2.1 Mean Characteristics of the Propeller Current and Turbulence by ADV	57
6.2.2 Structure of Turbulence above the Sediment Bed Measured by PIV	59
6.2.3 Erosion Rate	68
6.2.4 Critical Shear Stress	68
6.2.5 Graphic Version of Maynard's Model for Tugboat.....	71
6.2.6 Comparison of Field Data and Model Results	73
6.3 RESUSPENSION EVENTS.....	76
6.3.1 San Diego.....	76
6.3.2 Pearl Harbor.....	119
6.4 RESUSPENSION FROM A DEEP-DRAFT VESSEL.....	169
6.4.1 Field Observations using ADCP	169
6.4.2 Simulation Scenarios for DDG-51 Ship	170

6.4.3 FANS Model Simulation Results for DDG-51 Ship	172
6.5 SEDIMENT RECONTAMINATION POTENTIAL FOR PIER 7, SINCLAIR INLET, WA	182
6.5.1 Sediment Deposition Rates and Metal Concentrations.....	182
6.5.2 Sinclair Inlet Particle Resuspension Load and Deposition Rate.....	184
6.5.3 Metal Load and Fractionation.....	185
6.5.4 Sinclair Inlet Sediment Deposition Modeling Analysis	189
6.5.5 Sinclair Inlet Sediment Deposition Signature Analysis.....	195
6.6 DISCUSSION AND SUMMARY	197
6.6.1 Metals in Sediment Plumes.....	197
6.6.2 Resuspension Potential and Fate/Transport	197
6.6.3 Deposition at Pier 7, Sinclair Inlet, WA.....	198
7. COST ASSESSMENT.....	200
7.1 COST MODEL	200
7.2 COST DRIVERS	202
7.3 COST ANALYSIS.....	202
8. IMPLEMENTATION ISSUES	204

APPENDICES

A: POINTS OF CONTACT	A-1
B: THRUSTS ON NOZZLE PROPELLERS OF THE TRACTOR C-14 TUGBOAT FROM MEASUREMENTS AND THE FANS MODEL.....	B-1
C: SAN DIEGO BAY DATA	C-1
D: PEARL HARBOR DATA	D-1
E: GRAPHIC MAYNORD'S MODEL OUTPUT FILE AND FORMAT	E-1
F: FORMULAS USED TO SPECIFY INPUT CONCENTRATIONS OF METAL BINDING PHASES IN WHAM.....	F-1
G: SEDIMENT PROFILE IMAGE ANALYSIS RESULTS.....	G-1
H: DATA FOR SEDIMENT TRAP STUDY IN PIER 7, SINCLAIR INLET, WA	H-1

Figures

1-1. Study framework and components including both laboratory study, field work and modeling studies	1
1-2. Field and modeling effort in San Diego Bay	2
1-3. Field and modeling effort in Pearl Harbor	2
1-4. Field and modeling effort in Sinclair Inlet.....	3
5-1. Position of ADV measurements downstream of tug (red shape) operating at 100 RPM.....	15
5-2. Position of ADV measurements downstream of tug (red shape) operating at 200 RPM.....	15
5-3. Deployment of the UWMPIV frame in San Diego Bay	17
5-4. Sample PIV image: initiation of sediment resuspension	18
5-5. Diagram and photo of a resuspension event procedure induced by a tug	19
5-6. Flowchart of laboratory processing and analysis of the field samples for determination of CoC (i.e., metals or organic contaminants) concentrations in the total, sand, silt, clay, and dissolved fractions. Information in the middle represents the filtration sequence, information to the left are concentrations measured in the filtrated seawater (FS), and information to the right are masses retained by the respective filter.....	21
5-7. Photo of the resuspension event procedure induced by a tug and the <i>ECOS</i> sampling the plume in San Diego Bay.....	28
5-8. <i>ECOS</i> track and sampling locations for the resuspension event of 4 April 2012 at Naval Base San Diego, San Diego Bay, California.....	28
5-9. Photo of the resuspension event procedure induced by a tug and the <i>ECOS</i> sampling the plume at Oscar Pier in Pearl Harbor.....	29
5-10. Sampling and OBS locations for the two bottom sediment resuspension events in Pearl Harbor, HI	29
5-11. The hand-held, diver-deployed sediment profile camera used in Pearl Harbor.....	31
5-12. ADCP configuration as deployed from the Sea Engineering motor barge (left) ADCP mount in position while motoring to/from site (right) deployed in the measurement position	33
5-13. Calibration from backscatter to concentration for 28 August 2012.....	34
5-14. Sediment trap locations under Pier 7, PSNS&IMF. The stars are depicting the label and position of the sediment traps for both Pier 7 and the amendment cap on the sediment (gray area). Imagery ©2014 DigitalGlobe, U.S. Geographical Survey, USGS, Map data ©2014 Google Life mode Terms Privacy Report a problem	35
5-15. Sediment trap used for quantification of sediment particles and contaminants of concern over the sediment remedial cap located by Pier 7 at PSNS&IMF.....	36
5-16. Location for background sediment grab samples PSNS&IMF	37
5-17. Schematic plots of twin-nozzle propellers for a tug-boat in water of confined depth	41

5-18. Field study of tug-boat propeller wash at Pier 4-5 of Navy Base San Diego [(configuration of instruments in propeller plume, left, and tugboat Tractor C-14, right)	44
5-19. Tug-boat propeller speed during the field study (Hours 13.847–14.439, July 19, 2012) ...	44
5-20. Fate and transport CH3D model for San Diego Bay: model grid (lower left) and local grid at Piers 4 and 5 (upper right). Imagery ©2014 DigitalGlobe, U.S. Geographical Survey, USGS, Map data ©2014 Google Life mode Terms Privacy Report a problem.....	45
5-21. Fate and transport CH3D model for Pearl Harbor: model grid (top), and local grid at Bravo Pier (lower left), and Oscar Pier (lower right). Imagery ©2014 DigitalGlobe, U.S. Geographical Survey, USGS, Map data ©2014 Google Life mode Terms Privacy Report a problem.....	46
5-22. Fate and transport CH3D model for Sinclair Inlet: model grid (lower left) and local grid near Pier 7 (upper right). Imagery ©2014 DigitalGlobe, U.S. Geographical Survey, USGS, Map data ©2014 Google Life mode Terms Privacy Report a problem.....	47
6-1. Field and modelling efforts in San Diego Bay.....	51
6-2. Horizontal water velocities downstream of the tug propeller wash at 100 RPM and at various depths.....	53
6-3. Horizontal water velocities downstream of the tug propeller wash at 200 RPM and at various depths.....	54
6-4. Vertical cross-section of propeller wash velocity at 100 RPM and 200 RPM	55
6-5. Field study of tug-boat propeller wash at Pier 4-5 of Naval Base San Diego (configuration of instruments in propeller plume, left, and tug-boat Tractor C-14 in operation, right).....	56
6-6. Time series of velocities measured by the ADV, which was 110 m away from the propeller. The sample volume was about 12 cm above the sediment bed. Black dashed lines are the starting time of each RPM run. Pink dashed lines are estimated starting time for the change of propeller speed to affect the 110-m measurement site.....	57
6-7. Probability of the direction of the horizontal velocity recorded by the ADV probe	58
6-8. Change of mean velocities with the propeller RPM	59
6-9. Change of RMS of velocity variations with the propeller RPM.....	59
6-10. Time series of velocities measured concurrently by PIV and ADV. PIV signals were measured at $z = 11.5$ cm, while ADV data was at $z = 12.5$ cm	60
6-11. Vertical profile of the mean velocity measured by PIV between 14:00 and 14:01 (Section A). The red line is the fitted log-law with a shear velocity $u^* = 1.5$ cm/s.....	61
6-12. Vertical profiles of Reynolds stresses: (A) normal stresses; and (B) shear stresses measured between 14:00 and 14:01 (Section A).....	61
6-13. Vertical profile of the mean velocity measured by PIV between 14:01 and 14:02 (Section B). The red line is the fitted log-law with a shear velocity $u^* = 1.6$ cm/s.....	62
6-14. Vertical profiles of Reynolds stresses: (A) normal stresses; and (B) shear stresses measured between 14:01 and 14:02 (Section B).....	62
6-15. Vertical profiles of the TKE dissipation rate measured during Sections A and B.....	64
6-16. Mean velocity profiles averaged every 5 sec starting from 14:00	65
6-17. Time series of estimated bottom shear stress with different methods.....	66

6-18. Time series of estimated bottom shear stress from ADV measurement: (A) stress in linear scale, and (B) stress in log scale	67
6-19. Estimated cumulative bottom shear stress from ADV measurements	68
6-20. PIV images with visible sediment bed. The red line is the reconstructed bottom line from the bottom image.....	68
6-21. Sample images taken (a) when there was no significant erosion; (b)-(e) at the inception of erosion, and (f) after continuous erosion and resuspension	69
6-22. Cumulative erosion depth measured from PIV image analysis and modeling results with bottom shear stress obtained from ADV data.....	70
6-23. Graphical Maynard's model with input window and output graphics (right panels)	72
6-24. Comparison of velocity amplitudes for four propeller speeds between measurements and model results.....	74
6-25. Bottom shear stress from model results and estimation calculated based on measured velocity field during the propeller wash experiment	75
6-26. Cumulative shear stress over time between model results and estimation based on measured velocity field during the propeller wash experiment.....	76
6-27. Chromium, arsenic, nickel and silver distributions in the different particle size-fractions collected from the resuspension event of 4 April 2012 in San Diego Bay. The metal content in each fraction is calculated with the total fraction as the sum of all fractions	81
6-28. Copper, cadmium, zinc and lead distributions in the different particle size-fractions collected from the resuspension event of 4 April 2012 in San Diego Bay. The metal content in each fraction is calculated with the total fraction as the sum of all fractions	82
6-29. Chromium, arsenic, nickel and silver concentrations in the filtered solution (FS) for each different particle size-fractions collected from the resuspension event of 4 April 2012 in San Diego Bay. Ambient Total and Ambient Dissolved are from samples collected prior to the resuspension event. The USEPA Chronic Water Quality Criterion is provided as a measure of the potential concern derived from these quantifications	83
6-30. Copper, cadmium, zinc and lead concentrations in the filtered solution (FS) for each different particle size-fractions collected from the resuspension event of 4 April 2012 in San Diego Bay. Ambient Total and Ambient Dissolved are from samples collected prior to the resuspension event. The USEPA Chronic Water Quality Criterion is provided as a measure of the potential concern derived from these quantifications	84
6-31. Size-fraction distribution of metals for the resuspension event of 4 April 2012 in San Diego Bay. Each metal is provided as the percentage fraction for clay (grey), silt (green), sand (red) and total (blue), the same pattern is used in the following two figures.....	89
6-32. OBS output in nephelometer turbidity units versus measured TSS concentrations	90
6-33. ECOS boat track and OBS measurements (yellow), discrete pump samples (green dots), extrapolated TSS concentrations as colored contours, and CH3D model nodes (light blue disks)	93
6-34. ECOS boat track and OBS measurements (yellow), discrete pump samples (green dots), extrapolated copper on silt concentrations as colored contours.....	94
6-35. Simulated bottom velocity (top), bottom shear (middle) and erosion rate by Maynard's model for propeller speed of 150 RPM.....	95

6-36. Model predicted total eroded sediment mass during the 33-minute period	96
6-37. San Diego Bay Pier 4–5 region and the three locations (Segment 1, 2, and 3) for model/ data comparison and the representative inner bay and outer bay for model result analysis. Imagery ©2014 DigitalGlobe, U.S. Geographical Survey, USGS, Map data ©2014 Google Life mode Terms Privacy Report a problem.....	97
6-38. San Diego Bay sample locations. Main map shows locations of SPAWAR propeller wash samples. The inset map shows the transects and boxes from the Chadwick et al. (2005) sampling events. The prop wash area is highlighted in red in the inset map. Imagery ©2014 DigitalGlobe, U.S. Geographical Survey, USGS, Map data ©2014 Google Life mode Terms Privacy Report a problem.....	99
6-39. Summary of observed log K_D data from Chadwick et al. (2005) and the SPAWAR propeller wash sampling events. The boundary of the box closest to zero indicates the 25th percentile, the solid line within the box marks the median, the dashed line within the box indicates the mean, and the boundary of the box farthest from zero indicates the 75th percentile. The error bars above and below the box indicate the 95th and 5th percentiles values, respectively. Points represent values outside of the 5th and 95th percentile (i.e., outliers), respectively. Error bars and outliers are only calculated if a minimum number of data points exist	101
6-40. Performance assessment plot for copper (Cu, squares) and zinc (Zn, triangles) for the Chadwick et al. (2005) dataset (filled symbols and the SPAWAR prop wash dataset (hollow symbols The analysis was made using (A) default model parameters and (B) with hardness cation (calcium and magnesium) binding to DOC, POC, HFO, and HMO turned off.....	102
6-41. Correlation plot between partitioning model (Farley) and the linear equation from least- square method.....	105
6-42. Implemented metal (copper) partitioning algorithm (linear equation for look-up table) in CH3D	106
6-43. Predicted partitioning coefficients for copper in San Diego Bay by the linear equation (blue) and the field data (red)	106
6-44. Model/data comparison of clay (top), silt (middle), and sand (bottom) concentrations for the three locations (see Figure 6-33).....	108
6-45. Snapshots of water column concentrations of clay (top), silt (middle), and sand (bottom) between model (left) and field data (right) during 14:15–15:06, 4 April 2012	109
6-46. Simulated deposition mass (kilograms for each model segment) of clay, silt, sand, and total sediment particles from the propeller wash study	110
6-47. Time series of simulated dissolved (left) and total copper (right), and comparison with field data at the three representative locations	111
6-48. Snapshots of water column concentrations of dissolved copper between model (left) and field data (right) during 14:15–15:06, 4 April 2012	111
6-49. Snapshots of water column concentrations of total copper between model (left) and field data (right) during 14:15–15:06, 4 April 2012	111
6-50. Snapshots of water column concentrations of dissolved copper at Hr 68 (6th hour after resuspension) and Hr 240 (7.5th day after the resuspension)	112
6-51. Snapshots of water column concentrations of total copper at Hr 68 (6th hour after resuspension) and Hr 240 (7.5th day after the resuspension)	112

6-52. Deposited copper mass at Hr 63 (right after resuspension) and Hr 240 (7.5th day after resuspension)	113
6-53. Copper concentrations associated with clay, silt, and sand particles from the field data	114
6-54. Model/data comparison of copper concentrations bound by clay (top), silt (middle) and sand (bottom) particles, respectively for the three locations	115
6-55. Comparison between total deposited solids and total deposited copper.....	116
6-56. Comparison between total deposited solids and total deposited nickel	117
6-57. Percentages of deposition at the three regions (in-pier, outer bay and inner bay) of the particles and copper and nickel.....	118
6-58. Field and model studies in Pearl Harbor.....	119
6-59. Mass fraction (%) of the sand, silt, and clay fractions sampled in the three resuspension events	123
6-60. Average mass fraction (%) of the sand, silt, and clay fractions sampled in the three resuspension events on the left, and from background sediments sampled before the resuspension events on the right	124
6-61. Chromium, arsenic, nickel and silver distributions in the different particle size-fractions collected from the resuspension event of 28 August 2012 at Bravo 2 Pier in Pearl Harbor. The metal content in each fraction is calculated with the total fraction as the sum of all fractions	127
6-62. Copper, cadmium, zinc and lead distributions in the different particle size-fractions collected from the resuspension event of 28 August 2012 at Bravo 2 Pier in Pearl Harbor. The metal content in each fraction is calculated with the total fraction as the sum of all fractions.....	128
6-63. Chromium, arsenic, nickel, and silver distributions in the different particle size-fractions collected from the resuspension event of 29 August 2012 at Oscar 22 Pier in Pearl Harbor. The metal content in each fraction is calculated with the total fraction as the sum of all fractions	129
6-64. Copper, cadmium, zinc, and lead distributions in the different particle size-fractions collected from the resuspension event of 29 August 2012 at Oscar 22 Pier in Pearl Harbor. The metal content in each fraction is calculated with the total fraction as the sum of all fractions	130
6-65. Chromium, arsenic, nickel, and silver concentrations in the filtered solution (FS) for each different particle size-fractions collected from the resuspension event of 28 August 2012 at Bravo 2 Pier in Pearl Harbor. Ambient Total and Ambient Dissolved are from samples collected prior to the resuspension event. The USEPA Chronic Water Quality Criterion is provided as a measure of the potential concern derived from these quantifications.....	131
6-66. Copper, cadmium, zinc, and lead concentrations in the filtered solution (FS) for each different particle size-fractions collected from the resuspension event of 28 August 2012 at Bravo 2 Pier in Pearl Harbor. Ambient Total and Ambient Dissolved are from samples collected prior to the resuspension event. The USEPA Chronic Water Quality Criterion is provided as a measure of the potential concern derived from these quantifications.....	132

6-67. Chromium, arsenic, nickel, and silver concentrations in the filtered solution (FS) for each different particle size-fractions collected from the resuspension event of 28 August 2012 at Oscar 22 Pier in Pearl Harbor. Ambient Total and Ambient Dissolved are from samples collected prior to the resuspension event. The USEPA Chronic Water Quality Criterion is provided as a measure of the potential concern derived from these quantifications.....	133
6-68. Copper, cadmium, zinc, and lead concentrations in the filtered solution (FS) for each different particle size-fractions collected from the resuspension event of 28 August 2012 at Oscar 22 Pier in Pearl Harbor. Ambient Total and Ambient Dissolved are from samples collected prior to the resuspension event. The USEPA Chronic Water Quality Criterion is provided as a measure of the potential concern derived from these quantifications	134
6-69. Size-fraction distribution of metals for the resuspension event of 28 August 2012 at Bravo 2 Pier in Pearl Harbor	137
6-70. Size-fraction distribution of metals for the resuspension event of 28 August 2012 at Oscar 22 Pier in Pearl Harbor	138
6-71. Sediment profile image at the Bravo site at the start (left) and end (right) of the experiment. Scale: width of each image = 14.5 cm	139
6-72. Sediment profile image from the Oscar site at the start (left) and end (right) of the experiment. Scale: width of each image = 14.5 cm	140
6-73. One of the appearances of the crab over a 9-sec interval during the Oscar site deployment; each image taken 3 sec apart, starting at 15:02:49.....	141
6-74. Height of sediment and amount of suspended sediment in water column as a function of time during Bravo experiment	142
6-75. Height of sediment and amount of suspended sediment in water column as a function of time during Oscar experiment	142
6-76. Site map of Pearl Harbor with locations of Bravo and Oscar Piers where field experiments were conducted. Imagery ©2014 DigitalGlobe, U.S. Geographical Survey, USGS, Map data ©2014 Google Life mode Terms Privacy Report a problem.....	144
6-77. Space-time mapping of suspended sediment during the 28 Aug tug-generated plume. Aerial photo: Google. (Upper left) Site Map. (Upper Right) expanded site map with track line of the ADCP measurements. (Lower) vertical profiles of acoustic estimates of SSC (filled circles indicate physical samples, while line indicates position of the sediment bed, and colors indicate SSC (mg/L)). Imagery ©2014 DigitalGlobe, U.S. Geographical Survey, USGS, Map data ©2014 Google Life mode Terms Privacy Report a problem.....	145
6-78. OBS output as a function of pump-sampled TSS, measured at mid water column depth at Bravo and Oscar Piers	146
6-79. Bravo Pier boat track and OBS measurements (yellow), discrete pump samples (green dots),	151
6-80. Bravo Pier discrete pump samples (green dots), extrapolated copper on silt concentrations as colored contours.....	152
6-81. Oscar Pier boat track and OBS measurements (yellow), discrete pump samples (green dots),	153
6-82. Oscar Pier discrete pump samples (green dots), extrapolated copper on silt concentrations as colored contours.....	153

6-83. Water column particle size fractions and background sediment for clay (0.4 to 5 μm), silt (5 to 60 μm), and sand (>60 μm) for Bravo Pier in Pearl Harbor	154
6-84. Water column particle size fractions and background sediment for clay (0.4 to 5.0 μm), silt (5 to 60 μm), and sand >60 μm) for Oscar Pier in Pearl Harbor	155
6-85. Water column particle size fractions and background sediment for clay (0.4 to 5 μm), silt (5 to 60 μm), and sand (>60 μm) for San Diego Bay.....	156
6-86. Simulated dissolved copper concentrations at surface layer for CH3D fate and transport simulation at t = 0 (left) and t = 3 hours after resuspension from prop wash (color key applies to Figure 6-86 through Figure 6-88, inclusive)	158
6-87. Simulated dissolved copper concentrations at surface layer at t = 9 hours (left), and at t = 18 hours after prop-wash resuspension.....	158
6-88. Simulated dissolved copper concentrations at surface layer at t = 30 hours (left), and at t = 120 hours after prop-wash resuspension.....	159
6-89. Initial silt-particle-bound copper concentrations at surface layer for CH3D fate, and transport simulation at t = 0 after resuspension from prop wash (color key applies to Figure 6-89 through Figure 6-93, respectively)	159
6-90. Simulated silt-particle-bound copper concentrations at surface (left), and bottom layer (right) 3 hours after prop-wash resuspension	160
6-91. Simulated silt-particle-bound copper concentrations at surface (left), and bottom layer (right) 9 hours after prop-wash resuspension	160
6-92. Simulated silt-particle-bound copper concentrations at surface (left), and bottom layer (right) 18 hours after prop-wash resuspension	161
6-93. Simulated silt-particle-bound copper concentrations at bottom layer at t = 30 hours (left), and t = 120 hours (right) after prop-wash resuspension	161
6-94. Simulated silt-particle-bound deposits to the bottom bed at t = 3 hours (left), and at t = 9 hours after prop-wash resuspension (color key applies to Figure 6-94 through Figure 6-96)	162
6-95. Simulated silt-particle-bound deposits to the bottom bed at t = 18 hours (left), and at t = 30 hours after prop-wash resuspension.....	162
6-96. Simulated silt-particle-bound deposits to the bottom bed at t = 120 hours after prop-wash resuspension	163
6-97. Initial dissolved copper concentrations at Oscar Pier surface layer for CH3D simulation at t = 0 after resuspension from prop wash (color key applies to Figure 6-97 through Figure 6-100)	164
6-98. Figure 4-98. Simulated dissolved copper concentrations at Oscar Pier surface layer for CH3D simulation at t = 3 hours (left), and at t=9 hours after prop-wash resuspension	164
6-99. Simulated dissolved copper concentrations at Oscar Pier surface layer for CH3D simulation at t = 18 hours (left), and at t = 30 hours (right) after prop-wash resuspension.....	165
6-100. Simulated dissolved copper concentrations at Oscar Pier surface layer for CH3D simulation at t = 120 hours after prop-wash resuspension.....	165

6-101. Simulated silt-particle-bound copper concentrations at Oscar Pier bottom layer for CH3D simulation at t = 3 hours (left) and t = 9 hours after prop-wash resuspension	166
6-102. Simulated silt-particle-bound copper concentrations at Oscar Pier bottom layer for CH3D simulation at t = 18 hours after prop-wash resuspension.....	166
6-103. Simulated silt-particle-bound deposits to the Oscar Pier bottom bed at t = 3 hours (left) and t = 9 hours after prop-wash resuspension.....	167
6-104. Simulated silt-particle-bound deposits to the Oscar Pier bottom bed at t = 18 hours (left) and t = 30 hours after prop-wash resuspension.....	167
6-105. Simulated silt-particle-bound deposits to the bottom bed at t = 120 hours after prop-wash resuspension at Oscar Pier	168
6-106. Simulated water column TSS contours (left), TSS vertical profiles (center), and time series of TSS measured by ADCP (right) near the Oscar pier during the 11:23–12:45, 29 August 2012.....	169
6-107. ADCP track line with depth-averaged SSC (31 August 2012) indicated by color. Note that the track positions vary with time and do not indicate a snapshot in time. The sketched vessel positions indicate the approximate positions and sequence of vessel maneuvers during plume generation. Imagery ©2014 DigitalGlobe, U.S. Geographical Survey, USGS, Map data ©2014 Google Life mode Terms Privacy Report a problem.....	170
6-108. DDG-51 ship and P4876 propeller geometry.....	171
6-109. Computational domain and numerical grids	172
6-110. Longitudinal velocity contours and velocity vectors near seabed.....	173
6-111. Velocity profiles at the keel plane	174
6-112. Axial velocity contours and velocity vector plots around the propeller	174
6-113. Propeller-induced flow field at selected stations	175
6-114. Propeller-induced swirling flows	177
6-115. Shear stress distribution on the seabed	179
6-116. Surface plots of shear stresses on the seabed.....	180
6-117. Surface plots of seabed shear stresses around the twin-screw propellers.....	181
6-118. Field and model effort in Sinclair Inlet	182
6-119. Sediment deposition rate in the sediment traps by particle size and event	183
6-120. Deposition load and rate of sediments resuspended by sporadic (Event 1 and 2) and background or consistent activities (Event 3) in Sinclair Inlet, as measured from deposition onto the sediment remedial cap located in Pier 7 of PSNSY&IMF. Note that the symbols and colors in these plots are used in the plots within this chapter. Also note that thicker lines are used for the silt fraction measured in the three sampling events.....	185
6-121. Net deposition load (g/m^2) of metals measured in the different particle fractions collected with sediments traps on the sediment remediation cap in Pier 7. Note the different scales (g/m^2) in the ordinate (y-axis), of 0.80 for zinc and copper, 0.25 for lead, chromium, and nickel, and 0.10 for arsenic, silver, and cadmium. (Symbols and colors are the same as those in Figure 6-120).....	186

6-122. Metal deposition rates ($\text{g/m}^2 \text{ d}$) for metals in the different size-fractions measured in this effort. Note that a range to $0.016 \text{ g/m}^2 \text{ d}$ is used in the ordinate for zinc and copper, while 0.004 is used for the other metals. (Symbols and colors are the same as those in Figure 6-120)	187
6-123. Mercury concentrations measured at the ERDC Environmental Laboratory. These are only for Event 1	188
6-124. Deposition rates for silt (top), sand (middle) and TSS (bottom) from sediment plumes in Drydock 3.....	190
6-125. Deposition rates for silt (top), sand (middle) and TSS (bottom) from sediment plumes in Drydock 6.....	191
6-126. Measured and predicted sediment trap load for Event 1 and 2.....	192
6-127. Deposited copper (top) and nickel (bottom) from sediment plume in Drydock 3	194
6-128. Deposited copper (top) and nickel (bottom) from sediment plume in Drydock 6	195
6-129. Mean sediment trap particle concentration ($\mu\text{g/g}$) versus mean background sediment concentration ($\mu\text{g/g}$). Data are presented for each metal in the sand and silt fractions and for each of the three events.....	196
B-1. Ducted propeller geometry	1
B-2. Pressure distributions on the propeller blade, shaft and duct surfaces.....	2
E-1. MATLAB® Model GUI for the Graphic Maynard's Model	1
E-2. Graphic interface of model input and output of the Graphic Maynard's Model	2
E-3. Format of the output file (velocity field)	3

Tables

2-1. Field and model efforts used in the sediment resuspension and transport study	7
3-1. Performance objectives.....	10
5-1. Number and type of analytical samples for all three resuspension studies	20
5-2. Metal analysis in seawater samples, following methods suggested by USEPA (1994, 1999). Q-HNO ₃ is quartz-still grade nitric acid	22
5-3. Certified concentrations ($\mu\text{g/g}$ of dry sediment) for the standard reference materials (SRM) analyzed with the digestion procedure for resuspended and background sediments collected in this effort. NC indicates not certified	23
5-4. Mean blank ($n = 10$) concentrations and recoveries for SRMs BCSS-1, MESS-2 and PACS-1	24
5-5. Summary of QA/QC information for the analysis of metals by ICP-MS. Std. Dev. is standard deviation, NC means concentration is not certified, N/A is not applicable. Limit of detection is three times, and limit of reporting is 10 times the standard deviation of the blanks. LCS = SRM.....	25
5-6. Quality assurance/quality control for mercury analyses performed at the ERDC Environmental Laboratory. Laboratory control sample is synonymous to SRM. ND indicates that the analyte was not detected at or above the reporting limit	27
5-7. Calibration parameters for $\log_{10}(\text{SSC}) = a + b (\beta)$	34

5-8. Description of the three deployments events for quantification of particle and contaminants of concern deposited onto the sediment remedial cap in PSNS&IMF Pier 7	36
5-9. Methods for estimation of bottom shear stress (Biron et al., 2004)	39
6-1. Performance assessment results	49
6-2. Propeller information and operating conditions for ducted propeller	56
6-3. Key model input parameters for the Graphic Maynard's Model	72
6-4. Comparison of the calculated thrust and torque coefficients (in confined water) with the experimental data (open water) under bollard-pull condition	73
6-5. Sample identification, time, location, ancillary parameters, and mass fractions for samples collected at the San Diego Bay resuspension event of 4 April 2012 (S refers to surface, and M refers to mid-depth in the plume sample ID)	77
6-6. Metal concentrations measured in aqua regia digestates on background sediments from San Diego Bay. All data is provided in µg/g but for recoveries that are given as %. Certified are certified concentrations. Silver (Ag) is not certified in neither standard reference material (SRM)	79
6-7. Nationally recommended water quality criteria by the U.S. Environmental Protection Agency (USEPA). CMC = Criterion Maximum Concentration, CCC = Criterion Continuous Concentration (or Chronic Criterion)	86
6-8. Polycyclic aromatic hydrocarbons measured in selected fractions of a suite of samples from the San Diego Bay resuspension event of 4 April 2012. Note that values in italics with yellow background are the Method Limit of Detection, and is given for samples that were not detectable	87
6-9. Resuspended sediment and associated metal concentrations input values for San Diego Bay between piers 4 and 5. Metals not shown were below EPA's water quality standards	92
6-10. Eroded sediment particle masses from propeller wash experiment for fate/transport model simulation using CH3D and the settling velocities associated with the particles	97
6-11. Copper and zinc suspended matter/water log K_D summaries from literature data as compiled by Allison and Allison (2005)	101
6-12. Water quality parameters for San Diego Bay	103
6-13. Look-up table (red header with 15 datasets excerpted from 729 datasets in the original look-up table), the 7 coefficients (green header) derived from the 729 datasets, and the predicted partitioning by the linear equation (yellow header)	104
6-14. Average concentrations of copper and nickel associated with sand, silt, and clay particles based on field data	114
6-15. Sample identification, location, time and mass fractions of the different particle sizes measured in samples from the Pearl Harbor resuspension event of 28th August 2012 at Bravo Pier	121
6-16. Sample identification, location, time and mass fractions of the different particle sizes measured in samples from the earl arbor resuspension event of 29 August 2012 at Oscar Pier	122

6-17. Particle size fractionation and total organic carbon (TOC) measured prior to resuspension from the three sites selected for this study. Data for Oscar Pier is from one sample, and was not analyzed for TOC.....	124
6-18. Metal concentrations measured in aqua regia digestates from background sediments from Bravo Pier and Oscar Pier in Pearl Harbor. All data is provided in µg/gr, except for recoveries, which are given as %. Certified are certified concentrations. Silver is not certified in SRMs, BCSS-1, and PACS-1	126
6-19. Method detection limits (MDL, µg/L) for the samples analyzed for the NOAA-18 polychlorinated biphenyls (PCB) and pesticides from the Bravo Pier event of 28 August 2012. All the samples were qualified as undetected. B is background, 2 in the size-fraction column indicates that only the 2-mm fraction was analyzed, All is all the fractions analyzed, xmeans analyzed, - means not-analyzed	135
6-20. Method detection limits (MDL, µg/L) for the samples analyzed for the NOAA-18 PCB and pesticides from the Oscar Pier event of 29 August 2012. All the samples were qualified as undetected. B is background, 2 in the size-fraction column indicates that only the 2-mm fraction was analyzed, All is all the fractions analyzed,xmeans analyzed, - means not-analyzed	136
6-21. Resuspended sediment and associated metal concentrations input values for Bravo Pier. Metals not shown were below EPA's water quality standards	148
6-22. Resuspended sediment and associated metal concentrations input values for Oscar Pier	150
6-23. Propeller information for DDG-51 ship in FANS simulation	171
6-24. Maximum shear stresses in different regions of the seabed.....	181
6-25. Metal concentrations measured in aqua regia digestates on background sediments from PSNSY& IMF, Bremerton, Washington. All data is provided in µg/g, except for recoveries, which are given as %. Certified are certified concentrations. Silver is not certified (NC) in SRMs, BCSS-1, and PACS-1	184
6-26. Integrated deposition rate at Pier 7 between model results (g/m ²) and field data (g/m ² -day)	193
7-1. Costs model from the modeling development in San Diego Bay	200
7-2. Costs expected for the scenario of an embayment where basic hydrologic information is available, and there is a requirement for high resolution in the predicted fate and transport of particles resuspended by propeller wash.....	202
A-1 Points of contact	A-1
B-1. Propeller information and operating conditions for ducted propeller.....	B-1
B-2. Comparison of the calculated thrust and torque coefficients (in confined water) with the experimental data (open water) under bollard-pull condition	B-3
C-1. Size-fraction data	C-1
C-2. Chromium data for San Diego Bay Field Study, 4 April 2012.....	C-2
C-3. Nickel data for San Diego Bay Field Study, 4 April 2012	C-3
C-4. Copper data for San Diego Bay Field Study, 4 April 2012	C-4
C-5. Zinc data for San Diego Bay Field Study, 4 April 2012	C-5

C-6. Arsenic data for San Diego Bay Field Study, 4 April 2012	C-6
C-7. Silver data for San Diego Bay Field Study, 4 April 2012	C-7
C-8. Cadmium data for San Diego Bay Field Study, 4 April 2012.....	C-8
C-9. Lead data for San Diego Bay Field Study, 4 April 2012	C-9
D-1. Size-fraction data	D-1
D-2. Chromium data for Pearl Harbor Field Study, 29–29 August 2012	D-2
D-3. Nickel data for Pearl Harbor Field Study, 29–29 August 2012	D-3
D-4. Copper Data for Pearl Harbor Field Study, 29–29 August 2012.....	D-4
D-5. Zinc Data for Pearl Harbor Field Study, 29–29 August 2012.....	D-5
D-6. Arsenic Data for Pearl Harbor Field Study, 29–29 August 2012	D-6
D-7. Silver Data for Pearl Harbor Field Study, 29–29 August 2012	D-7
D-8. Cadmium Data for Pearl Harbor Field Study, 29–29 August 2012	D-8
D-9. Lead Data for Pearl Harbor Field Study, 29–29 August 2012	D-9
F-1. State variable for model input	F-2
F-2. WHAM input deck and outputs.....	F-19
G-1. Sediment Profile Image Analysis results	G-1
H-1. Particle and Metal Deposition Rates ($\text{g}/\text{m}^2 \text{ d}$) for Event 1	H-1

1. INTRODUCTION

Propeller wash induces disturbances to the bottom sediment in Department of Defense (DoD) harbors in multiple ways. Resuspension of bottom sediment by propeller wash in DoD harbors is a phenomenon constantly observed and occasionally reported. While these resuspension events occur frequently, their potential effects on erosion, transport, redeposition, and recontamination of bottom sediments have not been rigorously studied or quantified. At this point, we do not fully understand under what conditions propeller wash erodes and resuspends bottom sediment and how the eroded sediment plume is dispersed and redeposited in hydrodynamically energetic DoD harbors. This study aims to demonstrate and validate an innovative, quantitative method that integrates information from state of science measuring devices/tools with predictive models. These measuring devices have been used to measure and evaluate critical parameters that govern propeller wash resuspension and subsequent fate and transport of the eroded sediments in DoD harbors.

Figure 1-1 shows the overall framework and components of the study. First, measuring devices were calibrated and validated under laboratory conditions before they were deployed for field measurements. Water velocities and turbulence field disturbed by the propeller and subsequent resuspension of bottom sediment were measured to determine their fate and transport. For investigation of resuspension potential, Maynard's Model (1984) and the Finite Analytical Navier-Stoker Solver (FANS) model (Chen et al., 2003) were set up to simulate and evaluate flow velocities and bottom shear stress from propeller wash for a tugboat and a guided missile destroyer (DDG), respectively. Field data were used to support the fate and transport model, Curvilinear Hydrodynamics in 3D (CH3D), which was successfully calibrated for San Diego Bay, CA, Pearl Harbor, HI, and Sinclair Inlet, WA, in previous studies.

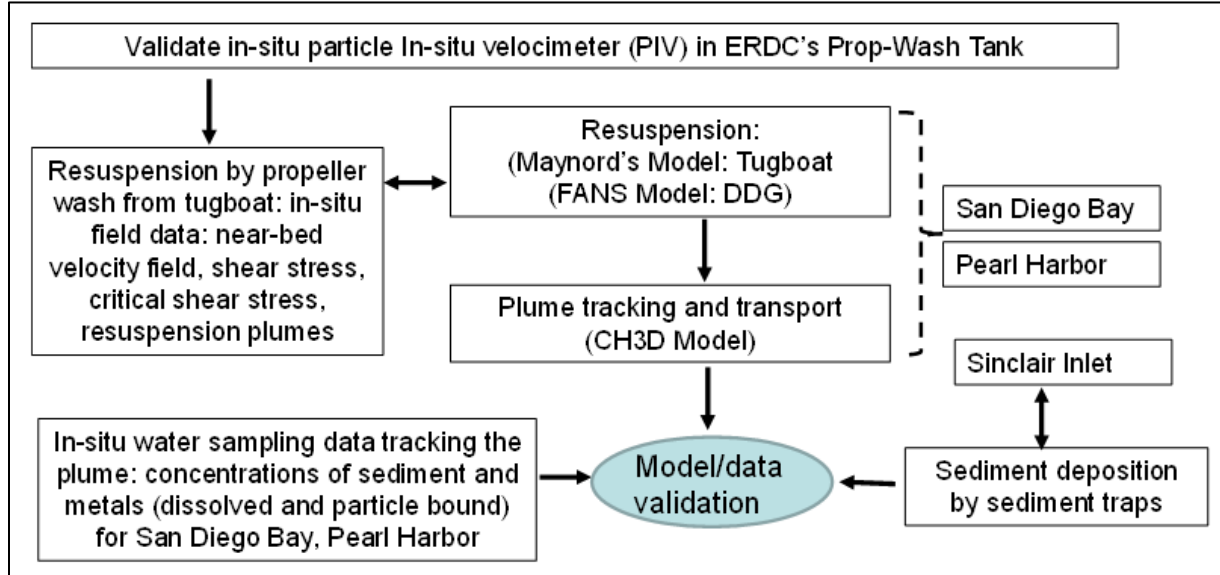


Figure 1-1. Study framework and components including both laboratory study, field work, and modeling studies.

Figure 1-2 shows the more detailed approach used in San Diego Bay between Piers 4 and 5 at the Naval Station San Diego. In the San Diego case, an additional metal partition model Tableau Input Coupled Kinetic Equilibrium Transport (TICKET) was added. In these figures, “cal” is shorthand for calibration, “val” is shorthand for validation. Calibration is process of setting up the model so that

output conforms to field observations. Validation is a subsequent model output test with an independent set of field observations. Figure 1-3 shows the approach used first at Bravo Pier, then Oscar Pier, in Pearl Harbor. Incidental observations of resuspension from underneath the guided missile destroyer USS *Chafee* via acoustic backscatter were used to validate predictions of the FANS model. Figure 1-4 shows the approach used at the Puget Sound Naval Shipyard in Sinclair Inlet, where sediment trap data showed that model assumptions predicting the effects of two tug assist events were not correct. At this site other, simultaneous sources of resuspended sediments were probably active.

San Diego Bay

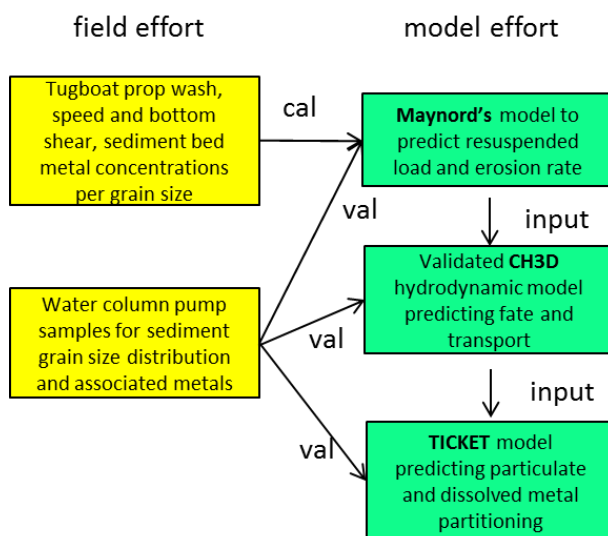


Figure 1-2. Field and modeling effort in San Diego Bay.

Pearl Harbor

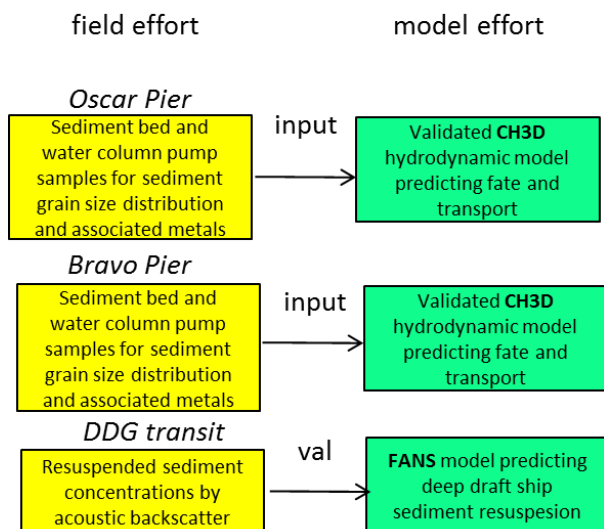


Figure 1-3. Field and modeling effort in Pearl Harbor.

Sinclair Inlet

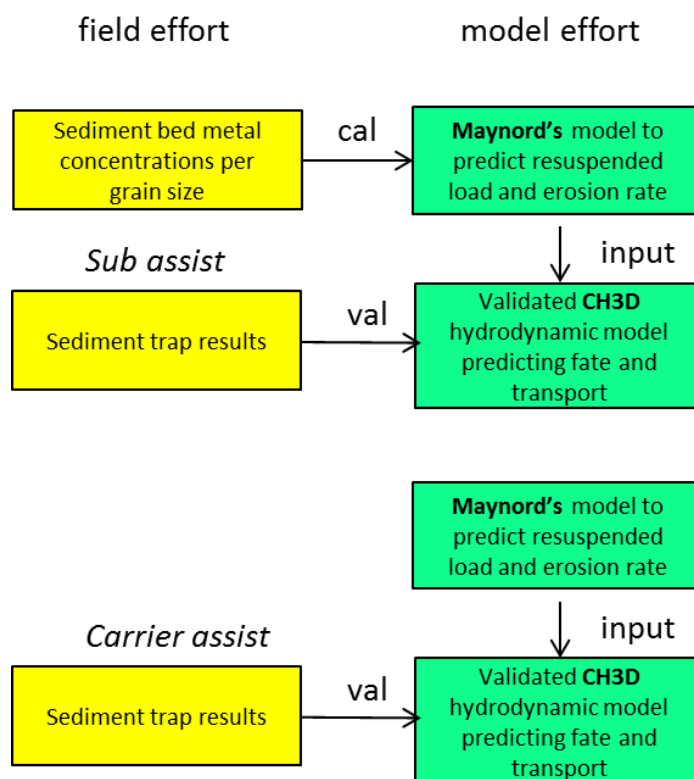


Figure 1-4. Field and modeling effort in Sinclair Inlet.

Based on this study, the following products have been published and delivered, which are in the public domain: Chen, and Wang, 2015; Liao, Wang, and Wang, 2013; Liao, Wang, and Wang, 2014; Wang, Farley, and Rivera, 2015; Wang, Cole, and Barua, 2015; Wang, Cole, and Barua, 2015; Wang et al., 2014; Wang, Liao, Bootsma, and Wang, 2012.

1.1 BACKGROUND

Over the past decade, we have witnessed a significant progress in identifying the scope and location of contaminated sediments in DoD harbors and waters. Equal amount of effort has been taken in remediation of these contaminated sediments with remedial actions that include, dredging, active or passive capping and natural recovery. However, as discussed in the “Strategic Environmental Research and Development Program (SERDP) and Environmental Security Technology Certificate Program (ESTCP) Workshop Report on Research and Development Needs for Long-Term Management of Contaminated Sediments” (SERDP-ESTCP, 2012), there is a lack of understanding on how effective these remedial efforts are in both the short and long term.

A major issue with these sediment remedial actions is the stability of the sediment’s three-dimensional structure. Long-term stability of this structure is required for the remedial action to have a significant effect on the sediment composition. Therefore, it’s important for the remedial actions to withstand resuspension as well as recontamination by sediments from a different site. However, there are observations and reports indicating that dredging, propeller wash, and extreme events (e.g.,

hurricanes) resuspended significant sediments in U.S. harbors (Stortz and Sydor, 1980; Kerfoot et al., 2004). These resuspension events occur at different time intervals, with propeller wash occurring daily around navigation channels and piers, dredging occurring most likely at contaminated sediment sites every few years and extreme storms taking place every several years. These events have a significant effect on the loading of particles to the water column, for example, a field study shows that berthing/docking at three naval piers in San Diego Bay resuspended a total of 26 tons/day of sediments into the water column (Wang et al., 2000). A modeling study shows that propeller wash from DoD vessels in transit resuspends ~54 tons/day of bottom sediments in Pearl Harbor (Wang et al., 2009), which is more than 10% of the total averaged daily suspended sediment load (TSSL) from the entire Pearl Harbor watershed. These resuspension events will affect sediment remediation sites by affecting its three-dimensional structure, and by bringing contaminated sediments to the top of the remediated sediment.

Tugboat activities and navigating deep-draft vessels, such as DDGs, are the major sources of propeller wash induced resuspension in DoD harbors. The graphic Maynard's model and the FANS model were implemented to predict the disturbances produced by tugboat and a DDG, respectively.

Propeller wash generates two impacts on a remediation bed: disturbances (e.g., shear stress) on the sediment bed inducing resuspension, and redeposition of sediment plumes over the bed of remediated sediments. Resuspension occurs when shear stress by prop wash exceeds the critical shear stress of the bed and sediment plumes enter into the water column and are subject to transport, chemical partitioning, remigration and redeposition. Redeposition is the result of resuspending sediments from a different site and having these particles settling down on the sediment under remediation. It is important to understand and quantify the processes of the sediment plumes from its resuspension origin, to remigration, redeposition and then, eventually being flushed out from the harbor domain.

For this study, we have applied both field study and modeling studies to simulate, and evaluate fate and transport of contaminated sediments resuspended from propeller wash in San Diego Bay, CA, two sites in Pearl Harbor, HI, and Sinclair Inlet, WA. The field work collected key data for analysis as well as for supporting the modeling study. Benefits of the study include (1) improved understanding of resuspension by propeller wash and its impact on bottom sediment in DoD harbors, (2) predictive capabilities for potential recontamination of contaminated sediment remedial sites, and (3) better information-based decision making in managing propeller wash-induced sediment resuspension, transport and recontamination potential.

1.2 OBJECTIVES OF THE DEMONSTRATION

The objectives of the study include (1) demonstrate and validate innovative methods to estimate erosion potential by propeller wash in two DoD harbors (source term), and (2) characterize, map and predict fate and transport of sediment plumes and contamination by propeller wash (fate and transport).

To achieve the first objective, we have conducted both laboratory and field studies to measure the parameters that govern propeller wash and its erosion potential, and then refine and validated Maynard's model for erosion potential evaluation. For the second objective, we have conducted field studies to measure concentrations of sediment particle sizes and metal concentrations from propeller wash plumes in San Diego Bay, CA, and Pearl Harbor, HI, and deployed sediment traps and measured sediment depositions at Pier 7 in Sinclair Inlet, WA. CH3D as the fate and transport model has been implemented to simulate the fate/transport and redeposition of the sediment plumes from propeller wash.

1.3 REGULATORY DRIVERS

Under the Federal Clean Water Act, Section 303(d), states are required to identify all water bodies that do not meet water quality standards. Identified impaired water bodies are included in the 303(d) list, and remedial strategies, water cleanup plans, or total maximum daily loads (TMDLs) must be developed to bring the water body back into compliance. Under the Comprehensive Environmental Response, Compensation, and Liability Act (CERCLA), federal agencies are liable for releases of hazardous material (contaminated sediments) and are required to take short-term removal of the material and/or long-term remedial actions.

2. TECHNOLOGY

2.1 TECHNOLOGY DESCRIPTION

The study includes a number of laboratory and field studies of which the results were used to calibrate/validate hydrodynamic models and/or provided input conditions to those models. The overall study framework is shown in Figure 1-1. Field studies measured water velocity, turbulence field, and resuspended sediment loads produced from propeller wash of tug-boats. Laboratory and field studies measured the concentration and particle size of resuspended sediment, as well as the concentration of contaminants (primarily metals) associated with those sediment. The models employed in this study include two models, Maynard and FANS, that predict sediment resuspension by the propeller wash from a tugboat and a DDG, respectively. The calibrated fate and transport model, CH3D, was used to predict the transport, migration, and eventual footprint of the resuspended sediment and associated contaminants downstream from the resuspension events. All data collection and model techniques rely on calibrated instruments and calibrated/validated models at the study sites in San Diego, CA (Figure 1-2), Pearl Harbor, HI (Figure 1-3), and Sinclair Inlet, WA (Figure 1-4). The field/laboratory techniques that fed input into the models are shown in Table 2-1.

Field studies consisted of five related activities: (1) tug propeller wash velocity measurements in the water column and near bottom in San Diego Bay, (2) measuring critical erosional velocities and erosion rate to calculate critical shear in San Diego Bay, (3) measuring sediment and contaminant concentrations in the water column downstream of the propeller wash in San Diego Bay and two sites in Pearl Harbor, (4) measuring resuspended sediment in the wake of a deep-draft vessel under tug escort in Pearl Harbor, and (5) collection of sediment from traps in Sinclair Inlet, deployed during tug operations over a 4-month period.

Field and laboratory instruments used in Tasks (1) and (2) in Table 2-1 were an acoustic Doppler velocimeter (ADV) that measures velocity in a small volume with high accuracy, a particle image velocimeter (PIV) to measure particle velocity profiles at high frequency on a vertical plane near the bottom. Field and laboratory instruments used in Tasks (3) and (4) were optical backscatter (OBS) devices to measure suspended sediment load, an acoustic Doppler current profiler (ADCP) that measures water velocity and resuspended sediment concentrations in the water column via acoustic backscatter, a sediment profile imaging system (SPI) for imagery of bottom sediment profiles before, during and after sediment erosion by propeller wash, deck pumps used to draw water samples, usually simultaneously from 1 m below the surface and at mid depth, sediment sieves and filters used to separate sediment and associated contaminants into gross size fractions in the laboratory, and a combination inductively-coupled plasma mass spectrometer device to measure metal contamination in the laboratory. In Task (5), nine vertical sediment traps were arranged on the bottom of Pier 7 in Sinclair Inlet to capture sediment load deposited over a six-month period (January–June 2014).

Table 2-1. Field and model efforts used in the sediment resuspension and transport study.

Task	Site and Date	Field/Laboratory Gear	Model(s)
(1) Measure tug wake velocity field	San Diego, CA December 2012	ADV	Maynard
(2) Measure critical shear stress	San Diego, CA March 2012	ADV PIV	Maynard
(3) Measure resuspension and transport of sediments and contaminants	San Diego, CA July 2012	OBS	Maynard and CH3D
		Deck pumps	
		Sediment sieves	
		ICP/mass spec	
(3) Measure resuspension and transport of sediments and contaminants	Bravo Pier, Pearl Harbor, HI August 2012	OBS	CH3D
		Deck pumps	
		Sediment sieves	
		ICP/mass spec	
		ADCP	
		SPI	
(3) Measure resuspension and transport of sediments and contaminants	Oscar Pier, Pearl Harbor, HI August 2012	OBS	CH3D
		Deck pumps	
		Sediment sieves	
		ICP/mass spec	
		ADCP	
		SPI	
(4) Resuspension by deep draft vessel	Bravo Pier, Pearl Harbor, HI August 2012	ADCP	FANS
(5) Measure resuspension and transport of sediments and contaminants	Sinclair Inlet, WA January-June 2014	Sediment traps Sediment sieves ICP/mass spec	Maynard and CH3D

For San Diego Bay, measurements of the tug wash resuspension potential were used to calculate bottom shear to calibrate the Maynard propeller wash model against measured velocities, bottom shear and total erosion rate. For the fate/transport study for San Diego Bay, the calibrated Maynard's model was then used to predict sediment and contaminant mass resuspended by the propeller wash from a tugboat under a controlled propeller running environment. Model-predicted sediment and contaminant mass from the tugboat were used as input to CH3D, a hydrodynamic model predicting sediment fate and transport. Predicted water column sediment and metal concentrations were compared with the field data measured at 17 stations in the vicinity of the pier region during the two-hour period following the resuspension event. The resuspended sediment acoustically detected behind a deep draft vessel was used to validate sediment resuspension predicted by the FANS model. Finally, the sediment caught in traps from the three deployments in Sinclair Inlet during January–June 2014 was compared with model-predicted footprint from potential resuspension events near the

site. Based on measured data and model results, analyses were conducted on the potential sources of resuspension/deposition scenarios. Field studies supporting Maynard, then CH3D model predictions are similar in the cases of San Diego and Sinclair Inlet. In Pearl Harbor, Maynard's model was not used. Resuspended sediments measured from pump samples were used as input to CH3D.

2.2 TECHNOLOGY/METHODOLOGY DEVELOPMENT

All of these instruments are commonly used in oceanographic and environmental studies. Additional information on gear and techniques are provided in the Test Design, Section 1.

Maynard's model (1984) is one of the few models that have been used to predict flow velocities and shear stresses near the sediment bed induced by a propeller. The model was initially developed for a single-screw propeller operating in an infinite flow domain and is approximated for deep water applications. For the current study, most traffic and propeller wash for Navy/DoD vessels are shallow water, high-energy activities, and Maynard's model has been implemented for this environment and was used to estimate the bed shear stress at the sediment bed induced by the propeller wash. Bed shear stress is the most important parameter that determines both the inception of resuspension (the critical shear stress exceeded) and the entrainment rate. Existing models for propeller wash, i.e., Maynard's model (Maynard 1984, 1998; Maynard et al., 2006), predict near-bed velocity that is then converted to a bed shear stress. This conversion is based on turbulent boundary layer theory in channel flows, usually under a uniform and steady flow condition. Similarly, the U.S. Army Corps of Engineers High Shear Stress flume (SEDflume) was utilized to establish the relationship between the erosion rate and the varying near-bed flow velocity in a confined channel where flow is relatively uniform. Almost all existing sediment entrainment models are obtained through laboratory flume studies with well-defined flow conditions. However, the flow field behind a propeller is extremely turbulent and unsteady, making it a special case that differs significantly from flow fields found in channels rivers, tidal current, flood flow, wind waves, etc.

Maynard's model (Maynard, 1984) was chosen for this study because it is often used for similar propeller wash studies. However, there are a number of limitations of the Maynard's model and one of the major limitations is that the model is applicable for deep water, for which the propeller should not be too close to the bottom. That is, the ratio of propeller diameter/shaft-to-bottom-distance D_p/H_p should be less than 1.2, as suggested by Maynard (1998). However, most deep-drafted vessels in DoD harbors operate in very shallow water conditions with D_p/H_p far exceeding 1.2. A literature search revealed that no published manuscripts/data could be found for validation of Maynard's model for the scenarios, $D_p/H_p > 1.2$, for which most naval vessels in DoD harbors operate. It has been observed and reported that resuspension by propeller wash in DoD harbors is primarily caused by two types of vessels: tugboats and deep-drafted vessels, such as DDGs and aircraft carriers (Wang et al., 2000). Tugboats are used for berthing, docking, and pushing vessels in the pier regions and large thrusts are generated, which generates turbulent flows to resuspend bottom sediment. The deep-drafted vessels, while navigating at low speed (< 5 knots), have been observed to resuspend bottom sediment because of the small clearance between the ship hull, the propellers, and the bottom. Therefore, we implemented the Maynard's model for evaluating the resuspension potential of propeller wash by a tugboat and the FANS model for a DDG.

The Finite-Analytic Navier-Stokes (FANS) code has been used extensively for the simulation of ship motions with and without propellers under very shallow water conditions. These applications include: berthing of DDG-51 and AOE-6 ships (Chen et al., 1998, 2000), mooring of LHD ships (Chen and Huang, 2003), performed berthing simulations for DDG-51 and AOE-6 ships. In these simulations, a very shallow water depth of 28 ft was used with the under keel clearance of the moored and docking ships to 1 ft or 3.7% of the ship draft (= 27 ft). More recently, the FANS code

has also been used by Huang and Chen (2007, 2010) for site-specific passing ship effects on a docked ship moored to a floating pier in Norfolk harbor. These simulation results clearly demonstrated the capability of the FANS code to model complex interactions between Navy harbor facilities and their client ships under real waterfront conditions. These site-specific conditions include bathymetry, shorelines, harbor geometry, navigation channels, hull shapes, and arbitrary ship motions, and the effects of propeller wash. The details of the FANS model applications for this study can be found in Chen and Wang (2014).

The numerical hydrodynamic fate and transport model applied for this study is CH3D. This model is a boundary-fitted finite difference, Z-coordinate model developed by the U.S. Army Corps of Engineers Waterways Experiment Station (Johnson et. al., 1995) to simulate physical processes in bays, rivers, lakes, and estuaries (Wang and Martin, 1991; Wang, 1992; Wang and McCutcheon, 1993; Wang et al., 1997, 1998; Johnson et al., 1995). The model simulates hydrodynamic currents in four dimensions (x, y, z, and time) and allows for the prediction of the fate and/or transport of metals, sediment, and other contaminants in estuarine and coastal environments under the forcing of tides, wind and freshwater inflows (Sheng et al., 1990; Wang and Richter, 1999). The CH3D model was implemented and applied to support the following relevant studies: (1) copper and other antifouling biocide concentrations from hull paint in San Diego Bay (Wang et al., 2006), concentrations of copper and its species in support of ESTCP's project for San Diego Bay and Pearl Harbor (Chadwick et al., 2008); and deposition of particulate contaminants from three creeks in San Diego Bay (Chadwick et al., 2013), and (2) sediment transport and deposition of sediment loads from the surrounding watersheds for Pearl Harbor (Wang et al., 2009), and (3) hydrodynamics modeling study for Sinclair Inlet (Wang, et al., 2003) and Total Maximum Daily Load (TMDL) for bacteria and combined sewage outfalls (CSO) in Sinclair Inlet (Wang et al., 2003). Further details about the model and results can be found in the references and the list of publications listed in Section 1. Section 1.

2.3 ADVANTAGES AND LIMITATIONS OF THE TECHNOLOGY/METHODOLOGY

Modeling, coupled with calibrating/validating field measurements, is the typical approach used to estimate dispersal in the water column. The main cost is the model setup, requiring data on initial conditions and a model tuned to site-specific conditions. The main benefit is broad applicability if the model is validated. The U. S. Army Corps of Engineers has been active in measuring and modeling transport of sediment, developing Maynard's model in 1984. They have also used CH3D, coupled with the U.S. Environmental Protection Agency model nutrient model Water Quality Analysis Simulation Program (WASP) for eutrophication studies in non-DoD harbors. This study is unique as far as we know in combining Maynard's model, CH3D and TICKET to predict the source, fate, and transport, and partitioning of resuspended sediments and contaminants in Navy harbors.

3. PERFORMANCE OBJECTIVES

The performance objectives of the study include both quantitative and qualitative metrics (Table 3-1). The quantitative objectives include sediment resuspension potential for tugboat, fate and transport of sediment plumes resuspended by propeller wash, and the linked fate and transport model (CH3D) and the metal partitioning model (TICKET). The qualitative objectives include the linked CH3D+TICKET model in its modeling framework by integrating the look-up table derived from TICKET into the CH3D model. The second qualitative objective is potential (incidental) detection of sediment plume generated by ship bow wake, instead of propeller wash for deep-draft vessel (USS *Chafee*). Table 3-1 lists these objectives, data requirements, and evaluation criteria for the stated objectives.

Table 3-1. Performance objectives.

Quantitative Objectives			
Performance Objectives	Metric	Data/Model Requirements	Success Criteria
Sediment resuspension model for tugboat	Calibrated resuspension model for San Diego Bay	Accuracy/comparison of measured velocity by PIV and ADV (field data)	Difference of Mean ($V_{piv} - V_{adv}$) < 5 cm/s or < 50%
		Velocity field by Maynard's model for four prop speeds	Mean velocity (model-data) < 10 cm/s or < 50%
		Bottom shear stress (cumulative)	Mean (model-data) < 0.1 Pa-Hr, or < 50 %
		Erosion rate (cumulative)	Measured-calculated cumulative erosion < 0.2 mm or < 50%
Fate and transport model of size-specific sediments resuspended in tug propeller wash	Calibrated and validated sediment fate and transport model for San Diego Bay	Water column sediment concentrations and sediment grain size	Difference (model-data) of water column sediment concentrations < 0.5 mg/L or < 50 %
		Water column dissolved and total copper concentrations	Difference (model-data) of water column dissolved and total copper concentrations < 3.1 µg/L or < 100 %
Linked CH3D+TICKET Model	Calibrated and validated contaminant partitioning model for San Diego Bay	Partitioning coefficient for copper between field data and look-up table	Difference (field data-estimated) of copper partitioning < 0.1 or < 75%
		Water column particulate copper concentrations	Difference (model-data) of water column copper concentrations bound by clay, silt, and sand < 3.1 µg/L or < 100 %

Table 3-1. Performance Objectives. (Continued)

Qualitative Objectives			
Performance Objectives	Metric	Data/Model Requirements	Success Criteria
Linked resuspension, fate and transport and partitioning models	Models linked	Compatible model input and output files	Models linked
Fate and transport model for Pearl Harbor	CH3D application for fate and transport for Pearl Harbor	TSS data tracking the bulk of the plumes	Model-simulated TSS concentrations compared with TSS, qualitatively
		Tracking (incidental) bow wake of USS Chafee	Incidental tracking and measured TSS plume in the wake of USS Chafee (deep draft), as predicted by FANS model

4. SITE DESCRIPTION

4.1 SITE LOCATION AND HISTORY

San Diego Bay is a natural harbor and deep water port located in San Diego County, California, near the U.S.–Mexico border. The bay, which is 12 mi (19 km) long and 1 to 3 mi (1.6 to 4.8 km) wide, is the third largest of the three large, protected natural bays on California's entire 840-mi (1,350-km) long coastline after San Francisco Bay and Humboldt Bay. The highly urbanized land adjacent to the bay includes the city of San Diego (eighth largest city in the United States) and four other cities, including National City, Chula Vista, Imperial Beach, and Coronado.

Considered one of the best natural harbors on the west coast of North America, it was colonized by Spain beginning in 1769. Later it served as base headquarters of major ships of the U.S. Navy in the Pacific until just before the U.S. entered World War II, when the newly organized U.S. Pacific Fleet's primary base was transferred to Pearl Harbor, Hawaii. However, San Diego Bay remains as a home port of major assets, including several aircraft carriers of the U.S. Pacific Fleet, and as a result of base closures beginning in the 1980s, facilities in San Diego Bay are the only remaining major naval base facilities still in operation in the entire State of California. Naval Base San Diego is the principal homeport of the U.S. Pacific Fleet, consisting of 46 Navy ships, one Coast Guard cutter, seven Military Sealift Command logistical support platforms, and several research and auxiliary vessels.

Pearl Harbor is located on the island of Oahu. The Pearl Harbor embayment, along the south coast, formed as the island sank ~360 m toward the end of the main shield building phase, drowning the river valleys that drain central Oahu. Pearl Harbor contains almost 50 km of shoreline backed by extensive wetlands through which highly-sedimented waters enter the harbor. The harbor has been a homeport to the U.S. Pacific Fleet for nearly 100 years. Navy Region Hawaii oversees the U.S. Navy's largest and most strategic island base in the Pacific. The Navy region extends over 23,000 acres of land and water on Oahu and Kauai and serves as the host for the headquarters of seven major Navy commands, including Commander, U.S. Pacific Fleet; Commander, Submarine Force, U.S. Pacific Fleet; Commander, Navy Region Hawaii; Commander, Naval Surface Group, Middle Pacific; and Commander, Naval Facilities Engineering Command (NAVFAC) Pacific. Established in 1908, the Pearl Harbor Naval Shipyard and Intermediate Maintenance Facility (PHNSY&IMF) provides regional maintenance at the depot and intermediate levels on U.S. Pacific Fleet's surface ships and submarines. Twenty-nine U.S. Navy surface ships and submarines are currently homeported at Naval Station Pearl Harbor.

Sinclair Inlet. Puget Sound Naval Shipyard was established in 1891 on Sinclair Inlet, WA, as a naval station and was designated Navy Yard Puget Sound in 1901. During World War I, the navy yard constructed ships, including 25 submarine chasers, seven submarines, two minesweepers, seven seagoing tugs, and two ammunition ships, as well as 1,700 small boats. During World War II, the shipyard's primary effort was the repair of battle damage to ships of the U.S. fleet and those of its allies. Following World War II, Navy Yard Puget Sound was designated Puget Sound Naval Shipyard. It engaged in an extensive program of modernizing carriers, including converting conventional flight decks to angle decks. During the Korean War, the shipyard was engaged in the activation of ships. In the late 1950s, it entered an era of new construction with the building of a new class of guided missile frigates. The historic district includes 22 contributing buildings and 42 contributing structures, as well as 49 non-contributing buildings, structures, and objects. A demonstration project is underway at Pier 7, Puget Sound Naval Shipyard and Intermediate Maintenance Facility, Bremerton, WA, under ESTCP project ER-201131. It is being conducted to demonstrate and validate placement, stability and performance of reactive amendments for the

treatment of contaminated sediments in an area with elevated polychlorinated biphenyl (PCB) and Hg contamination.

4.2 SITE CHARACTERISTICS

San Diego. Most of the piers for naval vessels are located at Naval Station San Diego along the northeast coast in the middle section of the bay. Docking, berthing, and tugging of naval vessels within the naval piers are routine activities, which result in resuspension of bottom sediments and sorbed contaminants. Tugging and docking activities are believed to be responsible for a major portion of bottom sediment resuspension in the region of Naval Station San Diego as well as in San Diego Bay in general (Wang et al., 2004). Once resuspended, sediments and sorbed contaminants are subject to transport by tidal currents and deposition to other regions of the bay, thus posing a concern for potential migration of these substances. While resuspension of bottom sediments during tugging and docking activities has frequently been observed in the field, quantitative descriptions of these processes are lacking. Pier 4-5 is chosen to be the first test site, where the majority of docking activities take place.

Pearl Harbor. The harbor has an entrance at the south and is fan-shaped with four subbasins: West Loch, Middle Loch, East Loch, and Southeast Loch. A navigation channel extends from the entrance 7.6 km (4.7 miles) northward to the northern boundary of East Loch. The distance of the west-to-east boundaries of the harbor is approximately 8.6 km (5.3 miles). The harbor has a total surface area of 19.3 km² (7.5 mile²), and an average depth of 9.2 meters (30.2 ft). Depths of the harbors vary in different regions, with ~14 meters (46 ft) near the entrance and ~11 meters (36 feet) in the navigation channel. Depths in West Loch and Middle Loch are approximately 3.5 and 7.6 meters (11.5 and 25 ft), respectively. Water depths in East Loch and Southeast Loch are in the range of 9–10 meters (29.5–32.8 ft). Surface water circulation is driven primarily by northeasterly trade winds. Maximum residence time for bottom waters has been calculated as about six days in Middle Loch. In major channel areas and throughout East Loch, however, surface water residence times average one to three days. Vessel traffic has been identified as a major harbor-water mixing mechanism (Grothoug, 1992).

Sinclair Inlet. The most prominent fluctuations in sea level and currents in Sinclair Inlet are caused by tides. The tidal range in sea level, up to 4 m, is about one-quarter of the water depth. The tidal currents associated with these sea-level oscillations typically have an 8 cm/s amplitude that is uniform with depth; hence, large volumes of water and material suspended across the entire water column move in and out of the inlet once or twice a day. The excursion length for this exchange is about 1.7 km, based on a typical 8 cm/s tidal current and a duration of 6 hours (from slack ebb to slack flood). The net exchange caused by these large fluctuations depends, in part, on (1) the mixing within the inlet caused by the large tides, and (2) by the strength of the currents that flow past the mouth of the inlet, either from Dyes Inlet or from the Port Orchard channel (Noble et al., 2013).

5. TEST DESIGN (METHODS)

This study resulted in multiple field and model designs in several Navy harbors. Rather than combining test designs and field results in one section, the design is described herein. How/whether performance objectives were met, as listed in Section 1, are described in Section 1, and supported by comparison of field data to model results. The test design section is laid out in two parts. Section 5.1 discusses how field samples, used to either calibrate or validate the models, was collected and processed. The field designs sequentially discussed are (1) tug propeller wash water column measurements, (2) tug wash bottom shear measurements, (3) processing of sediment and metal pump samples in general, (4) specific pump sample designs in San Diego and two sites in Pearl Harbor, (5) acoustic detection of resuspended sediments from USS *Chafee*, and (5) sediment traps deployed in Sinclair Inlet.

Section 5.2 discusses how the models were set up and populated with initial values. The model designs discussed are (1) Maynard's model for bottom shear for single and twin propellers under San Diego Bay conditions; (2) FANS model for a deep draft destroyer; (3) CH3D model for San Diego, the two sites in Pearl Harbor, and Sinclair Inlet; and (4) TICKET model to predict metal partitioning on resuspended sediment in San Diego Bay.

5.1 FIELD AND LABORATORY PROCEDURES

Field and laboratory procedures are discussed below. The first task is the deployment of the gear that measured and mapped out the tug wash velocity and turbulence field. Resuspension potential by tug wash involved deployment of ADV, ADCP, SPI, and OBS gear for evaluation of near-bottom disturbances including near-bottom velocity field, shear stress, critical shear stress and erosion rate under controlled tug wash conditions. The evaluation of the fate and transport of the plumes included water sampling, laboratory filter and analysis scheme, and the SPI and ADCP gear for the three resuspension events. The ADCP backscatter was used as a way of estimating suspended sediment load for the deep draft observations.

5.1.1 Tug Propeller Wash Velocities in San Diego Bay

The objective of this task was to map out the three-dimensional velocity field downstream of a moored tug rotating its propellers at 100 RPM and 200 RPM with an acoustic Doppler velocimeter (ADV), lowered from a small boat in the wake of the tug. These data would be later used to place the instrument platform to measure bottom velocity and calculated bottom shear. A C-14 Tractor was tied up at the stern against a quay wall between piers 4 and 5 at the Naval Station San Diego on Dec 21, 2012. Water depth was nominally 10 m. The tug has 360°-rotation twin-ducted, 2.28-m-diameter propellers located at the bottom of the boat at a depth of 5.5 m. The tug propellers were rotated to produce backward thrust, sending a powerful plume of water between the piers and out towards San Diego Bay. A small boat was secured by line to the tug bow and its outboard motor was used to swing the boat in arcs across the tug wake at various distances. Each swing was repeated several times as the ADV, on a weighted line, was lowered to two or three fixed depths. A GPS monitored the boat position through time. The ADV recorded instrument depth, water speed by Doppler shift and direction by magnetic compass through time. The two databases were later merged. Arcs of measurements were made from approximately 20 m to 100 m downstream of the tug by letting out the securing line (Figure 5-1 and Figure 5-2). The process was repeated at first 100 RPM, then 200 RPM of the tugs propellers – typical operating speeds during ship husbanding.

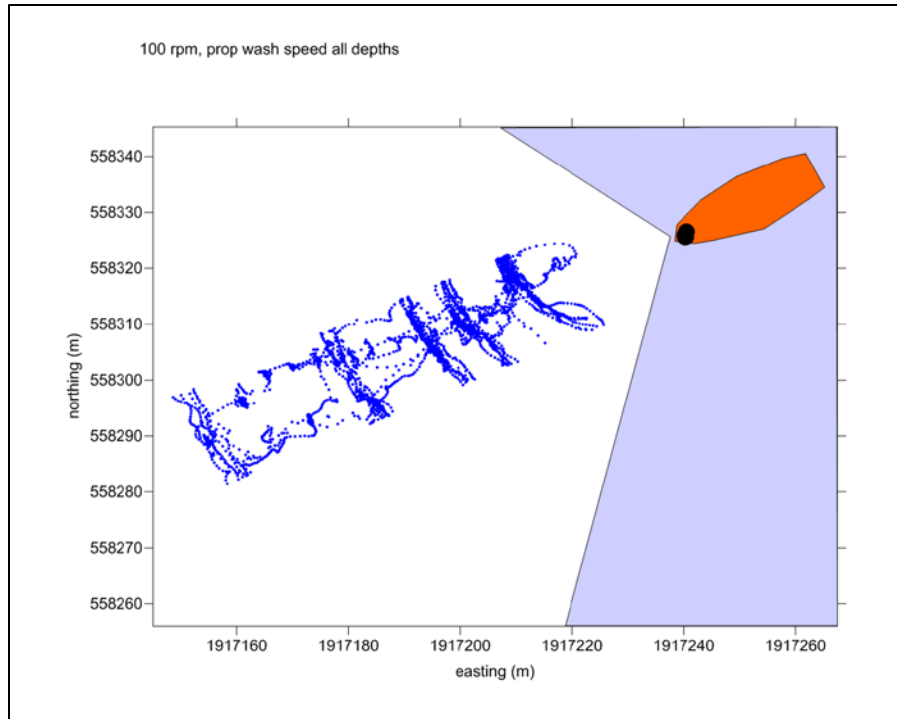


Figure 5-1. Position of ADV measurements downstream of tug (red shape) operating at 100 RPM.

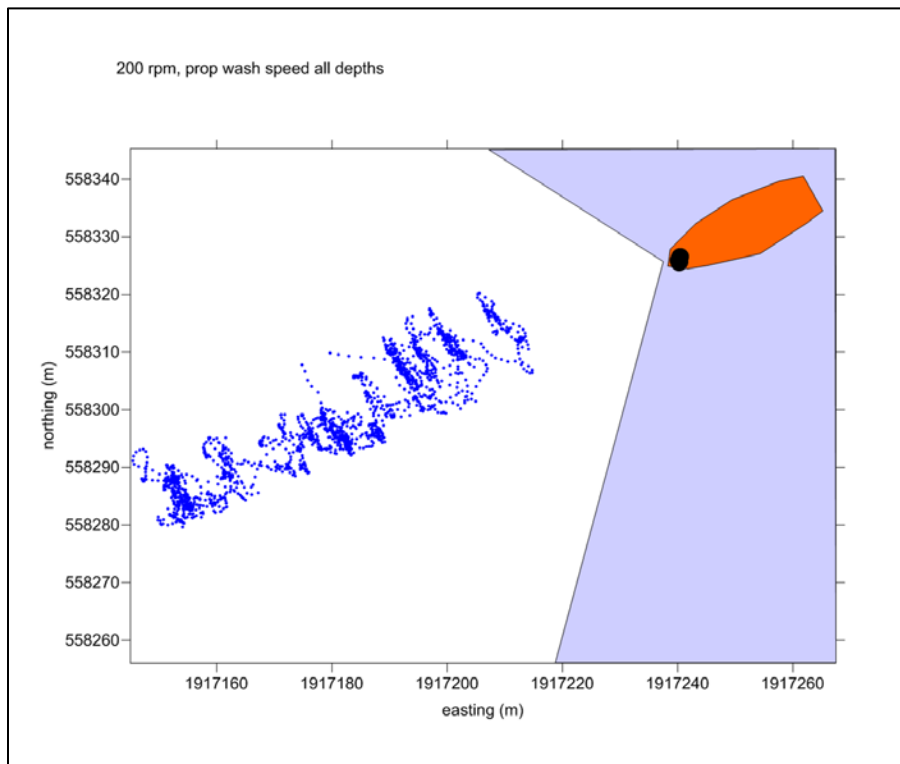


Figure 5-2. Position of ADV measurements downstream of tug (red shape) operating at 200 RPM.

5.1.2 Bottom Velocity and Shear in San Diego Bay

Bed shear stress is the most important parameter that determines both the inception of resuspension (the critical shear stress) and the entrainment rate. Existing models for propeller wash, i.e., Maynard's model (Maynard 1984, 1998; Maynard et al., 2006), predict the near bed velocity, which is then converted to a bed shear stress. Such a conversion is based on the theory of turbulent boundary layer in channel flows, usually under a uniform and steady flow condition. Similarly, SedFlume has been applied to establish the relation between the erosion rate and the varying near-bed flow velocity in a confined channel where flow is relatively uniform. Almost all existing sediment entrainment models are obtained through laboratory flume studies with well-defined flow conditions. The flow field behind a propeller is extremely turbulent and unsteady, which differs significantly from that in a channel or river, or flows induced by tidal current, flood flow, wind wave, etc.

The underwater PIV can measure instantaneous velocity field at high-frequency and high spatial resolution near the bottom, including the bottom boundary layer region. A number of fluid parameters, including the fluctuating velocity, energy dissipation rate, and the Reynold's stress (as a surrogate to the bottom shear stress) can be directly measured (Liao et al., 2009). There are no other existing methods that can measure these parameters simultaneously in the field. Simultaneous deployment with the SPI and ADCP has provided a relation among the sediment erosion rate, bed stress and the mean near-bed velocity distribution, specifically for the propeller wash. To establish this relation, we may also explore higher statistical moments of the measured Reynolds stress or energy dissipation rate (i.e., variance, skewness) that accounts for peak bed stress in addition to the mean value. The main purpose of these measurements is to provide "ground-truth" data that does not exist yet. These results were used to modify and calibrate existing models, such as the Maynard's model.

During past decades, many attempts were made to introduce the PIV technique into field applications. Several self-contained, fully or partially submersible in situ PIV systems were developed and applied in natural aquatic environments (Doron et al., 2001; Katiia et al., 2008). We employed a battery-powered, self-contained Under Water Miniature PIV (UWMPIV) system which has been successfully applied to measure small-scale hydrodynamics in the bottom boundary layer and surface boundary layer of Lake Michigan (Liao et al., 2009). A second generation UWMPIV was also developed for high-speed flow measurement with a dual-beam, dual-camera configuration (Wang et al., 2012). The current design of the UWMPIV is flexible. Primarily, it consists of two submersible units. The first is a laser unit with one or two continuous wave (CW) DPSS laser and a galvanometer (scanning mirror) that scans the laser beam into an effective laser "sheet." The power-supply unit that includes high-capacity lithium-ion batteries is also housed in the laser unit. The second unit is a camera unit with a CCD camera, a compact computer for streaming image data and a signal control unit. The power consumption of the entire system is about 30 W when running at the full rate.

The main objective of the field experiment is to quantify resuspension and erosion potential of contaminated sediments from propeller wash of a Navy tugboat. The battery-powered, self-contained UWMPIV, developed by Liao (Liao et al., 2009; Wang et al., 2013), was applied to measure and estimate critical shear stress while sediment resuspension was initiated. The instrument also was able to measure small-scale turbulence with good statistical properties at the water-sediment interface before, during, and after the resuspension. In this study, the two units of the PIV system were mounted on a steel frame. The laser unit was oriented vertically with the laser "sheet" shooting downward, parallel to the main direction of the propeller jet flow. The body of the camera housing

was parallel to the sea bottom, taking images of the laser “sheet.” Figure 5-3 shows the configuration of the PIV frame. An ADV probe (Nortek Victrino) was also mounted along on the PIV frame. The sample volume of the probe was about 12 ~13 cm above the sediment bed, as estimated through the “bottom check” function of the ADV probe. It was about 10 cm downstream (with respect to the propeller induce current) of the central point of the PIV image field of view (FOV), and 10 cm offside from the laser sheet, so it did not disturb the PIV measurements. Four 1×2 ft aluminum plates were mounted on the four legs of the steel frame to prevent the system from sinking down into the mud. During the deployment, a scuba diver inserted four 2-feet long steel bars into the sediment bed through each plate, which helped to hold the entire system from blowing down by the high speed current generated by the propeller.

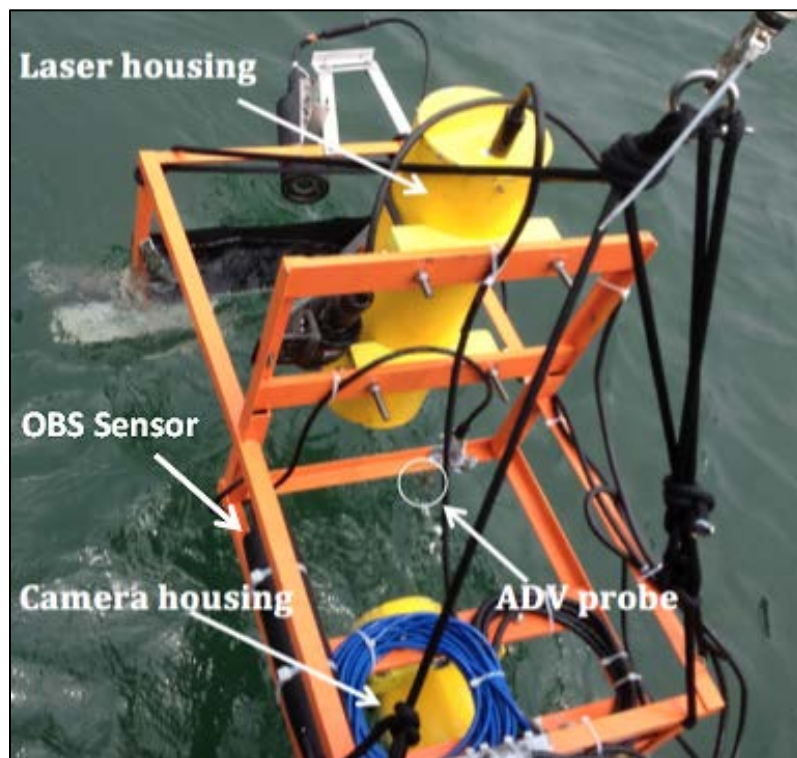


Figure 5-3. Deployment of the UWMPIV frame in San Diego Bay.

The experiment was conducted on 19 July 2012 at Pier 4–5 of Naval Station San Diego in San Diego, CA. The instrument platform was deployed at two sites behind the propeller of a tug-boat: 80 m and 110 m, respectively, based on results of water velocity maps obtained in Task 1. During the experiment, the propeller speed ramped up from 20 to 150 RPM (50 rpm, 100 rpm in between), and the corresponding near bed (12.5 cm above the bed) mean velocity changed from 0.25 to 0.52 m/s. The propeller speed was kept constant for about 10–15 min at each RPM. At the 80-m site, we noticed that the mean flow direction near the sediment bed was reversed for most of the time, suggesting that the propeller jet had not been able to touch the ground, and the near-bed flow was primarily due to the entrainment motion at the outer edge of the “jet”. Here, we present the results from the 110-m site, where the propeller jet flow had touched the ground and reached a fully developed state. For the 110-m site, 2 to ~ 3 sets of PIV images were acquired during each RPM, while the ADV was kept recording uninterrupted until the propeller stopped.

PIV data was acquired at a rate of 8 Hz, i.e., eight image pairs per second. Each data set recorded 1000 image pairs, i.e., 125 sec. The image size was set to 1360 (vertical) \times 800 (horizontal) pixels. With a resolution of 0.118 mm per pixel, that corresponded to a physical size of 16.0 \times 9.4 cm. The imaging system was adjusted such that the sediment/water interface was always visible in the FOV. The width of the laser sheet varies as it fans out from top to bottom. Eventually, the two-dimensional (2-D) velocity field measured by PIV was about 11.5 cm in the vertical direction and 7.8 cm in the horizontal direction, smaller than the image FOV. A multi-pass PIV interrogation algorithm with anti-aliasing method [19] was applied to reconstruct the 2-D velocity field. The size of the subwindow image of the final pass was set to 40 \times 40 pixels, or 4.7 \times 4.7 mm, with a 50% overlap. So the “effective” spatial resolution was about 2.4 mm. Figure 5-4 shows a sample PIV image and the 2-D velocity field revealed by PIV. The vector field represents the actual velocity field subtracting the mean streamwise velocity averaged over the entire measurement field at that moment, with the intention to present vertical structures of the turbulent flow field. It should also be noted that a sediment plume was stirred up by the flow, forming a slope that was about 45°, suggesting a typical wall layer turbulent coherent structure. In the analysis presented later, we had denote such a moment as the critical point for sediment resuspension, and the corresponding shear stress measured through PIV was assumed to be the “critical shear stress” for sediment entrainment.

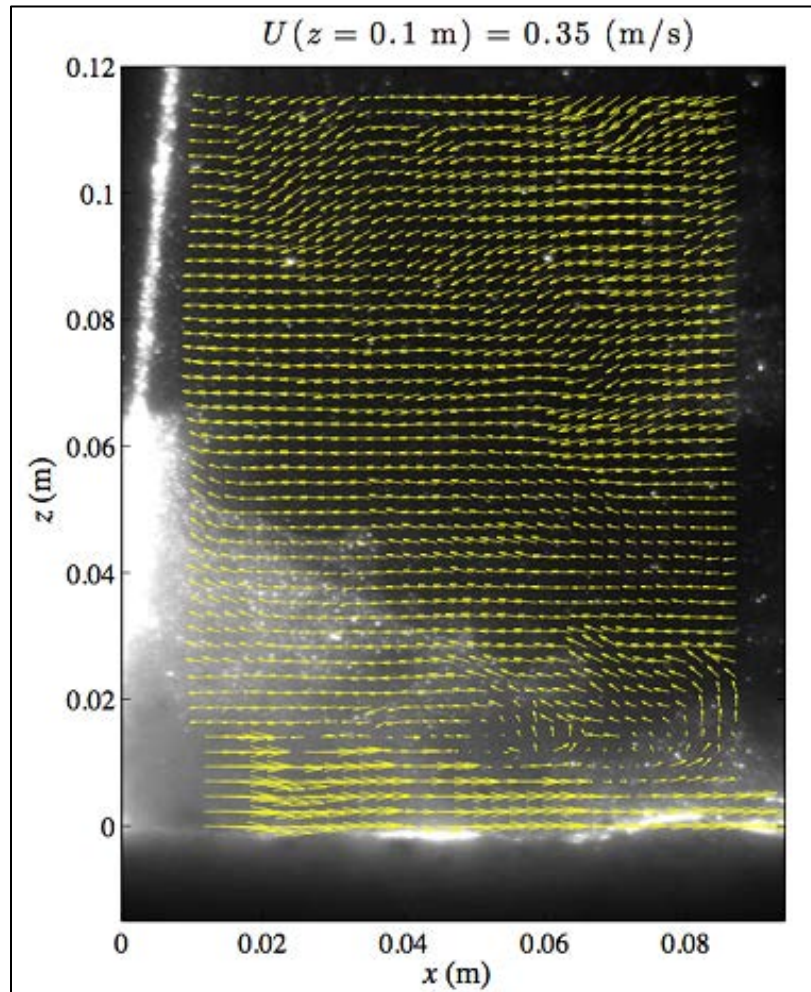


Figure 5-4. Sample PIV image: initiation of sediment resuspension.

For the 110-m site, the propeller started with a rotation speed of 20 RPM at 13:40 on 19 July 2012. Then the speed ramped up to 50, 100, and 150 RPM, respectively, and it stopped at 14:24. For each RPM, the propeller speed was held steady for about 10 min. Sets of 2 to ~ 3 sets of PIV images were acquired for each RPM, while the ADV was kept recording throughout the all experiments.

5.1.3 Resuspension Studies

This section describes the pump sample processing, analytical techniques and associated quality assurance and control that were used at all three resuspension sites and on samples collected from the sediment traps in Sinclair Inlet.

Three propeller wash resuspension studies were undertaken in this study, one in San Diego and two in Pearl Harbor. The first resuspension event took place on 4 April 2012 in San Diego Bay, CA, while the other two events were conducted 28 August (Bravo Pier) and 29 August 2012 (Oscar Pier) in Pearl Harbor, HI. Data from these field studies were used to compare and validate the propeller resuspension potential model and the fate and transport model. Use of these methods will lead to more informed evaluation of remedial options and to improve the predictive capabilities for potential recontamination of sediment remedial sites.

Background samples of sediment and water were collected prior to any resuspension event. A C-14 Tractor and a slightly smaller Tiger tug-boats were used in San Diego Bay and Pearl Harbor, respectively. Both vessels have 360°-rotation twin-ducted propellers of approximately the same size, located at the bottom of the boat. The revolution (RPM) of the propellers was operated and maintained at four speeds (20, 50, 100 and 150 RPM), each for about 5-10 minutes. At each place the tug-boat was moored adjacent and pointing into a quay wall. The starting time for each resuspension event was predetermined based on tide times. Once the time is achieved, the tug-boat operated the engines at a predetermined time and power, or RPM, sufficient to generate a visible surface plume of resuspended sediments. Once the tug-boat engine stopped, the sampling boat(s) started tracking and sampling the plume for about 2 hours. A diagram of the resuspension event procedure, including a schematic of the mapping is shown in Figure 5-5.

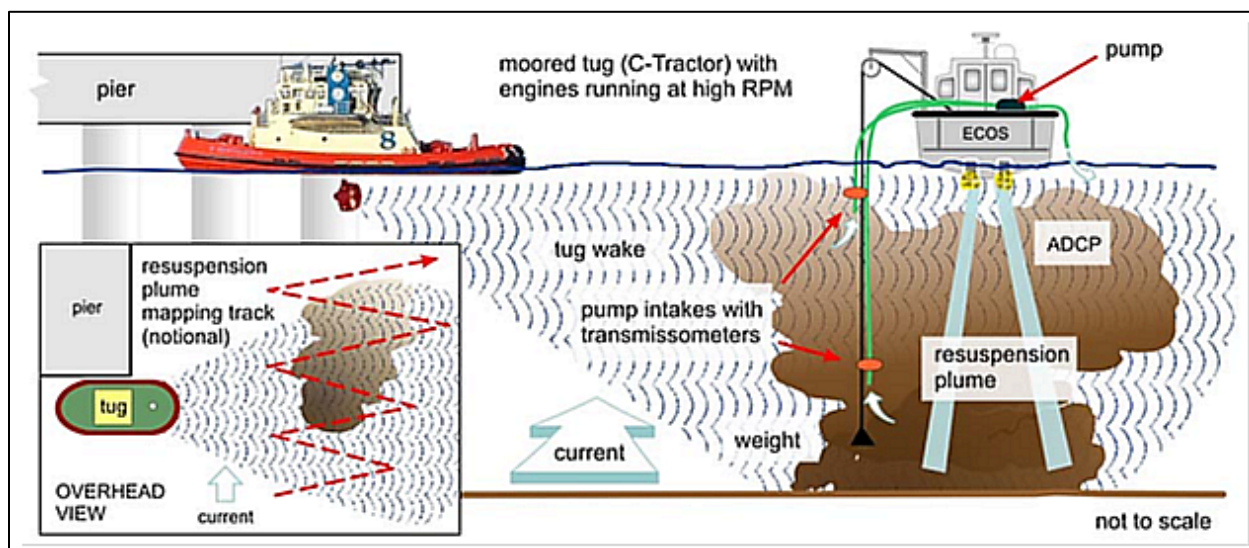


Figure 5-5. Diagram and photo of a resuspension event procedure induced by a tug.

5.1.3.1 Pump Sample Processing

Table 5-1 lists the types of background and plume samples that were collected for all three resuspension studies. The samples were subsampled in our laboratory facilities following the same procedure for each carboy, as explained below. Figure 5-6 shows the contaminants of concerns (CoCs) (i.e., metals and organic contaminants) analysis in a flow chart. Note that the numbers used in the figure are also displayed in the tables with data for identification. The blue boxes represent the CoCs concentration measured in the filtered seawater (FS) sample with particles for each size-fraction. CoCs concentrations for each fraction (blue boxes) were determined by subtracting the concentration derived from the next finer filter. The mass of particles retained by the 60- μm mesh (sand), and 5.0- μm (silt) and 0.4- μm (clay) filters (brown boxes), is quantified as dry weight by the difference between tare and dry weight. For practicality, the original water sample collected in the field may be sub-sampled to allow parallel filtrations for CoC concentrations and particle mass. Only total and dissolved CoCs are determined for the background water concentrations.

Table 5-1. Number and type of analytical samples for all three resuspension studies.

Task	Matrix	Location	Number of Sites	Analytes	Fractions
Background levels	Water	Resuspension site mid-depth	3	Metal and organic CoCs	Total and dissolved
	Sediment	Resuspension site surface sediments	3	Metal and organic CoCs	Total, sand, silt, clay
Plume levels	Water	Plume surface	Site & event dependent	Metal and organic CoCs	Total, sand, silt, clay, dissolved
	Water	Plume mid-depth	Site & event dependent	Metal and organic CoCs	Total, sand, silt, clay, dissolved

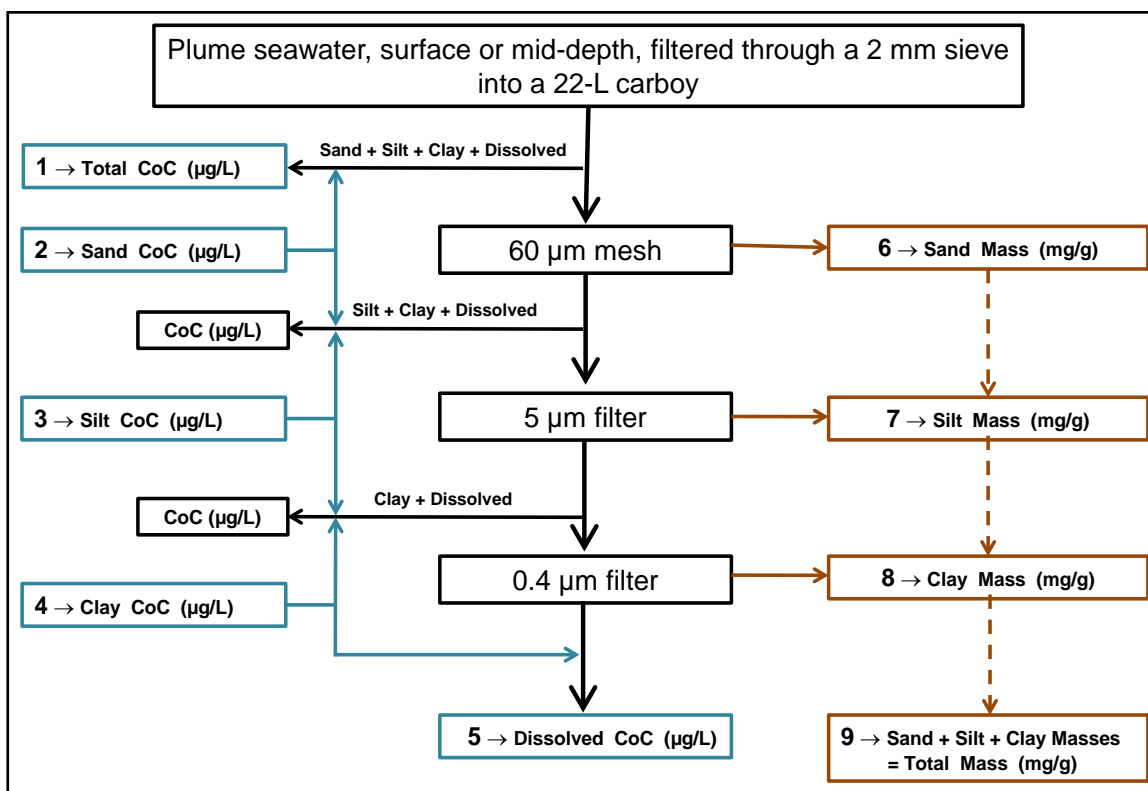


Figure 5-6. Flowchart of laboratory processing and analysis of the field samples for determination of CoC (i.e., metals or organic contaminants) concentrations in the total, sand, silt, clay, and dissolved fractions. Information in the middle represents the filtration sequence, information to the left are concentrations measured in the filtrated seawater (FS), and information to the right are masses retained by the respective filter.

Fractionation is done by filtering through sieves, meshes, or filters of the indicated pore-size. This process was not started immediately after sampling, with the samples being shipped in dark enclosures and delivered a week after sampling. The carboys were then stored in a laboratory at a constant temperature of 22 °C until processing in the same room. A maximum of two samples were processed per day, with about 14 days for completing the processing of all the samples for each field effort. Samples from the San Diego Bay resuspension event were processed from 24 July to 3 August 2012, or 110 to 120 days after sampling. Samples from the two Pearl Harbor resuspension events were processed from 10 to 26 September 2012, or 13 to 29 days after sampling. In the laboratory, each carboy is agitated manually for 1-min following the same pattern, and a 1-L sample is collected in a graduated cylinder as soon as possible using the spigot. This 1-L aliquot is then filtered through a clean, pre-weighed (i.e., tared) 60-µm mesh. Enough aliquots are filtered (about 5 L) to accumulate a measurable mass of sand on the mesh. The filtered sample is then used for filtration/ quantification in the other two smaller pore-size filters, filtering enough sample volume to accumulate a measurable amount of sediment in each phase. All the filters are tared and the mass of retained sediment is quantified after drying. Subsamples of 125 mL filtrated seawater plume samples are collected for each fraction and acidified to $\text{pH} \leq 2.0$ with quartz-still grade nitric acid (Q-HNO_3) on the day of filtration, and saved for metal quantification by inductively couple plasma with detection by mass spectrometry (ICP-MS). Alternatively, 1-L samples are collected from selected filtered samples in amber glass bottles for quantification of organic contaminants. The metals of interest and the analytical methods used for quantification are listed in Table 5-2. Polynuclear aromatic hydrocarbons

(PAHs) were measured at Columbia Analytical Services laboratory (now part of ALS Group) by sediment size fraction, using extraction method EPA 3520C and analysis method 8270D SIM.

Table 5-2. Metal analysis in seawater samples, following methods suggested by USEPA (1994, 1999). Q-HNO₃ is quartz-still grade nitric acid.

Metal	Method	Matrix	Preservation / Digestion	MRL	MDL	Units
Arsenic	6020/200.8	Seawater	Q-HNO ₃ pH ≤2.	0.5	0.04	µg/L
Cadmium	6020/200.8	Seawater	Q-HNO ₃ pH ≤2.	0.02	0.002	µg/L
Chromium	6020/200.8	Seawater	Q-HNO ₃ pH ≤2	0.2	0.03	µg/L
Copper	6020/200.8	Seawater	Q-HNO ₃ pH ≤2	0.1	0.004	µg/L
Lead	6020/200.8	Seawater	Q-HNO ₃ pH ≤2	0.02	0.009	µg/L
Nickel	6020/200.8	Seawater	Q-HNO ₃ pH ≤2	0.2	0.04	µg/L
Silver	6020/200.8	Seawater	Q-HNO ₃ pH ≤2	0.02	0.004	µg/L
Zinc	6020/200.8	Seawater	Q-HNO ₃ pH ≤2	0.5	0.06	µg/L

To reiterate, contaminants of concern (COC) were quantified in the suite of filtered seawater (FS) containing each of the particle-size classes and background sediments. These size classes include total (sieved through a 2-mm mesh to eliminate large size particles and organisms), and includes the sand, silt, clay, and dissolved fractions. The fraction that passes through a 60-µm mesh and is retained, termed silt, and includes the silt, clay, and dissolved fractions. The fraction that filters through a 5-µm pore size filter, termed clay, which includes the clay size and dissolved fractions. And the fraction that filters through a 0.45-µm pore-size filter, which is defined as the dissolved concentration of COC (Figure 5-6). Once isolated, the dry mass of each fraction was measured from the particles on the different filtering meshes or filters. Then a fraction of these dry particles or sediments were used for metal quantification after *aqua regia* digestion. The mass separated for the clay fraction in the settled particles was so minuscule that COC measurement was impossible, and these were evaluated from the concentration in the filtrate from the 5-µm pore-size filter. Clay and dissolved quantifications were performed after acidification with Q-HNO₃ to pH ≤2 of their respective solutions.

5.1.3.1.1 Acidic Extraction

In general, the *aqua regia* digestion was performed by isolating about 0.2 grams of the dry solids for each fraction in a 125-mL polyethylene wide-mouth bottle with cap, previously weighed. To the dry particles 1 mL of concentrated trace metal grade (TMG) hydrochloric acid and 0.5 mL of concentrated TMG nitric acid (HNO₃) were added, making sure to wet the particles with the mixture of these acids, known as *aqua regia*. The mixture was allowed to react overnight and extract the metals on the surface of the particles. The next day the slurries were set on a warm (~25 °C) hot plate for an hour. Once the mixture was at room temperature, then 1 N TMG HNO₃ is added to the neck of the bottle. The difference between the initial weight before adding the acids and the final weight with 1 N HNO₃ is a dilution factor used for quantification.

The digestates are further diluted prior to quantification by ICP-MS. A total of 100 µL of the digestates' supernatant is diluted with 5-mL 1 N Q-HNO₃ for a 51 dilution factor. ICP-MS analysis included blanks and the standard reference materials (SRM) from the National Research Council Canada, BCSS-1, MESS-2, and PACS-1; the former two are sediment collected in the Baie des Chaleurs, Gulf of Saint Lawrence, and the latter is sediment from Esquimalt Harbour, British Columbia. After collection, the SRM sediments were freeze-dried, screened through a 125-µm pore-size, blended, bottled, and radiation-sterilized. The certified concentrations for these SRMs are given in Table 5-3. Note that none of the SRMs is certified for silver.

Table 5-3. Certified concentrations (µg/g of dry sediment) for the standard reference materials (SRM) analyzed with the digestion procedure for resuspended and background sediments collected in this effort. NC indicates not certified.

Element	SRM BCSS-1 Certified Concentration (µg/g Dry Sediment)	SRM MESS-2 Certified Concentration (µg/g Dry Sediment)	SRM PACS-1 Certified Concentration (µg/g Dry Sediment)
Copper	18.5 ±2.7	39.3 ±2.0	452 ±16
Chromium	123 ±14	106 ±8	113 ±8
Nickel	55.3 ±3.6	49.3 ±1.8	44.1 ±2.0
Zinc	119 ±12	172 ±16	824 ±22
Arsenic	11.1 ±4	20.7 ±0.8	211 ±11
Silver	NC	NC	NC
Cadmium	0.25 ±0.04	0.24 ±0.01	2.38 ±0.20
Lead	22.7 ±3.4	21.9 ±1.2	404 ±20

Blank quantification is used to evaluate the addition of metal by the equipment and reagents used for the digestion of particles. The minimal metal concentration contributed by the digestion is indicated by the quantified blank concentrations, which are two to three orders of magnitude lower than the concentrations measured in the sand and silt fractions (Table 5-4). Note that the resuspended sediment concentrations in this report are not blank corrected or SRM corrected. The aqua regia digestion is designed for quantification of potentially bioavailable metal on the surface of the sediment particles, it is not a complete digestion of the solid matrix of the particles. Therefore, digestion recoveries are not expected to be 100% efficient; however, the precision (i.e., standard deviation) of the recovery provides an idea of the precision of the measurements. Table 5-4 shows the mean recoveries for the three SRMs, with those for zinc and arsenic being at about 100%, those for copper, nickel, and lead at about 80%, chromium between 20 and 47%, and cadmium from 127 to 166%. In general, the recoveries for SRM BCSS-1 show a 30% variation, and those for MESS-2 and PACS-1 at less than 10%.

Table 5-4. Mean blank (n = 10) concentrations and recoveries for SRMs BCSS-1, MESS-2 ,and PACS-1.

Element	Blank Average (µg/g)	Blank Standard Deviation (µg/g)	SRM BCSS-1 Average Recovery (%)	SRM BCSS-1 Standard Deviation Recovery (%)	SRM MESS-2 Average Recovery (%)	SRM MESS-2 Standard Deviation Recovery (%)	SRM PACS-1 Average Recovery (%)	SRM PACS-1 Standard Deviation Recovery (%)
Copper	0.027	0.017	79	27	87	1	93	3
Chromium	0.25	0.10	33	10	20	1	47	1
Nickel	0.11	0.10	81	28	75	4	67	1
Zinc	8.05	5.48	110	38	103	3	127	2
Arsenic	2.09	0.45	110	32	108	3	97	1
Silver	0.052	0.032	NC		NC		NC	
Cadmium	0.11	0.074	166	53	127	9	158	6
Lead	1.66	1.17	88	30	79	1	94	4

5.1.3.1.2 ICP-MS

Quality assurance/quality control (QA/QC) for ICP-MS quantifications is as follows. A duplicate sub-sample is obtained from a sample for each event. QA/QC for metal quantification includes calibration curves with correlation coefficients ≥ 0.999 , blanks made up of pH ≤ 2 18-M Ω /cm water, acidified with Q-HNO₃, and analyzed every five samples with a concentration within $\pm 10\%$ of zero background, a standard reference material (SRM) with a recovery of $\pm 15\%$ of certified concentration, a spiked sample per run with a recovery of $\pm 15\%$ of spiked concentration. Table 5-5 summarizes the QA/QC for the ICP-MS work performed for this effort. The two SRMs included were 1643e, Trace Elements in Water, from the National Institute of Standards and Technology, and CASS 4, Nearshore Seawater Reference Material for Trace Metals, from the National Research Council Canada. Note that silver concentration is not certified for CASS4.

Table 5-5. Summary of QA/QC information for the analysis of metals by ICP-MS. Std. Dev. is standard deviation, NC means concentration is not certified, N/A is not applicable. Limit of detection is three times, and limit of reporting is 10 times the standard deviation of the blanks. LCS = SRM.

Resuspended Sediment Samples									
		Units	Chromium	Nickel	Copper	Zinc	Arsenic	Silver	Cadmium
ICP-MS Blanks	Mean	µg/L	0.024	-0.064	-0.037	0.078	0.012	0.073	0.0090
	Std. Dev.	µg/L	0.063	0.010	0.006	0.128	0.010	0.010	0.0049
Limit of Detection		µg/L	0.188	0.029	0.017	0.38	0.029	0.031	0.015
Limit of Reporting		µg/L	0.625	0.096	0.057	1.28	0.095	0.103	0.049
1643e Certified concentration	Mean	µg/L	20.40	62.41	22.76	78.50	60.45	1.062	6.568
	Std. Dev.	µg/L	0.24	0.69	0.31	2.20	0.72	0.08	0.073
1643e Recovery	Mean	%	102.8	98.1	92.1	93.6	93.9	114.1	94.7
	Std. Dev.	%	2.37	1.49	1.71	1.97	2.15	3.99	1.89
Duplicate sample recovery	Mean	%	97	97	97	98	95	99	101
	Std. Dev.	%	3.85	5.44	3.28	4.12	3.04	2.56	10.35
Spiked sample recovery	Mean	%	105	103	104	267	120	89	113
	Std. Dev.	%	3.7	4.12	9.53	134	0.88	0.15	0.65
Slurries For Clay And Dissolved Samples									
		Units	Chromium	Nickel	Copper	Zinc	Arsenic	Silver	Cadmium
ICP-MS Blanks	Mean	µg/L	0.232	0.301	0.337	-0.59	1.226	-0.603	0.062
	Std. Dev.	µg/L	0.388	0.248	0.228	0.792	0.519	0.323	0.153
Limit of Detection		µg/L	1.16	0.74	0.69	2.37	1.56	0.97	0.46
Limit of Reporting		µg/L	3.88	2.48	2.28	7.92	5.19	3.23	1.53
CASS 4 Certified concentration	Mean	µg/L	0.144	0.314	0.592	0.381	1.11	NC	0.026
	Std. Dev.	µg/L	0.029	0.030	0.055	0.057	0.16	NC	0.003
CASS 4 Recovery	Mean	%	219	110	98	160	91		110
	Std. Dev.	%	214	5.2	8.4	251.6	28.0		13.7
Duplicate sample recovery	Mean	%	79	98	117	187	104	70	141
	Std. Dev.	%	35	2	23	168	15	11	23
Spiked sample recovery	Mean	%	95	106	255	149	118	171	129
	Std. Dev.	%		66	240	205	56	22	16

Table 5-5. Summary of QA/QC information for the analysis of metals by ICP-MS. (Continued)

Background Sediment Samples										
		Units	Chromium	Nickel	Copper	Zinc	Arsenic	Silver	Cadmium	Lead
ICP-MS Blanks	Mean	µg/L	-0.0002	-0.091	-0.014	-0.425	-0.026	0.054	-0.006	-0.005
	Std. Dev.	µg/L	0.069	0.020	0.026	0.039	0.004	0.005	0.001	0.004
Limit of Detection		µg/L	0.208	0.059	0.078	0.118	0.012	0.016	0.002	0.013
Limit of Reporting		µg/L	0.693	0.195	0.259	0.393	0.038	0.052	0.006	0.045
1643e Certified concentration	Mean	µg/L	20.40	62.41	22.76	78.50	60.45	1.062	6.568	19.63
	Std. Dev.	µg/L	0.24	0.69	0.31	2.20	0.72	0.08	0.073	0.21
1643e Recovery	Mean	%	90.3	87.7	85.1	87.6	88.1	85.9	87.4	85.6
	Std. Dev.	%	2.6	2.32	1.28	1.82	1.74	1.7	1.6	0.24
Duplicate sample recovery	Mean	%	104	98	97.8	93.3	105.3	98.2	175.7	100.7
	Std. Dev.	%	7.7	7.0	5.1	7.9	11.2	0.5	72.8	5.8
Spiked sample recovery	Mean	%	68	88	71	-90	80	55	81	84
	Std. Dev.	%	7.1	1.9	15.1	8.1	6.6	0.9	5.7	3.7

5.1.3.1.3 Mercury and PCB Concentrations in Particle Size-Fractions

Mercury and PCB congeners content in the different particle size-fractions was analyzed at the U.S. Army Corps of Engineers' Engineer Research and Development Center's Environmental Laboratory (ERDC) in Vicksburg, Mississippi. Mercury was analyzed following the U.S. Environmental Protection Agency's (USEPA) 6000/7000 Series Methods, and the QA/QC for the analysis is shown in Table 5-6.

Table 5-6. Quality assurance/quality control for mercury analyses performed at the ERDC Environmental Laboratory. Laboratory control sample is synonymous to SRM. ND indicates that the analyte was not detected at or above the reporting limit.

		Units	Mercury
Blanks		µg/L	ND
Limit of detection		µg/L	0.000005
Limit of reporting		µg/L	0.00001
Laboratory control sample (LCS)		µg/L	0.20
LCS recovery	Mean	%	109.7
	Std. Dev.	%	7.5
Duplicate sample recovery	Mean	%	93.1
	Std. Dev.	%	4.1
Matrix spike recovery	Mean	%	89.8
	Std. Dev.	%	6.5

5.1.3.2 San Diego Bay

The location for the study in San Diego Bay is between Piers 4 and 5 in approximately 11-m water depth at Naval Base San Diego (NBSD). A single controlled resuspension event with the tug-boat forcing resuspension by cranking up the engine for four consecutive periods, once the low tide was set from 13:40 to 14:08 for 28 min on 4 April 2012. Our sample boat *ECOS* started tracking the plume at 14:12, and 17 stations were sampled at two depths, surface and mid-depth (Figure 5-7). Figure 5-8 shows OBS (orange dots) and discrete sample (black dots) locations. Metal concentrations and mass fractions are quantified in all these samples. In contrast, total, > 60 µm and 5-µm fractions from five stations, one surface and four mid-depth, are quantified for PAHs, which are a CoC for this area of San Diego Bay (data presented in the results section). An attempt was made to set the sampling locations ahead of time; however, actual sampling locations were selected while tracking the plume. The actual path followed by the *ECOS* in mapping the resuspended plume of sediment, as well as the sampling locations is shown in Figure 5-8.



Figure 5-7. Photo of the resuspension event procedure induced by a tug and the *ECOS* sampling the plume in San Diego Bay.

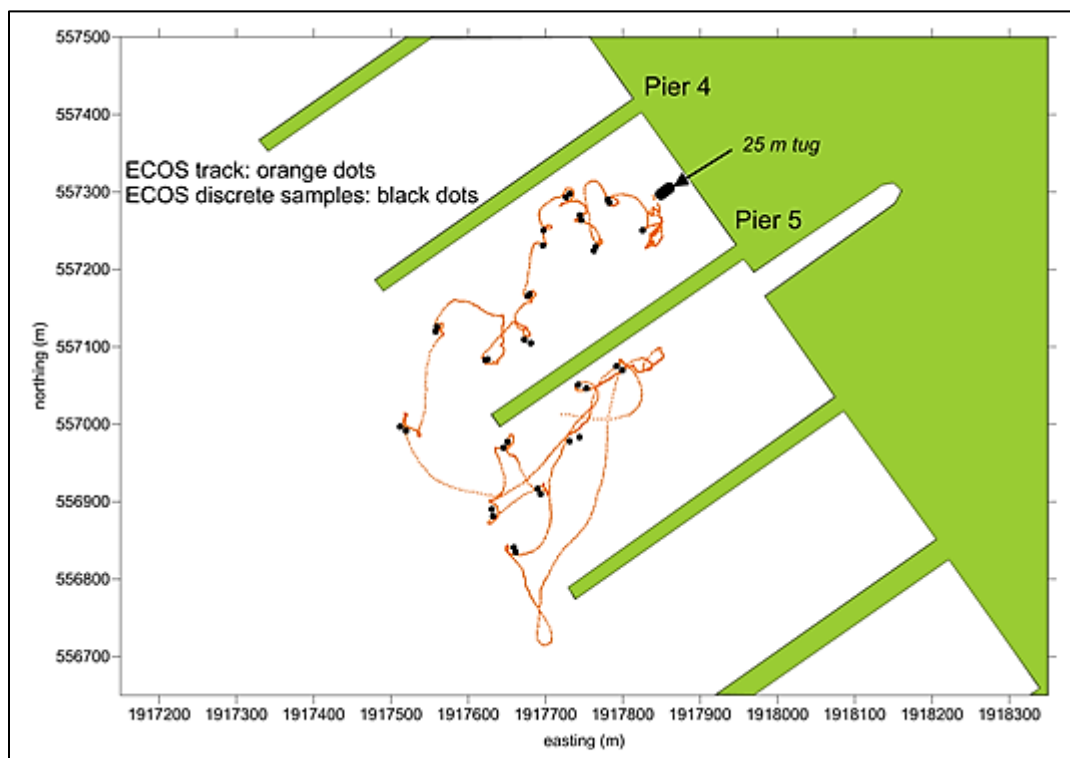


Figure 5-8. *ECOS* track and sampling locations for the resuspension event of 4 April 2012 at Naval Base San Diego, San Diego Bay, California.

Tracking of suspended sediments and contaminant concentrations is done by sampling the plume generated by a tug-boat. This tracking is done on a neap tide to have enough time to take a significant number of samples on the plume. The plume is tracked by a boat equipped with a pump fast enough to fill up a 22-L carboy in a couple of minutes. Thirty-four samples were pumped from about 1 m (3 ft) below the water surface, and from mid-depth (~ 5 m or 15 ft). Samples from bottom waters were

avoided as the sampling pump could induce resuspension from bottom sediments, affecting the concentrations in the plume. These water samples were analyzed in the laboratory for resuspended sediment concentration, size distribution, and associated contaminants.

Concentrations of TSS, particle size distributions (clay, silt, and sand fractions), and 13 priority pollutant metals associated with each particle size, as well as released into the water column as a dissolved fraction were measured in the laboratory from samples collected in the field. Data collected from the propeller wash events was used to calibrate and validate the Maynard and CH3D models. Characteristics of the plume, such as partitioning, settling of particulate metals, and transport of metals were estimated from this data.

5.1.3.3 Bravo Pier and Oscar Pier, Pearl Harbor

Two resuspension events were conducted in the waters surrounding Pearl Harbor Naval Shipyard and Intermediate Maintenance Facility (PHNSY&IMF). One event was by Bravo Pier on 28 August 2012, and the other was by Oscar Pier on 29 August 2012 (Figure 5-9). Figure 5-10 shows OBS (orange dots) and discrete sample (black dots) locations for both locations.



Figure 5-9. Photo of the resuspension event procedure induced by a tug and the *ECOS* sampling the plume at Oscar Pier in Pearl Harbor.

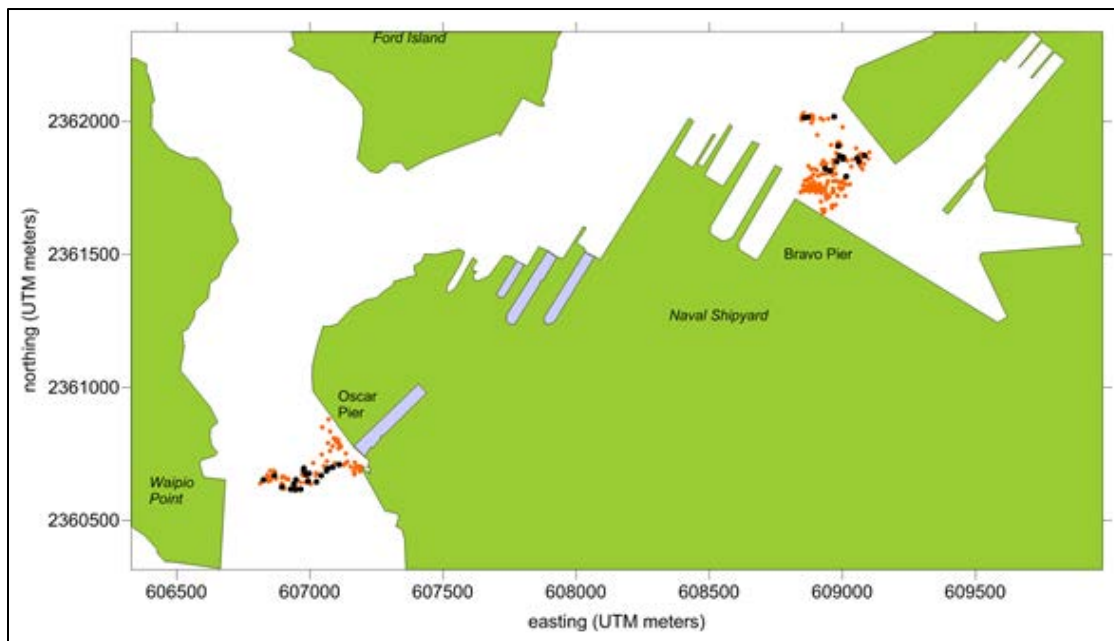


Figure 5-10. Sampling and OBS locations for the two bottom sediment resuspension events in Pearl Harbor, HI.

Similar to the study in San Diego, three background sediment and water samples were collected at each site prior to any resuspension, and there were three separate resuspension events. The first resuspension event was with the tug-boat forcing resuspension for 90 sec, after which water samples are collected at three stations from surface and mid-depth. The second resuspension event was a repetition of the first one. In the third resuspension event, the tug-boat forced resuspension of bottom sediment for 5 min, and samples were collected from eight stations at mid-depth only. All of these samples were fractionated and quantified for metal concentration and mass of sediment. In the same fashion, all the total samples, and the four size-fractions from selected samples were quantified for polychlorinated biphenyls (PCBs) and pesticides, and CoCs present in Pearl Harbor. Pearl Harbor data were directly input as initial conditions to CH3D set up for transport predictions off Bravo and Oscar piers.

As in the San Diego study, water samples were treated per Figure 5-6, Table 5-1, and Table 5-2. However, instead of PAHs, polychlorinated biphenyls (PCBs) as aroclors and pesticides were measured by Columbia Analytical Services using method EPA 8082.

The Sediment Profiling Imagery (SPI) camera was also deployed at both sites to capture a visible record of bottom erosion. On 28 August 2012, a SPI was deployed in the prop wash erosion experiment conducted at both Bravo and Oscar piers in Pearl Harbor, HI. SPI was used to collect 1500 sediment profile images at each of two stations. A lightweight aluminum, modified Ocean Imaging Systems Model 3731 sediment profile camera was used for the survey; the internal printed circuit card on the camera was redesigned so that the firing rate could be programmed at user-specified intervals for use in a time-lapse deployment.

SPI was developed almost four decades ago as a rapid reconnaissance tool for characterizing physical, chemical, and biological seafloor processes and has been used in numerous seafloor surveys throughout North America, Asia, Europe, and Africa (Rhoads and Germano, 1982, 1986, 1990; Revelas, Germano, and Rhoads, 1987; Diaz and Schaffner, 1988; Valente, Rhoads, Germano, and Cabelli, 1992; Germano et al., 2011). The sediment profile camera works like an inverted periscope. A Nikon® D7000 16.2-megapixel SLR camera with two 16-GB Secure Digital (SD) cards was mounted horizontally inside a watertight housing on top of a wedge-shaped prism.

The prism has a Plexiglas® faceplate at the front with a mirror placed at a 45° angle at the back. The camera lens looks down at the mirror, which is reflecting the image from the faceplate. The prism has an internal strobe mounted inside at the back of the wedge to provide illumination for the image; this chamber is filled with distilled water, so the camera always has an optically clear path. This wedge assembly was fitted with two side-handles, and an underwater trigger so that it could be inserted in the sediment at a specified location by a diver (Figure 5-11).



Figure 5-11. The hand-held, diver-deployed sediment profile camera used in Pearl Harbor.

The diver initially deployed the camera and took a test image so that the proper ISO and f-stop could be adjusted on the digital single lens reflex (DSLR) camera for the particular sediment bed. After the proper camera adjustments were made, the diver then inserted two pieces of perforated angle-iron into the sediment to keep the profile camera in place during the experiment; each piece was approximately 2 m in length and was inserted far enough so that only 50 cm of angle iron was projecting above the sediment–water interface. The camera prism was inserted in the seafloor and plastic tie-wraps were used to secure the camera prism to the angle iron. At the beginning of the survey, the time on the sediment profile camera's internal data logger was synchronized with Brad Davidson's timepiece (used for officially recording the progress and milestones of the experiment). Details of the camera settings for each digital image are available in the associated parameters file embedded in the electronic image file; for this survey, the ISO-equivalent was set at 640. The additional camera settings used were as follows: shutter speed was 1/250, f8, white balance set to flash, color mode to Adobe® RGB, sharpening to none, noise reduction off, and storage in Joint Photographic Expert Group (jpeg) files (approximately 3 MB each). The camera was programmed to take an image every 3 sec for 75 min after an initial 10-min delay after the diver depressed the trigger (20 images per minute, 1500 images for each experimental run). A spare camera and charged battery were carried in the field at all times to ensure uninterrupted sample acquisition. After deployment of the camera at each of the two stations, the frame counter was checked to make sure that the requisite number of replicates (1500) had been taken.

Back in the lab, the intensity histogram (RGB channel) for each image was adjusted in Adobe Photoshop® to maximize contrast without distortion. The jpeg images were then calibrated by measuring 1-cm gradations from the Kodak® Color Separation Guide that was photographed at the start of the experiment. This calibration information was applied to the SPI images analyzed from

each deployment: 885 images from the Bravo site and 552 from the Oscar site. Linear and area measurements were recorded as number of pixels and converted to scientific units using the calibration information. Measured parameters were recorded on a Microsoft® Excel® spreadsheet. Dr. J. Germano, Germano & Associates's senior scientist, subsequently checked all these data as an independent quality assurance/quality control review of the measurements before final interpretation was performed.

The SPI prism penetration depth was measured from the bottom of the image to the sediment–water interface. The area of the entire cross-sectional sedimentary portion of the image was digitized, and this number was divided by the calibrated linear width of the image to determine the average penetration depth. Linear maximum and minimum depths of penetration were also measured. All three measurements (maximum, minimum, and average penetration depths) were recorded in the data file. The particles of suspended sediment were digitized to get a relative estimation of the amount of suspended load in the water column as a function of time. Both the total number of pixels and the area of suspended sediment were recorded for each image.

In the case of the Pearl Harbor studies, resuspended plume loads were also estimated from acoustic backscatter levels that provided a more three-dimensional picture of the plumes. Acoustic backscatter was also used to observe resuspension plume caused by a deep-draft vessel in the next section. Suspended sediment concentration (SSC) was inferred from acoustic backscatter with a 1200-kHz RDI Workhorse Acoustic Doppler Current Profiler (ADCP) by personnel from the U.S. Army Corps of Engineers' Engineer Research and Development Center's Environmental Laboratory (ERDC) in Vicksburg, MS. Mercury was analyzed following the USEPA's 6000/7000 Series ERDC personnel. The ADCP was deployed with the acoustic transceivers oriented downward and positioned approximately 0.4 m below the water surface (Figure 5-12). The center of the first bin is 1.0 m from the transducer face and the bin spacing is 0.5 m. The sampling rate of the ADCP was approximately 2 Hz. A typical application of an ADCP is measure water velocity, but ADCPs also record the average echo intensity received with distance along each of the four beams. In clear water, beam spreading and acoustic attenuation cause echo intensity to decrease with distance from the transducer; however, an increase in concentration of acoustic scatterers (such as plankton or sediment particles) or a reflection from a boundary (such as the sediment bed) will cause the echo intensity to be somewhat higher than the expected value in clear water. Acoustic backscatter is a measure (in dB) of the received echo intensity versus the expected echo intensity. Given that the increased acoustic scattering is associated predominantly with suspended sediment in this study, a relationship between acoustic backscatter and SSC (from physical samples processed in the laboratory by American Society for Testing and Materials (ASTM) standard D 3977-97 (ASTM, 1997)) can be developed and applied to result in acoustic estimates of SSC over the full dataset.

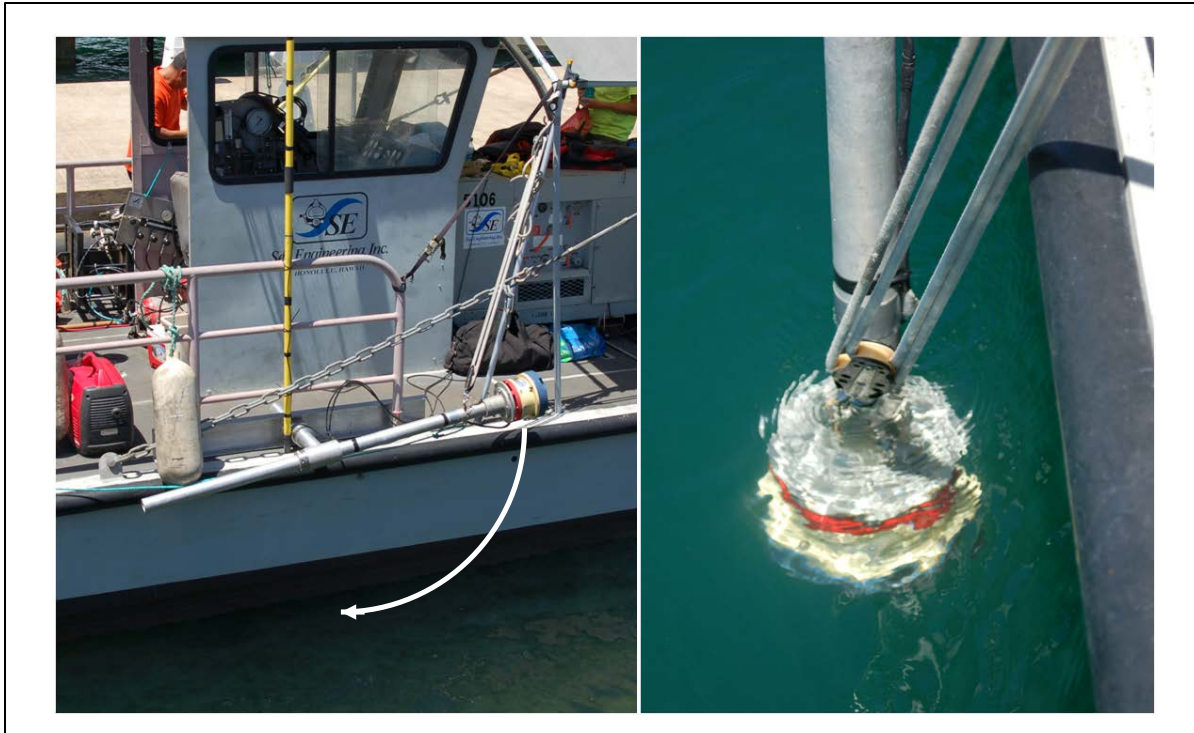


Figure 5-12. ADCP configuration as deployed from the Sea Engineering motor barge (left) ADCP mount in position while motoring to/from site (right) deployed in the measurement position.

The acoustic echo intensity data is first processed to separate valid and invalid samples. Invalid samples include influences of entrained air bubbles, reflections from the bed, channel margins, or other structures in the water column. Each beam is evaluated for the influence of bottom echo, and must also meet minimum thresholds for echo intensity (40 counts) and correlation (70 percent). The acoustic equation (RDI, 2007) including the acoustic attenuation of seawater (Ainslie and McCole, 1998) is applied to determine acoustic backscatter from the recorded echo intensities. The valid values of acoustic backscatter for each vertical bin are then averaged to produce time- and space-varying vertical profiles of acoustic backscatter. Acoustic backscatter data are time- and depth-paired with physical samples of SSC. The acoustic backscatter data were time-averaged over the 30-sec time interval of suspended sediment sample collection. A least-squares fit of $\log_{10}(SSC) = a + b \langle \beta \rangle$ is performed on the resulting pairs of SSC and time-averaged backscatter, $\langle \beta \rangle$. Where possible, the empirical fit parameters (a , b) are determined for each experimental dataset, considering the potential variation in scattering properties and vessel operations for each site. Figure 5-13 presents the paired SSC and $\langle \beta \rangle$ data and the empirical fit for the 28 August 2012 dataset. Table 5-7 provides the empirical fit parameters for each experimental dataset. Note that one calibration relationship is given for both experiments conducted on 31 August 2012. In this case, a procedural error in sample processing in the laboratory resulted in too few valid samples for the afternoon experiment of 31 August 2012. The correlation for 31 August 2012 was determined by pooling the SSC samples from the morning and afternoon experiments. Also note that the ADCP calibrations are not universal and must be performed on a site-, condition-, and instrument-specific basis.

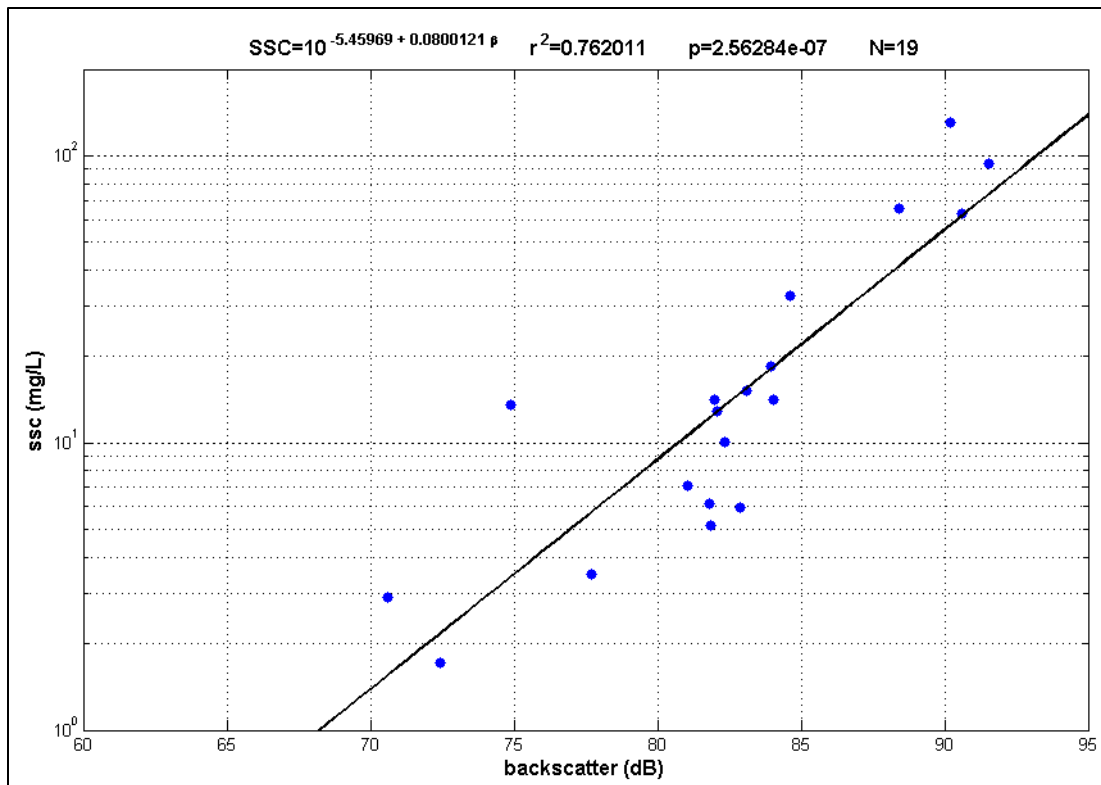


Figure 5-13. Calibration from backscatter to concentration for 28 August 2012.

Table 5-7. Calibration parameters for $\log_{10}(\text{SSC}) = a + b(\beta)$

Experiment	a	b	N	r^2	p
28 Aug 2012	-5.460	8.001×10^{-2}	19	0.76	2.5×10^{-7}
29 Aug 2012	-2.114	3.852×10^{-2}	38	0.32	7.7×10^{-5}
31 Aug 2012	-2.065	4.051×10^{-2}	10	0.70	6.8×10^{-4}

5.1.3.4 Deep-Draft Resuspension Study in Pearl Harbor

Acoustic backscatter and derived SSC was also measured by ERDC personnel on 31 August 2012 off Bravo Pier in the wake of USS *Chafee*, a guided missile destroyer (length 155 m, beam 20 m, loaded draft 9 m [us.navy.mil]). The vessel operations on the afternoon of 31 August 2012 (also from Bravo Pier) offered a contrasting case of plume generation. In this case, *Chafee* was pulled abeam from the Bravo Pier by two tugs. The tugs performed a turning maneuver in the basin and assisted *Chafee*'s departure from the berthing area. Incidental observation of SSC was used validate FANS predictions of sediment resuspension from a deep-draft vessel during tug assist.

5.1.3.5 Sediment Trap Study in Sinclair Inlet

Shore installations at Puget Sound Naval Shipyard & Intermediate Maintenance Facility (PSNS&IMF) include seven piers and six dry docks where ship repair and salvaging occur. The sediment remediation cap lies near the head of Pier 7, partially underneath the pier and partially exposed between Piers 7 and 6 (Figure 5-14). Pier 7 is the easternmost pier in PSNS&IMF, located near the Bremerton ferry terminal. There are a number of processes/activities that probably resuspend

sediment in the vicinity of the sediment cap at the end of PSNS&IMF Pier 7. These include tug-boat wakes, dry dock dewatering, caisson movement for opening, and closing of dry dock, commercial ferry operations, and occasional maintenance work such as pier piling replacement. Commercial ferry operations and wakes from vessels moving through the traffic channel are considered “normal” background conditions for the area, as they either are consistent (i.e., ferry operations) or occur in a daily basis with no specific control (i.e., traffic in and out of Sinclair Inlet). In contrast, occasionally, there are special operations that should have a larger effect on resuspension of sediments in the area, the field testing was designed specifically to capture these events. The sampling design was based on (1) a previous format already used at Navy piers in San Diego Bay and Pearl Harbor; (2) existing model development, calibration, and validation; and (3) limits to the project scope and funding.

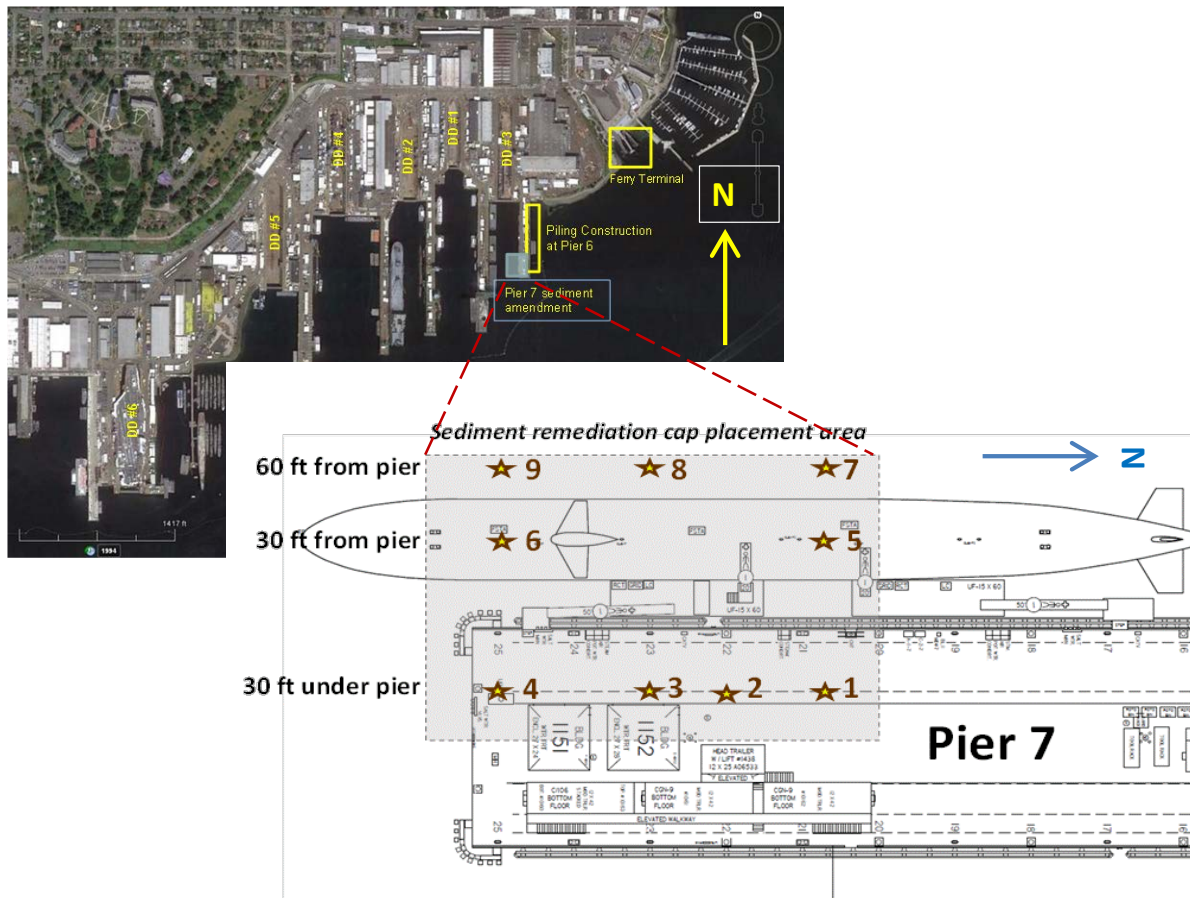


Figure 5-14. Sediment trap locations under Pier 7, PSNS&IMF. The stars are depicting the label and position of the sediment traps for both Pier 7 and the amendment cap on the sediment (gray area). Imagery ©2014 DigitalGlobe, U.S. Geographical Survey, USGS, Map data ©2014 Google Life mode Terms Privacy Report a problem.

Nine sediment traps (Figure 5-15) were deployed by divers at the locations over the sediment cap shown in Figure 5-14. Four traps (numbered 1 to 4) were deployed 30 feet under Pier 7, two traps (5 and 6) 30 feet from the pier side, and three traps (7 to 9) 60 feet from the pier side in the direction to Pier 6. The sediment traps are made up of 71.7 cm (4 feet) of 15.3 cm (6 inch) inside diameter PVC piping, with a PVC cap on the bottom end. The traps were deployed with the open side up by strapping to metal poles previously inserted on the cap. A plastic mesh with large openings (~ 2 cm or ½ inch) was secured on the top opening to keep large organisms from reaching into the trap. The

traps were covered with a plastic shower cap for retrieving to keep the particles in the trap. Once on the water surface, most of the clear water on the trap was disposed, and the rest of the water, as well as the deposited sediment particles, were collected in 2-L plastic containers. All of the collected water and particles were mixed together in the laboratory for subsampling and quantification of the different particle sizes, and contaminants of concern.



Figure 5-15. Sediment trap used for quantification of sediment particles and contaminants of concern over the sediment remedial cap located by Pier 7 at the PSNS&IMF.

The sampling plan to assess the deposition of contaminated sediment on the sediment cap under Pier 7 evolved based on the shipyard scheduling. In spite that the dry dock scheduling is set at least a year ahead of schedule, there were last minute modifications to the schedule that resulted in the final sampling scheme (Table 5-8). The first sampling interval included the effect of dry dock dewatering and tug's prop wash resuspension in the area between Piers 6 and 7 resulting from the docking of two submarines into Dry Dock 3 (DD3). The second sampling interval included the effect of tug/carrier resuspension while moving through the traffic channel, due to the undocking from Dry Dock 6 (DD6) of a carrier and its transit out of Sinclair Inlet. The third sampling interval captured the effect of sediment deposited under conditions considered normal operations, or background sources, as explained above.

Table 5-8. Description of the three deployments events for quantification of particle and contaminants of concern deposited onto the sediment remedial cap in PSNS&IMF Pier 7.

Sampling Event	Deployment dates (2014)	Deployment Period (Days)	Known deployment conditions
First (DD3)	22 January–8 April	76	Two submarines undocked from Pier 7 and docked into DD3
Second (DD6)	10 April–13 May	33	Carrier undocking from DD6 and transit out of Sinclair Inlet
Third (BCKGND)	14 May–24 June	40	Background conditions (normal Sinclair Inlet traffic & ferry operations)

The sediment traps were first deployed on 22 January 2014, with the objective of capturing background conditions, based on the schedule available from PSNS at deployment time. However, due to unexpected changes in the schedule, two submarines berthed at Pier 7 were docked into DD3 for salvage on the first week of April. As the sediment traps were retrieved on 8 April, the week after the submarine's docking, these samples of sedimentation for 76 days deployment period included the effect from tug operations around Pier 7 and the opening and closing of the caisson at DD3. The process for setting the submarines in the dry dock include filling up the dry dock with seawater,

moving the caisson out of the way, towing one submarine at a time with the help of tug-boats, setting the caisson back on the entrance of the dry dock, and dewatering of the dry dock by pumping the water to four discharges located on the water side of the dry dock, almost at bottom depth. All of these operations are highly conducive for sediment resuspension.

Sediment traps were redeployed on 10 April and retrieved on 13 May. This 33-day sampling period included the undocking of an aircraft carrier from DD6, and transit of this vessel through the traffic channel out of Sinclair Inlet. This process does not occur on a regular basis, and results in resuspension of sediments to the west of the sediment cap.

Sediment traps were redeployed on 14 May, and were recovered on 24 June. These are samples of sedimentation for 40-days deployment period that presumably included normal harbor operations, or background.

A separate set of sediment surface grabs was collected on 18 April at 12 locations. These sediment samples were collected for analysis of grain size and particle size associated contaminant concentrations. The 12 locations include two locations (inner – near dry dock caissons, and outer – between berthing areas of the piers) associated with each dry dock (Figure 5-16). These sediment samples were used for quantification of metal load associated with the different particle class-size studied in this effort.

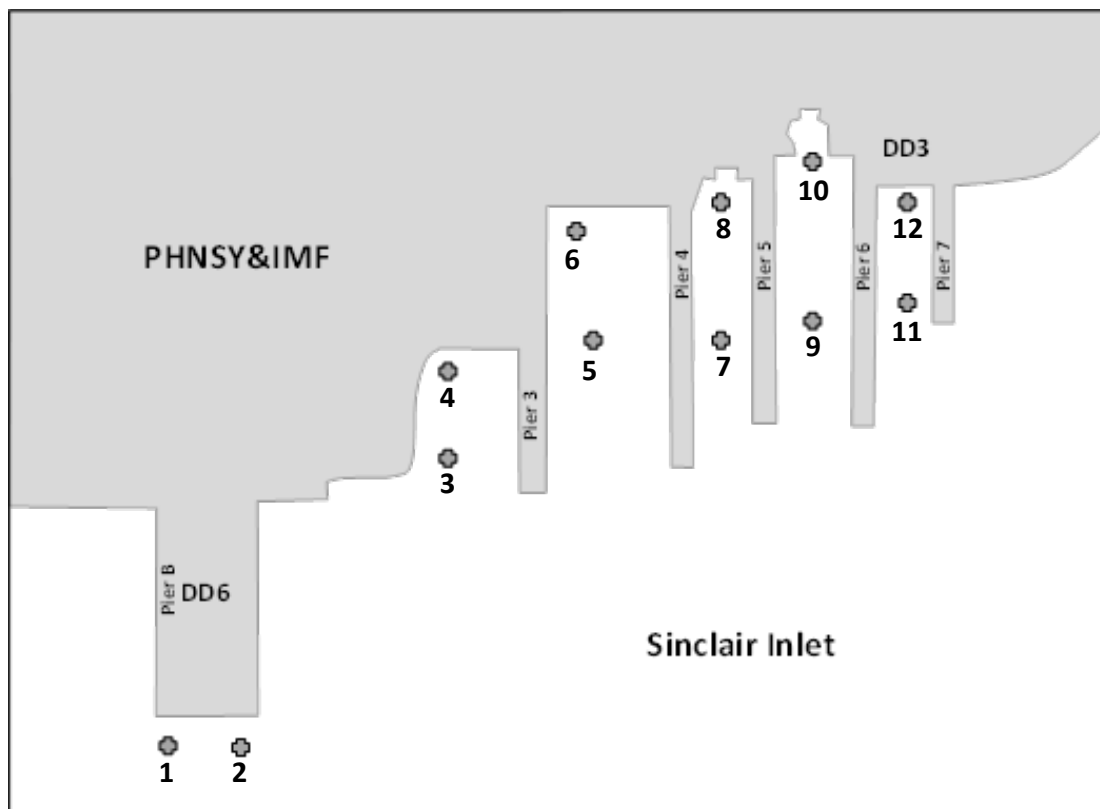


Figure 5-16. Location for background sediment grab samples at PSNS&IMF.

As in the San Diego study, water samples were treated per Figure 5-6, Table 5-1, and Table 5-2. However, instead of PAHs, total mercury was analyzed in whole samples (not size-fractionated) by ERDC following the USEPA's Method 6000/7000 Series.

5.2 MODEL PROCEDURES

The models employed in this study were Maynard's propeller resuspension model (Tasks 2, 3, and 5), FANS deep draft vessel model (Task 4), and CH3D fate and transport model (Tasks 3 and 5). The Maynard's model was calibrated using the data of tug wash velocity and shear measurements. The calibrated Maynard's model was then used to predict the sediment plume mass by tug wash in San Diego Bay and the estimated plume mass was then input to CH3D for predicting the fate and transport downstream. Model results were then compared with the sediment and metal data measured by the pump, sampling, and ADCP gears for the three resuspension events and the laboratory filtering and analysis scheme. In addition, the ADCP backscatter data was used as a way of estimating suspended sediment load for the deep draft observations in Pearl Harbor and three deployments of sediment traps were the nine sediment traps used in Sinclair Inlet.

5.2.1 Maynard's Resuspension Model

5.2.1.1 Bottom Shear Stress Estimation

Maynard developed equations for velocity field disturbed by propellers (Maynard, 1984, 1998, 2000). These equations are expressed and used with a number of model parameters to calculate the velocity field. For this study, we implemented Maynard's equations and refined the model parameters into a user-friendly model with graphic interface.

The bed shear stress is the most important parameter that links the flow condition to sediment transport. Estimated shear stress was used to determine both the inception of resuspension (the critical shear stress) and the subsequent entrainment rate. Existing models for propeller wash, i.e., Maynard's model (1984, 1998), predicts the near-bed velocity, which is then converted to a bed shear stress. Such a conversion is based on the theory of turbulent boundary layer in channel flows, usually under a uniform and steady flow condition. Almost all existing sediment entrainment models are obtained through laboratory flume studies with well-defined flow conditions. The flow field behind a propeller is extremely turbulent and unsteady as we have shown in Section 5.1.1, which differs significantly from that in a channel or river, or flows induced by tidal current, flood flow, wind wave, etc.

Despite the importance, the bottom shear stress and its relation to sediment transport is hard to quantify, particularly in a complex flow field where flow is highly three dimensional and transient, such as that in a propeller wash flow. Although methods exist to directly measure bottom shear stress with appropriate sensors, such as a shear plate (Rankin and Hires, 2000; Barnes et al., 2009), these methods are rarely applied in field experiments due to technical difficulties. In situ measurement of bottom shear stress usually relies on indirect estimation based on flow velocity measurements. These methods have been documented by Biron et al. (2004) and summarized in Table 5-9. Bottom shear stress is denoted as τ_0 , and the shearing velocity is defined as $u_* \equiv \sqrt{\frac{\tau_0}{\rho}}$, where ρ is the density of fluid.

Table 5-9. Methods for estimation of bottom shear stress (Biron et al., 2004).

Model	Description	Advantages	Disadvantages
“Law of the Wall” (LOG law)	Fit measured mean velocity with $u = \frac{u_*}{\kappa} \ln\left(\frac{z}{z_0}\right),$ where z_0 is the roughness height.	Can be used to map spatial patterns of shear stress as well as bottom roughness; standard error of regression can be provided as an estimate of error in u_* ; can be measured with an ADCP	Flow must conform with log velocity profile; result is sensitive to the measurement of height (z); requires measurement of velocity profile, thus can't be applied with point-wise instrument (e.g., an ADV)
Quadratic stress law	$\tau_0 = \rho C_d U^2,$ where C_d is the drag coefficient	Simple, only requires measurement of mean velocity at one point	Hard to accurately estimate the drag coefficient, generally a function of Reynolds number and geometry of the bottom
Direct estimate of the near-bed shear stress with the covariance method (COV)	$\tau_0 = -\rho \overline{u'w'},$ where u' and w' are the fluctuations of velocities in the streamwise and the vertical directions.	Direct measurement with least assumptions No need to estimate roughness height Can be obtained by point-wise instrument (e.g., an ADV)	No general rule for “How close to the bottom to measure” Sensitive to sensor tilt.
Turbulent Kinetic Energy (TKE) method	TKE: $k = \frac{1}{2} (\overline{u'^2} + \overline{v'^2} + \overline{w'^2})$ and $\tau_0 = C_1 \rho k,$ where $C_1 = 0.19$	No need to estimate roughness height Can be obtained by point-wise instrument (e.g., an ADV)	No general rule for “How close to the bottom to measure” Coefficient C_1 might be different for various environments (i.e., oceanic vs. riverine)
Modified TKE method	$\tau_0 = C_2 \rho \overline{w'^2},$ where $C_2 = 0.9$	No need to estimate roughness height Can be obtained by point-wise instrument (e.g., an ADV) For an ADV probe, the vertical velocity component w can be measured with higher accuracy and less noise level.	No general rule for “How close to the bottom to measure” Coefficient C_2 might be different for various environments (i.e., oceanic vs. riverine)

Note that all of these methods are indirect. The instantaneous bottom shear stress is itself a random variable. It is related to the near-bottom turbulence in a statistical sense, which depends on the temporal and spatial scales. We suppose that statistical values obtained over a longer period produces a mean shear stress with a lower uncertainty, but also will miss peak values that are significant for the prediction of sediment entrainment and erosion rate. For unsteady flows, such as the propeller jet induced current, longer sampling time may include the transient processes into the calculation of Reynolds stresses. We also suppose that statistics measured at a higher position above the bed

represents an average of bed stress over a larger area upstream, i.e., the “footprint” used to estimate water–sediment mass exchange using an “eddy correlation” approach (Berg et al., 2003).

In this study, we estimated the bed shear stress with both the ADV and PIV measurements. Taking the advantage of the high sampling rate of the ADV and high spatial resolution of the PIV, we explored to calculate the statistics of turbulence over a rather short period (a few seconds) to reduce the effects of unsteady flows on the estimation of the bed shear stress.

5.2.1.2 Maynard's Model for Single Propeller

Maynard's model is based on the empirical model developed by Blaauw and van de Kaa (1978), which follows the law of conservation of momentum. The power of the rotating propeller is equal to the momentum of the flow field in the wake of the propeller. The propeller-induced velocity can be expressed explicitly as

$$U(x, z) = AU_0 \left(\frac{D_0}{x} \right) e^{-B \left(\frac{z}{x} \right)^2}, \quad (1)$$

where x is the distance along the axial direction and z is the radial distance of the propeller. D_0 is the equivalent propeller diameter, and U_0 is the exit velocity of the propeller, which can be approximated by the power and diameter of the propeller (Blaauw and van de Kaa, 1978):

$$U_0 = C \left(\frac{P}{D_p} \right)^{1/3}, \quad (2)$$

where C is an empirical constant, P the engine power of the propeller in [horse power], and D_p is the propeller diameter.

In Equation (1), the two coefficients (constants), A and B , are obtained empirically. The model is for single-screw propellers in infinite flow domain. The velocities at the bottom are calculated by assigning the position (x, z) of the bottom to the equation, which means that the bottom is treated as a virtual bottom (transparent) in the model and the bottom effect to the hydrodynamics of the propeller wash is ignored. Maynard advised application of this method for propellers with the ratio of diameter/shaft-to-bottom distance D_p/H_p at low values (Maynard, 2000), less than 1.2, to reduce the effects of the bottom. However, most vessels in DoD harbors operate in very shallow water conditions with D_p/H_p far exceeding 1.2 (e.g., aircraft carriers, destroyers, etc.). For the destroyer (DDG) test case considered in the preliminary investigation, the ship draft was 31 ft and the water depth was 35 ft. The diameter of the twin-screw propeller was $D_p = 17$ ft, and the distance from propeller shaft to harbor bottom was $H_p = 15.3$ ft. This gives $D_p/H_p = 1.11$, which is near the threshold applicable range of Maynard's model. However, there is a strong interaction between the two counter-rotating propellers. Consequently, the bottom shear-stress distribution is drastically different from that induced by a single-screw propeller. We conducted a literature search and we could not find many published manuscripts/data for validation of Maynard's model for the scenarios, $D_p/H_p > 1.2$, which is more applicable for naval vessels operating in DoD harbors. In the application of Maynard's model (Maynard, 1998), two examples were discussed in the study of sand particle sizes for protecting the sediment caps for a commercial vessel traffic and a recreational vessel traffic.

For both applications, the ratios of D_p/H_p are less than 1.2, within the applicable range for Maynard's model. The range of applicability for Maynard's model is also emphasized by Jay (2002), where he suggested that Maynard's model should be applied only for deep water scenarios with a small D_p/H_p ratio, with best results from smaller ratios. The bottom effect would be reduced by

limiting application of the model to deep water, which is presumably more conformal to the model. However, for deep water scenarios, the propeller is closer to the free surface than to the bottom. Thus, the propeller jet should hit the free surface earlier than the bottom. The free surface effect would attenuate the propeller wash flow, and interfere with the conservation of momentum principle, on which Maynard's model is based (Blaauw and van de Kaa, 1978; Maynard, 1984).

5.2.1.3 Maynard's Model for Twin-Screw Propeller

Maynard (2000) presented two models to compute velocity magnitude near the sediment bed behind twin-screw propellers (tugboat). In these models, empirical values were measured for several model parameters. For this effort, our field study was conducted for tugboat pushing only in a stationary condition; therefore, the model for a stationary tugboat pushing condition is applied and presented. Figure 5-17 shows configurations of the twin-nozzle propellers from a side view (upper) and plane view (lower). Propeller-induced flows can be described in two zones, Zone 1 and Zone 2. Zone 1, less than 10 propeller diameters behind the propellers, includes the regions dominated by the jet flow from the propeller which is between the propeller and the end of transition distance ($X_p/D_p < 10$). Zone 2, greater than 10 propeller diameters behind the propellers, is dominated by the fully developed propeller flow, as described by Equations (3) and (4).

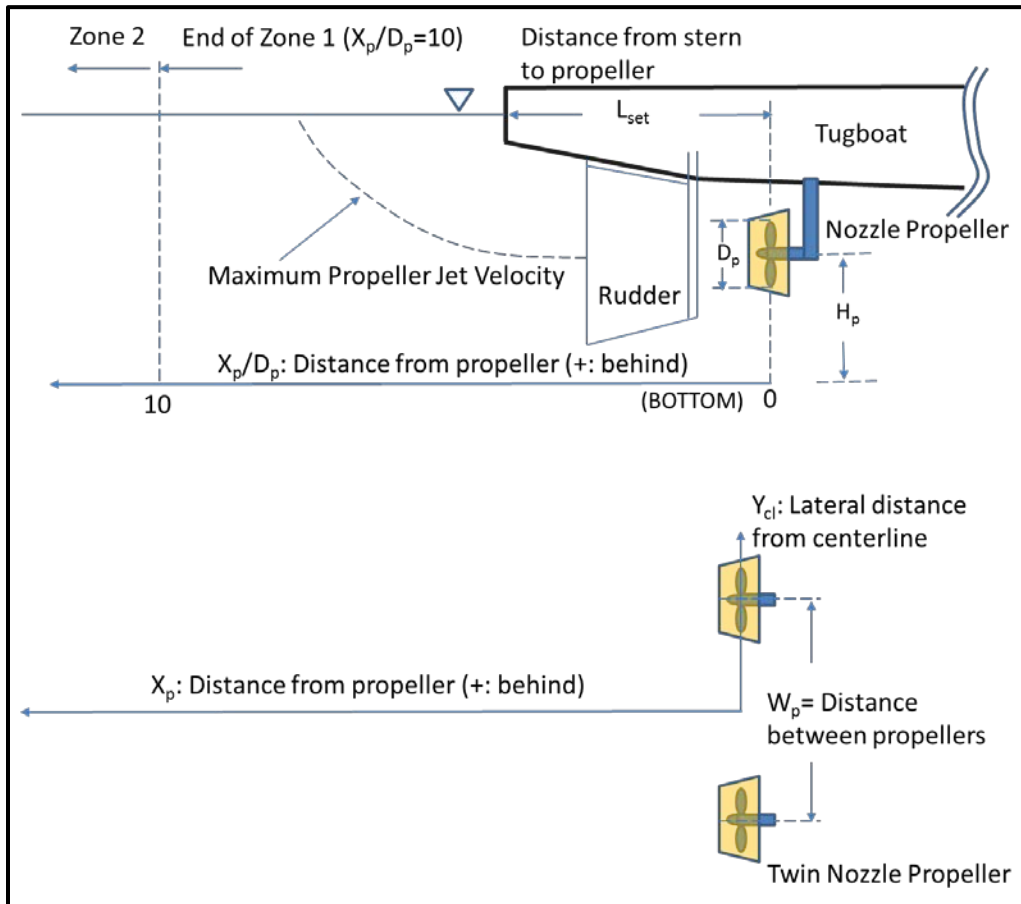


Figure 5-17. Schematic plots of twin-nozzle propellers for a tug-boat in water of confined depth.

Maynard model calculation of the flow field in Zone 1:

$$V_1(X_p, Y_{cl}) = AX_p^{-0.524} \left[e^{\frac{-15.4R_1^2}{X_p^2}} + e^{\frac{-15.4R_2^2}{X_p^2}} \right] \quad (3)$$

Maynard model calculation of the flow field in Zone 2:

$$V_2(X_p, Y_{cl}) = 0.34V_2C_1 \left(\frac{D_p}{H_p} \right)^{0.93} \left(\frac{X_p}{D_p} \right)^{0.24} e^{-\left(\frac{0.0178X_p}{D_p} + \frac{Y_{cl}^2}{2C_{Z2}^2X_p^2} \right)}, \quad (4)$$

where

$$A = 1.45V_2D_p^{0.524}$$

$$R_1^2 = (Y_{cl} - 0.5W_p)^2 + (H_p - C_j)^2$$

$$R_2^2 = (Y_{cl} + 0.5W_p)^2 + (H_p - C_j)^2$$

$$C_j = - \left[0.213 - 1.05 \left(\frac{C_p g}{V_2^2} \right) (X_p - 0.5L_{set}) \right] (X_p - 0.5L_{set}) = \text{vertical distance from propeller shaft to location of maximum velocity within the jet, in meters}$$

$$V_2 = \frac{1.13}{D_0} \sqrt{\frac{T}{\rho_w}}$$

T = Thrust of each propeller, N

$$C_p = \begin{cases} 0.12 \left(\frac{D_p}{H_p} \right)^{0.67} & \text{for open wheel propeller} \\ 0.04 & \text{for Kort nozzle propeller} \end{cases}$$

$$D_0 = \begin{cases} 0.71D_p & \text{for open wheel propeller} \\ D_p & \text{for Kort nozzle propeller} \end{cases}$$

and

X_p = Distance behind the propellers, m

Y_{cl} = Lateral distance from ship centerline, m

D_p = Propeller diameter, m

W_p = Distance between the twin propellers, m

L_{set} = Distance from ship stern to propeller, m

H_p = Distance from center of propeller axis to bottom, m

ρ_w = Density of water, Kg/m³

According to Maynard (2000), the bottom shear stress induced by the velocity field from the propellers can be calculated from Equation (5):

$$\tau = 0.5\rho_w C_{fs} V_{prop}^2, \quad (5)$$

where

$$C_{fs} = 0.01 \left(\frac{D_p}{H_p} \right)$$

and

C_{fs} = bottom friction factor for propeller wash,

τ = bottom shear stress (N/m²),

V_{PROP} = bottom velocity (m/s).

Erosion for cohesive sediment has been modeled based on the relationship between bottom shear stress and critical shear stress. When the bottom shear stress exceeds the critical shear stress of the bed, erosion occurs. The erosion rate can be simulated by the following equation:

$$E = \begin{cases} 0, & \tau < \tau_{cr} \\ \alpha(\tau - \tau_{cr})^n, & \tau \geq \tau_{cr} \end{cases}, \quad (6)$$

where E is the mass erosion rate with a dimension of [g m⁻² s⁻¹], α is the erosion rate constant, τ_{cr} is the critical shear stress, and n = 1 or 2. A linear relation (n = 1) was recommended for cohesive sediment by Kandiah (1974), while Lee et al. (2004), found n = 2 in their laboratory erosion experiments with undisturbed sediment cores from the Sheboygan River, WI.

Maynard (2000) introduced two forms of erosion rate formulae. Those two sets of equations are mathematically equivalent, and both are equivalent to Equation (6), above, with n = 1 (empirically obtained for this study). Note that the two erosion equations in Maynard (2000) and Equation (6), above, may have different units for the erosion constant.

5.2.1.4 Implementation of Maynard's Model for San Diego Bay

In the field study, a Navy-contracted tugboat (Tractor C-14, Figure 5-18) was used to provide the propeller wash under controlled conditions. The tugboat was moored at Pier 4–5 with the bow pushing against the pier wall and the propellers thrusting toward the pier water. The tugboat has twin-nozzle propellers and APPENDIX B lists the dimensions of the tugboat and the propellers. At 110 meters behind the tugboat, a PIV and an Acoustic Doppler Velocimeter (ADV) were mounted to a frame which was placed on the bottom before the experiment started. The PIV measured the water velocity profile near the bottom (0–15 cm), and the ADV measured the water velocity at 15 cm above the bottom, during the study period of 13.847–14.44 hours (since 00:00AM 19 July 2012).

The propellers were operated at four speeds (Figure 5-19), starting at 20 RPM for 5 min, the lowest RPM possible without stalling the engine). Speed was then increased to 50 RPM for about 11 min, followed by subsequent increase to 100 RPM for about 9 min and 150 RPM for about 8 min. These four speeds were estimated by the operator/driver of the tugboat, and include estimates of uncertainty. The operator/driver estimated these uncertainties to be relatively larger for low speeds and lower for high speeds.

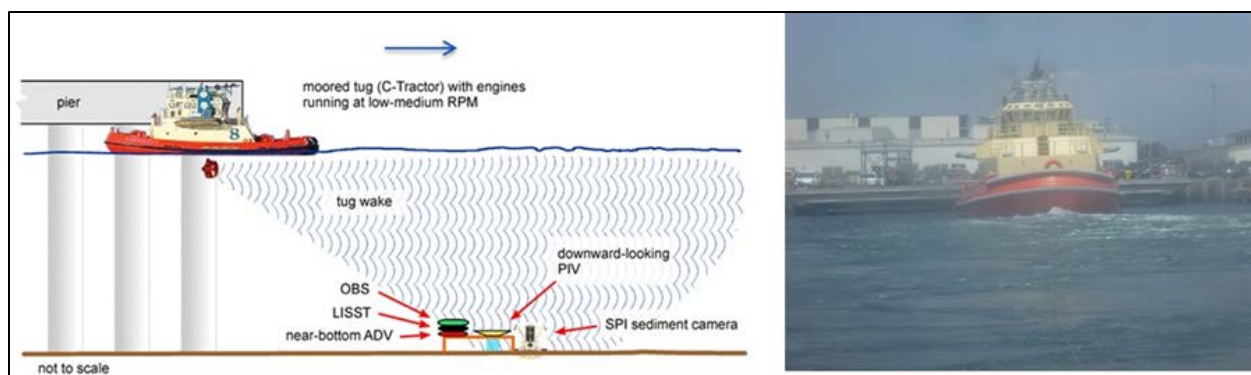


Figure 5-18. Field study of tug-boat propeller wash at Pier 4–5 of Navy Base San Diego (configuration of instruments in propeller plume, left, and tugboat Tractor C-14, right).

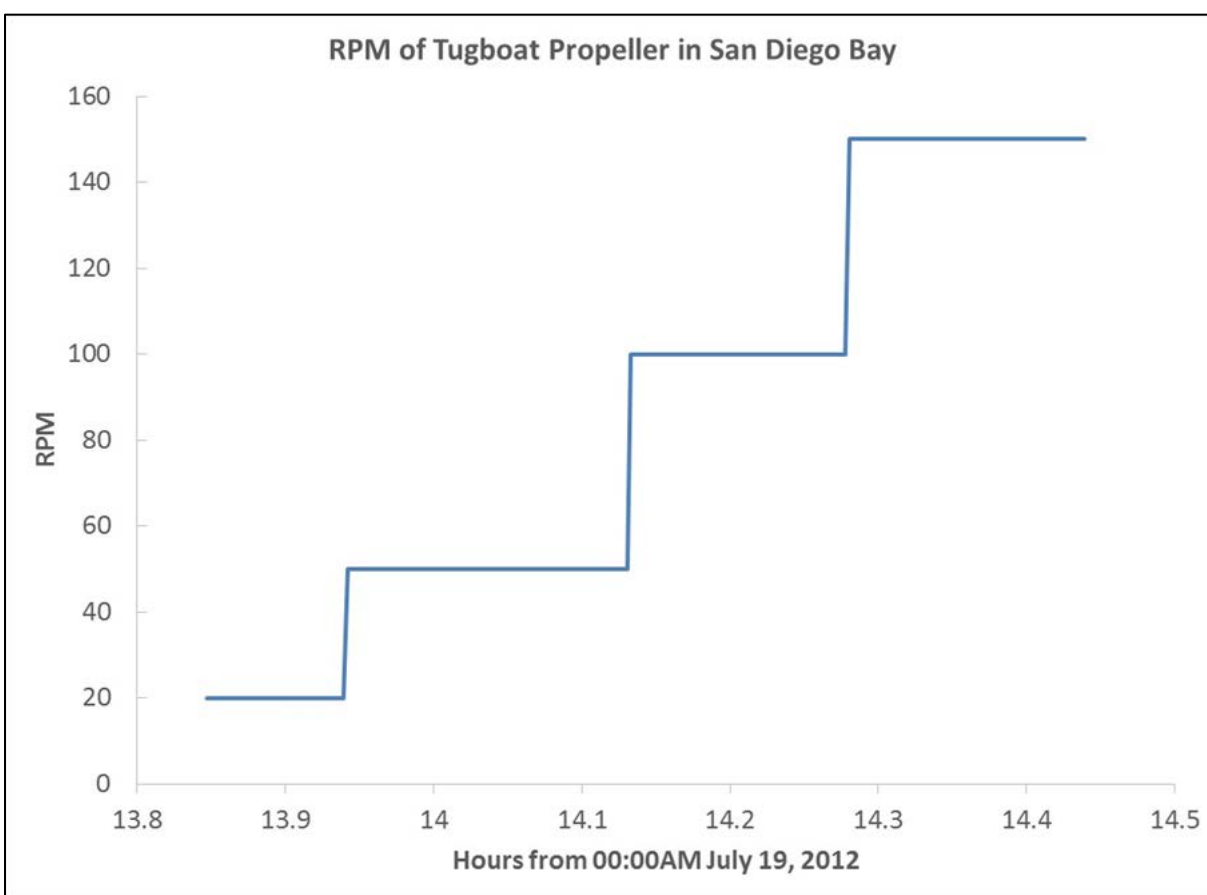


Figure 5-19. Tug-boat propeller speed during the field study (hours: 13.847–14.439, 19 July 2012).

The erosion constant and the critical shear stress were obtained empirically from the San Diego Bay study, are discussed in Section 6.2.

5.2.2 FANS Resuspension Model

The Finite-Analytic Navier-Stokes (FANS) code has been used extensively for the simulation of ship motions with and without propellers under very shallow water conditions. These applications include: berthing of DDG 51 and AOE 6 ships (Chen et al., 1998, 2000), mooring of LHD ships (Chen and Huang, 2003), performed berthing simulations for DDG 51 and AOE 6 ships. In these simulations, a very shallow water depth of 28 ft was used with the underkeel clearance of the moored and docking ships to 1 ft or 3.7% of the ship draft (= 27 ft). More recently, the FANS code has also been used by Huang and Chen (2007, 2010) for site-specific passing ship effects on a docked ship moored to a floating pier in Norfolk harbor. These simulation results clearly demonstrated the capability of the FANS code to model complex interactions between Navy harbor facilities and their client ships in a real waterfront ambience including site specific conditions such as sea bed bathymetry, shorelines, harbor geometry, navigation channels, hull shapes, and arbitrary ship motions, and the effects of propeller wash. The details of the FANS model applications for this study can be found in Chen and Wang (2014).

5.2.3 CH3D Fate and Transport Model

For this study, CH3D has been set up for simulating the fate and transport of plumes from the propeller wash in San Diego Bay, CA; Pearl Harbor, HI; and Sinclair Inlet, WA. Both models have been modified with increased resolutions, with the cell sizes decreased from 100–150 m to 20–50 m in the vicinity of the tug resuspension. The model was run for 5 to 10 days for San Diego Bay and Sinclair Inlet predictions, and 7 days for the two Pearl Harbor sites. The model grid for San Diego is shown in Figure 5-20, for Pearl Harbor in Figure 5-21, and for Sinclair Inlet in Figure 5-22.

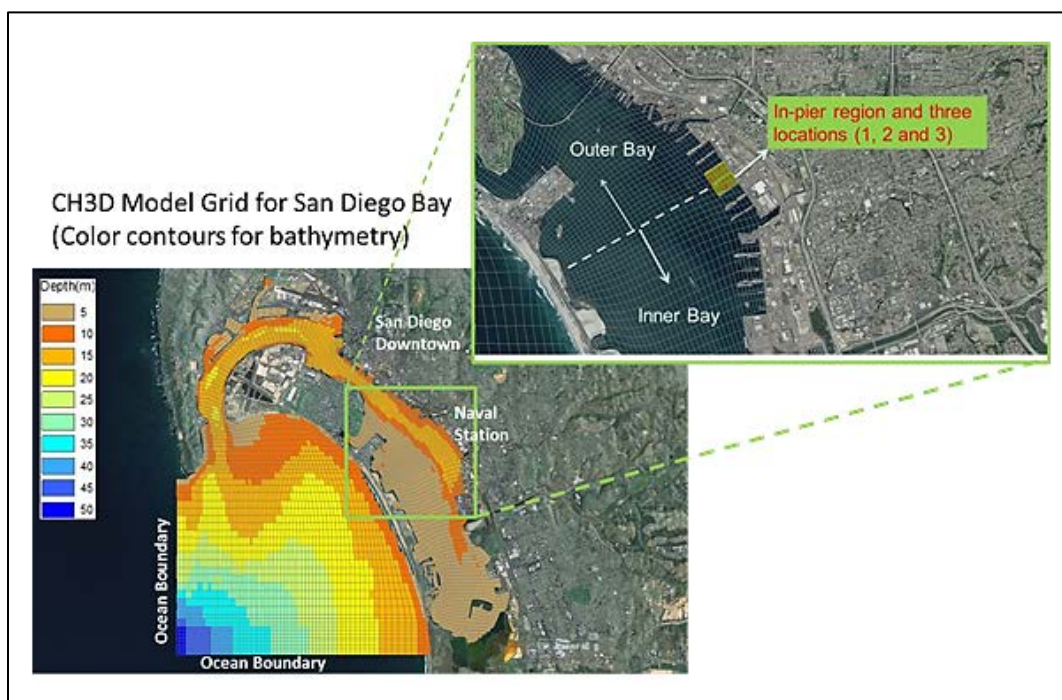


Figure 5-20. Fate and transport CH3D model for San Diego Bay: model grid (lower left) and local grid at Piers 4 and 5 (upper right). Imagery ©2014 DigitalGlobe, U.S. Geographical Survey, USGS, Map data ©2014 Google Life mode Terms Privacy Report a problem.

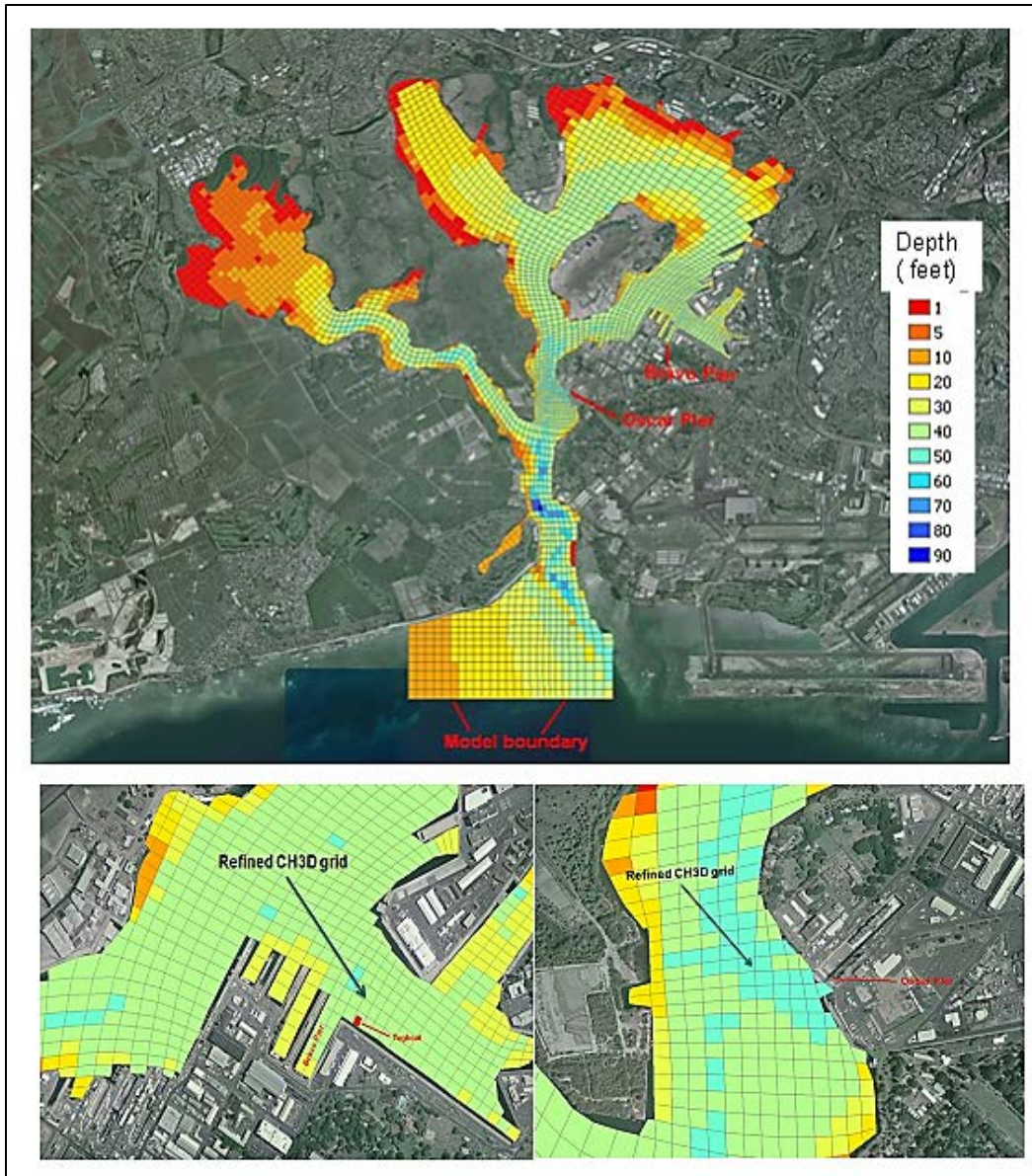


Figure 5-21. Fate and transport CH3D model for Pearl Harbor: model grid (top), and local grid at Bravo Pier (lower left), and Oscar Pier (lower right). Imagery ©2014 DigitalGlobe, U.S. Geographical Survey, USGS, Map data ©2014 Google Life mode Terms Privacy Report a problem.

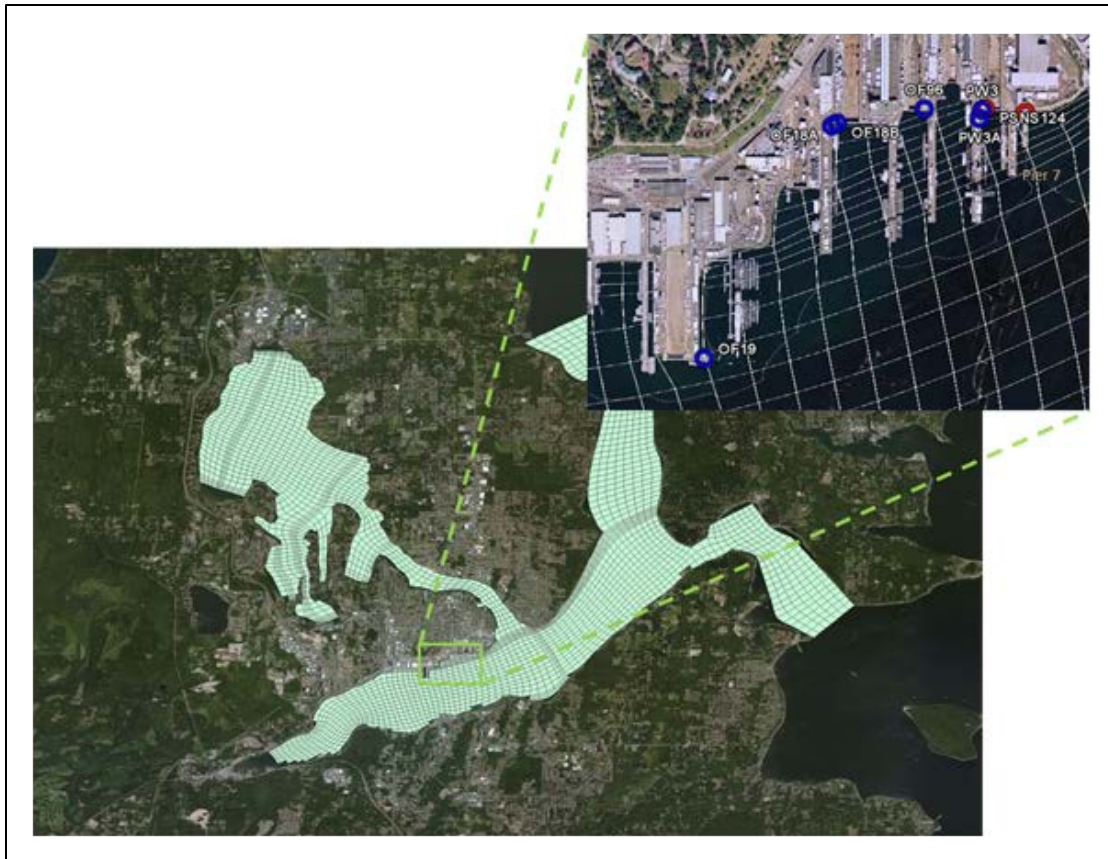


Figure 5-22. Fate and transport CH3D model for Sinclair Inlet: model grid (lower left) and local grid near Pier 7 (upper right). Imagery ©2014 DigitalGlobe, U.S. Geographical Survey, USGS, Map data ©2014 Google Life mode Terms Privacy Report a problem.

6. PERFORMANCE ASSESSMENT

Field and model results were compared to identify the performance of the models. Field and model results were compared to (1) evaluate Maynard's model predicting resuspension in San Diego Bay via pump samples, (2) evaluate the CH3D and TICKET coupled models predicting transport and partitioning in San Diego Bay via pump samples, (3) evaluate CH3D predicting transport in Pearl Harbor at Bravo and Oscar Piers via acoustic backscatter, (4) evaluate FANS predicting hull resuspension from the deep-draft USS *Chafee* via acoustic backscatter, and (5) evaluate CH3D predicting transport in Sinclair Inlet via sediment traps.

Table 6-1 presents a summary of the results and whether performance criteria were met. Details that support these conclusions are documented in comparisons of field data to model predictions in Sections 6.1 to 6.5. Sections 6.1 and 6.2 describe tug wash activities and validation of Maynard's model in San Diego. Section 6.3 describes validation of CH3D+TICKET predictions with pump samples in San Diego and of CH3D with acoustic backscatter in Pearl Harbor. Section 6.4 describes validation of the FANS model with acoustic backscatter in Pearl Harbor. Section 6.5 compares CH3D predictions with sediment trap results, suggesting that more than tug activity is resuspending sediments in Sinclair Inlet, WA.

Table 6-1. Performance assessment results.

Quantitative Objectives				
Performance Objectives	Metric	Data/Model Requirements	Success Criteria	Results
Sediment resuspension model for tugboat	Calibrated resuspension model for San Diego Bay	Accuracy/comparison of measured velocity by PIV and ADV (field data)	Difference of Mean ($V_{piv} - V_{adv}$) < 5 cm/s or < 50%	Criteria met for over 92% of data
		Velocity field by Maynard's model for four prop speeds	Mean velocity (model-data) < 10 cm/s or < 50%	Criteria met for all four prop speeds
		Bottom shear stress (cumulative)	Mean (model-data) < 0.1 Pa-Hr, or < 50 %	Criteria met for all four prop speeds during the 35-min test
		Erosion rate (cumulative)	Measured-calculated cumulative erosion < 0.2 mm or < 50%	Criteria met for 7 out of 9 data points, no corresponding model results for the other two field data, which were measured after prop stopped running
Fate and transport model of size-specific sediments resuspended in tug propeller wash	Calibrated and validated sediment fate and transport model for San Diego Bay	Water column sediment concentrations and sediment grain size	Difference (model-data) of water column sediment concentrations < 0.5 mg/L or < 50 %	Criteria met 89% of the data points for clay, silt, and sand in vicinity of the pier region
		Water column dissolved and total copper concentrations	Difference (model-data) of water column dissolved and total copper concentrations < 3.1 µg/L or < 100 %	Criteria met over 86% of the data points for dissolved copper, and over 81% of the data points for total copper
Linked CH3D+TICKET Model	Calibrated and validated contaminant partitioning model for San Diego Bay	Partitioning coefficient for copper between field data and look-up table	Difference (field data-estimated) of copper partitioning < 0.1 or < 75%	Criteria met for 23 out of 24 field data sets
		Water column particulate copper concentrations	Difference (model-data) of water column copper concentrations bound by clay, silt, and sand < 3.1 µg/L or < 100 %	Criteria met over 83% of the data points including copper concentrations bound by clay, silt, and sand

Table 6-1. Performance Assessment Results. (Continued)

Quantitative Objectives				
Performance Objectives	Metric	Data/Model Requirements	Success Criteria	Results
Linked resuspension, fate and transport and partitioning models	Models linked	Compatible model input and output files	Models linked	Linked CH3D+TICKET completed with look-up table derived from field data
Performance Objectives	Metric	Data/Model Requirements	Success Criteria	Results
Fate and transport model for Pearl Harbor	CH3D application for fate and transport for Pearl Harbor	TSS data tracking the bulk of the plumes	Model-simulated TSS concentrations compared with TSS, qualitatively	Model and data consistent in transport patterns
		Tracking (incidental) bow wake of USS <i>Chafee</i>	Incidental tracking and measured TSS plume in the wake of USS <i>Chafee</i> (deep draft), as predicted by FANS model	Sediment plumes from deep-draft USS <i>Chafee</i> predicted by the FANS model and measured by ADCP

6.1 TUG PROPELLER WASH VELOCITIES IN SAN DIEGO BAY

Figure 6-2 and Figure 6-3 map out extrapolated water velocities in the tug propeller wash in San Diego Bay at a number of depths and when the propeller was turning at 100 RPM and 200 RPM respectively. Blue dots represent locations of ADV measurements. Water depth was approximately 10 m. The depth of ADV measurements is approximate in these figures. Field conditions during measurements were akin to rafting down river rapids, perhaps Class 3. The water at the surface was composed of large, turbulent boils approximately 3 m across. Figure 6-4 represents the same data in cross section at 100 RPM and 200 RPM. The extrapolated contours are based on the average velocity data by depth and range downstream from the tug. The data were limited to measurements 10 m on either side of a boat axis line extending from the tug downstream to where our small measurement boat and represents the center of the plume. Variation in depth represents the actual depth of the ADV in the propeller wash. Although the ADV was weighted by 45 kg ballast, the wash was powerful enough to swing the suspended instrument around off the vertical, particularly at 200 RPM. Each data point represents a two second average of approximately 100 acoustic measurements so probably represents the mean of a relatively large volume of water.

The velocity contours in Figure 6-2 to Figure 6-4 exhibit highly turbulent patterns both in the horizontal direction and in the water column. Decay of the propeller jet flow was evident both for the 100 RPM and, even more evident, for the 200 RPM scenarios. Based on the contour level of the jet speed > 0.5 m/sec, the jet touched the bottom at a distance 80-100 m downstream the tug. These data were instrumental in the bottom placement of the ADV and PIV at 80 m, and then 110 m downstream of the tug to ensure that measured bottom velocities and critical shear were in the propeller plume.

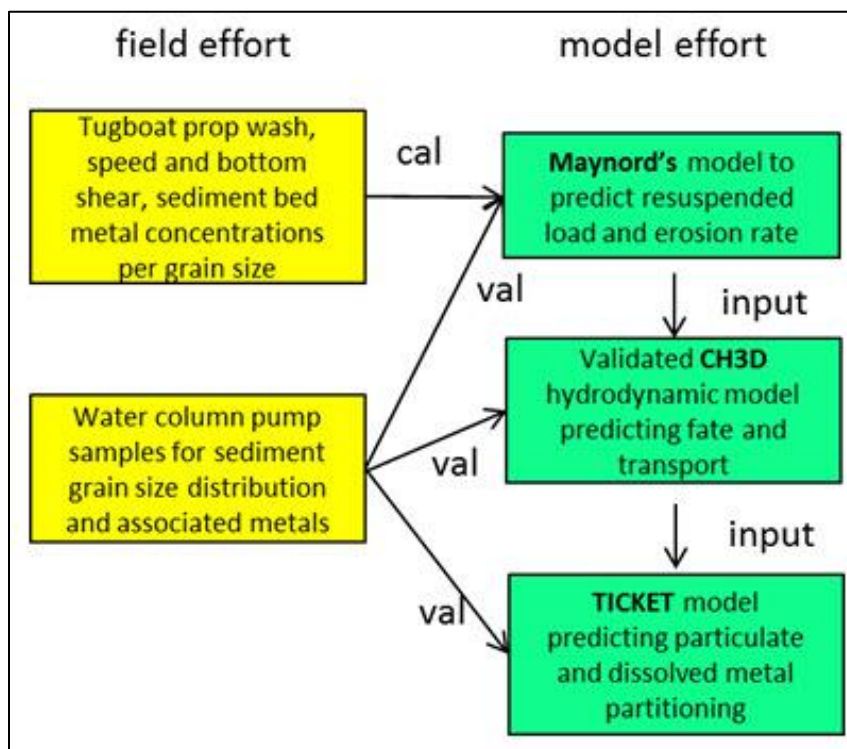


Figure 6-1. Field and modelling efforts in San Diego Bay.

Figure 6-2 and Figure 6-3 map out extrapolated water velocities in the tug propeller wash in San Diego Bay at a number of depths and when the propeller was turning at 100 RPM and 200 RPM respectively. Blue dots represent locations of ADV measurements. Water depth was approximately 10 m. The depth of ADV measurements is approximate in these figures. Field conditions during measurements were akin to rafting down river rapids, perhaps Class 3. The water at the surface was composed of large, turbulent boils approximately 3 m across. Figure 6-4 represents the same data in cross section at 100 RPM and 200 RPM. The extrapolated contours are based on the average velocity data by depth and range downstream from the tug. The data were limited to measurements 10 m on either side of a boat axis line extending from the tug downstream to where our small measurement boat and represents the center of the plume. Variation in depth represents the actual depth of the ADV in the propeller wash. Although the ADV was weighted by 45 kg ballast, the wash was powerful enough to swing the suspended instrument around off the vertical, particularly at 200 RPM. Each data point represents a two second average of approximately 100 acoustic measurements so probably represents the mean of a relatively large volume of water.

The velocity contours in Figure 6-2 to Figure 6-4 exhibit highly turbulent patterns both in the horizontal direction and in the water column. Decay of the propeller jet flow was evident both for the 100 RPM and, even more evident, for the 200 RPM scenarios. Based on the contour level of the jet speed > 0.5 m/sec, the jet touched the bottom at a distance 80–100 m downstream the tug. These data were instrumental in the bottom placement of the ADV and PIV at 80 m, and then 110 m downstream of the tug to ensure that measured bottom velocities and critical shear were in the propeller plume.

Propeller water velocity at 100 rpm by depth

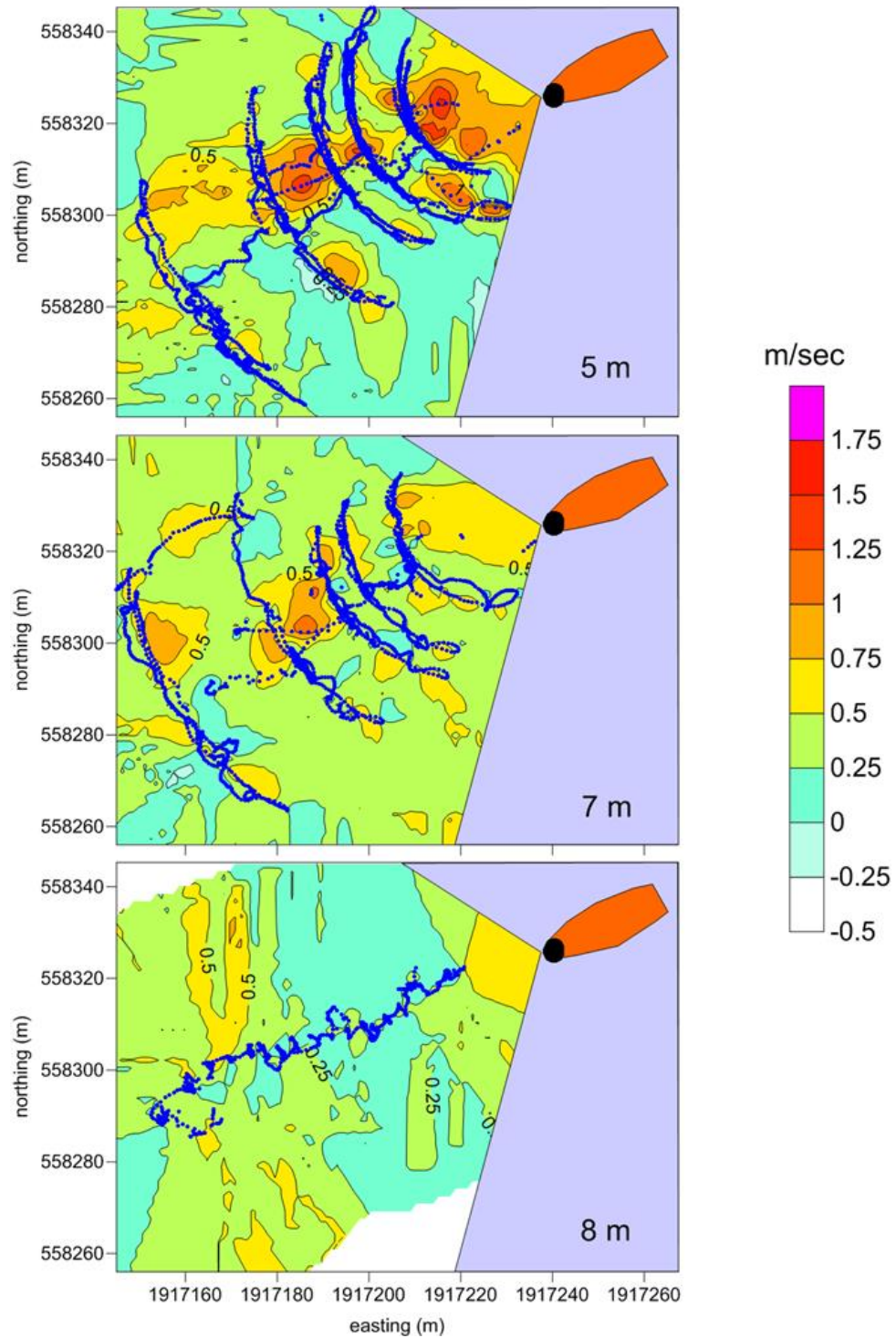


Figure 6-2. Horizontal water velocities downstream of the tug propeller wash at 100 RPM and at various depths.

Propeller water velocity at 200 rpm by depth

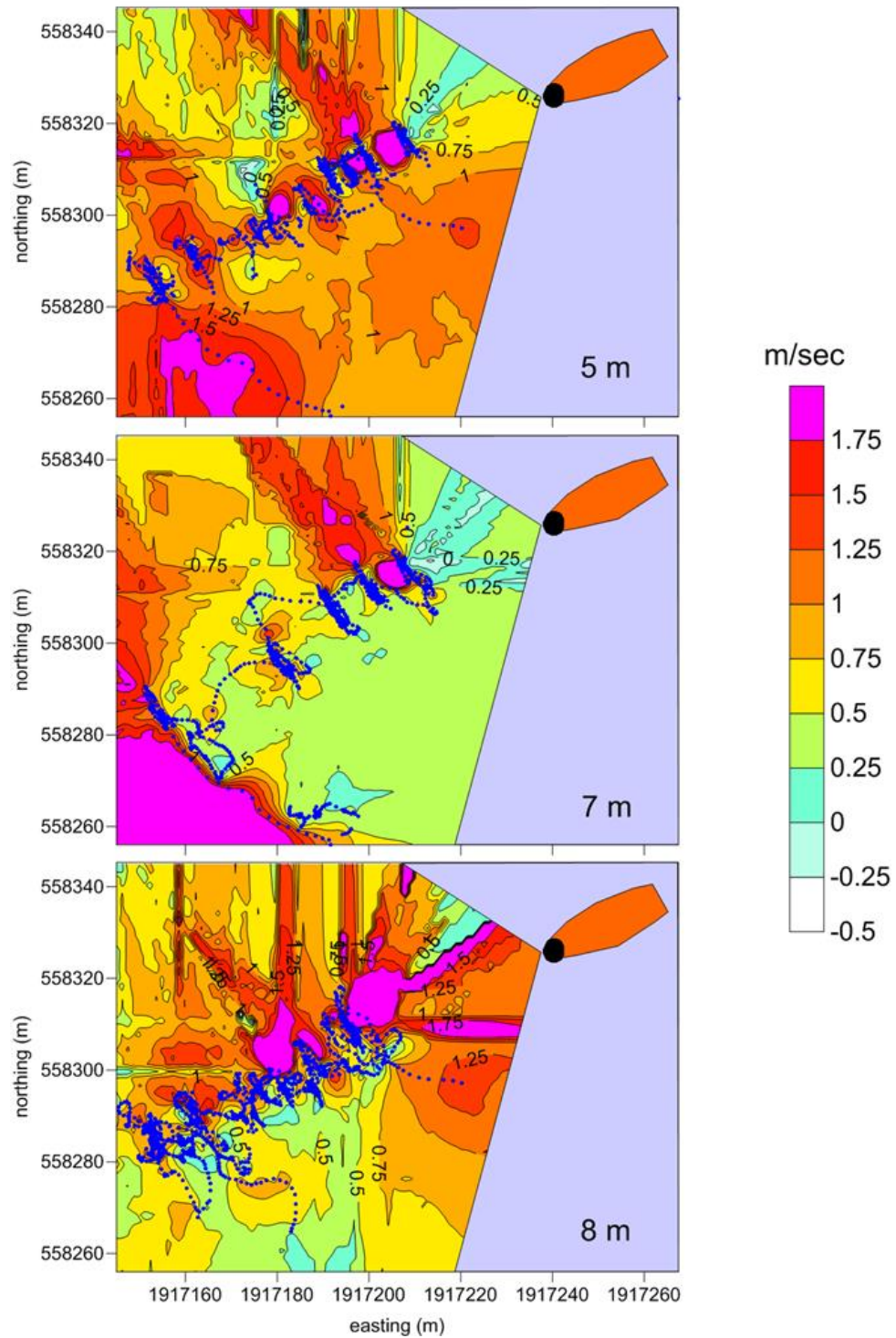


Figure 6-3. Horizontal water velocities downstream of the tug propeller wash at 200 RPM and at various depths.

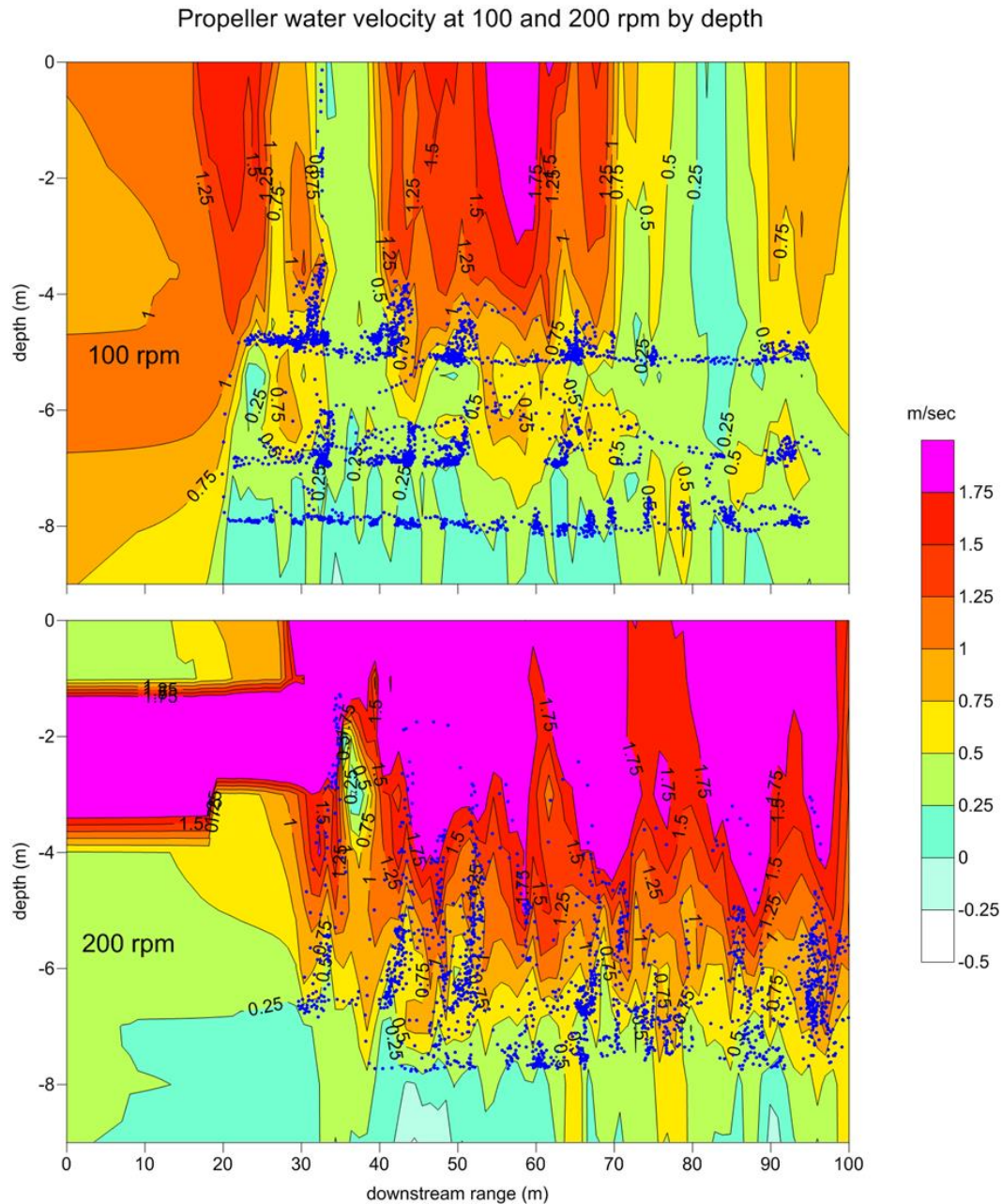


Figure 6-4. Vertical cross-section of propeller wash velocity at 100 RPM and 200 RPM.

6.2 IMPLEMENTATION OF MAYNORD'S MODEL FOR SAN DIEGO BAY

In the field study, a Navy-contracted tugboat (Tractor C-14, Figure 6-5) was used to provide the propeller wash under controlled conditions. The tugboat was moored between Pier 4–5 with the bow pushing against the pier wall and the propellers thrusting toward the pier water. The tugboat has twin-nozzle propellers and Table 6-2 lists the dimensions of the tugboat and the propellers. At 110 meters behind the tugboat, a PIV and an Acoustic Doppler Velocimeter (ADV) were mounted to a frame which was placed on the bottom before the experiment started (Figure 6-5). The PIV measured the water velocity profile near the bottom (0–15 cm), and the ADV measured the water velocity at 15 cm above the bottom, during the study period of 13.847–14.44 hours (since 00:00AM 19 July 2012).

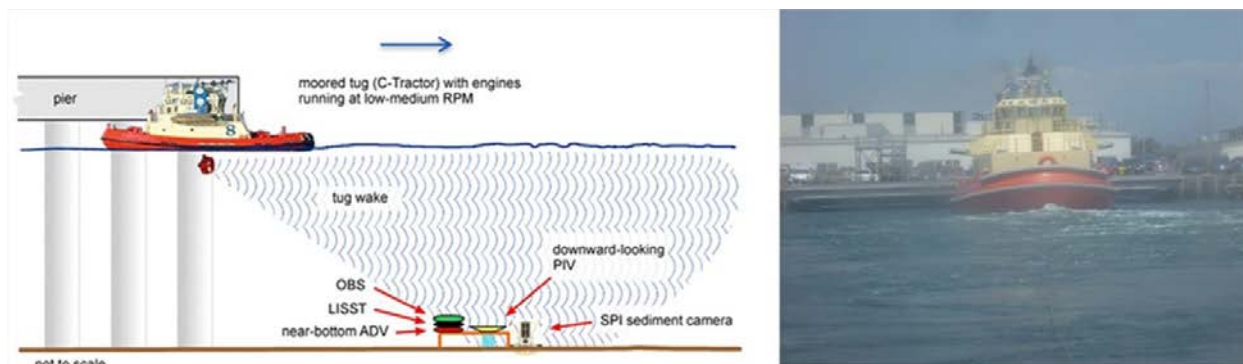


Figure 6-5. Field study of tugboat propeller wash at Pier 4–5 of Naval Base San Diego (configuration of instruments in propeller plume, left, and tug-boat Tractor C-14 in operation, right).

Table 6-2. Propeller information and operating conditions for ducted propeller.

Characteristics	Dimensions
Ship length L (m)	28.65 (94 ft)
Ship beam B (m)	10.36 (34 ft)
Ship draft (m)	3.353 (11 ft)
Water depth, H (m)	9.144 (30 ft)
Distance from ship bow to pier wall at waterline (m)	1.8288 (6 ft)
Distance from ship stern to pier wall at waterline (m)	30.48 (100 ft)
Clearance between ship sidewall and Pier wall (m)	Open water
Underkeel clearance (m)	2.997 (9.833 ft)
Propeller diameter, D_p (m)	2.286 (7.5 ft)
Distance between Propellers (W_p) (m)	4.8768 (16 ft)
Distance from ship stern to propeller (L_{set}) (m)	15.24 (50 ft)
Propeller depth (depth of the propeller axis) (m)	4.8768 (16 ft)
Distance from center of propeller axis to bottom (H_p) (m)	4.2672 (14 ft)
Gap clearance between propeller duct and tugboat bottom (m)	0.14 (0.46 ft)
Ship speed (knots)	0
Propeller RPM, n	20, 50, 100, 150 and 200
Characteristic time, T_o (s)	0.3
Characteristic velocity U_o (m/s)	1.016
Reynolds number based on characteristic length L_o (= 1 ft)	2.647×10^5
Reynolds number based on propeller diameter D	1.488×10^7

The propellers were operated at four speeds (Figure 5-19), starting at 20 RPM for 5 min, the lowest RPM possible without stalling the engine). Speed was then increased to 50 RPM for about 11 min, followed by subsequent increase to 100 RPM for about 9 min and 150 RPM for about 8 min. These four speeds were estimated by the operator/driver of the tugboat, and include estimates of

uncertainty. The operator/driver estimated these uncertainties to be relatively larger for low speeds and lower for high speeds.

Using the bottom check function of the Nortek ADV, we were able to determine the height of the ADV sample volume above the sediment bed, which varied from 12 to 13 cm at the 110-m site. The variation might be partly from the measurement error, or it might reflect the variation of the sediment bed due to resuspension and deposition.

Figure 6-6 shows the entire time series of velocities measured at the 110-m site. The abscissa represents the time in hours since midnight on 19 July 2012. Dashed black lines represent the starting time of each RPM. Since the probe was about 110 m away from the propeller, it would take several minutes for the ADV to detect the change of propeller speed after the change of RPM. We have estimated this time lag, and marked the effective starting time for each propeller speed, and they are shown as pink dashed lines in Figure 6-6.

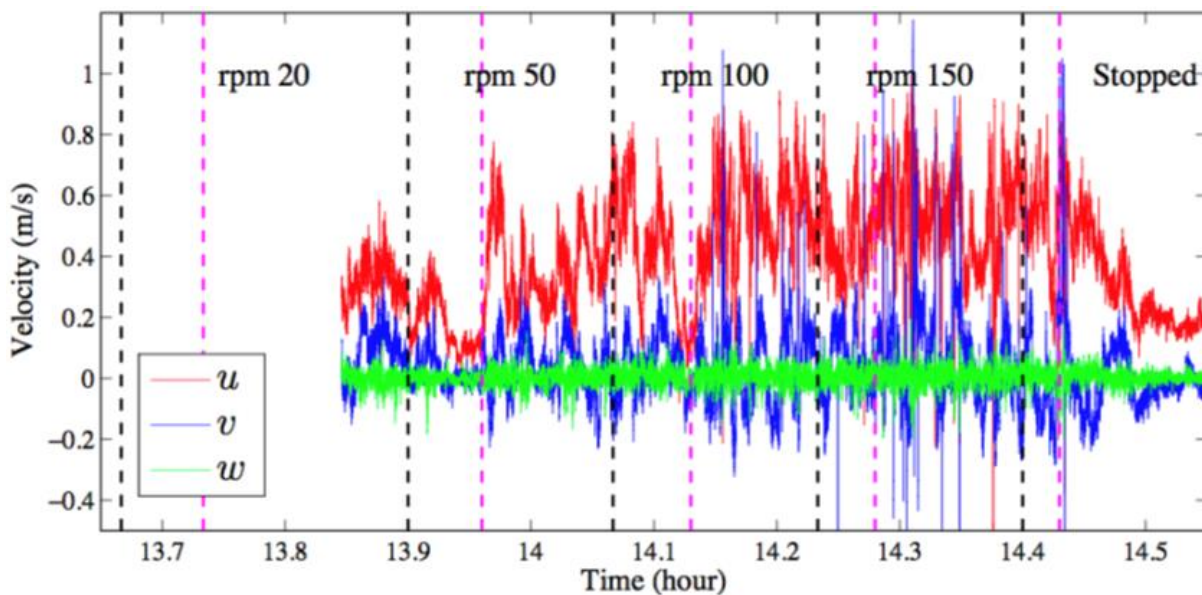


Figure 6-6. Time series of velocities measured by the ADV, which was 110 m away from the propeller. The sample volume was about 12 cm above the sediment bed. Black dashed lines are the starting time of each RPM run. Pink dashed lines are estimated starting time for the change of propeller speed to affect the 110-m measurement site.

6.2.1 Mean Characteristics of the Propeller Current and Turbulence by ADV

The near-bottom flow at the 110-m site was unsteady. Undulating patterns can be observed from the recorded time series of the two horizontal velocity components, which agreed with the meandering flow pattern we observed on the surface behind the propeller. Figure 6-7 shows the probability distribution of the direction of the horizontal flow as measured by the ADV over the entire measurement period. The meandering of the flow was, however, confined to a range of $\pm 30^\circ$ with respect to x. The root-mean-square (RMS) of the fluctuating velocities is calculated for each RPM run. The delineations of different RPM runs are the same as those pink dashed lines shown in Figure 6-6. Figure 6-8 shows the mean velocity components vs. the propeller speed. Error bars are drawn based on the standard deviation of the signal. The mean stream-wise velocity did increase with propeller RPM, while the increase was not linear. As the propeller speed increased from 100 pm to 150 RPM, the mean velocity only increased by 5 cm/s. The mean spanwise velocity was positive,

indicating that the instrument frame was not perfectly aligned with the mean flow direction, although the deviation is rather small, which can also be shown by the probability distribution of the flow direction, i.e., Figure 6-7. The mean vertical direction is negative for RPM = 20, suggesting a mean trend of sediment deposition. Sediment might be entrained at an upstream site, transported, and deposited to the 110-m site under this propeller speed. As the mean speed increased with RPM, the mean vertical velocity changed to positive and showed an increasing trend with RPM (Figure 6-9), which indicates a mean effect of resuspension.

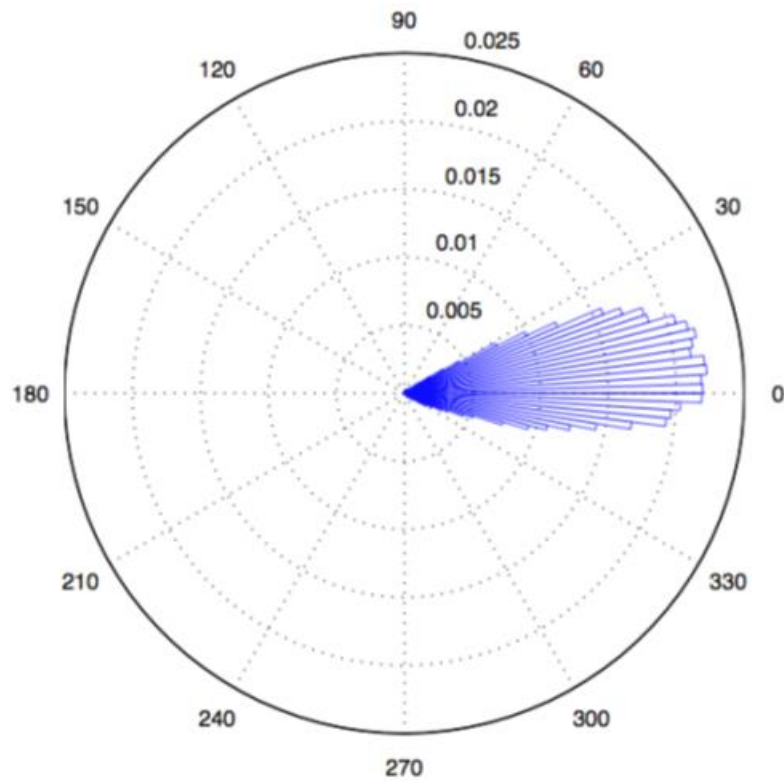


Figure 6-7. Probability of the direction of the horizontal velocity recorded by the ADV probe.

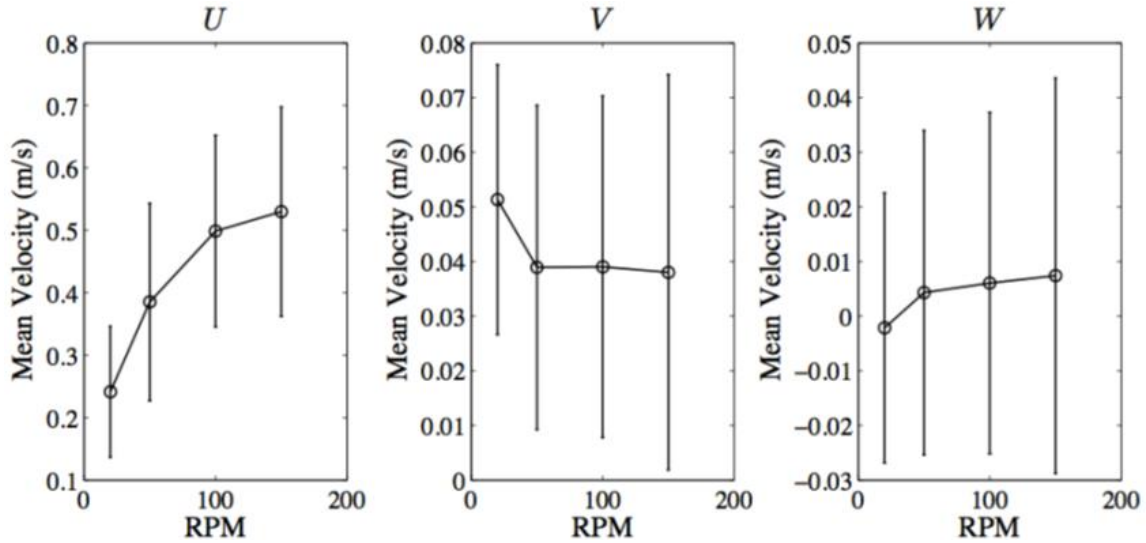


Figure 6-8. Change of mean velocities with the propeller RPM.

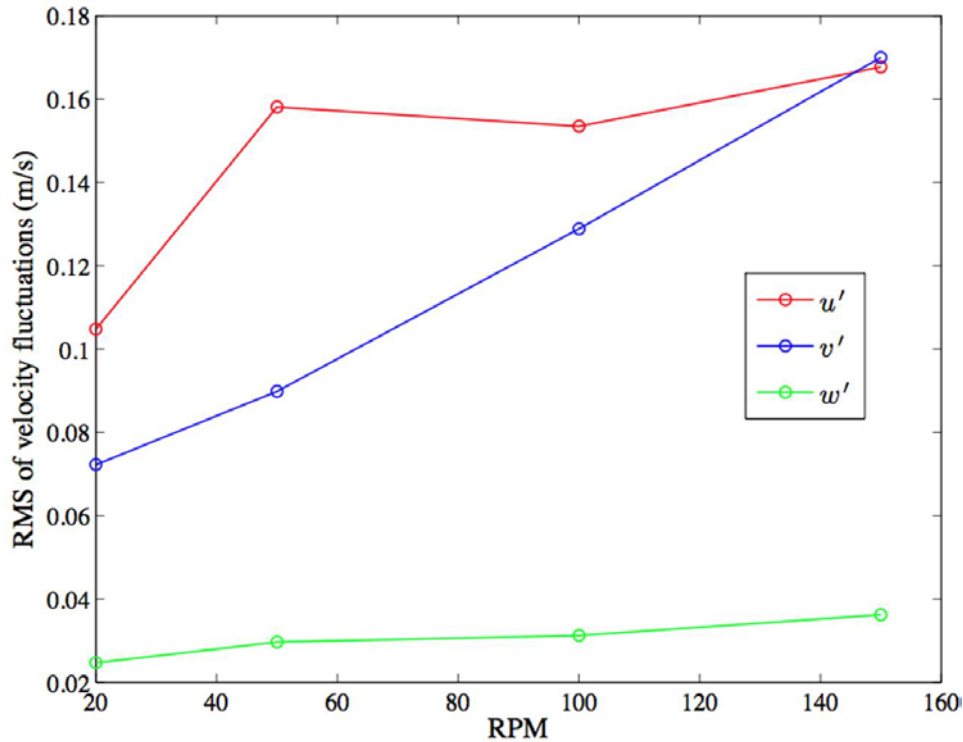


Figure 6-9. Change of RMS of velocity variations with the propeller RPM.

6.2.2 Structure of Turbulence above the Sediment Bed Measured by PIV

We observed that significant sediment resuspension occurred as the propeller speed ramped up to 50 rpm and above. High sediment concentration during resuspension made optical access to the laser sheet impossible. Most PIV measurements were not available during the experiment with high flows. However, we were able to capture the initiation of sediment entrainment through PIV images and make measurement on flow structures around that moment. PIV in this research is applied to validate

the ADV in estimating the bottom shear stress and to determine the critical shear stress for sediment resuspension. Figure 6-10 shows the time series of the velocities u and w measured by ADV and PIV at around 14:00 when the propeller rpm was 50, and initiation of sediment resuspension was observed. Signals from PIV were obtained at $z = 11.5$ cm, the highest position of PIV measurement, while the ADV's sample volume was approximately at $z = 12.5$ cm, and it was about 10 cm away from the PIV laser sheet in both x - and y - directions. Water velocity with the large temporal variations agreed well between the two instruments despite their spatial separation. Note that PIV data is unavailable during the interval between the 4.021 and 14.026 hour, when a strong sediment resuspension blocked the optical access. During that time we can observe a sudden increase of streamwise velocity from about 0.3 to 0.5 m/s, according to the ADV measurement.

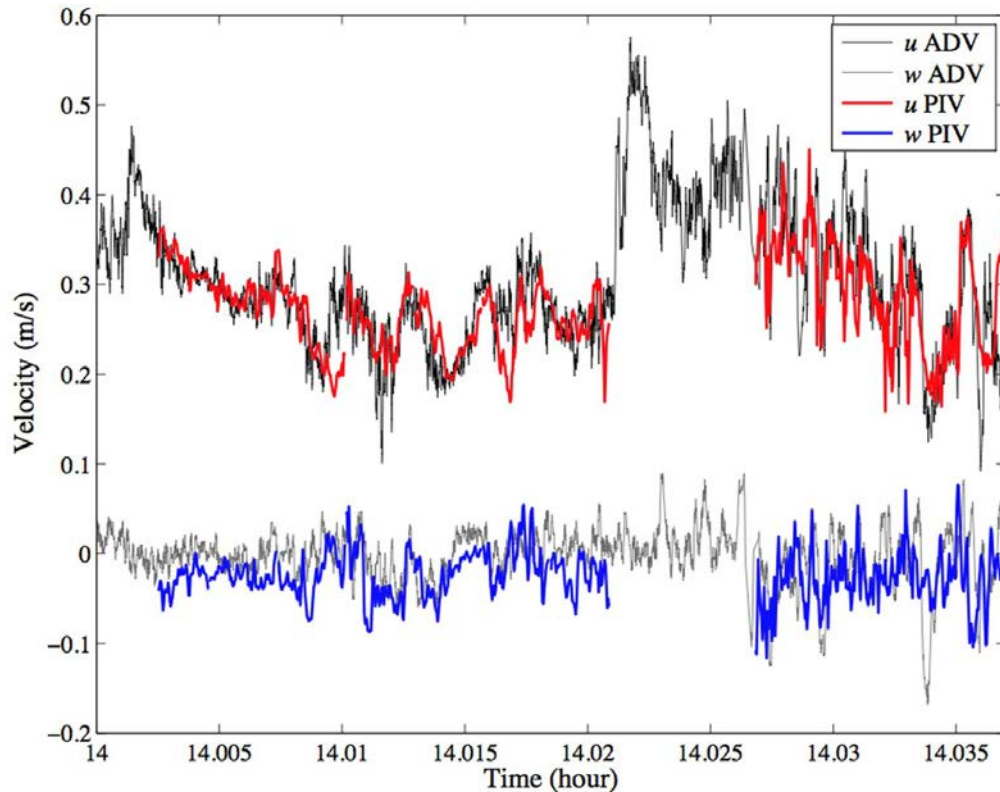


Figure 6-10. Time series of velocities measured concurrently by PIV and ADV. PIV signals were measured at $z = 11.5$ cm, while ADV data was at $z = 12.5$ cm.

From the PIV time series shown in Figure 6-10 we can see two distinct sections, here denoted as section A (from 14.005 to 14.021 hour) and section B (from 14.026 to 14.037 hour). Section A is characterized by a relatively steady flow, while section B shows a deceleration trend of u . Statistics of the turbulent flow were calculated for both Sections A and B. Profiles of mean velocity, variances of fluctuations, and the Reynolds shear stresses for the two sections are presented in Figure 6-11 through Figure 6-14.

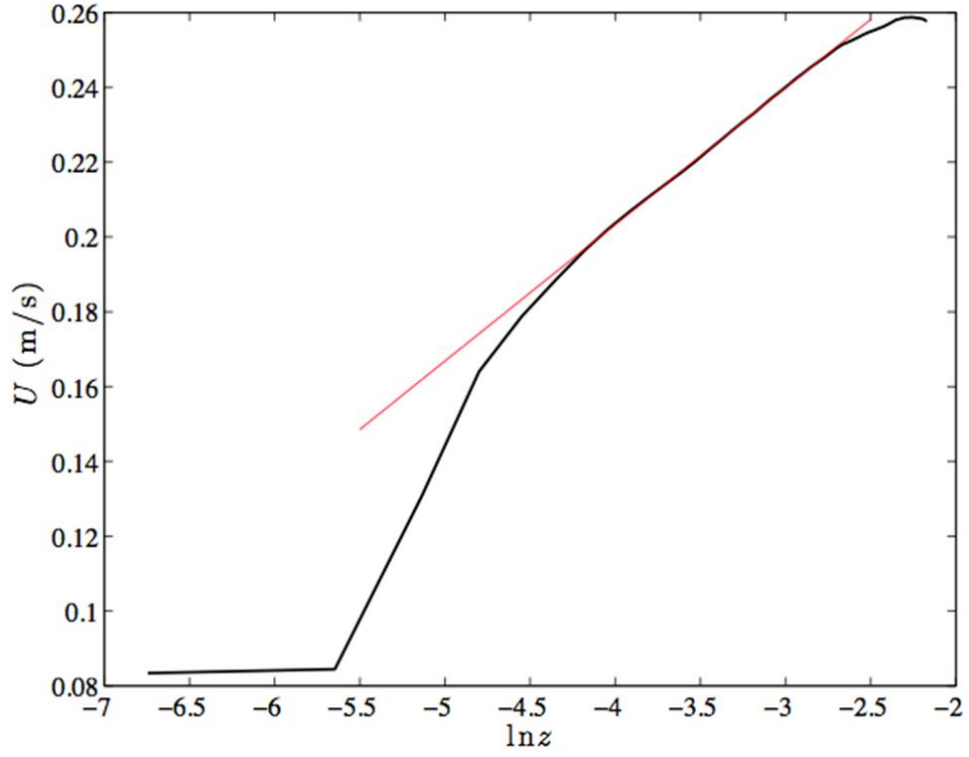


Figure 6-11. Vertical profile of the mean velocity measured by PIV between 14:00 and 14:01 (Section A). The red line is the fitted log-law with a shear velocity $u^* = 1.5$ cm/s.

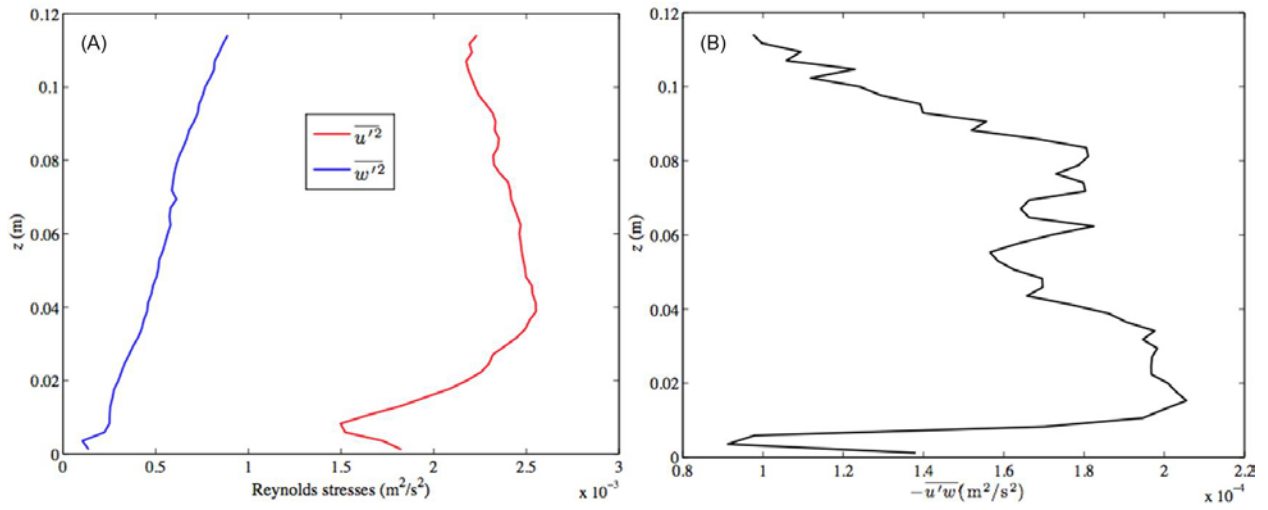


Figure 6-12. Vertical profiles of Reynolds stresses: (A) normal stresses, and (B) shear stresses measured between 14:00 and 14:01 (Section A).

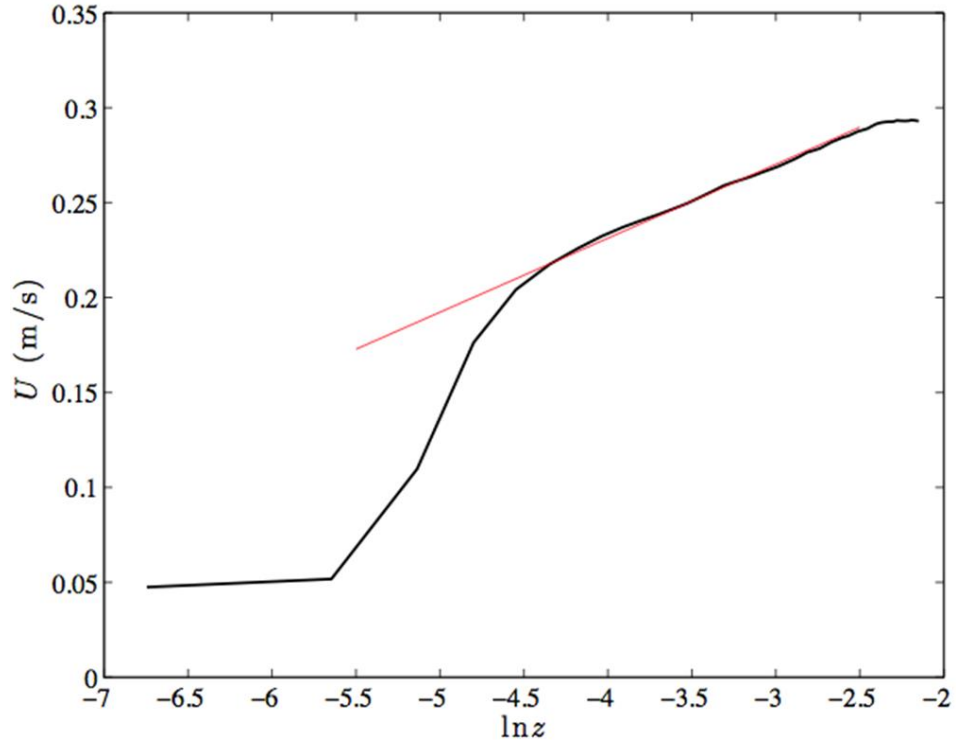


Figure 6-13. Vertical profile of the mean velocity measured by PIV between 14:01 and 14:02 (Section B). The red line is the fitted log-law with a shear velocity $u^* = 1.6$ cm/s.

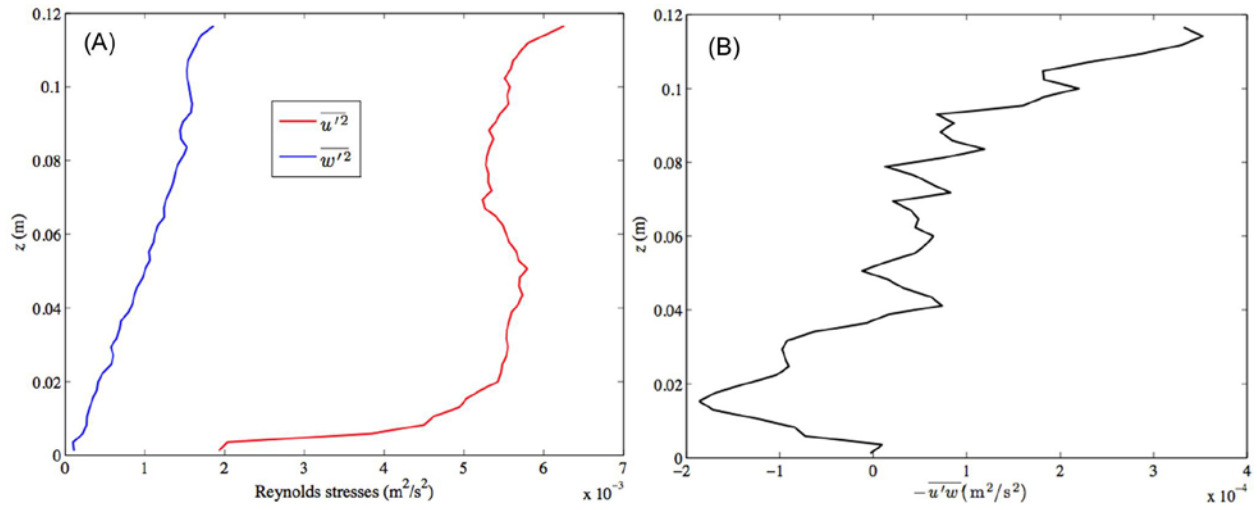


Figure 6-14. Vertical profiles of Reynolds stresses: (A) normal stresses; and (B) shear stresses measured between 14:01 and 14:02 (Section B).

The vertical profiles of the mean streamwise velocity are presented in Figure 4-11 in a semi-log plot. Profiles of U in both sections were well described by the log-law, i.e.,

$$U/u_* = 1/\kappa \ln[z/z_0] \quad (8)$$

Least square fit indicated that the shearing velocity $u_* = 0.015$ and 0.016 (m/s) for section A and B, respectively.

Vertical profiles of the Reynolds stresses $\overline{u'^2}$, $\overline{w'^2}$, and $-\overline{u'w'}$, are shown in Figure 6-12 and Figure 6-14 for Sections A and B, respectively. For Section A with a relatively stationary condition, these profiles showed a classic wall turbulence behavior (Figure 6-11). The fluctuation of the streamwise velocity peaked at about $z = 4$ cm and decreased with height. The Reynolds shear stress also had a peak value near the bottom. Taking a square root of the peak value as an estimate of the shear velocity, we have $u_* = 0.014$ (m/s), very close to the estimated value from the log-law fitting.

For Section B, the streamwise velocity profile could still be well described by the log-law despite the decelerating trend. The variances of turbulent fluctuations were about two times higher than those in Section A, and they both seemed to increase with z without distinguishable peaks. This observation can be explained by the flow unsteadiness. The Reynolds shear stress showed a negative value near the bottom, and it increases with height. No peak value was found within the entire height of PIV measurement, making it difficult to estimate the bottom shear stress (or the shear velocity). This, again, might be attributed to the unsteadiness of the mean flow.

The Reynolds shear stress had a peak value near the bottom. Taking a square root of the peak value as an estimate of the shear velocity, we have $u_* \approx \sqrt{-\overline{u'w'}_{peak}} = 0.0143$ (m/s), very close to the estimate from the log-law fitting.

For flow during Section B, the mean current profile can still be well described by a log-law despite the deceleration trend (Figure 6-13). The shear velocity was estimated to be $u_* = 0.016$ (m/s). The variances of turbulent fluctuations, $\overline{u'^2}$, $\overline{w'^2}$, were about two times higher, which can be attributed to the transient feature of the mean flow (Figure 6-13). The Reynolds shear stress showed a negative value near the bottom, and it increases with height. No peak value was found within the entire height of PIV measurement, making it difficult to estimate the bottom shear stress (or the shear velocity) based on the measurement of Reynolds shear stress. This, again, can be attributed to the unsteadiness of the mean flow.

The vertical profiles of the dissipation rate of TKE for the two sections are shown in Figure 6-15. Dissipation rate in section B was significantly higher than that in section A. For both sections, we did not see a decrease of dissipation rate with height z , while for canonical wall turbulence, we'd expect to see $\epsilon \sim z^{-1}$. The dissipation rate is rather uniform except a sharp increase very close to the sediment surface. This again suggested that the turbulence near the bottom could still be affected by the turbulence generated by the propeller and transported in the "free stream."

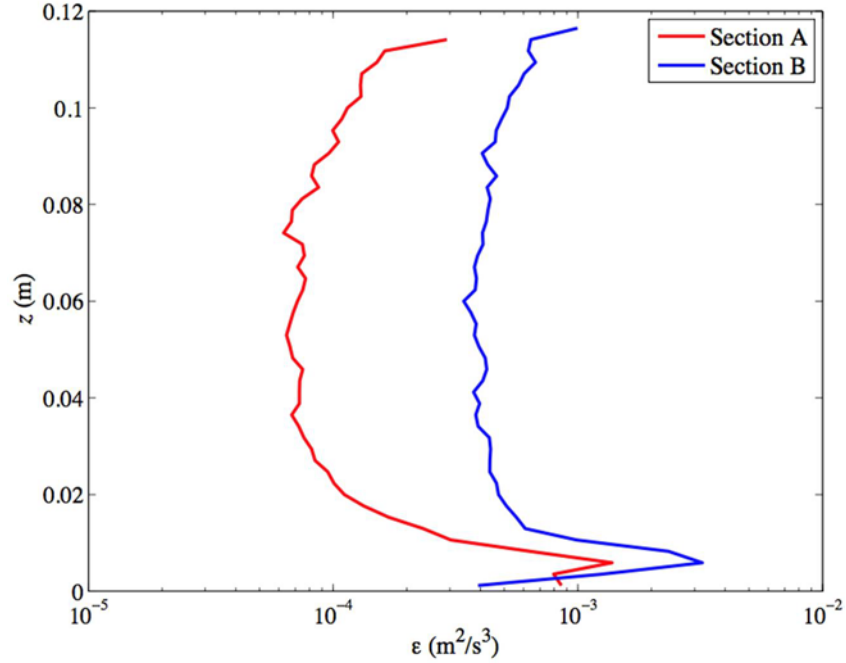


Figure 6-15. Vertical profiles of the TKE dissipation rate measured during Sections A and B.

Reiterating, in this study we tried to estimate the bed shear stress with both the ADV and PIV measurements. Taking the advantage of the high sampling rate of the ADV and high spatial resolution of the PIV, we explored to calculate the statistics of turbulence over a rather short period (a few seconds) to reduce the effects of unsteady flows on the estimation of the bed shear stress.

With available PIV data, we applied average on every 5 sec with a 50% overlap, which are 40 instantaneous 2-D flow fields. Spatial average was also applied over the horizontal direction to obtain the vertical profiles. Bed shear stress was estimated with both the log-law approach on the mean velocity, and the covariance method, i.e., the shear velocity was assumed to be the maximum of $\sqrt{-\overline{u'w'}}$ over 5 cm of water column above the sediment bed. Despite the short time averaging window, mean velocity profiles had always agreed well with a log-law. Figure 6-16 shows 60 mean velocity profiles measured during 2.5 min, starting from 14:00. After normalized with the estimated shear velocity, all profiles showed a log-linear trend with z for $z < 5$ cm.

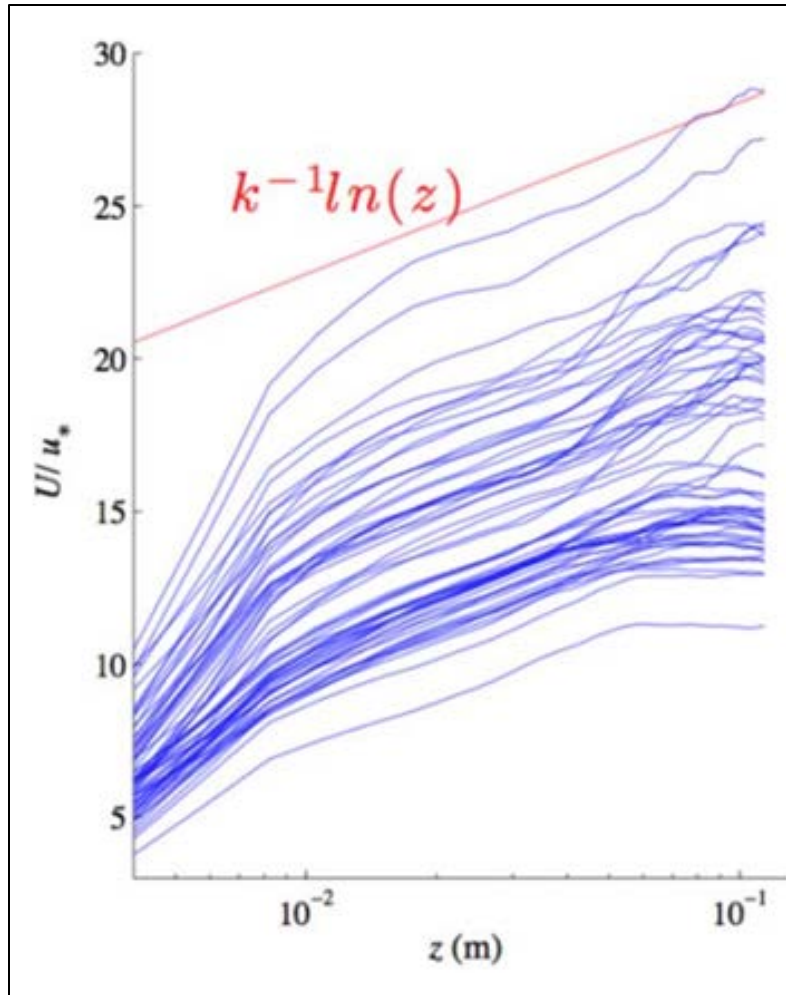


Figure 6-16. Mean velocity profiles averaged every 5 sec starting from 14:00.

With ADV measurements, bed shear stress was estimated with the direct covariance method, the TKE method, and the modified TKE method (see Table 5-9). Statistics were calculated over an averaging window of 10 sec, which corresponded to 300 data points with a sample rate of 30 Hz. Since all the three methods need a coefficient to account for the uncertainty about the optimal height of the sample volume, we calibrated the shear stress with that from PIV when it is available. Figure 6-17 shows the comparison among various methods for bottom shear stress estimation between 14:00 and 14:02, when both ADV and PIV results are available. In general, good agreements are found among all methods. Results from PIV were not available in a period when the bed stress was high than 0.8 (Pa), approximately due to sediment resuspension.

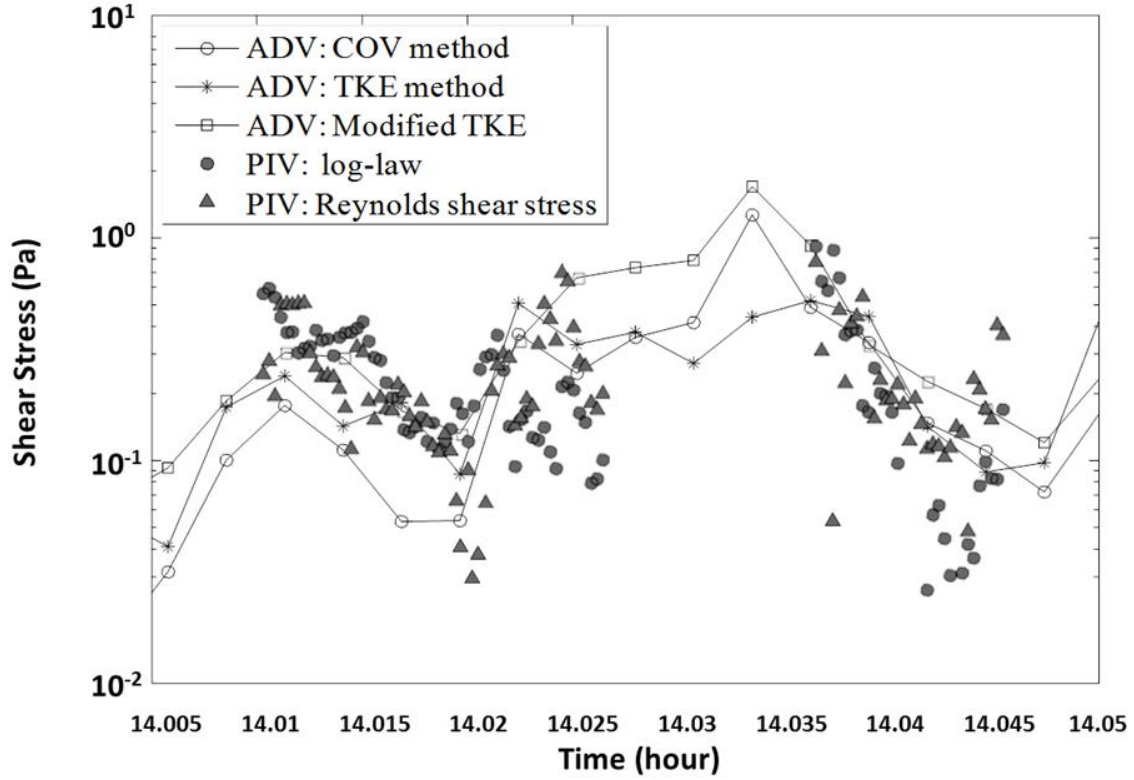


Figure 6-17. Time series of estimated bottom shear stress with different methods.

Model coefficients for ADV data were determined based on the best fit with PIV estimations. As a result, we have the following calibrated estimations from the ADV data series that were measured at $z = 12.5$ cm:

Direct covariance method (COV):

$$\tau_0 = -0.67\rho\overline{u'w'} \quad (9)$$

TKE method:

$$\tau_0 = 0.13\rho\left[\frac{1}{2}(\overline{u'^2} + \overline{v'^2} + \overline{w'^2})\right] \quad (10)$$

Modified TKE method:

$$\tau_0 = -0.67\rho\overline{u'w'} \quad (11)$$

Time series of the estimated bed shear stresses with Equations (2) through (4) over the entire period of measurement are plotted in Figure 6-18. Generally good agreements were found over the three different methods. Shear stress from COV and TKE methods produced several larger peaks at higher propeller rpm, while the estimate from the modified TKE method was much less “spiky” compared with the other two.

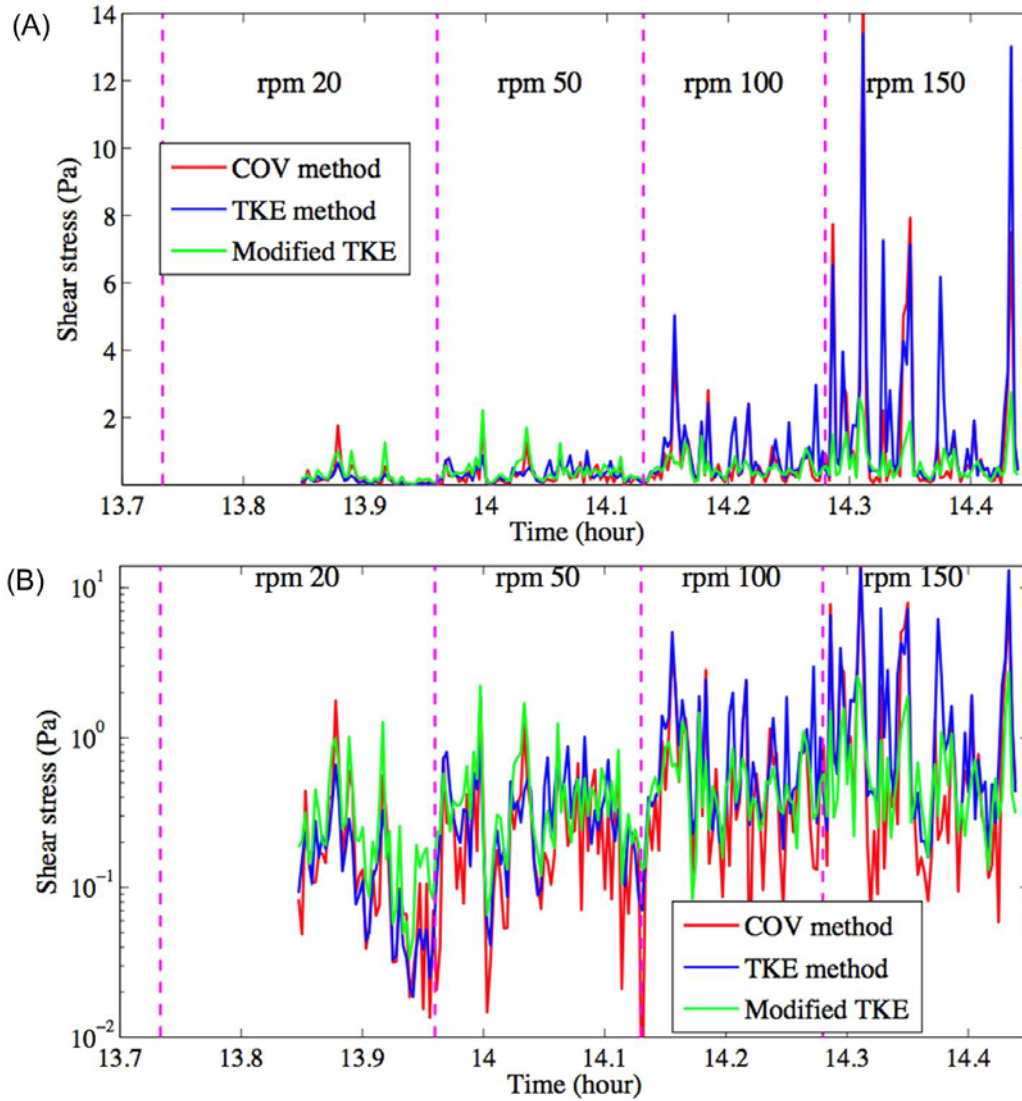


Figure 6-18. Time series of estimated bottom shear stress from ADV measurement: (A) stress in linear scale, and (B) stress in log scale.

Figure 6-19 shows the cumulative of the shear stress over the entire period of ADV measurements, about 35 min. As a result, the cumulative effects of the bottom shear were not significantly different until the rpm went up to 150. The major difference was found at the end of rpm 150. The highest cumulative is from the TKE method, which is about 81% higher than the modified TKE method. The result from the covariance method is about 40% higher than that of the modified TKE method.

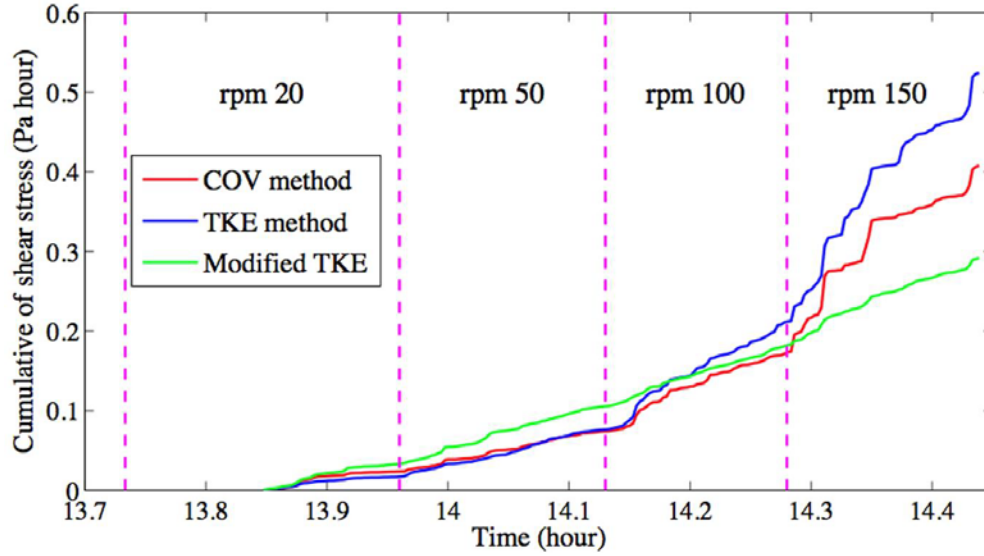


Figure 6-19. Estimated cumulative bottom shear stress from ADV measurements.

6.2.3 Erosion Rate

Although most PIV images were blurred or became completely dark with high sediment suspension at higher rpms, there were moments when the sediment bottom became visible. We have selected some images throughout the period of experiment to evaluate the sediment erosion rate. Figure 6-20 shows combined images acquired at different times when the sediment bed was visible. From these images we did observe a continuous erosion of the bed before the propeller stopped at 14.41 hour. After that, the sediment bed actually rose up slightly, probably due to sediment deposition. Assuming that the instrument frame did not sink as it stands on four large “feet” with stakes inserted deeply into the sediment bed, we could estimate the change of sea bottom as a function of time, as shown in Figure 6-20.

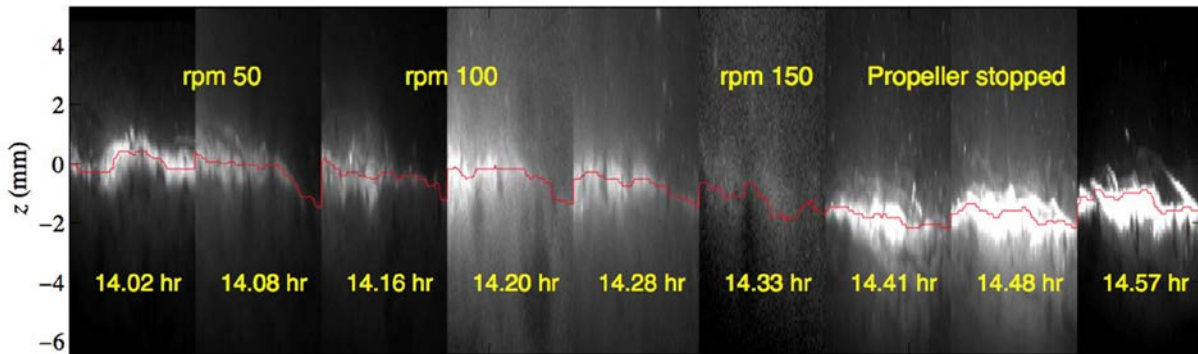


Figure 6-20. PIV images with visible sediment bed. The red line is the reconstructed bottom line from the bottom image.

6.2.4 Critical Shear Stress

Two parameters are needed to calculate erosion rate (Equation (6)), the critical shear stress (τ_{cr}) and the empirical erosion constant, a . These two constants were measured from the field study.

The critical shear stress was determined by visually checking PIV images for the initiation of sediment entrainment. Figure 6-21 presents sample images (I) when there was no significant sediment resuspension (Figure 6-21(a)) (II) at the inception of sediment entrainment (Figure 6-21 (b)-(e)) and (III) a short moment after resuspension (Figure 6-21 (d-f)). It is relatively easy to identify the moment of the inception of erosion, as a high concentration of sediment can be observed forming a “wedge”-like structure when they are lifted up by the shearing flow. The “edge” or “front” separating the sediment-laden flow and the overlaying clear fluid is sharp and signifies wall layer turbulent “eddies” (Figure 6-21 (b)-(e)). This suggests that the initial entrainment of sediment from the bed is largely due to the “ejection” of the low momentum near-bed fluid by “horse shoe” vortex structures, which are also major contributors to the Reynolds shear stress in boundary layer turbulent flows. Usually, several seconds after the observed inception of erosion, as the bed sediment was continuously eroded and resuspended, the enhanced scattering blocked the laser light and the image became blurred or completely dark (Figure 6-21(f)).

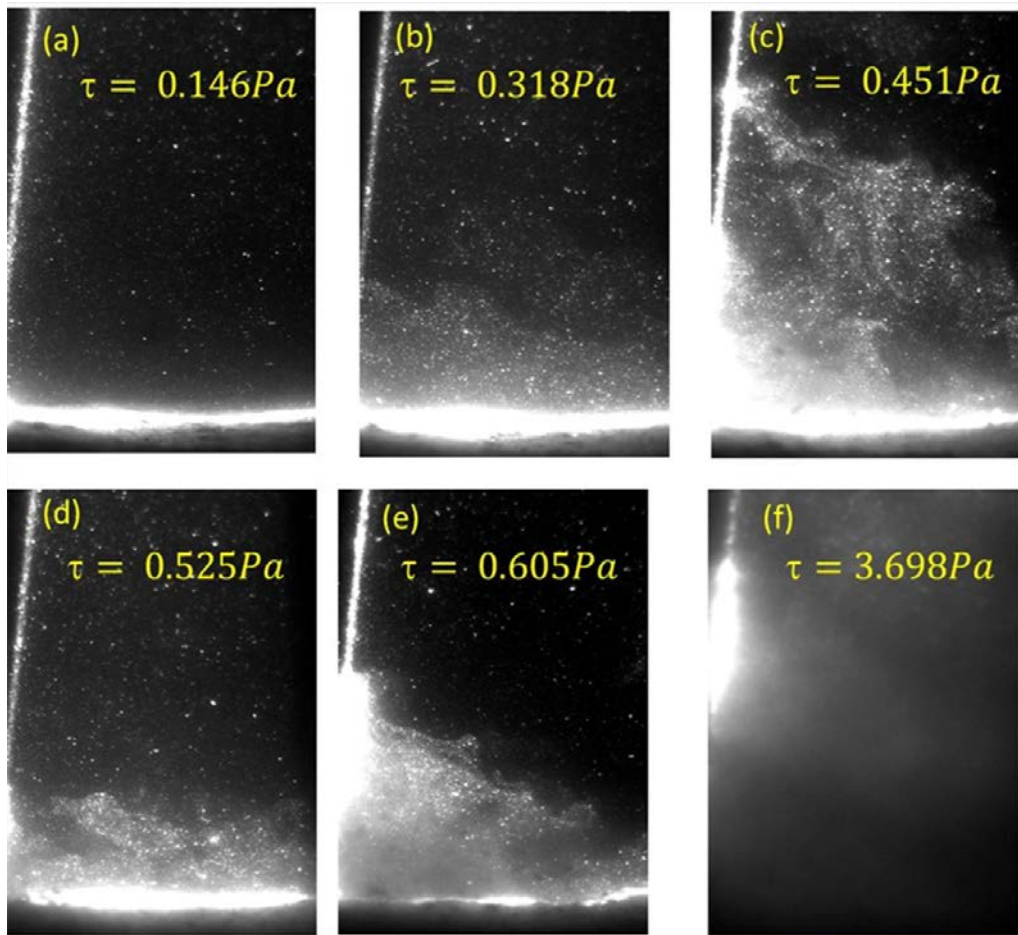


Figure 6-21. Sample images taken (a) when there was no significant erosion, (b)–(e) at the inception of erosion, and (f) after continuous erosion and resuspension.

The critical shear stress was estimated by calculating the mean velocity profile over a 5-second period around the moment when the initiation of resuspension was observed. The log-law profile fitting was applied to estimate the shear velocity, u_* . The bottom shear stress was then calculated as $\tau = \rho u_*^2$. With the available data, four cases were found that matched the selection criteria for the

estimation of critical shear stress when the propeller speed was between 20 and 50 RPM. The estimated bottom shear stresses are also shown in these figures. Note that the critical shear stress obtained in this way is also a statistical average, which may not represent the instantaneous shear stress that initiates the sediment resuspension. The estimated critical shear stress for the four selected cases varied from 0.32 to 0.60 (Pa) with a mean of 0.47 (Pa). Therefore, the critical shear stress for erosion for this site was estimated as $\tau_{cr}=0.47$ (Pa).

Mass erosion rate can be converted to the depth erosion rate (E_D [m/s]) with the following relation:

$$E = \rho_b E_D, \quad (12)$$

where ρ_b is the dry bulk density of the sediment. Therefore, the cumulative of the erosion depth can be modeled as

$$D(t) = \frac{\epsilon_M}{\rho_b} \int_0^t (\tau_0 - \tau_c)^\alpha dt'. \quad (13)$$

We have applied Equation (7) to fit the observed cumulative erosion depth to obtain the erosion rate constant ϵ_M . Bottom shear stress estimated with the three different methods, i.e., the covariance, TKE and modified TKE methods, were all applied. The parameter $\frac{\epsilon_M}{\rho}$ was obtained through least square fitting.

The best results are found when we select $\alpha = 1$. The correlation efficient (R^2) for the three methods are 51, 56 and 93%, respectively, which suggests that bottom shear stress estimated from the modified TKE is more reasonable. The cumulative erosion depth and the model results from Equation (7) are shown in Figure 6-22.

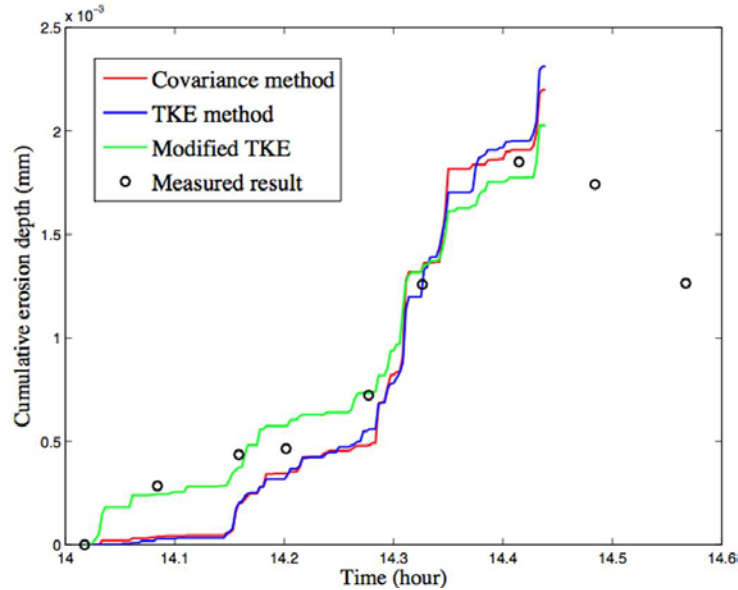


Figure 6-22. Cumulative erosion depth measured from PIV image analysis and modeling results with bottom shear stress obtained from ADV data.

Using the shear stress based on the modified TKE method, we have the rate of erosion depth E_D [mm s^{-1}] = $0.0079[\text{mm s}^{-1} \text{pa}^{-1}] \times (\tau_0 - \tau_b)$ [pa]. Taking a typical value for the dry bulk density of cohesive sediments, $\rho_b = 2000$ (kg m^{-3}), we have the erosion rate constant $\epsilon_b = 15.7$ ($\text{g m}^{-2} \text{s}^{-1} \text{pa}^{-1}$).

Both the critical shear stress ($\tau_{cr}=0.47$ Pa), and the erosion rate constant ($\epsilon_b = 15.7 \text{ g m}^{-2} \text{ s}^{-1} \text{ pa}^{-1}$), empirically obtained herein, were used to predict the sediment plume by tug wash for the fate/transport study in Section 6.2.6.

6.2.5 Graphic Version of Maynard's Model for Tugboat

We have investigated, analyzed, and implemented Maynard's model (Maynard, 1984; 2000) for investigation of propeller wash in DoD harbors. As discussed, Maynard's model is based on the theory of conservation of momentum and implemented for propellers with a single engine (Maynard 1984) and twin propellers (Maynard 2000). While convenient, Maynard's model has its application limitations, namely the ratio of propeller diameter to propeller-to-bottom distance, D_p/H_p , should be less than 1.2. Specifically, Maynard's model is applicable for propeller wash studies for tugboats and may not be applicable for deep-draft vessels, such as aircraft carriers and DDGs. Maynard's model was implemented with the user-friendly graphic model input and output interface (the "graphic Maynard's model"). The characteristics and dimensions of the tugboat propellers, including propeller diameters, distances between the propeller and the bottom, spacing of the propellers, horizontal distance between the stern and the propeller, and the thrust on the propeller provide the first set of model input for prediction of velocity field and shear stress near the bottom. Thrusts on the propellers were predicted by the FANS model, and predicted thrusts were validated by the field measurements (Baltazar et al., 2012). Both predicted velocity field and predicted bottom shear stress compared fairly well with measured values. The graphic Maynard's model also requires critical stress and erosion rate constants. These were derived from the empirical values obtained from the field study. We demonstrated that the graphic Maynard's model, with its user-friendly model input/output interface and added capability of calculating erosion potential from propeller wash, and validated by the field data of velocity and shear stress, can be a useful tool for propeller wash and related studies in DoD harbors.

As part of this study, a user-friendly graphic version of Maynard's model has been developed (Figure 6-23) for the twin-engine tugboat. Input parameters for the model include propeller type (Kort nozzle or traditional), propeller diameter, thrust, shaft to bottom distance and water depth. The model calculates velocity profiles and shear stress at the bottom sediment bed. Both visual output and ASCII data files are produced. Table 6-3 lists the input parameters for the graphic Maynard's model.

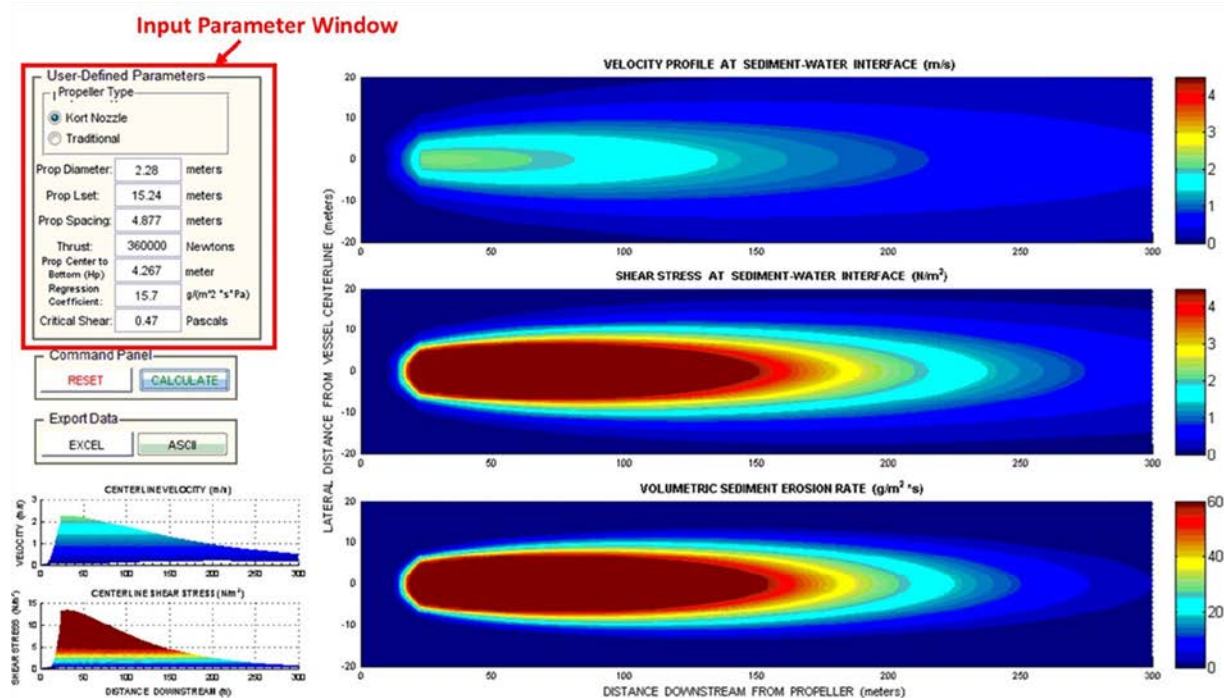


Figure 6-23. Graphical Maynard's model with input window and output graphics (right panels).

Table 6-3. Key model input parameters for the Graphic Maynard's Model.

Parameter	Variables	Values
Diameter of propellers	D_p	2.28m
Distance from stern to propeller	L_{set}	15.24m
Center of propeller to bottom	H_p	4.267m
Thrust on each propeller (plus nozzle)	T at 20 RPM (propeller)	1,228 Newtons
	T at 50 RPM (propeller)	7,673 Newtons
	T at 100 RPM (propeller)	30,773 Newtons
	T at 150 RPM (propeller)	69,466 Newtons
Propeller spacing	W_p	4.877m
Erosion constant	a	15.7g/(m ² -sec-Pa)
Critical shear stress	τ_{cr}	0.47 (Pa)

The first three model parameters are associated with the tugboat and the propellers. These numbers were provided by the driver of the tugboat, which should be considered as estimates with uncertainties. During the study, the propellers of the tugboat were operated running at four different speeds, described above, with each speed maintained for 8–9 minutes.

Thrusts on the propeller were estimated using a Finite Analytical Navier Stokes (FANS) model to simulate the tugboat operation at Pier 4–5. The propeller of the tugboat is Ka4-70 and the nozzle is based on the observed dimensions and shape from the picture we took. The propeller, including both

the blades and the nozzle, and the tugboat, were numerically segmented and simulated for the four propeller speeds used in the field study (20, 50, 100, and 150 RPM). Model results of the propeller thrust were compared with experimental results of open-water for propeller Ka4-70 in duct 19A (Baltazar et al., 2012) and can be found in APPENDIX B.

Table 6-4 shows the calculated thrusts and torques for the ducted propeller at rotating speeds of 20, 50, 100, 150, and 200 rpm. Note that the thrust and torque produced by the ducted propeller increase quadratically with the propeller rotating speed. With increasing propeller rotating speed from 20 to 200 rpm, the predicted propeller thrust coefficient K_{TP} increased slightly from 0.242 to 0.249 while the duct thrust coefficient K_{TD} reduced slightly from 0.151 to 0.147. The calculated propeller thrust coefficient K_{TP} was in excellent agreement with the experimental data. On the other hand, the predicted duct thrust coefficient K_{TD} was about 45% lower than the measured value of 0.27. The observed difference in K_{TD} can be attributed mainly to the blockage effect by the tugboat, and to a lesser degree the shallow water effect in a confined harbor.

Table 6-4. Comparison of the calculated thrust and torque coefficients (in confined water) with the experimental data (open water) under bollard-pull condition.

	K_{TP}	K_{TD}	K_T	K_Q
Experiment Open Water (rpm)	0.25 Propeller Thrust	0.27 Duct Thrust	0.52 Total Thrust	0.045 Total Torque
20	0.242 (756 N)	0.151 (472 N)	0.393 (1,228 N)	0.0483 (345 N-m)
50	0.243 (4,744 N)	0.150 (2,929 N)	0.393 (7,673 N)	0.0475 (2,123 N-m)
100	0.246 (19,240 N)	0.148 (11,533 N)	0.394 (30,773 N)	0.0454 (8,113 N-m)
150	0.248 (43,606 N)	0.147 (25,860 N)	0.395 (69,466 N)	0.0446 (17,940 N-m)
200	0.249 (77,763 N)	0.147 (45,982 N)	0.396 (123,745 N)	0.0441 (31,485 N-m)

6.2.6 Comparison of Field Data and Model Results

Figure 6-24 shows comparisons between the simulated and the measured velocity amplitudes near the bottom, between Piers 4 and 5, approximately 110m behind the tugboat. Velocity amplitudes were underestimated by the model when compared with field measurements for low propeller speeds at 20 RPM and 50 RPM. Simulated and measured velocity amplitudes were in good agreement for the 100 RPM case, but simulated velocities exceeded measured values for the 150 RPM scenario.

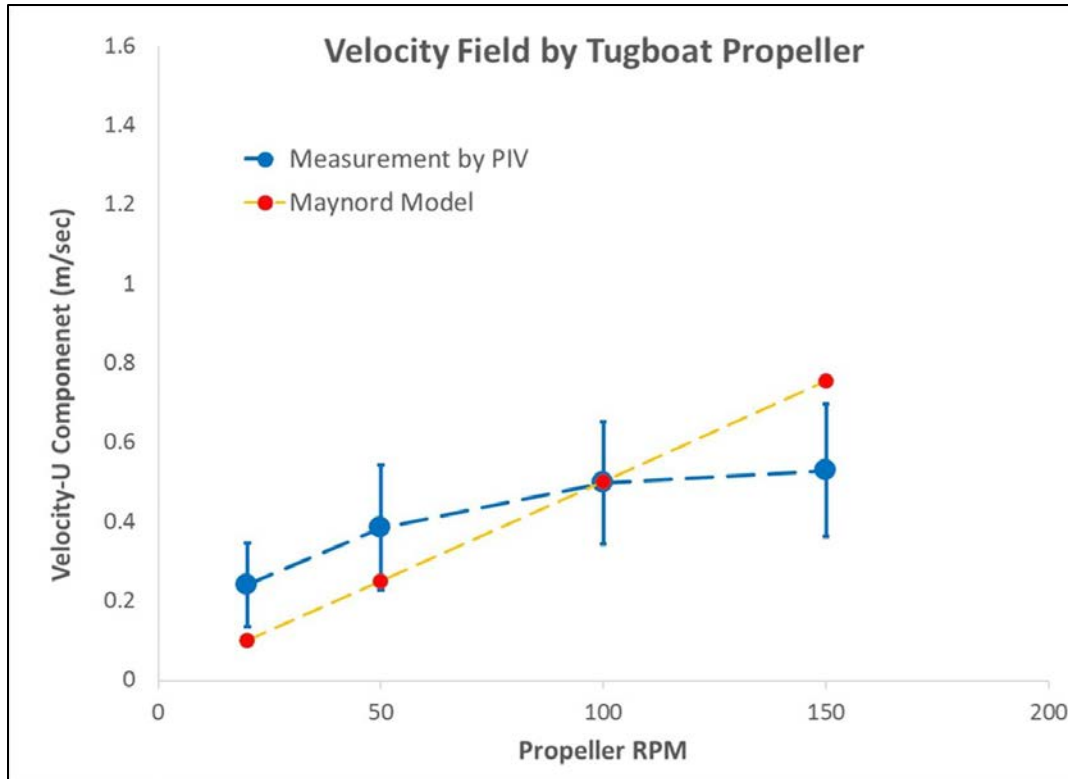


Figure 6-24. Comparison of velocity amplitudes for four propeller speeds between measurements and model results.

Simulated velocity amplitudes exhibited a linear relationship with the propeller speed, whereas our observed measurements showed non-linear behavior with increasing propeller speeds. Based on Equation (4), velocity fields disturbed by propeller wash were proportional to the square root of thrust, \sqrt{T} , which is proportional to square of the propeller speed (n), $T \propto n^2$. Therefore, velocity amplitude was predicted to behave linearly with respect to the propeller speed, as shown by the model. The nonlinear relationship observed between velocity amplitude and propeller speed may be caused by multiple factors. For example, the restricted water domain in the pier may generate complex return flows and circulations associated with finite water depth. We note also that Maynord's model applies to open water scenarios, and was not originally intended for restricted water domain.

Under-prediction of velocity amplitudes by the model at low propeller speeds may be attributed to the driver's uncertainty in propeller speed estimates. The driver of the tugboat had difficulty in accurately operating the speed of the propeller and the maintaining control of the driving wheel at low speed. In addition, the driver had difficulty in maintaining 20 RPM propeller speed without stalling the engine. Actual propeller speeds for the 20 and 50 RPM field study may be underestimated; the actual propeller speeds are likely to be greater than 20 and 50 RPM, respectively. Since there is no solid data to support these potential causes, we cannot comment reliably on the differences between the model and the measurements.

Bottom shear stress was calculated based on two sets of methods. The approach was based on the balance of total energy produced by the turbulence of the propeller wash and the dissipation by the bottom shear stress, which includes three different techniques to calculate bottom shear stress from the measured PIV velocity time series. The bottom shear stresses estimated from these three energy-

balanced methods were compared with the shear stress calculated by the Maynard's model (Figure 6-25). It showed that Maynard's model underestimates the bottom shear for propeller speeds at 20 and 50 RPM, though this could have been due to the uncertainties discussed previously for the discrepancies in velocity prediction. For the 100- and 150-RPM cases, Maynard's model compared relatively well with those calculated by the energy balance methods.

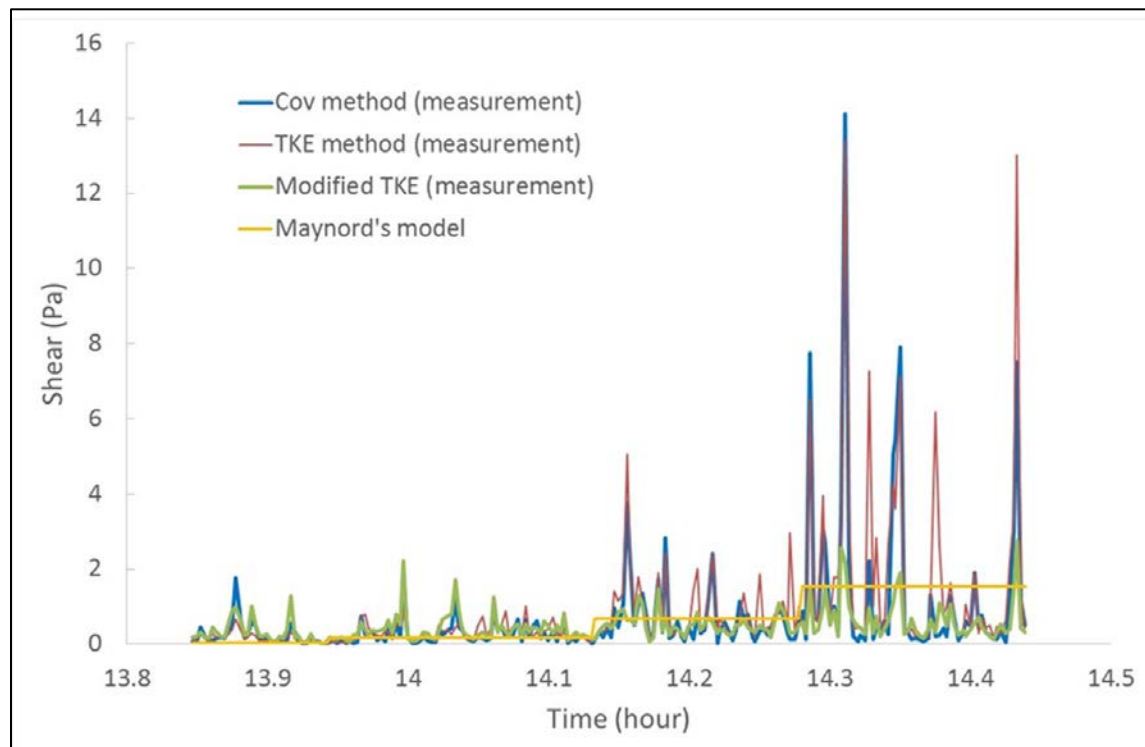


Figure 6-25. Bottom shear stress from model results and estimation calculated based on measured velocity field during the propeller wash experiment.

Figure 6-26 shows the cumulative bottom shear stress over time, an integration of the shear stress curve shown in Figure 6-25. Cumulative shear stress provides overall effects of the shear stress including the mean and temporal variations over time. As shown in Figure 6-26, Maynard's model results underpredicted the cumulative effect compared with the estimated values from the three energy-balanced methods.

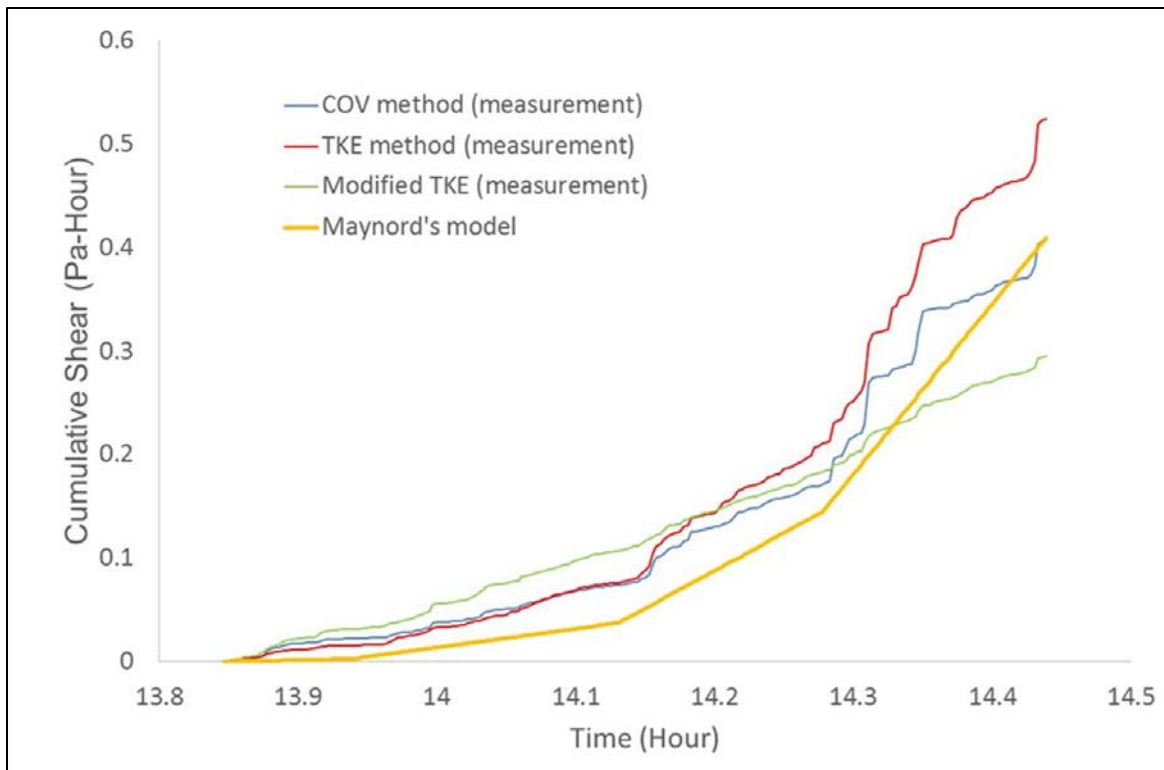


Figure 6-26. Cumulative shear stress over time between model results and estimation based on measured velocity field during the propeller wash experiment.

6.3 RESUSPENSION EVENTS

Results of the propeller wash resuspension studies are presented below. These three studies include one in San Diego Bay and two in Pearl Harbor. The first resuspension event took place on 4 April 2012 in San Diego Bay, CA, while the other two events were conducted 28 August (Bravo Pier) and 29 August 2012 (Oscar Pier) in Pearl Harbor, HI. Data from these field studies were used to compare and validate the propeller resuspension potential model and the fate and transport model.

6.3.1 San Diego

6.3.1.1 Sediment and Metal Concentrations

Important parameters are the background metal concentration in the suite of size-fractions in the resuspended sediment and in the background sediment before resuspension. To assess these parameters, background sediment samples were collected at each site prior to the resuspension event and slurry samples from the plume generated by the resuspension. These sediment samples were wet-sieved and filtered in the laboratory to separate the different size-fractions, which then were digested with aqua regia (Section 5.1.3.1.1) and analyzed by ICP-MS. Table 6-5 presents pump sampling resuspension data collected in San Diego Bay between Naval Station Piers 4 and 5 during the tug resuspension event of 4 April 2012. The resuspension study and the procedures are discussed under Section 5.1.3. The concentrations measured in the dry background sediment for San Diego Bay are given in Table 6-6.

Table 6-5. Sample identification, time, location, ancillary parameters, and mass fractions for samples collected at the San Diego Bay resuspension event of 4 April 2012 (S refers to surface and M refers to mid depth in the plume sample ID).

Sample ID	Time	Longitude	Latitude	Temp (°C)	Salinity	Trans- mission (%)	6 Sand 60 µm Mass Fraction (mg/L)	7 Silt 5 µm Mass Fraction (mg/L)	8 Clay 0.4 µm Mass Fraction (mg/L)	9 Total Mass Fraction (mg/L)
1S	14:14	-117.12663	32.68013	17.51	33.19	65.23	0.20	2.48	5.33	8.01
1M	14:15	-117.12662	32.68009	17.51	33.19	64.89	3.70	11.60	9.41	24.71
2S	14:19	-117.12680	32.67958	17.34	33.20	14.21	20.19	32.80	5.56	58.54
2M	14:19	-117.12682	32.67953	17.39	33.20	7.78	14.89	45.60	8.24	68.73
3S	14:21	-117.12700	32.67989	17.48	33.19	66.40	-0.02	2.04	4.27	6.29
3M	14:22	-117.12702	32.67994	17.45	33.20	65.91	0.29	2.71	4.27	7.27
4S	14:24	-117.12721	32.68015	17.47	33.19	60.74	1.61	3.40	3.29	8.30
4M	14:25	-117.12717	32.68019	17.46	33.19	60.75	-0.18	4.42	3.81	8.05
5 S	14:28	-117.12752	32.67976	17.48	33.19	63.13	0.57	14.50	6.05	21.12
5 M	14:28	-117.12753	32.67958	17.48	33.19	52.43	3.65	36.92	7.56	48.13
6 S	14:31	-117.12770	32.67902	17.42	33.19	24.75	5.16	17.33	3.10	25.59
6 M	14:31	-117.12773	32.67899	17.41	33.19	24.31	10.43	39.20	5.83	55.46
7 S	14:34	-117.12777	32.67849	17.43	33.20	32.31	3.68	2.80	3.24	9.72
7 M	14:35	-117.12768	32.67845	17.36	33.20	21.32	1.55	6.06	4.44	12.05
8S	14:38	-117.12831	32.67825	17.46	33.19	26.47	2.37	19.00	5.57	26.95
8M	14:38	-117.12827	32.67825	17.46	33.19	28.71	8.59	16.15	3.46	28.20
9S	14:44	-117.12898	32.67863	17.47	33.19	53.73	0.59	6.42	4.29	11.30
9M	14:45	-117.12900	32.67857	17.51	33.18	51.65	-0.32	5.75	4.07	9.50
10S	14:48	-117.12939	32.67741	17.51	33.20	7.53	0.01	22.22	5.79	28.02
10M	14:49	-117.12948	32.67746	17.50	33.20	8.28	8.25	53.33	12.50	74.08

Table 6-5. Sample identification, time, location, ancillary parameters and mass fractions for samples collected at the San Diego Bay resuspension event of 4 April 2012. (Continued)

Sample ID	Time	Longitude	Latitude	Temp (°C)	Salinity	Transmission (%)	6 Sand 60 µm Mass Fraction (mg/L)	7 Silt 5 µm Mass Fraction (mg/L)	8 Clay 0.4 µm Mass Fraction (mg/L)	9 Total Mass Fraction (mg/L)
11S	14:53	-117.12805	32.67723	17.55	33.18	42.15	1.49	7.67	3.10	12.26
11M	14:54	-117.12799	32.67729	17.57	33.17	46.22	0.99	11.00	2.33	14.33
12S	14:57	-117.12757	32.67675	17.60	33.16	53.13	0.05	3.20	0.77	4.02
12M	14:57	-117.12753	32.67669	17.62	33.16	57.99	3.46	1.86	0.00	5.32
13S	15:00	-117.12819	32.67643	17.65	33.16	57.68	1.46	2.17	2.00	5.62
13M	15:01	-117.12820	32.67651	17.63	33.16	56.92	1.80	6.67	3.64	12.10
14S	15:04	-117.12713	32.67731	17.61	33.16	57.95	0.08	2.83	1.60	4.52
14M	15:05	-117.12700	32.67736	17.64	33.16	59.26	0.02	8.71	3.09	11.83
15S	15:07	-117.12650	32.67818	17.69	33.16	54.41	0.44	2.04	1.00	3.49
15M	15:08	-117.12641	32.67814	17.72	33.16	56.96	0.32	2.00	1.84	4.15
16S	15:21	-117.12786	32.67601	17.54	33.19	48.04	0.20	6.25	1.59	8.04
16M	15:22	-117.12789	32.67607	17.50	33.19	47.90	1.05	9.60	2.57	13.23
17S	15:27	-117.12703	32.67797	17.61	33.17	51.29	0.47	5.20	2.68	8.35
17M	15:28	-117.12691	32.67793	17.60	33.17	51.40	3.90	3.52	1.40	8.81

Table 6-6. Metal concentrations measured in aqua regia digestates on background sediments from San Diego Bay. All data is provided in µg/g but for recoveries that are given as %. Certified are certified concentrations. Silver (Ag) is not certified in standard reference material (SRM).

		Cr (µg/g)	Ni (µg/g)	Cu (µg/g)	Zn (µg/g)	As (µg/g)	Ag (µg/g)	Cd (µg/g)
Total (n = 6)	Average	32.0	10.2	90.8	72.8	4.57	0.67	0.54
	Std. Dev.	5.7	1.7	24.8	17.4	1.00	0.21	0.07
63 µm (n = 5)	Average	39.6	12.7	100.7	73.7	5.30	0.70	0.59
	Std. Dev.	2.4	0.63	17.2	8.6	0.48	0.07	0.07
5 µm (n = 5)	Average	644.7	217.1	107.3	332.1	40.00	3.77	11.77
	Std. Dev.	445.6	147.8	69.5	234.4	27.92	2.39	8.10
Blank (n = 3)	Average	0.11	-0.0020	0.05	1.79	0.74	0.0035	0.000014
	Std. Dev.	0.0048	0.0015	0.040	0.55	0.046	0.00090	0.00022
SRM PACS-1 (n = 3)	Certified	113	44.1	452	824	211		2.38
	Average	39.6	19.7	135.6	226.6	69.6	0.69	1.26
	Std. Dev.	4.5	1.8	1.8	6.6	3.0	0.10	0.03
	Recovery (%)	35	45	30	27	33		53
SRM BCSS-1 (n = 3)	Certified	14	55.3	18.5	119	11.1		0.25
	Average	30.6	22.4	5.6	26.8	4.6	0.13	0.27
	Std. Dev.	5.8	2.2	0.3	1.3	0.4	0.04	0.08
	Recovery (%)	219	40	30	23	41		106

Two characteristics are readily derived from the information on the quantification of metals in the different particle size-fractions measured for the resuspension events, the distribution of each metal within the different particle size-fractions, and the potential environmental concern from each of these size-fraction concentrations. In the case of the resuspension event of 4 April 2012 in San Diego Bay, the percentage of metal content measured after acidification to pH² in the filtered solution (FS) for each fraction is presented in Figure 6-27 and Figure 6-28 and the concentrations measured in the FS from each size-fraction quantification is presented in Figure 6-29 and Figure 6-30.

The percentage of metal content in FS for each fraction (i.e., Figure 6-27 and Figure 6-28) is used for a comparison between these four fractions regarding their relative apportionment to the total metal load, and are calculated with two caveats. The first caveat is that the total concentration in all fractions is calculated as the sum of the fractions, and not directly from the measured total concentration (i.e., after filtration throughout 2-mm sieve and acidification), as the latter provided data considered erroneous with the total sum of the percent well above 100%, in contrast to the former which is normalized to the calculated total concentration always balancing out to 100%. The second caveat is that the amount of metal in the dissolved phase was normalized to the total mass of particles in the sample, as that should be the case in the water column. This normalization is done to present the dissolved metal data in similar units (i.e., $\mu\text{g}/\text{mg}$), allowing for a direct comparison on the order of magnitude of the metal load for each fraction.

These quantifications and calculations are also affected by storage time and manipulation of the samples prior to separation in the different fractions and acidification. Potential artifacts from storage and manipulation include changes in the redox conditions of the sample from oxic to anoxic, which will affect the distribution of metals between the particular and dissolved phases; representativeness of the subsample, as shaking of the 22-L carboy is cumbersome and quick collection of a 1-L sample representative of the whole 10+ liters remaining in the carboy is difficult at least. Artifacts from the analysis of the samples will also add some inaccuracy to the quantifications.

The combined effect of these and any other factor inducing differences between actual field conditions and quantifications after laboratory manipulation can be assessed by comparison to unfiltered and 0.45- μm filtered (i.e., dissolved) samples collected from the resuspension plumes. Unfortunately, collection of such samples was omitted due to the complexity of the field situation. Instead, ambient unfiltered and 0.45- μm seawater samples were collected in San Diego Bay on 28 March 2012, one week prior to the resuspension event there. While in the case of Pearl Harbor, only unfiltered samples were collected about 20 min prior to each of the two resuspension events there. The ambient sample is included in Appendix C and Appendix D. A rough comparison of the total and dissolved metal concentrations measured in the resuspended plumes in comparison to measured ambient concentrations for San Diego Bay indicate an increase of an order of magnitude for chromium, nickel, zinc, arsenic, and cadmium. The same comparison provides concentrations in the same order of magnitude for copper and lead. Silver concentrations are at undetected levels in both cases.

There is a greater difference between the total concentrations measured in the resuspension events with respect to total concentrations in ambient waters for Pearl Harbor. For the event in Bravo 22 Pier, resuspended samples were three orders of magnitude higher for chromium, two orders of magnitude higher for nickel and cadmium, one order of magnitude higher for copper, zinc, and arsenic. In the case of the event in Oscar 2 Pier, the resuspended samples were two orders of magnitude higher for chromium, nickel, and zinc, one order of magnitude higher for arsenic, and of the same order of magnitude for copper, zinc, and lead. Silver was at undetected levels for both pier events.

These differences should be better evaluated in future efforts. Collection of unfiltered and 0.45- μm filtered samples simultaneously to the 22-L carboys should provide a better baseline for comparison. A better solution could be to have an on-line system to separate all the different size fractions while sampling. However, these tasks were not considered for this effort.

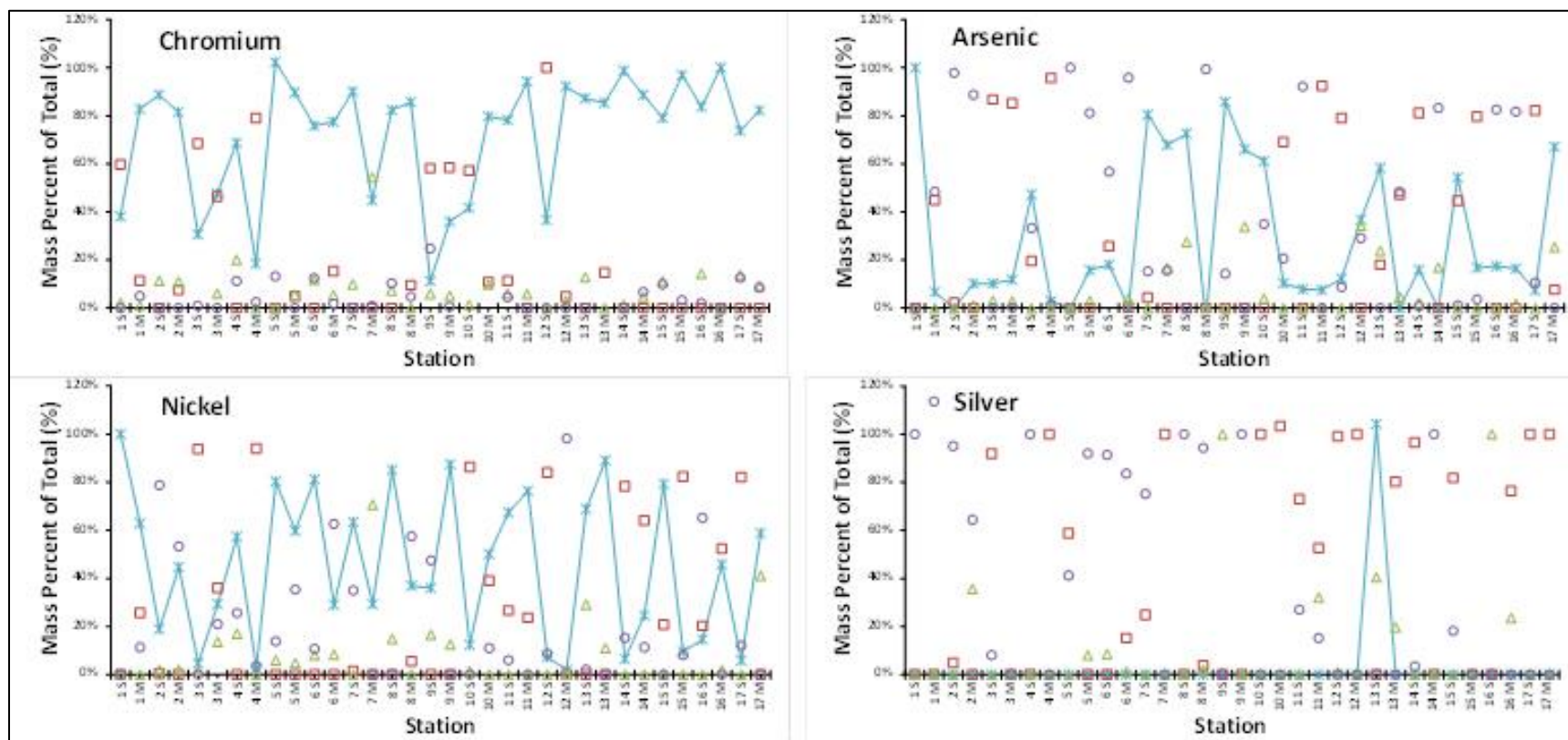


Figure 6-27. Chromium, arsenic, nickel, and silver distributions in the different particle size-fractions collected from the resuspension event of 4 April 2012 in San Diego Bay. The metal content in each fraction is calculated with the total fraction as the sum of all fractions.

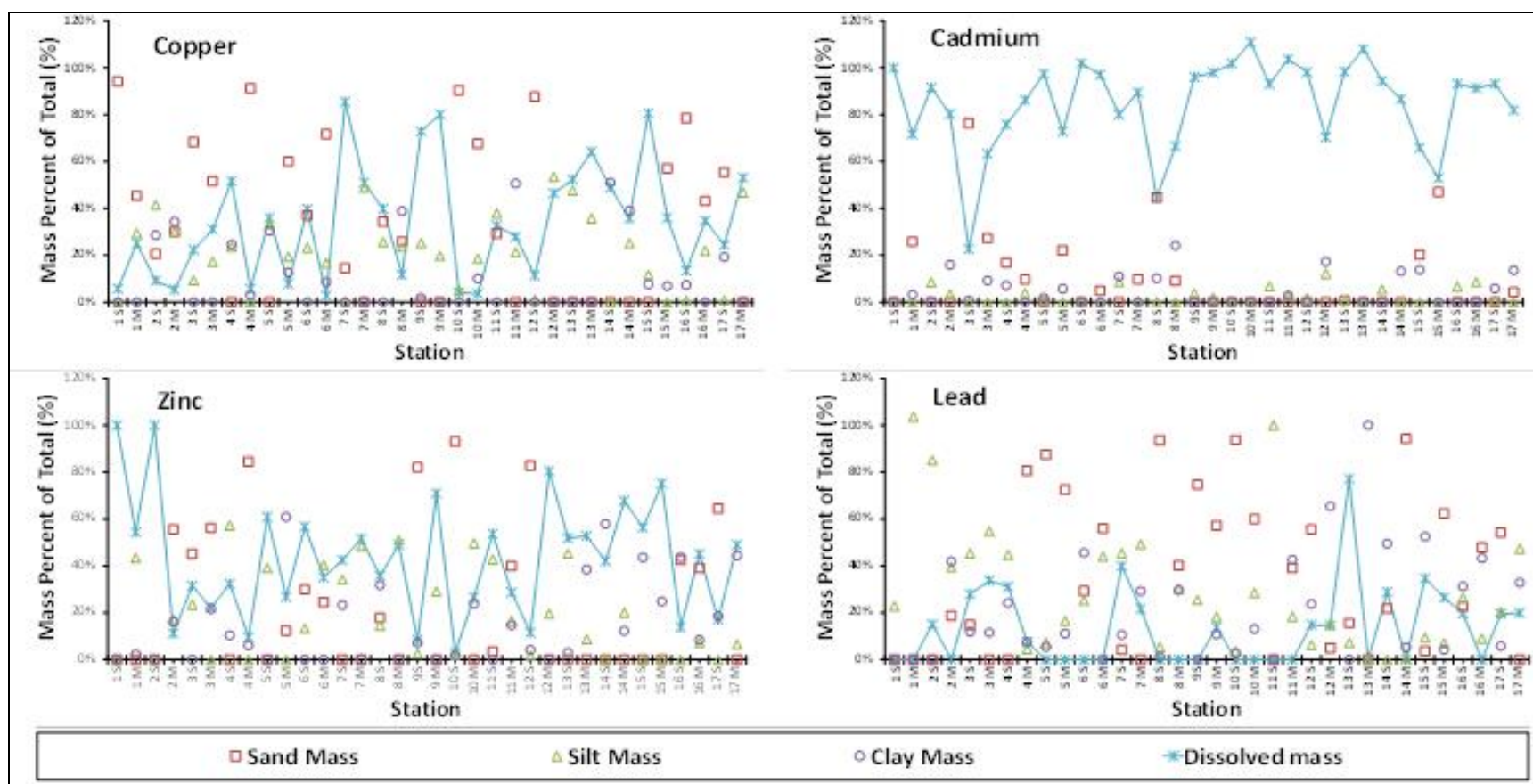


Figure 6-28. Copper, cadmium, zinc, and lead distributions in the different particle size-fractions collected from the resuspension event of 4 April 2012 in San Diego Bay. The metal content in each fraction is calculated with the total fraction as the sum of all fractions.

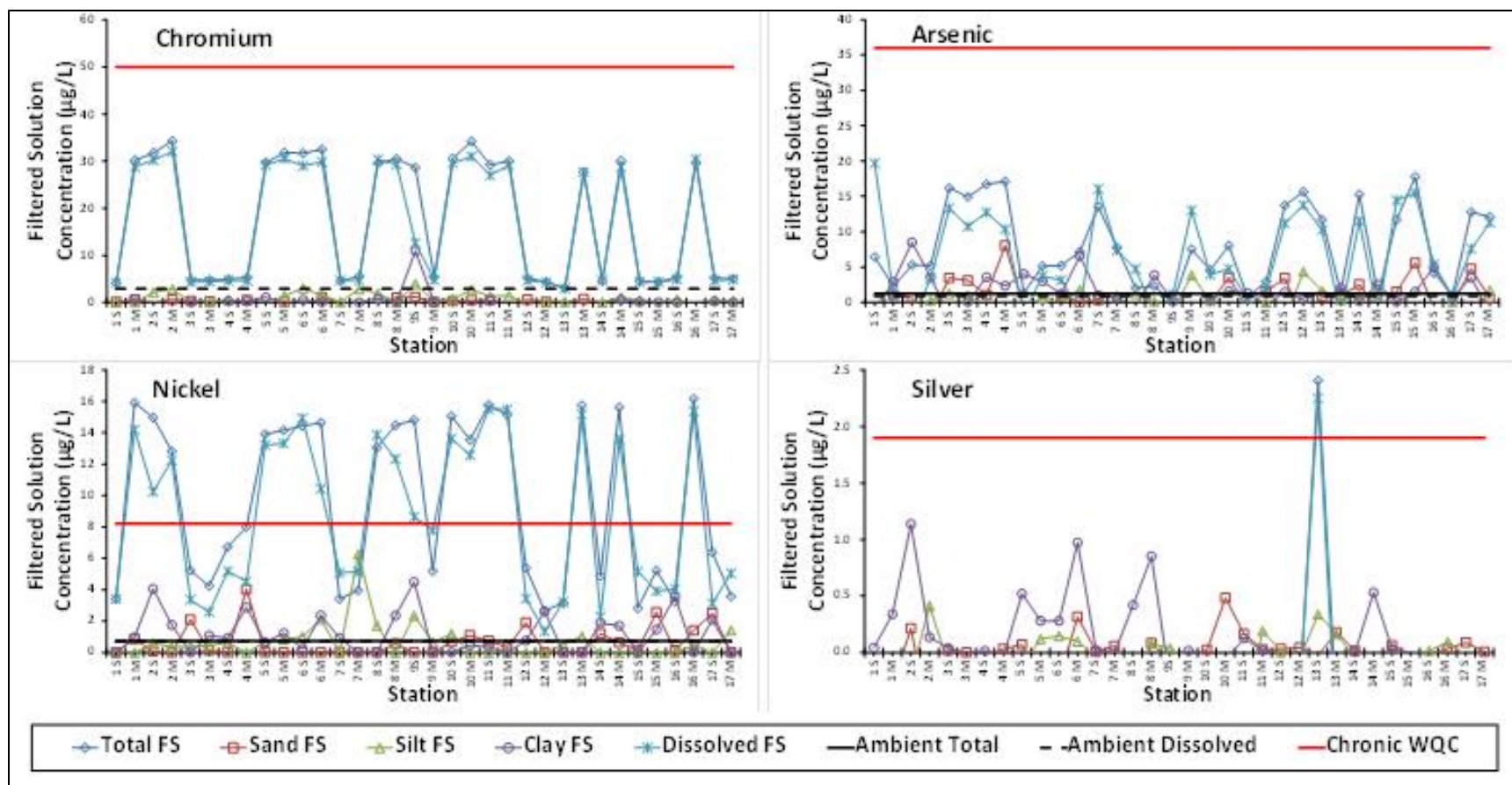


Figure 6-29. Chromium, arsenic, nickel and silver concentrations in the filtered solution (FS) for each different particle size-fractions collected from the resuspension event of 4 April 2012 in San Diego Bay. Ambient Total and Ambient Dissolved are from samples collected prior to the resuspension event. The USEPA Chronic Water Quality Criterion is provided as a measure of the potential concern derived from these quantifications.

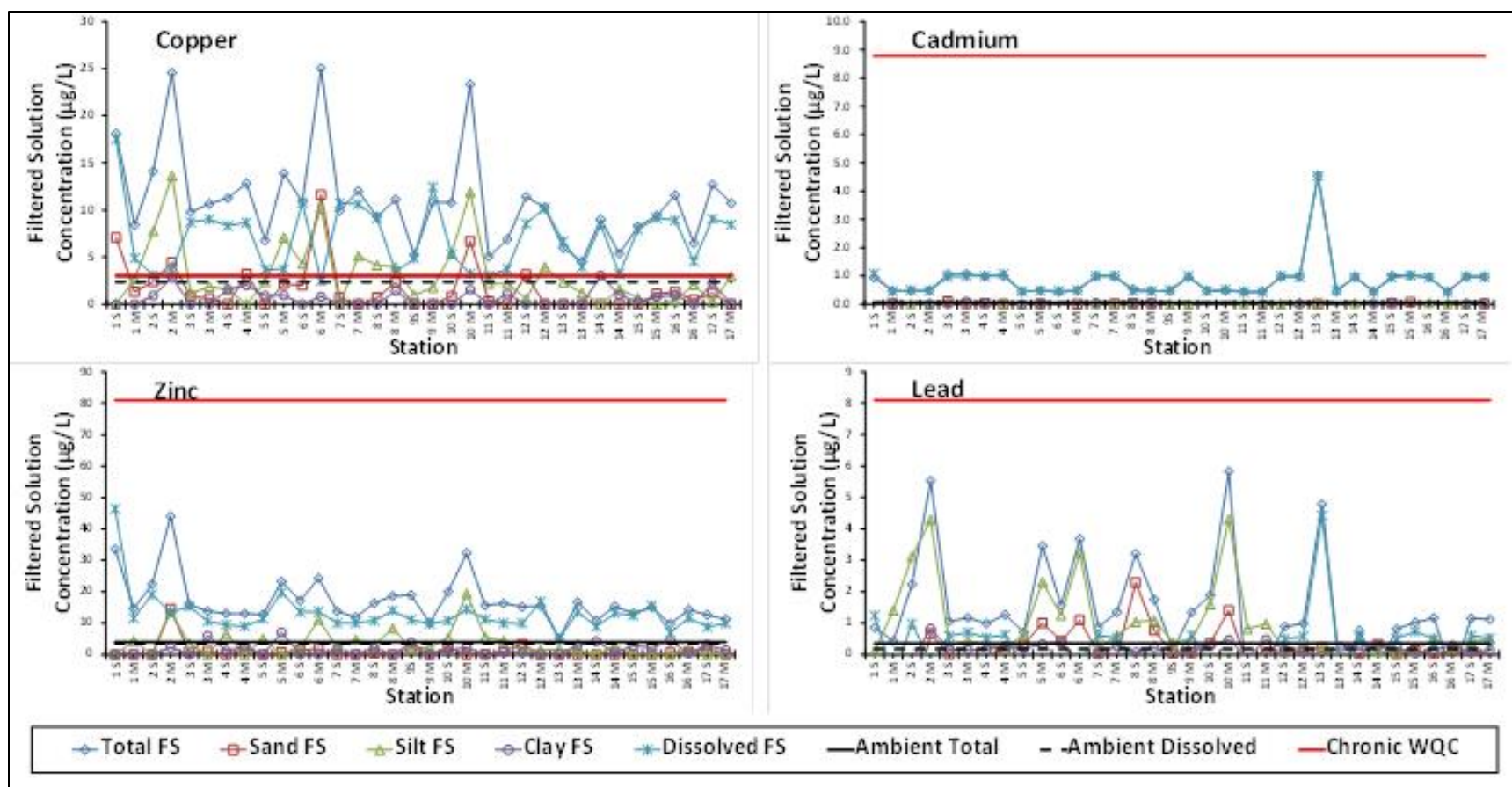


Figure 6-30. Copper, cadmium, zinc and lead concentrations in the filtered solution (FS) for each different particle size-fractions collected from the resuspension event of 4 April 2012 in San Diego Bay. Ambient Total and Ambient Dissolved are from samples collected prior to the resuspension event. The USEPA Chronic Water Quality Criterion is provided as a measure of the potential concern derived from these quantifications.

The distribution between the different fractions in this single resuspension event is metal dependent (Figure 6-27 and Figure 6-28). The most extreme distributions are for cadmium, which is mostly (>50%) in the dissolved (<0.4 μm) fraction, for silver, which is present mostly (>35%) in the sand (>60 μm) and clay (5 to 0.4 μm) fractions, and lead, which is mostly in the sand (>60 μm) and silt (5 to 60 μm). Chromium has a tendency to be mostly in the dissolved (<0.4 μm) fraction; but, few times (8 out of 34) is dominated by the sand (>60 μm) fraction. For most stations, arsenic is mostly present in either the sand (>60 μm) or clay (5 to 60 μm), and a few times (10 out of 34) has a significant presence in the dissolved (<0.4 μm) fraction. The other three metals, nickel, copper, and zinc, seem to be more evenly distributed between most of the fractions, with some predominance of the sand (>60 μm) fraction. In general, within these variability in size-distributions, the metals in the resuspended sediment have a strong association with the sand (>60 μm) fraction. The implication is that these metals will stay within a relatively smaller area of influence by the resuspension.

The potential contaminant concern is derived from comparison to the USEPA chronic water quality criteria (Figure 6-29 and Figure 6-30). In the case of the resuspension event of 4 April 2012 in San Diego Bay, only two metals were present at concentrations above the chronic water quality criteria, copper and nickel. However, while copper concentration above this criterion was for most of the fractions except the clay (5 to 60 μm) fraction, for nickel only the total and dissolved (<0.4 μm) fractions were above the criterion. therefore, for copper most fractions will have a potential effect, and probably will cover a relatively larger area. In the case of nickel, its concentration is mainly associated with the dissolved fraction (<0.4 μm), and it will undergo mixing/dilution with surrounding water. The implication here is that metals associated with particles will be advected, and could have an effect at some distance. In contrast, metals mostly in the dissolved (<0.4 μm) fraction, will undergo mixing and dilution, and their effect will be buffered by the surrounding waters with lower concentration of the same metal.

Because their concentrations are below the chronic water quality criteria, chromium, zinc, arsenic, silver, cadmium and lead should not have a potential concern of contaminating areas of deposition of resuspended sediments. A potential concern in these cases could be originated in the case of funneling of sediments to a relatively smaller area, where there is the potential to increase the metal loading as the particles are accumulated onto a smaller area than the source area.

To provide an idea of the potential contaminant concern generated by the resuspension events, the metal quantification data reported here is compared to the U.S. EPA nationally recommended water quality criteria for the protection of aquatic life and human health¹, which is provided in Table 6-7.

And, to provide the most conservative comparison, the chronic water quality criterion is used in the comparisons, despite the fact that some of the metal concentrations associated to the resuspension event are at levels not considered harmful; in San Diego Bay, all of the metals had dissolved concentrations above ambient concentrations measured prior to the resuspension event (Table 6-6, Figure 6-29, and Figure 6-30). Therefore, depending on the hydrodynamics of the site, propeller wash resuspension has the potential to affect ambient conditions. In the case of San Diego Bay, the hydrodynamic conditions allow for reestablishing of ambient conditions.

¹ U.S. Environmental Protection Agency.2016. "National Recommended Water Quality Criteria - Aquatic Life Criteria Table." Available online at <http://water.epa.gov/scitech/swguidance/standards/criteria/current/index.cfm>. Accessed 12 Jan 2016.

Table 6-7. Nationally recommended water quality criteria by the U.S. Environmental Protection Agency (USEPA). CMC = Criterion Maximum Concentration, CCC = Criterion Continuous Concentration (or Chronic Criterion).

Metal	Chemical Symbol	Priority Pollutant	CMC Acute (µg/L)	CCC Chronic (µg/L)	Publication Year	Notes
Chromium (VI)	Cr	Yes	1100	50	1995	D
Nickel	Ni	Yes	74	8.2	1995	D
Copper	Cu	Yes	4.8	3.1	2007	D, cc
Zinc	Zn	Yes	90	81	1995	D
Arsenic	As	Yes	69	36	1995	A,D
Silver	Ag	Yes	1.9		1980	D
Cadmium	Cd	Yes	40	8.8	2001	D
Lead	Pb	Yes	210	8.1	1980	D

- A** This recommended water quality criterion was derived from data for arsenic (III), but is applied here to total arsenic, which might imply that arsenic (III) and arsenic (V) are equally toxic to aquatic life and that their toxicities are additive. No data are known to be available concerning whether the toxicities of the forms of arsenic to aquatic organisms are additive. Please consult the criteria document for details.
- D** Freshwater and saltwater criteria for metals are expressed in terms of the dissolved metal in the water column. See "[Office of Water Policy and Technical Guidance on Interpretation and Implementation of Aquatic Life Metals Criteria](#)," October 1, 1993, by Martha G. Prothro, Acting Assistant Administrator for Water, available on [NSCEP's web site](#) and 40CFR§131.36(b)(1).
- cc** When the concentration of dissolved organic carbon is elevated, copper is substantially less toxic and use of Water-Effect Ratios might be appropriate.

No potential for toxicity was measured for organic contaminants resuspended in San Diego Bay. Polycyclic aromatic hydrocarbons (PAHs) were measured in selected fractions of a suite of samples from the resuspension event of 4 April 2012 in San Diego Bay (Table 6-8). Most PAH concentrations were lower than the method detection limit, and the rest were relatively low concentrations. The PAH benchmark calculation using the U.S. EPA PAH ESB approach² gave a sum of acute and chronic potential of less than one in the cases of calculation by particle size-fraction, and in the case of calculation by station; therefore, these calculations indicate that there is no potential for either acute or chronic toxicity.

² U.S. EPA Archive Document, "Explanation of PAH benchmark calculations using EPA PAH ESB approach," originally developed by Dave Mount, Office of Research and Development (ORD), Duluth, MN. Available online at <https://archive.epa.gov/bpspill/web/pdf/explanation-of-pah-benchmark-calculations-20100622.pdf>. Accessed 11 May 2016.

Table 6-8. Polycyclic aromatic hydrocarbons measured in selected fractions of a suite of samples from the San Diego Bay resuspension event of 4 April 2012. Note that values in italics with yellow background are the Method Limit of Detection, and is given for samples that were not detectable.

Sample ID →	6M	6M	6M	8M	8M	8M	10M	10M	10M
Fraction →	<2 mm	<60 µm	<5 µm	<2 mm	<60 µm	<5 µm	<2 mm	<60 µm	<5 µm
Analyze ↓	µg/L	µg/L	µg/L	µg/L	µg/L	µg/L	µg/L	µg/L	µg/L
Naphthalene	0.0078	0.0077	0.0180	0.0110	0.0082	0.0180	0.0074	0.0064	0.0270
2-Methylnaphthalene	<i>0.0023</i>	<i>0.0023</i>	<i>0.0024</i>	<i>0.0023</i>	<i>0.0023</i>	<i>0.0023</i>	0.0028	0.0025	0.0039
Acenaphthalene	0.0091	0.0058	0.0035	0.0050	0.0034	<i>0.0034</i>	0.0110	0.0040	<i>0.0039</i>
Acenaphthene	<i>0.0044</i>	<i>0.0049</i>	<i>0.0052</i>	<i>0.0059</i>	<i>0.0053</i>	<i>0.0061</i>	<i>0.0044</i>	<i>0.0044</i>	<i>0.0050</i>
Dibenzofuran	<i>0.0046</i>	<i>0.0046</i>	<i>0.0047</i>	<i>0.0046</i>	<i>0.0046</i>	<i>0.0046</i>	<i>0.0046</i>	<i>0.0046</i>	<i>0.0052</i>
Fluorene	<i>0.0038</i>	<i>0.0038</i>	<i>0.0039</i>	<i>0.0038</i>	<i>0.0038</i>	<i>0.0038</i>	<i>0.0038</i>	<i>0.0038</i>	<i>0.0043</i>
Phenanthrene	<i>0.0050</i>	<i>0.0050</i>	<i>0.0052</i>	<i>0.0050</i>	<i>0.0050</i>	<i>0.0050</i>	0.0140	0.0140	<i>0.0160</i>
Anthracene	0.0098	0.0057	<i>0.0037</i>	0.0069	<i>0.0036</i>	<i>0.0036</i>	0.0120	0.0053	<i>0.0041</i>
Fluoranthene	0.0081	0.0066	<i>0.0045</i>	0.0073	0.0050	<i>0.0044</i>	0.0110	0.0095	<i>0.0050</i>
Pyrene	0.0120	0.0090	<i>0.0036</i>	0.0100	0.0055	<i>0.0035</i>	0.0150	0.0110	<i>0.0040</i>
Benz(a)anthracene	0.0100	0.0062	<i>0.0027</i>	0.0059	0.0044	<i>0.0026</i>	0.0170	0.0110	<i>0.0030</i>
Chrysene	0.0150	0.0048	<i>0.0035</i>	0.0058	<i>0.0034</i>	<i>0.0034</i>	0.0380	0.0120	<i>0.0039</i>
Benzo(b)fluoranthene	0.0280	0.0200	<i>0.0024</i>	0.0150	0.0097	<i>0.0023</i>	0.0540	0.0380	<i>0.0026</i>
Benzo(k)fluoranthene	0.0110	0.0079	<i>0.0026</i>	0.0048	0.0041	<i>0.0025</i>	0.0180	0.0120	<i>0.0029</i>
Benzo(a)pyrene	0.0160	0.0120	<i>0.0044</i>	0.0094	0.0051	<i>0.0043</i>	0.0330	0.0220	<i>0.0049</i>
Indenol(1,2,3-cd)pyrene	0.0094	0.0064	<i>0.0027</i>	0.0057	0.0031	<i>0.0026</i>	0.0240	0.0180	<i>0.0030</i>
Dibenz(a,h)anthracene	<i>0.0025</i>	<i>0.0025</i>	<i>0.0026</i>	<i>0.0025</i>	<i>0.0025</i>	<i>0.0025</i>	0.0063	0.0042	<i>0.0029</i>
Benzo(g,h,i)perylene	0.0120	0.0083	<i>0.0030</i>	0.0078	0.0048	<i>0.0029</i>	0.0220	0.0180	<i>0.0033</i>

6.3.1.2 Size Fraction Distribution of Metals

There is a natural preference by metals to partition either in the dissolved or particulate phase. The partition of each metal between the water phase (i.e., dissolved) and the three particulate sizes (i.e., clay, silt, and sand) was assessed by plotting the ratio of dissolved to total concentrations versus the ratio of metal in each of the three particulate phases to the total concentration. Average concentrations were used for each resuspension event as a general approximation for these distributions, and the resulting plots are shown in Figure 6-31 for the resuspension events in San Diego Bay. In general, metals that plot high with respect to the abscissa (y-axis) are predominantly in the dissolved phase, those that plot lower with respect to the abscissa are predominantly in the particles, and the relative proportion of metals in the three particle sizes is represented by their distribution with respect to the ordinate (x-axis). The degree of precision of this approach is provided by the plotting of the total metal concentration (blue symbols) on the line for conservative bonding, that plots between the two points for 100%.

The tendency for copper, zinc, and lead for partitioning into the particulate phase is clearly observed, below 50% for San Diego Bay. These metals are distributed more or less equally between the three particle sizes in San Diego. Silver is highly partitioned to the particles in San Diego Bay, cadmium is highly in the dissolved phase for San Diego Bay, arsenic partitions at about equal percentage between the dissolved and particulate phases in San Diego Bay. Chromium is about 80% in the dissolved phase in San Diego Bay. This difference is driven by the high partition of chromium to the sand-size fraction in Oscar Pier, Pearl Harbor. Nickel partitions somewhat equally between the dissolved and particulate phases. A comparison of metal partitioning in San Diego Bay versus Pearl Harbor is discussed in Section 6.3.2.2.

The repercussions of the partitioning of the metals include the potential for advection into other areas within the harbors, or even outside the harbor. Those metals with a preference for the dissolved phase, will be found in lower concentrations in the area of influence as their concentrations are affected by mixing and advection of waters. In contrast, those metals with preferential partitioning into solid phases, should be transported as far as the particles are advected. With sand-size particles staying within a relatively small area surrounding the resuspension event, and clay-size particle being able for transporting even outside the harbor.

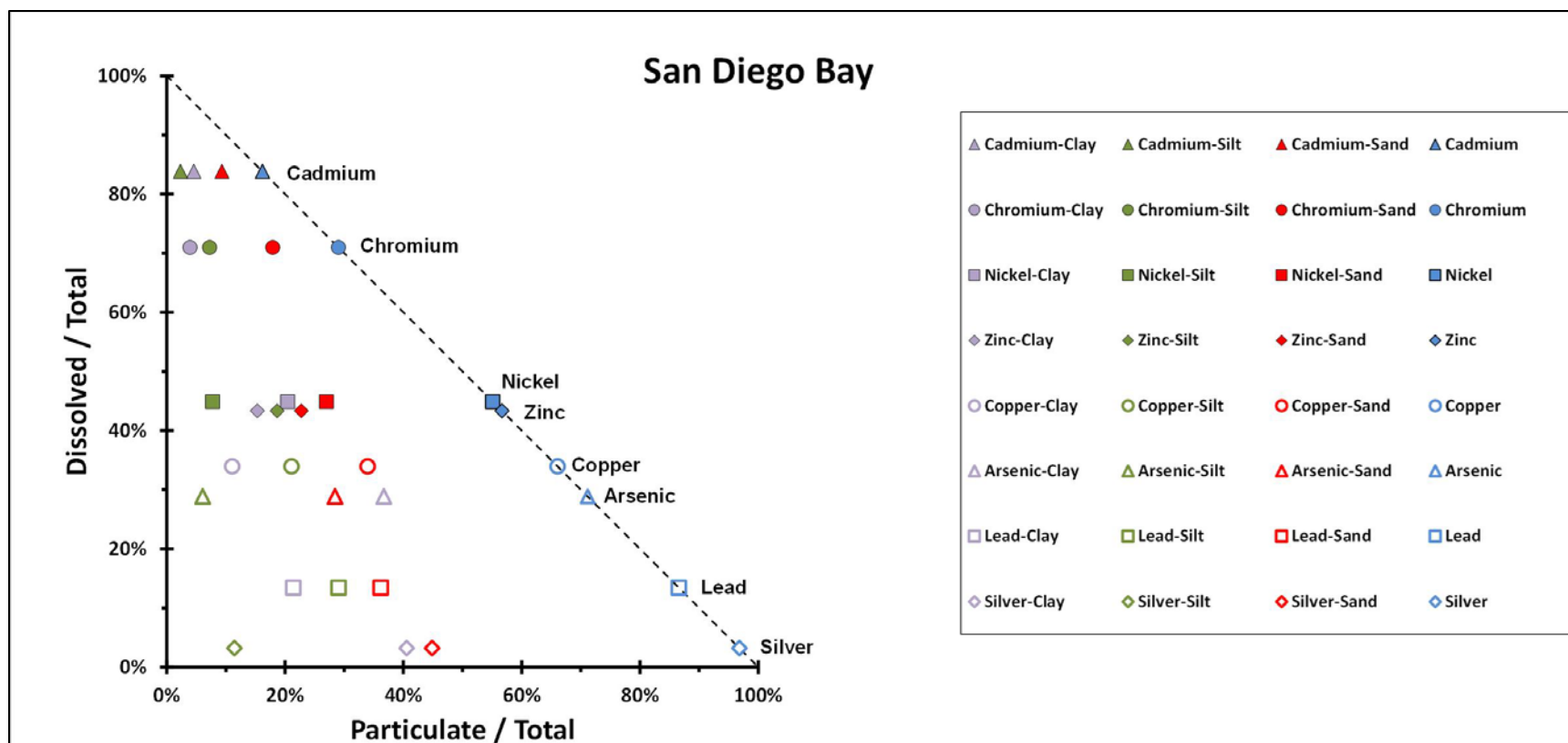


Figure 6-31. Size-fraction distribution of metals for the resuspension event of 4 April 2012 in San Diego Bay. Each metal is provided as the percentage fraction for clay (grey), silt (green), sand (red), and total (blue), the same pattern is used in the following two figures.

6.3.1.3 Preparing the Field Data for Fate/Transport Model Comparison

Figure 6-32 shows the relationship of OBS output as a function of pump-sampled TSS, measured at mid water column depth. This linear regression was used to extrapolate the few discrete TSS samples to all of the OBS output.

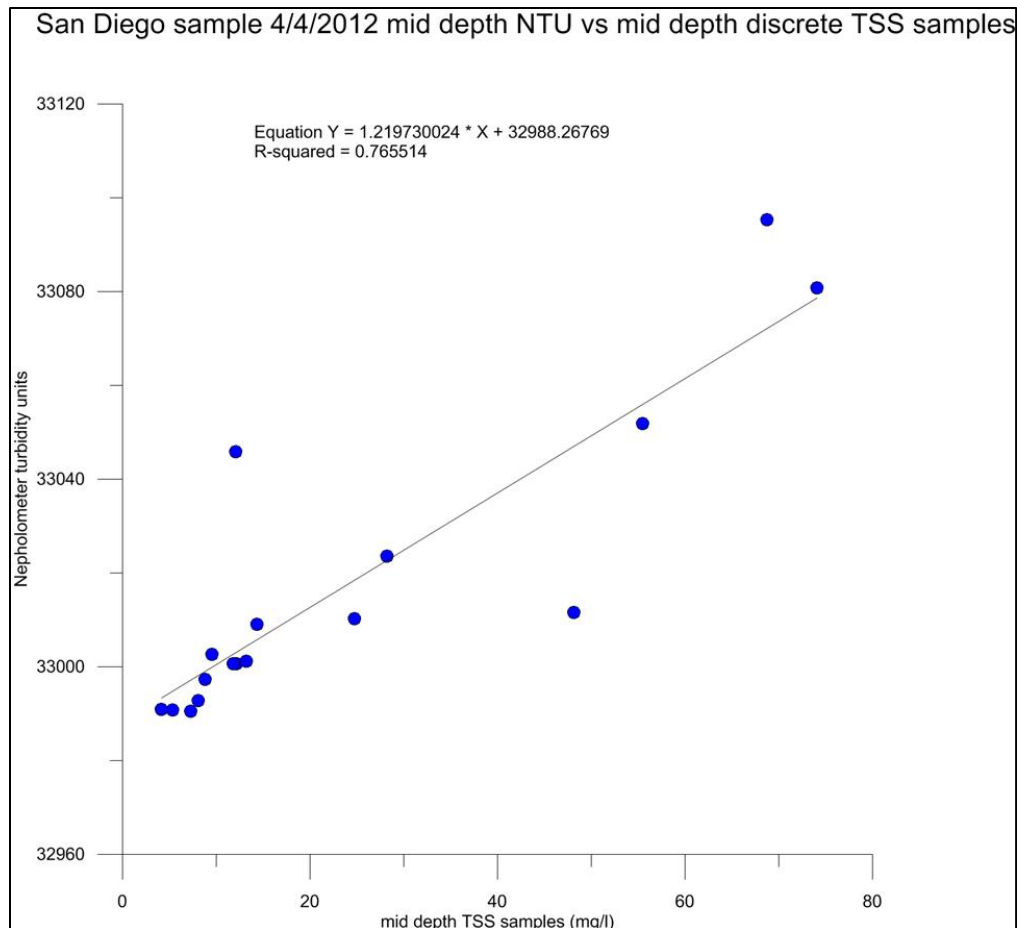


Figure 6-32. OBS output in nephelometer turbidity units versus measured TSS concentrations.

Most of the San Diego resuspension data provided as CH3D model validation come from two major sources: the nephelometry data collected from the ECOS at mid depth (5312 samples) and the discrete water sample data pump-collected at 17 stations at both the surface and mid depth (34 samples). From the discrete pump measurements, optical backscatter measurements were calibrated as TSS values, the mean fractions of sand, silt, and clay were assigned to these derived TSS values, and the mean metal concentrations associated with each sediment size fraction, as well as the dissolved fraction ($<0.4 \mu\text{m}$) were assigned to the derived TSS values. TSS and size fractions are reported as mg (sediment)/l (seawater). Average concentrations of sediment size fractions (sand $>60 \mu\text{m}$, $60 \mu\text{m} < \text{silt} < 5 \mu\text{m}$ and $<5 \mu\text{m} < \text{clay} < 0.43 \mu\text{m}$) were retained through all the processing steps below. The concentrations are reported as mg/l and were averaged over the water samples. Sand, silt, and clay made up 14, 57, and 29% of the resuspended TSS in San Diego, respectively.

Metals assigned to TSS, sand, silt, and clay size fractions were first reported as μg (metal)/mg (sediment), and then converted to μg (metal)/l (seawater) for model input. In the case of the dissolved metal fraction, the concentration of the metal was first reported as μg (metal)/mg (total TSS), then

converted to $\mu\text{g (metal)/l (seawater)}$. Since the metal concentrations for each of the sediment size-fractions was calculated by subtraction of the metal concentration in the next smaller size-fraction, it was possible to get negative concentrations for each water sample. If the average metal concentration per sediment size-fraction for all the water samples collected at each of the three sites was negative, it was considered as zero concentration. If the metal concentrations derived from the total load of sediment in the laboratory measurements did not exceed EPA's recommended chronic exposure level for seawater, the metal concentration was dropped from further processing. At the end of this step, the metals that were kept for further evaluation in the San Diego modeling were copper and nickel

The distributions of TSS, particle sizes, and their associated metal concentrations, as well as the dissolved metal concentrations that were derived from the original 17 stations (34 samples) were then interpolated/extrapolated on a regular grid evenly over a spatial area encompassing the tug-boat resuspension. The grid, derived in Golden Grapher Inc. SurferTM software, was approximately 100 points at 6-m spacing in the x (east–west) direction and 115 points at 7 m in the y (north–south) direction, yielding an 11,500 point grid. The derived grid values of TSS, particle sizes, and their associated metal concentrations were then assigned to the nearest hydrodynamic model grid point within 25 m. Twenty-four hydrodynamic model grid points were selected around the tug resuspension area to represent initial conditions for fate and transport. Those derived grid values further than 25 m from the chosen hydrodynamic grid points were discarded. The average derived values for TSS, particle sizes, and their associated metal concentrations assigned to each hydrodynamic grid point were averaged and these average values were provided as validation points at each of the 24 hydrodynamic grid points. Table 6-9 lists these values for the 24 model nodes.

Table 6-9. Resuspended sediment and associated metal concentrations input values for San Diego Bay between piers 4 and 5. Metals not shown were below EPA's water quality standards.

Node I	Node J	Easting (M)	Northing (M)	TSS (Mg/L)	Sand (Mg/L)	Silt (mg/l)	Clay (mg/l)	Cu Sand (µg/l)	Cu Silt (µg/l)	Cu Clay (µg/l)	Cu Diss (µg/l)	Ni Sand (µg/l)	Ni Silt (µg/l)	Ni Clay (µg/l)	Ni Diss (µg/l)
5	145	1917799.1	557397.9	2.02	0.28	1.16	0.58	0.79	0.38	0.12	1.68	0.58	0.11	0.42	1.25
5	146	1917868.7	557321.0	5.66	0.78	3.25	1.62	2.20	1.07	0.34	4.70	1.62	0.31	1.19	3.51
5	147	1917938.3	557224.5	6.42	0.89	3.69	1.84	2.49	1.22	0.39	5.33	1.84	0.35	1.35	3.98
5	148	1918009.6	557129.3	6.45	0.89	3.71	1.85	2.50	1.22	0.39	5.36	1.85	0.35	1.35	4.00
6	145	1917735.6	557360.0	6.88	0.95	3.96	1.97	2.67	1.31	0.41	5.71	1.98	0.38	1.44	4.27
6	146	1917801.2	557274.0	3.27	0.45	1.88	0.94	1.27	0.62	0.20	2.71	0.94	0.18	0.69	2.03
6	147	1917871.3	557182.3	6.52	0.90	3.75	1.87	2.53	1.24	0.39	5.41	1.87	0.36	1.37	4.04
6	148	1917942.9	557086.7	6.44	0.89	3.70	1.84	2.50	1.22	0.39	5.34	1.85	0.35	1.35	3.99
7	145	1917678.6	557314.4	7.91	1.10	4.55	2.27	3.07	1.50	0.48	6.56	2.27	0.43	1.66	4.90
7	146	1917740.0	557231.1	20.94	2.90	12.04	6.00	8.13	3.97	1.26	17.38	6.01	1.14	4.40	12.98
7	147	1917803.7	557140.9	9.18	1.27	5.28	2.63	3.56	1.74	0.55	7.62	2.64	0.50	1.93	5.69
7	148	1917874.3	557052.1	3.81	0.53	2.19	1.09	1.48	0.72	0.23	3.16	1.09	0.21	0.80	2.36
8	145	1917611.8	557270.3	9.59	1.33	5.51	2.75	3.72	1.82	0.58	7.96	2.75	0.52	2.01	5.95
8	146	1917673.2	557190.3	22.20	3.08	12.76	6.36	8.61	4.21	1.34	18.42	6.37	1.21	4.66	13.76
8	147	1917735.6	557103.0	15.57	2.16	8.95	4.46	6.04	2.95	0.94	12.92	4.47	0.85	3.27	9.65
8	148	1917801.0	557017.7	3.78	0.52	2.18	1.08	1.47	0.72	0.23	3.14	1.09	0.21	0.79	2.35
9	145	1917543.3	557229.0	8.27	1.15	4.75	2.37	3.21	1.57	0.50	6.86	2.37	0.45	1.74	5.13
9	146	1917605.2	557145.8	7.87	1.09	4.52	2.25	3.05	1.49	0.47	6.53	2.26	0.43	1.65	4.88
9	147	1917662.2	557068.1	19.16	2.66	11.02	5.49	7.44	3.64	1.15	15.90	5.50	1.05	4.02	11.88
9	148	1917727.7	556983.6	8.04	1.11	4.62	2.30	3.12	1.53	0.48	6.67	2.31	0.44	1.69	4.98
10	145	1917469.8	557187.1	7.97	1.10	4.58	2.28	3.09	1.51	0.48	6.62	2.29	0.44	1.67	4.94
10	146	1917527.1	557110.6	20.10	2.79	11.56	5.76	7.80	3.81	1.21	16.69	5.77	1.10	4.22	12.46
10	147	1917586.5	557031.6	3.22	0.45	1.85	0.92	1.25	0.61	0.19	2.68	0.93	0.18	0.68	2.00
10	148	1917649.6	556947.5	8.77	1.22	5.04	2.51	3.40	1.66	0.53	7.28	2.52	0.48	1.84	5.44

Figure 6-33 shows the *ECOS* tracks, discrete pump sample locations, TSS derived from OBS measurements as colored contours, and the 24 nodes of the CH3D model used for model validation. Numbers on the nodes are model coordinates. Figure 6-34 is a representative figure of copper associated with resuspended silt.

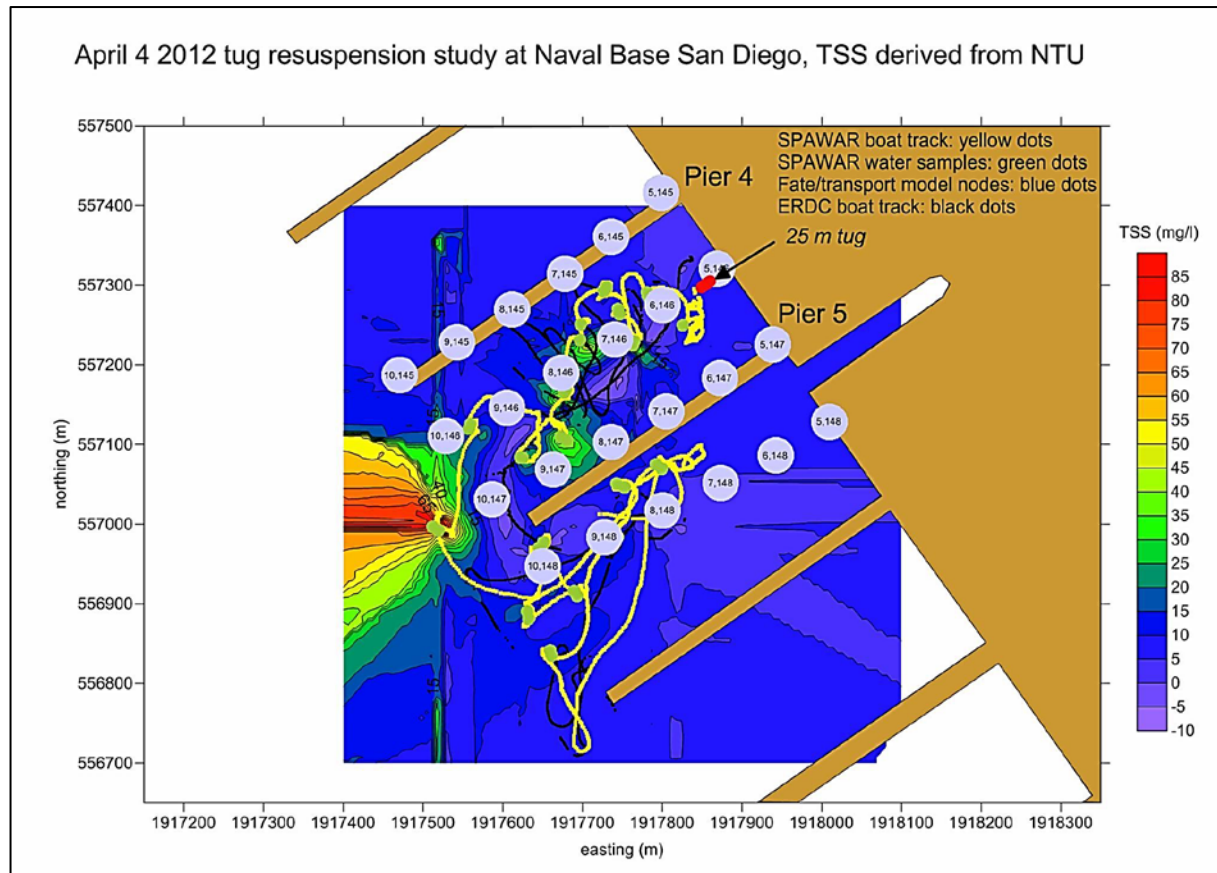


Figure 6-33. *ECOS* boat track and OBS measurements (yellow), discrete pump samples (green dots), extrapolated TSS concentrations as colored contours, and CH3D model nodes (light blue disks).

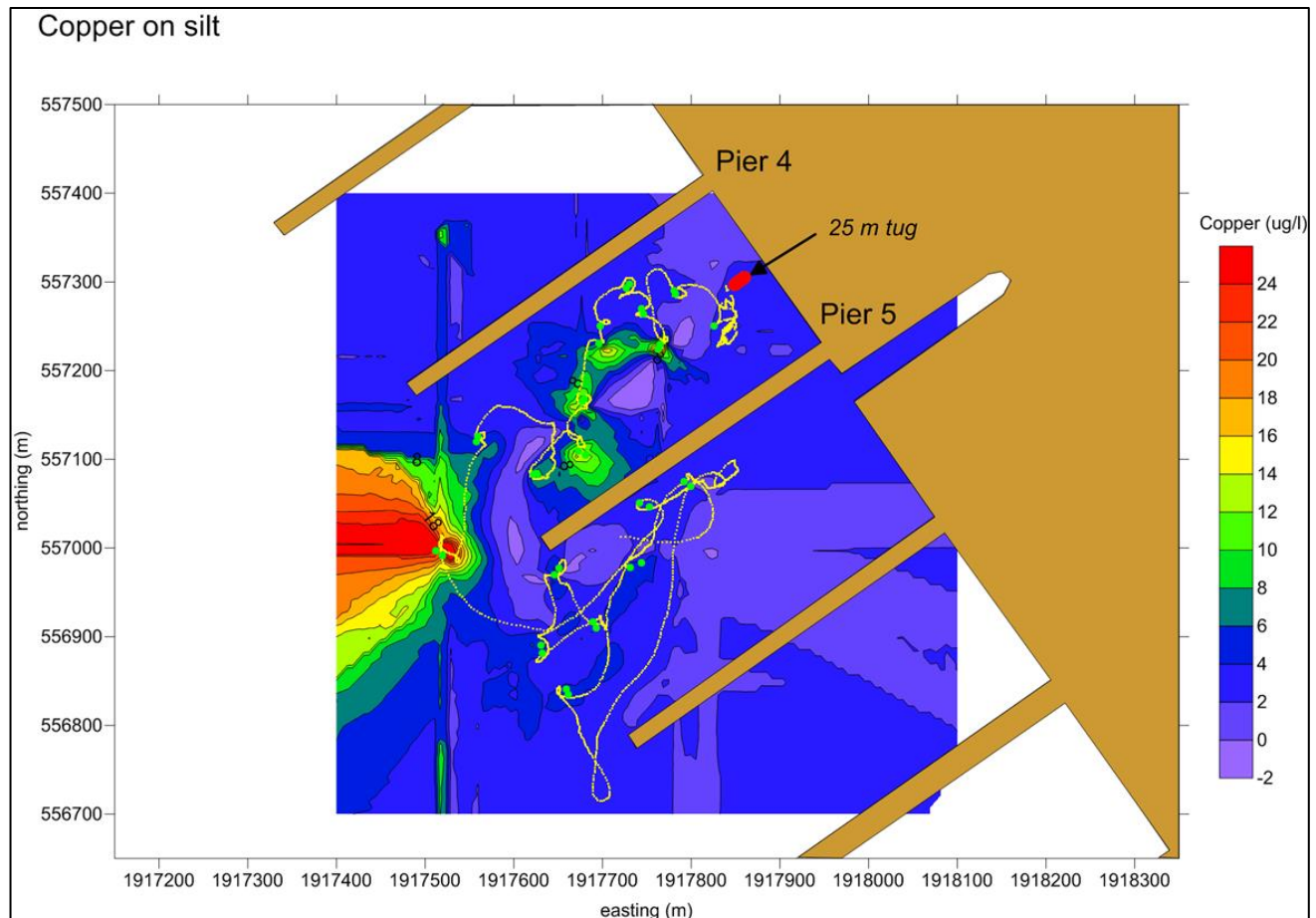


Figure 6-34. ECOS boat track and OBS measurements (yellow), discrete pump samples (green dots), extrapolated copper on silt concentrations as colored contours.

6.3.1.4 Comparison of Model and Field Results

The location for the study in San Diego Bay is between Piers 4 and 5 at Naval Base San Diego (NBSD), in the middle of the bay. A single controlled resuspension event with the tug-boat forcing resuspension by cranking up the engine for four consecutive 6–10 min intervals from 13:38 to 14:11 for 33 min was done in San Diego Bay on 4 April 2012. During the 33-minute period, the propeller started from 20 rpm for 6.6 min, then increased to 50 rpm for 10.2 min, then to 100 rpm for 9 min and then increased to and maintained at the highest speed, 150 rpm for 7.8 min. Then the propellers were shut off.

Maynard's model was used to simulate erosion rates by the designed propeller wash during the 33-min period. Figure 6-35 shows the simulated bottom velocity (top figure), bottom shear stress (middle), and erosion rate constants (grams/m²/sec) for the maximum propeller speed of 150 RPM. The other model parameters and propeller dimensions are the same as those used from the propeller erosion potential study and can be seen in Appendix E.

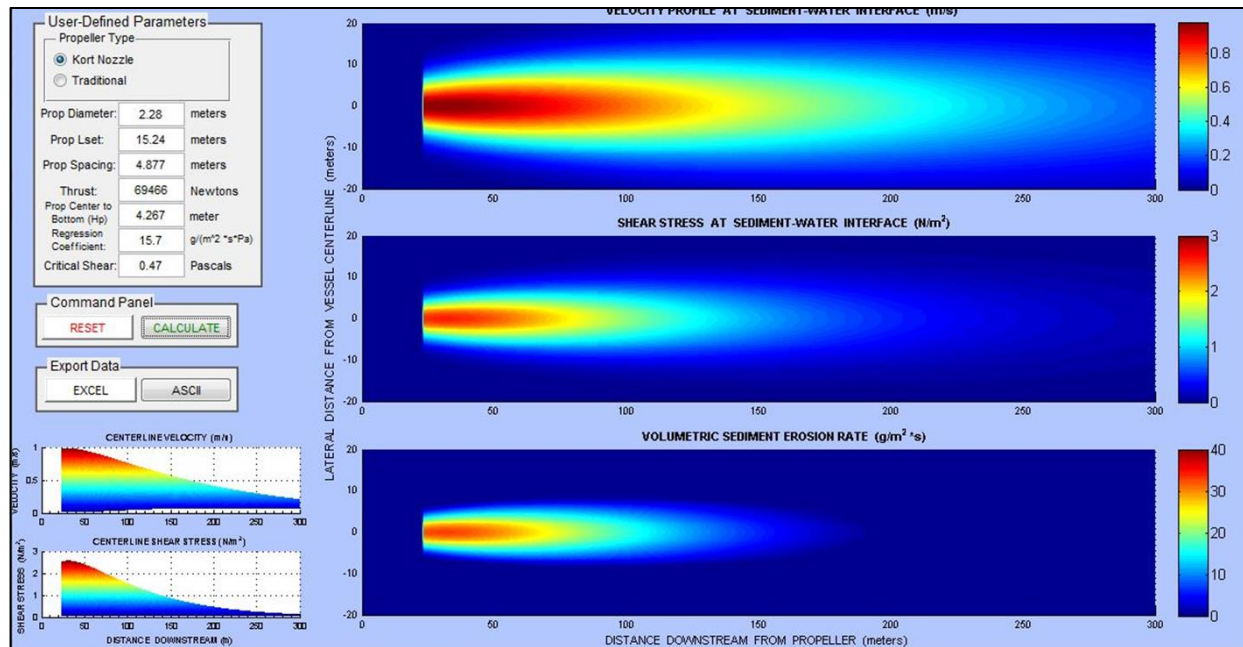


Figure 6-35. Simulated bottom velocity (top), bottom shear (middle), and erosion rate by Maynard's model for propeller speed of 150 RPM.

Figure 6-36 shows predicted total sediment erosion mass during the four propeller speeds. The erosion rate starts from $0.007 \text{ kg/m}^2/\text{sec}$ for the 20 RPM, to 0.44, 10.96 and $32.87 \text{ kg/m}^2/\text{sec}$ for the 50, 100, and 150 RPM, respectively. Therefore, major resuspension occurred during the periods of 100 RPM (5918 kg) and 150 rpm (15,383 kg). At the end of the propeller running period, 21571 kg of sediment mass was predicted to be eroded into the water column.

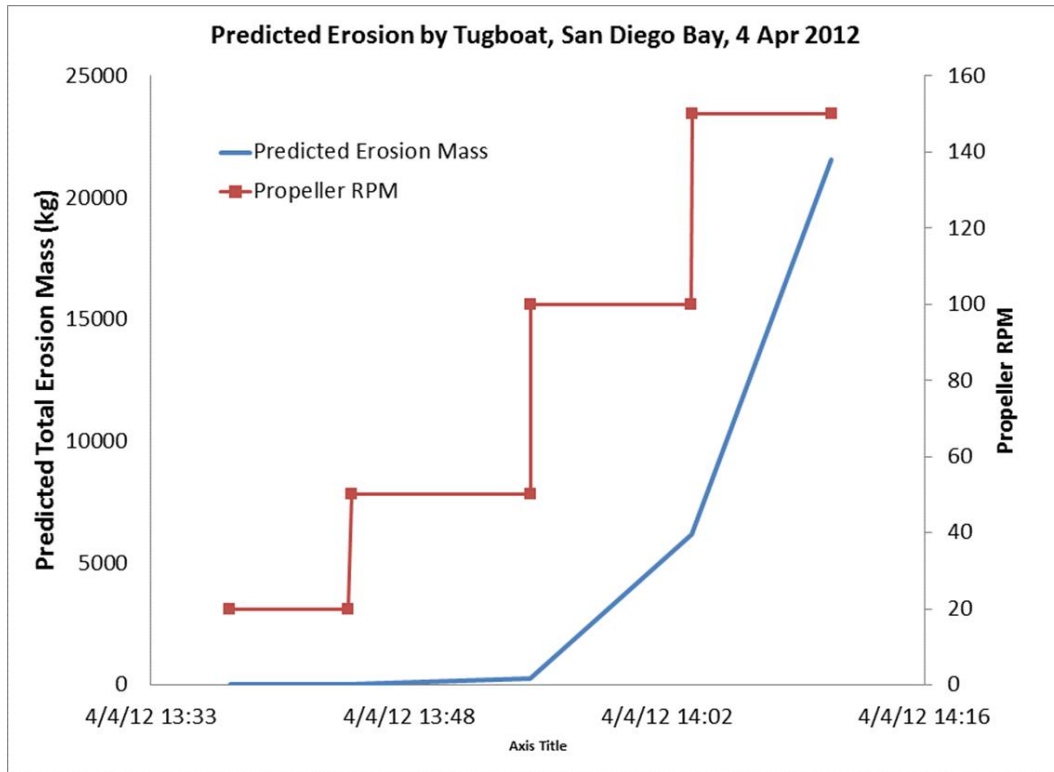


Figure 6-36. Model predicted total eroded sediment mass during the 33-minute period.

6.3.1.4.1 Fate/Transport for San Diego Bay

CH3D was set up to simulate the fate and transport of the sediment plume resuspended by the propeller wash from the tugboat. The CH3D model covers the entire San Diego Bay, the bay mouth and portions of the Pacific Ocean (Figure 6-37). The model uses curvilinear grids that conform to the bathymetry and the shorelines with adequate resolution and improved accuracy. The model grid covers the entire Pier 4–5 region with adequate grid resolution with minimal spatial variations to reduce numerical dispersion. The CH3D model simulation started from the midnight of 2 Apr 2012 (4/2/2012 0:00:00) and continued for about 2.5 days to eliminate any numerical transient errors from the cold start of the simulation. The model received the first pulse of eroded sediment plume at 4/4/2012 13:38 under the 20 RPM of the propeller (Figure 6-36). During the resuspension period, the eroded sediment mass was evenly and instantaneously distributed over the water column of the pier region, which is because flows in the pier region during the resuspension were highly turbulent, and were observed to be fully mixed in the water column. Since the near-field turbulent flow dynamics was not simulated, we assumed complete and instantaneous mixing of the water column for the near-field hydrodynamics induced by the propellers during the 33-minute resuspension period. During and after the resuspension period, CH3D simulated the fate and transport of the sediment plume for the next 5 days before the plumes settled to the bottom or were flushed out of the bay.

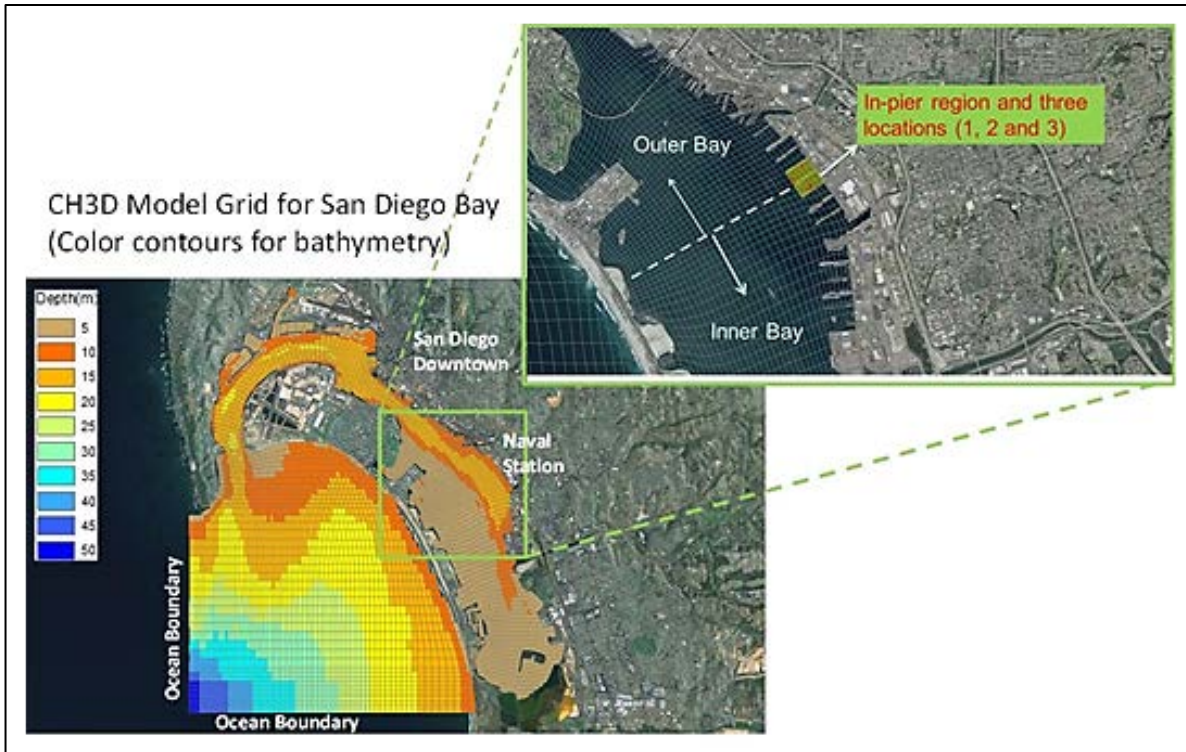


Figure 6-37. San Diego Bay Pier 4–5 region and the three locations (Segment 1, 2, and 3) for model/data comparison and the representative inner bay and outer bay for model result analysis. Imagery ©2014 DigitalGlobe, U.S. Geographical Survey, USGS, Map data ©2014 Google Life mode Terms Privacy Report a problem.

Sediment mass eroded during the propeller running period, as depicted in Figure 6-36, was fractionated into masses for three particle sizes, including sand, silt, and clay. Table 6-10 shows the percentages of the three-particle mass, which was derived from the background sediment data, and the settling velocities associated with the three particle sizes, based on the Stoke's Law.

Table 6-10. Eroded sediment particle masses from propeller wash experiment for fate/transport model simulation using CH3D and the settling velocities associated with the particles.

	Background Sediment Sample		Field Data	Settling Velocity
	Percentages of Particles Mass (%)	Refractionated Particles Mass (%)	Average Water Column Sample (%)	Stokes Law (cm/sec)
Sand	14.5	18.1	15.4	0.23
Silt	37.3	46.4	48.5	0.01
Clay	28.5	35.5	36.1	0.0014
Dissolved	19.6			
Clay+Silt+Sand	80.3	100		

6.3.1.4.2 Metal Partitioning

A detailed model describing changes in water chemistry and metal bioavailability that would occur during the early stages (e.g., 6–12 hours) of sediment oxidation was developed and demonstrated with the San Diego Bay propeller wash field data by Professor Kevin Farley from Manhattan College. This section describes the key processes of linkage of that model to the fate/transport model, CH3D.

Although it is possible to interface the simplified chemical model and CH3D by running the models in tandem, it was determined to be more expeditious to incorporate the time-variable portion of the simplified chemical model into the CH3D and to use a look-up table at each time step to determine partitioning of “labile” metal between the dissolved and particulate phases. For this purpose, a series of metal partitioning look-up tables were generated from a large array of chemical equilibrium model calculations that considered the effects of pH, hardness (or salinity), HFO, DOC, POC and “labile” metal concentrations on metal partitioning behavior. As part of the development of partitioning look-up tables, performance testing of the Windermere Humic Aqueous Model version 7 (WHAM7) (Tipping et al., 2011) was conducted using metal partitioning datasets from Delaware Bay and San Diego Bay. Final results for the incorporation of the simplified time-variable chemical calculations and the use of metal partitioning look-up tables into CH3D calculations are presented in Section 6.3.1.4.3.

6.3.1.4.2.1 Metal Partitioning Look-up Tables

Metal partitioning look-up tables offer a rapid and computationally efficient means of determining a distribution coefficient (K_D)³ within a transport model simulation. In this approach, potentially time- and cpu-intensive chemical speciation calculations are performed separate from the transport simulation using the range of key chemical parameters for a given site. Interpolation is used to select an appropriate K_D value from the table.

Assemblage chemical equilibrium speciation models quantify partitioning of metals to suspended solids by modeling the binding of metals to various constituents that make up suspended particulate matter (e.g., HFO, POC). These models predict metal partitioning based on water chemistry and therefore can be used to generate the look-up tables described above. One such model, WHAM7 (Tipping et al., 2011), can be used to simulate simultaneously the chemical speciation of a number of metals in the dissolved and particulate (i.e., adsorbed phases) and generate modeled K_D values based on a specified water chemistry. Typical input for the calculation includes pH, temperature, concentrations of dissolved/particulate organic carbon (i.e., DOC and POC), major cations (Na^+ , K^+ , Ca^{2+} , Mg^{2+}) and anions (Cl^- , SO_4^{2-} , CO_3^{2-}), amounts of hydrous ferric oxide (HFO), and hydrous manganese oxide (HMO). The particulate species POC, HFO, HMO, etc. are associated with the total suspended solids (TSS).

³ The distribution coefficient, K_D , defined as

$$K_D = \frac{v_M}{[M]_{\text{diss}}} = \frac{[M]_{\text{part}}}{[M]_{\text{diss}} \text{ TSS}},$$

where v_M is the solids-normalized particulate metal concentration [$\text{mol} \cdot \text{kg}^{-1}$], TSS is the total suspended solids concentration [$\text{kg} \cdot \text{L}^{-1}$], and $[M]_{\text{diss}}$ and $[M]_{\text{part}}$ are the molar dissolved and particulate metal concentrations [$\text{mol} \cdot \text{L}^{-1}$], respectively.

6.3.1.4.2.1.1 *San Diego Bay Datasets*

Two water column datasets from San Diego Bay were available for model testing: data from six sampling campaigns in the early 2000s (Chadwick et al., 2005) and data from an April 2012 propeller wash sampling event collected by the Space and Naval Warfare Systems Command (SPAWAR). Data from the early 2000s (Chadwick et al. 2005) included measurements of temperature, salinity, pH, TSS, DOC, alkalinity, and dissolved/total copper and zinc. Samples were collected along transects extending throughout the bay (Figure 6-38, inset), but only samples collected closest to the prop wash event were selected for this analysis. For the propeller wash sampling event, surface (3 feet) and mid-depth (15 feet) samples were collected from behind a tug-boat as it generated sediment plumes by pushing against the quay wall between Pier 4–5 at the eastern side of the bay (Figure 6-38). The data included measurements of total suspended solids, dissolved and particulate metals (associated with various size-fractions).

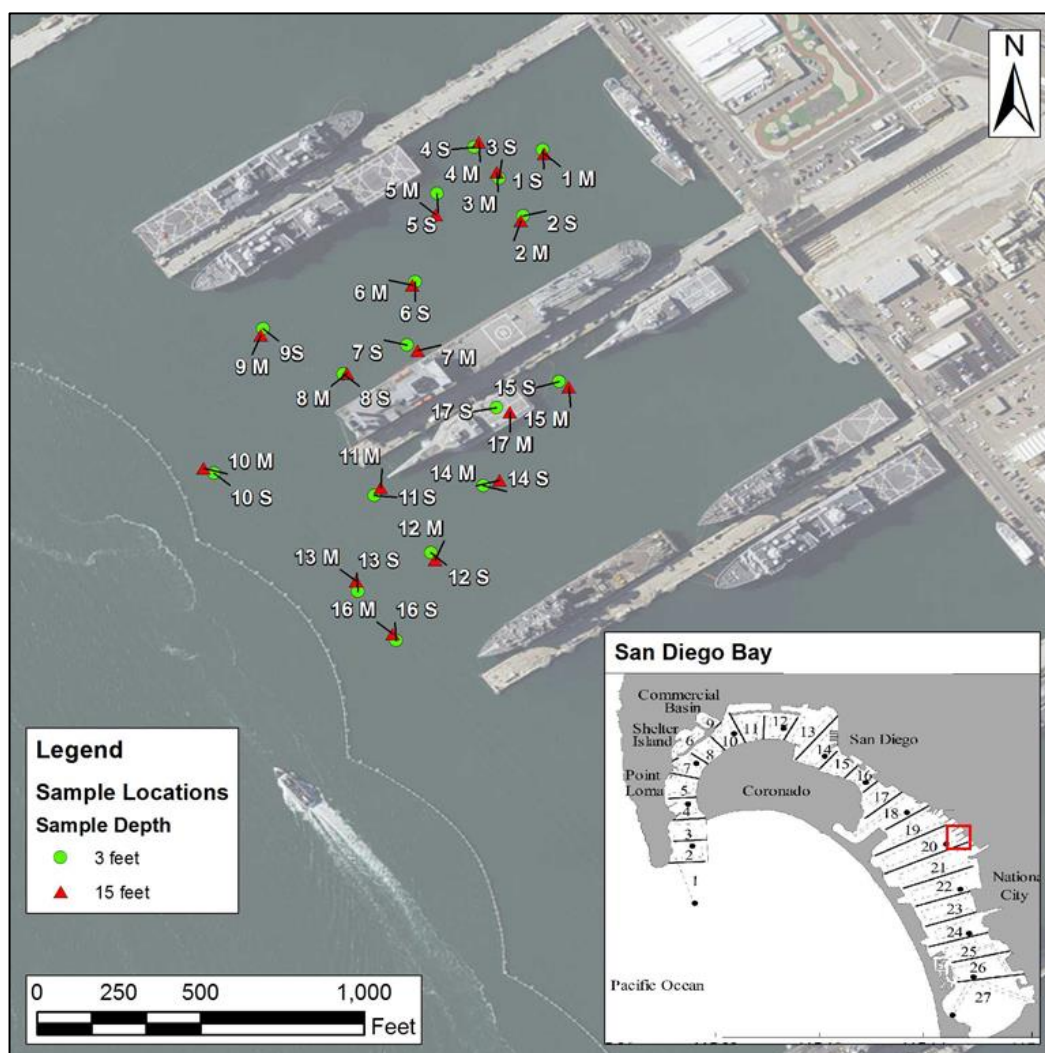


Figure 6-38. San Diego Bay sample locations. Main map shows locations of SPAWAR propeller wash samples. The inset map shows the transects and boxes from the Chadwick et al. (2005) sampling events. The prop wash area is highlighted in red in the inset map. Imagery ©2014 DigitalGlobe, U.S. Geographical Survey, USGS, Map data ©2014 Google Life mode Terms Privacy Report a problem.

Except for pH, DOC, and POC, input parameters for the WHAM7 calculations were specified based on concurrent field measurements. For pH and DOC, input values were estimated using data from other studies conducted in San Diego Bay, including Peng (2004), Chadwick et al. (1999), and Burton, Jr et al. (2012). For POC, input values were calculated as the product of the TSS and the fractional organic carbon content of the solids (f_{oc}). The quantities f_{oc} and POC were estimate using an approach based on the work of Turner (1996).⁴ Both San Diego Bay datasets utilize this relationship to obtain POC from TSS.

A summary of the observed (i.e., measured) copper and zinc log K_D values from the studies is provided in Figure 6-39. The median and mean log K_D values for both the Chadwick et al. (2005) and SPAWAR prop wash event are similar to observed log K_D values of 4.7 ± 0.4 for copper and 5.0 ± 0.5 that were reported for other sites (Table 6-11). Note, however, that log K_D values for copper and zinc observed in the Chadwick et al. (2005) study are higher than those from the SPAWAR study. This result is likely the result of lower organic carbon content in bedded sediments that were resuspended during the SPAWAR prop wash study.

⁴TSS was assumed to be comprised of (a) a permanently suspended fraction, TSS_{PS} with an $f_{oc,PS}$ and (b) a temporarily resuspended fraction, TSS_{TS} where ($TSS_{TS} = TSS_{Measured} - TSS_{PS}$) with an $f_{oc,TS}$ value of 0.02 mg/mg based on San Diego Bay sediment (Chadwick et al., 1999). The values of TSS_{PS} and $f_{oc,PS}$ were optimized using POC and TSS data from Peng, J. 2004. The f_{oc} varies with the measured TSS as the weighted average of the $f_{oc,TS}$ and $f_{oc,PS}$:

$$f_{oc} = [TSS_{PS} \times f_{oc,PS} + TSS_{TS} \times f_{oc,TS}] / TSS_{Measured}, \quad (1)$$

where TSS_{PS} is 0.246 mg/L, $TSS_{TS} = TSS_{Measured} - TSS_{PS}$, $f_{oc,PS} = 0.256$ mg/mg, $f_{oc,TS} = 0.02$ mg/mg. Since $POC = TSS_{Measured} \times f_{oc}$, the above equation can be expressed:

$$POC = [0.063 + (TSS_{Measured} - 0.246) \times 0.02], \quad (2)$$

where both TSS and POC are in mg/L.

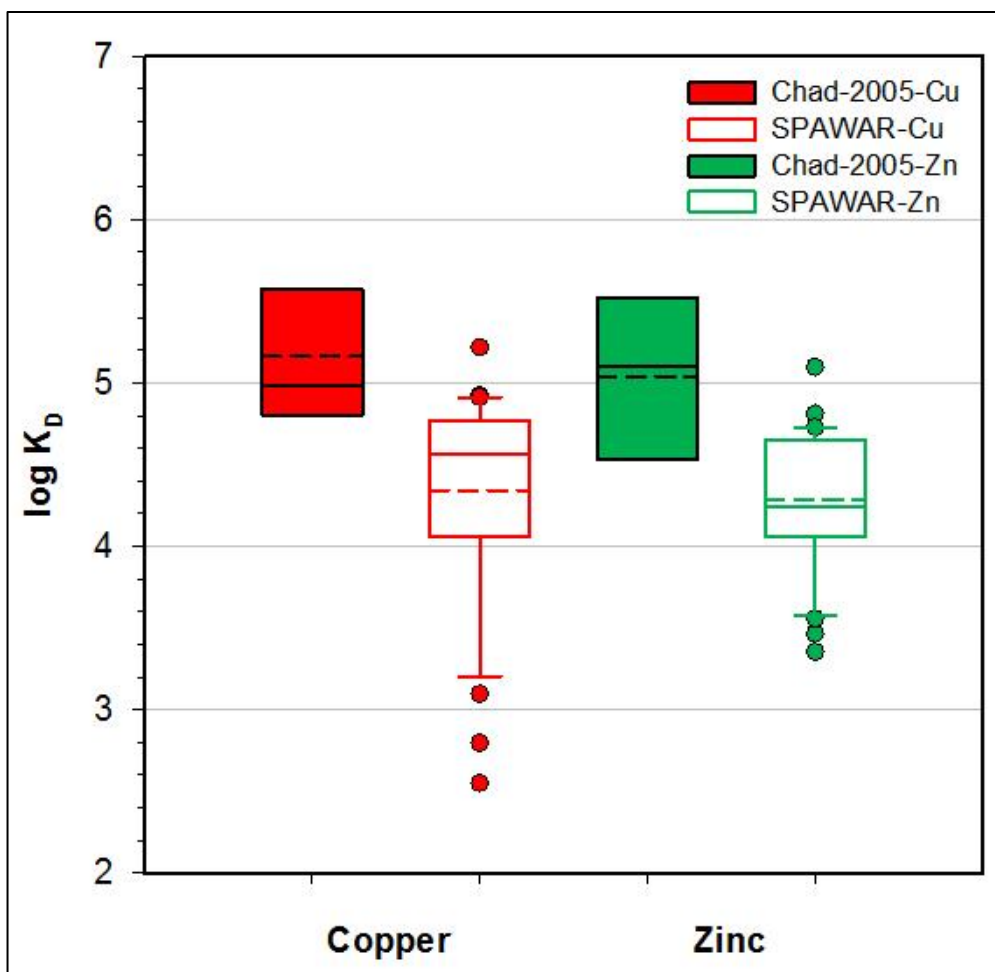


Figure 6-39. Summary of observed log K_D data from Chadwick et al. (2005) and the SPAWAR propeller wash sampling events. The boundary of the box closest to zero indicates the 25th percentile, the solid line within the box marks the median, the dashed line within the box indicates the mean, and the boundary of the box farthest from zero indicates the 75th percentile. The error bars above and below the box indicate the 95th and 5th percentiles values, respectively. Points represent values outside of the 5th and 95th percentile (i.e., outliers), respectively. Error bars and outliers are only calculated if a minimum number of data points exist.

Table 6-11. Copper and zinc suspended matter/water log K_D summaries from literature data as compiled by Allison and Allison (2005).

Metal	Median	Mean	Std. Dev.	Min	Max	Comments
Cu(I)	4.7	4.7	0.4	3.1	6.1	From literature data (edited, n=42); log-normal; CL=1
Zn(I)	5.1	5.0	0.5	3.5	6.9	From literature data (edited, n=47); log-normal; CL=1

A comparison of model-predicted and observed $\log K_D$ values is provided for copper and zinc (Figure 6-40A). As shown, the model-predicted $\log K_D$ values are generally within an order of magnitude of the observed $\log K_D$ values for copper. WHAM7 calculations however under predicted the observed $\log K_D$ values for zinc (i.e., values fell below the 1:1 line). Following the approach presented previously for Delaware Bay, cation competition to the WHAM7 binding sites was excluded in subsequent WHAM7 calculations (Figure 6-40B). As in the case of the Delaware Bay study, the exclusion of cation competition for DOC, POC, HFO, and HMO binding sites greatly improved the performance of WHAM7 in predicting $\log K_D$ values for zinc and had minimal effect on the $\log K_D$ calculations for copper. Based on these findings, the metal partitioning look-up tables for saline waters were developed using WHAM7 with Ca and Mg binding to DOC, POC, HFO and HMO excluded from the calculations.

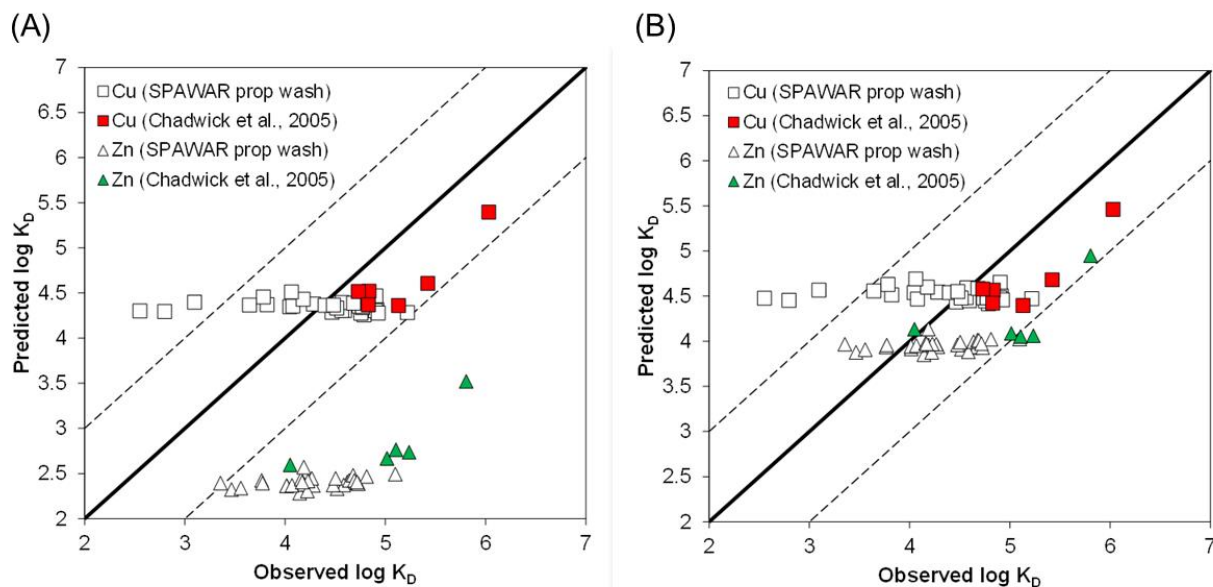


Figure 6-40. Performance assessment plot for copper (Cu, squares) and zinc (Zn, triangles) for the Chadwick et al. (2005) dataset (filled symbols) and the SPAWAR prop wash dataset (hollow symbols). The analysis was made using (A) default model parameters, and (B) with hardness cation (calcium and magnesium) binding to DOC, POC, HFO, and HMO turned off.

6.3.1.4.1.3 Look-Up Table Development

As a first step in producing a look-up table, it is necessary to select the key determinants (state variables) of metal partitioning and select relevant ranges over which to evaluate K_D values. These are the water quality parameters that affect the extent to which metal bind to TSS and would be expected to vary significantly at the site or type of site being modeled. For WHAM7, the input parameters listed above can all potentially impact metal partitioning. However, for conditions associated with a particular site or site-type, not all of these parameters necessarily impact the K_D calculation significantly, nor do they always vary enough to warrant inclusion as a state variable. For example, the major ion composition and pH would not be expected to vary considerably in full-salinity marine water.

Once the state variables and their ranges are selected, a model input deck must be generated that considers all the various permutations of the state variables as input parameters to the speciation

model. Once the model is run, the input and output values for K_D constitute the look-up table for the particular site.

6.3.1.4.2.1.3 *Application to San Diego Bay*

To better illustrate the process of look-up table generation, consider the following case of San Diego Bay. The salinity of San Diego Bay varies between approximately 32 and 35 practical salinity units (psu) (Chadwick et al., 2005). While this variation is generally small, it was nevertheless decided to use salinity as a state-variable since the concentration of key major ions can be related to this value through a simple end-member analysis (Di Toro et al., 2005). Table 6-12 presents water quality parameters (low, average, high) for San Diego Bay compiled from recent SPAWAR propeller wash resuspension field activities and earlier San Diego Bay reports (Chadwick et al., 1999; Chadwick et al., 2005).

Table 6-12. Water quality parameters for San Diego Bay.

	Total Copper, ($\mu\text{g/L}$)	pH	POC, (mg/L)	DOC, (mg/L)	Iron, (mg/L)	Salinity, (psu_
Value 1 (low)	4	7.8	0.04	0.75	0.05	32
Value 2 (average)	10	8.2	0.25	1.5	0.40	33.5
Value 3 (high)	26	8.6	1.6	4	3.25	35

Using the three values of the six state variables in Table 6-12, there are 729 possible parameter combinations. Visual Basic for Applications (VBA) code, accessible within Microsoft[®] Excel[®], was used to generate the WHAM7 input file with all parameter combinations. Details regarding the conversion of POC and DOC to particulate and colloidal humic and fulvic acid (i.e., the metal binding functional groups modeled in WHAM), and the conversion of iron to HFO can be found in Appendix F. The model was used to predict 729 realizations of the fraction particulate and the dimensionless distribution coefficient (K_D') that represent different water chemistries (i.e., different combinations of the input parameters). For these simulations hardness cation binding to DOC, POC, and HFO was excluded. The equation describing K_D , K_D' , and the fraction particulate (f_p) are presented in Appendix F.

Using the look-up table of the 729 datasets, we have developed a direct linear estimation of partitioning coefficient from the six variables:

$$f = C_0 + C_1[Cu]_{Total} + C_2[pH] + C_3[POC] + C_4[DOC] + C_5[p - Fe] + C_6[Salinity] \quad (14)$$

Table 6-13 shows 15 datasets excerpted from the 729 datasets of the look-up table (red header) with the predicted partitioning coefficients with the seven coefficients (equation above) obtained by the least-square method.

Table 6-13. Look-up table (red header with 15 datasets excerpted from 729 datasets in the original look-up table), the seven coefficients (green header) derived from the 729 datasets, and the predicted partitioning by the linear equation (yellow header).

Look-Up Table Developed by Farley								Least-Square Coefficients		Predicted by Least Square
STATE VARIABLES FOR MODEL INPUT						MODEL OUTPUT				
Total Cu (mol/L)	pH	POC (mg/L)	DOC (mg/L)	Particulate Iron (mg Fe/L)	Salinity (ppt)	$\log K_D = \log(K_D \times \text{TSS})$ (dimensionless)	Fract. Part. (dimensionless)		[c]-f	Y-f
1.259E-07	7.8	0.04	0.75	0.12	32	-1.17	0.064	c0	-0.53102635	0.173842698
1.259E-07	7.8	0.04	0.75	0.12	33.5	-1.17	0.063	c1	-1.017457E+05	0.170340509
1.259E-07	7.8	0.04	0.75	0.12	35	-1.18	0.062	c2	0.102671951	0.16683832
1.259E-07	7.8	0.04	0.75	0.6	32	-0.84	0.127	c3	0.279245993	0.206735655
1.259E-07	7.8	0.04	0.75	0.6	33.5	-0.85	0.123	c4	-3.712373E-02	0.203233465
1.259E-07	7.8	0.04	0.75	0.6	35	-0.87	0.120	c5	6.852699E-02	0.199731276
1.259E-07	7.8	0.04	0.75	3.25	32	-0.26	0.354	c6	-2.334793E-03	0.388332185
1.259E-07	7.8	0.04	0.75	3.25	33.5	-0.28	0.345			0.384829996
1.259E-07	7.8	0.04	0.75	3.25	35	-0.30	0.336			0.381327806
1.259E-07	7.8	0.04	1.5	0.12	32	-1.22	0.056			0.145999898
1.259E-07	7.8	0.04	1.5	0.12	33.5	-1.23	0.055			0.142497709
1.259E-07	7.8	0.04	1.5	0.12	35	-1.24	0.055			0.138995519
1.259E-07	7.8	0.04	1.5	0.6	32	-0.92	0.107			0.178892854
1.259E-07	7.8	0.04	1.5	0.6	33.5	-0.93	0.105			0.175390665
1.259E-07	7.8	0.04	1.5	0.6	35	-0.94	0.102			0.171888476

6.3.1.4.2.2 The Least-Square Method

Equation (15) can be applied to express the look-up table that contains 729 datasets:

$$f_i = C_0 + \sum_{j=1}^6 C_j [x_{ji}], \quad (15)$$

where $i = 1, 2, \dots, 729$, representing the the look-up table datasets, j represents the six variables, C_j is the coefficient associated with each water quality parameter, x_{ji} . The numerical values of the seven coefficients, C_i , $i=0,1,\dots, 6$, can be obtained by minimizing the ensamble errors from the equation:

$$E(C_0, C_1, \dots, C_7) = \sum_{i=1}^{729} \left(f_i - (C_0 + \sum_{j=1}^6 C_j [x_{ji}]) \right)^2 \quad (16)$$

$$\frac{\partial E}{\partial C_i} = 0, i = 0, 1, 2, \dots, 6 \quad (17)$$

The Lagrangian minimization requirement, as depicted by Equation (4) will result in the following set of seven linear equations for the solutions of C_i , $i=0, 1, 2, \dots, 6$:

$$\begin{aligned}
 & NC_0 + \sum_{j=1}^N x_{1j}C_1 + \sum_{j=1}^N x_{2j}C_2 + \sum_{j=1}^N x_{3j}C_3 + \dots + \sum_{j=1}^N x_{6j}C_6 = \sum_{j=1}^N f_i \\
 & \sum_{j=1}^N x_{1j}C_0 + \sum_{j=1}^N x_{1j}^2 C_1 + \sum_{j=1}^N x_{1j}x_{2j}C_2 + \sum_{j=1}^N x_{1j}x_{3j}C_3 + \dots + \sum_{j=1}^N x_{1j}x_{6j}C_6 = \sum_{j=1}^N x_{1j}f_i \\
 & \dots \\
 & \sum_{j=1}^N x_{6j}C_0 + \sum_{j=1}^N x_{1j}x_{6j}C_1 + \sum_{j=1}^N x_{6j}x_{2j}C_2 + \sum_{j=1}^N x_{6j}x_{3j}C_3 + \dots + \sum_{j=1}^N x_{6j}^2 C_6 = \sum_{j=1}^N x_{6j}f_i
 \end{aligned} \quad (18)$$

The numerical solution for the seven coefficients, C_0, C_1, \dots, C_6 , were obtained. Table 6-13 shows the seven coefficients obtained from the least-square methods using the complete look-up table (green header), with 15 representative datasets from the look-up table (red header), and the estimated partitioning coefficient using the linear equation, depicted by Equation (15). The units for the six variables are shown in Table 6-13.

In Figure 6-41, the partitioning coefficients for copper predicted by the model are plotted against those by the look-up table (linear equation). Good correlation is developed between the two datasets with $R^2 = 0.915$. These results demonstrate that it is valid and convenient to predict the partitioning coefficients from the look-up table by using the linear equation.

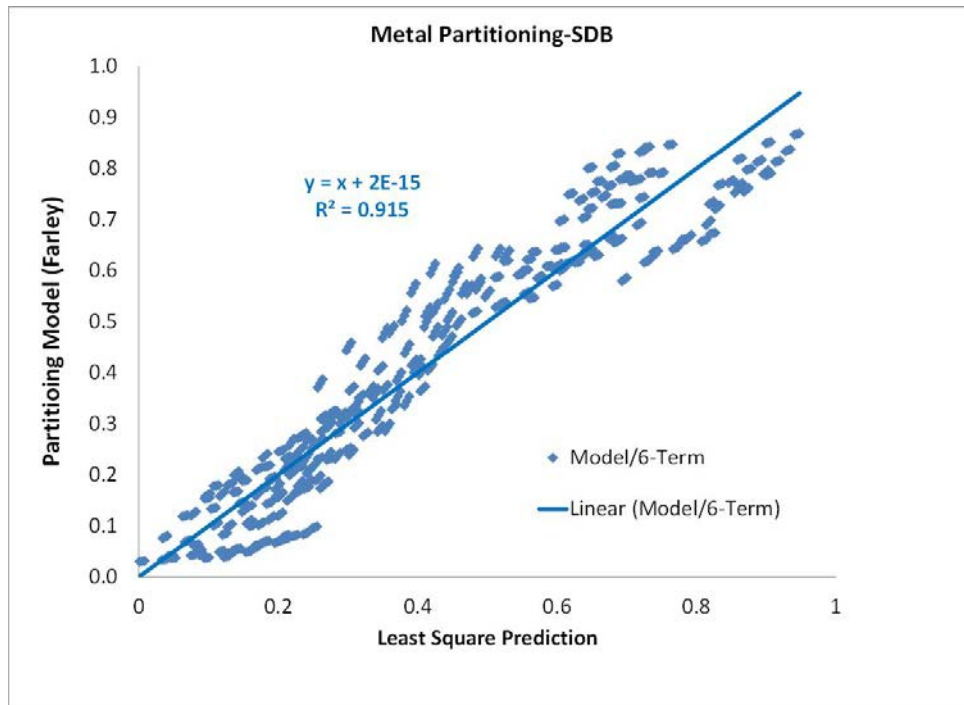


Figure 6-41. Correlation plot between partitioning model (Farley) and the linear equation from least-square method.

For the linked CH3D+TICKET model, the least-square equation for copper partitioning was inserted in the transport subroutine for copper (Figure 6-42). For each time step, the empirical equation was used to calculate the partitioning coefficient. As discussed previously, for this study, only metal concentrations were collected and measured, the other five water quality parameters were not measured. Therefore, we used historical (and representative) data for the other parameters, including pH, POC, DOC, iron, and salinity and used measured/predicted total copper concentrations to estimate the partitioning coefficient for copper. Figure 6-43 shows the comparison of predicted copper partitioning coefficients between the look-up table (blue) and the measured data (red) from the San Diego Bay field study. The figure shows that total copper concentration alone has significant contribution to the partitioning coefficient for copper.

CH3D-Model with Look-Up Table for Metal Partitioning

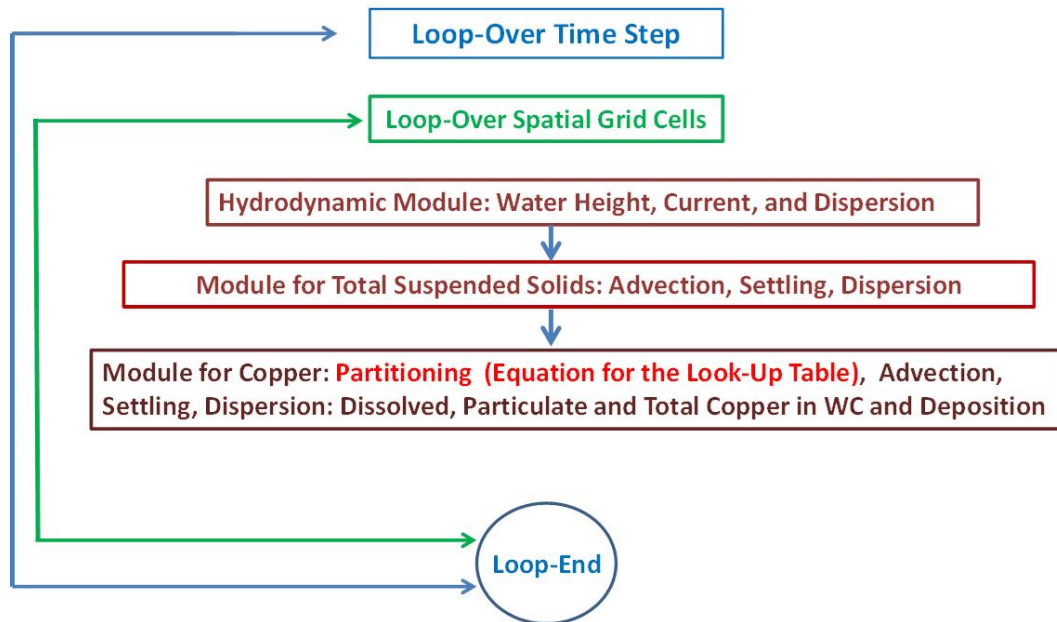


Figure 6-42. Implemented metal (copper) partitioning algorithm (linear equation for look-up table) in CH3D.

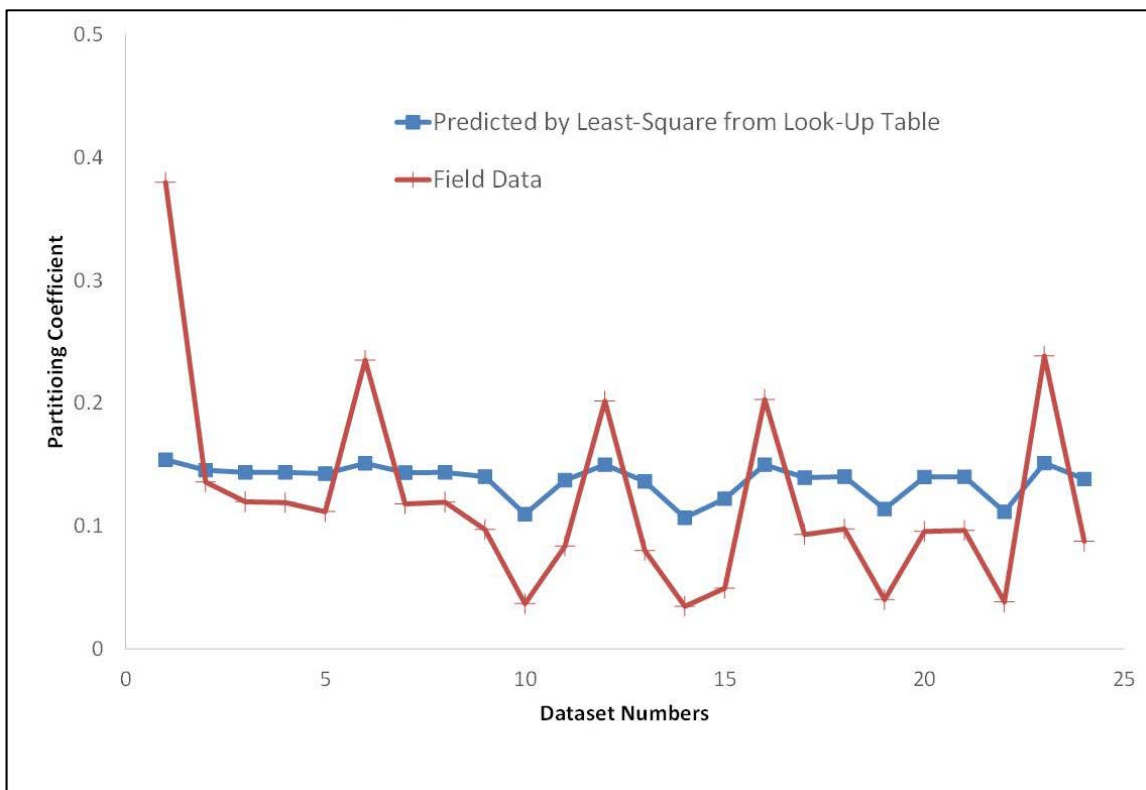


Figure 6-43. Predicted partitioning coefficients for copper in San Diego Bay by the linear equation (blue) and the field data (red).

6.3.1.4.3 CH3D+TICKET Model Results

6.3.1.4.3.1 Suspended Solids

Simulations with the linked CH3D+TICKET model was conducted for the period of 4/2/0:00 to 4/12/0:00, 2012 for a total of 10 days. Resuspension event occurred during 4/4/13:55–14:25, which was about 62 hours after the hydrodynamic model started, a time period long enough to eliminate any numerical dispersion due to the cold start of the simulation.

Figure 6-44 show the mode/data comparisons of clay, silt, and sand particle concentrations for three locations (Figure 6-33). These figures show that simulated concentrations of particles match well with the measured field data. The largest model/data differences occurred for Location #1 (Loc #1), with model predicted solid concentrations about 1.5 to 1.7 times of the field data. Once resuspended, the sediment plume in the pier region started to be flushed out of the region within 6 hours (half tidal cycle). After 6 hours, sediment concentrations decreased monotonically for the three particle sizes within the pier region, meaning the sediment was flushed out of the region and deposited to the bottom.

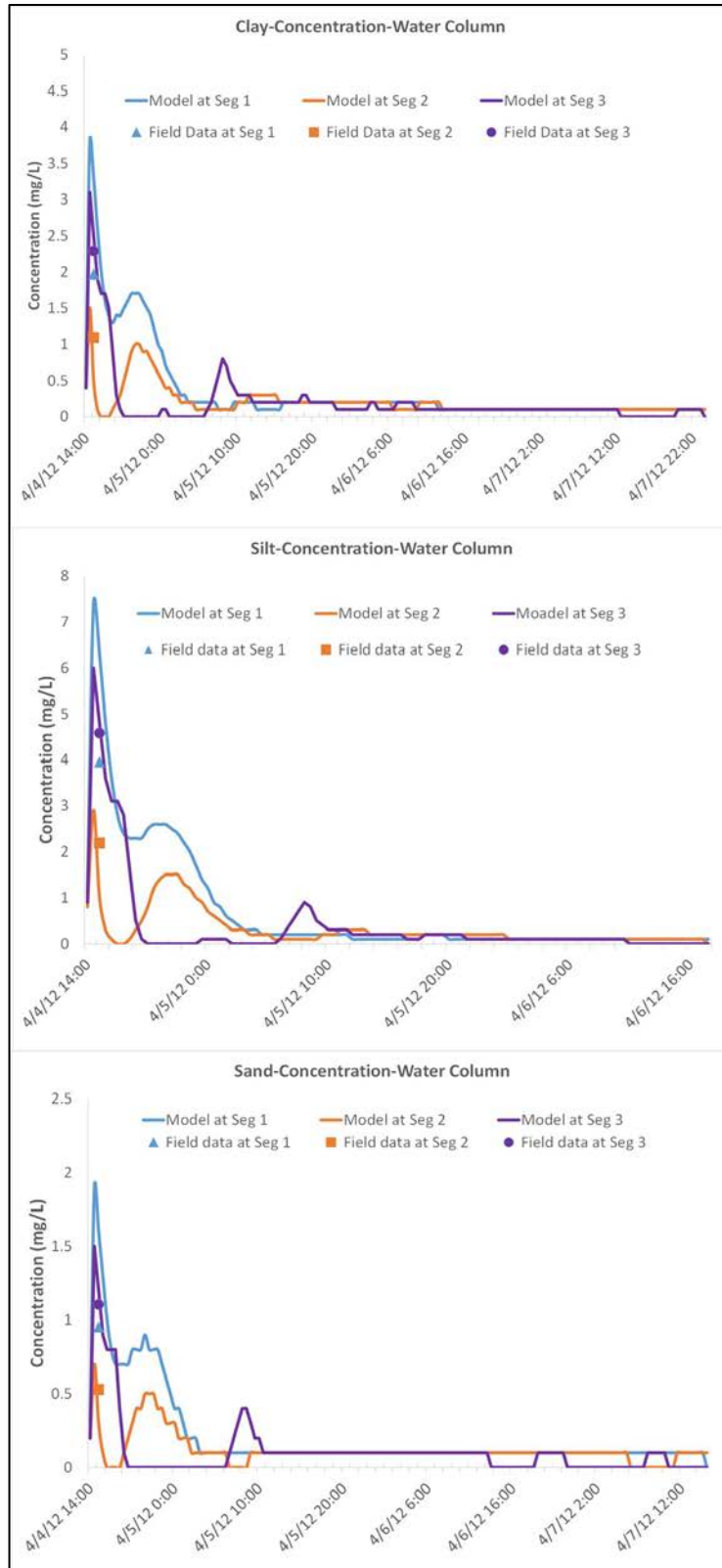


Figure 6-44. Model/data comparison of clay (top), silt (middle), and sand (bottom) concentrations for the three locations (see Figure 6-33).

Figure 6-45 shows the snapshots of simulated and measured water-column concentrations of clay, silt, and sand during the 1-hour period of field data sampling after the propeller resuspension (14:15–15:06, 4/4/2012). Both simulated and measured concentrations of clay, silt, and sand particles are within the same range (0–10 mg/L). The close agreement of concentrations (mass) of the sediment plumes between the model and field data suggests that the total eroded sediment mass, predicted by the Maynard's model, is accurate and close to the measured quantity. Predicted sediment concentrations are smoothly varying in the vicinity of the pier region, whereas measured data have larger spatial variations within the pier region. This is not surprising, since the in-pier flows still exhibited visible level of turbulence when the data were collected, and spatial variations of the data are expected in the near field pier region.

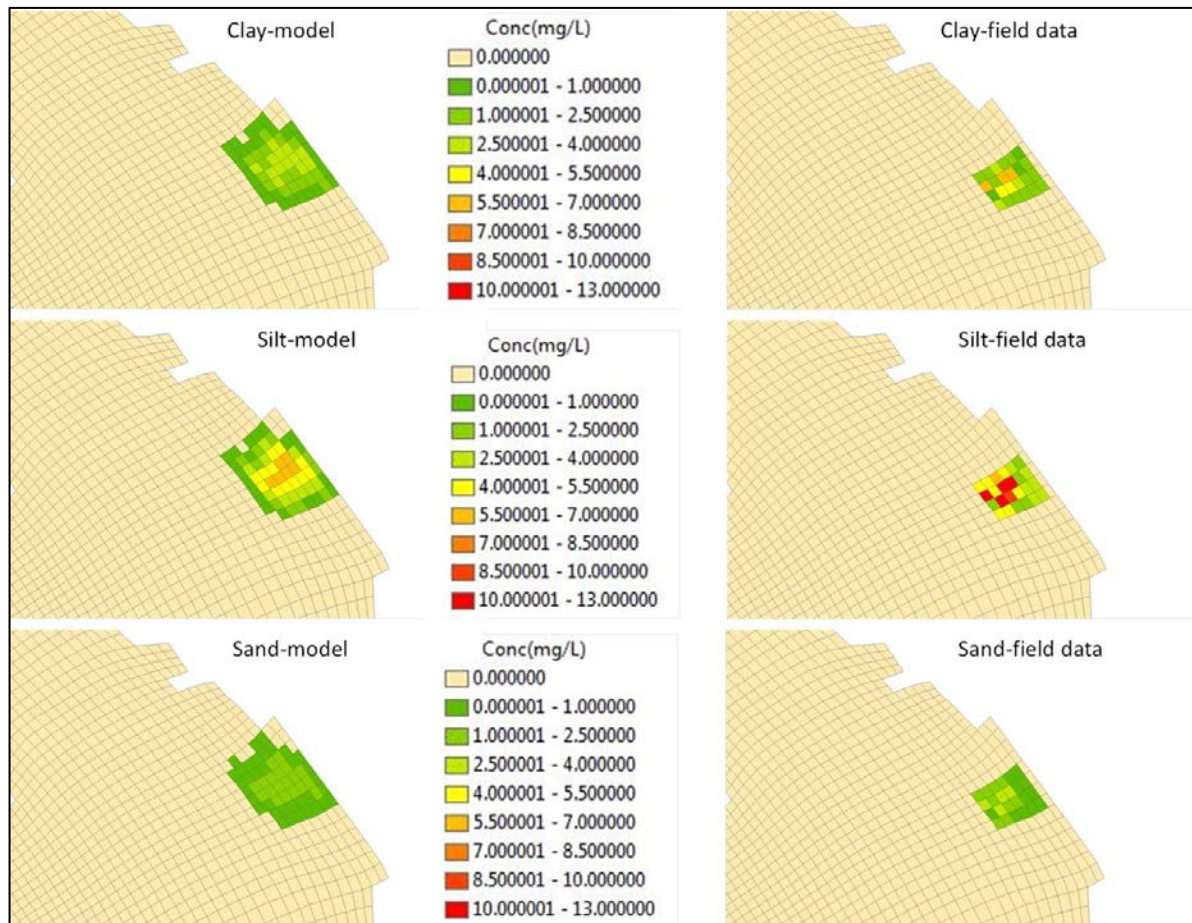


Figure 6-45. Snapshots of water column concentrations of clay (top), silt (middle), and sand (bottom) between model (left) and field data (right) during 14:15–15:06, 4 April 2012.

Figure 6-46 shows the deposition of clay, silt, sand and total sediment at the end of 7.5 days from the resuspension. Of the three particle sizes, clay particles tend to stay in the water column the longest before they were carried by currents and deposited to other regions of the bay, followed by silt, and sand. Sand particles tend to settle fast once the sediment is resuspended by the propellers; most of the sand deposits are in the vicinity of the locations where they are resuspended.

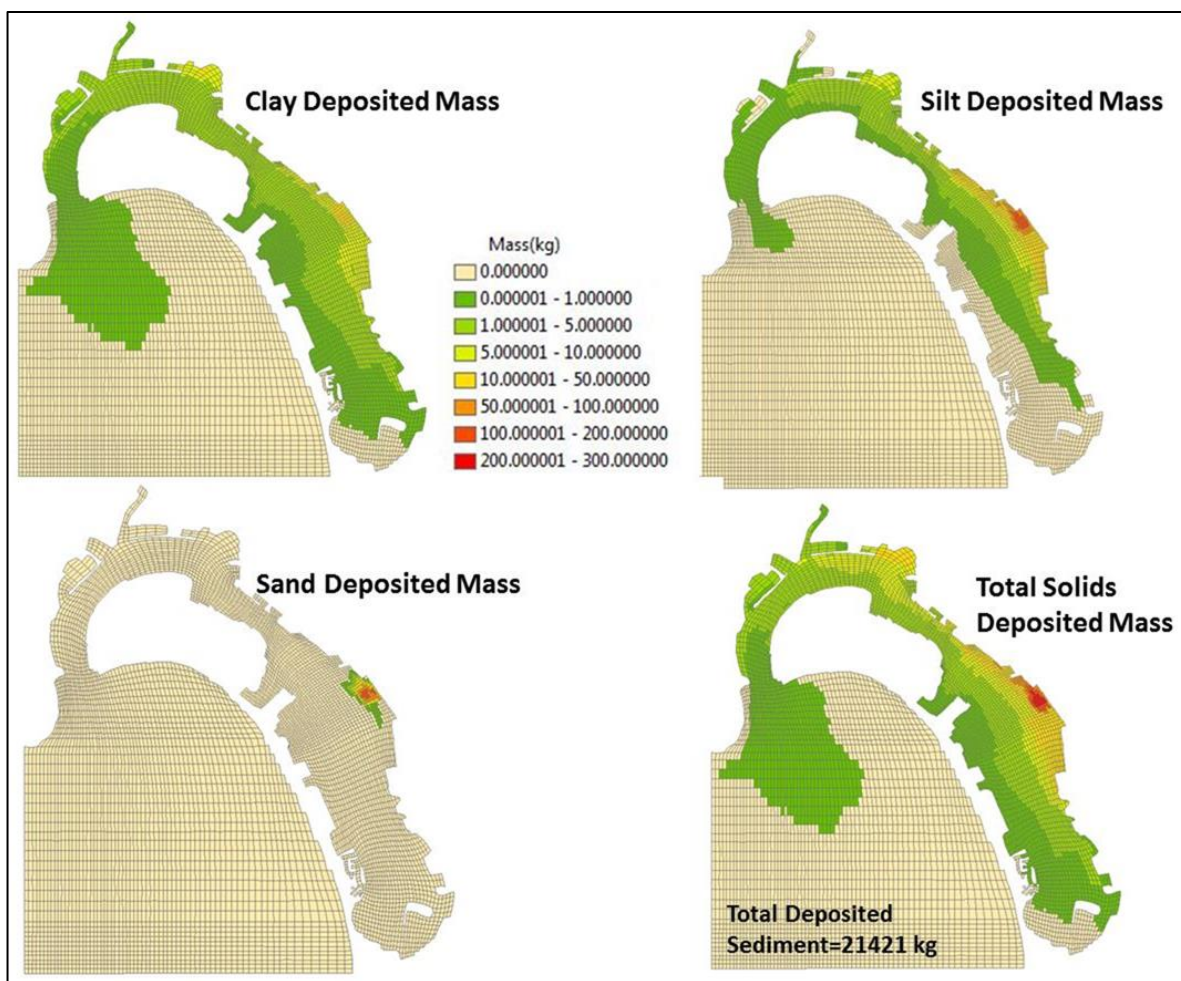


Figure 6-46. Simulated deposition mass (kilograms for each model segment) of clay, silt, sand and total sediment particles from the propeller wash study.

Figure 6-47 shows the time series and snapshots of simulated dissolved and total copper and the field data. Figure 6-48 shows the snapshot contours of predicted and measured dissolved copper in the water column during the 1-hour field data sampling period following the propeller resuspension. Figure 6-49 shows the corresponding contour plots for the total copper at Hr 63 and Hr 68. Figure 6-50 shows the snapshots of predicted dissolved copper concentrations at hour 68 (6 hours after resuspension) and Hr 240 (7.5 days after resuspension) and Figure 4-51 shows the corresponding contour plots for total copper. These figures show that both simulated and measured concentrations of dissolved and total copper are within the same range (0–10 $\mu\text{g/l}$ for dissolved copper and 0–20 $\mu\text{g/l}$ for total copper). For the three representative locations, simulated dissolved copper are 7.24 $\mu\text{g/l}$ (5.7 $\mu\text{g/l}$ for field data), 2.8 $\mu\text{g/l}$ (3.2 $\mu\text{g/l}$ for field data), and 5.5 $\mu\text{g/l}$ (6.6 $\mu\text{g/l}$ for field data), for location #1, #2 and #3, respectively. Simulated total copper range from 17.2 $\mu\text{g/l}$ (10.1 $\mu\text{g/l}$ for field data), to 3.6 $\mu\text{g/l}$ (5.6 $\mu\text{g/l}$ for field data) and 9.7 $\mu\text{g/l}$ (11.7 for field data), for location #1, #2, and #3, respectively.

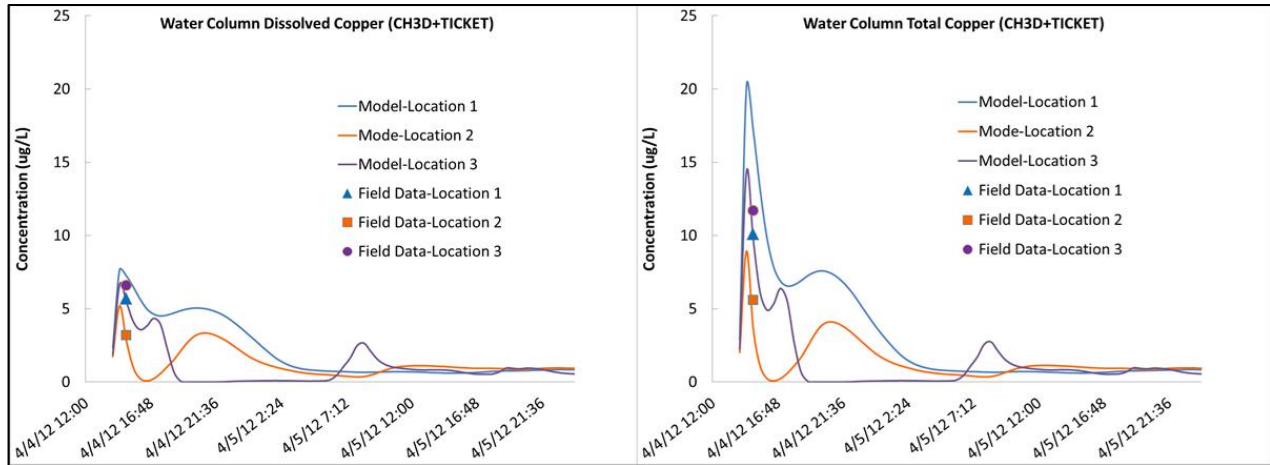


Figure 6-47. Time series of simulated dissolved (left) and total copper (right) and comparison with field data at the three representative locations.

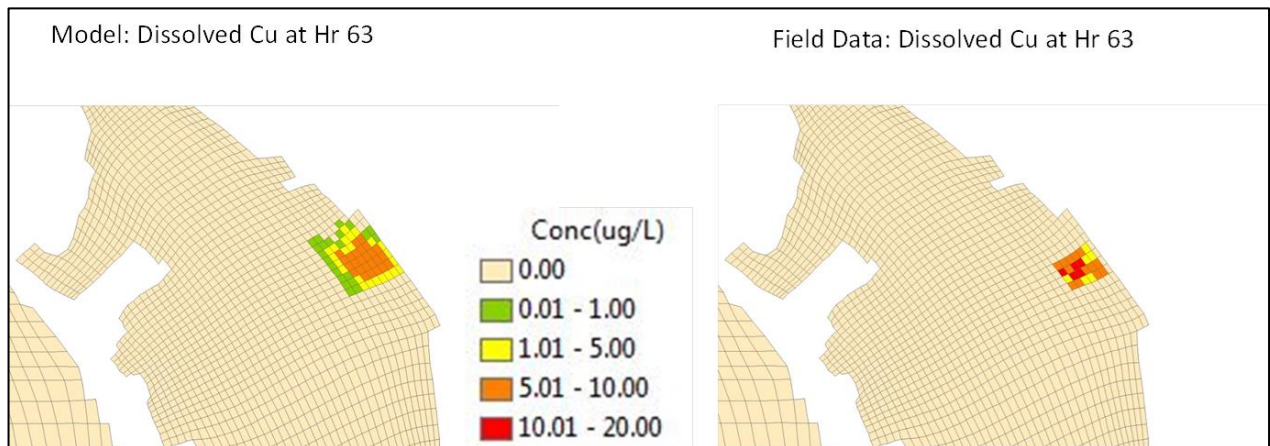


Figure 6-48. Snapshots of water column concentrations of dissolved copper between model (left) and field data (right) during 14:15–15:06, 4 April 2012.

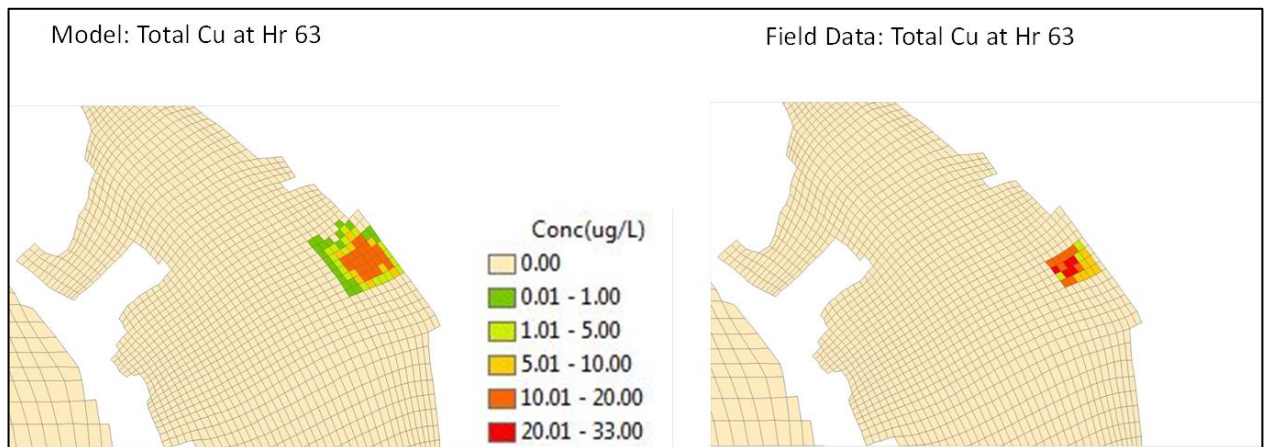


Figure 6-49. Snapshots of water column concentrations of total copper between model (left) and field data (right) during 14:15–15:06, 4 April 2012.

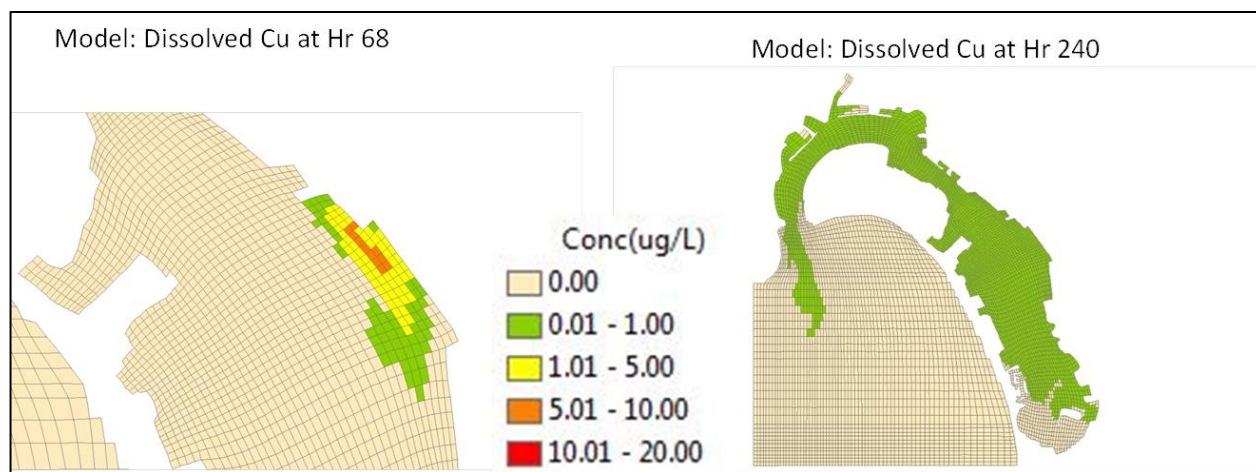


Figure 6-50. Snapshots of water column concentrations of dissolved copper at Hr 68 (6th hour after resuspension) and Hr 240 (7.5 days after the resuspension).

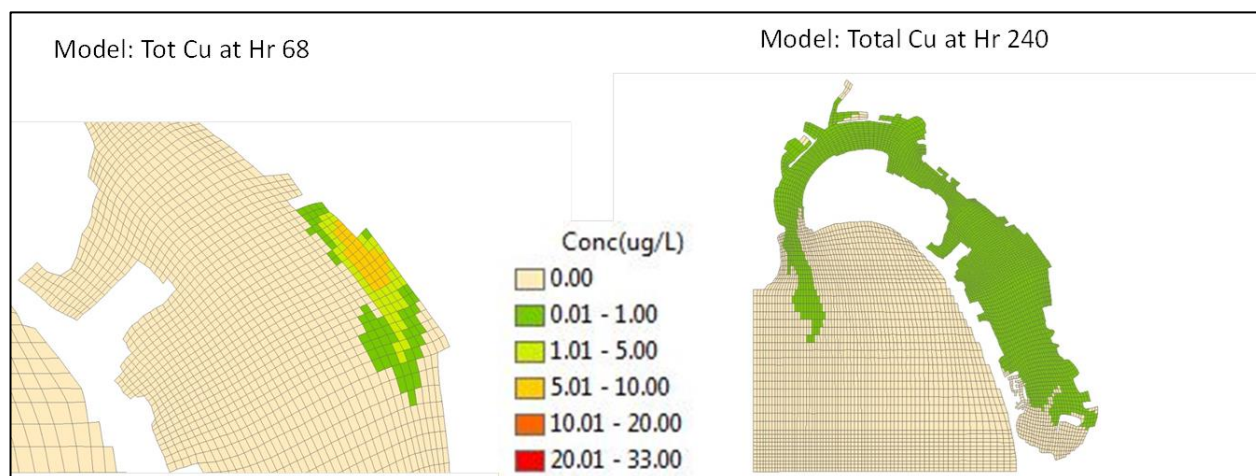


Figure 6-51. Snapshots of water column concentrations of total copper at Hr 68 (6th hour after resuspension) and Hr 240 (7.5 days after the resuspension).

The snapshot contour figures show that predicted copper concentrations are smoothly varying in the vicinity of the pier region, whereas measured data have larger spatial variations within the pier region, a phenomenon also reflected in the results of sediment for the same reasons of the near-field effect and the resolution of the model grid.

Figure 6-52 shows the deposited copper mass at Hr 63 and Hr 68. As discussed previously, deposition of the sediment plumes started right after they were resuspended. As the resuspension stopped and field measurement starts, deposition of copper already started, most of which occurred in the vicinity of the pier region. At 6 hours after the resuspension (Hr 68), deposition areas expand into the adjacent regions, with the high deposition rate centered in the pier region.

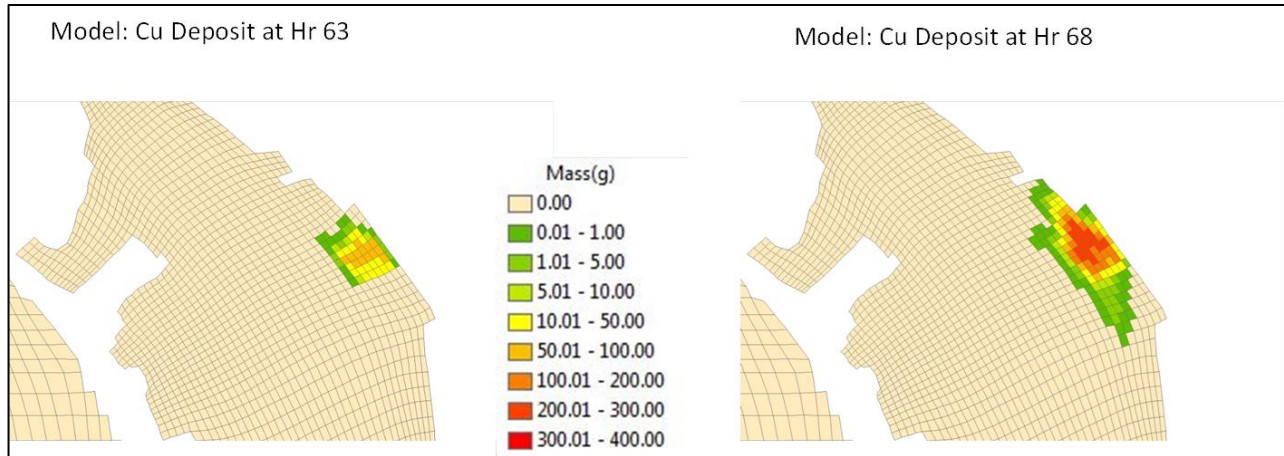


Figure 6-52. Deposited copper mass at Hr 63 (right after resuspension) and Hr 240 (7.5 days after resuspension).

The linked CH3D+TICKET has been demonstrated for its effectiveness of simulating fate/transport of copper for San Diego Bay with variable metal partitioning defined by the six water quality parameters. The values of the six water quality parameters can be either assigned or predicted. For this study, only the metal concentrations were measured and historical values were used for the other five parameters in the calculation of the copper partitioning during the transport simulation.

While the linked CH3D+TICKET demonstrated its capability of simulating the fate and transport of metal (copper) dynamically with both the metal partitioning and the hydrodynamic transport including settling and deposition, it associates particulate metal (copper) with TSS. In other words, TSS is the bulk and the only vehicle to carry the particulate copper during the fate/transport before it settles and deposits to the bottom. However, in reality, particulate metals and contaminants in general, are sorbed with different sizes of the particles, namely, clay, silt, and sand, each with different partitioning and concentrations. Furthermore, these three sizes of particles and the associated contaminants have different settling velocities, resulting in different deposition rates. To evaluate the impacts from different sediment particle sizes on the fate and transport of the sediment plumes, we conducted the following analysis.

Simulated depositions of copper and nickel associated with the clay, silt, and sand particles can be estimated from the simulated deposition of the three particles and measured metal concentrations:

$$M = S_{clay}[K_{clay}] + S_{silt}[K_{silt}] + S_{sand}[K_{sand}],$$

where M is the total deposited metal, S_{clay} , S_{silt} , S_{sand} represent the simulated sediment deposited mass for clay, silt, and sand, respectively, and K_s represent the measured concentrations of metal associated with each of the particles, as subscripted. Figure 6-53 shows the measured concentrations and the averaged concentrations of copper associated with the sand, silt, and clay particles. Table 6-14 shows the summary of the averaged concentrations for copper and nickel used in the analysis.

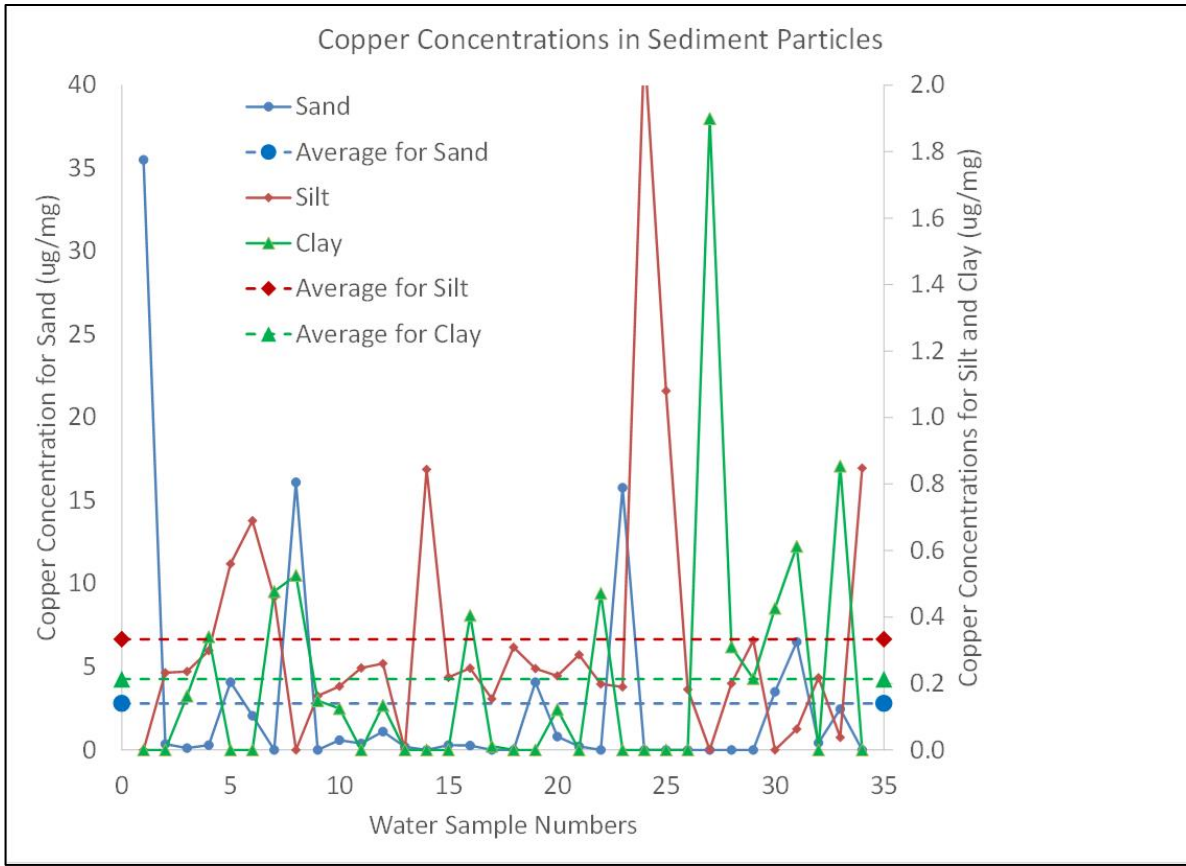


Figure 6-53. Copper concentrations associated with clay, silt, and sand particles from the field data.

Table 6-14. Average concentrations of copper and nickel associated with sand, silt, and clay particles based on field data.

	Copper ($\mu\text{g}/\text{mg}$)	Nickel ($\mu\text{g}/\text{mg}$)
Sand	2.80	2.07
Silt	0.33	0.10
Clay	0.21	0.73

Simulated dissolved and total copper concentrations were compared with measured values. Figure 6-54 shows the time series model results and the field data and Figure 6-55 shows the corresponding snapshot contours. Similar to those of the sediment results, simulated dissolved and total copper concentrations are in agreement with the measured values. Within one hour following the initial resuspension, copper concentrations in the resuspension pier region were in the range of [1–10 $\mu\text{g}/\text{l}$] for dissolved phase and in the range of [3–15 $\mu\text{g}/\text{l}$] for the total copper. Model predicted copper concentrations were smoothly varying in the vicinity of the pier region, whereas field data exhibits larger spatial variations. These variation have multiple causes. The near-field effect, which is not simulated by the model, was reflected in the field data. Spatial representation and resolution by the model grids also contribute to the spatial smoothness for the model results. In general, model-predicted copper concentrations in the water column compare well with the measured values, as shown in Figure 6-54 and Figure 6-55.

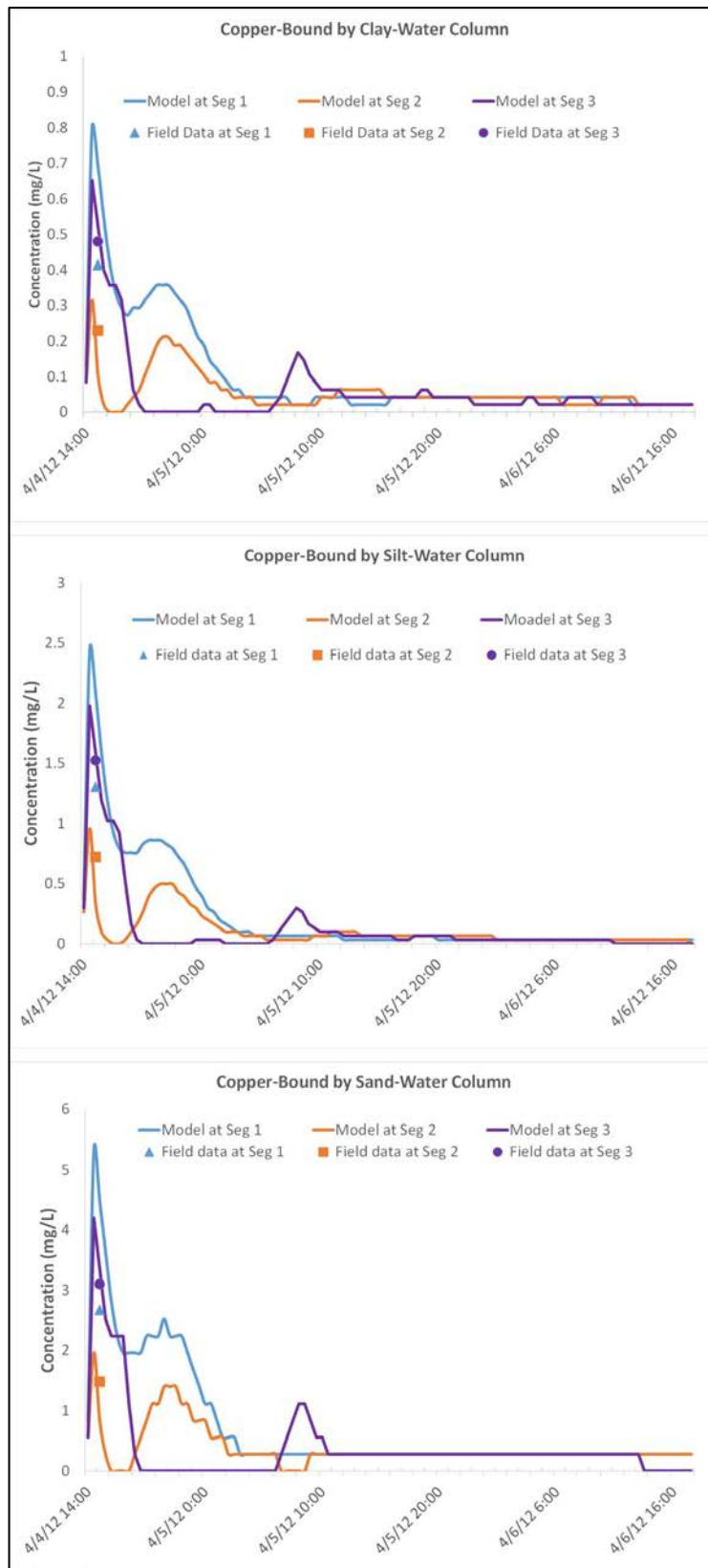


Figure 6-54. Model/data comparison of copper concentrations bound by clay (top), silt (middle), and sand (bottom) particles, respectively, for the three locations.

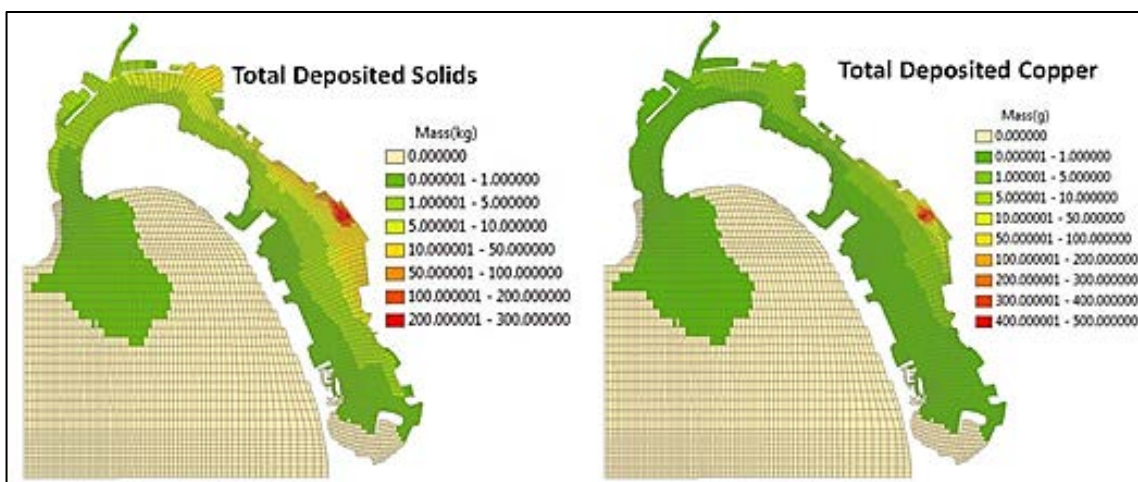


Figure 6-55. Comparison between total deposited solids and total deposited copper.

As discussed previously, once resuspended, the sediment plume in the pier region started to be flushed out of the region within 6 hours (half tidal cycle). After 6 hours, sediment concentrations decreased monotonically for the three particle sizes within the pier region, meaning the sediment was flushed out of the region and deposited to the bottom. After 24 hours following the resuspension event, copper concentrations of the pier water maintains at low values, less than 0.5, 0.2, and 0.1 $\mu\text{g/L}$, mostly in dissolved phases, before the end of the first day, second day, and third day, respectively.

The two primary reasons why the sediment plumes decayed fast within the pier region include the settling of the particles and the associated copper, and the hydrodynamic transport and dispersion. The metal contaminants in the sediment plumes resuspended by propeller wash are mostly associated with sediment particles. Once resuspended, these particles and the associated contaminants start settling and depositing to the bottom. This settling process removing contaminants from the water column dictated the decay of metal concentrations in the water column. Hydrodynamic processes further migrate and disperse the sediment plumes by the currents.

Figure 6-55 and Figure 6-56 show the comparison of deposition contours between TSS and copper and nickel, respectively. Concentrated deposition rate of TSS is centered around the pier region, and extends more toward the outer bay than the inner bay. Overall, deposited TSS mass is distributed in outer bay (62%), followed by inner bay (20%), and only 18% in the pier region, due to the relatively smaller area. In comparison, relative percentages of deposited copper (nickel) mass is highest in the outer bay at 50% (52%), followed by the in-pier region, 41% (34%), and only 9% (14%) gets deposited in the inner bay. The attenuated distribution of depositions between TSS and copper and nickel is due to the different partitioning and settling velocities among the three sizes of particles.

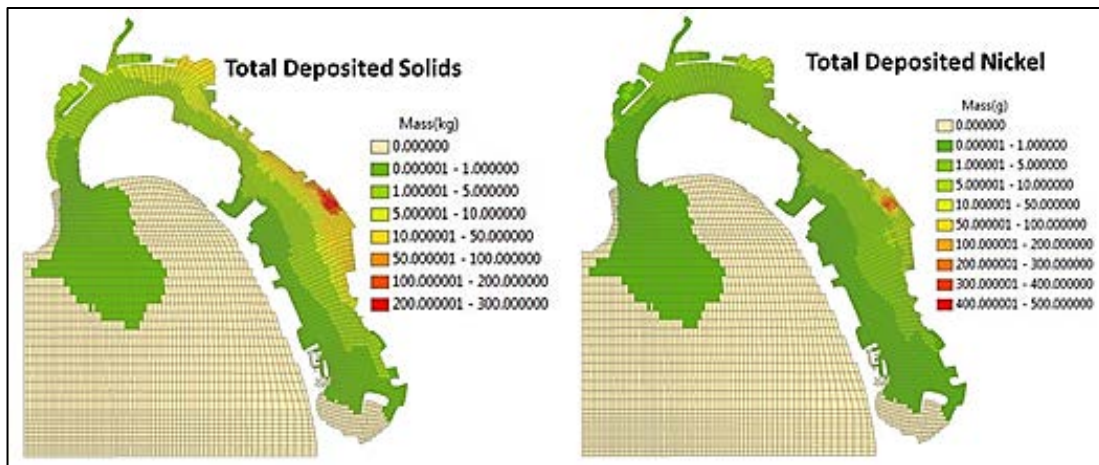


Figure 6-56. Comparison between total deposited solids and total deposited nickel.

Figure 6-57 shows the percentages of deposition from the resuspension in three different regions, the outer bay, the pier region and the inner bay. Most of the sand particles eroded by the propeller wash redeposited back into the pier region (60 %), with about 39.6% to the outer bay region, and only 0.6% to the inner bay, whereas only 4% of the clay particles redeposited back to the pier region, and the rest deposited into the outer and inner bay. Compared to the redeposition of the sediment mass, 40% of the particulate copper mass redeposited back into the pier region, and 50.3% and 9.1 % to the outer bay and inner bay, respectively. The uneven distribution of deposited copper masses between the outer bay and the inner bay primarily results from the asymmetry in flow patterns during the ebbing and flooding tides in San Diego Bay, a phenomenon observed and reported previously (Wang et al., 1998).

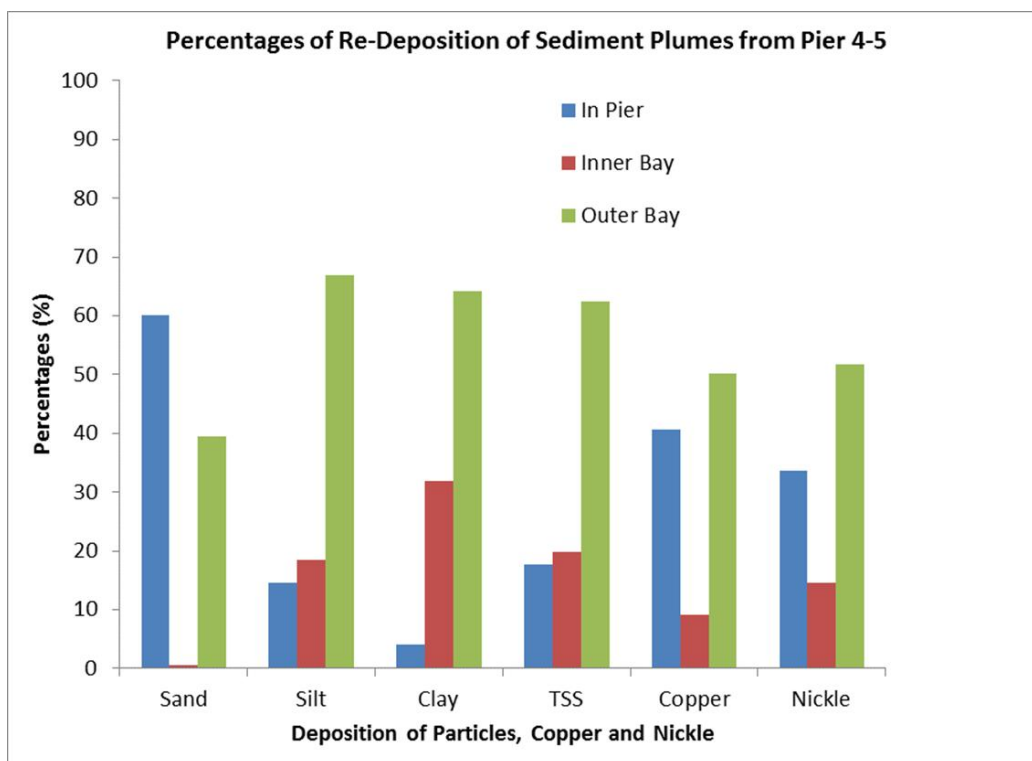


Figure 6-57. Percentages of deposition at the three regions (in-pier, outer bay, and inner bay) of the particles and copper and nickel.

The study for San Diego Bay includes two parts, resuspension potential by a tugboat and subsequent fate and transport of the sediment plumes. The Maynard's model, calibrated from the resuspension potential study (Section 6.2), was used to simulate resuspended sediment, copper, and nickel from the resuspension event, which took place with four controlled propeller speeds during the 33-min period on 4 April, 2012. Following the resuspension event, field data were measured during the 74-min window (14:14–15:28) at 17 stations in the vicinity of the pier region. It was observed (with photos) that during the period, the majority of the plume stayed within or in the vicinity of the entire pier region, defined by the pier wall and the lengths of the two piers. A sediment mass of 21571 kg, predicted by the Maynard's model, was introduced into the CH3D model to simulate subsequent fate and transport of the plume. Within the 74-min window when field data were measured, model-simulated water column concentrations of clay, silt, sand, and TSS were compared with the measured data with good agreement between the two. Such good agreement is significant because it validates the Maynard's model prediction of the 21,571 kg of sediment eroded by the tugboat, which is the first direct validation, that we know of, for the total eroded sediment mass by a tugboat using a validated model and field data. Second, the model/data agreement also validates the CH3D model for the three particles: clay, silt and sand, and the TSS. While CH3D has been demonstrated and validated with various hydrodynamic and/or water quality parameters in many previous studies, this is the first direct validation with three sediment particle sizes and TSS from the propeller wash study, all in good agreement with field data.

The linkage of CH3D with the metal partitioning model (Farley, 2015) is another new feature implemented and validated for this study. For collaboration, the metal chemistry data from the San Diego Bay field study were analyzed and processed into a format, which was sent to Professor Kevin Farley of the Manhattan College. Using the metal chemistry data, Professor Farley derived a

simple look-up table using the TICKET model that contains six variables, including total Cu, pH, DOC, POC, iron and salinity. To integrate the look-up table into CH3D, a simple equation was developed, based on the least-square method, which can readily calculate copper partitioning using the values of the six variables. The least-square equation was validated by comparing the results with the look-up table. A correlation of 100% between the estimates by the equation and the look-up table with $R^2 = 0.915$.

We applied the linked CH3D+TICKET model for the fate/transport of copper in the San Diego Bay study. Because only metal concentrations were measured for the field study, we used historical values for the other five variables, with the total copper concentrations as the only variable for the partitioning equation. Model results are in good agreement with field data for dissolved and total copper concentrations. Simulated particle-bound copper concentrations were also compared with measured data for clay, silt, and sand with similar levels of agreement. Trends of remigration and redeposition of the sediment plumes were simulated by the model as percentages of deposition in three regions, including in-pier, outer bay, and inner bay. As expected, sand particles tend to redeposit near the pier region where they were resuspended, clay and silt particles are more dispersed and redeposited over larger areas into the outer and inner bay. Compared to the TSS redeposition contour map, redeposited copper tends to concentrate in the vicinity of the pier region, due to the relatively larger copper concentrations associated with the sand particles.

6.3.2 Pearl Harbor

The Pearl Harbor effort had three notable differences from the work in San Diego Bay. The first was that the benthic SPI video camera was used to watch and measure bed erosion at the Bravo and Oscar Pier sites. The second was that the extrapolated sediment load and metal partitioning from the pump samples was used to provide initial conditions to CH3D model predictions, rather than validate CH3D predictions in San Diego Bay. The third difference is that suspended sediment concentrations (SSC), based on acoustic backscatter, were used as a qualitative check on CH3D predictions in Pearl Harbor. The other methods used in San Diego Bay are essentially identical to those used in Pearl Harbor (Figure 6-58).

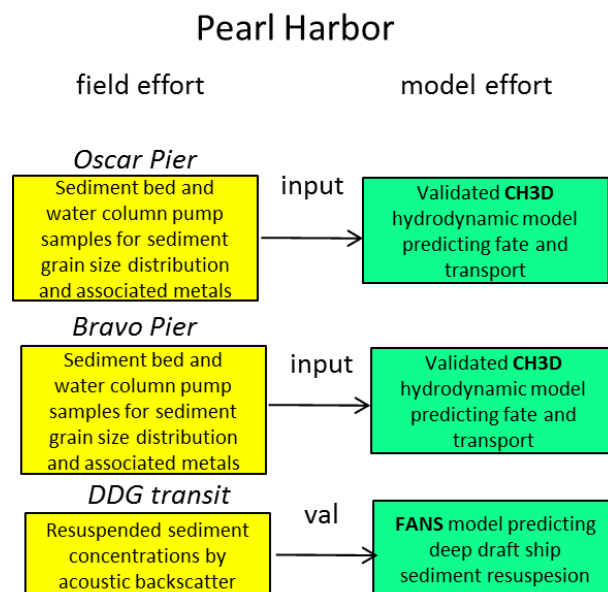


Figure 6-58. Field and model studies in Pearl Harbor.

6.3.2.1 Pump Sampled Resuspended Sediments

Pump samples similar to the one described above for San Diego Bay were collected at the multiple resuspension events of Bravo Pier and Oscar Pier in Pearl Harbor, HI, on 28 and 29 August 2012, respectively (Table 6-15 and Table 6-16). Pump samples were processed as they were in San Diego, where metal concentrations associated with sediment size fractions and in the dissolved state (passing a 0.4- μ m filter) were identified. Figure 6-59, Figure 6-60, and Table 6-17 compare the sediment size fractions and total organic carbon (TOC) between the San Diego Bay and Pearl Harbor sites, as well as between bed sediments and resuspended sediments captured in the pump samples.

Table 6-15. Sample identification, location, time, and mass fractions of the different particle sizes measured in samples from the Pearl Harbor resuspension event of 28 August 2012 at Bravo Pier.

Bravo Pier, Pearl Harbor, 28 August 2012						6 Sand	7 Silt	8 Clay	9 Total
Event	Sample ID	Sampling depth (ft)	Sampling Date and Time	Latitude	Longitude	60 μ m Mass Fraction (mg/L)	5 μ m Mass Fraction (mg/L)	0.4 μ m Mass Fraction (mg/L)	Total Mass Fraction (mg/L)
First Resuspension Event	1	3	8/28/12 10:40	21.35519	-157.94936	22.03	55.12	5.04	82.18
	2	15	8/28/12 10:41	21.35519	-157.94936	0.97	6.40	2.86	10.23
	3	3	8/28/12 10:45	21.35562	-157.94884	5.63	18.33	4.91	28.87
	4	15	8/28/12 10:46	21.35562	-157.94884	3.37	11.33	4.60	19.30
	5	3	8/28/12 10:50	21.35559	-157.94874	14.28	39.50	5.50	59.28
	6	15	8/28/12 10:51	21.35559	-157.94874	8.33	30.00	4.07	42.40
Second Resuspension Event	7	3	8/28/12 11:03	21.35492	-157.94861	7.54	35.91	2.40	45.85
	8	15	8/28/12 11:04	21.35492	-157.94861	13.19	40.00	4.60	57.79
	9	3	8/28/12 11:05	21.35542	-157.94893	38.10	70.00	7.60	115.70
	10	15	8/28/12 11:06	21.35542	-157.94893	2.73	25.00	8.00	35.73
	11	3	8/28/12 11:07	21.35595	-157.94889	14.30	19.20	5.14	38.64
	12	15	8/28/12 11:08	21.35595	-157.94889	10.58	37.33	6.60	54.51
Third Resuspension Event	13	15	8/28/12 11:51	21.35512	-157.94920	8.17	28.00	5.80	41.97
	14	15	8/28/12 11:53	21.35550	-157.94871	24.25	63.00	9.00	96.25
	15	15	8/28/12 11:55	21.35542	-157.94815	41.57	80.67	9.20	131.44
	16	15	8/28/12 11:56	21.35554	-157.94820	36.63	68.67	2.40	107.69
	17	15	8/28/12 0:04	21.35562	-157.94794	17.60	43.00	2.80	63.40
	18	15	8/28/12 0:11	21.35696	-157.94902	6.60	27.33	1.80	35.73
	19	15	8/28/12 0:19	21.35694	-157.94997	11.70	5.20	0.40	17.30
	20	15	8/28/12 0:27	21.35693	-157.95011	2.21	14.00	1.79	18.00

Table 6-16. Sample identification, location, time, and mass fractions of the different particle sizes measured in samples from the Pearl Harbor resuspension event of 29 August 2012 at Oscar Pier.

Oscar Pier, Pearl Harbor, 29 August 2012						6 Sand	7 Silt	8 Clay	9 Total
Event	Sample ID	Sampling depth (ft)	Sampling Date and Time	Latitude	Longitude	60 μ m Mass Fraction (mg/L)	5 μ m Mass Fraction (mg/L)	0.4 μ m Mass Fraction (mg/L)	Total Mass Fraction (mg/L)
First Resuspension Event	21	3	8/29/12 9:31	21.34516	-157.96727	2.19	13.40	0.85	16.44
	22	15	8/29/12 9:32	21.34505	-157.96750	0.66	2.59	0.30	3.55
	23	3	8/29/12 9:34	21.34495	-157.96813	13.74	23.50	1.44	38.68
	24	15	8/29/12 9:35	21.34492	-157.96824	2.97	9.22	0.80	12.99
	25	3	8/29/12 9:37	21.34475	-157.96860	1.27	5.76	0.50	7.53
	26	15	8/29/12 9:38	21.34460	-157.96868	0.07	1.80	0.22	2.09
Second Resuspension Event	27	3	8/29/12 10:34	21.34526	-157.96704	0.03	3.80	0.53	4.37
	28	15	8/29/12 10:35	21.34512	-157.96745	3.59	9.36	0.00	12.95
	29	3	8/29/12 10:36	21.34488	-157.96768	1.64	8.00	0.11	9.75
	30	15	8/29/12 10:37	21.34466	-157.96786	0.60	1.66	0.97	3.23
	31	3	8/29/12 10:41	21.34506	-157.96832	2.94	6.30	0.75	9.99
	32	15	8/29/12 10:42	21.34513	-157.96831	1.49	6.12	0.13	7.74
Third Resuspension Event	33	15	8/29/12 11:36	21.34469	-157.96816	3.11	7.78	0.12	11.01
	34	15	8/29/12 11:37	21.34442	-157.96844	5.19	16.15	0.14	21.49
	35	15	8/29/12 11:39	21.34441	-157.96863	3.23	9.37	0.00	12.60
	36	15	8/29/12 11:40	21.34440	-157.96863	0.07	5.78	0.65	6.50
	37	15	8/29/12 11:41	21.34442	-157.96880	1.41	8.25	0.44	10.10
	38	15	8/29/12 11:43	21.34450	-157.96912	3.35	6.71	0.11	10.17
	39	15	8/29/12 11:54	21.34489	-157.96939	0.00	3.03	2.00	5.03
	40	15	8/29/12 12:01	21.34475	-157.96978	0.00	2.22	1.50	3.72

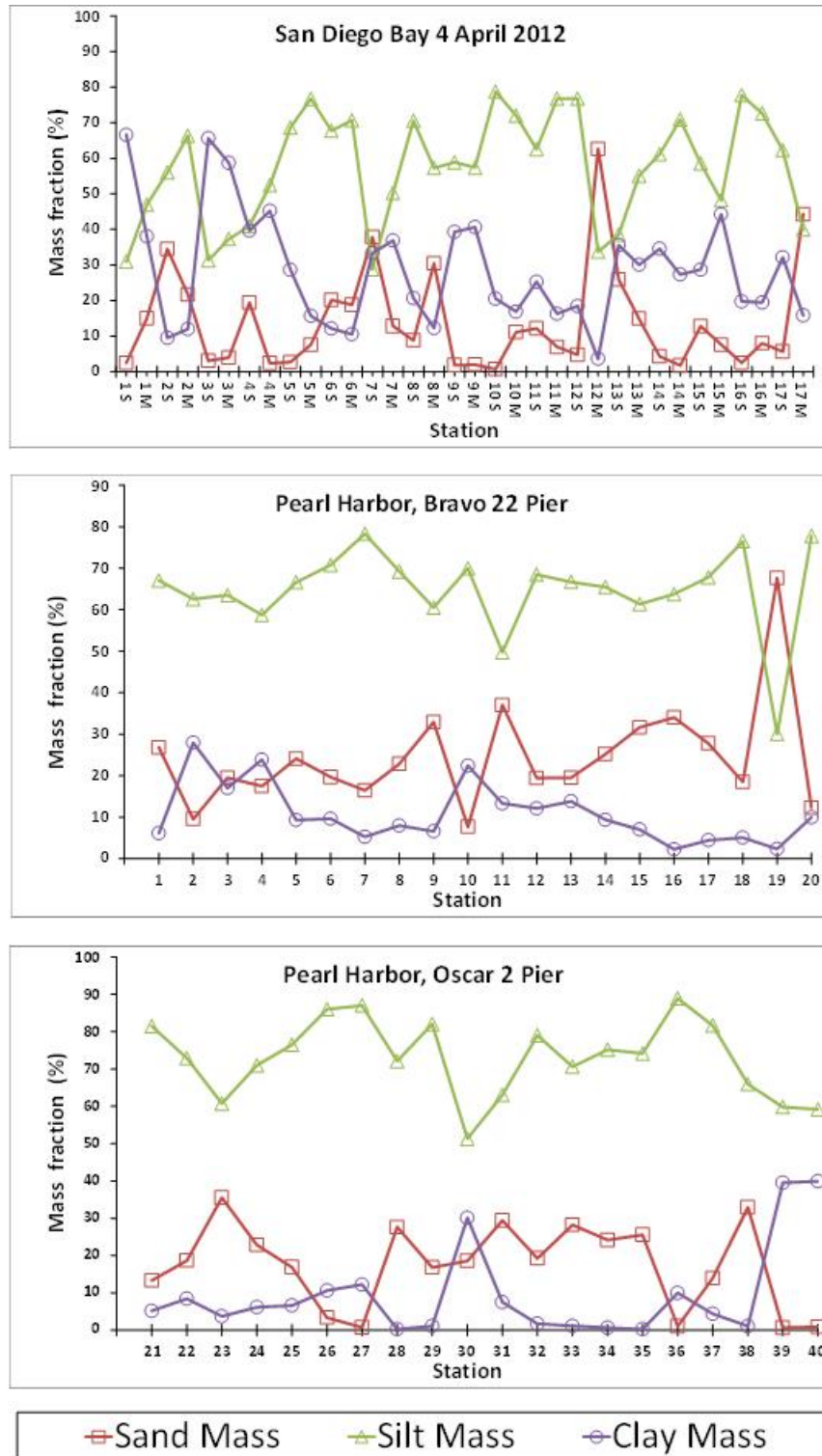


Figure 6-59. Mass fraction (%) of the sand, silt, and clay fractions sampled in the three resuspension events.

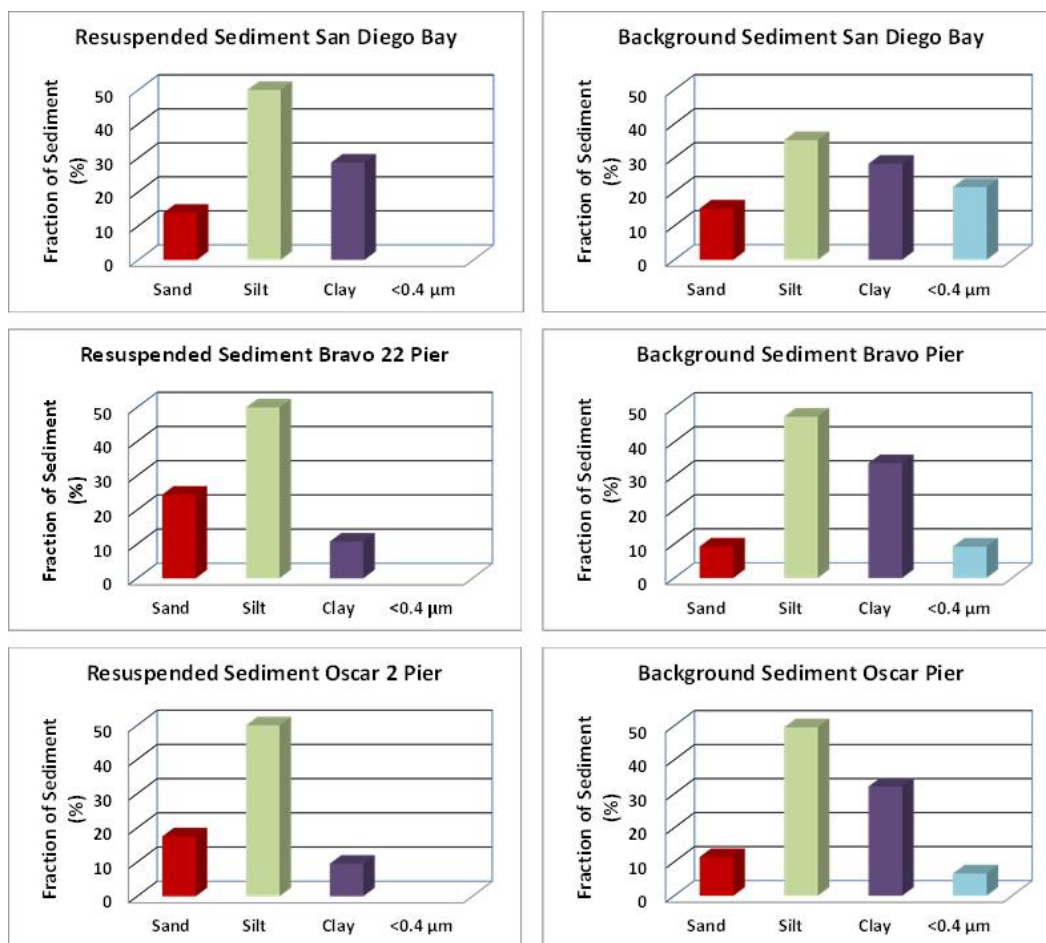


Figure 6-60. Average mass fraction (%) of the sand, silt, and clay fractions sampled in the three resuspension events on the left, and from background sediments sampled before the resuspension events on the right.

Table 6-17. Particle size fractionation and total organic carbon (TOC) measured prior to resuspension from the three sites selected for this study. Data for Oscar Pier is from one sample, and was not analyzed for TOC.

	San Diego Bay, CA		Bravo Pier, HI		Oscar Pier, HI	
	Average (%)	Std. Dev. (%)	Average (%)	Std. Dev. (%)	Average (%)	Std. Dev. (%)
Sand (>60μm)	15.10	4.88	9.3	3.77	11.4	N/A
Silt (5 to 60 μm)	35.2	3.43	47.4	0.22	49.6	N/A
Clay (0.4 to 5 μm)	28.3	2.32	33.7	2.40	32.1	N/A
<0.4 μm	21.4	5.92	9.2	1.26	6.6	N/A
TOC	1.8	0.15	1.5	0.32	N/A	N/A

6.3.2.2 Size Fraction Distribution of Metals

Table 6-18 lists background metal concentrations at the two piers. Figure 6-61 through Figure 6-64 show the mass percent of the recovered metals distributed among the sediment size classes. Note that the resuspension events in Pearl Harbor were done in triplicate at each site, and even with this replication, the metal distribution between the different particle size-fractions is dependent on the metal as well. Chromium, nickel, and silver are mostly (~80%) present in the dissolved (<0.4 μm) fraction in both resuspension sites (Figure 6-61 and Figure 6-63), although, there were some instances when their distributions were dominated by the sand (>60 μm) or clay (0.4 to 5 μm) size-fractions during the resuspension events at Oscar Pier (Figure 6-63). Cadmium also appears dominated by both the dissolved (<0.4 μm) and the sand (>60 μm) fractions, with a short time period also by the clay (0.4 to 5 μm) fraction, especially in the Bravo Pier resuspension events (Figure 6-62). Lead distribution in both Pearl Harbor sites is dominated by the particle fractions, with minimal contribution by the dissolved (<0.4 μm) fraction. Copper, arsenic, and zinc are distributed more evenly between the four size-fractions, which is more evident in the distributions from Bravo Pier than in those from Oscar Pier.

Most metals were present at levels considered with low potential for concern as compared to accepted water quality criteria (Table 6-7). Figure 6-65 through Figure 6-68). Zinc, arsenic, silver, and cadmium were present at concentrations below the USEPA water quality criteria. Copper is above the USEPA water quality criteria in the resuspension events at Bravo Pier, but below or similar at Oscar Pier. Lead had few concentrations similar to the USEPA water quality criterion at Bravo Pier, but below this criterion at Oscar Pier. Only chromium and nickel were consistently over their respective water quality criteria in the six resuspension events studied in Pearl Harbor.

Once again, resuspension events caused by propeller wash in Pearl Harbor are able to affect metal concentrations above ambient conditions. Similar to the San Diego Bay resuspension event, all the metals had concentrations above ambient levels in all the resuspension events in Pearl Harbor. The only metal with concentration at the same levels as ambient was cadmium in the resuspension events at Bravo Pier.

Concentrations of organic COCs were undetectable. PCBs were believed to be a potential CoC in Pearl Harbor. Selected PCBs and pesticides measured in samples from the resuspension events from both Pearl Harbor sites were below the laboratory method detection level (Table 6-19 and Table 6-20).

These results indicate that concentrations of these organic COCs should be of no concern with respect to sediment resuspension events, at least for the two sites tested.

Table 6-18. Metal concentrations measured in aqua regia digestates from background sediments from Bravo Pier and Oscar Pier in Pearl Harbor. All data is provided in µg/gr but for recoveries that are given as %. Certified are certified concentrations. Silver is not certified in SRMs BCSS-1 and PACS-1.

		Cr (µg/g)	Ni (µg/g)	Cu (µg/g)	Zn (µg/g)	As (µg/g)	Ag (µg/g)	Cd (µg/g)	Pb (µg/g)
Bravo Pier Total	Average	86.4	54.0	97.8	290	13.0	0.67	0.82	53.0
	Std. Dev.	5.5	3.8	62.2	100	1.1	0.43	0.20	35.1
Bravo Pier <60µm	Average	89.9	56.2	93.3	344	13.8	0.84	1.10	52.8
	Std. Dev.	1.4	2.4	40.3	82	0.5	0.56	0.25	32.2
Bravo Pier <0.4µm	Average	27.9	14.1	29.3	1165	33.7	1.70	5.31	25.3
	Std. Dev.	7.5	3.3	4.7	220	3.4	0.23	0.62	15.2
Oscar Pier Total	Average	51.8	33.2	49.0	225	10.5	0.32	0.41	41.8
	Std. Dev.	9.2	6.2	8.6	34	2.7	0.06	0.09	4.7
Oscar Pier <60µm	Average	44.2	28.6	41.4	207	9.5	0.32	0.47	31.5
	Std. Dev.	2.9	0.7	10.8	19	0.4	0.02	0.05	3.9
Oscar Pier <0.4µm	Average	22.9	11.1	24.3	1406	32.9	1.32	4.90	10.4
	Std. Dev.	5.2	2.2	6.5	263	5.9	0.09	0.79	2.9
Blanks (n = 5)	Average	0.062	0.080	0.60	16.3	0.58	0.0052	0.081	0.050
	Std. Dev.	0.039	0.0031	0.21	9.2	0.039	0.0029	0.0025	0.0077
BCSS-1 (n = 3)	Certified	123	55.3	18.5	119	11.1		0.25	22.7
	Average	27.6	32.0	12.3	175	10.0	0.09	0.5	14.2
	Std. Dev.	1.8	1.7	0.7	2	0.6	0.02	0.0	1.1
	Recovery (%)	22	58	67	147	90		208	63
MESS-2 (n = 3)	Certified	106	49.3	39.3	172	20.7	0.18	0.24	21.9
	Average	15.1	29.6	29.0	219	17.3	0.10	0.5	13.0
	Std. Dev.	1.0	3.5	1.9	29	1.2	0.02	0.1	0.7
	Recovery (%)	14	60	74	127	83	56	217	59
PACS-1 (n = 3)	Certified	113	44.1	452	824	211		2.38	404
	Average	34.2	22.9	291.8	835	140	1.19	2.95	268
	Std. Dev.	2.3	1.7	21.1	9	5	0.04	0.13	19
	Recovery (%)	30	52	65	101	66		124	66

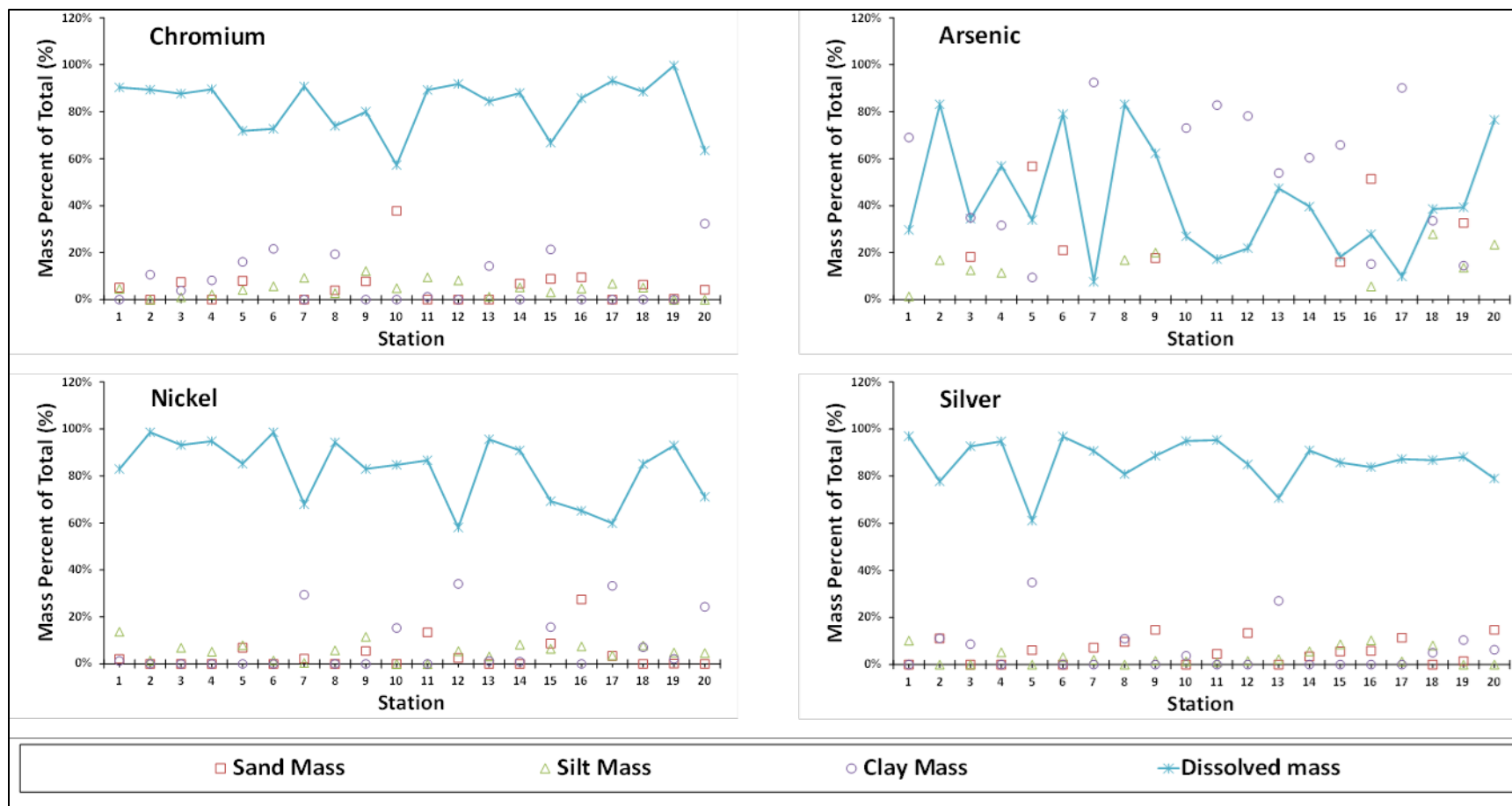


Figure 6-61. Chromium, arsenic, nickel, and silver distributions in the different particle size-fractions collected from the resuspension event of 28 August 2012 at Bravo 2 Pier in Pearl Harbor. The metal content in each fraction is calculated with the total fraction as the sum of all fractions.

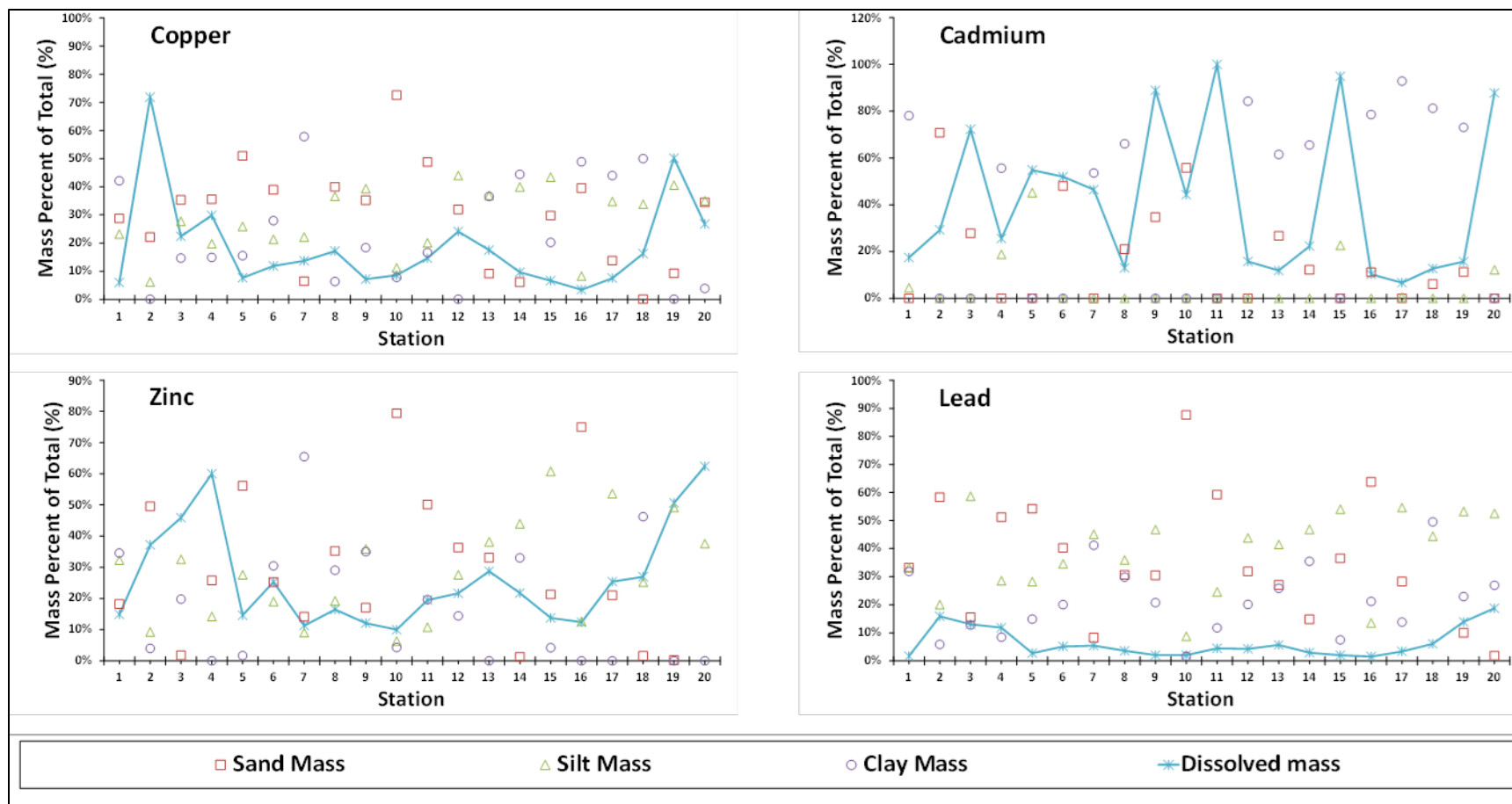


Figure 6-62. Copper, cadmium, zinc, and lead distributions in the different particle size-fractions collected from the resuspension event of 28 August 2012 at Bravo 2 Pier in Pearl Harbor. The metal content in each fraction is calculated with the total fraction as the sum of all fractions.

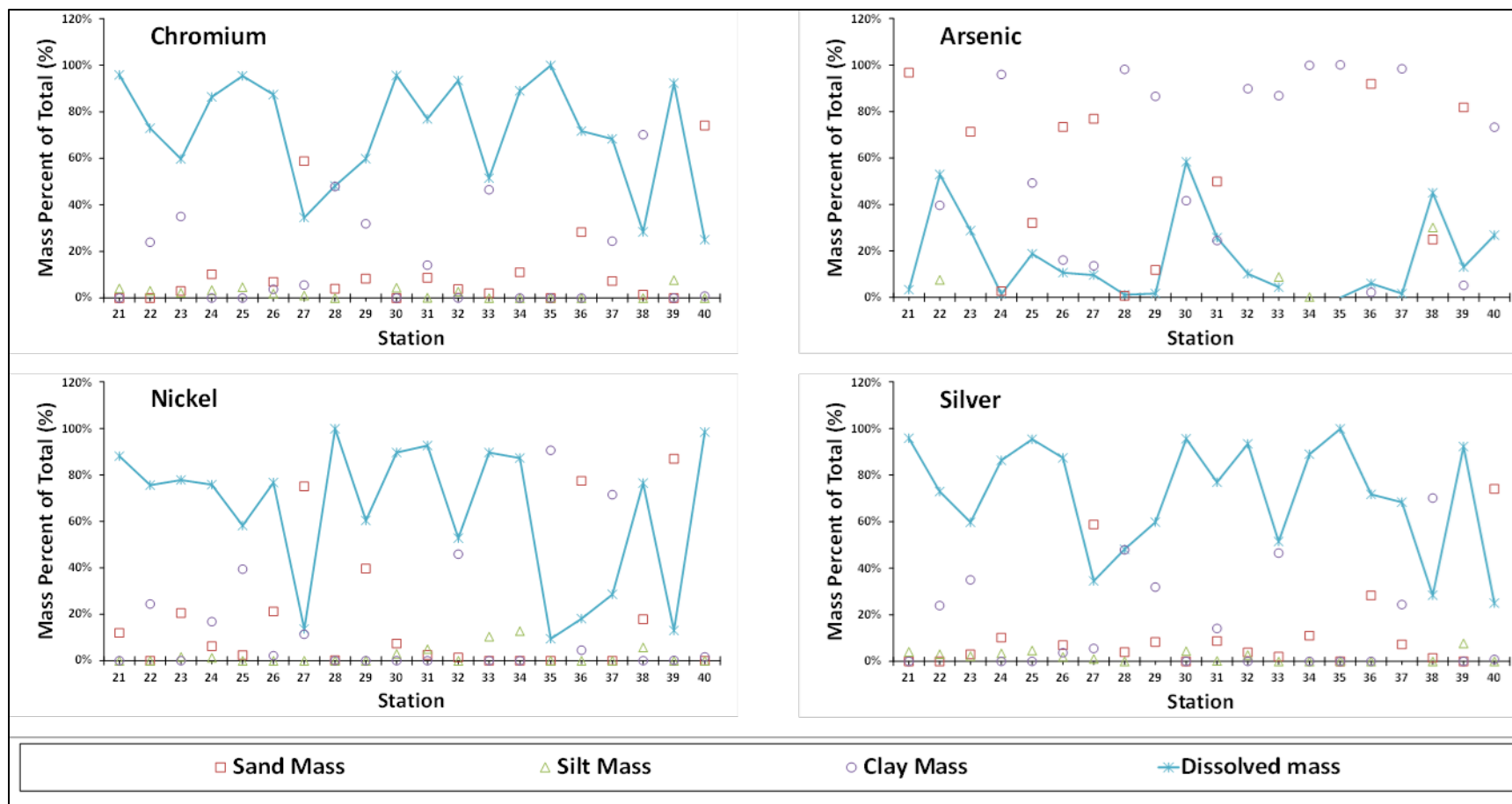


Figure 6-63. Chromium, arsenic, nickel, and silver distributions in the different particle size-fractions collected from the resuspension event of 29 August 2012 at Oscar 22 Pier in Pearl Harbor. The metal content in each fraction is calculated with the total fraction as the sum of all fractions.

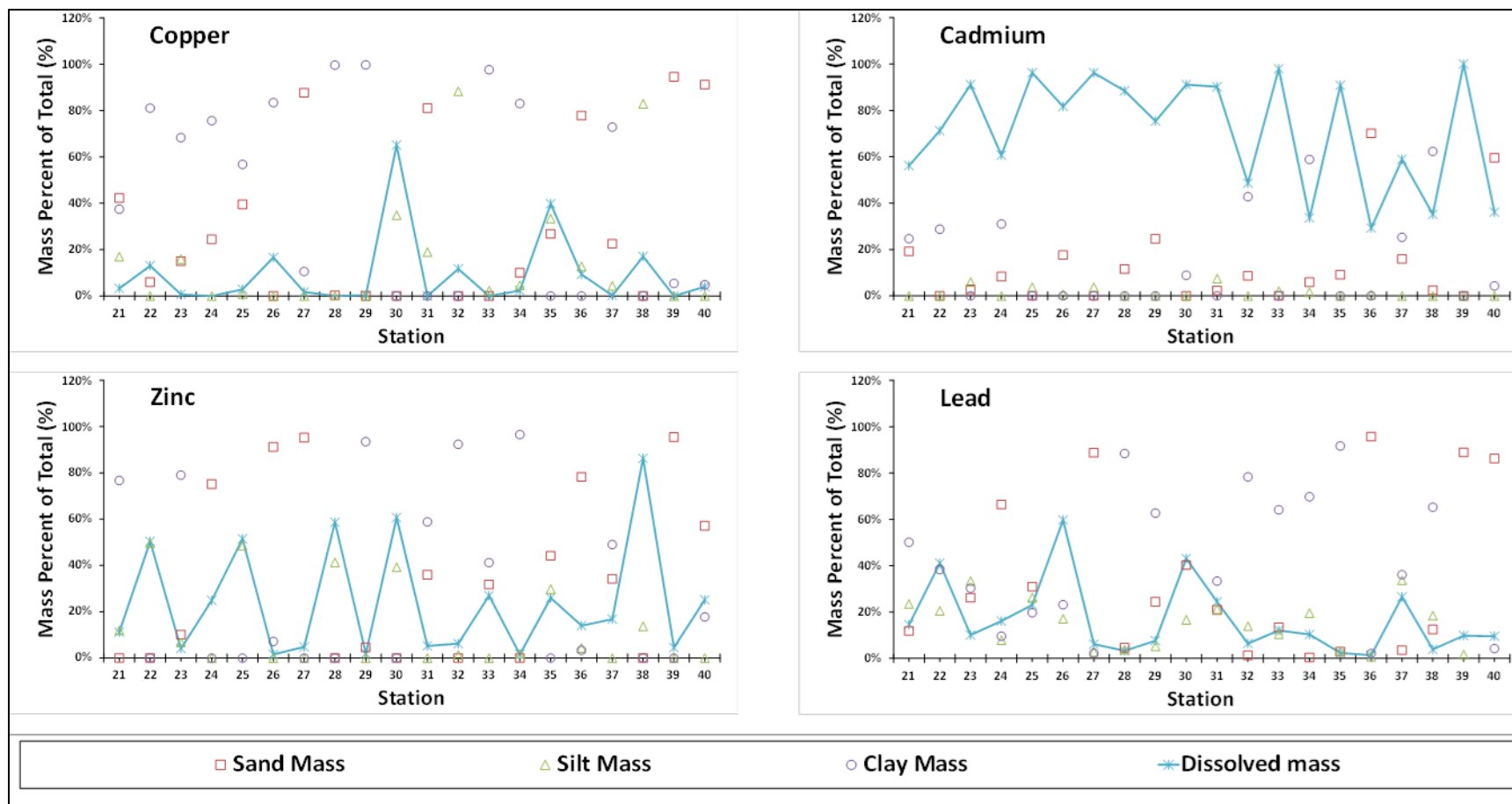


Figure 6-64. Copper, cadmium, zinc, and lead distributions in the different particle size-fractions collected from the resuspension event of 29 August 2012 at Oscar 22 Pier in Pearl Harbor. The metal content in each fraction is calculated with the total fraction as the sum of all fractions.

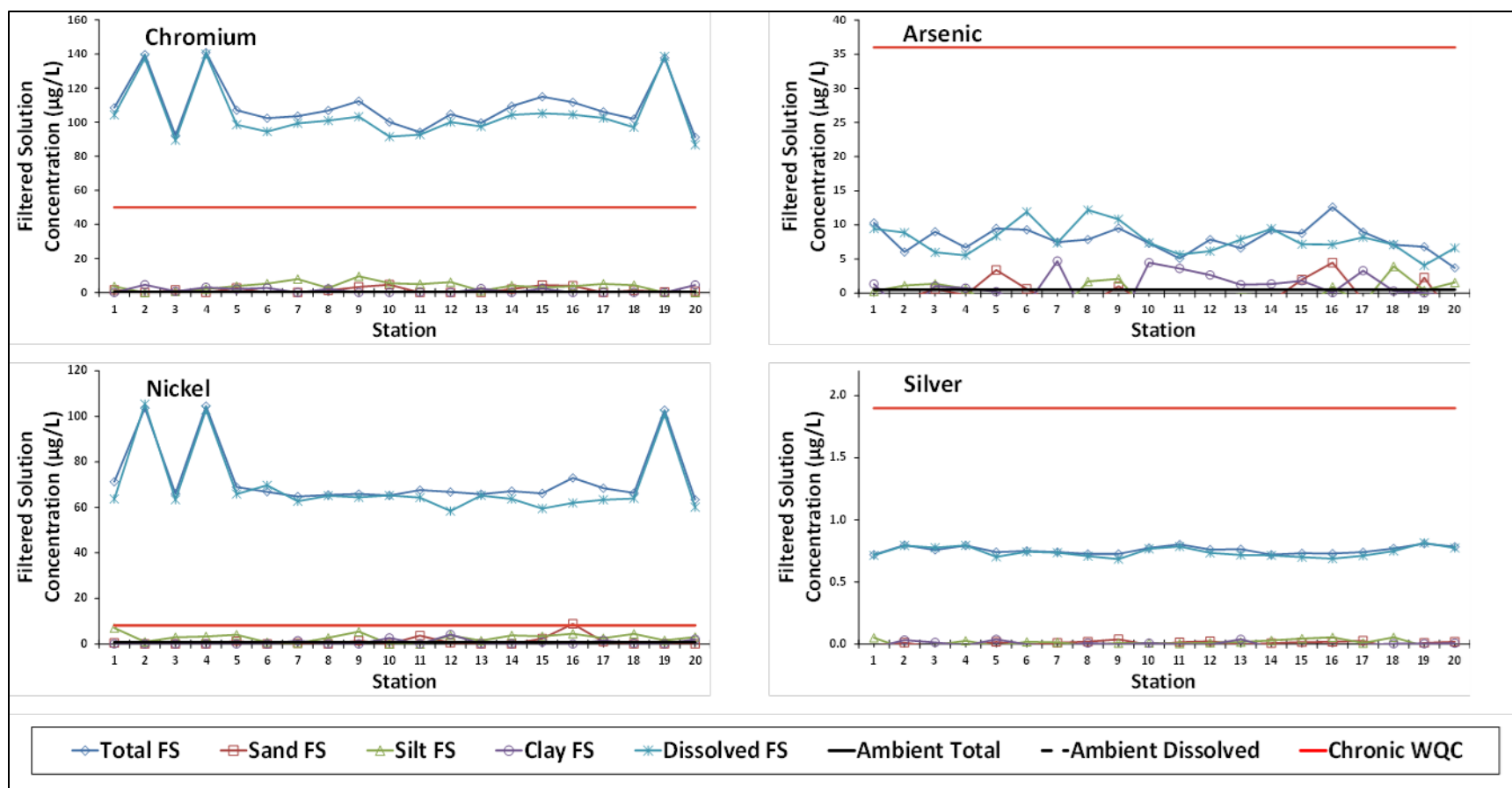


Figure 6-65. Chromium, arsenic, nickel, and silver concentrations in the filtered solution (FS) for each different particle size-fractions collected from the resuspension event of 28 August 2012 at Bravo 2 Pier in Pearl Harbor. Ambient Total and Ambient Dissolved are from samples collected prior to the resuspension event. The USEPA Chronic Water Quality Criterion is provided as a measure of the potential concern derived from these quantifications.

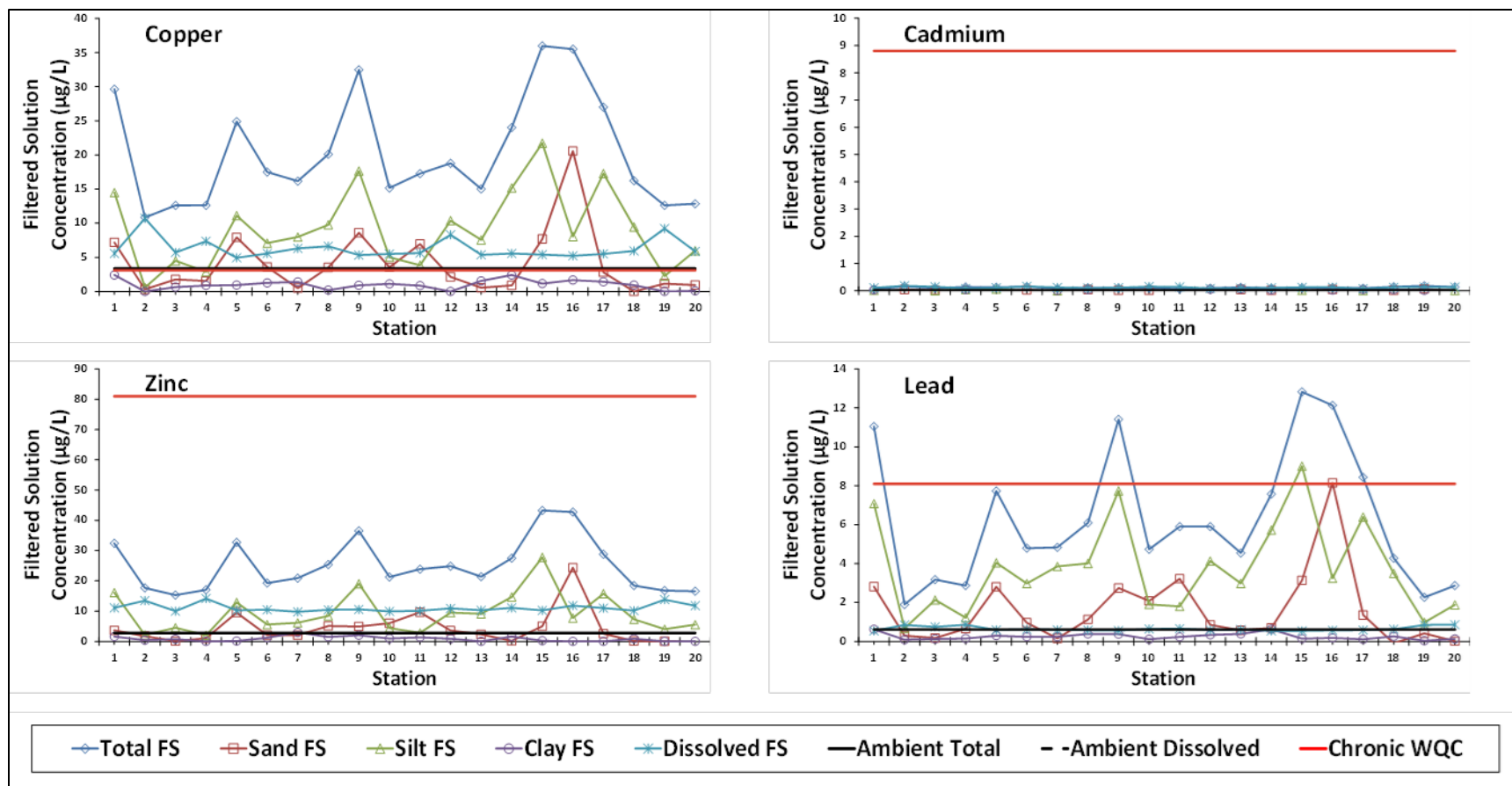


Figure 6-66. Copper, cadmium, zinc and lead concentrations in the filtered solution (FS) for each different particle size-fractions collected from the resuspension event of 28 August 2012 at Bravo 2 Pier in Pearl Harbor. Ambient Total and Ambient Dissolved are from samples collected prior to the resuspension event. The USEPA Chronic Water Quality Criterion is provided as a measure of the potential concern derived from these quantifications.

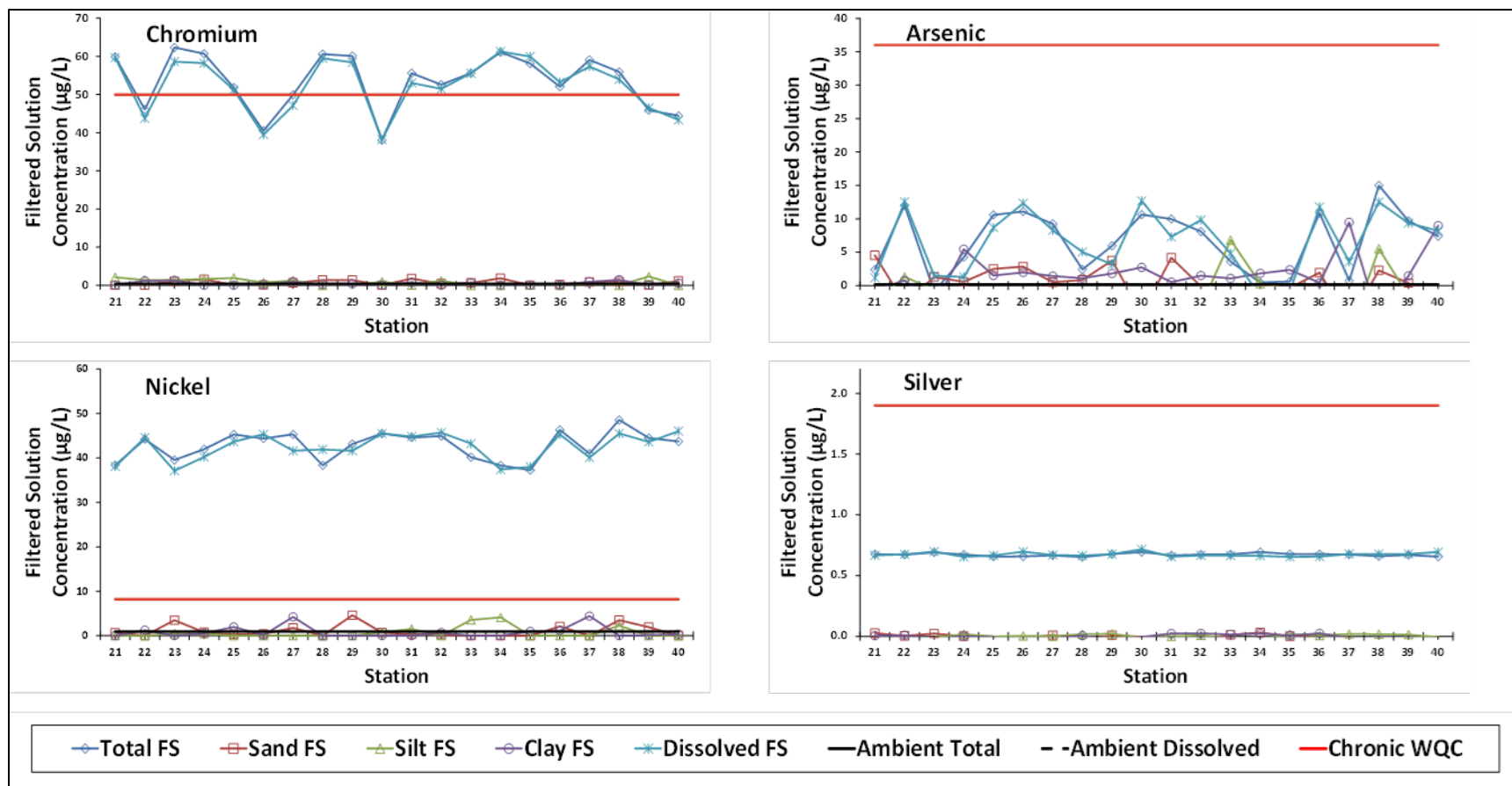


Figure 6-67. Chromium, arsenic, nickel, and silver concentrations in the filtered solution (FS) for each different particle size-fractions collected from the resuspension event of 28 August 2012 at Oscar 22 Pier in Pearl Harbor. Ambient Total and Ambient Dissolved are from samples collected prior to the resuspension event. The USEPA Chronic Water Quality Criterion is provided as a measure of the potential concern derived from these quantifications.

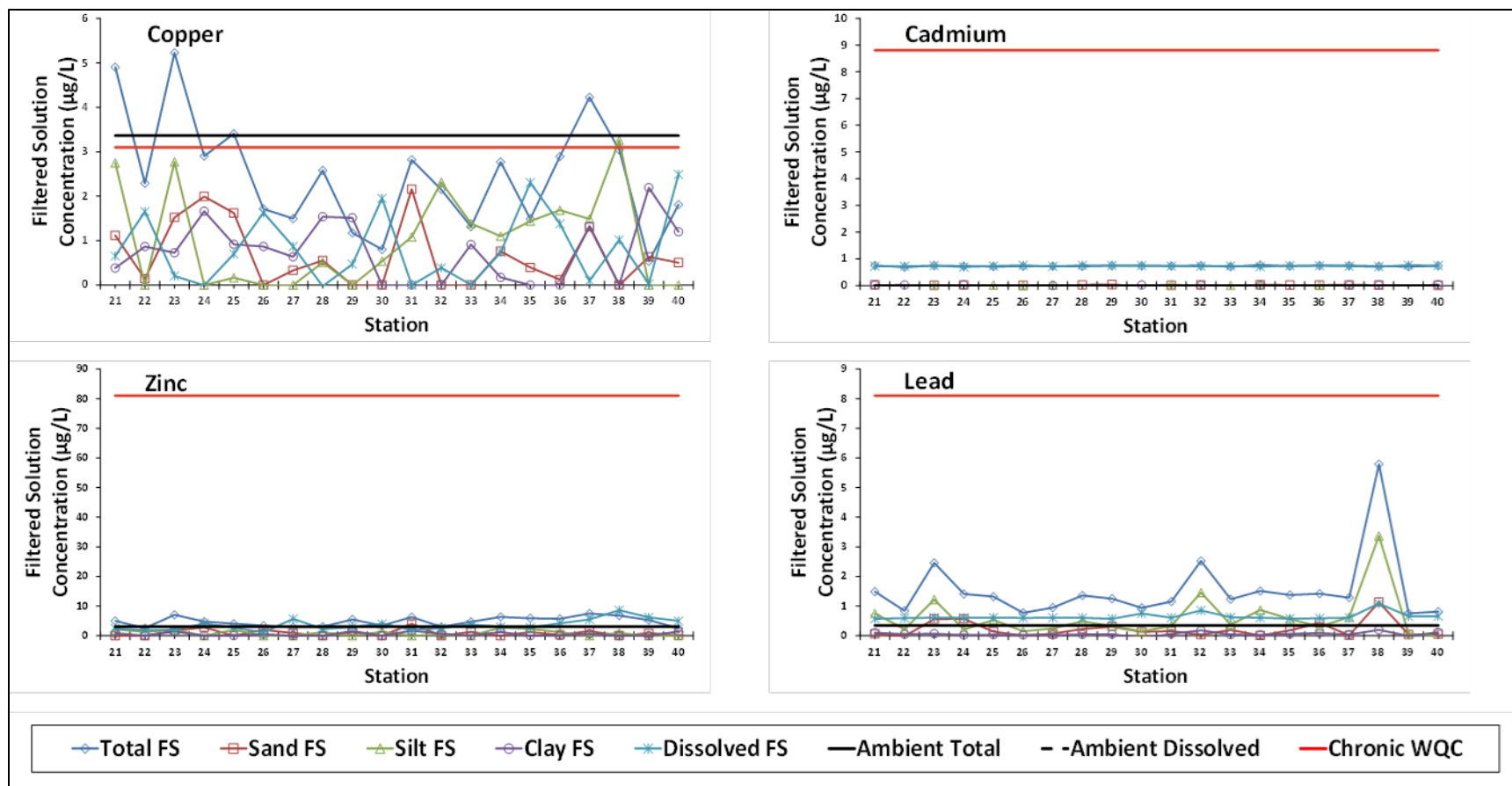


Figure 6-68. Copper, cadmium, zinc and lead concentrations in the filtered solution (FS) for each different particle size-fractions collected from the resuspension event of 28 August 2012 at Oscar 22 Pier in Pearl Harbor. Ambient Total and Ambient Dissolved are from samples collected prior to the resuspension event. The USEPA Chronic Water Quality Criterion is provided as a measure of the potential concern derived from these quantifications.

Table 6-19. Method detection limits (MDL, µg/L) for the samples analyzed for the NOAA-18 polychlorinated biphenyls (PCB) and pesticides from the Bravo Pier event of 28 August 2012. All the samples were qualified as undetected. B is background, 2 in the Size-Fraction column indicates that only the 2-mm fraction was analyzed, All is all the fractions analyzed, x means analyzed, - means not-analyzed.

Sample ID	Sampling Event	Sample Depth (ft)	Size-Fraction (2 mm or All)	TOTAL PCB NOAA-18	PCB-101	PCB-105	PCB-118	PCB-128	PCB-138	PCB-153	PCB-170	PCB-18	PCB-180	PCB-187	PCB-195	PCB-206	PCB-206	PCB-28	PCB-44	PCB-52	PCB-66	PCB-8	DIELDRIN	ENDOSULFAN I	ENDOSULFAN II	ENDOSULFAN SULFATE	TOTAL ENDOSULFAN
MDL				0.360	0.390	0.390	0.520	0.400	0.500	0.360	0.500	0.460	0.390	0.390	0.490	0.530	0.380	0.420	0.530	0.460	0.430	0.460	0.010	0.010	0.004	0.010	0.004
1		3	2	x	x	x	x	x	x	x	x	x	x	x	x	x	x	x	x	x	x	x	-	-	-	-	-
1	1	3	All	x	x	x	x	x	x	x	x	x	x	x	x	x	x	x	x	x	x	x	-	-	-	-	-
2	1	15	2	x	x	x	x	x	x	x	x	x	x	x	x	x	x	x	x	x	x	x	-	-	-	-	-
3	1	3	2	x	x	x	x	x	x	x	x	x	x	x	x	x	x	x	x	x	x	x	-	-	-	-	-
4	1	15	2	x	x	x	x	x	x	x	x	x	x	x	x	x	x	x	x	x	x	x	-	-	-	-	-
5	1	3	2	x	x	x	x	x	x	x	x	x	x	x	x	x	x	x	x	x	x	x	-	-	-	-	-
6	1	15	2	x	x	x	x	x	x	x	x	x	x	x	x	x	x	x	x	x	x	x	-	-	-	-	-
7	2	3	2	x	x	x	x	x	x	x	x	x	x	x	x	x	x	x	x	x	x	x	-	-	-	-	-
8	2	15	2	x	x	x	x	x	x	x	x	x	x	x	x	x	x	x	x	x	x	x	-	-	-	-	-
9	2	3	2	x	x	x	x	x	x	x	x	x	x	x	x	x	x	x	x	x	x	x	-	-	-	-	-
10	2	15	2	x	x	x	x	x	x	x	x	x	x	x	x	x	x	x	x	x	x	x	-	-	-	-	-
11	2	3	2	x	x	x	x	x	x	x	x	x	x	x	x	x	x	x	x	x	x	x	-	-	-	-	-
12	2	15	2	x	x	x	x	x	x	x	x	x	x	x	x	x	x	x	x	x	x	x	-	-	-	-	-
13	3	15	All	x	x	x	x	x	x	x	x	x	x	x	x	x	x	x	x	x	x	x	x	x	x	x	x
14	3	15	2	x	x	x	x	x	x	x	x	x	x	x	x	x	x	x	x	x	x	x	-	-	-	-	-
15	3	15	2	x	x	x	x	x	x	x	x	x	x	x	x	x	x	x	x	x	x	x	-	-	-	-	-
16	3	15	All	x	x	x	x	x	x	x	x	x	x	x	x	x	x	x	x	x	x	x	-	-	-	-	-
17	3	15	2	x	x	x	x	x	x	x	x	x	x	x	x	x	x	x	x	x	x	x	-	-	-	-	-
18	3	15	2	x	x	x	x	x	x	x	x	x	x	x	x	x	x	x	x	x	x	x	-	-	-	-	-
19	3	15	2	x	x	x	x	x	x	x	x	x	x	x	x	x	x	x	x	x	x	x	-	-	-	-	-
20	3	15	2	x	x	x	x	x	x	x	x	x	x	x	x	x	x	x	x	x	x	x	-	-	-	-	-

Table 6-20. Method detection limits (MDL, µg/L) for the samples analyzed for the NOAA-18 PCB and pesticides from the Oscar Pier event of 29 August 2012. All the samples were qualified as undetected. B is background, 2 in the Size-Fraction column indicates that only the 2-mm fraction was analyzed, All is all the fractions analyzed, x means analyzed, - means not-analyzed.

Sample ID				MDL	TOTAL PCB NOAA-18	PCB-101	PCB-105	PCB-118	PCB-128	PCB-138	PCB-153	PCB-170	PCB-18	PCB-180	PCB-187	PCB-195	PCB-206	PCB-206	PCB-28	PCB-44	PCB-52	PCB-66	PCB-8	DIELDRIN	ENDOSULFAN I	ENDOSULFAN II	ENDOSULFAN SULFATE	TOTAL ENDOSULFAN
Sampling Event																												
Sample Depth (ft)																												
Size-Fraction (2 mm or All)																												
B		3	2	x	x	x	x	x	x	x	x	x	x	x	x	x	x	x	x	x	x	x	x	-	-	-	-	
21	1	3	All	x	x	x	x	x	x	x	x	x	x	x	x	x	x	x	x	x	x	x	x	-	-	-	-	
22	1	15	All	x	x	x	x	x	x	x	x	x	x	x	x	x	x	x	x	x	x	x	x	-	-	-	-	
23	1	3	2	x	x	x	x	x	x	x	x	x	x	x	x	x	x	x	x	x	x	x	x	-	-	-	-	
24	1	15	2	x	x	x	x	x	x	x	x	x	x	x	x	x	x	x	x	x	x	x	x	-	-	-	-	
25	1	3	2	x	x	x	x	x	x	x	x	x	x	x	x	x	x	x	x	x	x	x	x	-	-	-	-	
26	1	15	2	x	x	x	x	x	x	x	x	x	x	x	x	x	x	x	x	x	x	x	x	-	-	-	-	
27	2	3	All	x	x	x	x	x	x	x	x	x	x	x	x	x	x	x	x	x	x	x	x	-	-	-	-	
28	2	15	2	x	x	x	x	x	x	x	x	x	x	x	x	x	x	x	x	x	x	x	x	x	x	x	x	
29	2	3	2	x	x	x	x	x	x	x	x	x	x	x	x	x	x	x	x	x	x	x	x	x	x	x	x	
30	2	15	2	x	x	x	x	x	x	x	x	x	x	x	x	x	x	x	x	x	x	x	x	-	-	-	-	
31	2	3	2	x	x	x	x	x	x	x	x	x	x	x	x	x	x	x	x	x	x	x	x	-	-	-	-	
32	2	15	2	x	x	x	x	x	x	x	x	x	x	x	x	x	x	x	x	x	x	x	x	-	-	-	-	
33	3	15	2	x	x	x	x	x	x	x	x	x	x	x	x	x	x	x	x	x	x	x	x	-	-	-	-	
34	3	15	2	x	x	x	x	x	x	x	x	x	x	x	x	x	x	x	x	x	x	x	x	-	-	-	-	
35	3	15	2	x	x	x	x	x	x	x	x	x	x	x	x	x	x	x	x	x	x	x	x	-	-	-	-	
36	3	15	2	x	x	x	x	x	x	x	x	x	x	x	x	x	x	x	x	x	x	x	x	-	-	-	-	
37	3	15	2	x	x	x	x	x	x	x	x	x	x	x	x	x	x	x	x	x	x	x	x	-	-	-	-	
38	3	15	2	x	x	x	x	x	x	x	x	x	x	x	x	x	x	x	x	x	x	x	x	-	-	-	-	
39	3	15	2	x	x	x	x	x	x	x	x	x	x	x	x	x	x	x	x	x	x	x	x	-	-	-	-	
40	3	15	2	x	x	x	x	x	x	x	x	x	x	x	x	x	x	x	x	x	x	x	x	-	-	-	-	

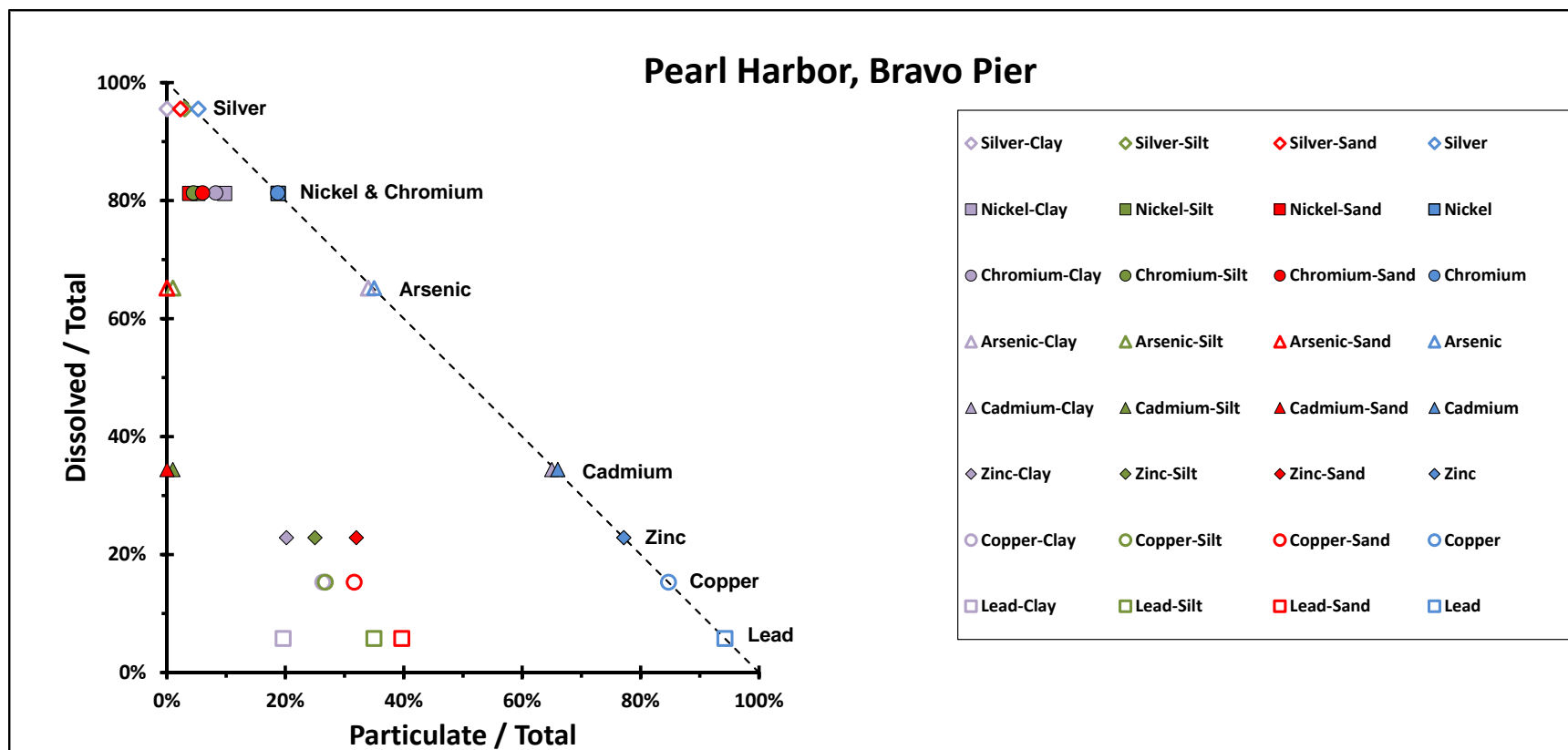


Figure 6-69. Size-fraction distribution of metals for the resuspension event of 28 August 2012 at Bravo 2 Pier in Pearl Harbor.

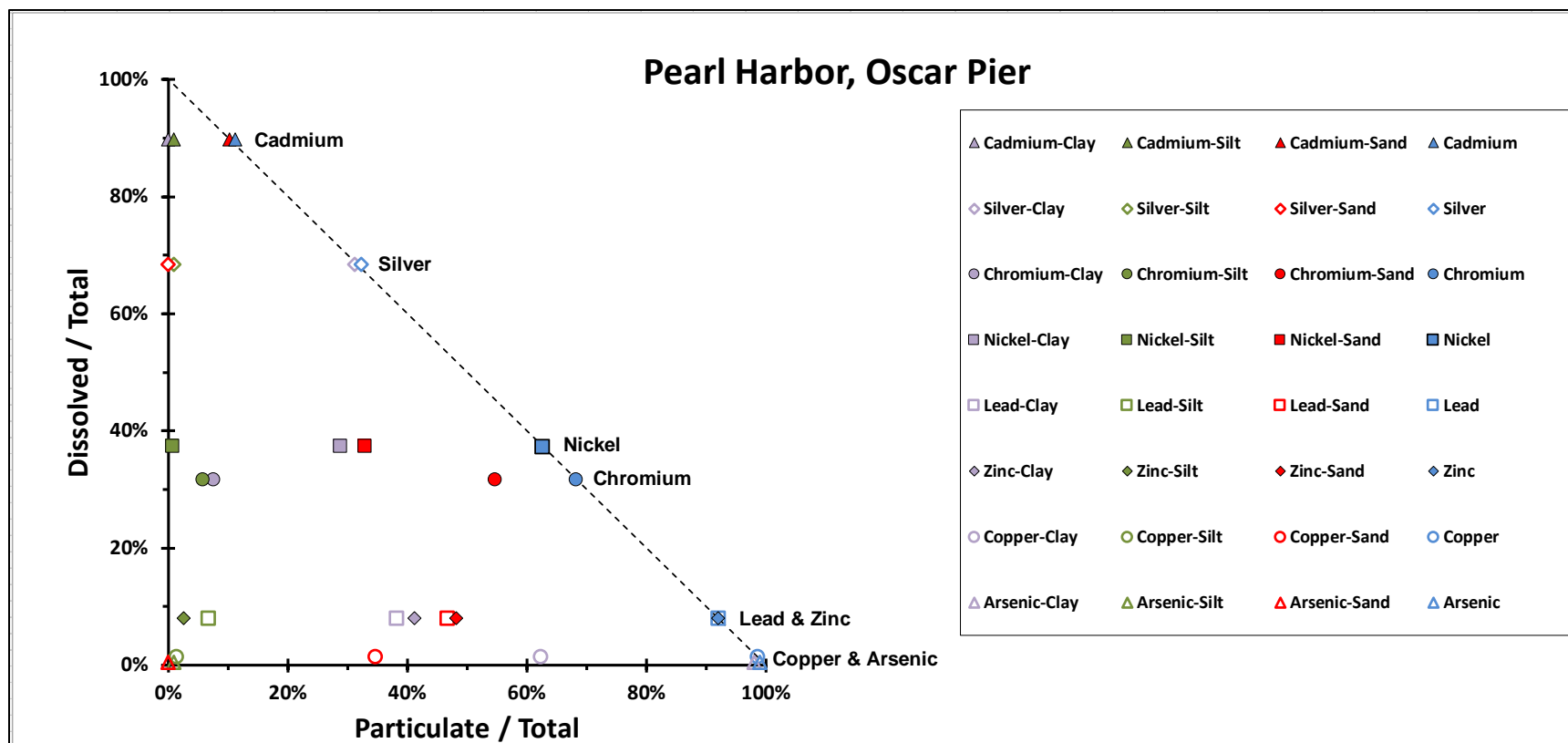


Figure 6-70. Size-fraction distribution of metals for the resuspension event of 28 August 2012 at Oscar 22 Pier in Pearl Harbor.

6.3.2.3 Sediment Profiling Imagery (SPI) for Pearl Harbor

A complete set of all the summary data measured from each image is presented in Appendix G. Animated time-lapse movies were made of all 1500 images from each site and delivered to the client under separate cover.

The Bravo site, which was the first experiment performed that day, had the instrument array closer to the stern of the tug-boat than at the Bravo site. The sediments at the Bravo site were primarily silt-clay particles (< 62 microns) with a layer of fine to medium sand on the surface. At the start of the experiment, the camera prism was inserted to the full depth of the faceplate window, with the average height of the imaged sediment cross section at 21.15 cm (Figure 6-71; see Appendix G). At the conclusion of the experiment, the cross-sectional height of the sediment was 4.93 (Figure 6-71), meaning a surface layer slightly exceeding 16 cm had eroded away from this particular location as a result of the propeller wash at the Bravo site.

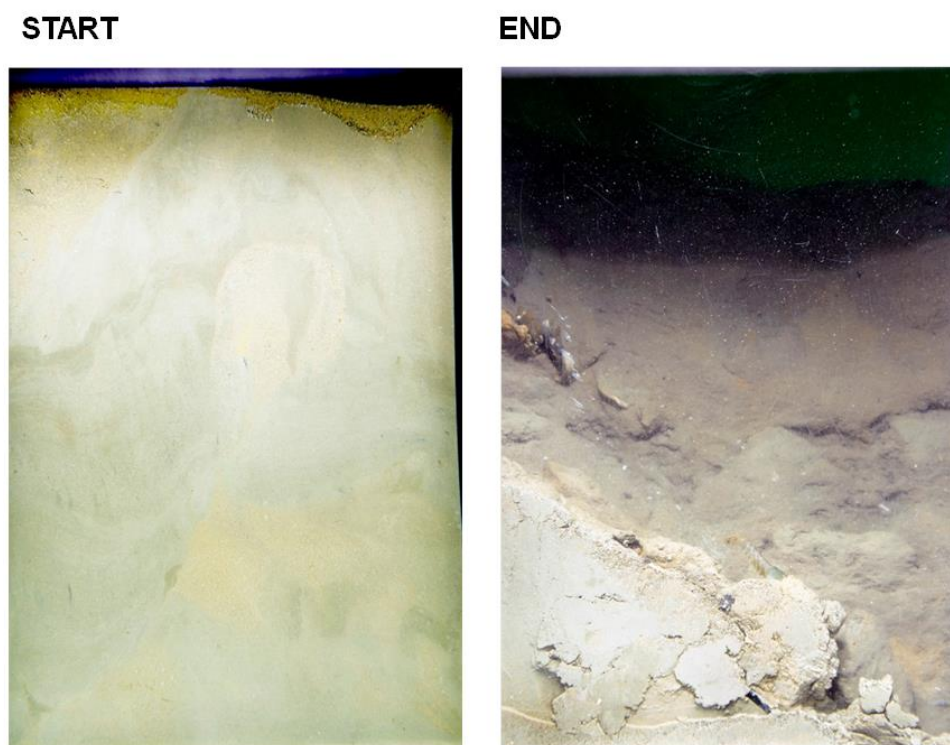
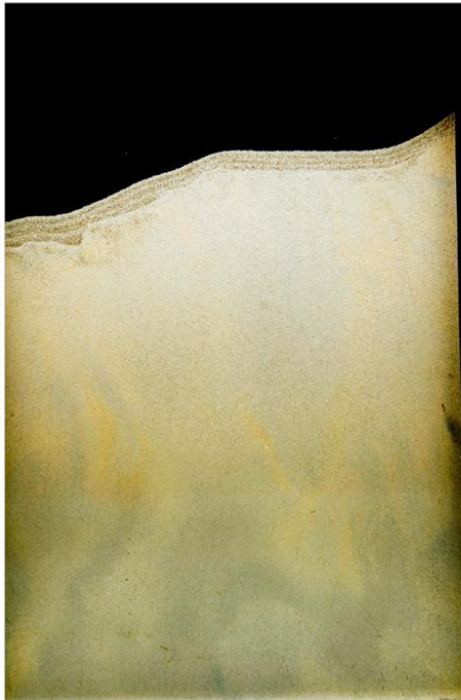


Figure 6-71. Sediment profile image at the Bravo site at the start (left) and end (right) of the experiment. Scale: width of each image = 14.5 cm.

The instrument deployment at the Oscar site was at a greater distance from the tug stern, and the sediments at this location site consisted of silty, very fine to fine sands (Figure 6-72); at the start of the experiment, the average height of the sediment column was 16.73 cm (Appendix G). The last image of the sediment cross-section recorded by the SPI camera had an average height of 14.28 cm, so an average of 2.45 cm of sediment was eroded from the surface during the course of the experiment. On two different occasions a long-eyed swimming (aka sentinel) crab (*Podophthalmus vigil*) was recorded walking across the sediment in front of the faceplate (at 14:38 and 15:02—see Figure 6-73 and the comment field in Appendix G).

START



END

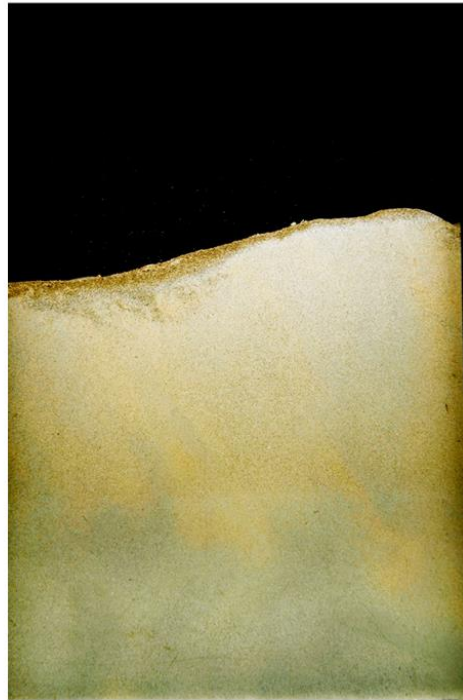


Figure 6-72. Sediment profile image from the Oscar site at the start (left) and end (right) of the experiment. Scale: width of each image = 14.5 cm.

There appeared to be two different types of erosion occurring: a steady, gradual loss of sediment particles from the sediment–water interface (the characteristic dynamic at the Oscar site), or occasional saltational erosion “events,” when a large amount of sediment would erode or be lifted up into the water column and a “new” sediment–water interface would be established from that point onward (both of these types of dynamics happened at the Bravo site). Fracturing events in the muds at the Bravo site could be visualized periodically, and it is unclear whether or not this was an artifact from the sediment being pressed up against the camera faceplate or was an accurate reflection of what was happening at other locations in the bed. Sometimes sediment that had been resuspended would resettle on the surface and be incorporated back into the sediment column; this resulted in occasional increases in the sediment height at times, followed over time by steady decreases (see Appendix G and Figure 6-74 and Figure 6-75).

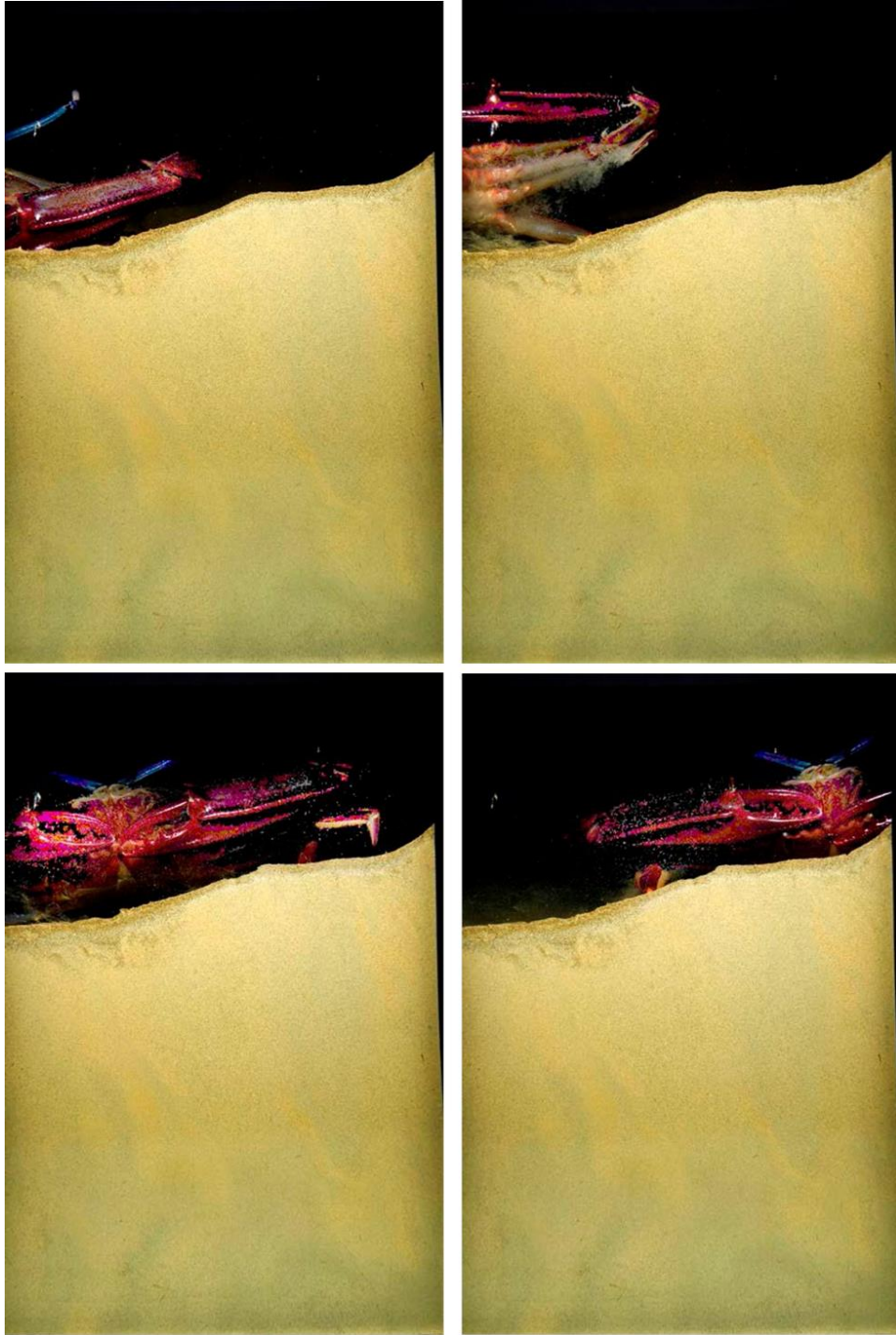


Figure 6-73. One of the appearances of the crab over a 9-sec interval during the Oscar site deployment; each image taken 3 sec apart, starting at 15:02:49.

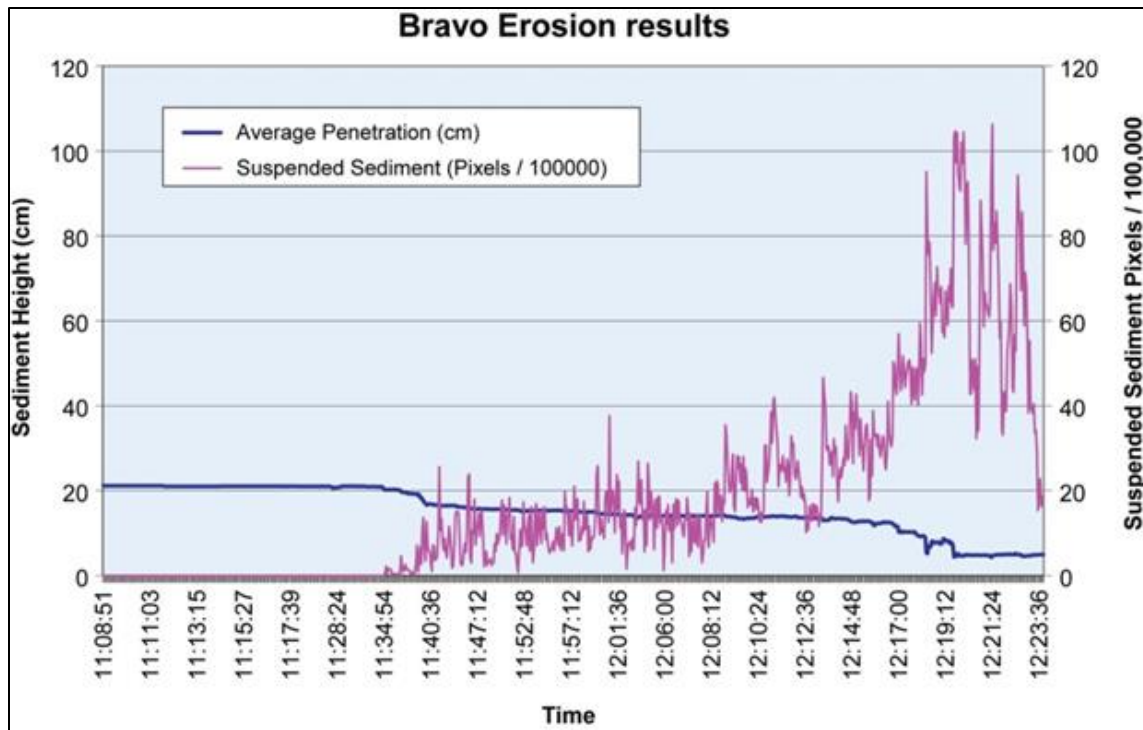


Figure 6-74. Height of sediment and amount of suspended sediment in water column as a function of time during Bravo experiment.

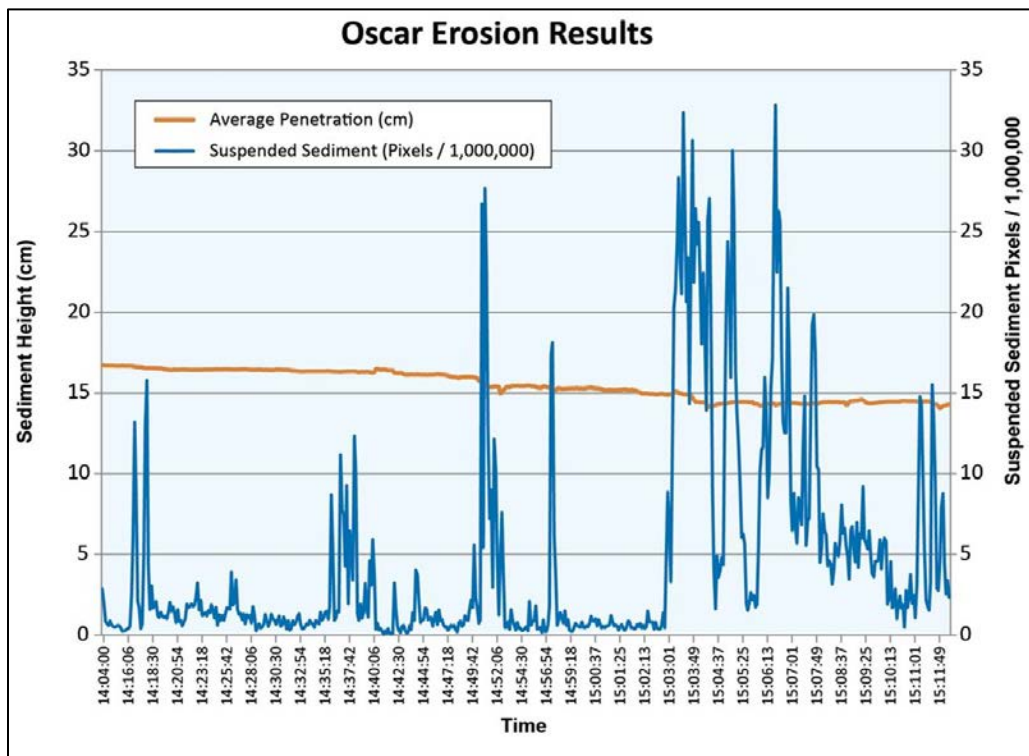


Figure 6-75. Height of sediment and amount of suspended sediment in water column as a function of time during Oscar experiment.

There were varying amounts of suspended sediments measured in the water column as a function of time, corresponding to planned adjustments in the propeller speed; the peaks in suspended sediment reflected the initial reaction of the sediment bed to the changes in speed until the final decline in suspended sediment load at the end of the experiment (Figure 6-74, Figure 6-75). At the Bravo site, large sediment chunks were on the surface or in the background that were excluded from the measurement of the suspended sediment particles. The amount of particles in the water column immediately over the sediment bed appeared to be much greater at the Bravo site (Figure 6-74) than at the Oscar site (Figure 6-75); this was to be expected, given the closer position of the instrument array to the tug stern at the Bravo site as compared with the Oscar site (stronger currents and more erosion measured at the Bravo deployment as compared with the Oscar experiment).

6.3.2.4 Tracking of Pearl Harbor Propeller Wash Plumes Using Acoustic Backscatter

As part of the field study at the two pier sites in Pearl Harbor (28–29 August 2012), tracking of the plumes resuspended by propeller wash was conducted near Bravo and Oscar Piers of Pearl Harbor, Hawaii (Figure 6-76). The depths near the piers are about 12–13 m, and the mean tide range is 0.40 m. Instrumentation was deployed from a 30-ft motor barge operated by Sea Engineering. On 28–29 August 2012, a Tiger tugboat pushed against the pier pilings at Bravo and Oscar Piers, respectively, generating a prop jet which suspended sediments from the bed. In each case, the tug pushed against the pier in three intervals of 5 min separated by approximately 15 min for observations. During the observational period, the Sea Engineering barge operated in tandem with a pontoon supporting research activities of the Navy SPAWAR team. On 31 August 2012, the ERDC-CHL team conducted measurements in plumes generated by two departing vessels in the vicinity of Bravo Pier. During these vessel operations, tugboats assisted the departing naval vessels in leaving the pier or berth, turning the vessel, and getting underway during harbor departure.



Figure 6-76. Site map of Pearl Harbor with locations of Bravo and Oscar Piers where field experiments were conducted. Imagery ©2014 DigitalGlobe, U.S. Geological Survey, USGS, Map data ©2014 Google Life mode Terms Privacy Report a problem.

The general approach in defining the characteristics of the sediment plumes and the suspended sediment within the plume was to first define the initial extent of the subsurface plume by acoustic backscatter. Then, periodically, a profiling frame was cast through the water column to permit suspended sediment sampling and measurements of temperature, salinity, suspended particle size, and settling velocity. The acoustic mapping and vertical casts of the profiling frame continued alternately until the sediment plume became very diffuse and difficult to discern from ambient conditions by acoustic backscatter (typically, several hours).

The calibrations of SSC to acoustic backscatter were applied to the corresponding datasets to produce a space-time mapping of backscatter-estimated SSC. An example period of SSC data estimated from the ADCP backscatter is provided in Figure 6-77. The data are from the 28 August 2012 tug experiment at Bravo Pier, and the vertical profiles displayed in the lower panel correspond to 20 to 25 min after the second tug pulse generating a suspended sediment plume. The solid white line in the lower panel indicates the bed position relative to the transducer, and the darkest blue color indicates data that didn't pass the data validation filters. The colored track lines in the upper right panel of Figure 6-77 show the relative position of the vessel corresponding to the profile data in the lower panel, and the red marker indicates the approximate position of the tug that generated the suspended sediment plume. A complete dataset of each experiment's acoustically estimated SSC was generated (including horizontal position, vertical position, time, and SSC) for each acoustic sample, resulting in a total of approximately 2×10^6 samples.

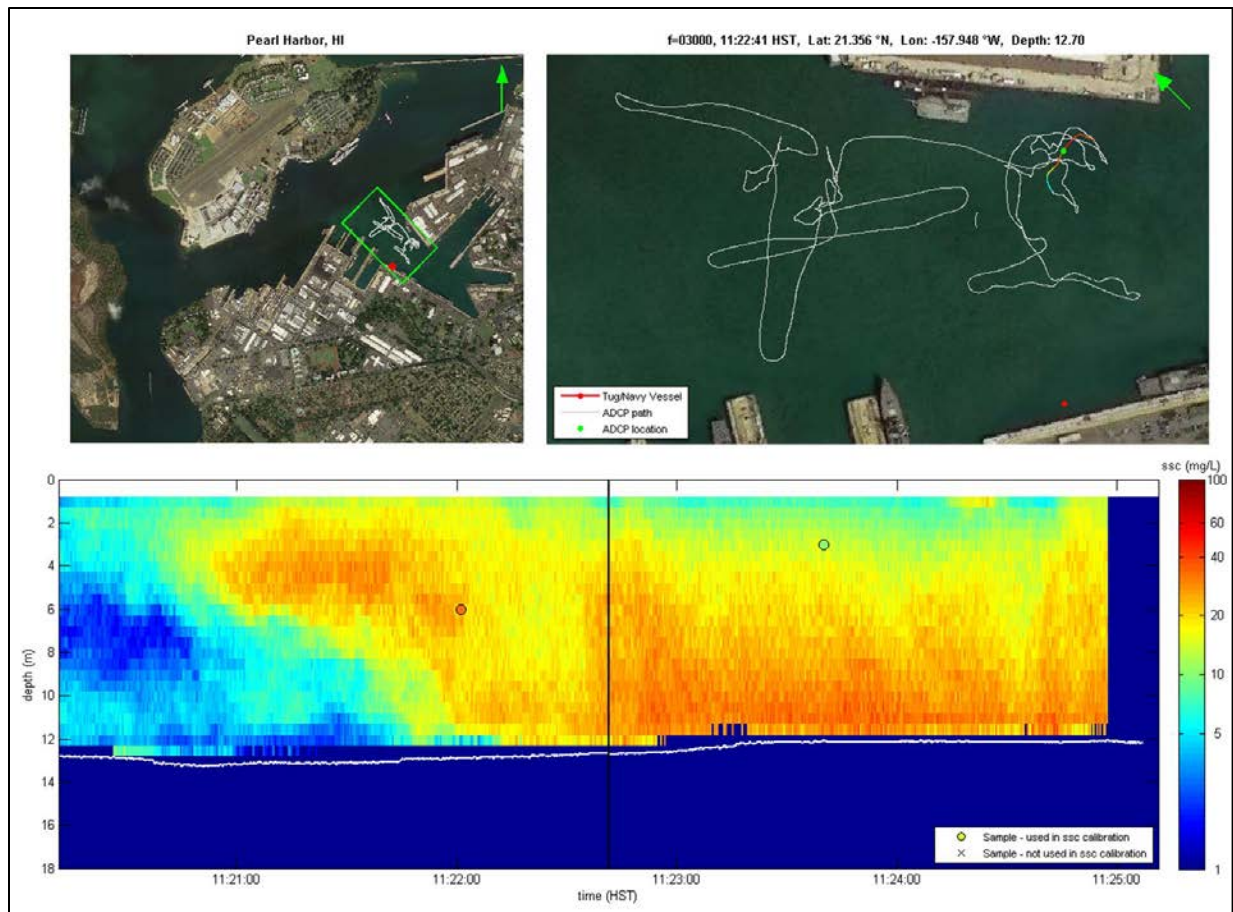


Figure 6-77. Space-time mapping of suspended sediment during the 28 August 2012 tug-generated plume. Aerial photo: Google. (Upper left) Site Map. (Upper Right) expanded site map with track line of the ADCP measurements. (Lower) vertical profiles of acoustic estimates of SSC (filled circles indicate physical samples, while line indicates position of the sediment bed, and colors indicate SSC (mg/L)). Imagery ©2014 DigitalGlobe, U.S. Geographical Survey, USGS, Map data ©2014 Google Life mode Terms Privacy Report a problem.

6.3.2.5 Preparing the Field Data for Model Comparison

Like the San Diego data, resuspension data for Bravo Pier provided as model input come from two major sources: the nephelometry data collected from the *ECOS* at mid-depth (193 samples) and 20 discrete water sample data pump-collected primarily at mid-depth. The smaller number of optical measurements, relative to those in San Diego Bay, was due to a lower instrument sampling rate. From the discrete pump measurements, optical backscatter measurements were calibrated as TSS values, the mean fractions of sand, silt, and clay were assigned to these derived TSS values, and the mean metal concentrations associated with each sediment size fraction, as well as the dissolved fraction ($<0.4 \mu\text{m}$) were assigned to the derived TSS values. TSS and size-fractions are reported as mg (sediment)/l (seawater). Sand, silt, and clay made up 24, 67, and 10% of the resuspended TSS at Bravo Pier, respectively.

Figure 6-78 shows the relationships of OBS output as a function of pump-sampled TSS, measured at mid water column depth at Bravo and Oscar Piers. Output from the OBS was scaled a bit differently from the unit used in San Diego, but the output is assumed to be linearly related to TSS

concentration. These linear regressions were used to extrapolate the few discrete TSS samples to all of the OBS output.

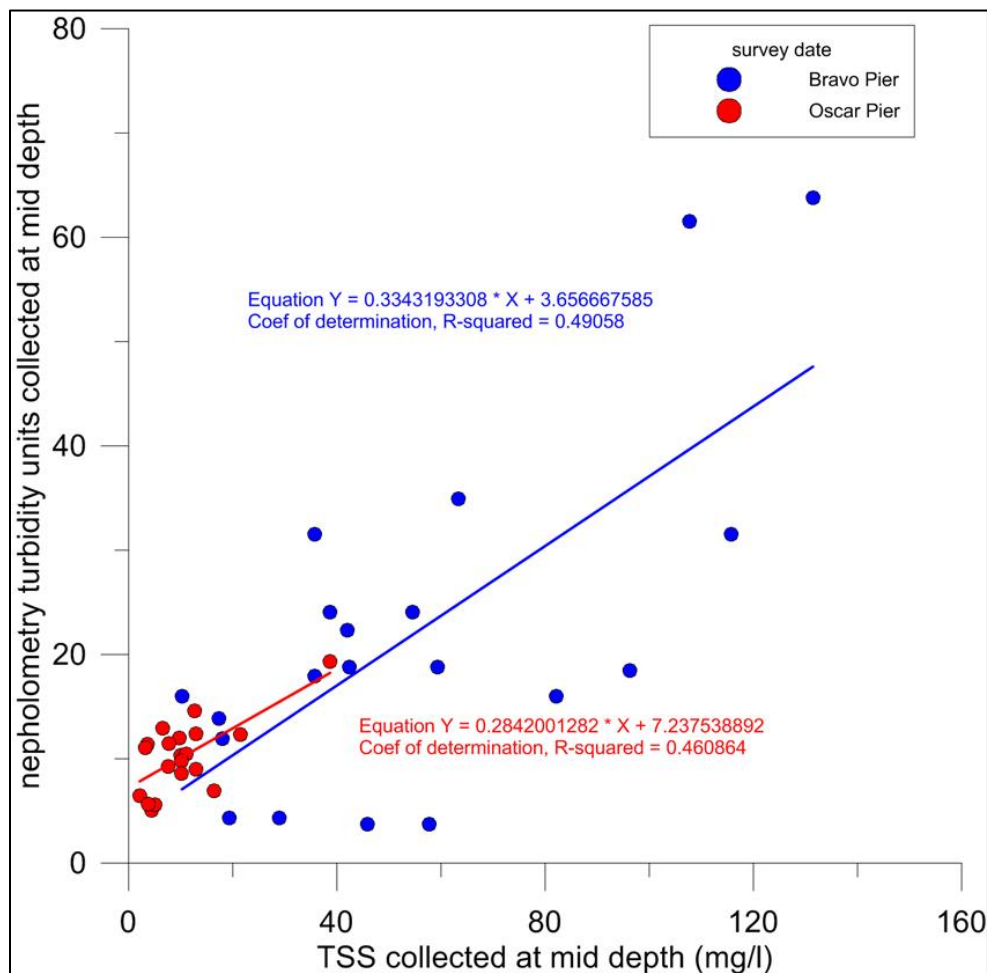


Figure 6-78. OBS output as a function of pump-sampled TSS, measured at mid-water column depth at Bravo and Oscar Piers.

Metals assigned to TSS, sand, silt, and clay size-fractions were first reported as μg (metal)/mg (sediment), and then converted to μg (metal)/l (seawater) for model input. Total chromium, copper, nickel, and lead were kept for modeling off Bravo Pier.

The distributions of TSS, particle sizes, and their associated metal concentrations, as well as the dissolved metal concentrations that were derived from the original 20 samples, were then interpolated/extrapolated on a regular grid evenly over a spatial area encompassing the tug-boat resuspension. The grid, derived in Golden Grapher Inc. Surfer[™] software, was approximately 100 points at 6 m spacing in the x (east–west) direction and 215 points at 7 m in the y (north–south) direction, yielding an 21,500 point grid. The derived grid values of TSS, particle sizes, and their associated metal concentrations were then assigned to the nearest hydrodynamic model grid point within 25 m. Sixty-eight hydrodynamic model grid points were selected around the tug resuspension area to represent initial conditions for fate and transport predictions. Those derived grid values further than 25 m from the chosen hydrodynamic grid points were discarded. The average derived values for TSS, particle sizes, and their associated metal concentrations assigned to each

hydrodynamic grid point were averaged and these average values were provided as “initial conditions” at each of the 68 hydrodynamic grid points. The initial condition data are shown in Table 6-21.

Resuspension data for Oscar Pier provided as model input come from nephelometry data collected from the *ECOS* at mid-depth (203 samples) and 20 discrete water samples collected primarily at mid-depth. From the discrete pump measurements, optical backscatter measurements were calibrated as TSS values, the mean fractions of sand, silt, and clay were assigned to these derived TSS values, and the mean metal concentrations associated with each sediment size-fraction, as well as the dissolved fraction ($<0.4\ \mu\text{m}$), were assigned to the derived TSS values. TSS and size-fractions are reported as mg (sediment)/l (seawater). Sand, silt, and clay made up 18, 73, and 10% of the resuspended TSS at Oscar Pier, respectively.

The distributions of TSS, particle sizes, and their associated metal concentrations, as well as the dissolved metal concentrations that were derived from the original 20 samples, were then interpolated/extrapolated on a regular grid evenly over a spatial area encompassing the tug-boat resuspension. The grid, derived in Golden Grapher Inc. Surfer[™] software, was approximately 100 points at 4.6-m spacing in the x (east–west) direction and 86 points at 4.6 m in the y (north–south) direction, yielding an 8600 point grid. The derived grid values of TSS, particle sizes, and their associated metal concentrations were then assigned to the nearest hydrodynamic model grid point within 25 m. Forty three hydrodynamic model grid points were selected around the tug resuspension area to represent initial conditions for fate and transport predictions. Those derived grid values further than 25 m from the chosen hydrodynamic grid points were discarded. The average derived values for TSS, particle sizes, and their associated metal concentrations assigned to each hydrodynamic grid point were averaged and these average values were provided as ‘initial conditions’ at each of the 43 hydrodynamic grid points. The initial condition data are shown below in Table 6-22. Again, of only chromium and copper were included in the fate and transport model for Oscar Pier.

Table 6-21. Resuspended sediment and associated metal concentrations input values for Bravo Pier. Metals not shown were below EPA's water quality standards.

i	j	easting (m)	northing (m)	TSS (mg/l)	sand (mg/l)	silt (mg/l)	clay (mg/l)	Cu sand (µg/l)	Cu silt (µg/l)	Cu clay (µg/l)	Cu diss (µg/l)	Ni sand (µg/l)	Ni silt (µg/l)	Ni clay (µg/l)	Ni diss (µg/l)	Cr sand (µg/l)	Cr silt (µg/l)	Cr clay (µg/l)	Cr diss (µg/l)	Pb sand (µg/l)	Pb silt (µg/l)	Pb clay (µg/l)	Pb diss (µg/l)
100	77	608800.2	2361956.1	32.46	7.95	21.02	3.50	2.54	5.46	0.73	6.49	0	2.10	0	71.74	0	1.89	0.84	102.26	1.11	2.31	0.21	0.65
100	78	608828.0	2361994.0	37.01	9.06	23.96	3.99	2.90	6.23	0.84	7.40	0	2.40	0	81.78	0	2.16	0.96	116.57	1.27	2.64	0.24	0.74
100	79	608855.1	2362026.1	41.70	10.21	27.00	4.49	3.27	7.02	0.94	8.34	0	2.70	0	92.16	0	2.43	1.08	131.36	1.43	2.97	0.27	0.83
100	80	608884.1	2362057.7	48.48	11.87	31.39	5.22	3.80	8.16	1.10	9.70	0	3.14	0	107.15	0	2.82	1.25	152.72	1.66	3.45	0.31	0.97
100	81	608913.4	2362087.1	52.06	12.75	33.71	5.61	4.08	8.76	1.18	10.41	0	3.37	0	115.06	0	3.03	1.35	164.00	1.78	3.71	0.34	1.04
100	82	608946.3	2362120.5	53.81	13.17	34.84	5.80	4.22	9.06	1.22	10.76	0	3.48	0	118.93	0	3.14	1.39	169.51	1.84	3.83	0.35	1.08
101	77	608853.7	2361932.4	30.83	7.55	19.96	3.32	2.42	5.19	0.70	6.17	0	2.00	0	68.13	0	1.80	0.80	97.11	1.06	2.20	0.20	0.62
101	78	608881.3	2361968.2	33.86	8.29	21.92	3.65	2.65	5.70	0.77	6.77	0	2.19	0	74.84	0	1.97	0.88	106.67	1.16	2.41	0.22	0.68
101	79	608907.5	2362001.8	42.56	10.42	27.56	4.58	3.33	7.16	0.96	8.51	0	2.76	0	94.06	0	2.48	1.10	134.07	1.46	3.03	0.28	0.85
101	80	608936.4	2362031.3	51.87	12.70	33.58	5.59	4.06	8.73	1.17	10.37	0	3.36	0	114.63	0	3.02	1.34	163.39	1.78	3.69	0.34	1.04
101	81	608962.5	2362062.1	52.75	12.91	34.15	5.68	4.13	8.88	1.19	10.55	0	3.42	0	116.58	0	3.07	1.36	166.16	1.81	3.76	0.34	1.06
101	82	608988.7	2362093.4	53.64	13.13	34.73	5.78	4.20	9.03	1.21	10.73	0	3.47	0	118.55	0	3.13	1.39	168.98	1.84	3.82	0.35	1.07
102	77	608891.2	2361913.0	30.16	7.38	19.53	3.25	2.36	5.08	0.68	6.03	0	1.95	0	66.66	0	1.76	0.78	95.01	1.03	2.15	0.19	0.60
102	78	608918.4	2361949.9	30.48	7.46	19.73	3.28	2.39	5.13	0.69	6.10	0	1.97	0	67.37	0	1.78	0.79	96.02	1.04	2.17	0.20	0.61
102	79	608942.5	2361982.2	39.31	9.62	25.45	4.23	3.08	6.62	0.89	7.86	0	2.54	0	86.88	0	2.29	1.02	123.83	1.35	2.80	0.25	0.79
102	80	608969.9	2362015.0	47.25	11.57	30.59	5.09	3.70	7.95	1.07	9.45	0	3.06	0	104.43	0	2.75	1.22	148.85	1.62	3.37	0.31	0.95
102	81	608998.9	2362047.4	49.61	12.14	32.12	5.34	3.89	8.35	1.12	9.92	0	3.21	0	109.63	0	2.89	1.28	156.27	1.70	3.53	0.32	0.99
103	75	608877.6	2361811.6	24.05	5.89	15.57	2.59	1.88	4.05	0.54	4.81	0	1.56	0	53.15	0	1.40	0.62	75.76	0.82	1.71	0.16	0.48
103	76	608903.9	2361854.8	34.90	8.54	22.60	3.76	2.73	5.88	0.79	6.98	0	2.26	0	77.14	0	2.03	0.90	109.95	1.20	2.49	0.23	0.70
103	77	608931.1	2361894.5	34.24	8.38	22.17	3.69	2.68	5.76	0.77	6.85	0	2.22	0	75.67	0	2.00	0.89	107.86	1.17	2.44	0.22	0.68
103	78	608956.0	2361929.6	27.72	6.78	17.94	2.98	2.17	4.67	0.63	5.54	0	1.79	0	61.25	0	1.61	0.72	87.30	0.95	1.97	0.18	0.55
103	79	608979.5	2361962.5	33.39	8.17	21.62	3.60	2.62	5.62	0.76	6.68	0	2.16	0	73.80	0	1.95	0.86	105.19	1.14	2.38	0.22	0.67
103	80	609001.6	2361992.9	36.48	8.93	23.62	3.93	2.86	6.14	0.83	7.30	0	2.36	0	80.62	0	2.13	0.94	114.91	1.25	2.60	0.24	0.73
103	81	609022.3	2362017.7	44.19	10.82	28.61	4.76	3.46	7.44	1.00	8.84	0	2.86	0	97.67	0	2.57	1.14	139.21	1.51	3.15	0.29	0.88
104	73	608867.4	2361698.0	26.33	6.44	17.04	2.84	2.06	4.43	0.60	5.27	0	1.70	0	58.18	0	1.53	0.68	82.92	0.90	1.87	0.17	0.53
104	74	608895.9	2361742.6	26.54	6.50	17.18	2.86	2.08	4.47	0.60	5.31	0	1.72	0	58.64	0	1.55	0.69	83.59	0.91	1.89	0.17	0.53
104	75	608923.0	2361790.1	28.80	7.05	18.65	3.10	2.26	4.85	0.65	5.76	0	1.86	0	63.65	0	1.68	0.74	90.72	0.99	2.05	0.19	0.58
104	76	608947.2	2361832.1	45.87	11.23	29.70	4.94	3.59	7.72	1.04	9.17	0	2.97	0	101.37	0	2.67	1.19	144.49	1.57	3.27	0.30	0.92
104	77	608973.4	2361871.0	45.53	11.14	29.47	4.90	3.57	7.66	1.03	9.11	0	2.95	0	100.61	0	2.65	1.18	143.41	1.56	3.24	0.29	0.91
104	78	608996.0	2361906.2	53.94	13.20	34.92	5.81	4.23	9.08	1.22	10.79	0	3.49	0	119.21	0	3.14	1.39	169.91	1.85	3.84	0.35	1.08
104	79	609017.0	2361939.4	42.86	10.49	27.75	4.62	3.36	7.21	0.97	8.57	0	2.77	0	94.73	0	2.50	1.11	135.02	1.47	3.05	0.28	0.86
104	80	609039.5	2361965.6	41.90	10.26	27.13	4.51	3.28	7.05	0.95	8.38	0	2.71	0	92.61	0	2.44	1.08	132.00	1.44	2.98	0.27	0.84
104	81	609051.1	2361987.3	45.59	11.16	29.52	4.91	3.57	7.67	1.03	9.12	0	2.95	0	100.76	0	2.66	1.18	143.62	1.56	3.25	0.29	0.91
105	73	608909.7	2361674.8	27.33	6.69	17.69	2.94	2.14	4.60	0.62	5.47	0	1.77	0	60.40	0	1.59	0.71	86.09	0.94	1.95	0.18	0.55
105	74	608936.2	2361720.3	27.48	6.73	17.79	2.96	2.15	4.63	0.62	5.50	0	1.78	0	60.74	0	1.60	0.71	86.57	0.94	1.96	0.18	0.55
105	75	608962.5	2361767.4	29.17	7.14	18.89	3.14	2.29	4.91	0.66	5.83	0	1.89	0	64.47	0	1.70	0.75	91.89	1.00	2.08	0.19	0.58
105	76	608987.6	2361809.1	34.12	8.35	22.09	3.68	2.67	5.74	0.77	6.82	0	2.21	0	75.41	0	1.99	0.88	107.49	1.17	2.43	0.22	0.68
105	77	609011.7	2361846.1	63.87	15.64	41.35	6.88	5.00	10.75	1.44	12.77	0	4.14	0	141.16	0	3.72	1.65	201.20	2.19	4.55	0.41	1.28
105	78	609035.0	2361880.6	79.15	19.38	51.24	8.52	6.20	13.32	1.79	15.83	0	5.12	0	174.93	0	4.61	2.05	249.33	2.71	5.64	0.51	1.58
105	79	609053.4	2361911.4	51.00	12.49	33.02	5.49	4.00	8.58	1.15	10.20	0	3.30	0	112.72	0	2.97	1.32	160.66	1.75	3.63	0.33	1.02
105	80	609074.8	2361943.8	55.59	13.61	35.99	5.99	4.35	9.36	1.26	11.12	0	3.60	0	122.86	0	3.24	1.44	175.11	1.91	3.96	0.36	1.11

Table 6-21. Resuspended sediment and associated metal concentrations input values for Bravo Pier. (Continued)

i	j	easting (m)	northing (m)	TSS (mg/l)	sand (mg/l)	silt (mg/l)	clay (mg/l)	Cu sand (µg/l)	Cu silt (µg/l)	Cu clay (µg/l)	Cu diss (µg/l)	Ni sand (µg/l)	Ni silt (µg/l)	Ni clay (µg/l)	Ni diss (µg/l)	Cr sand (µg/l)	Cr silt (µg/l)	Cr clay (µg/l)	Cr diss (µg/l)	Pb sand (µg/l)	Pb silt (µg/l)	Pb clay (µg/l)	Pb diss (µg/l)
106	73	608945.3	2361654.6	27.45	6.72	17.77	2.96	2.15	4.62	0.62	5.49	0	1.78	0	60.65	0	1.60	0.71	86.45	0.94	1.95	0.18	0.55
106	74	608973.5	2361699.9	27.68	6.78	17.92	2.98	2.17	4.66	0.63	5.54	0	1.79	0	61.17	0	1.61	0.72	87.18	0.95	1.97	0.18	0.55
106	75	609002.2	2361745.2	27.94	6.84	18.09	3.01	2.19	4.70	0.63	5.59	0	1.81	0	61.75	0	1.63	0.72	88.01	0.96	1.99	0.18	0.56
106	76	609028.2	2361784.1	28.47	6.97	18.43	3.07	2.23	4.79	0.64	5.69	0	1.84	0	62.93	0	1.66	0.74	89.69	0.98	2.03	0.18	0.57
106	77	609051.4	2361820.4	47.60	11.65	30.82	5.13	3.73	8.01	1.08	9.52	0	3.08	0	105.20	0	2.77	1.23	149.94	1.63	3.39	0.31	0.95
106	78	609073.0	2361853.1	80.44	19.69	52.08	8.66	6.30	13.54	1.82	16.09	0	5.21	0	177.78	0	4.69	2.08	253.39	2.76	5.73	0.52	1.61
106	79	609093.5	2361881.8	86.71	21.23	56.14	9.34	6.79	14.60	1.96	17.34	0	5.61	0	191.64	0	5.05	2.24	273.15	2.97	6.18	0.56	1.73
106	80	609110.8	2361912.3	79.81	19.54	51.67	8.60	6.25	13.43	1.81	15.96	0	5.17	0	176.38	0	4.65	2.06	251.40	2.74	5.68	0.52	1.60
107	73	608986.6	2361634.3	27.37	6.70	17.72	2.95	2.14	4.61	0.62	5.47	0	1.77	0	60.49	0	1.59	0.71	86.22	0.94	1.95	0.18	0.55
107	74	609014.6	2361676.8	27.46	6.72	17.78	2.96	2.15	4.62	0.62	5.49	0	1.78	0	60.68	0	1.60	0.71	86.49	0.94	1.96	0.18	0.55
107	75	609042.7	2361719.2	26.90	6.59	17.42	2.90	2.11	4.53	0.61	5.38	0	1.74	0	59.45	0	1.57	0.70	84.74	0.92	1.92	0.17	0.54
107	76	609070.2	2361759.4	25.89	6.34	16.76	2.79	2.03	4.36	0.59	5.18	0	1.68	0	57.21	0	1.51	0.67	81.54	0.89	1.84	0.17	0.52
107	77	609093.3	2361794.8	30.63	7.50	19.83	3.30	2.40	5.16	0.69	6.13	0	1.98	0	67.68	0	1.78	0.79	96.47	1.05	2.18	0.20	0.61
107	78	609114.7	2361826.1	56.47	13.83	36.56	6.08	4.42	9.51	1.28	11.29	0	3.66	0	124.81	0	3.29	1.46	177.90	1.94	4.02	0.36	1.13
107	79	609135.0	2361851.9	71.27	17.45	46.14	7.68	5.58	12.00	1.61	14.25	0	4.61	0	157.51	0	4.15	1.84	224.51	2.44	5.08	0.46	1.43
107	80	609152.4	2361877.0	76.62	18.76	49.61	8.25	6.00	12.90	1.73	15.32	0	4.96	0	169.34	0	4.46	1.98	241.37	2.63	5.46	0.50	1.53
108	73	609033.2	2361600.3	27.83	6.81	18.02	3.00	2.18	4.69	0.63	5.57	0	1.80	0	61.51	0	1.62	0.72	87.68	0.95	1.98	0.18	0.56
108	74	609064.9	2361642.8	28.34	6.94	18.35	3.05	2.22	4.77	0.64	5.67	0	1.83	0	62.63	0	1.65	0.73	89.27	0.97	2.02	0.18	0.57
108	75	609094.0	2361685.3	29.15	7.14	18.87	3.14	2.28	4.91	0.66	5.83	0	1.89	0	64.43	0	1.70	0.75	91.83	1.00	2.08	0.19	0.58
108	76	609122.4	2361724.2	32.05	7.85	20.75	3.45	2.51	5.39	0.72	6.41	0	2.07	0	70.83	0	1.87	0.83	100.96	1.10	2.28	0.21	0.64
108	77	609149.0	2361757.8	39.32	9.62	25.45	4.23	3.08	6.62	0.89	7.86	0	2.55	0	86.89	0	2.29	1.02	123.85	1.35	2.80	0.25	0.79
108	78	609173.4	2361787.9	49.40	12.09	31.98	5.32	3.87	8.32	1.12	9.88	0	3.20	0	109.18	0	2.88	1.28	155.61	1.69	3.52	0.32	0.99
108	79	609199.3	2361816.7	58.32	14.28	37.75	6.28	4.57	9.82	1.32	11.66	0	3.78	0	128.88	0	3.40	1.51	183.70	2.00	4.15	0.38	1.17
109	76	609188.9	2361682.1	38.08	9.32	24.65	4.10	2.98	6.41	0.86	7.62	0	2.47	0	84.16	0	2.22	0.98	119.96	1.31	2.71	0.25	0.76
109	77	609213.4	2361713.9	42.92	10.51	27.78	4.62	3.36	7.22	0.97	8.58	0	2.78	0	94.85	0	2.50	1.11	135.19	1.47	3.06	0.28	0.86
109	78	609238.8	2361746.0	48.64	11.91	31.49	5.24	3.81	8.19	1.10	9.73	0	3.15	0	107.50	0	2.83	1.26	153.22	1.67	3.46	0.31	0.97
109	79	609263.2	2361775.8	53.79	13.17	34.82	5.79	4.21	9.05	1.22	10.76	0	3.48	0	118.87	0	3.13	1.39	169.43	1.84	3.83	0.35	1.08

Table 6-22. Resuspended sediment and associated metal concentrations input values for Oscar Pier.

i	j	easting (m)	northing (m)	TSS (mg/l)	sand (mg/l)	silt (mg/l)	clay (mg/l)	Cu sand (µg/l)	Cu silt (µg/l)	Cu clay (µg/l)	Cu diss (µg/l)	Ni sand (µg/l)	Ni silt (µg/l)	Ni clay (µg/l)	Ni diss (µg/l)	Cr sand (µg/l)	Cr silt (µg/l)	Cr clay (µg/l)	Cr diss (µg/l)	Pb sand (µg/l)	Pb silt (µg/l)	Pb clay (µg/l)	Pb diss (µg/l)
76	46	606786.9	2360553.2	7.41	1.30	5.40	0.71	2.61	0.11	0	1.26	6.54	0	0	40.37	2.09	0.70	0.81	53.85	0.80	0.49	0.28	0.59
76	47	606784.9	2360594.3	5.43	0.95	3.96	0.52	1.91	0.08	0	0.92	4.80	0	0	29.60	1.53	0.52	0.59	39.49	0.59	0.36	0.21	0.43
76	48	606782.4	2360637.0	3.44	0.60	2.51	0.33	1.21	0.05	0	0.59	3.04	0	0	18.77	0.97	0.33	0.37	25.04	0.37	0.23	0.13	0.28
77	46	606834.2	2360554.7	9.30	1.63	6.78	0.89	3.28	0.14	0	1.58	8.22	0	0	50.69	2.62	0.88	1.01	67.62	1.01	0.61	0.35	0.74
77	47	606831.9	2360596.7	7.06	1.24	5.15	0.67	2.49	0.10	0	1.20	6.24	0	0	38.49	1.99	0.67	0.77	51.34	0.77	0.46	0.27	0.57
77	48	606829.0	2360639.3	4.16	0.73	3.04	0.40	1.47	0.06	0	0.71	3.68	0	0	22.68	1.17	0.39	0.45	30.25	0.45	0.27	0.16	0.33
77	49	606826.9	2360678.9	3.77	0.66	2.75	0.36	1.33	0.06	0	0.64	3.33	0	0	20.56	1.06	0.36	0.41	27.43	0.41	0.25	0.14	0.30
78	46	606887.4	2360555.0	12.41	2.17	9.05	1.18	4.37	0.18	0	2.11	10.96	0	0	67.62	3.50	1.18	1.35	90.20	1.35	0.81	0.47	0.99
78	47	606886.2	2360598.5	10.86	1.90	7.92	1.04	3.82	0.16	0	1.85	9.59	0	0	59.17	3.06	1.03	1.18	78.93	1.18	0.71	0.41	0.87
78	48	606883.1	2360643.1	7.69	1.35	5.61	0.73	2.71	0.11	0	1.31	6.79	0	0	41.91	2.17	0.73	0.84	55.91	0.84	0.50	0.29	0.62
78	49	606882.0	2360681.9	3.20	0.56	2.34	0.31	1.13	0.05	0	0.54	2.83	0	0	17.46	0.90	0.30	0.35	23.28	0.35	0.21	0.12	0.26
78	50	606880.2	2360723.8	2.03	0.36	1.48	0.19	0.71	0.03	0	0.35	1.79	0	0	11.06	0.57	0.19	0.22	14.76	0.22	0.13	0.08	0.16
79	46	606942.2	2360555.3	14.69	2.57	10.71	1.40	5.17	0.21	0	2.50	12.97	0	0	80.03	4.14	1.39	1.60	106.76	1.60	0.96	0.56	1.17
79	47	606940.1	2360599.3	14.09	2.47	10.28	1.34	4.96	0.21	0	2.40	12.45	0	0	76.80	3.98	1.34	1.53	102.45	1.53	0.93	0.54	1.13
79	48	606937.8	2360643.7	6.08	1.07	4.44	0.58	2.14	0.09	0	1.03	5.37	0	0	33.15	1.72	0.58	0.66	44.22	0.66	0.40	0.23	0.49
79	49	606937.3	2360684.6	9.05	1.59	6.60	0.86	3.19	0.13	0	1.54	8.00	0	0	49.34	2.55	0.86	0.98	65.82	0.98	0.59	0.35	0.72
79	50	606934.4	2360727.8	5.87	1.03	4.28	0.56	2.07	0.09	0	1.00	5.19	0	0	32.00	1.66	0.56	0.64	42.69	0.64	0.39	0.22	0.47
80	46	606993.1	2360555.2	13.55	2.37	9.88	1.29	4.77	0.20	0	2.30	11.97	0	0	73.84	3.82	1.28	1.47	98.50	1.47	0.89	0.52	1.08
80	47	606991.1	2360599.3	11.23	1.97	8.19	1.07	3.96	0.16	0	1.91	9.92	0	0	61.20	3.17	1.06	1.22	81.64	1.22	0.74	0.43	0.90
80	48	606990.0	2360645.2	5.50	0.96	4.01	0.52	1.94	0.08	0	0.93	4.86	0	0	29.96	1.55	0.52	0.60	39.97	0.60	0.36	0.21	0.44
80	49	606987.3	2360686.9	13.12	2.30	9.57	1.25	4.62	0.19	0	2.23	11.59	0	0	71.48	3.70	1.24	1.43	95.35	1.43	0.86	0.50	1.05
80	50	606984.5	2360730.5	6.79	1.19	4.95	0.65	2.39	0.10	0	1.15	6.00	0	0	37.02	1.92	0.64	0.74	49.38	0.74	0.45	0.26	0.54
81	47	607044.0	2360600.2	11.07	1.94	8.07	1.06	3.90	0.16	0	1.88	9.77	0	0	60.31	3.12	1.05	1.20	80.45	1.20	0.73	0.42	0.89
81	48	607043.2	2360646.4	11.68	2.05	8.52	1.11	4.12	0.17	0	1.99	10.32	0	0	63.67	3.30	1.11	1.27	84.93	1.27	0.77	0.45	0.93
81	49	607039.4	2360688.8	7.32	1.28	5.34	0.70	2.58	0.11	0	1.25	6.47	0	0	39.92	2.07	0.69	0.80	53.25	0.80	0.48	0.28	0.59
81	50	607037.6	2360732.5	1.60	0.28	1.17	0.15	0.56	0.02	0	0.27	1.41	0	0	8.71	0.45	0.15	0.17	11.62	0.17	0.10	0.06	0.13
81	51	607034.7	2360776.2	-0.59	-0.10	-0.43	-0.06	-0.21	-0.01	0	-0.10	-0.52	0	0	-3.19	-0.17	-0.06	-0.06	-4.26	-0.06	-0.04	-0.02	-0.05
81	52	607027.9	2360820.6	-2.26	-0.40	-1.65	-0.22	-0.80	-0.03	0	-0.38	-1.99	0	0	-12.31	-0.64	-0.21	-0.25	-16.42	-0.25	-0.15	-0.09	-0.18
81	53	607022.8	2360866.6	-1.93	-0.34	-1.40	-0.18	-0.68	-0.03	0	-0.33	-1.70	0	0	-10.50	-0.54	-0.18	-0.21	-14.00	-0.21	-0.13	-0.07	-0.15
82	48	607091.5	2360646.4	9.81	1.72	7.15	0.93	3.45	0.14	0	1.67	8.66	0	0	53.44	2.77	0.93	1.07	71.28	1.07	0.64	0.37	0.78
82	49	607088.4	2360690.2	7.31	1.28	5.33	0.70	2.57	0.11	0	1.24	6.46	0	0	39.83	2.06	0.69	0.79	53.13	0.79	0.48	0.28	0.58
82	50	607085.7	2360733.8	-0.15	-0.03	-0.11	-0.01	-0.05	0.00	0	-0.03	-0.13	0	0	-0.83	-0.04	-0.01	-0.02	-1.11	-0.02	-0.01	-0.01	-0.01
82	51	607081.4	2360779.1	0.08	0.01	0.06	0.01	0.03	0.00	0	0.01	0.07	0	0	0.43	0.02	0.01	0.01	0.57	0.01	0.01	0.00	0.01
82	52	607077.5	2360825.3	-0.60	-0.10	-0.43	-0.06	-0.21	-0.01	0	-0.10	-0.53	0	0	-3.25	-0.17	-0.06	-0.06	-4.33	-0.06	-0.04	-0.02	-0.05
82	53	607065.8	2360870.1	-2.18	-0.38	-1.59	-0.21	-0.77	-0.03	0	-0.37	-1.93	0	0	-11.89	-0.62	-0.21	-0.24	-15.85	-0.24	-0.14	-0.08	-0.17
83	48	607141.2	2360647.2	3.77	0.66	2.75	0.36	1.33	0.06	0	0.64	3.33	0	0	20.56	1.06	0.36	0.41	27.42	0.41	0.25	0.14	0.30
83	49	607133.6	2360691.5	1.14	0.20	0.83	0.11	0.40	0.02	0	0.19	1.01	0	0	6.24	0.32	0.11	0.12	8.32	0.12	0.08	0.04	0.09
83	50	607123.4	2360735.5	0.01	0.00	0.01	0.00	0.00	0.00	0	0.00	0.01	0	0	0.06	0.00	0.00	0.00	0.08	0.00	0.00	0.00	0.00
83	51	607120.3	2360781.1	-1.06	-0.19	-0.77	-0.10	-0.37	-0.02	0	-0.18	-0.93	0	0	-5.76	-0.30	-0.10	-0.11	-7.68	-0.11	-0.07	-0.04	-0.08
84	47	607196.9	2360601.8	3.43	0.60	2.51	0.33	1.21	0.05	0	0.58	3.03	0	0	18.72	0.97	0.33	0.37	24.97	0.37	0.23	0.13	0.27
84	48	607191.2	2360648.7	0.93	0.16	0.67	0.09	0.33	0.01	0	0.16	0.82	0	0	5.04	0.26	0.09	0.10	6.72	0.10	0.06	0.04	0.07
84	49	607178.1	2360692.7	-0.56	-0.10	-0.41	-0.05	-0.20	-0.01	0	-0.10	-0.50	0	0	-3.07	-0.16	-0.05	-0.06	-4.09	-0.06	-0.04	-0.02	-0.05
84	50	607157.2	2360736.3	-0.31	-0.05	-0.22	-0.03	-0.11	0.00	0	-0.05	-0.27	0	0	-1.68	-0.09	-0.03	-0.03	-2.24	-0.03	-0.02	-0.01	-0.02

Figure 6-79 shows the *ECOS* tracks, discrete pump sample locations, TSS derived from OBS measurements as colored contours, and the 68 nodes of the CH3D model used for model validation at Bravo Pier. Numbers on the nodes are model coordinates. Figure 6-80 is a representative figure of copper associated with resuspended silt at Bravo Pier.

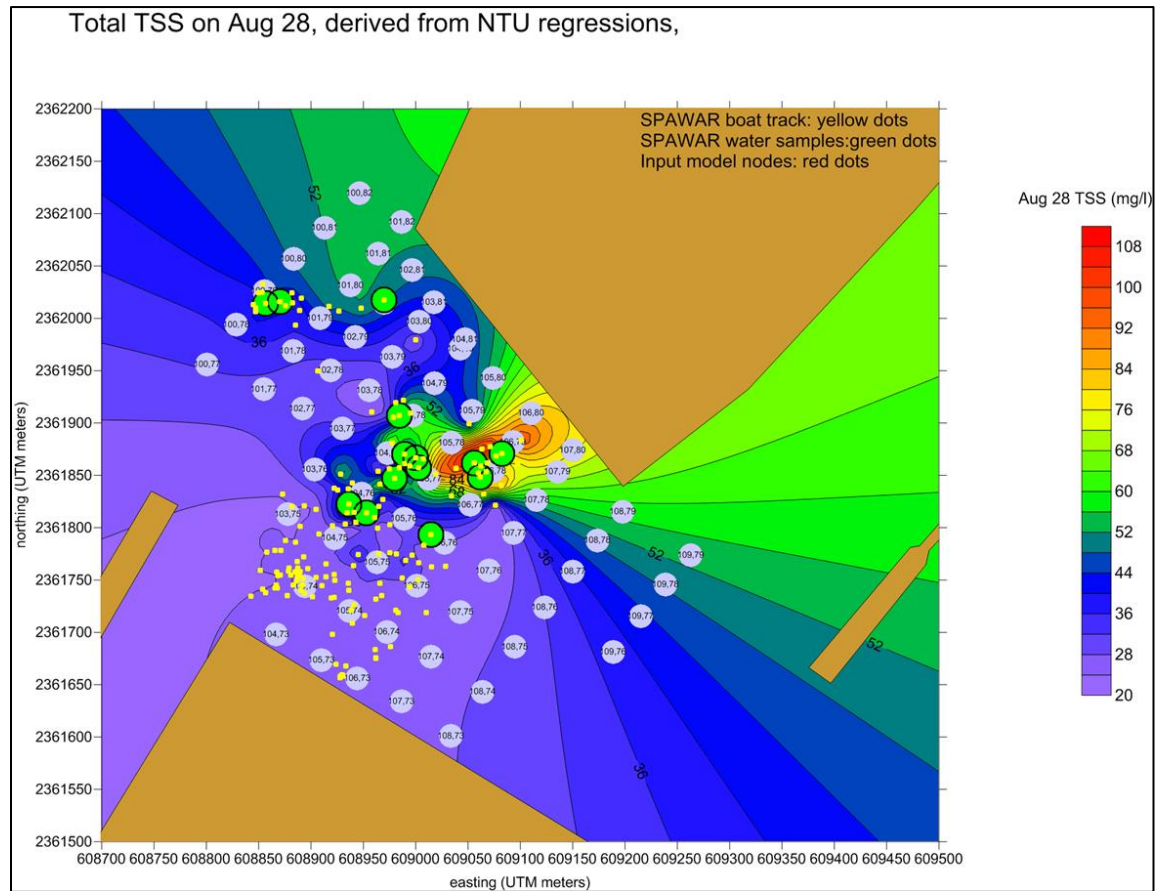


Figure 6-79. Bravo Pier boat track and OBS measurements (yellow), and discrete pump samples (green dots),

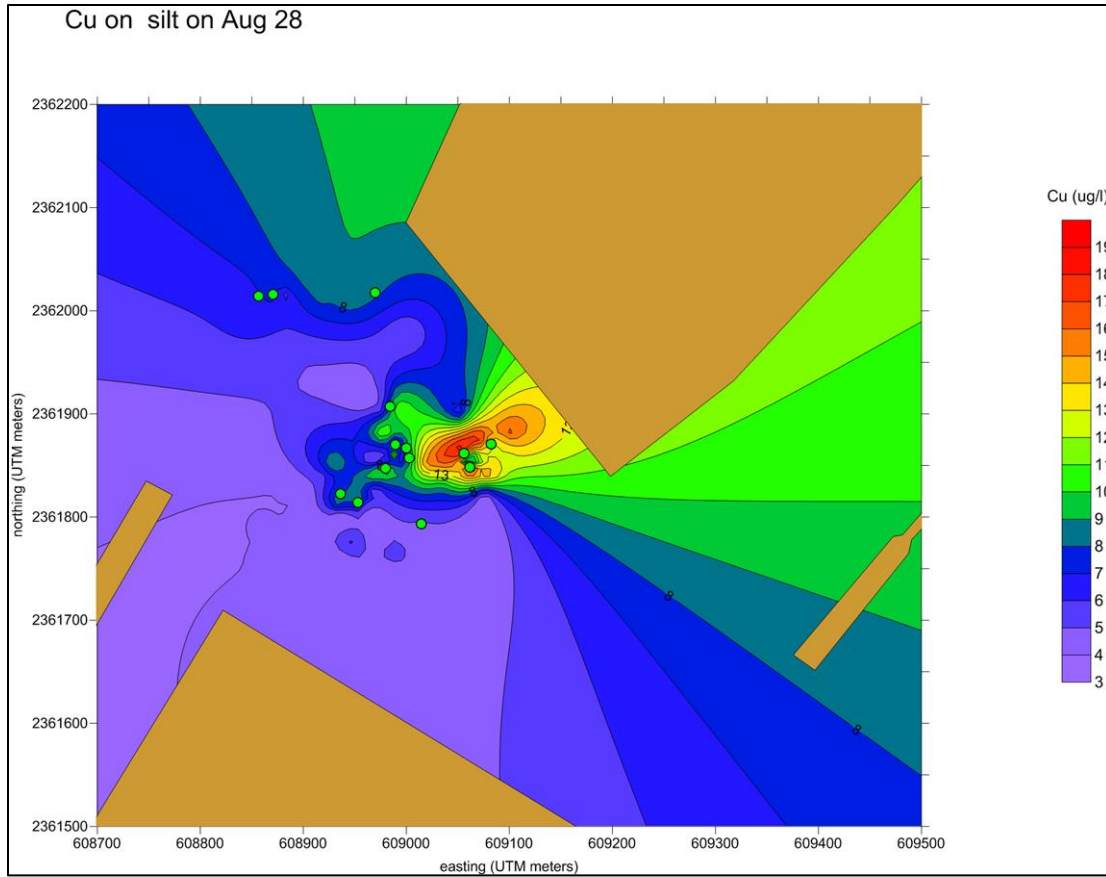


Figure 6-80. Bravo Pier discrete pump samples (green dots), and extrapolated copper on silt concentrations as colored contours.

Figure 6-81 shows the *ECOS* tracks, discrete pump sample locations, TSS derived from OBS measurements as colored contours, and the 43 nodes of the CH3D model used for model validation at Oscar Pier. Numbers on the nodes are model coordinates. Figure 6-82 is a representative figure of copper associated with resuspended silt at Oscar Pier.

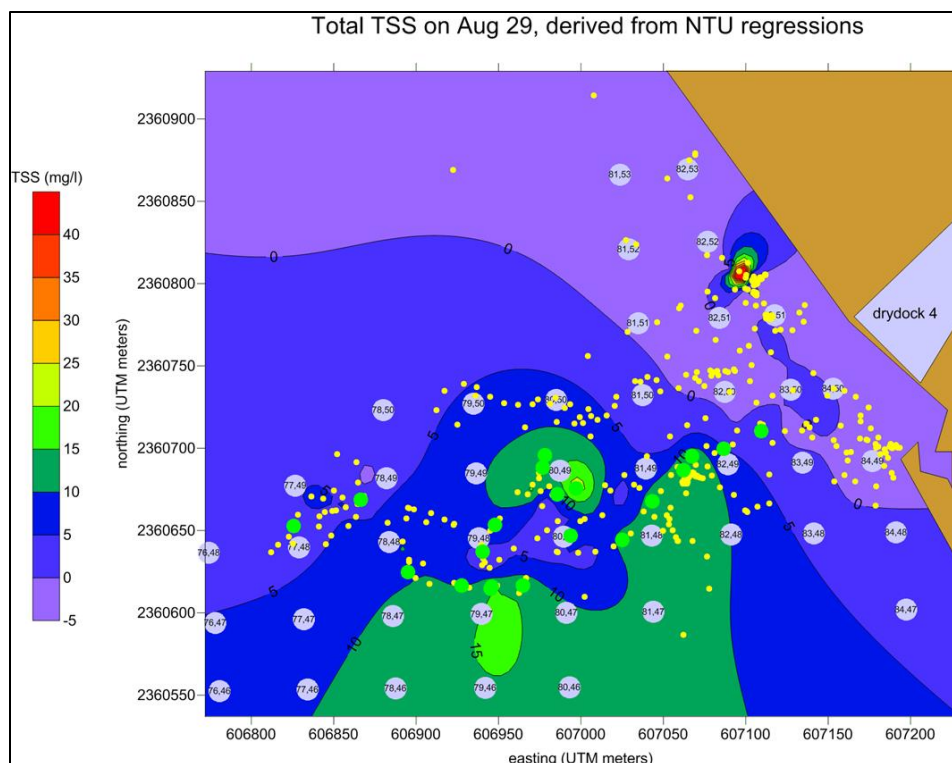


Figure 6-81. Oscar Pier boat track and OBS measurements (yellow), and discrete pump samples (green dots),

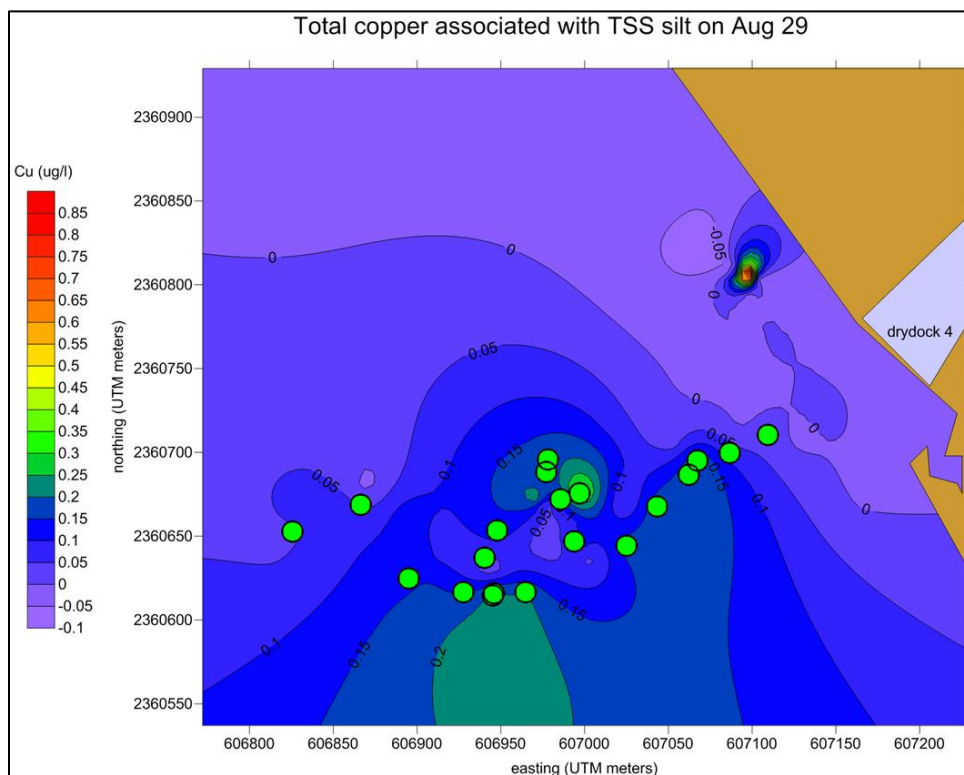


Figure 6-82. Oscar Pier discrete pump samples (green dots) and extrapolated copper on silt concentrations as colored contours.

6.3.2.6 Comparison of Model and Field Results

The hydrodynamic model, CH3D, was implemented with fate and transport of dissolved and particulate metals. Eight metals were measured and simulated fate and transport of dissolved and silt-bound copper concentrations are demonstrated for Bravo Pier and Oscar Pier. At both piers, silt particles were the predominant particles (~70%), followed by sand (~20%) and clay (<10%) (Figure 6-83 and Figure 6-84). These percent fractions contrast with those found in San Diego, which had a higher clay content and lower silt, and sand content (Figure 6-85).

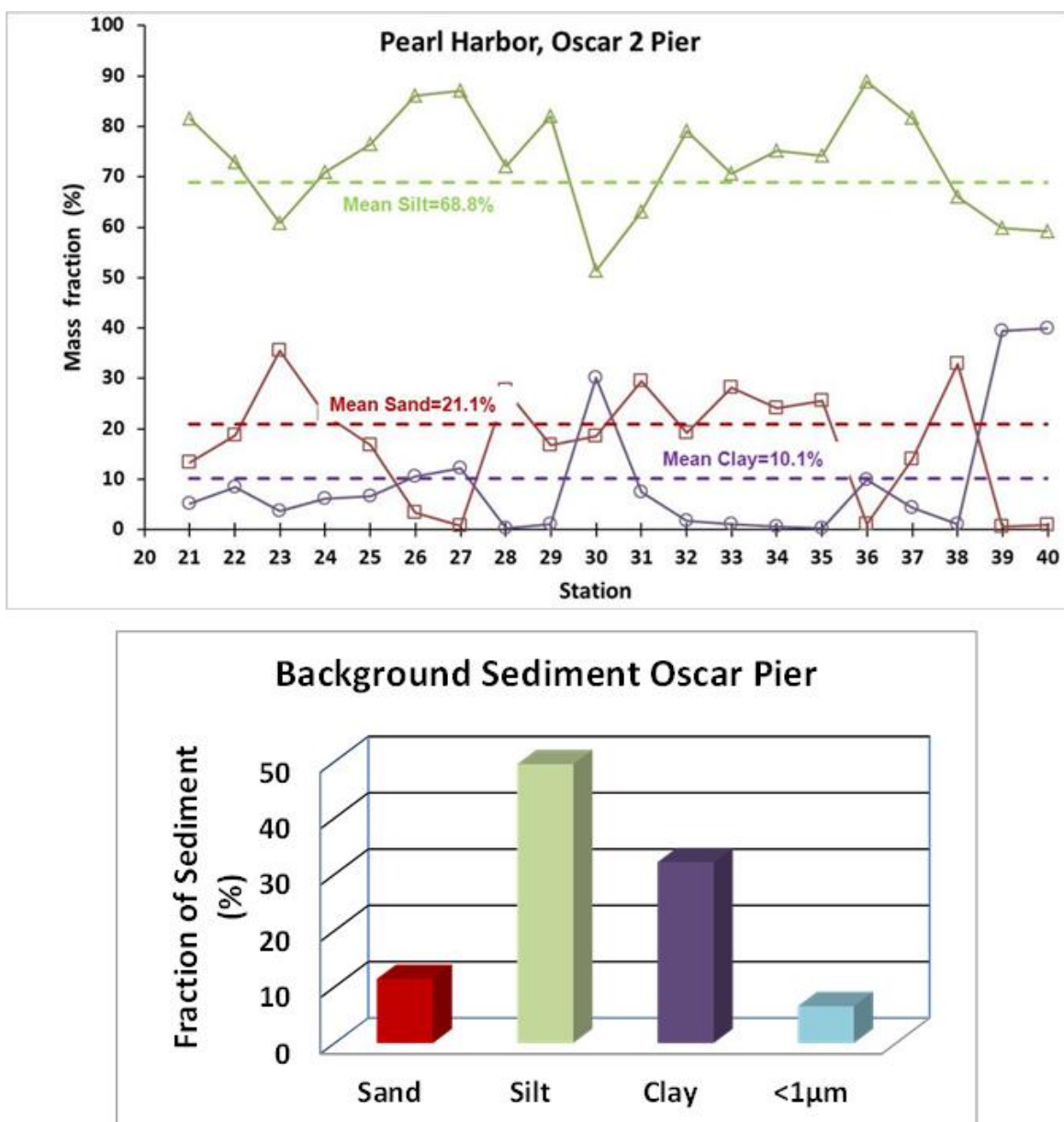


Figure 6-83. Water column particle size fractions and background sediment for clay (0.4 to 5 µm), silt (5 to 60 µm), and sand (>60 µm) for Bravo Pier in Pearl Harbor.

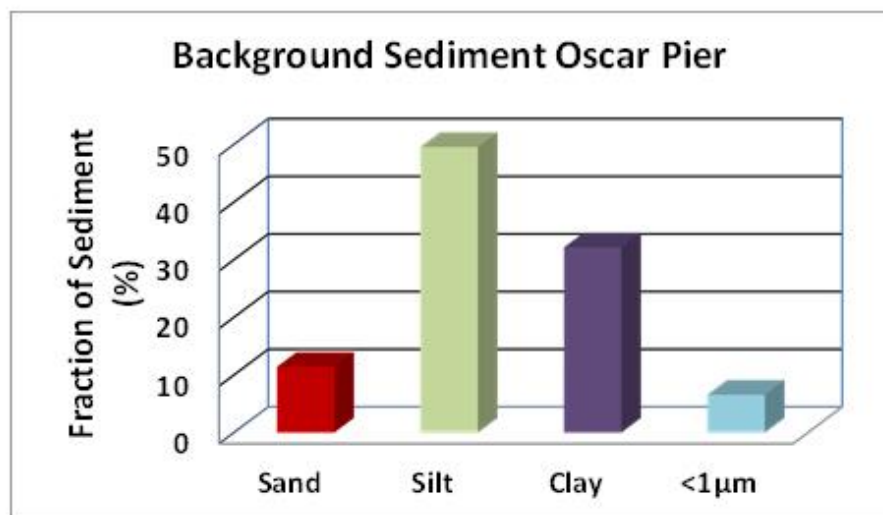
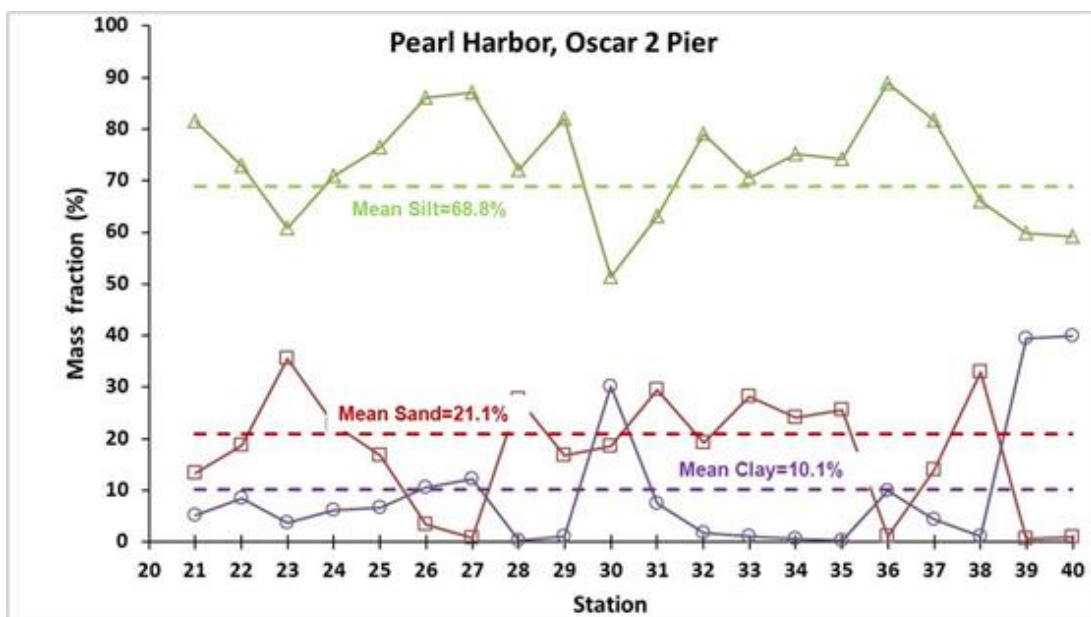


Figure 6-84. Water column particle size-fractions and background sediment for clay (0.4 to 5.0 μm), silt (5 to 60 μm), and sand (>60 μm) for Oscar Pier in Pearl Harbor.

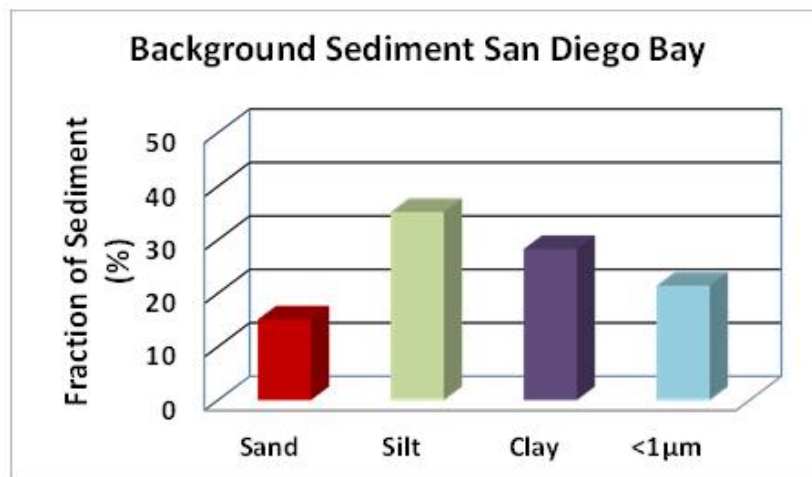
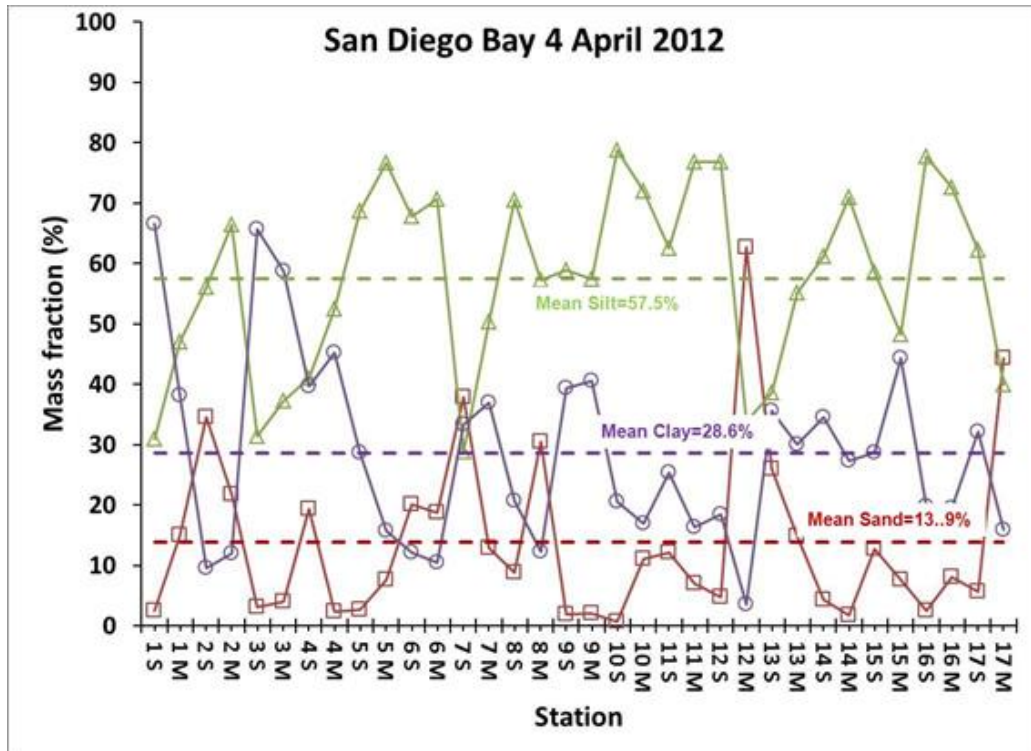


Figure 6-85. Water column particle size fractions and background sediment for clay (0.4 to 5 µm), silt (5 to 60 µm), and sand (>60 µm) for San Diego Bay.

Unlike the fate and transport modeling study for San Diego Bay, for the Pearl Harbor study, CH3D used the TSS and copper data measured during the resuspension studies at the Bravo Pier and the Oscar Pier as the initial conditions. For San Diego Bay, we used the Maynard's model, which was calibrated for the San Diego Bay resuspension potential study, to predict the eroded sediment and metal masses from the resuspension by the tugboat (C-14 Tractor). From the calibration of Maynard's model, the critical shear stress was deduced from the field data. In contrast, for Pearl Harbor, the resuspension potential study was not conducted and the critical shear stress at the Bravo Pier and Oscar Pier were unknown. Furthermore, the tugboat used for the Pearl Harbor was of the Tiger type, which is smaller in both the boat length and the propeller size than those of the C-14

Tractor tugboat, used for the San Diego Bay study. Therefore, the same modeling study framework used for San Diego Bay cannot be repeated for Pearl Harbor. Instead, we used the field data measured during the first 2 hours following the resuspension event as the initial conditions to drive the CH3D fate and transport model. This method will underestimate the model results, compared to the field data, to unknown degree. Therefore, we need to be cautious not to overinterpret model results, from which we strive to learn qualitative fate and transport patterns.

The measured size-specific TSS and copper concentrations associated with sediment and in the dissolved state at Bravo Pier and Oscar Pier were interpolated and assigned to the model grid as the initial conditions for the model (light blue circles in Figure 6-79 and Figure 6-81). The model started the hydrodynamic simulation from a state of zero motion (zero forcing) from 00:00 26 August 2012 with tidal forcing from the mouth of the harbor. Model simulation continued for 60 hours before the initial copper concentrations were assigned for the Bravo Pier at 12:00 28 August 2012, and for 84 hours before the initial copper concentrations were assigned for the Oscar Pier at 12:00 29 August 2012. Simulation continued until 23:00 2 September 2012. Model output of dissolved and silt-bound concentrations in the water column and silt-bound deposits to the sediment bed were analyzed.

6.3.2.6.1 *Bravo Pier*

The propellers of the tug-boat were turned on at the Bravo Pier between 10:36 and 11:00, 28 August 2-12. Between 11:02–12:20, water samples were collected by chasing after the plumes. Metal concentrations measured during the period were used and interpolated as the initial conditions for the subsequent fate and transport of the plume by the tidal currents.

Figure 6-86 through Figure 6-88 show the simulated transport patterns of dissolved copper in the surface layer at six selected times, $t = 0$ (initial condition), 3, 9, 18, 30, and 120 hours after the propeller wash, respectively. The propeller wash took place at the end of a flooding tide, and fate and transport was initiated during the ebbing tide. Figure 6-86 shows during the first 3 hours, ebbing tides transport the plume out of the naval station channel going first westward and then northward. As time progresses, the plume starts to go through tidal dispersion processes, oscillating during tidal cycles with the plume expanding to other regions. Dilution and expansion of the plume can be visualized from these figures. At the end of 5th day (Figure 6-88), the dissolved copper concentrations are diluted from an initial concentration of ~ 12 to ~ 0 to $0.2 \mu\text{g/L}$ values, a reduction of 98.5% in concentrations, whereas the domain of the plume expanding to almost entire harbor.

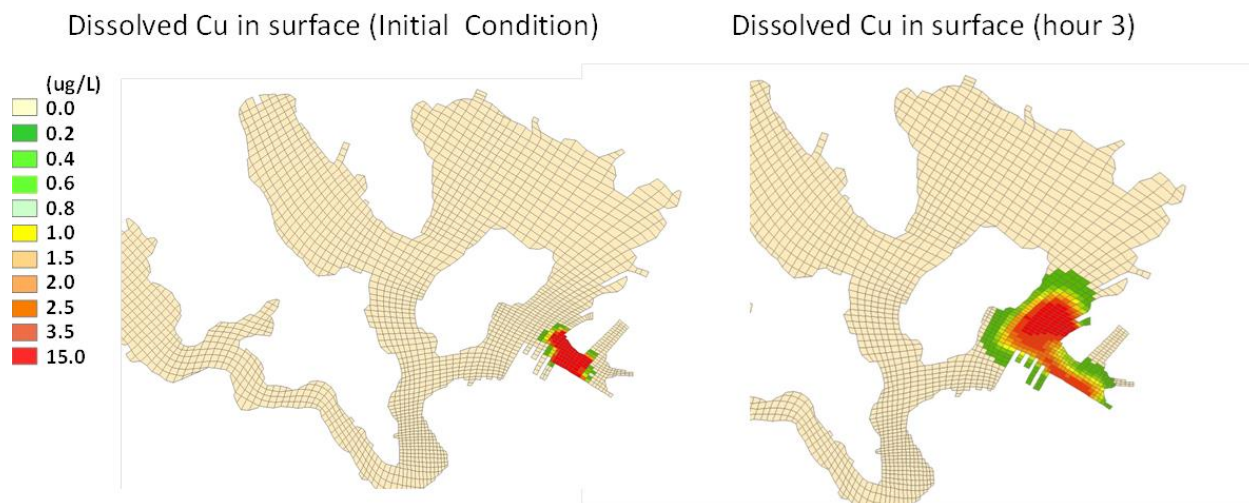


Figure 6-86. Simulated dissolved copper concentrations at surface layer for CH3D fate and transport simulation at $t = 0$ (left), and $t = 3$ hours after resuspension from prop wash (color key applies to Figure 6-86 through Figure 6-88, inclusive).

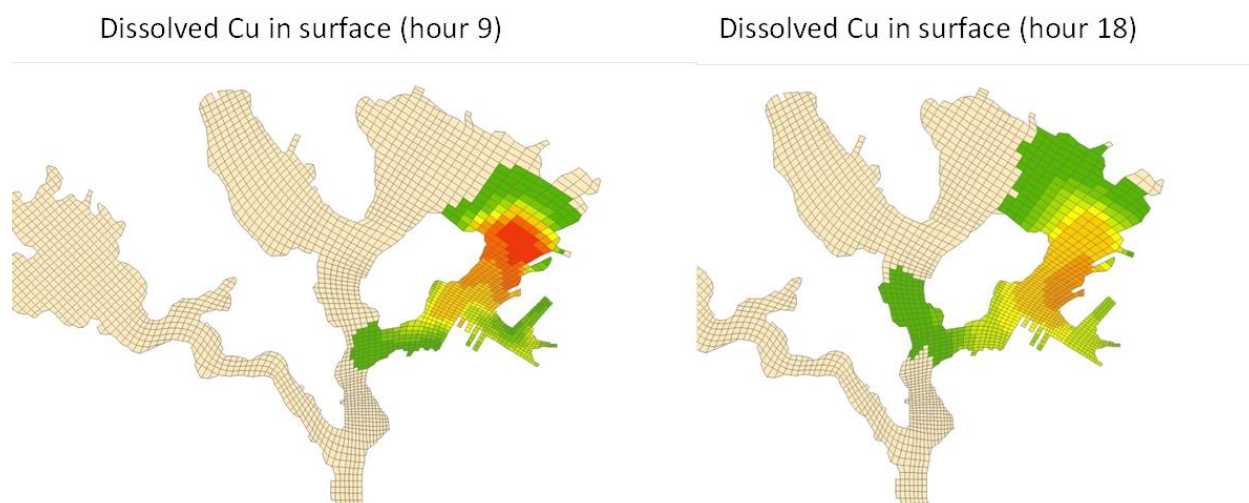


Figure 6-87. Simulated dissolved copper concentrations at surface layer at $t = 9$ hours (left), and at $t = 18$ hours after prop-wash resuspension.

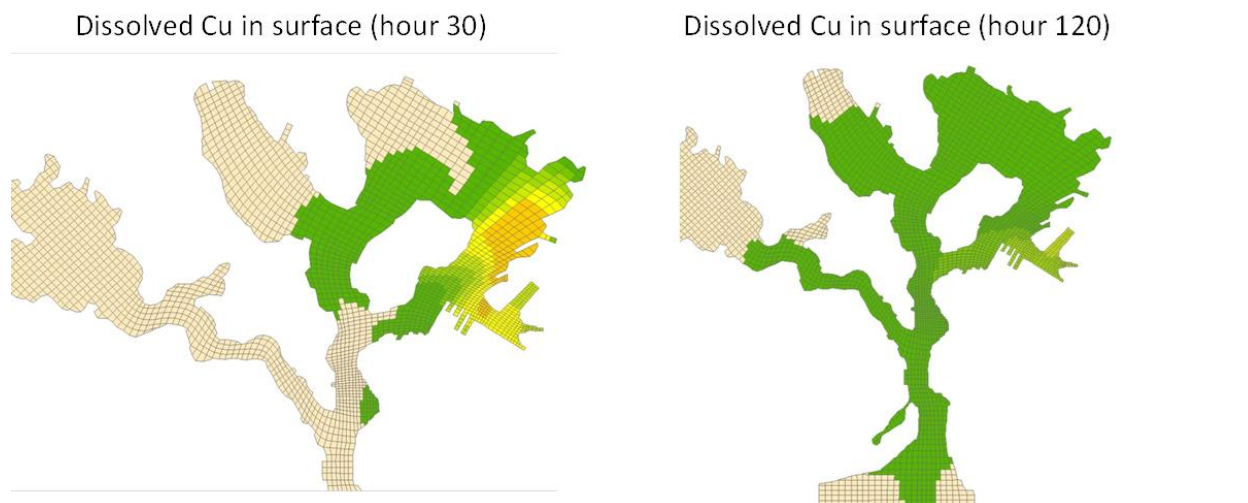


Figure 6-88. Simulated dissolved copper concentrations at surface layer at $t = 30$ hours (left), and at $t = 120$ hours after prop-wash resuspension.

In addition to the advection transport for dissolved copper, silt-particle-bound copper is subject to settling of the silt particles, which remove silt-bound copper from the water column to the bottom sediment bed. Figure 6-89 through Figure 6-92 show simulated silt-particle-bound copper concentrations at the surface layer and the bottom layer at the times of $t=0$ (initial condition), 3, 9, and 18 hours, respectively. The transport patterns are similar to those for dissolved copper, except that silt-bound concentrations decay fast during the transport. At 9 hours, simulated silt-bound copper concentrations reduce to a 0.0- to 0.2- $\mu\text{g/L}$ level (Figure 6-91), whereas dissolved copper retains a highest concentration at $\sim 10 \mu\text{g/L}$ (Figure 6-87). At 18 hours, silt-bound copper concentrations reduce to zero in the surface layer (Figure 6-92).

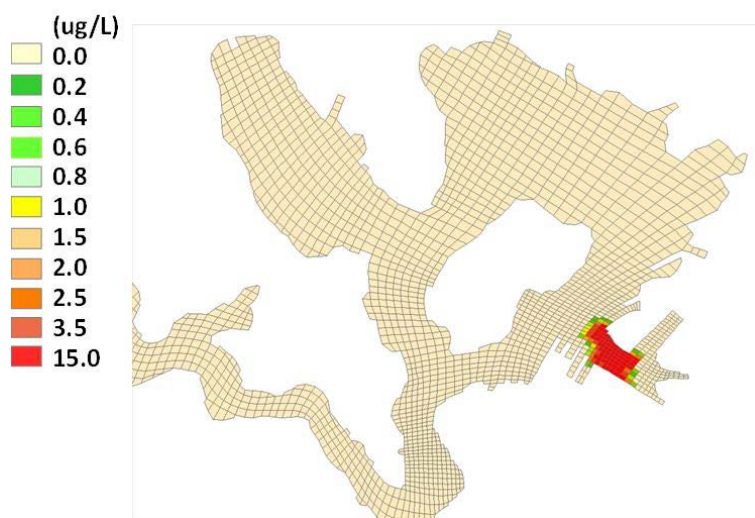


Figure 6-89. Initial silt-particle-bound copper concentrations at surface layer for CH3D fate and transport simulation at $t = 0$ after resuspension from prop wash (color key applies to Figure 6-89 through Figure 6-93, respectively).

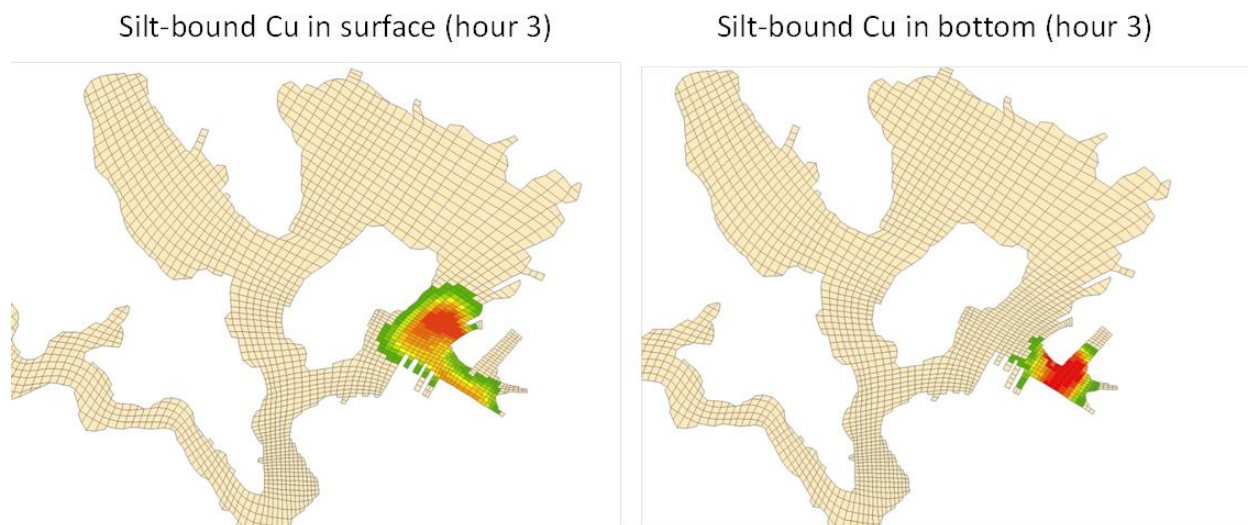


Figure 6-90. Simulated silt-particle-bound copper concentrations at surface (left), and bottom layer (right) 3 hours after prop-wash resuspension.

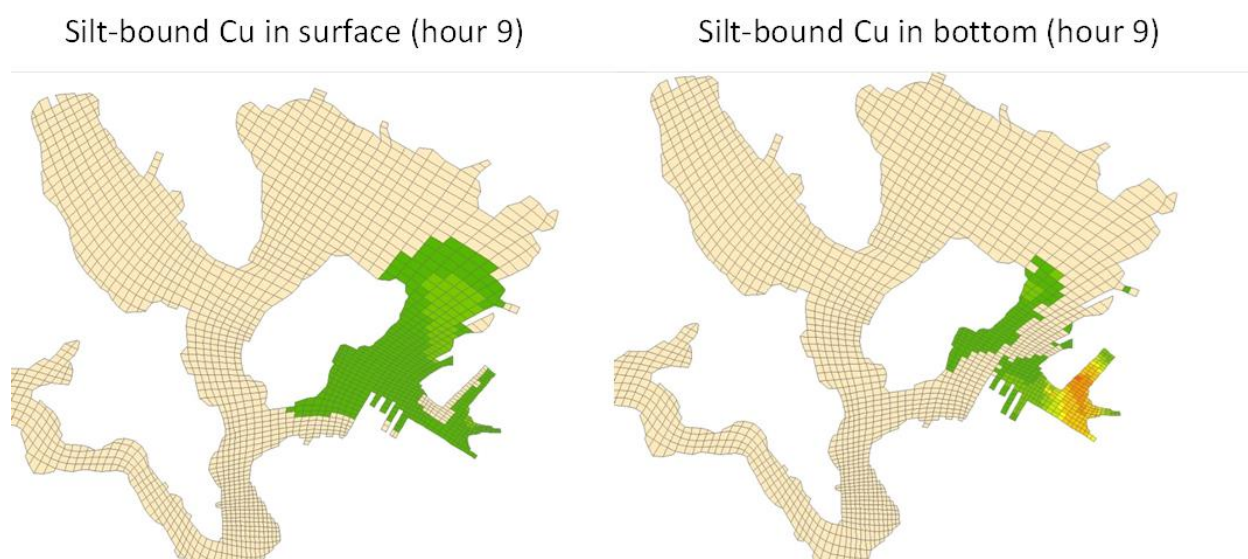


Figure 6-91. Simulated silt-particle-bound copper concentrations at surface (left), and bottom layer (right) 9 hours after prop-wash resuspension.

Silt-bound Cu in surface (hour 18)



Silt-bound Cu in bottom (hour 18)



Figure 6-92. Simulated silt-particle-bound copper concentrations at surface (left), and bottom layer (right) 18 hours after prop-wash resuspension.

Silt-bound concentrations in the bottom layer behave in a way similar to that in the surface layer, except that they decay with a much slower rate. This is because, due to settling, silt-bound copper concentrations in the bottom layer lose mass to the bottom, they also receive copper mass settled in from the upper layers. Therefore, the loss rate at the bottom layer is much slower than that for the surface layer. Silt-bound copper concentrations still retain a level of 0 to 0.3 $\mu\text{g/L}$ at 30 hours (Figure 6-93, left). The submerged plume loses its total mass by 120 hour (Figure 6-93, right).

Silt-bound Cu in bottom (hour 30)



Silt-bound Cu in bottom (hour 120)



Figure 6-93. Simulated silt-particle-bound copper concentrations at bottom layer at $t = 30$ hours (left), and $t = 120$ hours (right) after prop-wash resuspension.

Figure 6-94 through Figure 6-96 show simulated silt-bound copper deposits (footprint) from the propeller wash plume during the first 5 days. Figure 6-94 shows that the initial plume deposits a major portion of the mass during the first 3 to 9 hours toward the inner channel (sub-base). As time progresses with the plume migrating, the deposit increases both in magnitude and in domain. The general deposition pattern starts from the resuspension site extending toward the Southeast Loch from the channel east of Ford Island and then toward the central channel, between Naval Reservation and Ford Island. At 120 hours, the deposition domain has extended to the water surrounding Ford Island and further toward the mouth. Simulated deposition patterns reveal that while prop wash may be a local activity (occurring at the pier for this study), the fate and transport of the sediment plume may result in remigration and deposition patterns that extend beyond the local site.

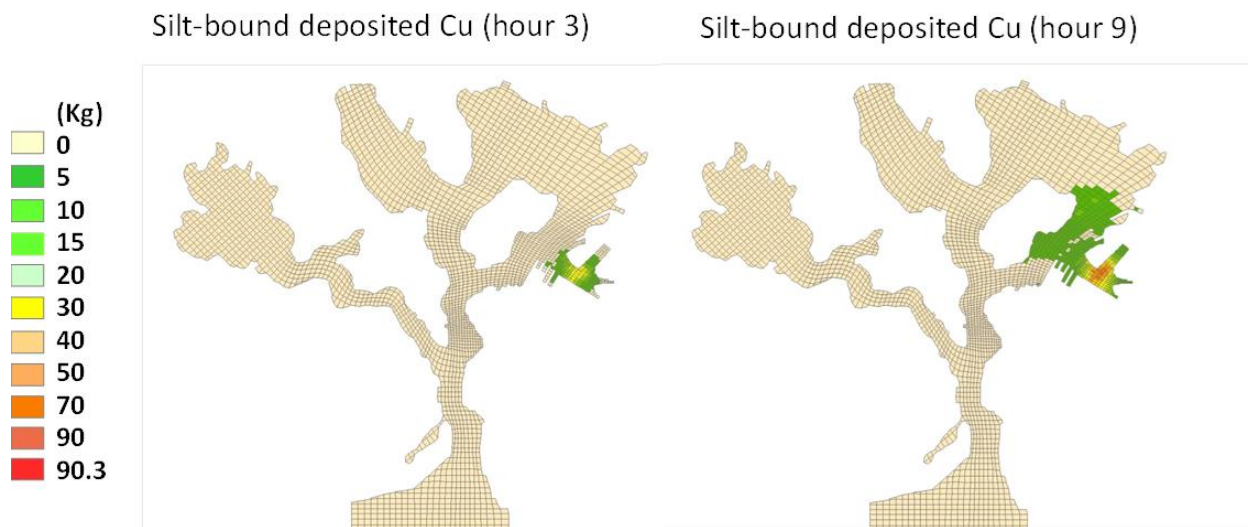


Figure 6-94. Simulated silt-particle-bound deposits to the bottom bed at $t = 3$ hours (left), and at $t = 9$ hours after prop-wash resuspension (color key applies to Figure 6-94 through Figure 6-96).

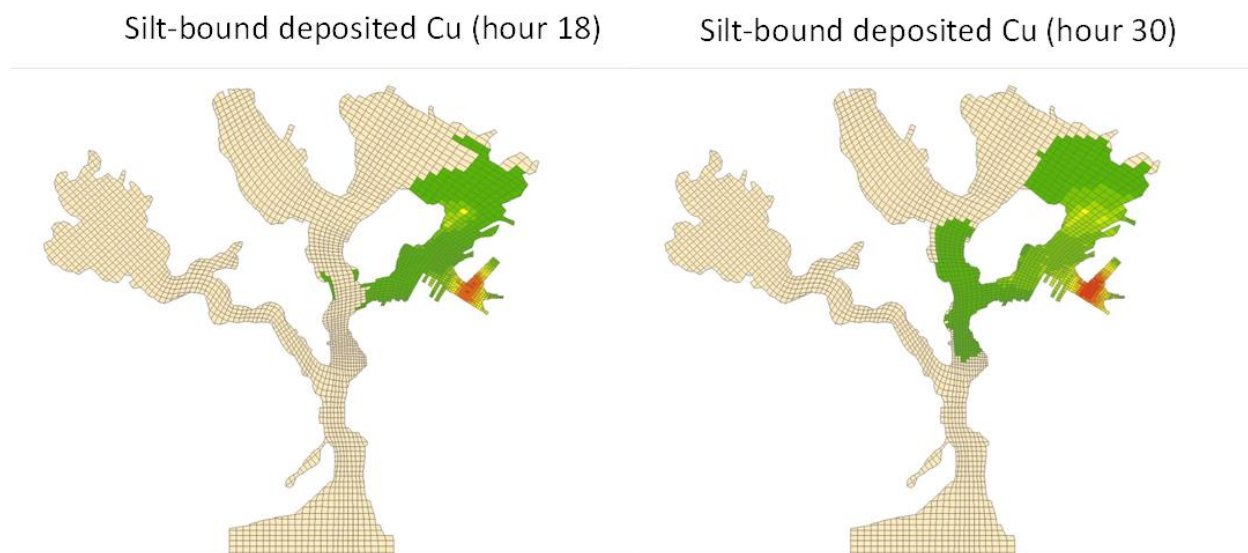


Figure 6-95. Simulated silt-particle-bound deposits to the bottom bed at $t = 18$ hours (left), and at $t = 30$ hours after prop-wash resuspension.

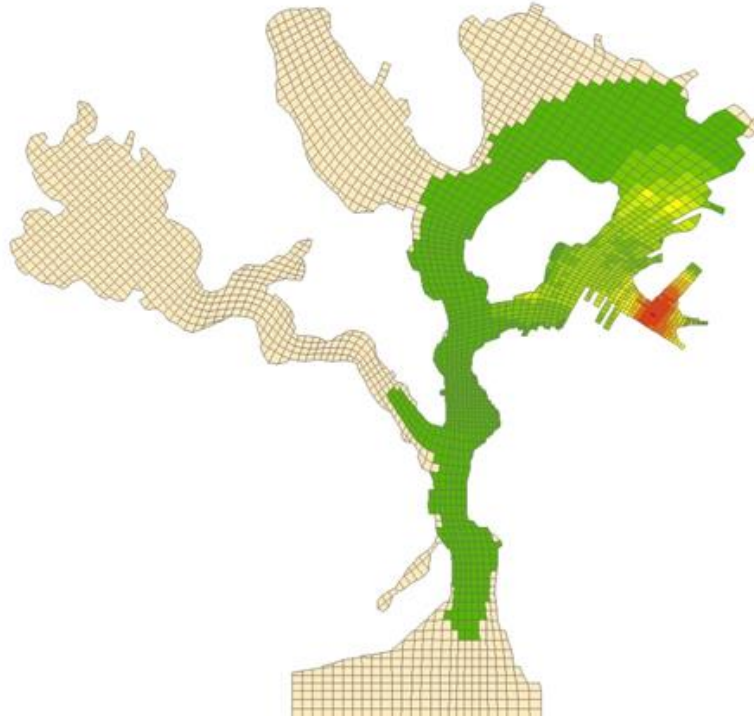


Figure 6-96. Simulated silt-particle-bound deposits to the bottom bed at $t = 120$ hours after prop-wash resuspension.

6.3.2.6.2 *Oscar Pier*

The propellers of the tug-boat were turned on at the Oscar Pier between 10:25 and 11:30, 29 August 2012. Between 11:30–13:08, water samples were collected by chasing after the plumes. Metal concentrations measured during the period were used and interpolated as the initial conditions for the subsequent fate and transport of the plume by the tidal currents.

Figure 6-97 through Figure 6-100 show the simulated transport patterns of dissolved copper in the surface layer at six selected times: $t = 0$ (initial condition), 3, 9, 18, 30, and 120 hours after the propeller wash, respectively. The propeller wash took place during the flooding tide, and fate and transport was initiated during the flooding tide. Figure 6-98 shows that, during the first 3 hours, flooding tides push the plume northward, toward Ford Island along the west channel. As time progresses, the plume starts to going through tidal dispersion processes, oscillating during tidal cycles with the plume expanding to other regions. Dilution and expansion of the plume can be seen from these figures. At the end of the 5th day (Figure 6-100), the dissolved copper concentrations are diluted from an initial concentration of $\sim 1 \mu\text{g/L}$ to ~ 0 to $0.2 \mu\text{g/L}$ values, a reduction of 90% in concentrations, whereas the domain of the plume expanding to a larger domain including a major portion of East Loch and Middle Loch, and the channels west of Ford Island.



Figure 6-97. Initial dissolved copper concentrations at Oscar Pier surface layer for CH3D simulation at $t = 0$ after resuspension from prop wash (color key applies to Figure 6-97 through Figure 6-100).

Dissolved Cu in surface Oscar (hour 3)

Dissolved Cu in surface Oscar (hour 9)



Figure 6-98. Figure 4-98. Simulated dissolved copper concentrations at Oscar Pier surface layer for CH3D simulation at $t = 3$ hours (left), and at $t = 9$ hours after prop-wash resuspension.

Dissolved Cu in surface Oscar (hour 18)

Dissolved Cu in surface Oscar (hour 30)

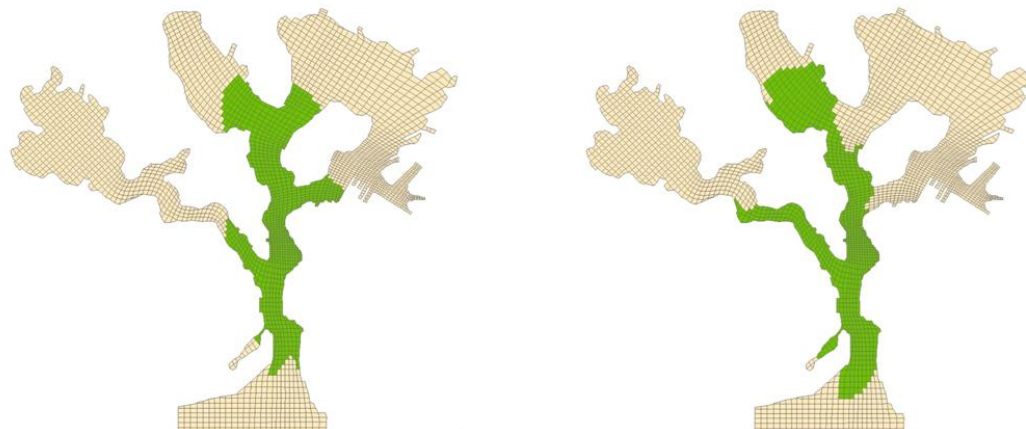


Figure 6-99. Simulated dissolved copper concentrations at Oscar Pier surface layer for CH3D simulation at $t = 18$ hours (left), and at $t = 30$ hours (right) after prop-wash resuspension.

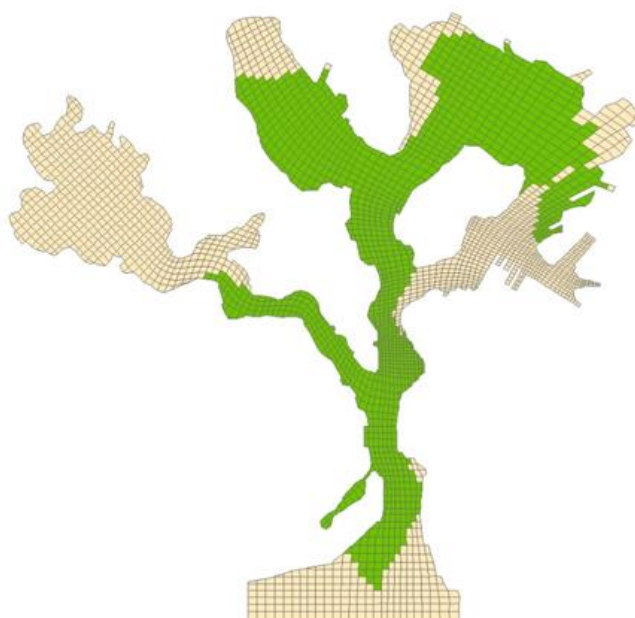


Figure 6-100. Simulated dissolved copper concentrations at Oscar Pier surface layer for CH3D simulation at $t = 120$ hours after prop-wash resuspension.

Compared to the resuspension sediment plume for Bravo Pier, the Oscar Pier plume is much smaller in magnitude. The color spectrum shows that approximately the highest concentration of the plume is $1 \mu\text{g/L}$ for the Oscar Pier test, compared to $\sim 15 \mu\text{g/L}$ for the Bravo Pier plume.

Therefore, Figure 6-101 and Figure 6-102 show that silt-bound copper concentrations are low throughout the first few hours of the plume. The surface silt-bound plume loses its major mass before 9 hours and bottom layer loses its mass before 18 hours throughout the harbor.

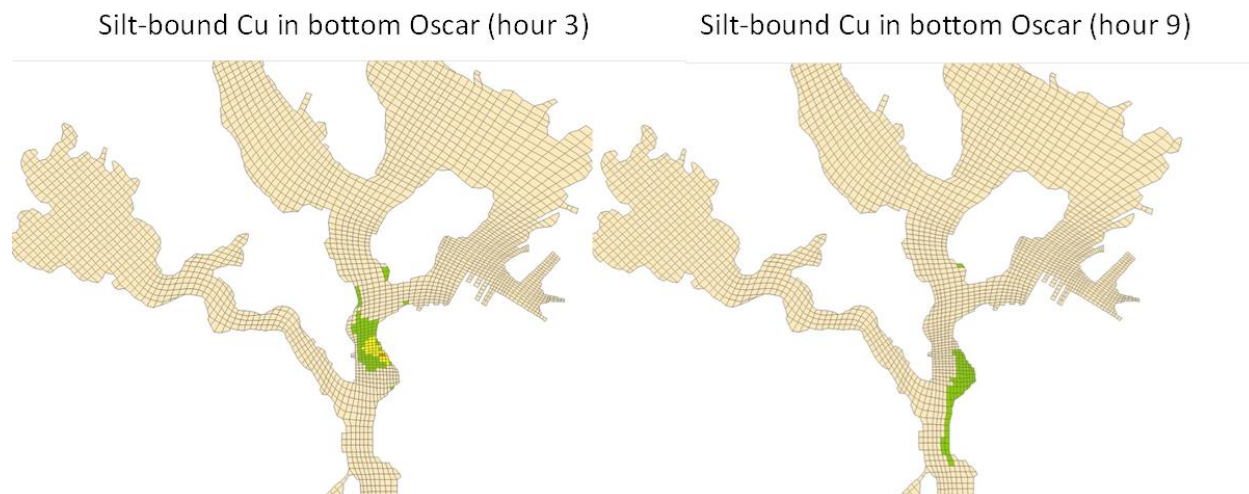


Figure 6-101. Simulated silt-particle-bound copper concentrations at Oscar Pier bottom layer for CH3D simulation at $t = 3$ hours (left), and $t = 9$ hours after prop-wash resuspension.

Silt-bound Cu in bottom Oscar (hour 18)

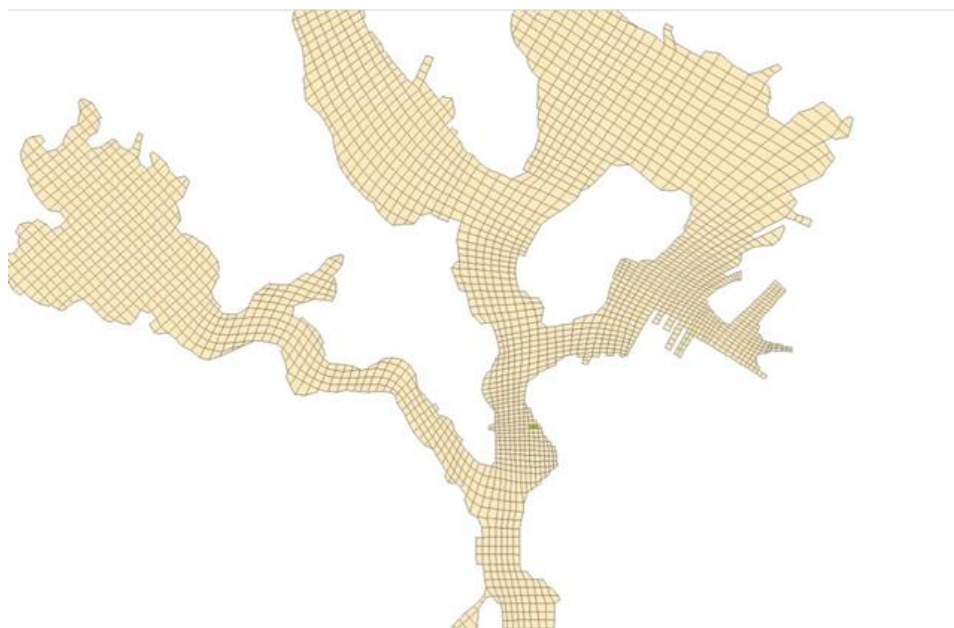


Figure 6-102. Simulated silt-particle-bound copper concentrations at Oscar Pier bottom layer for CH3D simulation at $t = 18$ hours after prop-wash resuspension.

The Oscar Pier plume deposits its majority of mass of the silt particles and the associated copper mass during the first 18 hours (Figure 6-103 through Figure 6-105). However, deposition of the low-concentration plume of the water column continues during the first 30 hours (Figure 6-104). Between 30 and 120 hours, the deposition patterns only increase slightly in the East Loch.

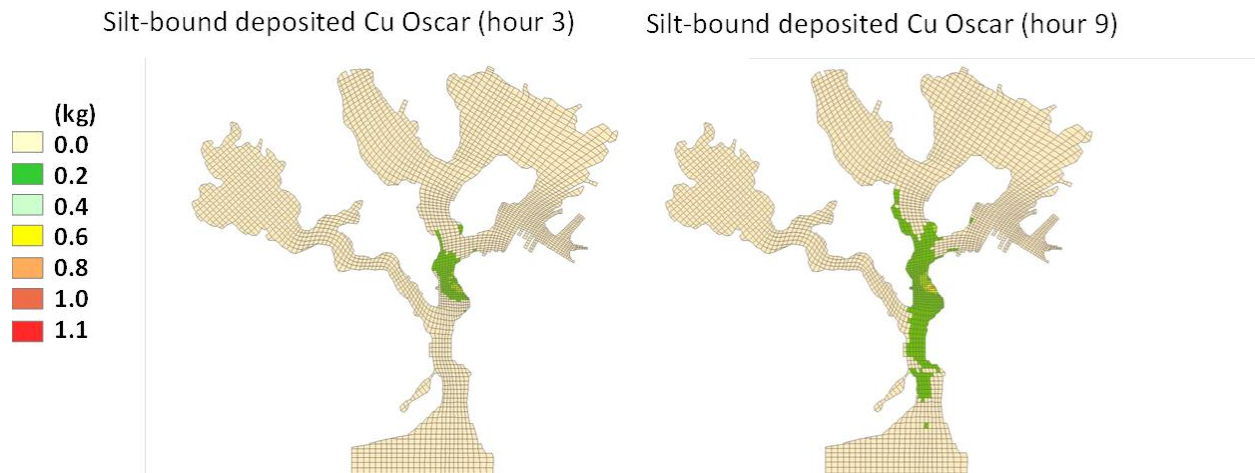


Figure 6-103. Simulated silt-particle-bound deposits to the Oscar Pier bottom bed at $t = 3$ hours (left), and $t = 9$ hours after prop-wash resuspension.

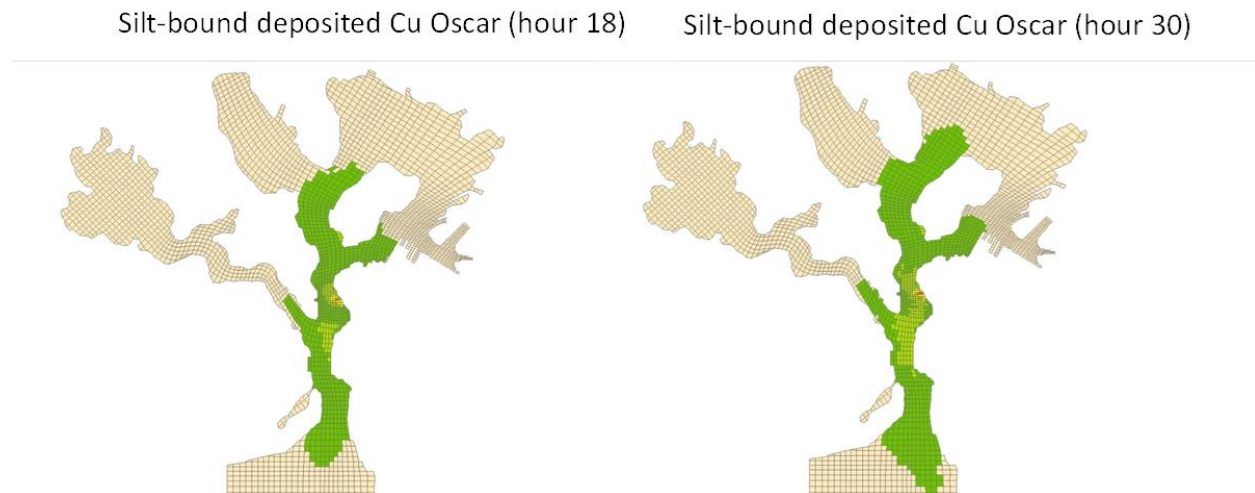


Figure 6-104. Simulated silt-particle-bound deposits to the Oscar Pier bottom bed at $t = 18$ hours (left), and $t = 30$ hours after prop-wash resuspension.

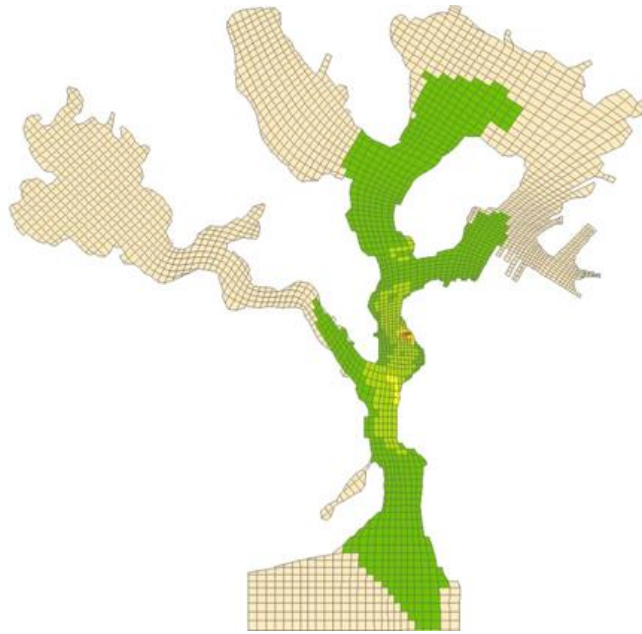


Figure 6-105. Simulated silt-particle-bound deposits to the bottom bed at $t = 120$ hours after prop-wash resuspension at Oscar Pier.

Once resuspended by propeller wash, the sediment plumes in the water column started the settling process. Model results show the plume in the surface layer decay at a speed faster than that for the bottom layer, due to the settling process discussed above. Figure 6-106 shows such variations in the water column from both the model results and field data. During the time-window of 11:23–12:45, 29 August 2012, the survey boat was around the Oscar Pier taking ADCP backscattering for TSS concentrations. Figure 6-106 shows the TSS by ADCP (right) which exhibits weak vertical variation with TSS concentrations higher at the bottom layer than at the surface layer. Model results during the period also show similar vertical variations (left and middle) between the surface layer and the bottom layer.

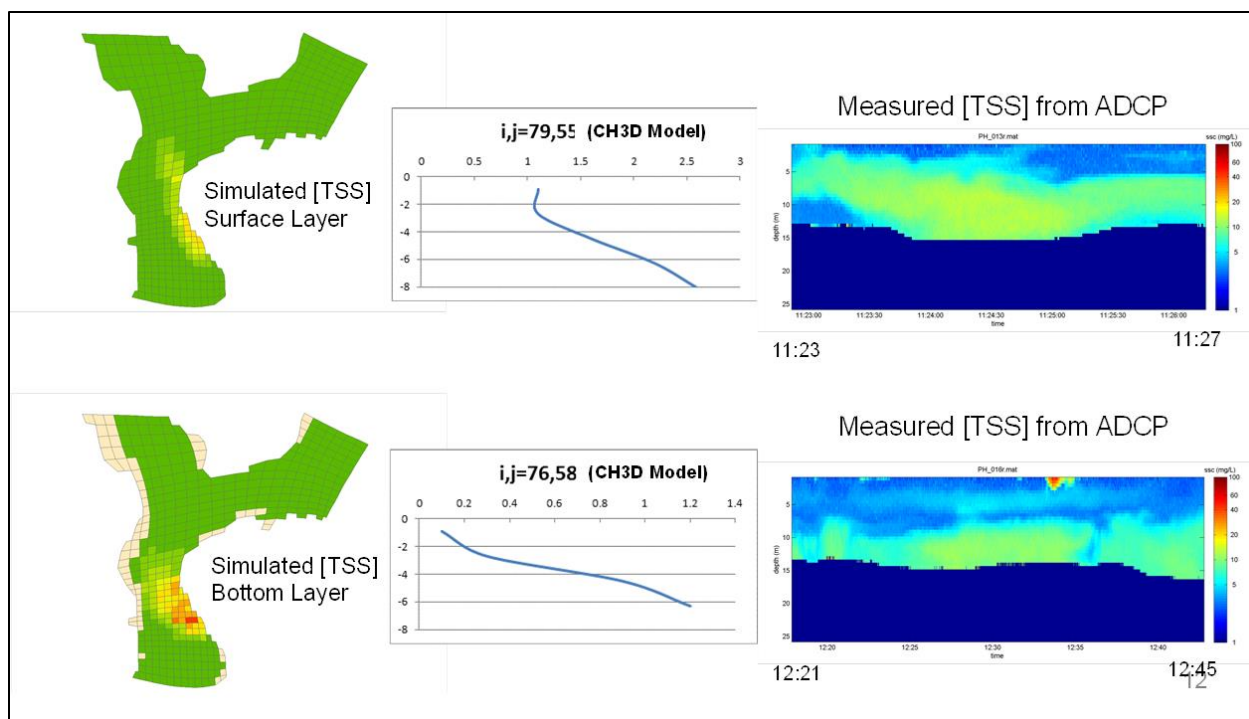


Figure 6-106. Simulated water column TSS contours (left), TSS vertical profiles (center), and time series of TSS measured by ADCP (right) near the Oscar pier during the 11:23–12:45, 29 August 2012.

6.4 RESUSPENSION FROM A DEEP-DRAFT VESSEL

6.4.1 Field Observations using ADCP

The vessel operations on the afternoon of 31 August 2012 (also from Bravo Pier) offer a contrasting case of plume generation, relative to the plumes generated by the tugs at Bravo and Oscar Piers. In this case (Figure 6-107), USS *Chafee* (length: 155 m; beam: 20 m; loaded draft: 9 m⁵) was pulled abeam from the pier by two tugs. The tugs performed a turning maneuver in the basin and assisted *Chafee*'s departure from the berthing area. A large, turbid surface plume was observed during the turning maneuver. Approximately 13 min after the vessel operation commenced, the ADCP survey began and measured SSC values on the order of 80 mg/L with a longitudinal scale of approximately 500 m (several times the length of *Chafee*). The subsurface plume extended well into the turning basin and persisted with concentrations on the order of 20–30 mg/L at 1 hour and 10–15 mg/L at approximately 3 hours. The horizontal scales and initial sediment distribution of the plume and the locations of maximum concentration suggest that the plume was generated predominantly by under keel flows of *Chafee*, instead of tug jets, since the dominant plume centers took place in the wake of *Chafee*. These observed plume patterns are consistent with the FANS model results for the deep-drafted vessel, i.e., DDG, to be discussed in Section 6.4.2.

⁵ The US Navy -- Fact File: Destroyers - DDG, http://www.navy.mil/navydata/fact_display.asp?cid=4200&tid=900&ct=4, accessed 13 Jan 2016.

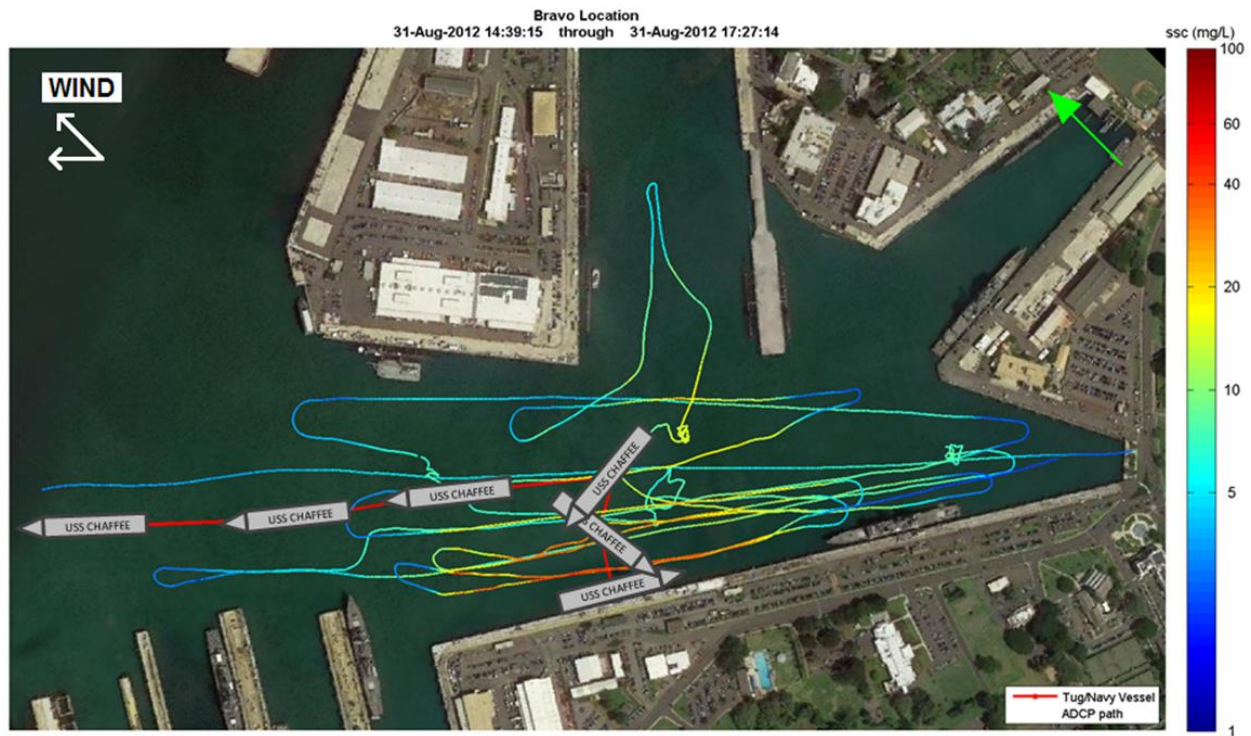


Figure 6-107. ADCP track line with depth-averaged SSC (31 August 2012) indicated by color. Note that the track positions vary with time and do not indicate a snapshot in time. The sketched vessel positions indicate the approximate positions and sequence of vessel maneuvers during plume generation. Imagery ©2014 DigitalGlobe, U.S. Geographical Survey, USGS, Map data ©2014 Google Life mode Terms Privacy Report a problem.

6.4.2 Simulation Scenarios for DDG-51 Ship

FANS simulation were performed for a DDG-51 ship as shown in Figure 6-108 under two different water depths (10.0588 m and 11.5824 m) and two different propeller rotating speeds (26 and 51 RPM). The length of the DDG-51 ship is 142.04 m (466 ft) and the designed draft is 9.4488 m. The diameter of the twin-screw propellers is 5.4864 m (18 ft), and the center of propeller axis is located at 5.7912 m below the mean water level. For the shallow water case with 10.0584 m (33 ft) water depth, the under keel clearance is only 0.6096 m (2 ft) beneath the sonar dome and the minimum gap between the propeller tip and the sea bottom is 1.524 m (5 ft). The propeller rotating speed is 26 rpm when the ship speed is 5 knots. The ship speed increases to 10 knots when the propeller is rotating at 51 rpm. Detailed information of DDG-51 ship and P4876 propellers are summarized in Table 6-23.

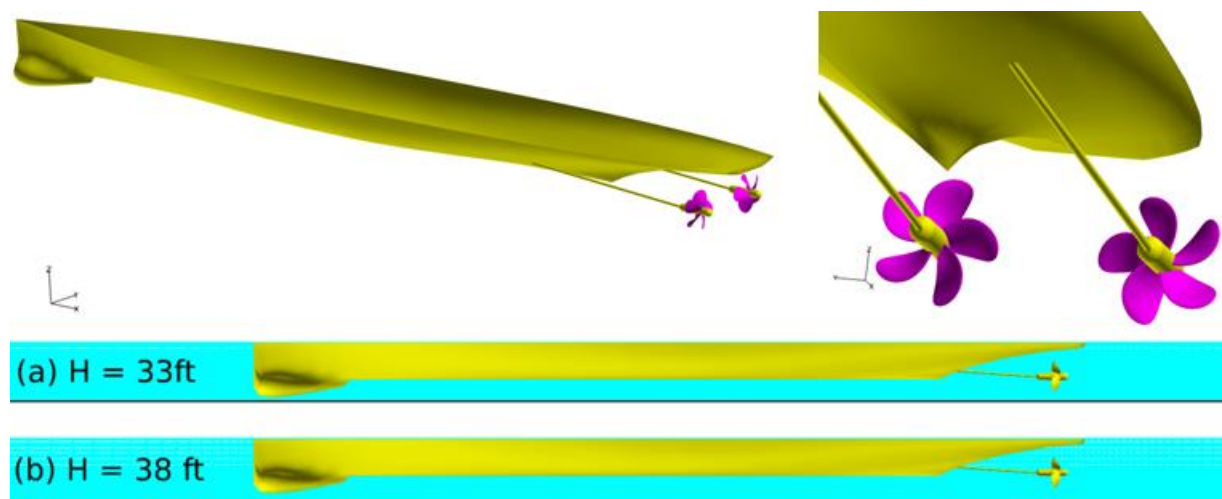


Figure 6-108. DDG-51 ship and P4876 propeller geometry.

Table 6-23. Propeller information for DDG-51 ship in FANS simulation.

Case #	1	2	3	4
Ship length L (m)	142.04 (466 ft)	142.04 (466 ft)	142.04 (466 ft)	142.04 (466 ft)
Ship Draft (m)	9.4488 (31 ft)	9.4488 (31 ft)	9.4488 (31 ft)	9.4488 (31 ft)
Water depth, H (m)	10.0584 (33 ft)	11.5824 (38 ft)	10.0584 (33 ft)	11.5824 (38 ft)
Underkeel clearance (m)	0.6096 (2 ft)	0.6096 (2 ft)	2.1336 (7 ft)	2.1336 (7 ft)
Propeller Diameter, D (m)	5.4864 (18 ft)	5.4864 (18 ft)	5.4864 (18 ft)	5.4864 (18 ft)
Distance between Propellers (m)	9.8755 (32.4 ft)	9.8755 (32.4 ft)	9.8755 (32.4 ft)	9.8755 (32.4 ft)
Distance from ship stern to propeller (m)	4.8768 (16 ft)	4.8768 (16 ft)	4.8768 (16 ft)	4.8768 (16 ft)
Propeller Depth (depth of the propeller axis)	5.7912 (19 ft)	5.7912 (19 ft)	5.7912 (19 ft)	5.7912 (19 ft)
Distance from center of propeller axis to bottom	4.2672 (14 ft)	4.2672 (14 ft)	5.7912 (19 ft)	5.7912 (19 ft)
Forward Thrust (N)	47314	47314	175307	175307
Ship speed (knots)	5	5	10	10
Propeller rpm, n	26	26	51	51
Propeller advance coefficient	1.082	1.082	1.103	1.103
Characteristic velocity, nD (m/s)	2.3774	2.3774	4.6634	4.6634
Reynolds number based on propeller diameter D	1.115×10^7	1.115×10^7	2.187×10^7	2.187×10^7
Reynolds number based on ship length L	3.262×10^8	3.262×10^8	6.245×10^8	3.262×10^8

6.4.3 FANS Model Simulation Results for DDG-51 Ship

Figure 6-109 shows the computational domain and multi-block overset grids used in the present study. The overset grid system consists of 15 computational blocks and 7 phantom grid blocks with a total of 2,369,549 grid points covering half of the solution domain. A near-wall spacing of 5.4864×10^{-6} m was used near the sea bottom to provide accurate resolution of the turbulent boundary layer flow. Since the first grid point is located within the laminar sublayer, it allows us to calculate the shear stresses on the seabed directly without relying on the wall-function approximations.

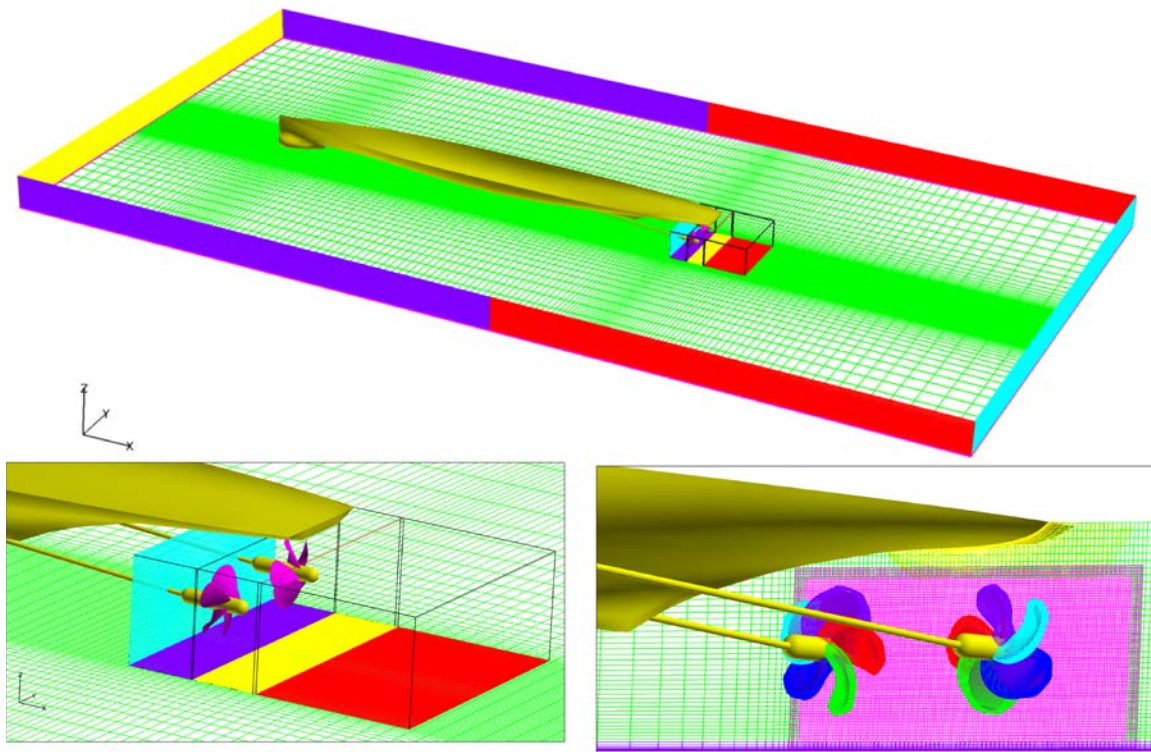


Figure 6-109. Computational domain and numerical grids.

All calculations were performed for 4,000 time steps (i.e., 100 propeller revolutions) using 12 CPUs on a Linux cluster. For the 5-knot cases, the ship travels 230.8 sec and a total distance of 594 m. When the ship speed was increased to 10 knots, it took approximately 117.7 sec for the ship to travel total distance of 605 m over 100 propeller revolutions. The simulation results clearly indicated that the propeller-induced shear stresses reached a periodic pattern in less than 50 propeller revolutions.

6.4.3.1 Disturbed Velocity Profiles

Figure 6-110 shows the predicted velocity contours and velocity vectors adjacent to the sea bottom. For completeness, the velocity vectors at the keel plane is also shown in Figure 6-111 to provide a more detailed understanding of the three-dimensional flow field induced by the ship motions. For simplicity, the velocities are normalized by a characteristic velocity $V_o = nD$, given in Table 6-23, where n is the propeller rotating speed (rps) and D is the propeller diameter (m). Note that the ship is traveling in the negative x -direction on an earth-fixed frame, which is equivalent to a positive current in the x -direction on a ship-fixed reference frame. It is clearly seen from

Figure 6-110 and Figure 6-111 that there is strong flow acceleration beneath the sonar dome when the water is forced to pass through the narrow underkeel clearance below the sonar dome, which resulted in positive velocities (in the opposite direction of the ship motion) and high shear stresses beneath the sonar dome.

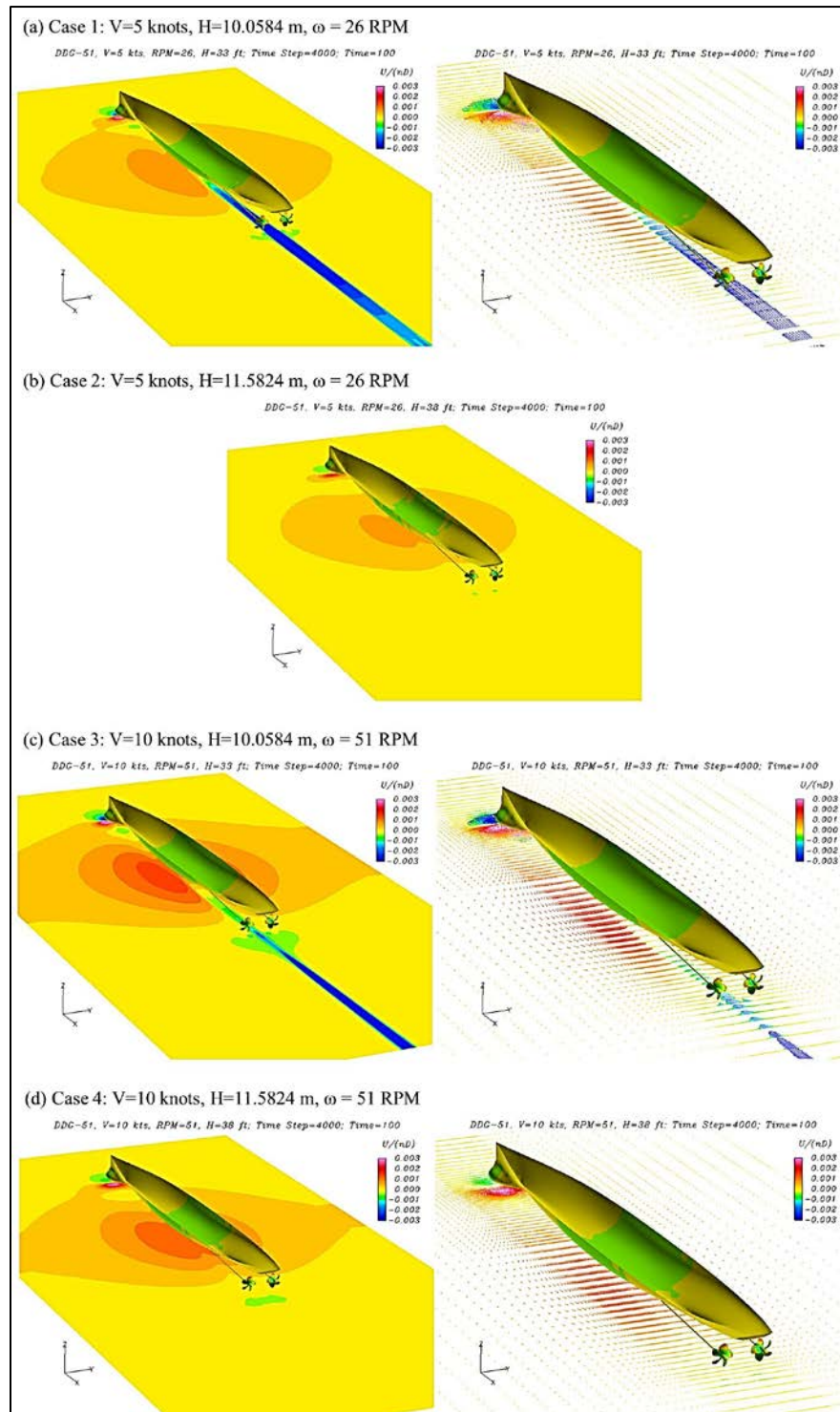


Figure 6-110. Longitudinal velocity contours and velocity vectors near seabed.

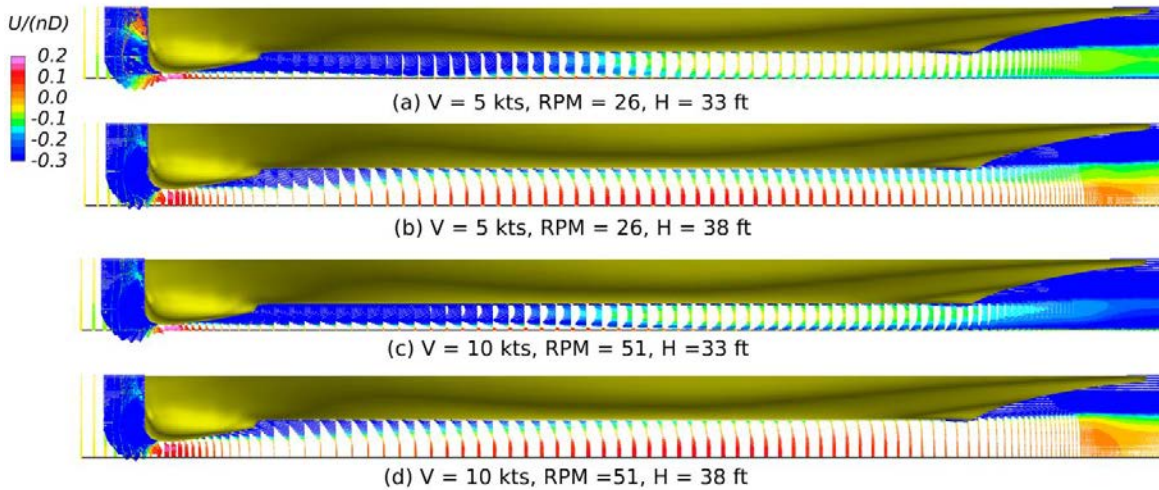


Figure 6-111. Velocity profiles at the keel plane.

Figure 6-112 shows the propeller induced velocity distribution along the center plane of the propeller axis. The axial velocity contours at five selected cross-sections are also shown in Figure 6-113 to provide a better understanding of the swirling flow pattern induced by the propeller rotation. It is seen that the propeller rotation induced strong swirling flow immediately downstream of the propeller. The axial flow induced by the propeller thrust force remains strong for more than 15 propeller diameters behind the ship stern even though a rather coarse grid was used in the far wake. This strong axial flow is expected to carry the suspended sediment for a long distance downstream of the twin-screw propellers.

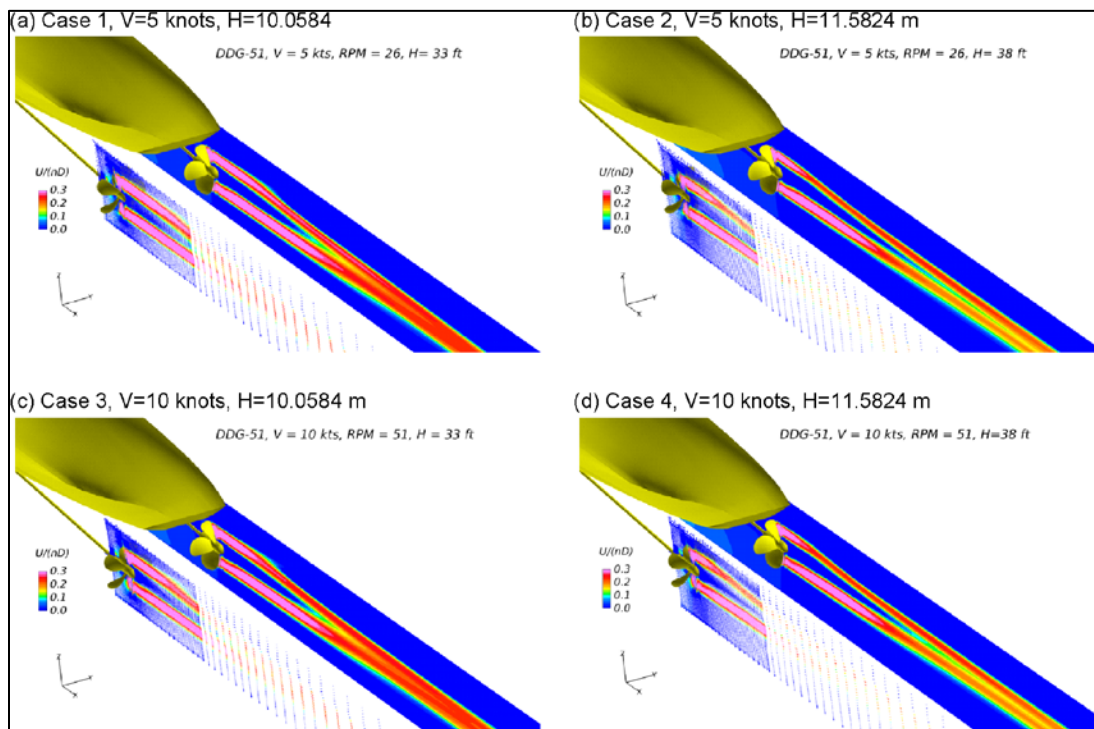


Figure 6-112. Axial velocity contours and velocity vector plots around the propeller.

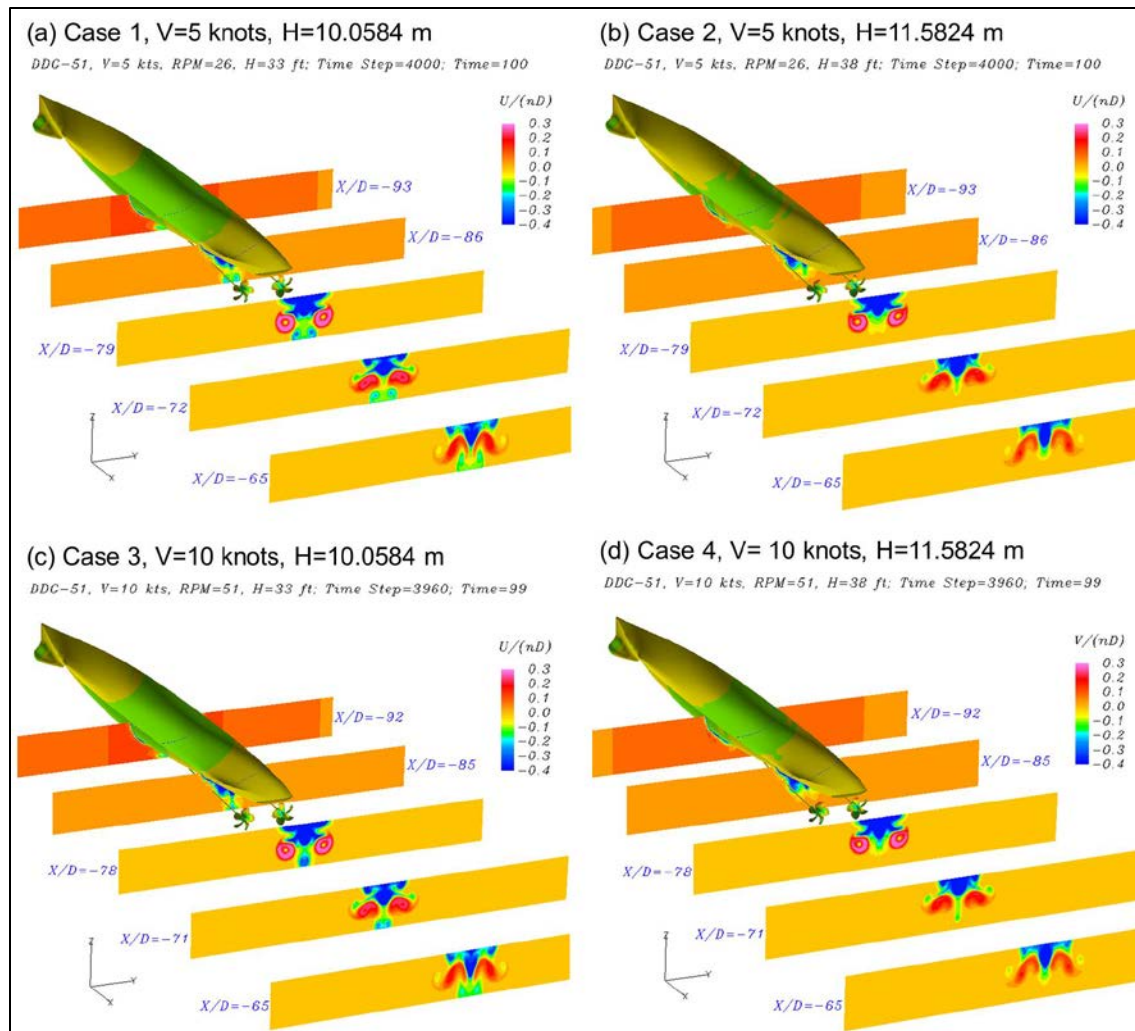


Figure 6-113. Propeller-induced flow field at selected stations.

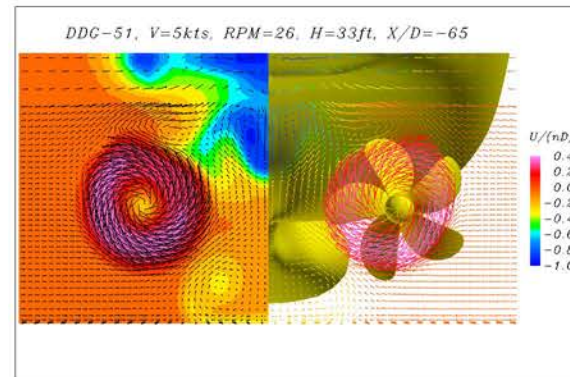
It is seen from Figure 6-112(b) and Figure 6-112(d) for the deep water cases with $H = 11.5824$ m, a significant portion of the flow is pushed underneath the bow due to local flow acceleration around the sonar dome. This produces a large flow recirculation region (in earth-fixed reference frame) at the keel plane with a fairly weak return flow near the sea bottom.

When the water depth was reduced to $H = 10.0584$ m, there was a much larger resistance to push the flow beneath the sonar dome. Consequently, most of the surrounding water tends to move laterally around the sonar dome and the flow recirculation near the seabed was confined to a fairly small region immediately downstream of the bow, as shown in Figure 6-111(a) and Figure 6-111(c). It is clearly seen from Figure 6-110(a) and Figure 6-110(c) that the ship induced a strong trailing water flow (in the same direction of the ship motion) beneath the ship keel that extends beyond the propeller plane and well into the far wake. The high velocity (and high shear stress) regions around the bow and mid-ship are induced by the ship hull movement, but not directly related to the propeller wash. Note that the effect of propeller thrust and torque are confined to the ship stern and wake regions.

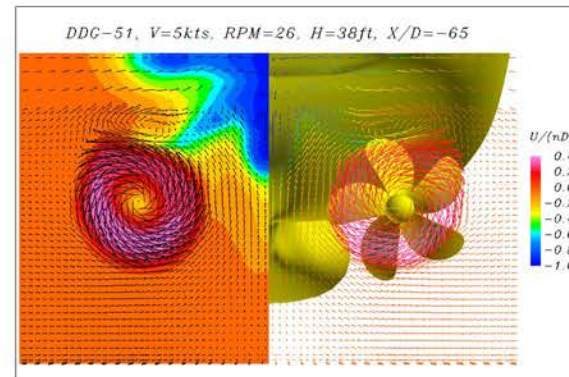
In addition to the axial flow profiles in Figure 6-112 and Figure 6-113, the swirling flows at selected cross-sections are also shown in Figure 6-114 to provide a complete description of the three-

dimensional flow field induced by the propeller rotation. It is seen that the propeller induced swirling flow patterns are quite similar immediately downstream of the propeller. However, the propeller swirl is somewhat stronger in the far wake for shallow water cases with $H = 10.0584$ m. Also note that there is a second pair of counter-rotating vortices near the center plane of symmetry. This vortex pair was generated in the narrow gap region around the sonar dome, and remains visible in the far wake.

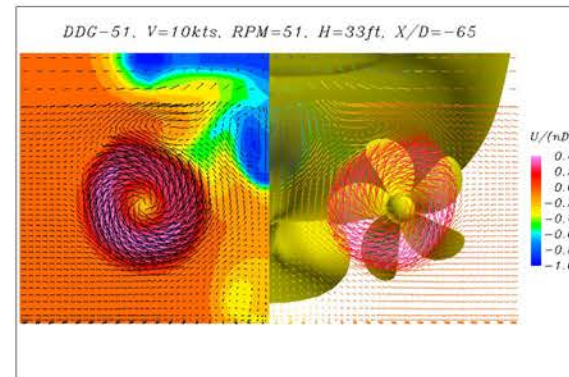
(a) Case 1, $V=5$ knots, $H=10.0584$ m



(b) Case 2, $V=5$ knots, $H=11.5824$ m



(c) Case 3, $V=10$ knots, $H=10.0584$ m



(d) Case 4, $V=10$ knots, $H=11.5824$ m

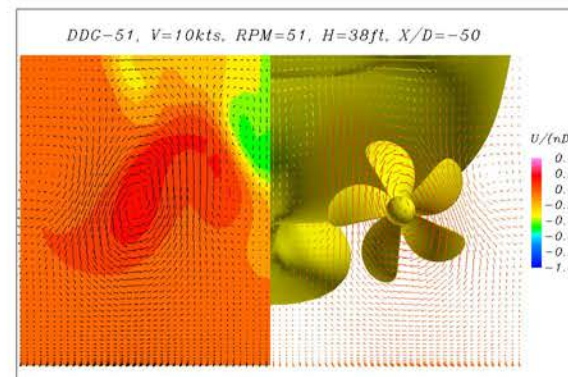
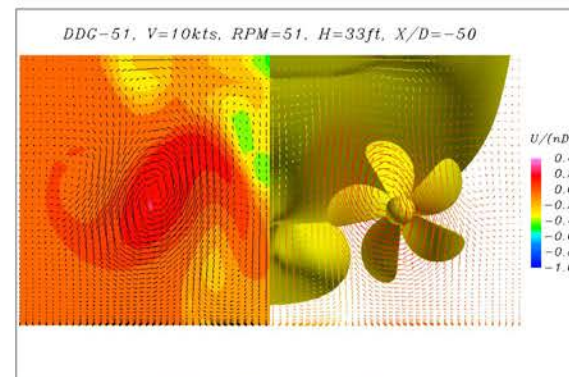
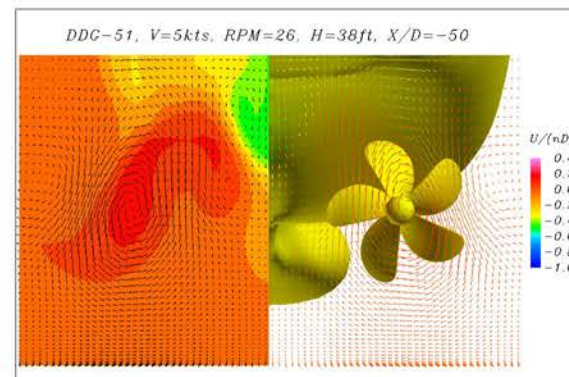
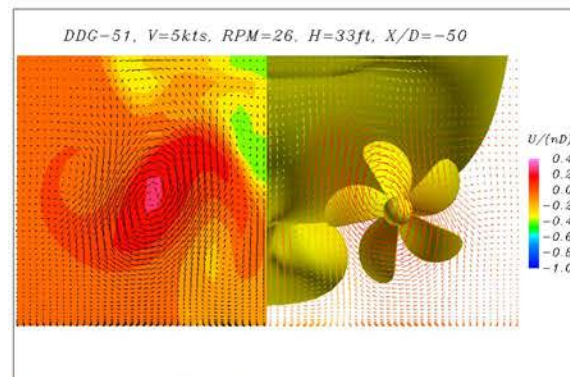
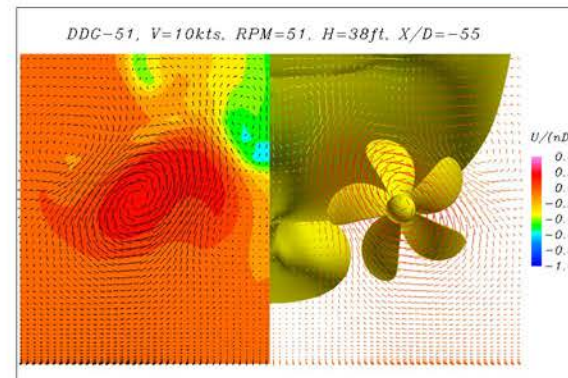
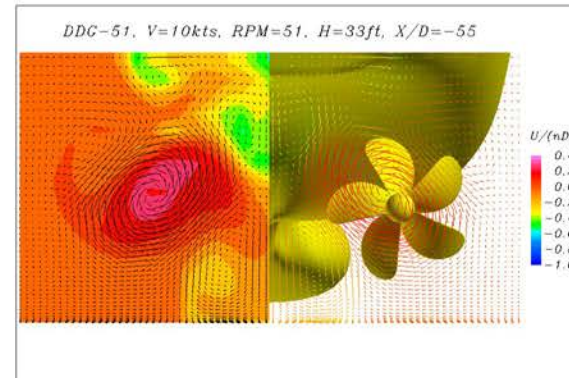
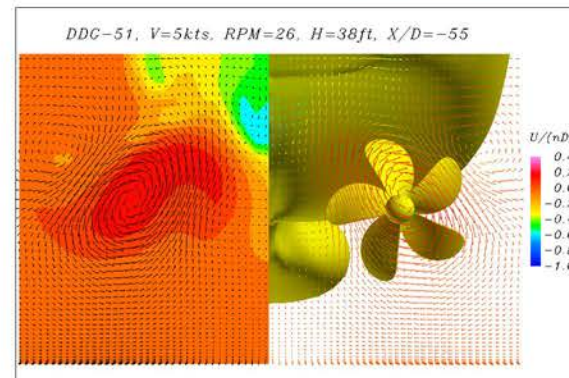
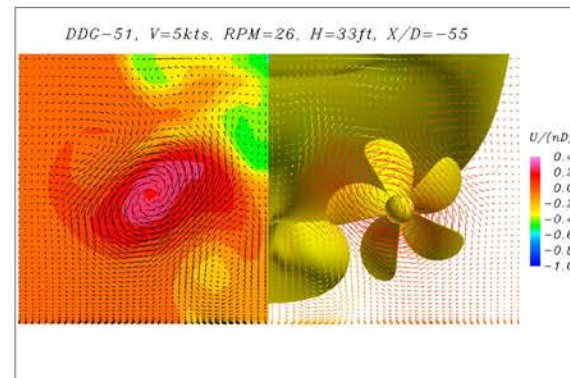
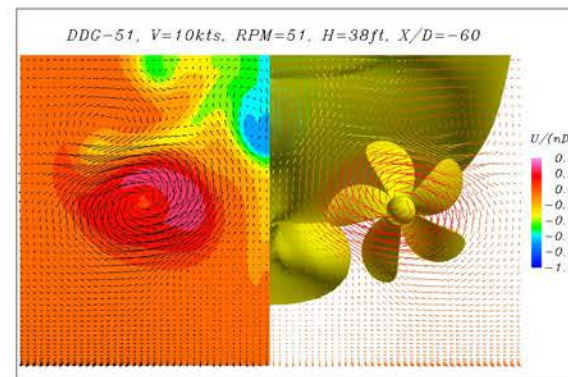
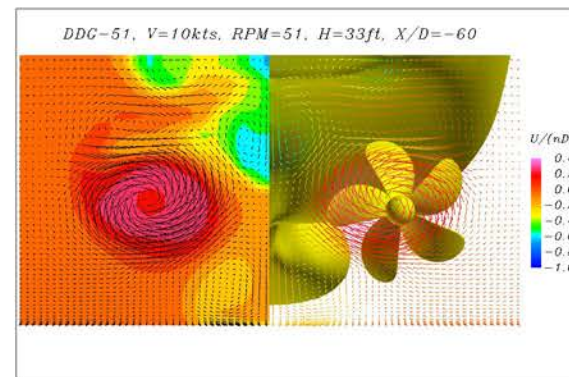
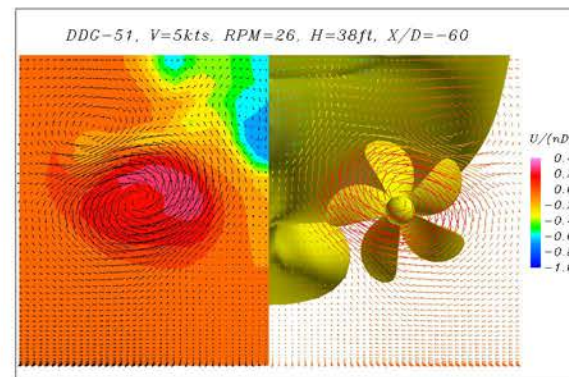
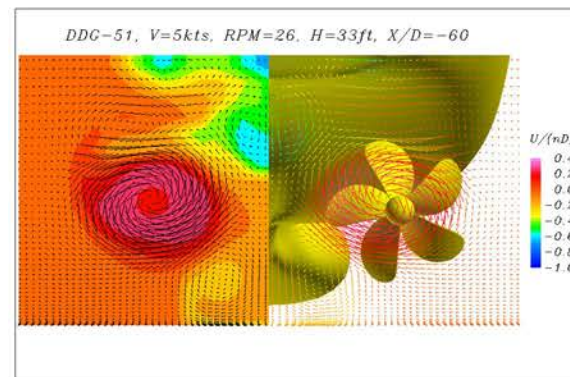
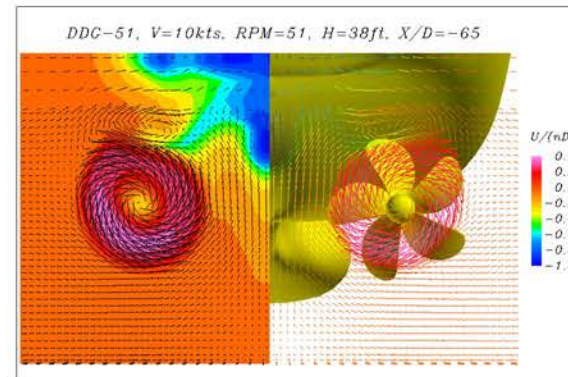


Figure 6-114. Propeller-induced swirling flows.

A detailed examination of the velocity profiles near sea bottom (see Figure 6-110 and Figure 6-111) indicated that the propeller wash effect is negligible for the deep water cases since the swirling flow decreases quickly in the radial direction away from the propeller tip as shown in Figure 6-114. The effect of propeller wash grew considerably stronger under shallow water conditions when the minimum gap below the propeller tip was reduced from 3.048 m (10 ft) to 1.524 m (5 ft).

6.4.3.2 Estimated Bottom Shear Stresses

Figure 6-115 shows the shear stress distributions on the sea bottom for all four test cases considered in the present study. Note that different color bar scales were used since the bottom shear stresses for Case 2 are considerably smaller than the other three cases. In general, the bottom shear stress increases with the propeller rpm and ship speed. Under deep water conditions, the maximum shear stress occurred beneath the sonar dome due to strong flow acceleration through the narrow passage between the sonar dome and sea bottom. High shear stress regions were also observed around the mid-ship due to large block coefficient of the DDG 51 hull cross-section area. It is seen that the propeller induced shear stresses are not as high as those induced by the ship motion. Furthermore, the propeller wash effects are confined to a rather small region directly below the twin-screw propellers. For shallow water cases with $H = 10.0584$ m, the highest shear stress also occurred underneath the sonar dome. However, the shear stresses in the stern region are also very high due to the presence of strong underkeel current (see Figure 6-111) induced by the ship motion.

The excessive bottom shear stress generated by the underkeel flow is consistent with the observed plume patterns in the wake of USS *Chafee* in Pearl Harbor (Figure 6-107).

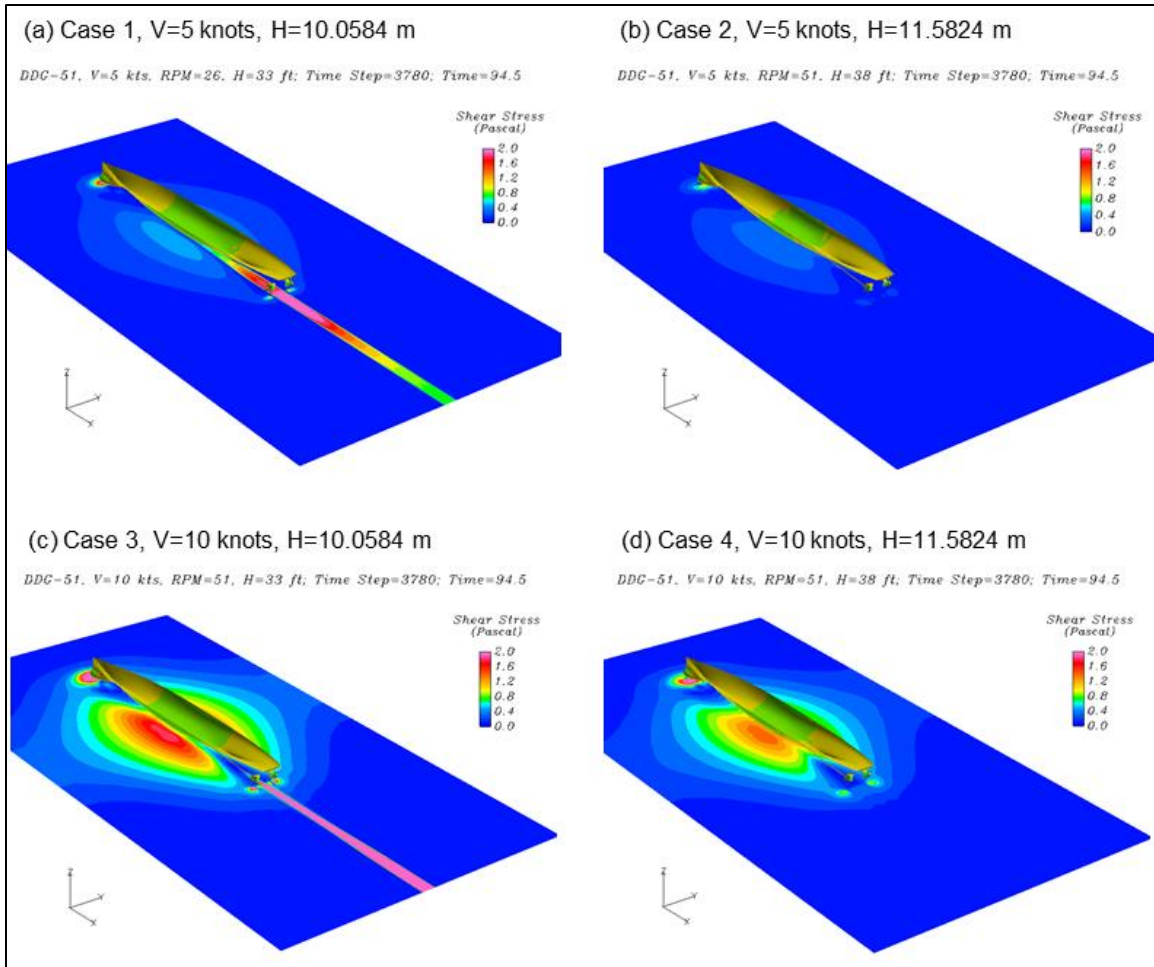


Figure 6-115. Shear stress distribution on the seabed.

Figure 6-116 shows the surface plots of seabed shear stress distributions under different water depths and different ship speeds. For clarity, the shear stress scales were adjusted for each case to provide a detailed comparison of the shear stress patterns in the bow, mid-ship, propeller, and ship stern regions. As noted earlier, the highest shear stress occurred beneath the sonar dome for all four test cases considered. For deeper water cases, the propeller induced shear stresses are considerably smaller than those induced by the ship hull motion. However, the bottom shear stress distributions changed drastically when the water depth was reduced to $H = 10.0584$ m with a very small underkeel clearance of 0.6096 m. The high shear stresses in the ship wake regions were induced primarily by the trailing water in the narrow gap between the keel and seabed. The simulation results clearly demonstrated that the blockage effect (i.e., block coefficient) of the ship hull in shallow water is the dominant parameter in determining the sea bottom shear stress distributions.

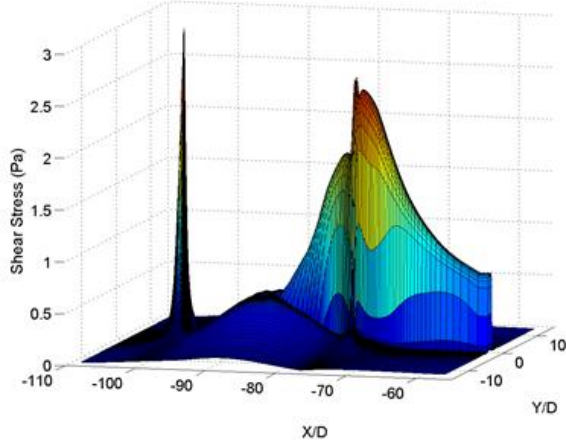
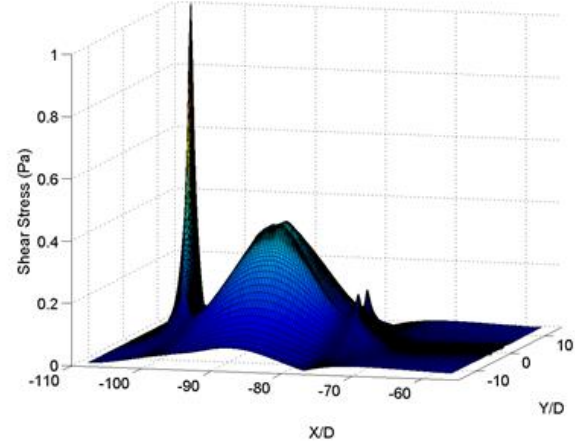
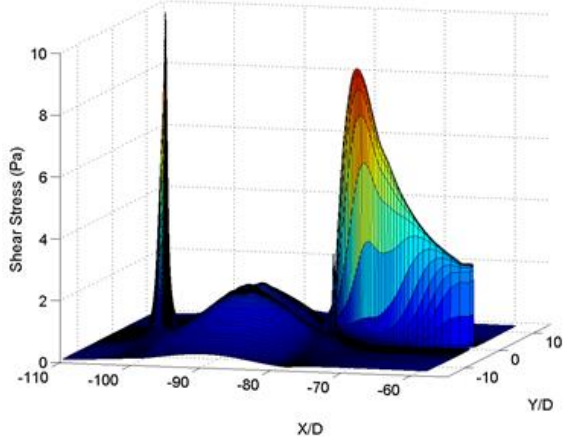
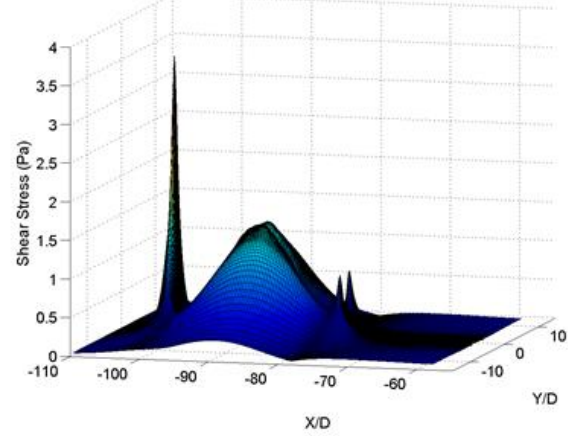
(a) Case 1, $V=5$ knots, $H=10.0584$ m(b) Case 2, $V=5$ knots, $H=11.5824$ m(c) Case 3, $V=10$ knots, $H=10.0584$ m(d) Case 4, $V=10$ knots, $H=11.5824$ m

Figure 6-116. Surface plots of shear stresses on the seabed.

Enlarged views of the seabed shear stress distributions around the twin-screw propellers and the ship stern regions are shown in Figure 6-117 to provide a detailed assessment of the propeller wash effects. In addition, the maximum shear stresses at various locations of the seabed were also summarized in Table 6-24. It is clearly seen that the propeller-induced shear stresses are much smaller than the hull-induced shear stresses under shallow water conditions. The maximum shear stress in the ship wake exceeded 8.9 Pa for Case 3 when the ship speed was 10 knots. Even for the lower speed case with $V = 5$ knots (Case 1), the bottom shear stress in Case 1 still reached nearly 2.5 Pa in the ship wake. The maximum shear stresses in ship wake region are about three times of those induced by the propeller rotation. It is quite obvious that the large blockage effect of sonar dome under shallow water condition is the primary cause of the strong trailing water and high shear stresses in the narrow gap between the ship keel and sea bottom. However, the shear stress induced by the ship hull is strongly dependent on the ship size, hull form, and water depth. Therefore, it will be necessary to perform numerical simulations for each individual ship to quantify the water depth effect for different type of ships.

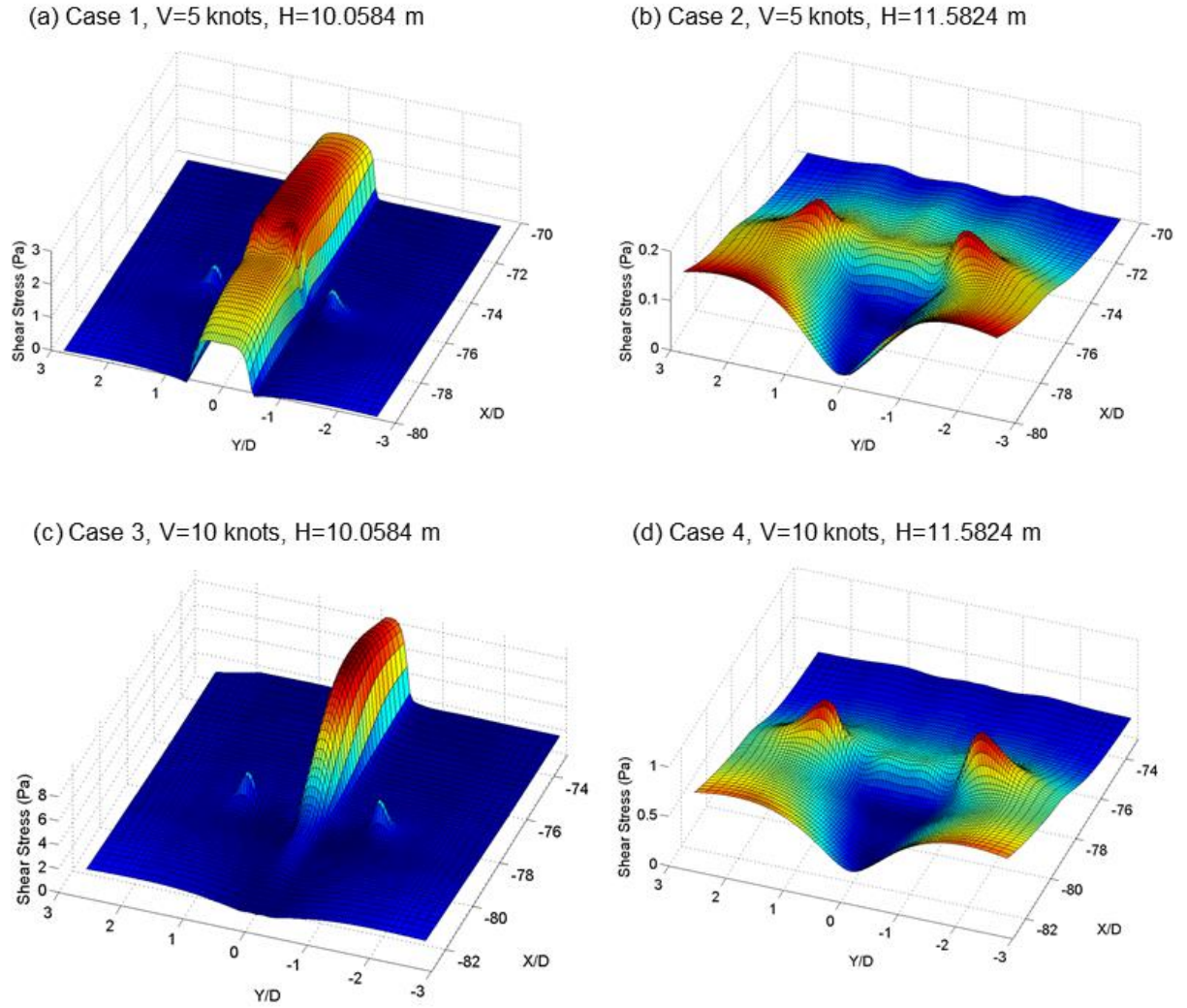


Figure 6-117. Surface plots of seabed shear stresses around the twin-screw propellers.

Table 6-24. Maximum shear stresses in different regions of the seabed.

Case #	1	2	3	4
Bow	3.02 Pa	1.09 Pa	10.53 Pa	3.57 Pa
Mid-ship	0.51 Pa	0.39 Pa	1.85 Pa	1.46 Pa
Propeller	0.85 Pa	0.18 Pa	3.00 Pa	0.85 Pa
Ship wake	2.49 Pa	0.14 Pa	8.94 Pa	0.37 Pa

6.5 SEDIMENT RECONTAMINATION POTENTIAL FOR PIER 7, SINCLAIR INLET, WA

Figure 6-118 summarizes the field and modeling effort in Sinclair Inlet to predict the effects of two tug-assisted movements of two submarines and a carrier on sediment resuspension and subsequent settling in the vicinity of a capped remediation site adjacent to Pier 7.

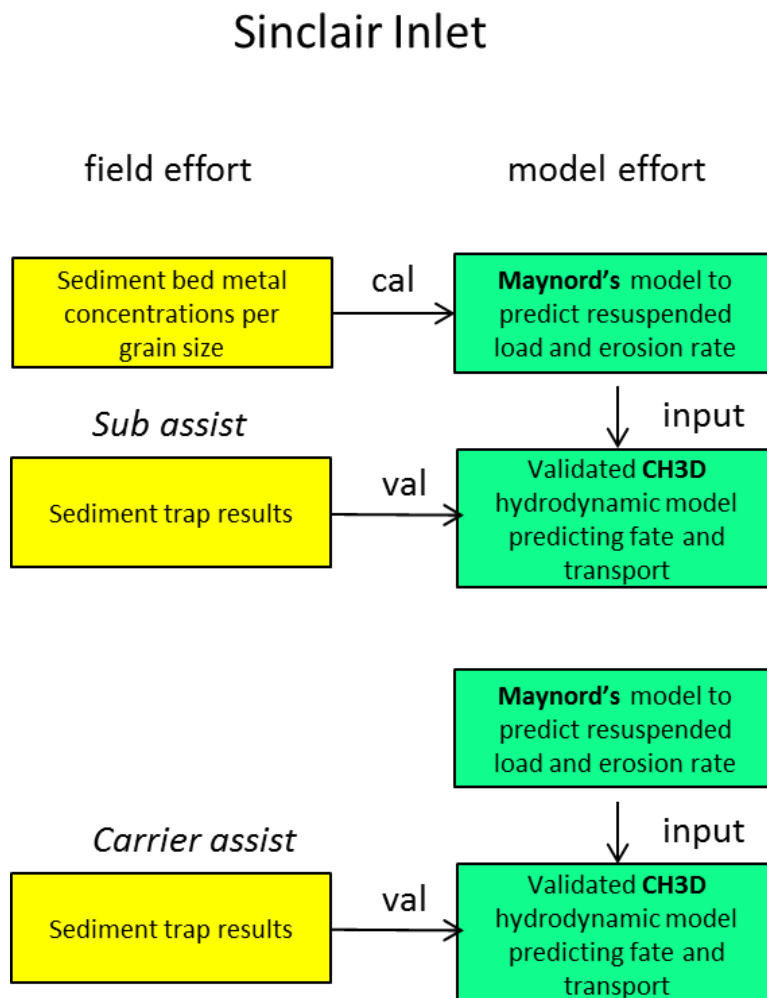


Figure 6-118. Field and model effort in Sinclair Inlet.

6.5.1 Sediment Deposition Rates and Metal Concentrations

To reiterate from Table 5-8, the sediment traps were sampled at the end of three time periods: (1) 22 January to 8 April 2014, when two submarines were undocked from Pier 7 and led into Drydock 3; (2) 10 April to 13 May 2014, when a carrier from Drydock 6 transited out of Sinclair Inlet; and (3) 14 May to 24 June 2014, when background conditions (probably dominated by activity at the nearby ferry dock) were presumably measured. Sediment trap sample locations are shown in Figure 5-14 and background sediment sample locations are shown in Figure 5-16, with data provided in Appendix H. Sediment deposition rates as a function of particle size by event and sediment trap is shown Figure 6-119. Metal concentrations in background sediments are shown in Table 6-25.

Sediment deposition rate by grain size and event

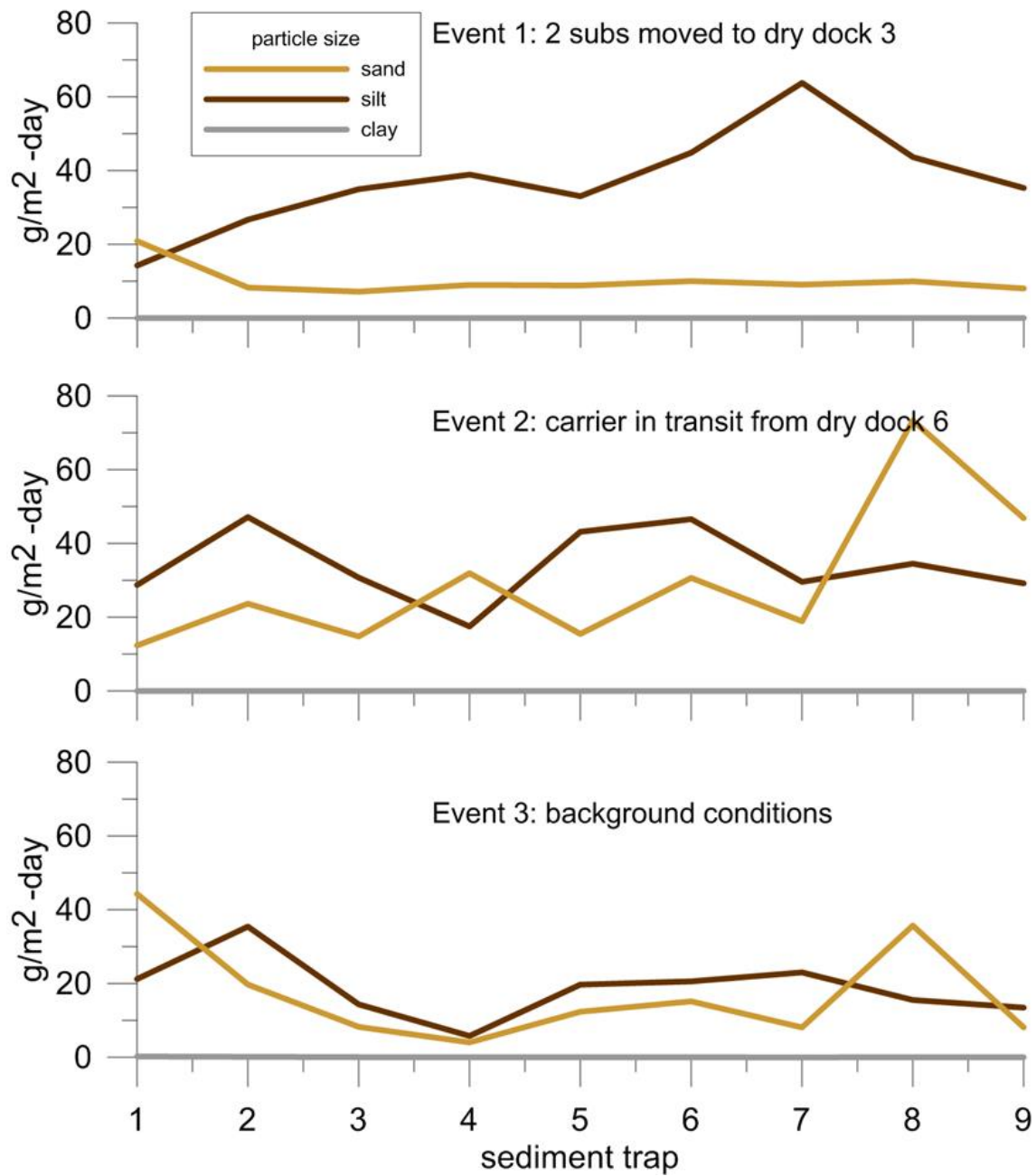


Figure 6-119. Sediment deposition rate in the sediment traps by particle size and event.

Table 6-25. Metal concentrations measured in aqua regia digestates on background sediments from PSNSY& IMF, Bremerton, Washington. All data is provided in µg/g. but for recoveries, are given as %. Certified are certified concentrations. Silver is not certified (NC) in SRMs BCSS-1 and PACS-1.

Sample ID	Size fraction		Cr (µg/g)	Ni (µg/g)	Cu (µg/g)	Zn (µg/g)	As (µg/g)	Ag (µg/g)	Cd (µg/g)
1 & 2	Sand	Average	68	29	68	278	8.1	1.6	0.6
		Std. Dev.	20	1.4	2.9	24.1	0.13	0.16	0.04
3 & 4	Sand		44	31	114	250	12.5	1.8	1.1
5 & 6	Sand		60	33	221	456	24.4	1.9	2.5
7 & 8	Sand	Average	39	27	102	257	11.2	1.5	1.5
		Std. Dev.	0.62	0.7	12.7	10.9	0.45	0.08	0.19
9 & 10	Sand		38	24	75	183	9.1	1.8	1.6
11 & 12	Sand		40	26	56	189	9.1	1.6	1.1
1 & 2	Silt		49	33	118	252	14.0	1.8	1.3
3 & 4	Silt		53	35	123	234	13.7	1.7	1.6
5 & 6	Silt	Average	52	34	277	272	18.6	2.0	1.8
		Std. Dev.	1.2	1.0	2.2	2.5	1.21	0.03	0.01
7 & 8	Silt		42	28	107	244	12.0	1.5	1.8
9 & 10	Silt		48	30	92	207	11.3	1.7	2.3
11 & 12	Silt	Average	46	32	99	258	12.0	1.5	1.6
		Std. Dev.	0.13	0.1	2.5	7.2	0.24	0.02	0.12
SRM PACS-1 (n=3)		Certified	113	44.1	452	824	211	NC	2.38
		Average	53	29.6	423	1049	204.4	3.1	3.7
		Std. Dev.	1.1	0.6	11.6	13.4	2.0	0.6	0.1
		Recovery (%)	47	26	67	127	97	NC	158
SRM BCSS-1 (n=3)		Certified	123	55.3	18.5	119	11.1	NC	0.25
		Average	40	44.6	14.5	131	12.2	1.8	0.41
		Std. Dev.	12.8	15.3	4.9	45.3	3.6	0.4	0.13
		Recovery (%)	33	36	81	110	110	NC	166
SRM MESS-2 (n=3)		Certified	106	49.3	39.3	49.3	20.7	0.18	0.24
		Average	21.3	37.1	34.2	178	22.4	1.7	0.30
		Std. Dev.	0.7	1.8	0.54	5.6	0.6	0.4	0.02
		Recovery (%)	20	26	75	361	108	951	127

6.5.2 Sinclair Inlet Particle Resuspension Load and Deposition Rate

The silt (60 to 5 µm) particle size fraction is the major component of the load settled onto the sediment remedial cap under Pier 7, PSNSY&IMF. This is similar to the resuspension events in San Diego Bay and Pearl Harbor, where the silt fraction also was the major component in sediment resuspended under controlled conditions.

Figure 6-120 shows the net (difference between observed and background) deposition load (g/m^2) and the deposition rate ($\text{g/m}^2 \text{ d}$) measured in the dry particle fractions from the slurry collected in the sediment traps. The plot for the net deposition load clearly shows that the silt fraction is the major constituent for the first and second events, and only the sand fraction ($< 2 \text{ mm}$ to $60 \mu\text{m}$) for the second event is present at similar levels. Note that the information for the twelve measured fractions is included in each plot; however, due to the order of magnitude difference between the quantities for the different fractions, only a subset of them, generally six fractions, are clearly shown in the plots, as the other six fractions plot at the 0 value for the ordinate (y-axis) all the time. These six particle size fractions with minimal concentrations are the clay (5 to $0.45 \mu\text{m}$) and dissolved ($< 0.45 \mu\text{m}$) fractions in the three events. The deposition load of different particle fractions is affected by both the relative distribution of these fractions in the background sediment, and by the differences in the advection of these different particle fractions in the water column. The differences in the load of sediment particle fractions observed here could result from silt being the major component of the resuspended sediment, or of clay and dissolved fractions being transported to longer distances, creating a dilution effect on the quantity of these particles when settling on a specific site. The information on net particle deposition load (Figure 6-120) indicates the predominance of the silt fraction in the sediments resuspended by the opening and closing of Drydock 3 (Event 1), which is as much as three times the load from the transit of a carrier out of Sinclair Inlet (Event 2).

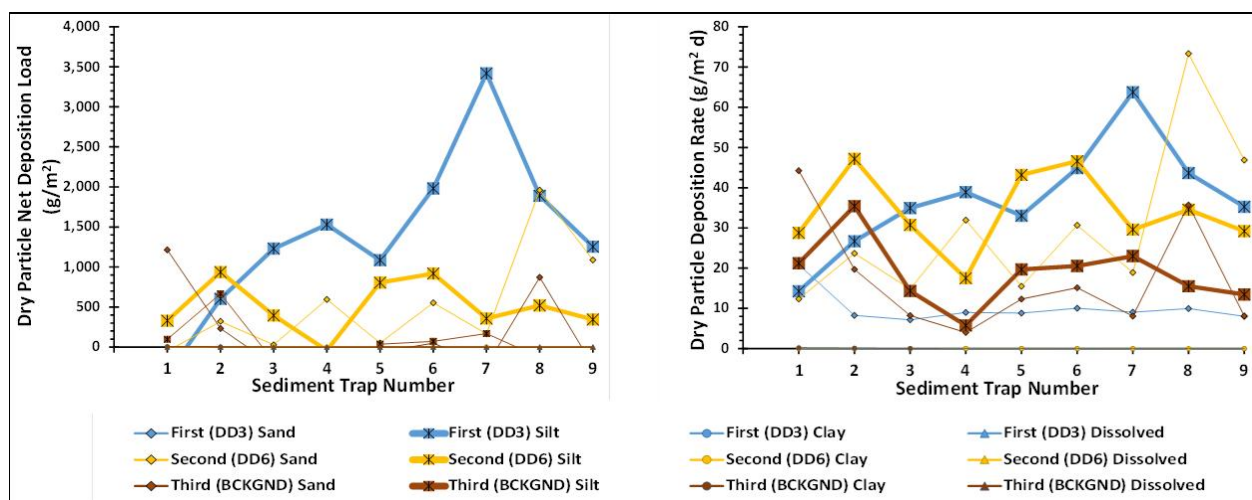


Figure 6-120. Deposition load and rate of sediments resuspended by sporadic (First and Second events) and background or consistent activities (Event 3) in Sinclair Inlet, as measured from deposition onto the sediment remedial cap located in Pier 7 of PSNSY&IMF. Note that the symbols and colors in these plots are used in the plots within this section. Also note that thicker lines are used for the silt fraction measured in the three sampling events.

6.5.3 Metal Load and Fractionation

The silt fraction is the major component in the metal load in the Events 1 and 2, denoting unknown resuspension processes in Sinclair Inlet, as expected from the net load of the different particle fractions (Figure 6-120 and Figure 6-121). In a similar fashion, the silt fraction is predominant in Event 1, but similar to the sand fraction in Events 2 and 3 (Figure 6-121). Between the metals, copper, and zinc have the larger load to about 0.5 g/m^2 , chromium and lead loads are lower at about 0.15 g/m^2 , while arsenic, silver, and cadmium loads are the lowest at less than 0.1 g/m^2 . The difference in the metal loads must be due to the predominance of copper and zinc in background sediment, and in sediments associated to industrial processes in the dry docks. Copper and zinc are

the major components of antifouling coatings used in Navy boat hulls. Usually these coatings are stripped off during dry dock operations.

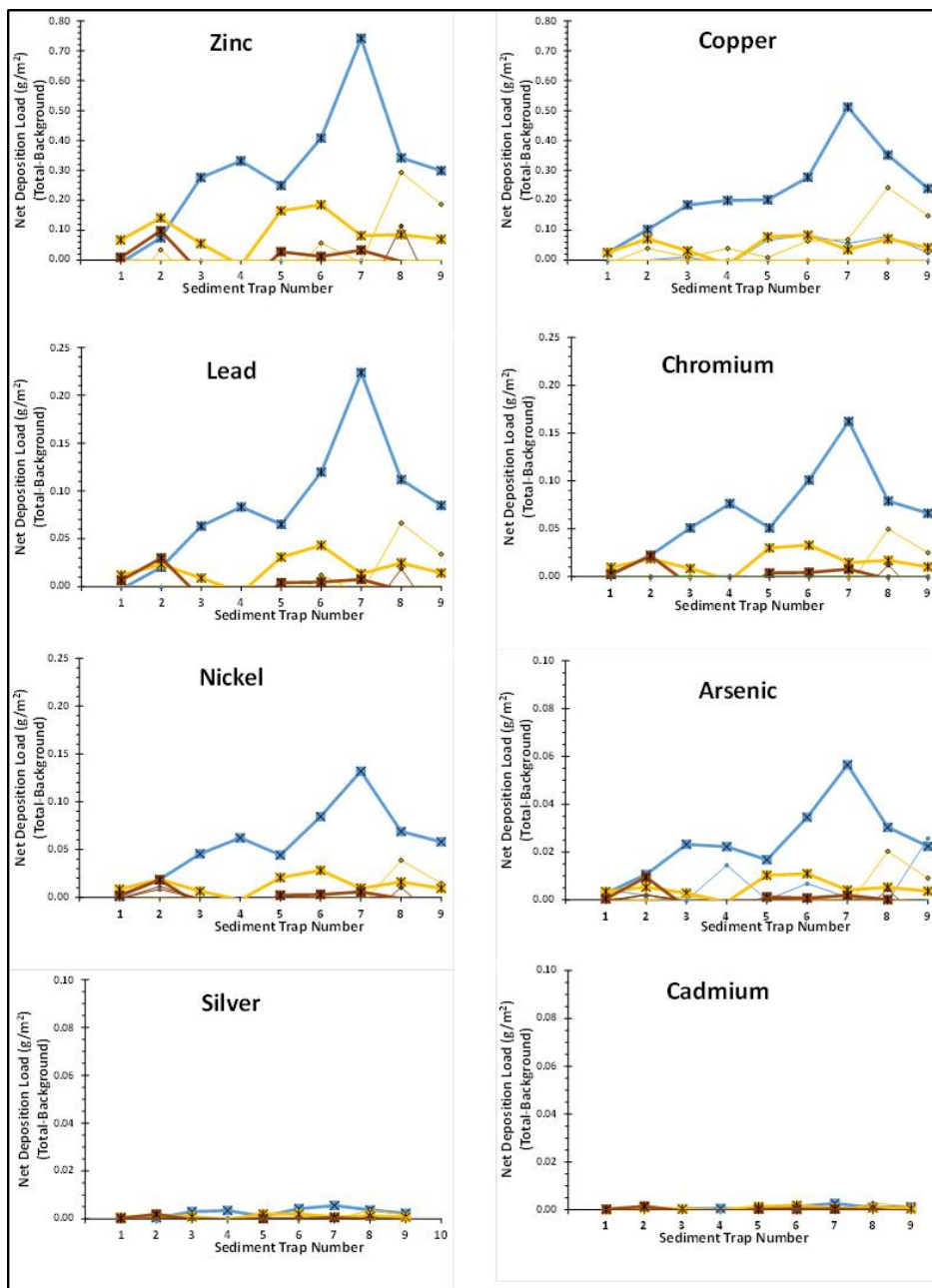


Figure 6-121. Net deposition load (g/m^2) of metals measured in the different particle fractions collected with sediments traps on the sediment remediation cap in Pier 7. Note the different scales (g/m^2) in the ordinate (y-axis): 0.80 for zinc and copper; 0.25 for lead, chromium, and nickel; and 0.10 for arsenic, silver, and cadmium. (Symbols and colors are the same as those in Figure 6-120).

The silt and sand fractions are also the major components of the metal deposition rates normalized by day ($\text{g}/\text{m}^2 \text{ d}$, Figure 6-122). The predominance of the silt fraction over the sand fraction in the first event is also shown for the metals, while the similarity within the loads from these fractions is shown for the second and third events. The load from resuspension seems to be more significant in sediment traps 7, 8, and 9, located at the eastern edge of the cap, in the middle between Piers 6 and 7. With the strongest effect in sediment trap 7, located closer to Drydock3 (away from the main channel). Mercury loads are three to four orders of magnitude lower than those for other metals.

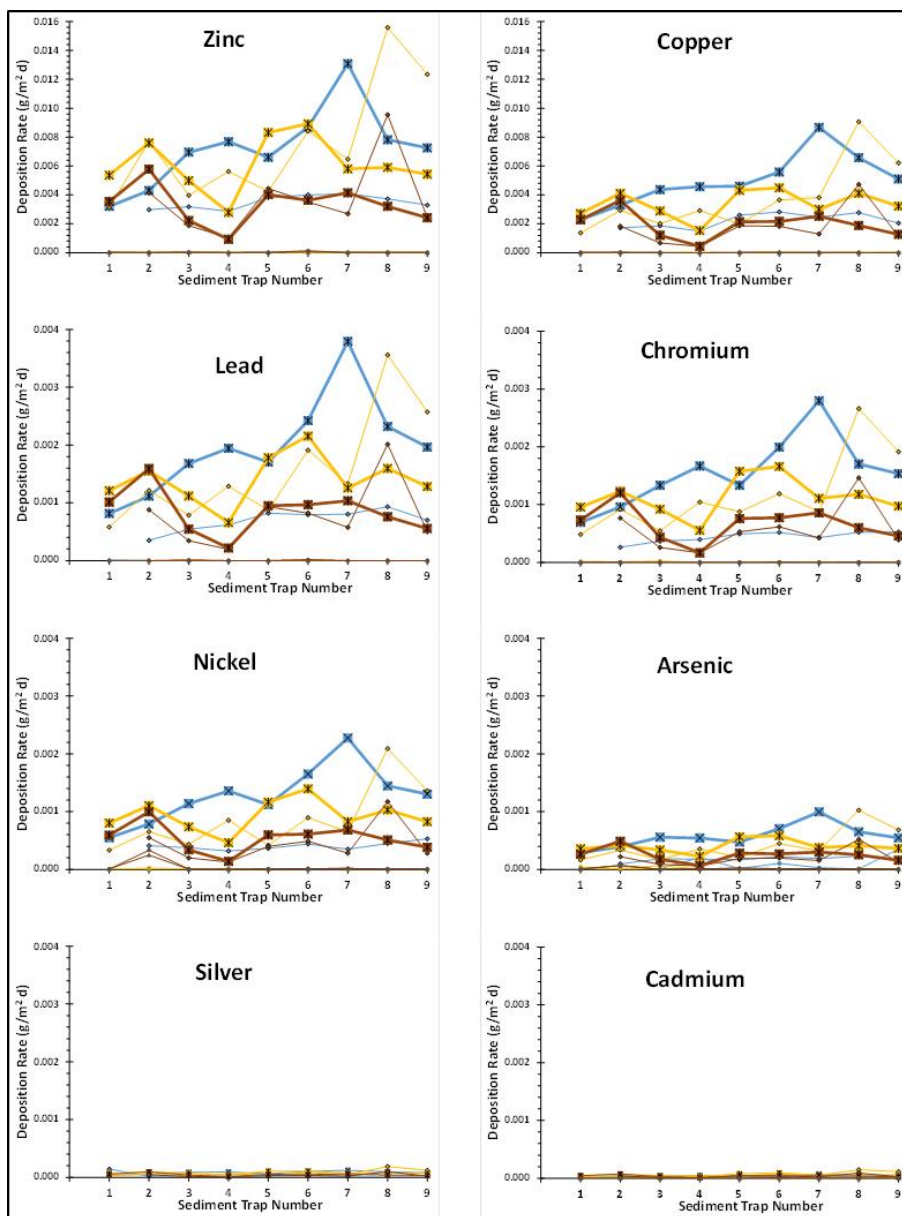


Figure 6-122. Metal deposition rates ($\text{g}/\text{m}^2 \text{ d}$) for metals in the different size fractions measured in this effort. Note that a range to 0.016 $\text{g}/\text{m}^2 \text{ d}$ is used in the ordinate for zinc and copper, while 0.004 is used for the other metals. (Symbols and colors are the same as those in Figure 6-120).

Figure 6-123 shows the net deposition load of mercury (g/m^2). There are several caveats to these calculations; the concentrations were measured at the ERDC Environmental Laboratory, on samples provided after fractionation. During the separation of the fractions by filtration, the samples were exposed to air, with the potential loss of mercury to the atmosphere. Due to the small amount of particles separated for each fraction, analyses of mercury were performed on the slurry, and the measured concentrations are provided as mg/L . The mass of particles is required to calculate the load; the average particle mass collected for analysis of the other metals was used for mercury, which was considered acceptable, as the other metal and mercury samples are aliquots of the same sample. Despite these caveats, the estimated net load of mercury in the settled particles is on the order of $1 \mu\text{g}/\text{m}^2$, and this is only for the case of silt in Event 1, which is the predominant particle size class for all the events.

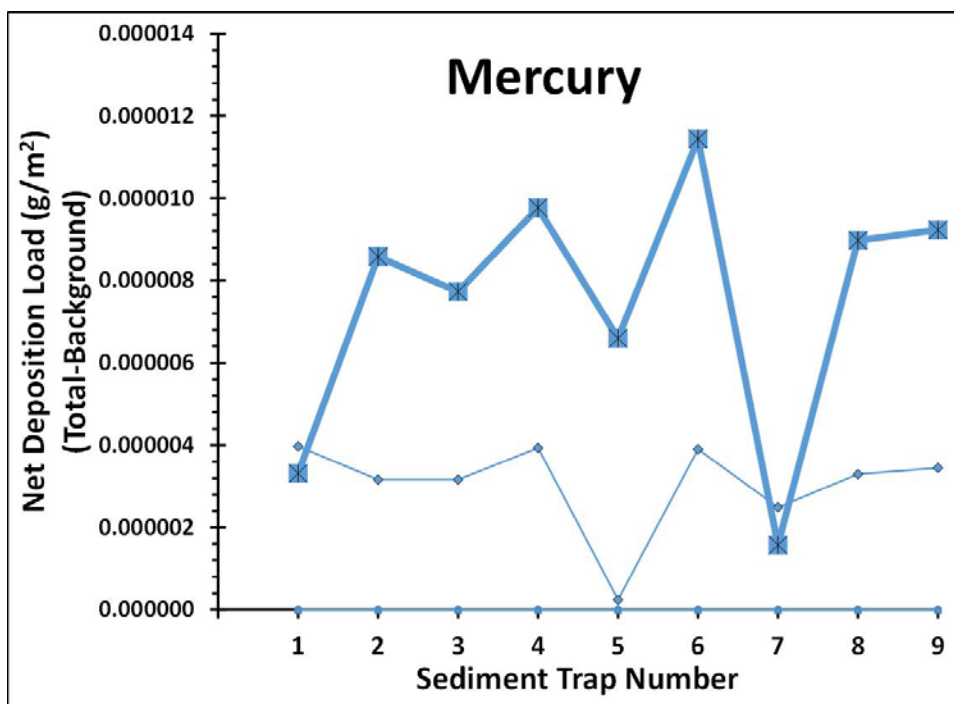


Figure 6-123. Mercury concentrations measured at the ERDC Environmental Laboratory. These are only for Event 1.

There is a consensus between background sediment particle distribution and the resuspended sediment collected in the traps. Background sediments were mainly sand and silt, with minimal clay. Silt and sand are the main components of the resuspended sediment collected in the sediment traps, although there is a measurable, but minimal, contribution to the metal load from the clay and dissolved fractions in the sediment traps. Probably due to the difference in the settling of the resuspended clay- and sand-size particles, the load measured in the sand size-fraction was lower than that for the silt size-fraction. The distance from the resuspension event to the location of the sediment traps on the remediated sediment area also plays a role in the measured load. Event 1 is the closest to the location, as it included the flooding, opening, and closing of the caisson into Drydock 3, and the towing of two submarines into the dry dock. This event is the one with the highest load of silt-size particles, and the metals associated with this fraction. Event 2 was the opening and closing of Drydock 6 for undocking of a carrier, and transiting of the carrier out of Sinclair Inlet. This event has lower silt-size load, with the sand-size load being of similar level to the silt-size. Note that the metal

concentrations measured in the background sediments are very similar for the silt and sand fractions; therefore, the metal loads observed in Bremerton cannot be attributed to differences in metal loading between these particle-size fractions.

6.5.4 Sinclair Inlet Sediment Deposition Modeling Analysis

The primary effort for the Sinclair Inlet study was the sediment trap study. As discussed previously, sediment transport dynamics in Sinclair Inlet is complex. Multiple sources/processes of sediments are components for this complex system. To evaluate and provide further insight to the sediment/metal data collected from the sediment traps, we attempted to use CH3D for some baseline modeling and evaluate the model results with the measured data. For the three sediment trap events, information about the potential tug-boat activities were provided verbally and no specific knowledge was available, such as specificity of the tug-boats or operational records during the period. Therefore, it is difficult to quantitatively estimate sediment erosion from the berthing of two submarines and drydocking of a carrier for Events 1 and 2, respectively. To make our analysis meaningful, the same sediment erosion mass (i.e., 21,571 kg), which was predicted for San Diego Bay using the Maynard's model, was assumed and used as eroded sediments from Drydock 3 and 6, respectively. For each event, CH3D was used to simulate for 7 days, during which 99% of sediments have been deposited to the bottom.

Figure 6-124 shows the total deposition rates (grams/m^2) for silt, sand particles, and TSS from the initial resuspended sediment at Drydock 3. Overall, the primary deposition zones center around Drydock 3, with values reaching over 100 g/m^2 . Deposition rate at Pier 7 are $25.2 \text{ (g/m}^2\text{)}$ for silt, and $20.3 \text{ (g/m}^2\text{)}$ for sand particles. For the Drydock 6 event of drydocking a carrier, Figure 6-125 shows the total deposition rates for silt, sand particles, and TSS from an initial resuspension plume generated at Drydock 6. Similar to the deposition patterns from the Drydock 3 event, major deposition centers around the dry dock region have the highest deposition rate of $\sim 100 \text{ g/m}^2$. Deposition extends along the pier walls, but decays fast with the deposition rates of $\sim 0.6 \text{ g/m}^2$ and 2.7 g/m^2 for silt and sand, respectively at Pier 7. These deposition rates are one order of magnitude less than the daily deposition rate from the data, which ranges between an average of $20 \text{ g/m}^2/\text{day}$, and $30 \text{ g/m}^2/\text{day}$ for silt and sand, respectively. Again, note the different units between the model (g/m^2 for the event) and the field data ($\text{g/m}^2/\text{day}$).

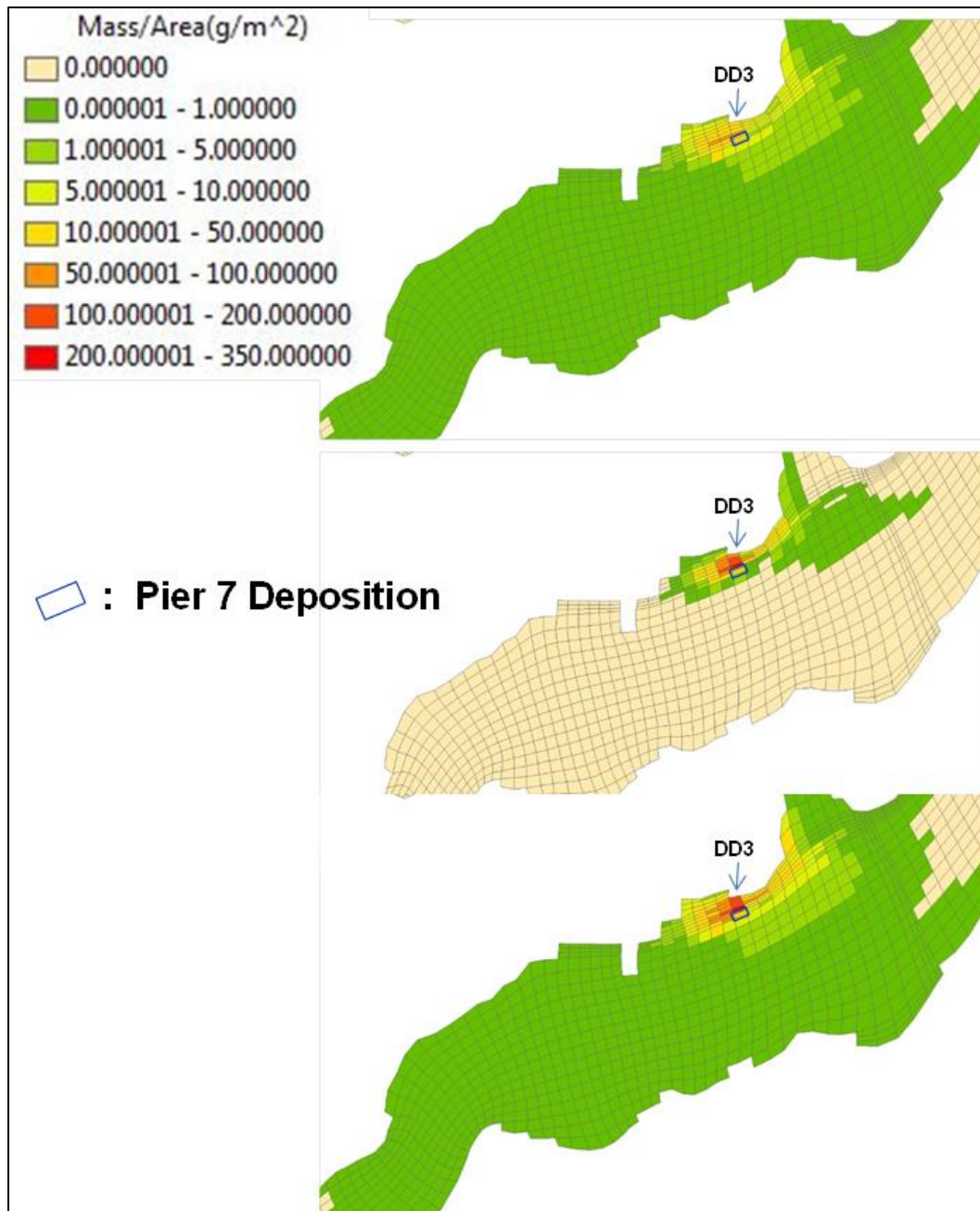


Figure 6-124. Deposition rates for silt (top), sand (middle), and TSS (bottom) from sediment plumes in Drydock 3.

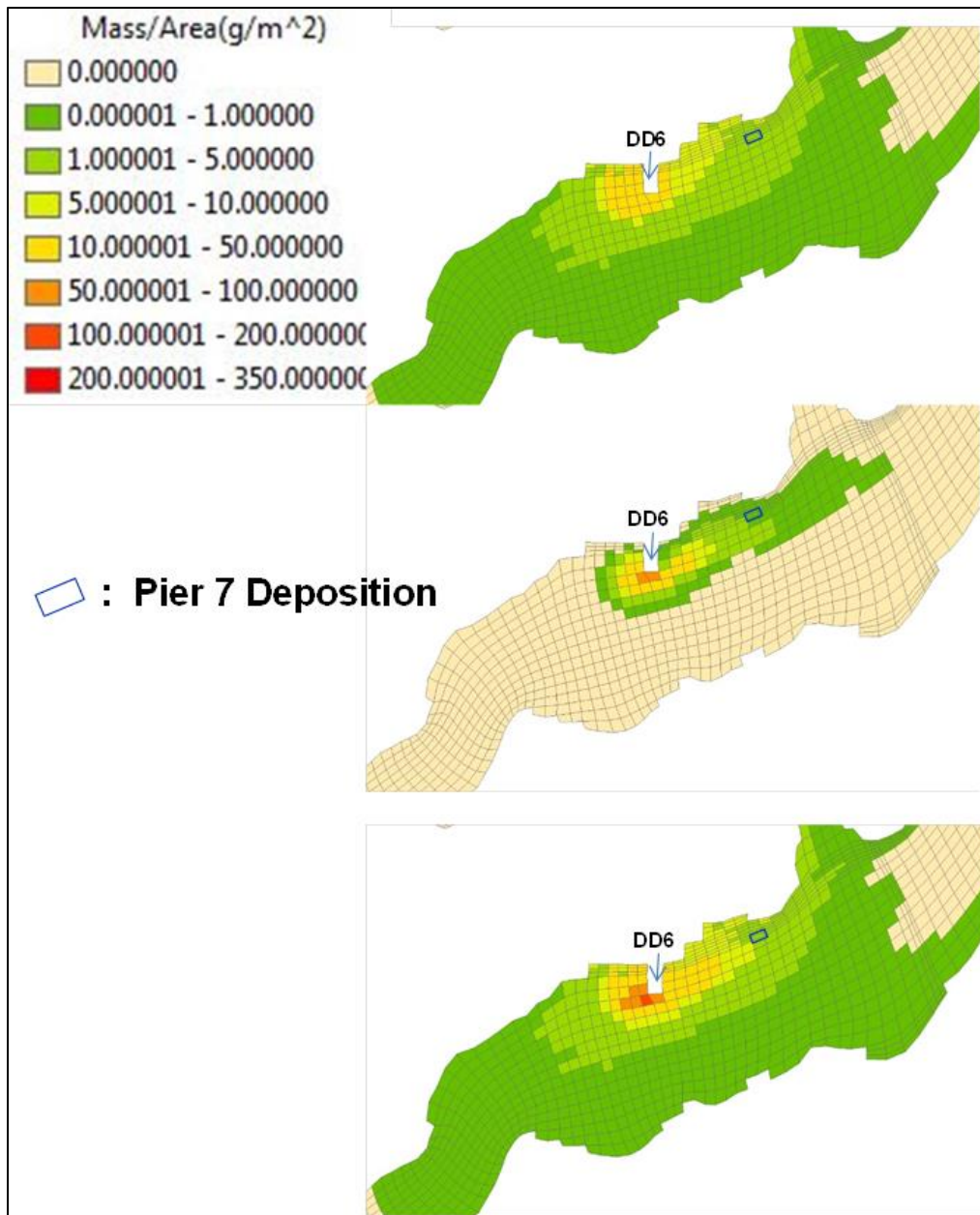


Figure 6-125. Deposition rates for silt (top), sand (middle), and TSS (bottom) from sediment plumes in Drydock 6.

Figure 6-126 shows model/data comparison for the deposition rates, although for the Drydock 3 event, the deposition rates between the model and field data are close for both silt and sand; note that the field data was averaged over the deployment period of 76 days and bears a unit of g/m²/day, whereas model results were based on the assumption of 21,571 kg of initial resuspended sediment near Drydock 3. The information was that two submarines were dry-docked the first week of April 2014, and our sediment traps were retrieved on 8 April 2014. Although it was likely that the sediment mass collected in the traps were mainly from the deposition of the plume from dry-docking the two submarines, there existed uncertainty of unknown magnitude as to the level of significance for the agreement between the model and field data.

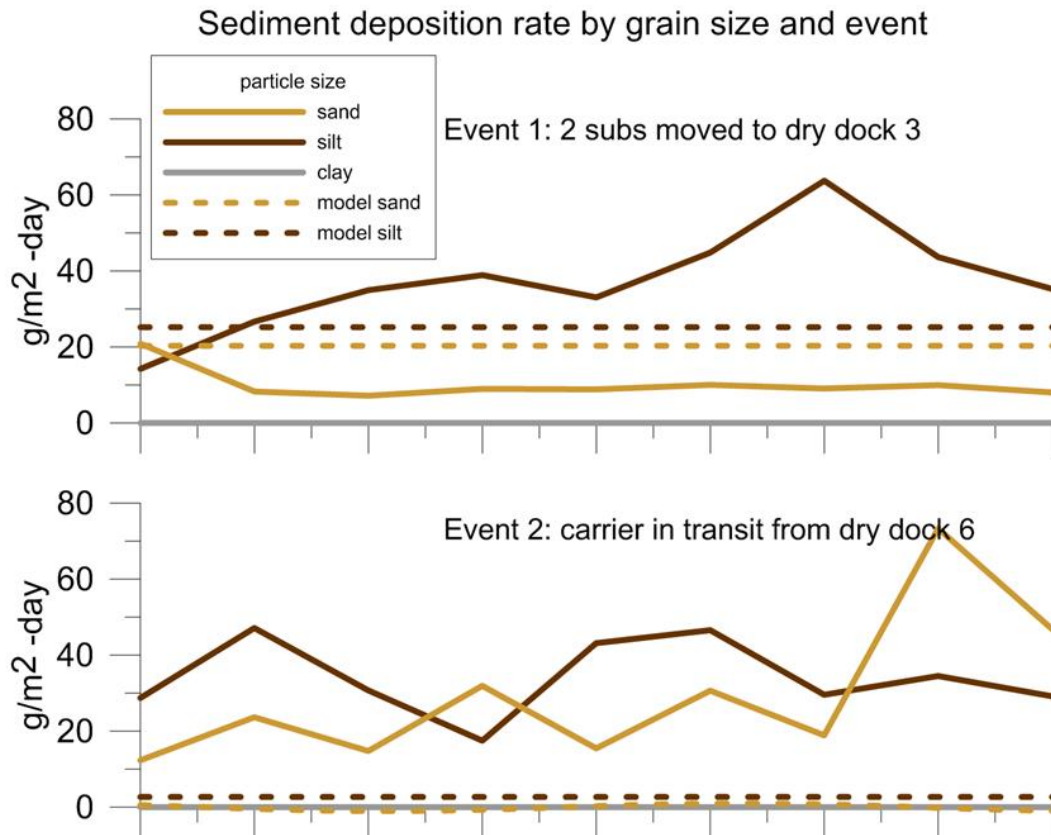


Figure 6-126. Measured and predicted sediment trap load for events 1 and 2.

The difference of deposition rates between the model and the sediment trap data for the Drydock 6 event have multiple potential reasons. Note that, due to the lack of information about the undocking of a carrier, 21,571 kg of sediment mass was assumed to the eroded sediment mass at Drydock 6 and model results of deposition at Pier 7 were recorded. The 21,571 kg of sediment mass was assumed to be the same mass of the sediment plume produced by one tug-boat for the San Diego Bay study. It is unknown how the undocking at Drydock 6 was conducted, and how many tug-boats were used for how long. As discussed, there are a number of processes/activities that could resuspend sediment in the vicinity of the sediment cap at the end of PSNS&IMF Pier 7. These include tug-boat wakes, drydock dewatering, caisson movement for opening and closing of dry dock, commercial ferry operations, and occasional maintenance work such as pier piling replacement. Most of these activities have the potential to disturb and resuspend bottom sediment in ways that are quite different than that for tug wash, and the amount of sediment resuspension from those activities remains unknown.

Table 6-26 shows comparison of averaged deposition rates at Pier 7 between the Drydock 3 and 6 events. Simulated deposition rates from Drydock 3 resuspension event were close between silt (20.3 g/m^2) and sand (25.2 g/m^2), comparable to the measured data of $9.5 \text{ (g/m}^2\text{-day)}$ for silt, and $40.8 \text{ (g/m}^2\text{-day)}$ for sand. Simulated deposition from the Drydock 6 event is only about 2% of that from the Drydock 3 event for silt, and 13% for sand particles. As shown in Figure 6-124 and Figure 6-125, the plumes from those two resuspension events got dispersed over distance from the resuspension sites. The distance between Drydock 6 and Pier 7 is about 1,200 m compared to the distance of ~50 m between Drydock 3 and Pier 7. The differences of simulated deposition rates between Drydock 3 and Drydock 6 resuspension events should be attributed to the differences of distance between the two dry docks and Pier 7.

Table 6-26. Integrated deposition rate at Pier 7 between model results (g/m^2) and field data ($\text{g/m}^2\text{-day}$).

	Event 1		Event 2		Event 3
Deposition Rate	Model (g/m^2)	Data ($\text{g/m}^2\text{-day}$)	Model (g/m^2)	Data ($\text{g/m}^2\text{-day}$)	Data ($\text{g/m}^2\text{-day}$)
Sand	20.3	40.8	2.7	34.7	29.8
Silt	25.2	9.5	0.6	27.6	19.4
Clay	~0	~0	~0	~0	~0

Figure 6-127 and Figure 6-128 show the predicted total deposited rate of copper and nickel (mg/m^2), associated with the deposited particles for the Drydock 3 and 6 events, respectively. For Drydock 3 event, highest deposition rates center around the dry dock, with values in the range of 5–10 mg/m^2 for copper and 3–8 mg/m^2 for nickel. For the Drydock 6 event, the highest deposition rates center around the dry dock with values in the range of 1–7 mg/m^2 for copper and < 4 mg/m^2 for nickel.

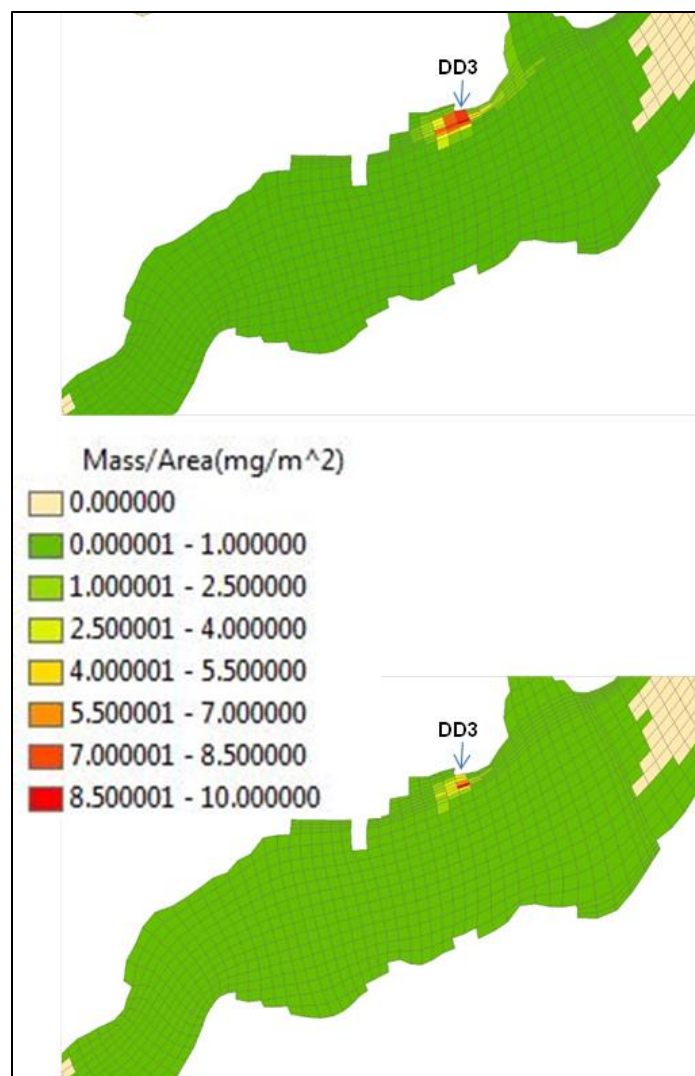


Figure 6-127. Deposited copper (top) and nickel (bottom) from sediment plume in Drydock 3.

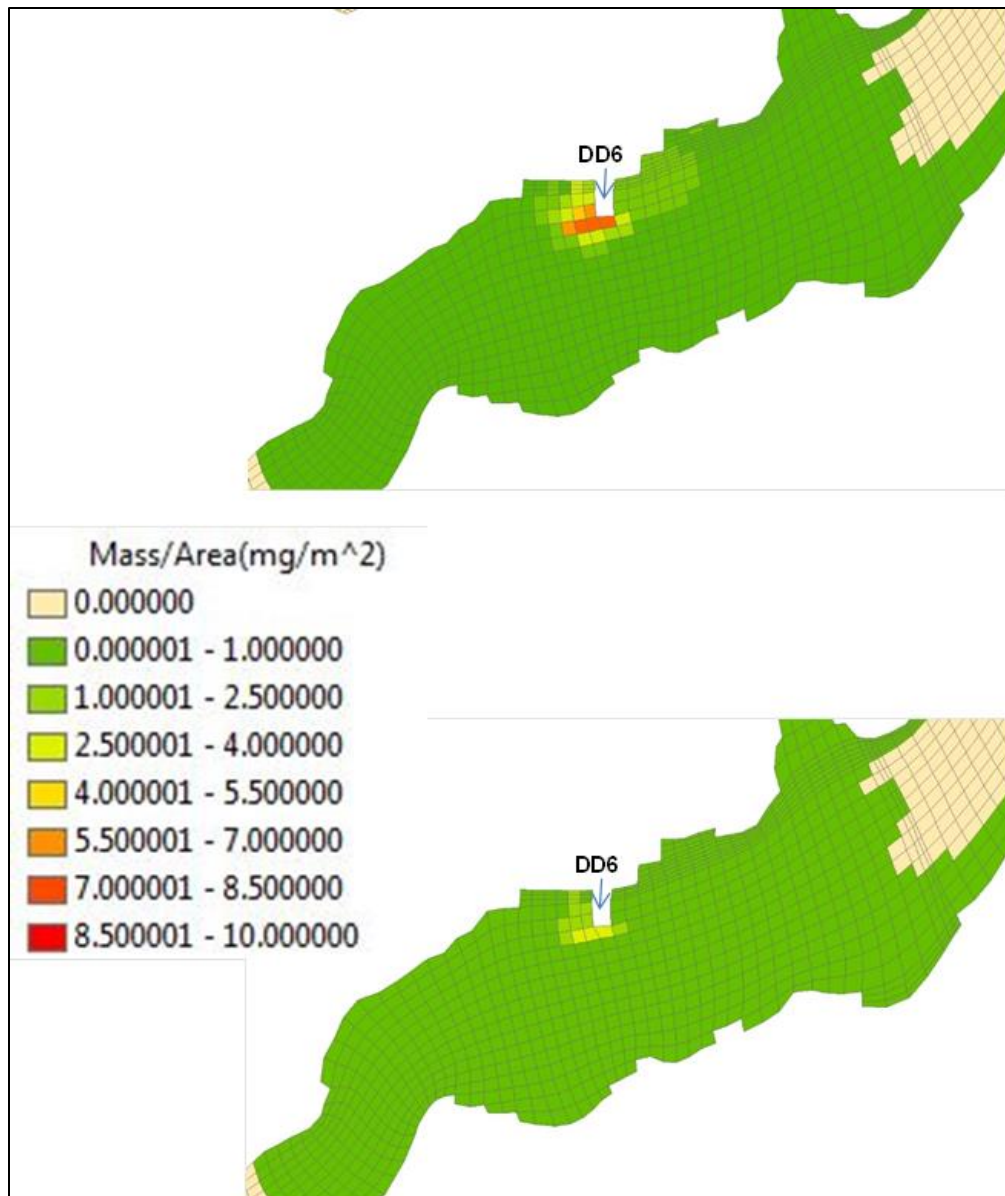


Figure 6-128. Deposited copper (top) and nickel (bottom) from sediment plume in Drydock 6.

6.5.5 Sinclair Inlet Sediment Deposition Signature Analysis

The comparison between the metal concentrations ($\mu\text{g/g}$) in the particles collected by the sediment traps and those in the background sediment provides evidence of the provenance of the particles. Figure 6-129 is the plot of the average metal concentration measured in each of the three events versus the average metal concentration in the background sediments collected by and in between the piers in PSNSY& IMF. If the source of the collected particles was the background sediment, then the data should align along the line depicting a 1:1 ratio, which is the case for the metals with the lowest concentrations in both matrices: silver, cadmium, and arsenic. However, deviations from the 1:1 relationship is obvious for the other five metals that have larger concentrations: nickel, chromium, lead, copper, and zinc.

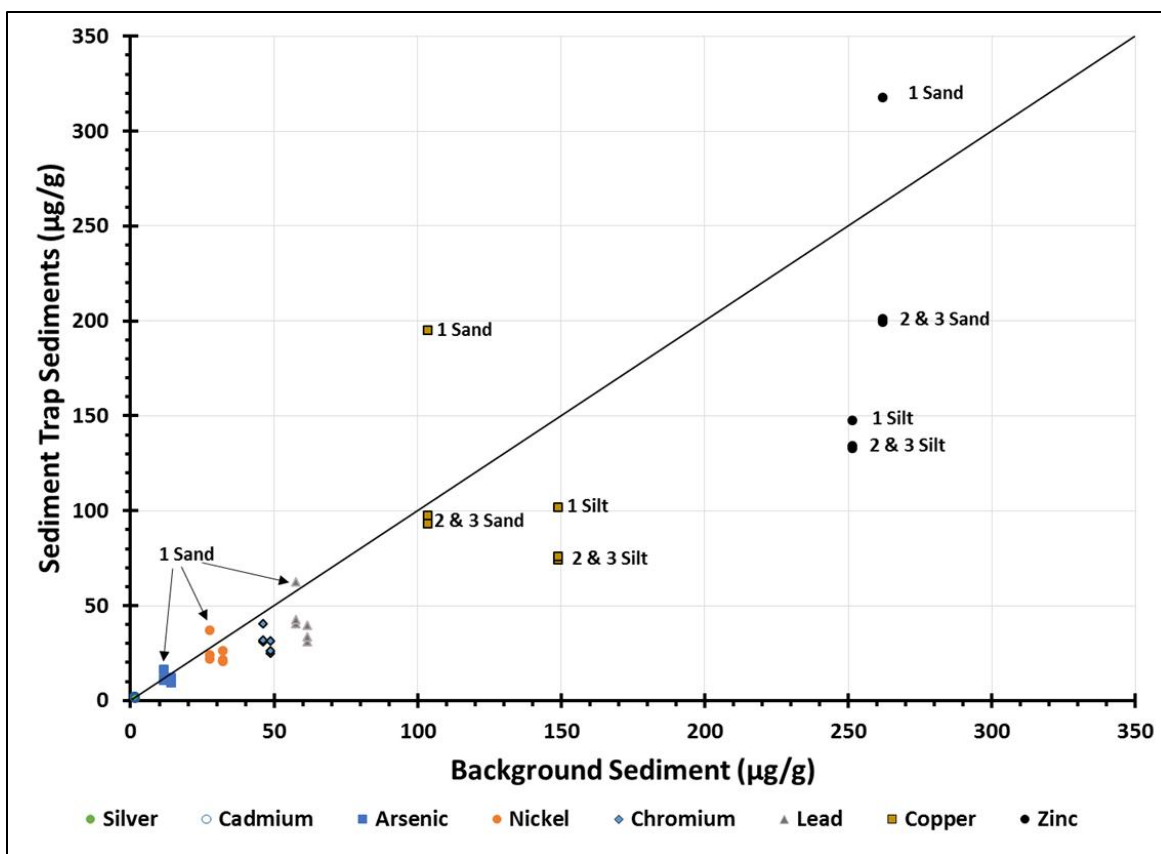


Figure 6-129. Mean sediment trap particle concentration (µg/g) versus mean background sediment concentration (µg/g). Data are presented for each metal in the sand and silt fractions and for each of the three events.

There is a deviation to the positive side of the 1:1 relationship for copper and zinc in the sand fraction of Event 1 (Drydock 3). Copper concentration in the sand-size particles in average are about twice the concentration in background sediment, while the difference in zinc is about 1.2. In general most of the other metals also show a larger concentration in the particles for the sand fraction in Event 1 (Drydock 3), which indicates that the particles originated, at least in part, from a different source, with larger concentration of these and the other metals. The most probable source is sediment closer to Drydock 3. The shuttling of the two submarines, previously docked in Pier 7, to Drydock 3 resulted in resuspension of larger particles (sand) in the area closer to the dry dock. The resuspended sand had relatively high levels of copper and zinc relative to background (Figure 6-129), which may be due to the opening and closing of the caisson, combined with the effect of tug-boats pushing the submarines into position for docking, as well as the dewatering of the dry dock. These larger particles could derive from industrial activities on antifouling paints in the dry dock.

The silt fraction for Event 1, and the two fractions (sand and silt) for the Event 2 and Event 3 show a negative deviation from the 1:1 relationship (i.e., they plot below the 1:1 line in Figure 6-129). Event 2 and 3 have similar concentrations in the plot for each fraction, which indicates that there is/are another source(s) of sediments that has lower metal concentration than the background sediment for those fractions. These sources could be sediment from the daily transit of ferries in the area just east of Pier 7, and the resuspension of sediment from the transit channel area in Sinclair Inlet by the carrier leaving Drydock 6 in Event 2.

The last result also indicates that the source of the silt fraction is from a larger area or a longer deposition time. The dissimilarity between the sand and silt fractions for copper and zinc in the first event indicates that sand should come from a closer source with higher metal concentration (sediments by the caisson as discussed above). In contrast, the silt fraction for Event 1 is not as different to the silt concentrations in Events 2 and 3, indicating that the source of the silt fraction is more similar, or that the proportion between the silt generated and deposited in Event 1 has a stronger effect from silt resuspended in other areas of the inlet (i.e., ferry and vessel transit, other anthropogenic or natural phenomena resulting in resuspension of sediment) than the sand fraction. This is evidence that the particles collected in the sediment traps under Pier 7 are affected by processes occurring beyond piers of PSNS& IMF.

6.6 DISCUSSION AND SUMMARY

Resuspension of bottom sediment by propeller wash in DoD harbors is a phenomenon constantly observed and occasionally reported. Current regulatory laws require the development of better scientific knowledge about this phenomenon for its potential impacts on erosion, transport, redeposition, and recontamination. This study was conducted to evaluate the following impacts from propeller wash: resuspension potential, fate and transport, and remigration and recontamination potential of the sediment plumes from propeller wash in DoD harbors.

6.6.1 Metals in Sediment Plumes

During the fate/transport study, water samples were collected from the sediment plumes and analyzed. Results show that for San Diego Bay, only two metals were present at concentrations above the chronic water quality criteria, copper and nickel. Copper concentration above this criterion was for most of the fractions but the clay (5 to 60 μm) fraction. For nickel, only the total and dissolved ($<0.4 \mu\text{m}$) fractions were above the criterion. Therefore, for copper most fractions will have a potential effect, and probably will cover a relatively larger area. In the case of nickel, its concentration is mainly associated with the dissolved fraction ($<0.4 \mu\text{m}$), and it will undergo mixing/dilution with surrounding water. The implication here is that metals associated with particles will be advected, and could have an effect at some distance. In contrast, metals mostly in the dissolved ($<0.4 \mu\text{m}$) fraction will undergo mixing and dilution, and their effect will be buffered by the surrounding waters with lower concentration of the same metal.

For Pearl Harbor, most metals in the sediment plumes were present at levels considered with low potential for concern as compared to accepted water quality. Zinc, arsenic, silver, and cadmium were present at concentrations below the USEPA water quality criteria. Copper was above the USEPA water quality criteria in the resuspension events at Bravo Pier, but below or similar at Oscar Pier. Lead had few concentrations similar to the USEPA water quality criterion at Bravo Pier; but below this criterion at Oscar Pier. Only chromium and nickel were consistently over their respective water quality criteria in the six resuspension events performed in Pearl Harbor.

6.6.2 Resuspension Potential and Fate/Transport

In DoD harbors, resuspension by propeller wash in DoD harbors arises from two activities: berthing/docking by tug-boats and navigating deep-drafted vessels such as DDGs and/or aircraft carriers. For the resuspension potential study, we applied and calibrated Maynard's model for tug wash in San Diego Bay. Field data of velocity and near-bottom turbulence field, along with laser snapshots of bed erosion profiles during the resuspension field study were used to calibrate the Maynard's model and further extend its capability in predicting erosion from tug wash. Model-predicted sediment plumes, which was estimated to be 21,571 kg and produced by the tug-boat

during the fate/transport study was used to drive the fate and transport model, CH3D. Good agreement of model/data comparison was achieved for water column sediment and metal concentrations. Such good agreement is significant because it validates the Maynard's model prediction of the 21,571 kg of sediment eroded by the tug-boat. This is the first direct validation, that we know of, for the total eroded sediment mass by a tug-boat using a validated model and field data. Second, the model/data agreement also validates the CH3D model for the three particles, clay, silt, and sand, and the TSS. While CH3D has been demonstrated and validated with various hydrodynamic and/or water quality parameters in many previous studies, this is the first direct validation with three sediment particle sizes, and TSS from the propeller wash study, all in good agreement with field data.

Model results show that sediment plumes from tug wash contains mostly silt particles for all the three harbors, including San Diego Bay, Pearl Harbor, and Sinclair Inlet. The sediment plumes were transported by ambient tidal currents with settling to the bottom. Most of the plume decayed from settling to the bottom fast. In 6–10 hours, the plumes disappeared from the pier regions where they were resuspended. In 24 hours (two tidal cycles), most of the sand and silt particles and the associated metals settled to the bottom. Clay particles stayed in the water column for another 4 to 5 days before they either finally settled to the bottom or were flushed out the bay. These transport and deposition patterns were consistent for both San Diego Bay and Pearl Harbor.

Unlike the San Diego Bay study in which Maynard's model and the CH3D model were both calibrated for simulation of resuspension potential and subsequent fate and transport of the sediment plumes by tug wash, the Pearl Harbor study did not include similar field measurements. Instead, CH3D was used to simulate fate/transport of the sediment plumes from tug wash in Pearl Harbor and results were analyzed and characterized qualitatively. Sediment plumes in Bravo Pier and Oscar Pier were both advected by the background currents, which are weaker than those for San Diego Bay. Similar to the deposition patterns in San Diego Bay, most silt particles deposited to the bottom during the first 24 hours (2 tidal cycles).

On 31 Aug 2012, the last day of our field work in Pearl Harbor, the sediment plumes produced from tug-assisted undocking of USS *Chafee* (draft: 9 m) in Bravo Pier were, coincidentally, and perhaps, accidentally, detected and recorded by the ADCP survey. Recorded data were analyzed and it was found that the horizontal scales and initial sediment distribution of the plume and the locations of maximum concentration suggest that the plume was generated predominantly by underkeel flows of *Chafee*, instead of tug jets. Unlike plumes by tug wash, plumes generated by deep-drafted vessels, which often navigate at low speed, would tend to stay in the bottom layer water column before they resettle back, and therefore these subsurface sediment plumes were not as visible as plumes from tug wash. These observed plume patterns are consistent with the FANS model results for the deep-drafted vessel, i.e., DDG, discussed in Section 6.4. This provides another qualitative confirmation of the fact that deep-drafted vessels produce sediment resuspension in DoD harbors, due to its low clearance between the keel and propeller, and the bottom.

6.6.3 Deposition at Pier 7, Sinclair Inlet, WA

Sediment data collected from the sediment traps at Pier 7, Sinclair Inlet, provided direct measurements of deposition of sediment in the area. The comparison between the metal concentrations ($\mu\text{g/g}$) in the particles collected by the sediment traps and those in the background sediment exhibited deviation to the positive side of the 1:1 relationship for copper and zinc in the sand fraction of Event 1 (Drydock 3). Copper concentration in the sand-size particles in average are about twice the concentration in background sediment, while the difference in zinc is about 1.2, which indicates the particles might originate from a different source with a larger concentration of

these particles. The most probable source is sediment closer to Drydock 3. The shuttling of the two submarines, previously docked in Pier 7 to Drydock 3 resulted in resuspension of larger particles (sand) in the area closer to the dry dock. The resuspended sand had relatively high levels of copper and zinc relative to background, which may be due to the opening and closing of the caisson, combined with the effect of tug-boats pushing the submarines into position for docking, as well as the dewatering of the dry dock. These larger particles could derive from industrial activities on antifouling paints in the dry dock.

The silt fraction for Event 1, and the two fractions (sand and silt) for Events 2 and 3 show a negative deviation from the 1:1 relationship (i.e., they plot below the 1:1 line in Figure 6-129). Events 2 and 3 have similar concentrations in the plot for each fraction, which indicates that there is/are another source(s) of sediments that has lower metal concentration than the background sediment for those fractions. These sources could be sediment from the daily transit of ferries in the area just east of Pier 7, and the resuspension of sediment from the transit channel area in Sinclair Inlet by the carrier leaving Drydock 6 in Event 2.

The last result also indicates that the source of the silt fraction is from a larger area or a longer deposition time. The dissimilarity between the sand and silt fractions for copper and zinc in Event 1 indicates that sand should come from a closer source, with higher metal concentration (sediments by the caisson as discussed above). In contrast, the silt fraction for Event 1 is not as different to the silt concentrations in Events 2 and 3, indicating that the source of the silt fraction is more similar, or that the proportion between the silt generated and deposited in Event 1 has a stronger effect from silt resuspended in other areas of the inlet (i.e., ferry and vessel transit, other anthropogenic or natural phenomena resulting in resuspension of sediment) than the sand fraction. This is evidence that the particles collected in the sediment traps under Pier 7 are affected by processes occurring beyond piers of PSNS&IMF.

7. COST ASSESSMENT

In this project, we have developed, calibrated, and validated the modeling of the fate and transport of sediment particles resuspended by propeller wash in three DoD embayments. This effort identified the parameters required for the application of this modeling. In this section, we strive to present the costs that would be incurred for applying this modeling to a different body of water.

Prediction of the fate of contaminant load associated with particles resuspended by propeller wash must include the setting up, calibration, validation, and application of the two main models developed in this effort, the Graphic Maynard's Model and the CH3D/TICKET Model. There will be minimal confidence in any predictions resulting from a least expensive option of applying these models to a different body of water without calibration. Furthermore, calibration could be accomplished by having a single resuspension event, similar to those accomplished in San Diego Bay and Pearl Harbor as part of this project.

7.1 COST MODEL

As the approach for development, calibration, and validation of the models followed in this project was similar for the three DoD harbors, the cost model presented here is for the effort in San Diego Bay. Table 7-1 show the costs incurred in the development, calibration, and application of the models in San Diego Bay, and it is divided in different cost elements for each of the separate tasks required for application of the models. These cost elements are described below.

Table 7-1. Cost model from the modeling development in San Diego Bay.

Cost Element	Data Tracked During the Demonstration	Costs		
		Description	Qty	Units
Instruments rental/purchase and laboratory calibration	Personnel and labor	Lab technician		Hours
		Certified Engineer		Hours
	Equipment	ADV		Rental
		ADCP		Purchase
		PIV shear detector		Purchase
		SPI camera system		Rental
	Materials	Filters, etc.		Cost
Resuspension event and background sediment sampling	Personnel and labor	Captain		Hours
		Sampling boat driver		Hours
		Two ADCP operators		Hours
		Three sampling technicians		Hours
	Equipment	Boats rental		Rental
		Tug-boat rental		Hours
		Tug-boat fuel		Cost
	Materials	Sampling equipment		Cost

Qty = quantity.

Cost was used to identify a group of materials and/or fuel consumption by the tug-boat as a lump sum.

Table 7-1. Costs model from the modeling development in San Diego Bay. (Continued)

Cost Element	Data Tracked During the Demonstration	Costs		
		Description	Qty	Units
Laboratory preparation and analysis	Personnel and labor	Lab technician		Hours
	Analytical costs	Materials		Cost
		Organics		Cost
		Metals		Cost
Graphics Maynard's Model	Personnel and labor	Modeler		Hours
		Computer technician		Hours
CH3D/TICKET Model	Personnel and labor	Modeler		Hours
		Computer technician		Hours
Report	Personnel and labor	Modeler		Hours

Qty = quantity.

Cost was used to identify a group of materials and/or fuel consumption by the tug-boat as a lump sum.

Instrument rental/purchase and calibration in laboratory. These costs are associated with rental fees, purchasing, calibration, and preparation of the suite of instruments required for resuspension field measurements. These instruments include ADV, ADCP(s), PIV shear detector, SPI camera system, pumps, and hoses for sampling of resuspended sediment, carboys/containers for sample, etc. In the case of San Diego Bay, some of these instruments required purchasing.

Resuspension event and background sediment sampling. These illustrate the operational costs for taking three cores of background sediments prior to the resuspension event, having a tug-boat tied to a pier and cranking up the propeller to different speeds for determination of the shear speed that resuspends the sediment, collecting 10 samples from the plume of resuspended sediment, and collecting data associated with the currents generated by the tug-boat during the resuspension. This process was followed in the resuspension events performed in San Diego Bay and Pearl Harbor as part of this project.

Laboratory Preparation and Analysis. This describes the labor costs for separation of the background sediments and resuspended sediment samples into the four grain-size classes investigated in this project as shown in Figure 5-6, and the costs associated for quantification of organic and metals CoCs in these fractions.

Graphic Maynard's Model. These are the costs expected from setting up the Graphic Maynard's Model to the body of water, as well as calibration, validation, and application of the model.

CH3D/TICKET Model. Similar to above, these are the costs expected for setting up, calibration, validation, and application of the CH3D/TICKET Model to the body of water.

Report. These costs are expected for analysis and explanation of results from the two models, and prediction of fate of contaminants of concern (CoC) after resuspension in the body of water.

Our estimates may be different that those from private industry or academia. Our cost estimates are based on the assumption that these are performed by personnel with similar salaries as those of the personnel at SSC Pacific that performed these tasks for this project. Therefore, differences in costs should be expected for organizations with personnel within a different range of salaries. Another difference can arise from having the instrumentation already available (i.e., no need for purchasing).

The estimates presented here do not include some costs. These include costs for traveling back and forth to the body of water from the organization place. Shipping costs of instrumentation or samples are not included, as well as administrative costs. As the two models were developed as part of this ESTCP-funded effort, costs for development of the models are not included for future endeavors.

7.2 COST DRIVERS

Management of contaminated sediments is the main driver for implementing prop wash resuspension modeling in DoD harbors. Modeling of sediment resuspension by propeller wash is applicable to bodies of water with strong evidence or confirmed presence of contaminated sediments. This modeling is pertinent to the management and remediation of these contaminated sediments, and should indicate the most efficient, cost-effective, long-term management approaches in that specific body of water. Most probably, the application of this modeling is a response to regulatory scrutiny, and a desire for improving public opinion.

7.3 COST ANALYSIS

The cost model presented here is for sampling and quantification of required data, and costs associated with setting up, calibration, application, and description of the modeling results to a different DoD harbor. Assumptions for this scenario include the case in a body of water where environmental information required for modeling (i.e., currents' speed and direction, bathymetry, tidal information, etc.) is available. There is a requirement of assessing background sediments for particle size distribution and associated metal mass loading, which will be accomplished by sampling, manipulation (i.e., grain size separation in four classes), and analysis of three sediment cores. There also is a requirement for the highest confidence in the results from the modeling, which will be accomplished by calibration with data from one resuspension event. With sampling, manipulation, and analysis of 10 samples of resuspended sediments for calibration of the models. Table 7-2 shows the costs expected for this scenario. This cost scenario does not include any comparison, as we are not aware of any other available modeling of prop wash resuspension. Furthermore, costs, savings, and improvements on environmental condition and public opinion are difficult to evaluate.

Table 7-2. Costs expected for the scenario of an embayment where basic hydrologic information is available, and there is a requirement for high resolution in the predicted fate and transport of particles resuspended by propeller wash.

Cost Element	Data Tracked During the Demonstration	Costs				
		Description	Qty	Units	Price/ unit (\$)	Price/ item (\$)
Instruments rental/purchase and laboratory calibration	Personnel and labor	Lab technician	80	Hours	118	9,418
		Certified engineer	24	Hours	118	2,825
	Equipment	ADV	1	Rental	5,000	5,000
		ADCP	2	Purchase	20,000	40,000
		PIV shear detector	1	Purchase	5,000	5,000
		SPI camera system	1	Rental	5,000	\$5,000
	Materials	Filters, etc.	1	Cost	2,000	\$2,000
	Subtotal					\$69,243

Table 7-2. Costs expected for the scenario of an embayment. where basic hydrologic information is available, and there is a requirement for high resolution in the predicted fate and transport of particles resuspended by propeller wash. (Continued)

Cost Element	Data Tracked During the Demonstration	Costs				
		Description	Qty	Units	Price/ unit (\$)	Price/ item (\$)
Resuspension event and background sediment sampling	Personnel and labor	Captain	8	Hours	118	942
		Sampling boat driver	8	Hours	118	942
		Two ADCP operators	16	Hours	118	1,884
		Three sampling technicians	24	Hours	118	2,825
	Equipment	Boats rental	2	Rental	2,500	5,000
		Tug-boat rental	8	Hours	1,200	9,600
		Tug-boat fuel	1	Cost	3,000	3,000
	Materials	Sampling equipment	1	Cost	5,000	5,000
	Subtotal					29,192
Laboratory preparation and analysis	Personnel and labor	Lab technician	480	Hours	118	\$56,506
	Analytical costs	Materials	1	Cost	3,000	\$3,000
		Organics	1	Cost	30,000	\$30,000
		Metals	1	Cost	10,000	\$10,000
	Subtotal					\$99,506
Graphics Maynard's Model	Personnel and labor	Modeler	200	Hours	118	\$23,544
		Computer technician	320	Hours	118	\$37,670
	Subtotal					\$61,214
CH3D/TICKET Model	Personnel and labor	Modeler	320	Hours	118	\$37,670
		Computer technician	560	Hours	18	\$65,923
	Subtotal					\$103,594
Report	Personnel and labor	Modeler	480	Hours	118	\$56,506
	Subtotal					\$56,506
GRAND TOTAL						\$419,254

Qty = quantity.

Cost was used to identify a group of materials and fuel consumption by the tug-boat.

8. IMPLEMENTATION ISSUES

We have conducted a study to evaluate impacts of propeller wash in DoD harbors. With this study, we have collected important and essential field data and developed tools (models) for prediction and evaluation of the impacts. Lessons learned during the demonstration study are provided below.

- Collection of field data of propeller wash is challenging, due to the highly turbulent flow and dynamic boat and propeller movements during the study
- Good coordination and cooperation with the boat crew, in particular, the driver of the boat is important so that the tug wash experiment can be conducted under controlled conditions.
- Good logistical support and coordination are needed for field study
- Field data are important and costly and collection and analysis are laborious. It is necessary to plan well and identify the types of data based on priorities and budget
- Models can be effective, if calibrated and validated against field data
- Models need to be more user-friendly so that they can be used by people other than the developer(s) of the models. This can be effectively achieved in two ways:
 - Make graphic user interfaces for easy model input and model output
 - Provide users' manuals for the models
- Further research needed for long term impacts with and without propeller wash on sediment dynamics and remediation options in DoD harbors.

REFERENCES

- Barnes, M.P., T. O'Donoghue, J.M. Alsina, and T.E. Baldock. (2009), "Direct bed shear stress measurements in bore-driven swash", *Coastal Engineering*, 56:853-867.
- Berg, P., H. Røy, F. Janssen, V. Meyer, B.B. Jørgensen, M. Huettel, and D. de Beer, 2003. "Oxygen Uptake by Aquatic Sediments Measured with a Novel non-Invasive Eddy-correlation Technique," *Marine Ecology Progress Series* 261:75–83.
- Biron, P.M., C. Robson, M.F. Lapointe, and S.J. Gaskin. 2004, "Comparing Different Methods of Bed Shear Stress Estimates in Simple and Complex Flow Fields," *Earth Surface Processes and Landforms* 29:1403–1415.
- Blaauw, H.B. and E.J. Va de Kaa. 1978. "Erosion of Bottom and Sloping Banks caused by the Screw-race of Maneuvering Ships," Publication 202. *Delft, The Netherlands*.
- Chadwick, D.B., I. Rivera-Duarte, G. Rosen, P.F. Wang, R.C. Santore, A.C. Ryan, P.R. Paquin, S.D. Hafner, and W. H. Choi. 2008. "Demonstration of an Integrated Compliance Model for Predicting Copper Fate and Effects in DoD Harbors," Environmental Security Technology Certification Program, Project ER-0523. Technical Report 1973, SPAWAR Systems Center Pacific, San Diego, CA.
- Chen, H.C., and E.T. Huang. 2003. "Time-Domain Simulation of Floating Pier and Multiple-Vessel Interactions by a Chimera RANS Method." 7th International Symposium on Fluid Control, Measurement and Visualization, 25–28 August, Sorrento, Italy.
- Chen, H.C., and P.F., Wang, 2015. FANS Simulation of Propeller Wash at Navy Harbors and FANS-3D User's Guide, SSC PAC Technical Report, pp 203, submitted to the ESTCP Program Office. ([https://www.serdp-estcp.org/Program-Areas/Environmental-Restoration/Contaminated-Sediments/ER-201031/ER-201031/\(language\)/eng-US](https://www.serdp-estcp.org/Program-Areas/Environmental-Restoration/Contaminated-Sediments/ER-201031/ER-201031/(language)/eng-US)).
- Diaz, R.J., and L.C. Schaffner. 1988. " Comparison of Sediment Landscapes in the Chesapeake Bay as Seen by Surface and Profile Imaging. *In* Understanding the Estuary: Advances in Chesapeake Bay Research," pp. 222–240, M.P. Lynch and E.C. Krome, eds. Chesapeake Bay Research Consortium Publication 129, Chesapeake Bay Program 24/88.
- Doron, P., L. Bertuccioli, J. Katz, and T. Osborn. 2001. Turbulence characteristics and dissipation estimates in the coastal ocean bottom boundary layer from PIV data. *Journal of Physical Oceanography* 31 (2001) 2108–2134.
- Germano, J.D., D.C. Rhoads, R.M. Valente, D.A. Carey, and M. Solan. 2011. The Use of Sediment Profile Imaging (SPI) for Environmental Impact Assessments and Monitoring Studies—Lessons Learned from the Past Four Decades. *Oceanography and Marine Biology: An Annual Review* 49:247–310.
- Grovhoug, J.G. 1992. Evaluation of sediment contamination in Pearl Harbor. Naval Command Control and Ocean Surveillance Center Tech Report 1502, June 1992.
- Jay, D. 2002. "An Analysis of Propwash, Spillage and Sediment Transport Impacts of the Maury Island, Glacier Northwest Gravel Mine", Technical Report, OGI School of Science and Engineering, Oregon Health & Science University, Beaverton, OR.
- Johnson, B.H., H.V. Wang, and K.W. Kim. 1995. "Can Numerical Estuarine Models Be Driven at the Estuary Mouth." *ASCE Estuarine and Coastal Modeling*, pp. 255–267, American Society of Civilian Engineering, New York, NY.

- Johnston, R.K., P.F. Wang, B.E. Skahill, C.W. May, V. Cullinan, M. Roberts, and S. Lawrence. 2007. "Integrated Modeling and Monitoring to Assess the Impact of Runoff at the Watershed Scale." ERF 2007, Estuarine Research Federation, Conference, Nov. 4–8, Providence, RI.
- Kandiah, A. 1974. Fundamental Aspects of Surface Erosion of Cohesive Soils. *Ph.D. thesis*, University of California, Davis, Davis, CA.
- Katija, K., and J. Dabiri. 2008. In situ field measurements of aquatic animal-fluid interaction using a self-contained underwater velocimetry apparatus (SCUVA). *Limnol. Oceanogr.-Meth.* 6 (2008).
- Kerfoot, W.C., J.W. Budd, B.J Eadie, H.A. Vanderploeg, and M. Agy. 2004. Winter Storms: Sequential Sediment Traps Record *Daphnia ephippial* Production, Resuspension, and Sediment Interactions. *Limnology and Oceanography* 49(4, part 2):1365–1382.
- Liao, Q. and E.A. Cowen. 2005. An efficient anti-aliasing spectral continuous window shifting technique for PIV. *Experiments in Fluids* 38(2): 197-208.
- Liao, Q., H.A. Bootsma, J.E. Xiao, J.V. Klump, A. Hume, M.H. Long, and P. Berg. 2009. Development of an in situ Underwater Particle Image Velocimetry (UWPIV) System. *Limnology Oceanography:Methods* 7:169–184.
- Liao, Q., B. Wang, and P.F., Wang, 2013. "In situ PIV measurement of sediment resuspension by a propeller wash in a US Navy harbor", *Proceedings of 2013 IAHR World Congress*.
- Liao, Q., B. Wang, and P.F., Wang, 2014. "In Situ Measurement of sediment resuspension caused by propeller wash with an underwater Particle Image Velocimetry and an Acoustic Doppler Velocimeter", manuscript submitted to *Flow Measurement and Instrumentation*.
- Maynard, S.T. 1984. "Riprap Protection on Navigable Waterways." Technical Report HL–84–3. U.S. Army Engineers Waterways Experiment Station. Vicksburg, MS.
- Maynard, S.T. 1998. "Guidance for In-Situ Subaqueous Capping of Contaminated Sediments: Appendix A: Armor Layer Design." Technical Draft. U.S. Army Division for U.S. EPA.
- Maynard, S., J. Hite, and M. Sanchez. 2006. "Atkinson Island Mooring Basin Alternatives, Houston Ship Channel." U.S. Army Corps of Engineers, Engineer Research and Development Center, Report CHLTR06-09, Vicksburg, MS.
- Maynard's Model in San Diego Bay Model Description and User's Manual", submitted to ESTCP Program Office, pp 41.
- Noble, M.A., K.J. Rosenberger, A.J. Paulson, and A.L. Gartner. 2013. Circulation and Exchange Patterns in Sinclair Inlet, Washington. U.S. Geological Survey Open-File Report 2013-1117.
- Plumb, R.H. Jr. 1981. "Procedures for Handling and Chemical Analysis of Sediment and Water Samples." Technical Report EPA/CE-81-1. Prepared by Great Lakes Laboratory, State University College at Buffalo, Buffalo, NY, for the U.S. Environmental Protection Agency/U.S. Army Corps of Engineers Technical Committee on Criteria for Dredged and Fill Material. U.S. Army Engineer Waterways Experiment Station, CE, Vicksburg, MS.
- Rankin, K.J., and R.I. Hires. 2000. Laboratory Measurement of Bottom Shear Stress on a Movable Bed. *Journal of Geophysical Research* 105(C7):17,011–17,019.
- Revelas, E.C., J.D. Germano, and D.C. Rhoads. 1987. "REMOTS Reconnaissance of Benthic Environments." *Coastal Zone '87 Proceedings* (pp. 2069–2083). 26–29 May, Seattle, WA. American Society of Civil Engineers, WW Division.

- Rhoads, D.C., and J.D. Germano. 1986. Interpreting Long-term Changes in Benthic Community Structure: A New Protocol. *Hydrobiologia* 142:291–308.
- Rhoads, D.C., and J.D. Germano. 1990. The use of REMOTS® Imaging Technology for Disposal Site Selection and Monitoring. In *Geotechnical Engineering of Ocean Waste Disposal*, pp. 50–64, K. Demars and R. Chaney, Eds. American Society for Testing and Materials, West Conshocken, PA.
- Rhoads, D.C., and J.D. Germano. 1982. Characterization of Benthic Processes using Sediment Profile Imaging: An Efficient Method of Remote Ecological Monitoring of the Seafloor (REMOTS® System). *Marine Ecology Progress Series* 8:115–128.
- Stortz, K.R., and M. Sydor. 1980. Transport in the Duluth-Superior Harbor. *Journal of Great Lakes Research* 6(3):223–231. Delf University of Technology, SWAN home page: www.swan.tudelft.nl.
- SERDP, and ESTCP. 2012. Workshop Report on Research and Development Needs for Long-Term Management of Contaminated Sediments. <https://clu-in.org/download/.../sediments/Sediment-Workshop-2012.pdf> (accessed 25 May 2016)
- U.S. Environmental Protection Agency. 1994. “Method 6020. Inductively Coupled Plasma - Mass Spectrometry: Revision 0.” Environmental Monitoring Systems Laboratory, Office of Research and Development, Cincinnati, OH.
- U.S. Environmental Protection Agency. 1999. Method 200.8. “Determination of Trace Elements in Waters and Wastes by Inductively Coupled Plasma - Mass Spectrometry: Revision 5.4.” Environmental Monitoring Systems Laboratory, Office of Research and Development, Cincinnati, OH.
- U.S. Environmental Protection Agency. 2006. “Guidance on Systematic Planning Using the Data Quality Objectives Process (EPA QA/G-4).” EPA/240/B-06/001. Available at <http://www.epa.gov/quality/qs-docs/g4-final.pdf> [accessed 9 June 2011].
- Valente, R.M., D.C. Rhoads, J.D. Germano, and V.J. Cabelli. 1992. Mapping of Benthic Enrichment Patterns in Narragansett Bay, RI. *Estuaries* 15:1–17.
- Wang, B., Q. Liao, H. Bootsma, and P. Wang. 2012. A dual-beam-dual-camera method for battery-powered in situ piv system, *Experiments in Fluids* 52 (2012) 1401–1414.
- Wang, B., Q. Liao, J. Xiao, and H. Bootsma. 2013. A free-floating PIV system: measurements of small-scale turbulence under the wind wave surface. *Journal of Atmospheric and Oceanic Technology* 30 (2013) 1494–1510.
- Wang, P-F, B. E. Skahill, and H. Samaitis. 2002. A GIS-Based Artificial Neural Network Forecasting Watershed Runoff in Sinclair and Dyes Inlet, WA. Paper presented at The Watershed 2002 Conference.
- Wang, P-F, D. Sutton, K. Richter, and B. Chadwick, 2000, “Modeling Migration of Sediment and Sorbed Contaminants Resuspended by Ship Docking in San Diego Bay”, Proceedings in the 4th International Conference on Hydrosience & Engineering., Seoul, Korea.
- Wang, P-F, Bart Chadwick, and Woo-Hee Choi. 2007. Integrated TMDL Model for Particle-Bound Contaminants from Three Watersheds in San Diego, Battelle 4th International Conference on Remediation of Contaminated Sediments, Savannah, GA.

- Wang, P-F, Ignacio Rivera-Duarte, Bart Chadwick, Gunther Rosen, Woo-Hee Choi, Robert Santore, Adam Ryan, and Paul Paquin. 2007. The Linked Transport Model (CH3D) and the Biotic Ligand Model (BLM) for Copper Species in San Diego Bay, SETAC Annual Conference, 2007.
- Wang, P-F, Bart Chadwick, Woo-Hee Choi, Craig Jones, Wendell Wen, and Michelle Yoshioka. 2009. Evaluation of sediment transport in Pearl Harbor using numerical models. Battelle 5th Int'l Conference on Remediation of Contaminated Sediment, Jacksonville, FL.
- Wang, P-F, K. Richter, I. Rivera-Duarte, B. Davidson, B. Wild, R. Barua, Q. Liao, J. Germano, K. Markillie, and J. Gailani. 2014. Evaluation of Resuspension from Propeller Wash in Pearl Harbor and San Diego Bay. SPAWAR Systems Center Pacific Technical Report 2036.
- Wang, P-F, B. Cole, and R. Barua, 2015. Tugboat-Induced Flows and Sediment Bed Erosion: Application of Maynord's Model in San Diego Bay, Model Description and User's Manual, SSC PAC Technical Report, pp 33, submitted to the ESTCP Program Office. ([https://www.serdp-estcp.org/Program-Areas/Environmental-Restoration/Contaminated-Sediments/ER-201031/ER-201031/\(language\)/eng-US](https://www.serdp-estcp.org/Program-Areas/Environmental-Restoration/Contaminated-Sediments/ER-201031/ER-201031/(language)/eng-US)).
- Wang, P.F., K. Farley and I. Rivera, 2015. A linked fate and transport model with metal partitioning for propeller wash in San Diego Bay, manuscript (in preparation) for peer-reviewed publication.
- Wang, P.F., B. Cole, and R. Barua, 2015. Graphic Maynod's Model, Installation Package for Windows PC, submitted to the ESTCP Program Office.

APPENDIX A

POINTS OF CONTACT

Table A-1 Points of contact

Point Of Contact Name	Organization Name/Address	Phone Fax E-Mail	Role In Project
Pei-Fang Wang	SSC PAC 53475 Strothe Road San Diego, CA 92152	619-553-9192 Pei-fang.wang@navy.mil	Principal Investigator: Oversight of technical/management activities
Ignacio Rivera- Duarte	SSC PAC	619-553-2373 iriverad@spawar.navy.mil	Co-PI: Field chemistry data collection and analysis
Ken Richter	SSC PAC	619-553-2780 richter@spawar.navy.mil	Co-PI: Field work, design of frames for ADCP and other instruments
Qian Liao	Dept of Civil Engineering and Mechanics University of Wisconsin-Milwaukee, WI	414-229-4228 liao@uwm.edu	Co-PI: PIV, ADV instruments for tug wakes/plumes, empirical bottom shear stress and erosion rate
Kevin Farley	Manhattan College Dept of Civil and Envir Eng of Manhattan College Riverdale, NY 10471	718-862-7383 kevin.farley@manhattan.edu	Co-PI: Developed look-up table for metal partitioning with the San Diego Bay copper chemistry data for linkage with CH3D
Hamn-Chin Chen	Texas A&M University 3136 TAMU College Station, TX 77843-3136	979-847-9468 hcchen@civil.tamu.edu	Co-PI: Implemented FANS model for resuspension by deep-drafted vessels
Joe Germano	Germano & Associates 12100 SE 46th PI Bellevue, WA 98006	425-865-0199 joe@remots.com	Co-PI: SPI instrument deployment and image processing
Kimberly Markillie	NAVFAC-HI 258 Makalapa Dr Ste 100 Pearl Harbor, HI	(808) 472-1465 kimberly.markillie@navy.mil	Co-PI: Provide logistical support for field study in Pearl Harbor
Joe Gailani	ERDC 3909 Halls Ferry Road Vicksburg, MS 39180-6199	(601) 634-4851 joe.z.gailani@usace.army.mil	Co-PI: Conducted ADCP survey in Pearl Harbor

APPENDIX B:

THRUSTS ON NOZZLE PROPELLERS OF THE TRACTOR C-14 TUGBOAT FROM MEASUREMENTS AND THE FANS MODEL

To simulate the flow field induced by the twin-engine tugboat (Tractor C-14), we selected a typical ducted propeller with the four-bladed Ka4-70 propeller inside a 19A duct as shown in Figure B-1. The propeller specifications and the operating conditions are summarized in Table B-1. The FANS model was employed to calculate the thrust and torque produced by the ducted propeller at five different rotating speeds (20, 50, 100, 150, and 200 rpm) under bollard-pull conditions.

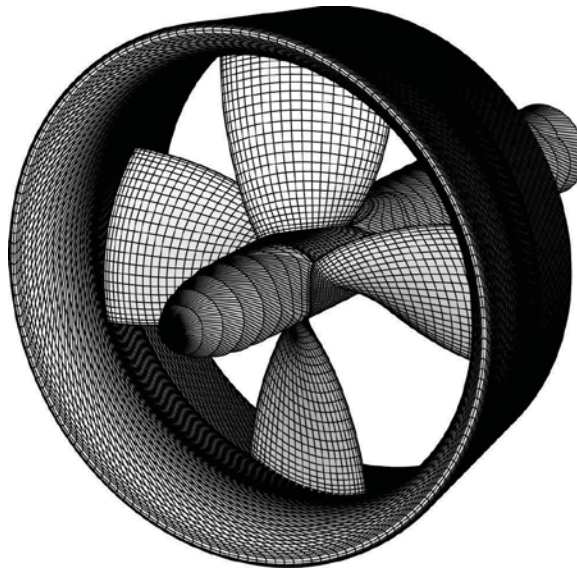


Figure B-1. Ducted propeller geometry.

Table B-1. Propeller information and operating conditions for ducted propeller.

Characteristics	Dimensions
Ship length L (m)	28.65 (94 ft)
Ship Beam B (m)	10.36 (34 ft)
Ship Draft (m)	3.353 (11 ft)
Water depth, H (m)	9.144 (30 ft)
Distance from ship bow to pier wall at waterline (m)	1.8288 (6 ft)
Distance from ship stern to pier wall at waterline (m)	30.48 (100 ft)
Clearance between ship sidewall and Pier wall (m)	Open water
Underkeel clearance (m)	2.997 (9.833 ft)
Propeller Diameter, D_p (m)	<u>2.286 (7.5 ft)</u>

Characteristics	Dimensions
Distance between Propellers (W_p) (m)	<u>4.8768 (16 ft)</u>
Distance from ship stern to propeller (L_{set}) (m)	<u>15.24 (50 ft)</u>
Propeller Depth (depth of the propeller axis) (m)	4.8768 (16 ft)
Distance from center of propeller axis to bottom (H_p) (m)	<u>4.2672 (14 ft)</u>
gap clearance between propeller duct and tugboat bottom (m)	<u>0.14 (0.46 ft)</u>
Ship speed (knots)	0
Propeller rpm, n	20, 50, 100, 150 and 200
Characteristic time, T_o (s)	0.3
Characteristic velocity U_o (m/s)	1.016
Reynolds number based on characteristic length L_o ($= 1$ ft)	2.647×10^5
Reynolds number based on propeller diameter D	1.488×10^7

Figure B-2 shows the surface pressure distributions on the propeller blade, shaft and duct surfaces for the 100 rpm case. It should be noted that the pressure is normalized by $P_o = \rho n^2 D_p^2$, where $\rho = 1030 \text{ kg/m}^3$ is the density of seawater, n is the propeller rotating speed, and $D = 2.286 \text{ m}$ (7.5 ft) is the propeller diameter. Figure B-2 clearly shows that the propeller rotation induced a strong negative pressure on the suction side of the propeller blade and a relatively mild positive pressure on the pressure side. The net forces and torques acting on the ducted propeller can be obtained by numerical integration of the surface pressures and shear stresses over the blade, shaft, and duct surfaces. The dimensionless thrust and torque of the ducted propeller are given by the propeller thrust coefficient K_{TP} , the duct thrust coefficient K_{TD} , and the torque coefficient K_Q defined below:

$$1.0 \quad K_{TP} = \frac{T_p}{\rho n^2 D^4}, \quad K_{TD} = \frac{T_D}{\rho n^2 D^4}, \quad K_Q = \frac{Q}{\rho n^2 D^5}$$

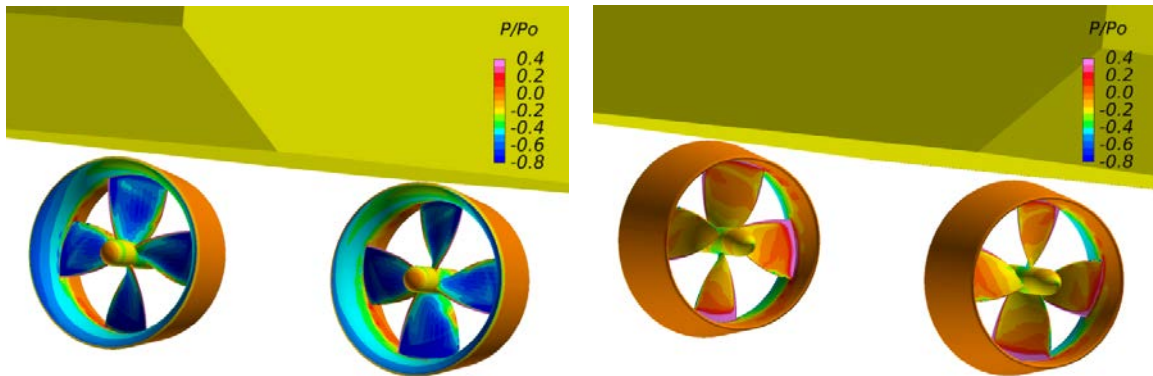


Figure B-2. Pressure distributions on the propeller blade, shaft, and duct surfaces.

Table B-2 shows the calculated thrusts and torques for the ducted propeller at rotating speeds of 20 rpm, 50, 100, 150 and 200 rpm. It was noted that the thrust and torque produced by the ducted propeller increase quadratically with the propeller rotating speed. With increasing propeller rotating speed from 20 to 200 rpm, the predicted propeller thrust coefficient K_{TP} increased slightly from 0.242 to 0.249 while the duct thrust coefficient K_{TD} reduced slightly from 0.151 to 0.147. The calculated propeller thrust coefficient K_{TP} was in excellent agreement with the experimental data. On the other hand, the predicted duct thrust coefficient K_{TD} was about 45% lower than the measured value of 0.27. The observed difference in K_{TD} can be attributed mainly to the blockage effect by the tugboat, and to a lesser degree the shallow water effect in a confined harbor. As noted in Table B-1, the minimum gap clearance between the propeller duct and the tug-boat bottom is only 0.14 m (0.46 ft) or about 6% of the propeller diameter. It is clearly seen from Figure B-2 that the suction pressure on the duct inner surface is significantly weaker in the vicinity of the tugboat bottom surface due to the effect of narrow gap clearance. This resulted in a significant reduction of the thrust force acting on the duct compared to open water conditions. Consequently, the total thrust force produced by the ducted propeller was about 20% lower in a confined harbor with the presence of tug-boat and seabed boundaries.

For completeness, a comparison of the calculated and measured torque coefficients is provided in Table B-2. Torque coefficient reduces from 0.0483 to 0.0441 when the rotating speed was increased from 20 to 200 rpm, which is also in excellent agreement with the measured K_Q value of 0.045. The present simulation results indicate that the tug-boat blockage and shallow water effects do not alter the overall performance of the propeller thrust (K_{TP}) and torque (K_Q) since the propeller is shielded inside the duct. However, the thrust force induced by the duct (nozzle) is significantly reduced as a result of the tug-boat blockage.

Table B-2. Comparison of the calculated thrust and torque coefficients (in confined water) with the experimental data (open water) under bollard-pull condition.

	K_{TP}	K_{TD}	K_T	K_Q
Experiment (open water)	0.25 (propeller thrust)	0.27 (duct thrust)	0.52 (total thrust)	0.045 (total torque)
20 rpm	0.242 (756 N)	0.151 (472 N)	0.393 (1,228 N)	0.0483 (345 N-m)
50 rpm	0.243 (4,744 N)	0.150 (2,929 N)	0.393 (7,673 N)	0.0475 (2,123 N-m)
100 rpm	0.246 (19,240 N)	0.148 (11,533 N)	0.394 (30,773 N)	0.0454 (8,113 N-m)
150 rpm	0.248 (43,606 N)	0.147 (25,860 N)	0.395 (69,466 N)	0.0446 (17,940 N-m)
200 rpm	0.249 (77,763 N)	0.147 (45,982 N)	0.396 (123,745 N)	0.0441 (31,485 N-m)

APPENDIX C

SAN DIEGO BAY DATA

Table C-1. Size-fraction Data.

	SAND	SILT	CLAY	TOTAL	SAND	SILT	CLAY
	6	7	8	9			
Sample ID	SAND 60 µm Mass Fraction (mg/L)	SILT 5 µm Mass Fraction (mg/L)	CLAY 0.4 µm Mass Fraction (mg/L)	TOTAL Mass Fraction (mg/L)	SAND 60 µm Mass Fraction (%)	SILT 5 µm Mass Fraction (%)	CLAY 0.4 µm Mass Fraction (%)
1 S	0.20	2.48	5.33	8.01	2.5	30.9	66.6
1 M	3.70	11.60	9.41	24.71	15.0	46.9	38.1
2 S	20.19	32.80	5.56	58.54	34.5	56.0	9.5
2 M	14.89	45.60	8.24	68.73	21.7	66.4	12.0
3 S	0.20	2.04	4.27	6.51	3.1	31.3	65.6
3 M	0.29	2.71	4.27	7.27	4.0	37.3	58.7
4 S	1.61	3.40	3.29	8.30	19.4	41.0	39.6
4 M	0.20	4.42	3.81	8.43	2.4	52.4	45.2
5 S	0.57	14.50	6.05	21.12	2.7	68.7	28.6
5 M	3.65	36.92	7.56	48.13	7.6	76.7	15.7
6 S	5.16	17.33	3.10	25.59	20.1	67.7	12.1
6 M	10.43	39.20	5.83	55.46	18.8	70.7	10.5
7 S	3.68	2.80	3.24	9.72	37.9	28.8	33.3
7 M	1.55	6.06	4.44	12.05	12.8	50.3	36.9
8 S	2.37	19.00	5.57	26.95	8.8	70.5	20.7
8 M	8.59	16.15	3.46	28.20	30.5	57.3	12.3
9 S	0.20	6.42	4.29	10.90	1.8	58.9	39.3
9 M	0.20	5.75	4.07	10.02	2.0	57.4	40.6
10 S	0.20	22.22	5.79	28.21	0.7	78.8	20.5
10 M	8.25	53.33	12.50	74.08	11.1	72.0	16.9
11 S	1.49	7.67	3.10	12.26	12.2	62.6	25.3
11 M	0.99	11.00	2.33	14.33	6.9	76.8	16.3
12 S	0.20	3.20	0.77	4.17	4.8	76.8	18.5
12 M	3.46	1.86	0.20	5.52	62.6	33.8	3.6
13 S	1.46	2.17	2.00	5.62	25.9	38.5	35.6
13 M	1.80	6.67	3.64	12.10	14.9	55.1	30.0
14 S	0.20	2.83	1.60	4.63	4.3	61.2	34.5
14 M	0.20	8.02	3.09	11.31	1.8	70.9	27.3
15 S	0.44	2.04	1.00	3.49	12.8	58.5	28.7
15 M	0.32	2.00	1.84	4.15	7.6	48.2	44.2
16 S	0.20	6.25	1.59	8.04	2.5	77.8	19.7
16 M	1.05	9.60	2.57	13.23	8.0	72.6	19.4
17 S	0.47	5.20	2.68	8.35	5.6	62.3	32.1
17 M	3.90	3.52	1.40	8.81	44.2	39.9	15.8
Average					13.9	57.5	28.6
Standard deviation					14.2	15.3	15.6

Table C-2. Chromium data for San Diego Bay Field Study, 4 April 2012.

San Diego Bay		Chromium			1	2	3	4	5	6	7	8	9					
Station	Depth (ft)	Sampling date and time	Latitude	Longitude	TOTAL Filtered solution (µg/L)	SAND Filtered solution (µg/L)	SILT Filtered solution (µg/L)	CLAY Filtered solution (µg/L)	DISSOLVED Filtered solution (µg/L)	Mass of metal in SAND fraction (µg/mg)	Mass of metal in SILT fraction (µg/mg)	Mass of metal in CLAY fraction (µg/mg)	Mass of metal in TOTAL fraction (µg/mg)	TOTAL as Summ of fractions (µg/mg)	Mass of metal in SAND fraction (%)	Mass of metal in SILT fraction (%)	Mass of metal in CLAY fraction (%)	Mass of DISSOLVED metal associated to TOTAL fraction (%)
					< 2 mm	≥ 60 µm	60 µm to 5 µm	5 µm to 0.4 µm	< 0.4 µm	≥ 60 µm	60 µm to 5 µm	5 µm to 0.4 µm	< 2 mm		≥ 60 µm	60 µm to 5 µm	5 µm to 0.4 µm	< 0.4 µm
1 S	3	4/4/2012 14:14	32.68013	-117.12663	4.18	0.16	0.07	-0.24	4.18	0.82	0.03	-0.05	0.52	1.37	60%	2%	0%	38%
1 M	15	4/4/2012 14:15	32.68009	-117.12662	30.21	0.59	0.14	0.66	28.81	0.16	0.01	0.07	1.22	1.41	11%	1%	5%	83%
2 S	3	4/4/2012 14:19	32.67958	-117.12680	31.78	-0.12	2.16	-0.50	30.23	-0.01	0.07	-0.09	0.54	0.58	0%	11%	0%	89%
2 M	15	4/4/2012 14:19	32.67953	-117.12682	34.31	0.64	2.87	-1.23	32.03	0.04	0.06	-0.15	0.50	0.57	8%	11%	0%	81%
3 S	3	4/4/2012 14:21	32.67989	-117.12700	4.73	0.30	-0.02	0.09	4.36	1.50	-0.01	0.02	0.73	2.19	68%	0%	1%	31%
3 M	15	4/4/2012 14:22	32.67994	-117.12702	4.75	0.17	0.21	-0.07	4.44	0.59	0.08	-0.02	0.65	1.28	46%	6%	0%	48%
4 S	3	4/4/2012 14:24	32.68015	-117.12721	4.95	-0.59	0.56	0.30	4.68	-0.36	0.16	0.09	0.60	0.82	0%	20%	11%	69%
4 M	15	4/4/2012 14:25	32.68019	-117.12717	5.28	0.47	-0.07	0.28	4.60	2.34	-0.02	0.07	0.63	2.96	79%	0%	2%	18%
5 S	3	4/4/2012 14:28	32.67976	-117.12752	29.71	-0.12	-0.45	1.08	29.20	-0.21	-0.03	0.18	1.41	1.35	0%	0%	13%	102%
5 M	15	4/4/2012 14:28	32.67958	-117.12753	31.81	0.13	1.42	-0.25	30.52	0.03	0.04	-0.03	0.66	0.71	5%	5%	0%	90%
6 S	3	4/4/2012 14:31	32.67902	-117.12770	31.70	-0.91	3.04	0.58	29.00	-0.18	0.18	0.19	1.24	1.49	0%	12%	12%	76%
6 M	15	4/4/2012 14:31	32.67899	-117.12773	32.50	1.11	1.48	0.08	29.84	0.11	0.04	0.01	0.59	0.70	15%	5%	2%	77%
7 S	3	4/4/2012 14:34	32.67849	-117.12777	4.61	-0.13	0.15	-0.12	4.70	-0.03	0.05	-0.04	0.47	0.54	0%	10%	0%	90%
7 M	15	4/4/2012 14:35	32.67845	-117.12768	5.51	-2.09	2.87	0.03	4.70	-1.35	0.47	0.01	0.46	0.87	0%	54%	1%	45%
8 S	3	4/4/2012 14:38	32.67825	-117.12831	29.55	-3.49	1.92	0.78	30.34	-1.47	0.10	0.14	1.10	1.37	0%	7%	10%	82%
8 M	15	4/4/2012 14:38	32.67825	-117.12827	30.50	0.99	0.02	0.20	29.30	0.12	0.00	0.06	1.08	1.21	10%	0%	5%	86%
9 S	3	4/4/2012 14:44	32.67863	-117.12898	28.66	1.19	3.92	10.93	12.61	5.98	0.61	2.55	2.63	10.30	58%	6%	25%	11%
9 M	15	4/4/2012 14:45	32.67857	-117.12900	5.33	0.15	0.39	0.03	4.76	0.77	0.07	0.01	0.53	1.32	58%	5%	1%	36%
10 S	3	4/4/2012 14:48	32.67741	-117.12939	30.55	0.29	0.71	-0.02	29.57	1.44	0.03	0.00	1.08	2.52	57%	1%	0%	42%
10 M	15	4/4/2012 14:49	32.67746	-117.12948	34.20	0.47	2.74	-0.02	31.01	0.06	0.05	0.00	0.46	0.53	11%	10%	0%	80%
11 S	3	4/4/2012 14:53	32.67723	-117.12805	29.20	0.47	1.31	0.40	27.02	0.32	0.17	0.13	2.38	2.82	11%	6%	5%	78%
11 M	15	4/4/2012 14:54	32.67729	-117.12799	30.03	-0.33	1.39	-0.17	29.14	-0.33	0.13	-0.07	2.10	2.16	0%	6%	0%	94%
12 S	3	4/4/2012 14:57	32.67675	-117.12757	5.17	0.61	-0.09	-0.02	4.67	3.06	-0.03	-0.03	1.24	3.06	100%	0%	0%	37%
12 M	15	4/4/2012 14:57	32.67669	-117.12753	4.36	0.14	0.05	-0.04	4.21	0.04	0.02	-0.21	0.79	0.83	5%	3%	0%	92%
13 S	3	4/4/2012 15:00	32.67643	-117.12819	3.08	-0.03	0.17	-0.03	2.97	-0.02	0.08	-0.01	0.55	0.61	0%	13%	0%	87%
13 M	15	4/4/2012 15:01	32.67651	-117.12820	27.68	0.71	-0.71	-0.03	27.71	0.39	-0.11	-0.01	2.29	2.68	15%	0%	0%	85%
14 S	3	4/4/2012 15:04	32.67731	-117.12713	4.61	-0.03	0.04	-0.06	4.66	-0.16	0.01	-0.04	0.99	1.02	0%	1%	0%	99%
14 M	15	4/4/2012 15:05	32.67736	-117.12700	30.09	-0.31	1.08	0.59	28.73	-1.54	0.13	0.19	2.66	2.86	0%	5%	7%	89%
15 S	3	4/4/2012 15:07	32.67818	-117.12650	4.60	-0.23	0.35	0.15	4.32	-0.51	0.17	0.15	1.32	1.57	0%	11%	10%	79%
15 M	15	4/4/2012 15:08	32.67814	-117.12641	4.38	-0.05	0.00	0.07	4.37	-0.16	0.00	0.04	1.06	1.09	0%	0%	3%	97%
16 S	3	4/4/2012 15:21	32.67601	-117.12786	5.37	-0.10	0.64	0.02	4.82	-0.51	0.10	0.01	0.67	0.72	0%	14%	2%	84%
16 M	15	4/4/2012 15:22	32.67607	-117.12789	29.78	-0.05	-0.44	-0.12	30.39	-0.05	-0.05	-0.05	2.25	2.30	0%	0%	0%	100%
17 S	3	4/4/2012 15:27	32.67797	-117.12703	5.22	-0.15	0.53	0.25	4.59	-0.33	0.10	0.09	0.63	0.75	0%	14%	13%	74%
17 M	15	4/4/2012 15:28	32.67793	-117.12691	5.03	-0.12	0.22	0.08	4.85	-0.03	0.06	0.06	0.57	0.67	0%	9%	8%	82%
Ambient SDB 1S					0.39				0.02									
Ambient SDB 2S					0.26				0.00									
Ambient SDB 3S					4.40				1.84									
Ambient SDB 4S					12.02				0.75									
Ambient SDB 5S					4.54				2.03									
Average					2.40				0.93									
Standard deviation					2.391				0.970									
Ambient SDB 1B					0.53				0.01									
Ambient SDB 2B					1.55				-0.05									
Ambient SDB 3B					3.61				5.67									
Ambient SDB 4B					18.06				8.02									
Ambient SDB 5B					11.45				12.86									
Average					4.29				3.42									
Standard deviation					4.95				4.079									
Overall Average					3.17				2.91									
Overall Standard Deviation					3.84				4.72									

Table C-3. Nickel Data for San Diego Bay Field Study, 4 April 2012.

San Diego Bay					Nickel	1	2	3	4	5	6	7	8	9					
Station	Depth (ft)	Sampling date and time	Latitude	Longitude	TOTAL Filtered solution (µg/L)	SAND Filtered solution (µg/L)	SILT Filtered solution (µg/L)	CLAY Filtered solution (µg/L)	DISSOLVED Filtered solution (µg/L)	Mass of metal in SAND fraction (µg/mg)	Mass of metal in SILT fraction (µg/mg)	Mass of metal in CLAY fraction (µg/mg)	Mass of metal in TOTAL fraction (µg/mg)	TOTAL Summ of fractions (µg/mg)	as	Mass of metal in SAND fraction (%)	Mass of metal in SILT fraction (%)	Mass of metal in CLAY fraction (%)	Mass of DISSOLVED metal associated to TOTAL fraction (%)
					< 2 mm	≥ 60 µm	60 µm to 5 µm	5 µm to 0.4 µm	< 0.4 µm	≥ 60 µm	60 µm to 5 µm	5 µm to 0.4 µm	< 2 mm			≥ 60 µm	60 µm to 5 µm	5 µm to 0.4 µm	< 0.4 µm
1 S	3	4/4/3912 14:14	32.68013	-117.12663	3.42	0.00	0.00	0.00	3.42	0.00	0.00	0.00	-0.13	0.43		0%	0%	0%	100%
1 M	15	4/4/3912 14:15	32.68009	-117.12662	15.92	0.87	0.00	0.97	14.18	0.23	0.00	0.10	0.64	0.91		26%	0%	11%	63%
2 S	3	4/4/3912 14:19	32.67958	-117.12680	14.97	0.07	0.59	4.06	10.25	0.00	0.02	0.73	0.26	0.93		0%	2%	79%	19%
2 M	15	4/4/3912 14:19	32.67953	-117.12682	12.81	0.00	0.36	1.75	12.24	0.00	0.01	0.21	0.19	0.40		0%	2%	53%	45%
3 S	3	4/4/3912 14:21	32.67989	-117.12700	5.23	2.10	0.38	0.00	3.36	10.53	0.19	0.00	0.80	11.23		94%	2%	0%	5%
3 M	15	4/4/3912 14:22	32.67994	-117.12702	4.24	0.13	0.45	1.09	2.58	0.44	0.16	0.25	0.58	1.21		36%	14%	21%	29%
4 S	3	4/4/3912 14:24	32.68015	-117.12721	6.72	0.00	0.63	0.92	5.19	0.00	0.19	0.28	0.81	1.09		0%	17%	26%	57%
4 M	15	4/4/3912 14:25	32.68019	-117.12717	8.00	4.03	0.00	2.88	4.51	20.26	0.00	0.75	0.95	21.55		94%	0%	4%	2%
5 S	3	4/4/3912 14:28	32.67976	-117.12752	13.91	0.00	0.67	0.65	13.22	0.00	0.05	0.11	0.66	0.78		0%	6%	14%	80%
5 M	15	4/4/3912 14:28	32.67958	-117.12753	14.16	0.00	0.82	1.24	13.31	0.00	0.02	0.16	0.29	0.46		0%	5%	35%	60%
6 S	3	4/4/3912 14:31	32.67902	-117.12770	14.44	0.00	1.01	0.24	14.92	0.00	0.06	0.08	0.56	0.72		0%	8%	11%	81%
6 M	15	4/4/3912 14:31	32.67899	-117.12773	14.63	0.00	2.11	2.37	10.43	0.00	0.05	0.41	0.26	0.65		0%	8%	63%	29%
7 S	3	4/4/3912 14:34	32.67849	-117.12777	3.42	0.05	0.00	0.93	5.07	0.01	0.00	0.29	0.35	0.82		2%	0%	35%	63%
7 M	15	4/4/3912 14:35	32.67845	-117.12768	3.96	0.00	6.26	0.00	5.15	0.00	1.03	0.00	0.33	1.46		0%	71%	0%	29%
8 S	3	4/4/3912 14:38	32.67825	-117.12831	13.06	0.00	1.71	0.00	13.88	0.00	0.09	0.00	0.48	0.61		0%	15%	0%	85%
8 M	15	4/4/3912 14:38	32.67825	-117.12827	14.47	0.56	0.00	2.35	12.33	0.07	0.00	0.68	0.51	1.18		6%	0%	57%	37%
9S	3	4/4/3912 14:44	32.67863	-117.12898	14.81	0.00	2.35	4.49	8.65	0.00	0.37	1.05	1.36	2.21		0%	17%	47%	36%
9 M	15	4/4/3912 14:45	32.67857	-117.12900	5.18	0.00	0.65	0.00	7.79	0.00	0.11	0.00	0.52	0.89		0%	13%	0%	87%
10 S	3	4/4/3912 14:48	32.67741	-117.12939	15.05	0.67	1.19	0.00	13.63	3.39	0.05	0.00	0.53	3.92		86%	1%	0%	12%
10 M	15	4/4/3912 14:49	32.67746	-117.12948	13.54	1.09	0.00	0.47	12.57	0.13	0.00	0.04	0.18	0.34		39%	0%	11%	50%
11 S	3	4/4/3912 14:53	32.67723	-117.12805	15.77	0.74	0.00	0.35	15.51	0.50	0.00	0.11	1.29	1.88		27%	0%	6%	67%
11 M	15	4/4/3912 14:54	32.67729	-117.12799	15.14	0.33	0.00	0.00	15.49	0.33	0.00	0.00	1.06	1.42		24%	0%	0%	76%
12 S	3	4/4/3912 14:57	32.67675	-117.12757	5.38	1.90	0.00	0.76	3.42	9.53	0.00	0.99	1.29	11.33		84%	0%	9%	7%
12 M	15	4/4/3912 14:57	32.67669	-117.12753	2.66	0.00	0.00	2.61	1.35	0.00	0.00	13.10	0.48	13.35		0%	0%	98%	2%
13 S	3	4/4/3912 15:00	32.67643	-117.12819	3.17	0.00	0.52	0.03	3.21	0.00	0.24	0.02	0.56	0.83		0%	29%	2%	69%
13 M	15	4/4/3912 15:01	32.67651	-117.12820	15.74	0.00	1.03	0.00	15.17	0.00	0.15	0.00	1.30	1.41		0%	11%	0%	89%
14 S	3	4/4/3912 15:04	32.67731	-117.12713	4.88	1.20	0.00	1.88	2.29	6.02	0.00	1.17	1.05	7.68		78%	0%	15%	6%
14 M	15	4/4/3912 15:05	32.67736	-117.12700	15.62	0.62	0.00	1.70	13.57	3.12	0.00	0.55	1.38	4.87		64%	0%	11%	25%
15 S	3	4/4/3912 15:07	32.67818	-117.12650	2.82	0.17	0.00	0.00	5.17	0.39	0.00	0.00	0.81	1.87		21%	0%	0%	79%
15 M	15	4/4/3912 15:08	32.67814	-117.12641	5.22	2.56	0.00	1.47	3.92	8.14	0.00	0.80	1.26	9.88		82%	0%	8%	10%
16 S	3	4/4/3912 15:21	32.67601	-117.12786	3.24	0.14	0.00	3.57	4.04	0.70	0.00	2.25	0.40	3.45		20%	0%	65%	15%
16 M	15	4/4/3912 15:22	32.67607	-117.12789	16.16	1.40	0.45	0.00	15.37	1.33	0.05	0.00	1.22	2.53		52%	2%	0%	46%
17 S	3	4/4/3912 15:27	32.67797	-117.12703	6.39	2.49	0.00	2.10	3.14	5.30	0.00	0.78	0.76	6.46		82%	0%	12%	6%
17 M	15	4/4/3912 15:28	32.67793	-117.12691	3.57	0.00	1.41	0.00	5.05	0.00	0.40	0.00	0.41	0.97		0%	41%	0%	59%
Ambient SDB 1S					0.98				0.75										
Ambient SDB 2S					0.72				0.65										
Ambient SDB 3S					0.81				0.71										
Ambient SDB 4S					0.88				0.68										
Ambient SDB 5S					0.73				0.93										
Average					0.83				0.74										
Standard deviation					0.107				0.110										
Ambient SDB 1B					0.68				0.84										
Ambient SDB 2B					0.71				0.74										
Ambient SDB 3B					0.71				0.86										
Ambient SDB 4B					0.98				0.83										
Ambient SDB 5B					0.83				0.83										
Average					0.78				0.82										
Standard deviation					0.12				0.046										
Overall Average					0.73				0.71										
Overall Standard Deviation					0.11				0.09										

Table C-4. Copper data for San Diego Bay Field Study, 4 April 2012.

San Diego Bay		Copper			1	2	3	4	5	6	7	8	9						
Station	Depth (ft)	Sampling date and time	Latitude	Longitude	TOTAL Filtered solution (µg/L)	SAND Filtered solution (µg/L)	SILT Filtered solution (µg/L)	CLAY Filtered solution (µg/L)	DISSOLVED Filtered solution (µg/L)	Mass of metal in SAND fraction (µg/mg)	Mass of metal in SILT fraction (µg/mg)	Mass of metal in CLAY fraction (µg/mg)	Mass of metal in TOTAL fraction (µg/mg)	TOTAL Summ of fractions (µg/mg)	as	Mass of metal in SAND fraction (%)	Mass of metal in SILT fraction (%)	Mass of metal in CLAY fraction (%)	Mass of DISSOLVED metal associated to TOTAL fraction (%)
					< 2 mm	≥ 60 µm	60 µm to 5 µm	5 µm to 0.4 µm	< 0.4 µm	≥ 60 µm	60 µm to 5 µm	5 µm to 0.4 µm	< 2 mm			≥ 60 µm	60 µm to 5 µm	5 µm to 0.4 µm	< 0.4 µm
1 S	3	4/4/3912 14:14	32.68013	-117.12663	18.12	7.07	0.00	0.00	17.50	35.50	0.00	0.00	2.26	37.69		94%	0%	0%	6%
1 M	15	4/4/3912 14:15	32.68009	-117.12662	8.40	1.32	2.70	0.00	4.88	0.36	0.23	0.00	0.34	0.79		45%	30%	0%	25%
2 S	3	4/4/3912 14:19	32.67958	-117.12680	14.11	2.37	7.75	0.90	3.09	0.12	0.24	0.16	0.24	0.57		21%	42%	29%	9%
2 M	15	4/4/3912 14:19	32.67953	-117.12682	24.57	4.44	13.62	2.81	3.71	0.30	0.30	0.34	0.36	0.99		30%	30%	34%	5%
3 S	3	4/4/3912 14:21	32.67989	-117.12700	9.80	0.81	1.14	0.00	8.71	4.09	0.56	0.00	1.51	5.98		68%	9%	0%	22%
3 M	15	4/4/3912 14:22	32.67994	-117.12702	10.65	0.60	1.87	0.00	9.01	2.06	0.69	0.00	1.46	3.99		52%	17%	0%	31%
4 S	3	4/4/3912 14:24	32.68015	-117.12721	11.26	0.00	1.56	1.57	8.34	0.00	0.46	0.00	1.36	1.94		0%	24%	25%	52%
4 M	15	4/4/3912 14:25	32.68019	-117.12717	12.84	3.21	0.00	2.00	8.68	16.11	0.00	0.53	1.52	17.67		91%	0%	3%	6%
5 S	3	4/4/3912 14:28	32.67976	-117.12752	6.76	0.00	2.36	0.90	3.70	0.00	0.16	0.15	0.32	0.49		0%	33%	31%	36%
5 M	15	4/4/3912 14:28	32.67958	-117.12753	13.90	2.16	7.08	0.95	3.72	0.59	0.19	0.13	0.29	0.99		60%	19%	13%	8%
6 S	3	4/4/3912 14:31	32.67902	-117.12770	10.86	2.03	4.27	0.00	10.77	0.39	0.25	0.00	0.42	1.06		37%	23%	0%	40%
6 M	15	4/4/3912 14:31	32.67899	-117.12773	25.05	11.60	10.20	0.78	2.46	1.11	0.26	0.13	0.45	1.55		72%	17%	9%	3%
7 S	3	4/4/3912 14:34	32.67849	-117.12777	9.93	0.69	0.00	0.00	10.73	0.19	0.00	0.00	1.02	1.29		15%	0%	0%	85%
7 M	15	4/4/3912 14:35	32.67845	-117.12768	12.03	0.00	5.12	0.00	10.61	0.00	0.84	0.00	1.00	1.72		0%	49%	0%	51%
8 S	3	4/4/3912 14:38	32.67825	-117.12831	9.29	0.69	4.15	0.00	9.14	0.29	0.22	0.00	0.34	0.85		34%	26%	0%	40%
8 M	15	4/4/3912 14:38	32.67825	-117.12827	11.12	2.31	3.97	1.40	3.43	0.27	0.25	0.40	0.39	1.04		26%	24%	39%	12%
9S	3	4/4/3912 14:44	32.67863	-117.12898	5.21	0.00	0.99	0.05	4.86	0.00	0.15	0.01	0.48	0.61		0%	25%	2%	73%
9 M	15	4/4/3912 14:45	32.67857	-117.12900	10.88	0.00	1.78	0.00	12.46	0.00	0.31	0.00	1.09	1.55		0%	20%	0%	80%
10 S	3	4/4/3912 14:48	32.67741	-117.12939	10.77	0.81	5.44	0.00	5.29	4.08	0.24	0.00	0.38	4.51		90%	5%	0%	4%
10 M	15	4/4/3912 14:49	32.67746	-117.12948	23.33	6.69	11.90	1.53	3.22	0.81	0.22	0.12	0.31	1.20		68%	19%	10%	4%
11 S	3	4/4/3912 14:53	32.67723	-117.12805	5.04	0.33	2.19	0.00	3.02	0.22	0.29	0.00	0.41	0.75		29%	38%	0%	33%
11 M	15	4/4/3912 14:54	32.67729	-117.12799	6.89	0.00	2.19	1.10	3.73	0.00	0.20	0.47	0.48	0.93		0%	21%	51%	28%
12 S	3	4/4/3912 14:57	32.67675	-117.12757	11.42	3.14	0.61	0.00	8.55	15.78	0.19	0.00	2.74	18.02		88%	1%	0%	11%
12 M	15	4/4/3912 14:57	32.67669	-117.12753	10.26	0.00	3.96	0.00	10.19	0.00	2.12	0.00	1.86	3.97		0%	53%	0%	47%
13 S	3	4/4/3912 15:00	32.67643	-117.12819	5.95	0.00	2.34	0.00	6.67	0.00	1.08	0.00	1.06	2.27		0%	48%	0%	52%
13 M	15	4/4/3912 15:01	32.67651	-117.12820	4.52	0.00	1.21	0.00	3.95	0.00	0.18	0.00	0.37	0.51		0%	36%	0%	64%
14 S	3	4/4/3912 15:04	32.67731	-117.12713	9.02	0.00	0.00	3.04	8.43	0.00	0.00	1.90	1.95	3.72		0%	0%	51%	49%
14 M	15	4/4/3912 15:05	32.67736	-117.12700	5.36	0.00	1.60	0.96	3.21	0.00	0.20	0.31	0.47	0.79		0%	25%	39%	36%
15 S	3	4/4/3912 15:07	32.67818	-117.12650	8.24	0.00	0.67	0.22	7.92	0.00	0.33	0.22	2.36	2.82		0%	12%	8%	81%
15 M	15	4/4/3912 15:08	32.67814	-117.12641	9.39	1.10	0.00	0.78	9.15	3.50	0.00	0.43	2.26	6.13		57%	0%	7%	36%
16 S	3	4/4/3912 15:21	32.67601	-117.12786	11.57	1.30	0.39	0.97	8.91	6.50	0.06	0.61	1.44	8.28		78%	1%	7%	13%
16 M	15	4/4/3912 15:22	32.67607	-117.12789	6.48	0.45	2.09	0.00	4.53	0.43	0.22	0.00	0.49	0.99		43%	22%	0%	35%
17 S	3	4/4/3912 15:27	32.67797	-117.12703	12.70	1.15	0.20	2.29	9.06	2.46	0.04	0.85	1.52	4.43		55%	1%	19%	24%
17 M	15	4/4/3912 15:28	32.67793	-117.12691	10.71	0.00	2.98	0.00	8.46	0.00	0.85	0.00	1.22	1.81		0%	47%	0%	53%
Ambient SDB 1S					3/28/2012					3.52				2.52					
Ambient SDB 2S					3/28/2012					2.88				2.46					
Ambient SDB 3S					3/28/2012					3.10				2.54					
Ambient SDB 4S					3/28/2012					2.93				2.38					
Ambient SDB 5S					3/28/2012					2.88				2.18					
					Average	3.06								2.42					
					Standard deviation	0.271								0.146					
Ambient SDB 1B					3/28/2012					4.01				3.34					
Ambient SDB 2B					3/28/2012					4.05				3.21					
Ambient SDB 3B					3/28/2012					3.33				2.78					
Ambient SDB 4B					3/28/2012					3.27				2.72					
Ambient SDB 5B					3/28/2012					3.23				2.32					
					Average	3.58								2.87					
					Standard deviation	0.41								0.409					
					Overall Average	3.02								2.40					
					Overall Standard Deviation	0.38								0.30					

Table C-5. Zinc data for San Diego Bay Field Study, 4 April 2012.

San Diego Bay		Zinc			1	2	3	4	5	6	7	8	9					
Station	Depth (ft)	Sampling date and time	Latitude	Longitude	TOTAL Filtered solution (µg/L)	SAND Filtered solution (µg/L)	SILT Filtered solution (µg/L)	CLAY Filtered solution (µg/L)	DISSOLVED Filtered solution (µg/L)	Mass of metal in SAND fraction (µg/mg)	Mass of metal in SILT fraction (µg/mg)	Mass of metal in CLAY fraction (µg/mg)	Mass of metal in TOTAL fraction (µg/mg)	TOTAL Summ of fractions (µg/mg)	Mass of metal in SAND fraction (%)	Mass of metal in SILT fraction (%)	Mass of metal in CLAY fraction (%)	Mass of DISSOLVED metal associated to TOTAL fraction (%)
					< 2 mm	≥ 60 µm	60 µm to 5 µm	5 µm to 0.4 µm	< 0.4 µm	≥ 60 µm	60 µm to 5 µm	5 µm to 0.4 µm	< 2 mm		≥ 60 µm	60 µm to 5 µm	5 µm to 0.4 µm	< 0.4 µm
1 S	3	4/4/3912 14:14	32.68013	-117.12663	33.58	0.00	0.00	0.00	46.41	0.00	0.00	0.00	4.19	5.79	0%	0%	0%	100%
1 M	15	4/4/3912 14:15	32.68009	-117.12662	14.66	0.00	4.37	0.19	11.66	0.00	0.38	0.02	0.59	0.87	0%	43%	2%	54%
2 S	3	4/4/3912 14:19	32.67958	-117.12680	22.40	0.00	0.00	0.00	19.13	0.00	0.00	0.00	0.38	0.33	0%	0%	0%	100%
2 M	15	4/4/3912 14:19	32.67953	-117.12682	44.04	14.52	13.70	2.34	13.48	0.98	0.30	0.28	0.64	1.76	56%	17%	16%	11%
3 S	3	4/4/3912 14:21	32.67989	-117.12700	15.93	0.67	3.57	0.00	15.35	3.37	1.75	0.00	2.45	7.48	45%	23%	0%	32%
3 M	15	4/4/3912 14:22	32.67994	-117.12702	13.83	1.07	0.00	6.08	10.61	3.70	0.00	1.42	1.90	6.58	56%	0%	22%	22%
4 S	3	4/4/3912 14:24	32.68015	-117.12721	13.11	0.00	6.84	1.21	9.45	0.00	2.01	0.37	1.58	3.52	0%	57%	10%	32%
4 M	15	4/4/3912 14:25	32.68019	-117.12717	13.07	1.88	0.00	2.59	9.00	9.42	0.00	0.68	1.55	11.17	84%	0%	6%	10%
5 S	3	4/4/3912 14:28	32.67976	-117.12752	12.81	0.00	5.02	0.00	11.39	0.00	0.35	0.00	0.61	0.89	0%	39%	0%	61%
5 M	15	4/4/3912 14:28	32.67958	-117.12753	23.25	0.70	0.00	7.08	19.81	0.19	0.00	0.94	0.48	1.54	12%	0%	61%	27%
6 S	3	4/4/3912 14:31	32.67902	-117.12770	17.21	1.45	2.17	0.00	13.61	0.28	0.13	0.00	0.67	0.94	30%	13%	0%	57%
6 M	15	4/4/3912 14:31	32.67899	-117.12773	24.32	1.80	11.12	0.00	13.71	0.17	0.28	0.00	0.44	0.70	25%	40%	0%	35%
7 S	3	4/4/3912 14:34	32.67849	-117.12777	13.78	0.00	2.32	1.83	10.03	0.00	0.83	0.56	1.42	2.43	0%	34%	23%	43%
7 M	15	4/4/3912 14:35	32.67845	-117.12768	11.91	0.00	4.74	0.00	10.03	0.00	0.78	0.00	0.99	1.61	0%	48%	0%	52%
8 S	3	4/4/3912 14:38	32.67825	-117.12831	16.40	0.48	3.11	1.99	10.83	0.20	0.16	0.36	0.61	1.12	18%	15%	32%	36%
8 M	15	4/4/3912 14:38	32.67825	-117.12827	18.68	0.00	8.37	0.00	14.04	0.00	0.52	0.00	0.66	1.02	0%	51%	0%	49%
9 S	3	4/4/3912 14:44	32.67863	-117.12898	18.95	2.02	2.01	3.83	11.09	10.14	0.31	0.89	1.74	12.36	82%	3%	7%	8%
9 M	15	4/4/3912 14:45	32.67857	-117.12900	10.08	0.00	2.32	0.00	9.85	0.00	0.40	0.00	1.01	1.39	0%	29%	0%	71%
10 S	3	4/4/3912 14:48	32.67741	-117.12939	20.01	2.34	5.38	1.46	10.82	11.77	0.24	0.25	0.71	12.64	93%	2%	2%	3%
10 M	15	4/4/3912 14:49	32.67746	-117.12948	32.34	0.00	19.40	2.17	14.47	0.00	0.36	0.17	0.44	0.73	0%	50%	24%	27%
11 S	3	4/4/3912 14:53	32.67723	-117.12805	15.66	0.09	5.62	0.00	11.25	0.06	0.73	0.00	1.28	1.71	3%	43%	0%	54%
11 M	15	4/4/3912 14:54	32.67729	-117.12799	16.29	0.97	4.45	0.84	10.03	0.97	0.40	0.36	1.14	2.44	40%	17%	15%	29%
12 S	3	4/4/3912 14:57	32.67675	-117.12757	15.21	3.44	1.12	0.67	9.99	17.28	0.35	0.87	3.65	20.89	83%	2%	4%	11%
12 M	15	4/4/3912 14:57	32.67669	-117.12753	15.48	0.00	1.39	0.00	16.87	0.00	0.74	0.00	2.80	3.80	0%	20%	0%	80%
13 S	3	4/4/3912 15:00	32.67643	-117.12819	5.06	0.00	1.70	0.10	5.06	0.00	0.79	0.05	0.90	1.74	0%	45%	3%	52%
13 M	15	4/4/3912 15:01	32.67651	-117.12820	16.69	0.00	1.25	2.99	13.65	0.00	0.19	0.82	1.38	2.14	0%	9%	38%	53%
14 S	3	4/4/3912 15:04	32.67731	-117.12713	10.88	0.00	0.00	4.25	8.91	0.00	0.00	2.65	2.35	4.58	0%	0%	58%	42%
14 M	15	4/4/3912 15:05	32.67736	-117.12700	15.38	0.00	2.77	0.66	13.22	0.00	0.35	0.21	1.36	1.73	0%	20%	12%	68%
15 S	3	4/4/3912 15:07	32.67818	-117.12650	13.16	0.00	0.00	2.77	12.49	0.00	0.00	2.77	3.78	6.35	0%	0%	44%	56%
15 M	15	4/4/3912 15:08	32.67814	-117.12641	15.08	0.00	0.00	2.28	15.62	0.00	0.00	1.24	3.63	5.00	0%	0%	25%	75%
16 S	3	4/4/3912 15:21	32.67601	-117.12786	9.81	0.54	0.00	4.38	7.04	2.68	0.00	2.76	1.22	6.32	42%	0%	44%	14%
16 M	15	4/4/3912 15:22	32.67607	-117.12789	14.33	0.81	1.38	0.42	11.71	0.77	0.14	0.16	1.08	1.96	39%	7%	8%	45%
17 S	3	4/4/3912 15:27	32.67797	-117.12703	12.67	1.88	0.00	3.08	8.82	3.99	0.00	1.15	1.52	6.20	64%	0%	19%	17%
17 M	15	4/4/3912 15:28	32.67793	-117.12691	11.24	0.00	0.54	1.43	9.94	0.00	0.15	1.02	1.28	2.31	0%	7%	44%	49%
Ambient SDB 1S					5.03				3.92									
Ambient SDB 2S					4.08				3.91									
Ambient SDB 3S					4.58				4.37									
Ambient SDB 4S					4.20				4.19									
Ambient SDB 5S					4.66				3.52									
Average					4.51				3.98									
Standard deviation					0.381				0.324									
Ambient SDB 1B					4.34				4.23									
Ambient SDB 2B					4.26				3.89									
Ambient SDB 3B					4.41				4.14									
Ambient SDB 4B					4.15				4.41									
Ambient SDB 5B					4.31				2.85									
Average					4.30				3.91									
Standard deviation					0.10				0.618									
Overall Average					4.00				3.59									
Overall Standard Deviation					0.30				0.48									

Table C-6. Arsenic data for San Diego Bay Field Study, 4 April 2012.

San Diego Bay		Arsenic			1	2	3	4	5	6	7	8	9						
Station	Depth (ft)	Sampling date and time	Latitude	Longitude	TOTAL Filtered solution (µg/L)	SAND Filtered solution (µg/L)	SILT Filtered solution (µg/L)	CLAY Filtered solution (µg/L)	DISSOLVED Filtered solution (µg/L)	Mass of metal in SAND fraction (µg/mg)	Mass of metal in SILT fraction (µg/mg)	Mass of metal in CLAY fraction (µg/mg)	Mass of metal in TOTAL fraction (µg/mg)	TOTAL Summ of fractions (µg/mg)	as	Mass of metal in SAND fraction (%)	Mass of metal in SILT fraction (%)	Mass of metal in CLAY fraction (%)	Mass of DISSOLVED metal associated to TOTAL fraction (%)
					< 2 mm	≥ 60 µm	60 µm to 5 µm	5 µm to 0.4 µm	< 0.4 µm	≥ 60 µm	60 µm to 5 µm	5 µm to 0.4 µm	< 2 mm			≥ 60 µm	60 µm to 5 µm	5 µm to 0.4 µm	< 0.4 µm
1 S	3	4/4/3912 14:14	32.68013	-117.12663	6	-6	-6	-1	20	-32.40	-2.40	-0.16	0.80	2.46		0%	0%	0%	100%
1 M	15	4/4/3912 14:15	32.68009	-117.12662	2	1	-3	3	1	0.28	-0.23	0.31	0.09	0.63		45%	0%	48%	7%
2 S	3	4/4/3912 14:19	32.67958	-117.12680	5	1	-1	8	-2	0.03	-0.04	1.53	0.09	1.56		2%	0%	98%	0%
2 M	15	4/4/3912 14:19	32.67953	-117.12682	5	-2	0	4	3	-0.13	0.01	0.43	0.08	0.49		0%	1%	89%	10%
3 S	3	4/4/3912 14:21	32.67989	-117.12700	16	3	1	-2	13	17.42	0.61	-0.43	2.49	20.08		87%	3%	0%	10%
3 M	15	4/4/3912 14:22	32.67994	-117.12702	15	3	1	0	11	10.70	0.37	0.02	2.05	12.57		85%	3%	0%	12%
4 S	3	4/4/3912 14:24	32.68015	-117.12721	17	1	-1	4	13	0.63	-0.18	1.08	2.01	3.25		20%	0%	33%	47%
4 M	15	4/4/3912 14:25	32.68019	-117.12717	17	8	-4	2	10	40.35	-0.81	0.61	2.03	42.19		96%	0%	1%	3%
5 S	3	4/4/3912 14:28	32.67976	-117.12752	1	-1	0	4	-2	-1.16	-0.03	0.66	0.06	0.66		0%	0%	100%	0%
5 M	15	4/4/3912 14:28	32.67958	-117.12753	5	-2	1	3	4	-0.60	0.02	0.40	0.11	0.49		0%	3%	81%	16%
6 S	3	4/4/3912 14:31	32.67902	-117.12770	5	1	0	1	3	0.18	0.00	0.39	0.20	0.68		26%	0%	57%	18%
6 M	15	4/4/3912 14:31	32.67899	-117.12773	7	0	2	7	-1	0.00	0.05	1.13	0.13	1.17		0%	4%	96%	0%
7 S	3	4/4/3912 14:34	32.67849	-117.12777	14	0	-4	1	16	0.09	-1.38	0.31	1.39	2.06		4%	0%	15%	80%
7 M	15	4/4/3912 14:35	32.67845	-117.12768	8	-1	1	1	7	-0.75	0.15	0.14	0.64	0.90		0%	17%	16%	68%
8 S	3	4/4/3912 14:38	32.67825	-117.12831	2	-3	1	-1	5	-1.42	0.07	-0.11	0.08	0.24		0%	27%	0%	73%
8 M	15	4/4/3912 14:38	32.67825	-117.12827	2	0	0	4	-2	-0.01	0.01	1.11	0.08	1.12		0%	1%	99%	-5%
9 S	3	4/4/3912 14:44	32.67863	-117.12898	0	0	-1	0	1	-0.87	-0.17	0.02	0.00	0.13		0%	0%	14%	86%
9 M	15	4/4/3912 14:45	32.67857	-117.12900	8	-7	4	-3	13	-33.70	0.67	-0.65	0.75	1.97		0%	34%	0%	66%
10 S	3	4/4/3912 14:48	32.67741	-117.12939	5	0	0	0	4	-0.29	0.01	0.08	0.16	0.23		0%	4%	35%	61%
10 M	15	4/4/3912 14:49	32.67746	-117.12948	8	4	-2	2	5	0.43	-0.03	0.13	0.11	0.62		69%	0%	21%	10%
11 S	3	4/4/3912 14:53	32.67723	-117.12805	1	-1	0	1	0	-0.59	-0.02	0.43	0.06	0.46		0%	0%	92%	8%
11 M	15	4/4/3912 14:54	32.67729	-117.12799	3	2	0	0	2	1.54	0.00	-0.17	0.21	1.66		0%	0%	0%	8%
12 S	3	4/4/3912 14:57	32.67675	-117.12757	14	3	-2	1	11	17.23	-0.73	1.88	3.29	21.80		79%	0%	9%	12%
12 M	15	4/4/3912 14:57	32.67669	-117.12753	16	-3	4	0	14	-0.81	2.32	1.97	2.83	6.78		0%	34%	29%	37%
13 S	3	4/4/3912 15:00	32.67643	-117.12819	12	1	2	-1	10	0.56	0.74	-0.50	2.08	3.13		18%	24%	0%	58%
13 M	15	4/4/3912 15:01	32.67651	-117.12820	1	1	0	2	-2	0.53	0.05	0.54	0.12	1.13		47%	5%	48%	0%
14 S	3	4/4/3912 15:04	32.67731	-117.12713	15	3	1	0	12	12.71	0.36	0.11	3.29	15.67		81%	2%	1%	16%
14 M	15	4/4/3912 15:05	32.67736	-117.12700	1	-1	1	3	-2	-5.21	0.17	0.82	0.09	0.99		0%	17%	83%	0%
15 S	3	4/4/3912 15:07	32.67818	-117.12650	12	2	-4	0	14	3.41	-2.13	0.09	3.36	7.65		45%	0%	1%	54%
15 M	15	4/4/3912 15:08	32.67814	-117.12641	18	6	-5	1	15	17.72	-2.40	0.81	4.28	22.26		80%	0%	4%	17%
16 S	3	4/4/3912 15:21	32.67601	-117.12786	4	-1	-5	5	5	-3.93	-0.86	3.15	0.52	3.82		0%	0%	83%	17%
16 M	15	4/4/3912 15:22	32.67607	-117.12789	1	0	0	1	1	-0.40	0.01	0.27	0.08	0.32		0%	2%	82%	16%
17 S	3	4/4/3912 15:27	32.67797	-117.12703	13	5	-3	3	8	10.14	-0.58	1.30	1.53	12.35		82%	0%	11%	7%
17 M	15	4/4/3912 15:28	32.67793	-117.12691	12	1	2	-1	11	0.14	0.48	-1.04	1.37	1.91		8%	25%	0%	67%
Ambient SDB 1S					1.06				0.51										
Ambient SDB 2S					1.17				0.70										
Ambient SDB 3S					1.16				1.07										
Ambient SDB 4S					1.61				1.13										
Ambient SDB 5S					1.34				1.34										
Average					1.27				0.95										
Standard deviation					0.215				0.335										
Ambient SDB 1B					0.99				0.68										
Ambient SDB 2B					1.52				0.81										
Ambient SDB 3B					1.35				1.06										
Ambient SDB 4B					1.77				1.38										
Ambient SDB 5B					1.44				1.40										
Average					1.41				1.06										
Standard deviation					0.28				0.324										
Overall Average					1.22				0.92										
Overall Standard Deviation					0.23				0.31										

Table C-7. Silver data for San Diego Bay Field Study, 4 April 2012.

San Diego Bay					Silver		1	2	3	4	5	6	7	8	9					
Station	Depth (ft)	Sampling date and time	Latitude	Longitude	TOTAL Filtered solution (µg/L)	SAND Filtered solution (µg/L)	SILT Filtered solution (µg/L)	CLAY Filtered solution (µg/L)	DISSOLVED Filtered solution (µg/L)	Mass of metal in SAND fraction (µg/mg)	Mass of metal in SILT fraction (µg/mg)	Mass of metal in CLAY fraction (µg/mg)	Mass of metal in TOTAL fraction (µg/mg)	TOTAL Summ of fractions (µg/mg)	as Mass of metal in SAND fraction (%)	Mass of metal in SILT fraction (%)	Mass of metal in CLAY fraction (%)	Mass of DISSOLVED metal associated to TOTAL fraction (%)		
					< 2 mm	≥ 60 µm	60 µm to 5 µm	5 µm to 0.4 µm	< 0.4 µm	≥ 60 µm	60 µm to 5 µm	5 µm to 0.4 µm	< 2 mm		≥ 60 µm	60 µm to 5 µm	5 µm to 0.4 µm	< 0.4 µm		
1 S	3	4/4/3912 14:14	32.68013	-117.12663	-0.38	0.00	-0.09	0.04	-0.33	-0.012	-0.037	0.008	-0.05	0.01	0%	0%	100%	0%		
1 M	15	4/4/3912 14:15	32.68009	-117.12662	-0.71	-0.29	-0.05	0.34	-0.71	-0.078	-0.004	0.036	-0.03	0.03	0%	0%	114%	0%		
2 S	3	4/4/3912 14:19	32.67958	-117.12680	-0.38	0.21	-0.22	1.14	-1.50	0.011	-0.007	0.205	-0.01	0.22	5%	0%	95%	0%		
2 M	15	4/4/3912 14:19	32.67953	-117.12682	-0.70	-0.61	0.41	0.13	-0.64	-0.041	0.009	0.016	-0.01	0.03	0%	36%	64%	0%		
3 S	3	4/4/3912 14:21	32.67989	-117.12700	-0.40	0.02	-0.09	0.04	-0.37	0.104	-0.046	0.009	-0.06	0.11	92%	0%	8%	0%		
3 M	15	4/4/3912 14:22	32.67994	-117.12702	-0.42	0.00	-0.07	0.00	-0.35	0.000	-0.027	-0.001	-0.06	0.00	0%	0%	0%	0%		
4 S	3	4/4/3912 14:24	32.68015	-117.12721	-0.41	-0.03	-0.01	0.02	-0.39	-0.021	-0.002	0.005	-0.05	0.00	0%	0%	100%	0%		
4 M	15	4/4/3912 14:25	32.68019	-117.12717	-0.39	0.03	-0.03	-0.03	-0.37	0.162	-0.007	-0.008	-0.05	0.16	100%	0%	0%	0%		
5 S	3	4/4/3912 14:28	32.67976	-117.12752	-0.52	0.07	-0.12	0.52	-0.99	0.123	-0.008	0.086	-0.02	0.21	59%	0%	41%	0%		
5 M	15	4/4/3912 14:28	32.67958	-117.12753	-0.43	-0.31	0.12	0.28	-0.52	-0.085	0.003	0.037	-0.01	0.04	0%	8%	92%	0%		
6 S	3	4/4/3912 14:31	32.67902	-117.12770	-0.56	-0.24	0.15	0.28	-0.75	-0.046	0.008	0.090	-0.02	0.10	0%	9%	91%	0%		
6 M	15	4/4/3912 14:31	32.67899	-117.12773	-0.02	0.32	0.10	0.97	-1.41	0.030	0.003	0.167	0.00	0.20	15%	1%	84%	0%		
7 S	3	4/4/3912 14:34	32.67849	-117.12777	-0.40	0.01	-0.04	0.02	-0.39	0.002	-0.013	0.006	-0.04	0.01	25%	0%	75%	0%		
7 M	15	4/4/3912 14:35	32.67845	-117.12768	-0.38	0.06	-0.05	0.00	-0.38	0.037	-0.009	-0.001	-0.03	0.04	100%	0%	0%	0%		
8 S	3	4/4/3912 14:38	32.67825	-117.12831	-0.97	-0.50	-0.22	0.42	-0.68	-0.209	-0.011	0.075	-0.04	0.08	0%	0%	100%	0%		
8 M	15	4/4/3912 14:38	32.67825	-117.12827	-0.31	0.08	0.08	0.85	-1.32	0.010	0.005	0.246	-0.01	0.26	4%	2%	94%	0%		
9S	3	4/4/3912 14:44	32.67863	-117.12898	-1.14	-0.09	0.04	-0.27	-0.82	-0.449	0.006	-0.062	-0.10	0.01	0%	100%	0%	0%		
9 M	15	4/4/3912 14:45	32.67857	-117.12900	-0.43	-0.03	-0.06	0.02	-0.35	-0.174	-0.010	0.004	-0.04	0.00	0%	0%	100%	0%		
10 S	3	4/4/3912 14:48	32.67741	-117.12939	-0.48	0.02	-0.12	-0.01	-0.37	0.124	-0.006	-0.002	-0.02	0.12	100%	0%	0%	0%		
10 M	15	4/4/3912 14:49	32.67746	-117.12948	-0.29	0.48	-0.10	-0.07	-0.59	0.059	-0.002	-0.006	0.00	0.06	103%	0%	0%	0%		
11 S	3	4/4/3912 14:53	32.67723	-117.12805	-0.76	0.16	-0.52	0.13	-0.53	0.110	-0.068	0.041	-0.06	0.15	73%	0%	27%	0%		
11 M	15	4/4/3912 14:54	32.67729	-117.12799	-0.33	0.03	0.19	0.02	-0.57	0.028	0.017	0.008	-0.02	0.05	53%	32%	15%	0%		
12 S	3	4/4/3912 14:57	32.67675	-117.12757	-0.38	0.03	0.00	-0.02	-0.40	0.151	0.001	-0.021	-0.09	0.15	99%	1%	0%	0%		
12 M	15	4/4/3912 14:57	32.67669	-117.12753	-0.37	0.04	-0.05	-0.02	-0.34	0.013	-0.028	-0.093	-0.07	0.01	100%	0%	0%	0%		
13 S	3	4/4/3912 15:00	32.67643	-117.12819	2.41	-0.02	0.34	-0.16	2.25	-0.016	0.156	-0.079	0.43	0.38	0%	40%	0%	104%		
13 M	15	4/4/3912 15:01	32.67651	-117.12820	-0.52	0.18	0.16	-0.05	-0.81	0.100	0.025	-0.015	-0.04	0.12	80%	20%	0%	0%		
14 S	3	4/4/3912 15:04	32.67731	-117.12713	-0.40	0.02	-0.04	0.00	-0.38	0.081	-0.015	0.003	-0.09	0.08	97%	0%	3%	0%		
14 M	15	4/4/3912 15:05	32.67736	-117.12700	-0.86	-0.11	-0.09	0.53	-1.20	-0.531	-0.011	0.172	-0.08	0.17	0%	0%	100%	0%		
15 S	3	4/4/3912 15:07	32.67818	-117.12650	-0.37	0.06	-0.06	0.03	-0.42	0.145	-0.027	0.032	-0.11	0.18	82%	0%	18%	0%		
15 M	15	4/4/3912 15:08	32.67814	-117.12641	-0.42	-0.01	-0.03	-0.01	-0.37	-0.037	-0.013	-0.008	-0.10	0.00	0%	0%	0%	0%		
16 S	3	4/4/3912 15:21	32.67601	-117.12786	-0.42	-0.02	0.02	0.00	-0.41	-0.115	0.003	-0.001	-0.05	0.00	0%	100%	0%	0%		
16 M	15	4/4/3912 15:22	32.67607	-117.12789	-0.55	0.03	0.09	-0.19	-0.48	0.031	0.010	-0.073	-0.04	0.04	76%	24%	0%	0%		
17 S	3	4/4/3912 15:27	32.67797	-117.12703	-0.33	0.09	-0.03	-0.03	-0.36	0.189	-0.005	-0.013	-0.04	0.19	100%	0%	0%	0%		
17 M	15	4/4/3912 15:28	32.67793	-117.12691	-0.41	0.01	-0.02	-0.02	-0.38	0.002	-0.005	-0.013	-0.05	0.00	100%	0%	0%	0%		
Ambient SDB 1S					-2.87				-3.30											
Ambient SDB 2S					-2.44				-3.04											
Ambient SDB 3S					7.91				-3.63											
Ambient SDB 4S					-0.09				-2.31											
Ambient SDB 5S					-2.90				-2.18											
Average					-0.08				-2.89											
Standard deviation					4.615				0.630											
Ambient SDB 1B					-2.87				-2.04											
Ambient SDB 2B					12.61				-2.71											
Ambient SDB 3B					-3.63				-2.01											
Ambient SDB 4B					-3.07				-2.47											
Ambient SDB 5B					-3.40				-2.04											
Average					-0.07				-2.26											
Standard deviation					7.09				0.316											
Overall Average					-0.07				-2.34											
Overall Standard Deviation					5.89				0.58											

Table C-8. Cadmium data for San Diego Bay Field Study, 4 April 2012.

San Diego Bay		Cadmium			1	2	3	4	5	6	7	8	9						
Station	Depth (ft)	Sampling date and time	Latitude	Longitude	TOTAL Filtered solution (µg/L)	SAND Filtered solution (µg/L)	SILT Filtered solution (µg/L)	CLAY Filtered solution (µg/L)	DISSOLVED Filtered solution (µg/L)	Mass of metal in SAND fraction (µg/mg)	Mass of metal in SILT fraction (µg/mg)	Mass of metal in CLAY fraction (µg/mg)	Mass of metal in TOTAL fraction (µg/mg)	TOTAL Summ of fractions (µg/mg)	as	Mass of metal in SAND fraction (%)	Mass of metal in SILT fraction (%)	Mass of metal in CLAY fraction (%)	Mass of DISSOLVED metal associated to TOTAL fraction (%)
					< 2 mm	≥ 60 µm	60 µm to 5 µm	5 µm to 0.4 µm	< 0.4 µm	≥ 60 µm	60 µm to 5 µm	5 µm to 0.4 µm	< 2 mm			≥ 60 µm	60 µm to 5 µm	5 µm to 0.4 µm	< 0.4 µm
1 S	3	4/4/3912 14:14	32.68013	-117.12663	0.95	-0.05	-0.04	-0.04	1.08	-0.273	-0.015	-0.007	0.12	0.13		0%	0%	0%	100%
1 M	15	4/4/3912 14:15	32.68009	-117.12662	0.48	0.02	0.00	0.01	0.45	0.007	0.000	0.001	0.02	0.03		26%	0%	3%	72%
2 S	3	4/4/3912 14:19	32.67958	-117.12680	0.47	-0.03	0.03	-0.03	0.51	-0.001	0.001	-0.005	0.01	0.01		0%	8%	0%	92%
2 M	15	4/4/3912 14:19	32.67953	-117.12682	0.50	-0.01	0.01	0.01	0.48	-0.001	0.000	0.001	0.01	0.01		0%	4%	16%	80%
3 S	3	4/4/3912 14:21	32.67989	-117.12700	1.06	0.10	-0.04	0.02	0.98	0.503	-0.018	0.005	0.16	0.66		76%	0%	1%	23%
3 M	15	4/4/3912 14:22	32.67994	-117.12702	1.07	0.02	-0.02	0.09	0.99	0.059	-0.008	0.020	0.15	0.22		27%	0%	9%	63%
4 S	3	4/4/3912 14:24	32.68015	-117.12721	1.00	0.04	-0.07	0.04	0.99	0.027	-0.022	0.011	0.12	0.16		17%	0%	7%	76%
4 M	15	4/4/3912 14:25	32.68019	-117.12717	1.00	0.00	0.03	-0.10	1.07	0.014	0.006	-0.026	0.12	0.15		10%	4%	0%	86%
5 S	3	4/4/3912 14:28	32.67976	-117.12752	0.46	-0.01	0.00	0.00	0.46	-0.018	0.000	0.000	0.02	0.02		0%	1%	2%	97%
5 M	15	4/4/3912 14:28	32.67958	-117.12753	0.49	0.01	0.00	0.01	0.48	0.003	0.000	0.001	0.01	0.01		22%	0%	6%	73%
6 S	3	4/4/3912 14:31	32.67902	-117.12770	0.44	-0.04	0.00	0.00	0.48	-0.007	0.000	0.000	0.02	0.02		0%	0%	0%	102%
6 M	15	4/4/3912 14:31	32.67899	-117.12773	0.49	0.00	-0.01	0.00	0.49	0.000	0.000	-0.001	0.01	0.01		5%	0%	0%	97%
7 S	3	4/4/3912 14:34	32.67849	-117.12777	1.01	-0.06	0.03	0.05	0.99	-0.017	0.011	0.014	0.10	0.13		0%	9%	11%	80%
7 M	15	4/4/3912 14:35	32.67845	-117.12768	1.00	0.01	0.00	-0.03	1.01	0.009	0.000	-0.006	0.08	0.09		10%	1%	0%	90%
8 S	3	4/4/3912 14:38	32.67825	-117.12831	0.53	0.04	0.00	0.02	0.47	0.017	0.000	0.004	0.02	0.04		45%	0%	10%	45%
8 M	15	4/4/3912 14:38	32.67825	-117.12827	0.48	0.02	-0.01	0.02	0.45	0.002	-0.001	0.006	0.02	0.02		9%	0%	24%	67%
9 S	3	4/4/3912 14:44	32.67863	-117.12898	0.47	-0.04	0.01	-0.01	0.50	-0.190	0.002	-0.003	0.04	0.05		0%	4%	0%	96%
9 M	15	4/4/3912 14:45	32.67857	-117.12900	0.97	-0.03	0.01	-0.01	1.00	-0.144	0.002	-0.002	0.10	0.10		0%	2%	0%	98%
10 S	3	4/4/3912 14:48	32.67741	-117.12939	0.47	0.00	0.00	0.00	0.48	-0.024	0.000	0.000	0.02	0.02		0%	0%	0%	102%
10 M	15	4/4/3912 14:49	32.67746	-117.12948	0.48	0.00	-0.02	-0.02	0.52	0.000	0.000	-0.002	0.01	0.01		0%	0%	0%	111%
11 S	3	4/4/3912 14:53	32.67723	-117.12805	0.44	-0.01	0.02	-0.01	0.44	-0.008	0.003	-0.003	0.04	0.04		0%	7%	0%	93%
11 M	15	4/4/3912 14:54	32.67729	-117.12799	0.45	0.00	0.01	0.00	0.44	-0.003	0.001	0.001	0.03	0.03		0%	3%	3%	104%
12 S	3	4/4/3912 14:57	32.67675	-117.12757	0.99	-0.01	0.01	-0.01	1.00	-0.043	0.004	-0.019	0.24	0.24		0%	2%	0%	98%
12 M	15	4/4/3912 14:57	32.67669	-117.12753	0.98	-0.05	0.06	0.01	0.97	-0.015	0.031	0.043	0.18	0.25		0%	12%	17%	70%
13 S	3	4/4/3912 15:00	32.67643	-117.12819	4.56	0.01	0.02	-0.01	4.54	0.005	0.008	-0.003	0.81	0.82		1%	1%	0%	98%
13 M	15	4/4/3912 15:01	32.67651	-117.12820	0.46	-0.01	-0.02	-0.01	0.49	-0.003	-0.003	-0.002	0.04	0.04		0%	0%	0%	108%
14 S	3	4/4/3912 15:04	32.67731	-117.12713	0.98	-0.01	0.03	-0.01	0.96	-0.029	0.012	-0.005	0.21	0.22		0%	6%	0%	94%
14 M	15	4/4/3912 15:05	32.67736	-117.12700	0.44	-0.01	-0.01	0.02	0.45	-0.050	-0.001	0.006	0.04	0.05		0%	0%	13%	87%
15 S	3	4/4/3912 15:07	32.67818	-117.12650	1.02	0.04	-0.03	0.06	0.95	0.084	-0.013	0.057	0.29	0.41		20%	0%	14%	66%
15 M	15	4/4/3912 15:08	32.67814	-117.12641	1.03	0.07	-0.04	-0.01	1.02	0.218	-0.021	-0.008	0.25	0.46		47%	0%	0%	53%
16 S	3	4/4/3912 15:21	32.67601	-117.12786	0.96	-0.05	0.05	0.00	0.96	-0.258	0.009	-0.002	0.12	0.13		0%	7%	0%	93%
16 M	15	4/4/3912 15:22	32.67607	-117.12789	0.43	-0.02	0.03	-0.02	0.44	-0.018	0.003	-0.008	0.03	0.04		0%	9%	0%	91%
17 S	3	4/4/3912 15:27	32.67797	-117.12703	0.99	-0.01	0.01	0.02	0.98	-0.030	0.001	0.007	0.12	0.13		0%	1%	6%	93%
17 M	15	4/4/3912 15:28	32.67793	-117.12691	0.97	0.02	-0.05	0.03	0.97	0.006	-0.014	0.018	0.11	0.13		4%	0%	14%	82%
Ambient SDB 1S					0.06				0.053										
Ambient SDB 2S					0.06				0.064										
Ambient SDB 3S					0.08				0.076										
Ambient SDB 4S					0.06				0.069										
Ambient SDB 5S					0.07				0.061										
Average					0.07				0.065										
Standard deviation					0.008				0.0086										
Ambient SDB 1B					0.06				0.062										
Ambient SDB 2B					0.06				0.066										
Ambient SDB 3B					0.06				0.072										
Ambient SDB 4B					0.07				0.072										
Ambient SDB 5B					0.06				0.062										
Average					0.06				0.067										
Standard deviation					0.00				0.0048										
Overall Average					0.06				0.060										
Overall Standard Deviation					0.01				0.0069										

Table C-9. Lead data for San Diego Bay Field Study, 4 April 2012.

San Diego Bay		Lead			1	2	3	4	5	6	7	8	9						
Station	Depth (ft)	Sampling date and time	Latitude	Longitude	TOTAL Filtered solution (µg/L)	SAND Filtered solution (µg/L)	SILT Filtered solution (µg/L)	CLAY Filtered solution (µg/L)	DISSOLVED Filtered solution (µg/L)	Mass of metal in SAND fraction (µg/mg)	Mass of metal in SILT fraction (µg/mg)	Mass of metal in CLAY fraction (µg/mg)	Mass of metal in TOTAL fraction (µg/mg)	TOTAL Summ of fractions (µg/mg)	as	Mass of metal in SAND fraction (%)	Mass of metal in SILT fraction (%)	Mass of metal in CLAY fraction (%)	Mass of DISSOLVED metal associated to TOTAL fraction (%)
					< 2 mm	≥ 60 µm	60 µm to 5 µm	5 µm to 0.4 µm	< 0.4 µm	≥ 60 µm	60 µm to 5 µm	5 µm to 0.4 µm	< 2 mm			≥ 60 µm	60 µm to 5 µm	5 µm to 0.4 µm	< 0.4 µm
1 S	3	4/4/3912 14:14	32.68013	-117.12663	0.86	-0.12	0.11	-0.38	1.24	-0.592	0.046	-0.071	0.11	0.20		0%	23%	0%	0%
1 M	15	4/4/3912 14:15	32.68009	-117.12662	0.43	-0.02	1.40	-0.25	-0.71	-0.004	0.121	-0.027	0.02	0.12		0%	104%	0%	0%
2 S	3	4/4/3912 14:19	32.67958	-117.12680	2.23	-1.72	3.12	-0.15	0.98	-0.085	0.095	-0.028	0.04	0.11		0%	85%	0%	15%
2 M	15	4/4/3912 14:19	32.67953	-117.12682	5.53	0.66	4.29	0.82	-0.24	0.044	0.094	0.100	0.08	0.24		19%	39%	42%	0%
3 S	3	4/4/3912 14:21	32.67989	-117.12700	1.06	0.01	0.30	0.16	0.59	0.048	0.146	0.038	0.16	0.32		15%	45%	12%	28%
3 M	15	4/4/3912 14:22	32.67994	-117.12702	1.17	-0.11	0.43	0.14	0.71	-0.374	0.158	0.033	0.16	0.29		0%	55%	12%	34%
4 S	3	4/4/3912 14:24	32.68015	-117.12721	0.99	-0.02	0.31	0.16	0.53	-0.014	0.092	0.050	0.12	0.21		0%	45%	24%	31%
4 M	15	4/4/3912 14:25	32.68019	-117.12717	1.27	0.16	0.20	0.28	0.63	0.797	0.045	0.073	0.15	0.99		80%	5%	7%	8%
5 S	3	4/4/3912 14:28	32.67976	-117.12752	0.70	0.31	0.65	0.20	-0.45	0.535	0.045	0.033	0.03	0.61		87%	7%	5%	0%
5 M	15	4/4/3912 14:28	32.67958	-117.12753	3.46	1.00	2.31	0.32	-0.17	0.275	0.063	0.042	0.07	0.38		72%	16%	11%	0%
6 S	3	4/4/3912 14:31	32.67902	-117.12770	1.57	0.43	1.25	0.40	-0.51	0.083	0.072	0.129	0.06	0.28		29%	25%	46%	0%
6 M	15	4/4/3912 14:31	32.67899	-117.12773	3.68	1.09	3.23	-0.51	-0.14	0.105	0.082	-0.087	0.07	0.19		56%	44%	0%	0%
7 S	3	4/4/3912 14:34	32.67849	-117.12777	0.88	0.02	0.20	0.05	0.60	0.007	0.071	0.016	0.09	0.16		4%	45%	11%	40%
7 M	15	4/4/3912 14:35	32.67845	-117.12768	1.35	-0.06	0.61	0.26	0.53	-0.039	0.100	0.060	0.11	0.20		0%	49%	29%	22%
8 S	3	4/4/3912 14:38	32.67825	-117.12831	3.21	2.29	1.03	0.07	-0.18	0.966	0.054	0.012	1.03			94%	5%	1%	0%
8 M	15	4/4/3912 14:38	32.67825	-117.12827	1.75	0.77	1.09	0.23	-0.34	0.089	0.067	0.066	0.06	0.22		40%	30%	30%	0%
9 S	3	4/4/3912 14:44	32.67863	-117.12898	0.16	0.04	0.39	-0.11	-0.16	0.177	0.061	-0.025	0.01	0.24		75%	25%	0%	0%
9 M	15	4/4/3912 14:45	32.67857	-117.12900	1.35	0.05	0.47	0.20	0.62	0.258	0.082	0.13	0.45			57%	18%	11%	14%
10 S	3	4/4/3912 14:48	32.67741	-117.12939	1.89	0.37	1.59	0.31	-0.38	1.845	0.072	0.053	0.07	1.97		94%	4%	3%	0%
10 M	15	4/4/3912 14:49	32.67746	-117.12948	5.83	1.40	4.31	0.46	-0.34	0.170	0.081	0.037	0.08	0.28		60%	29%	13%	0%
11 S	3	4/4/3912 14:53	32.67723	-117.12805	-1.45	-0.32	0.82	-0.09	-1.86	-0.218	0.107	-0.028	-0.12	0.11		0%	100%	0%	0%
11 M	15	4/4/3912 14:54	32.67729	-117.12799	-0.26	0.19	0.97	0.48	-1.90	0.188	0.088	0.204	-0.02	0.48		39%	18%	43%	0%
12 S	3	4/4/3912 14:57	32.67675	-117.12757	0.89	0.09	0.16	0.15	0.50	0.446	0.049	0.190	0.21	0.81		55%	6%	24%	15%
12 M	15	4/4/3912 14:57	32.67669	-117.12753	0.98	0.12	0.20	0.09	0.57	0.035	0.107	0.463	0.18	0.71		5%	15%	65%	15%
13 S	3	4/4/3912 15:00	32.67643	-117.12819	4.79	0.23	0.16	-0.03	4.42	0.159	0.075	-0.016	0.85	1.02		16%	7%	0%	77%
13 M	15	4/4/3912 15:01	32.67651	-117.12820	-0.73	-0.10	-0.02	0.24	-0.86	-0.054	-0.003	0.067	-0.06	0.07		0%	0%	100%	0%
14 S	3	4/4/3912 15:04	32.67731	-117.12713	0.76	0.02	-0.10	0.32	0.53	0.087	-0.036	0.198	0.16	0.40		22%	0%	49%	29%
14 M	15	4/4/3912 15:05	32.67736	-117.12700	-0.43	0.33	0.09	0.28	-1.14	1.652	0.012	0.091	-0.04	1.75		94%	1%	5%	0%
15 S	3	4/4/3912 15:07	32.67818	-117.12650	0.81	0.01	0.08	0.22	0.51	0.015	0.039	0.219	0.23	0.42		4%	9%	52%	35%
15 M	15	4/4/3912 15:08	32.67814	-117.12641	1.02	0.13	0.09	0.05	0.74	0.420	0.047	0.028	0.25	0.67		62%	7%	4%	26%
16 S	3	4/4/3912 15:21	32.67601	-117.12786	1.17	0.01	0.51	0.15	0.49	0.070	0.082	0.096	0.15	0.31		23%	26%	31%	20%
16 M	15	4/4/3912 15:22	32.67607	-117.12789	-0.68	0.13	0.22	0.29	-1.32	0.124	0.023	0.112	-0.05	0.26		48%	9%	43%	0%
17 S	3	4/4/3912 15:27	32.67797	-117.12703	1.15	0.09	0.39	0.06	0.61	0.201	0.076	0.021	0.14	0.37		54%	20%	6%	20%
17 M	15	4/4/3912 15:28	32.67793	-117.12691	1.12	-0.03	0.49	0.14	0.52	-0.008	0.141	0.098	0.13	0.30		0%	47%	33%	20%
Ambient SDB 1S					0.44				0.17										
Ambient SDB 2S					0.33				0.13										
Ambient SDB 3S					0.39				0.15										
Ambient SDB 4S					0.33				0.16										
Ambient SDB 5S					0.36				0.25										
Average					0.37				0.17										
Standard deviation					0.047				0.045										
Ambient SDB 1B					0.39				0.19										
Ambient SDB 2B					0.36				0.17										
Ambient SDB 3B					0.38				0.21										
Ambient SDB 4B					0.42				0.22										
Ambient SDB 5B					0.43				0.26										
Average					0.39				0.21										
Standard deviation					0.03				0.035										
Overall Average					0.35				0.17										
Overall Standard Deviation					0.04				0.045										

APPENDIX D

PEARL HARBOR DATA

Table D-1. Size-fraction data.

Pearl Harbor	SAND	SILT	CLAY	TOTAL	SAND	SILT	CLAY
	5	6	7	8			
	Mass in filter	Mass in filter	Mass in filter	Total = 5+6+7			
Sample ID	60 µm Mass Fraction (mg/L)	5 µm Mass Fraction (mg/L)	0.4 µm Mass Fraction (mg/L)	Total Mass Fraction (mg/L)	60 µm Mass Fraction (%)	5 µm Mass Fraction (%)	0.4 µm Mass Fraction (%)
1	22.03	55.12	5.04	82.18	26.8	67.1	6.1
2	0.97	6.40	2.86	10.23	9.5	62.6	27.9
3	5.63	18.33	4.91	28.87	19.5	63.5	17.0
4	3.37	11.33	4.60	19.30	17.5	58.7	23.8
5	14.28	39.50	5.50	59.28	24.1	66.6	9.3
6	8.33	30.00	4.07	42.40	19.6	70.8	9.6
7	7.54	35.91	2.40	45.85	16.4	78.3	5.2
8	13.19	40.00	4.60	57.79	22.8	69.2	8.0
9	38.10	70.00	7.60	115.70	32.9	60.5	6.6
10	2.73	25.00	8.00	35.73	7.6	70.0	22.4
11	14.30	19.20	5.14	38.64	37.0	49.7	13.3
12	10.58	37.33	6.60	54.51	19.4	68.5	12.1
13	8.17	28.00	5.80	41.97	19.5	66.7	13.8
14	24.25	63.00	9.00	96.25	25.2	65.5	9.4
15	41.57	80.67	9.20	131.44	31.6	61.4	7.0
16	36.63	68.67	2.40	107.69	34.0	63.8	2.2
17	17.60	43.00	2.80	63.40	27.8	67.8	4.4
18	6.60	27.33	1.80	35.73	18.5	76.5	5.0
19	11.70	5.20	0.40	17.30	67.6	30.1	2.3
20	2.21	14.00	1.79	18.00	12.3	77.8	9.9
Average					24.5	64.7	10.8
Std Dev					12.9	10.6	7.2
21	2.19	13.40	0.85	16.44	13.3	81.5	5.2
22	0.66	2.59	0.30	3.55	18.7	72.9	8.4
23	13.74	23.50	1.44	38.68	35.5	60.7	3.7
24	2.97	9.22	0.80	12.99	22.9	71.0	6.2
25	1.27	5.76	0.50	7.53	16.9	76.5	6.6
26	0.07	1.80	0.22	2.09	3.3	86.0	10.6
27	0.03	3.80	0.53	4.37	0.8	87.0	12.2
28	3.59	9.36	0.03	12.98	27.6	72.1	0.3
29	1.64	8.00	0.11	9.75	16.8	82.1	1.1
30	0.60	1.66	0.97	3.23	18.6	51.3	30.1
31	2.94	6.30	0.75	9.99	29.4	63.1	7.5
32	1.49	6.12	0.13	7.74	19.2	79.0	1.7
33	3.11	7.78	0.12	11.01	28.2	70.6	1.1
34	5.19	16.15	0.14	21.49	24.2	75.2	0.7
35	3.23	9.37	0.03	12.64	25.6	74.2	0.3
36	0.07	5.78	0.65	6.50	1.1	88.9	10.0
37	1.41	8.25	0.44	10.10	14.0	81.6	4.4
38	3.35	6.71	0.11	10.17	32.9	66.0	1.1
39	0.03	3.03	2.00	5.06	0.7	59.8	39.5
40	0.03	2.22	1.50	3.76	0.9	59.2	39.9
Average					17.5	72.9	9.5
Std Dev					11.3	10.4	12.3

Table D-2. Chromium data for Pearl Harbor Field Study, 28–29 August 2012.

Pearl Harbor			Chromium			1	2	3	4	5	6	7	8	9						
	Station	Depth (ft)	Sampling date and time	Latitude	Longitude	TOTAL Filtered solution (µg/L)	SAND Filtered solution (µg/L)	SILT Filtered solution (µg/L)	CLAY Filtered solution (µg/L)	DISSOLVED Filtered solution (µg/L)	Mass of metal in SAND fraction (µg/mg)	Mass of metal in SILT fraction (µg/mg)	Mass of metal in CLAY fraction (µg/mg)	Mass of metal in TOTAL fraction (µg/mg)	TOTAL Summ of fractions (µg/mg)	as	Mass of metal in SAND fraction (%)	Mass of metal in SILT fraction (%)	Mass of metal in CLAY fraction (%)	Mass of DISSOLVED metal associated to TOTAL fraction (%)
						< 2 mm	≥ 60 µm	60 µm to µm	5	5 µm to 0.4 µm	< 0.4 µm	≥ 60 µm	60 µm to 5 µm	5 µm to 0.4 µm	< 2 mm		≥ 60 µm	60 µm to 5 µm	5 µm to 0.4 µm	< 0.4 µm
Bravo 22 Pier																				
Plume Event One	1	3	8/28/2012 10:40	21.35519	-157.94936	108.5	1.6	3.6	0.0	104.3	0.07	0.06	0.00	1.32	1.41		5%	5%	0%	90%
	2	15	8/28/2012 10:41	21.35519	-157.94936	139.7	0.0	0.0	4.6	137.7	0.00	0.00	1.60	13.66	15.07		0%	0%	11%	89%
	3	3	8/28/2012 10:45	21.35562	-157.94884	92.3	1.5	0.7	0.7	89.4	0.26	0.04	0.14	3.20	3.53		7%	1%	4%	88%
	4	15	8/28/2012 10:46	21.35562	-157.94884	140.9	0.0	2.1	3.0	140.0	0.00	0.18	0.66	7.30	8.10		0%	2%	8%	90%
	5	3	8/28/2012 10:50	21.35559	-157.94874	107.1	2.6	3.8	2.0	98.6	0.19	0.10	0.37	1.81	2.32		8%	4%	16%	72%
Plume Event Two	6	15	8/28/2012 10:51	21.35559	-157.94874	102.4	0.0	5.2	2.7	94.5	-0.01	0.17	0.66	2.41	3.07		0%	6%	22%	73%
	7	3	8/28/2012 11:03	21.35492	-157.94861	103.6	0.0	7.9	0.0	99.4	0.00	0.22	0.00	2.26	2.39		0%	9%	0%	91%
	8	15	8/28/2012 11:04	21.35492	-157.94861	106.9	1.2	2.6	2.1	100.9	0.09	0.07	0.46	1.85	2.36		4%	3%	19%	74%
	9	3	8/28/2012 11:05	21.35542	-157.94893	112.4	3.3	9.5	0.0	103.3	0.09	0.14	0.00	0.97	1.12		8%	12%	0%	80%
	10	15	8/28/2012 11:06	21.35542	-157.94893	100.1	4.6	5.5	0.0	91.5	1.69	0.22	0.00	2.80	4.47		38%	5%	0%	57%
Plume Event Three	11	3	8/28/2012 11:07	21.35595	-157.94889	94.1	0.0	4.9	0.2	92.7	0.00	0.26	0.03	2.44	2.69		0%	10%	1%	89%
	12	15	8/28/2012 11:08	21.35595	-157.94889	104.7	0.0	6.1	0.0	100.1	0.00	0.16	0.00	1.92	2.00		0%	8%	0%	92%
	13	15	8/28/2012 11:51	21.35512	-157.94920	99.7	0.0	1.0	2.3	97.5	0.00	0.03	0.39	2.37	2.75		0%	1%	14%	84%
	14	15	8/28/2012 11:53	21.35550	-157.94871	109.5	2.0	4.1	0.0	104.3	0.08	0.06	0.00	1.14	1.23		7%	5%	0%	88%
	15	15	8/28/2012 11:55	21.35542	-157.94815	115.0	4.4	3.0	2.4	105.2	0.11	0.04	0.26	0.87	1.20		9%	3%	21%	67%
	16	15	8/28/2012 11:56	21.35554	-157.94820	111.8	3.9	3.7	0.0	104.5	0.11	0.05	0.00	1.04	1.13		9%	5%	0%	86%
	17	15	8/28/2012 0:04	21.35562	-157.94794	106.1	0.0	5.1	0.0	102.5	0.00	0.12	0.00	1.67	1.74		0%	7%	0%	93%
	18	15	8/28/2012 0:11	21.35696	-157.94902	101.9	1.3	4.3	0.0	97.0	0.19	0.16	0.00	2.85	3.07		6%	5%	0%	88%
	19	15	8/28/2012 0:19	21.35694	-157.94997	137.8	0.4	0.0	0.0	138.7	0.03	0.00	0.00	7.96	8.05		0%	0%	0%	100%
	20	15	8/28/2012 0:27	21.35693	-157.95011	91.2	0.7	0.0	4.4	86.8	0.32	0.00	2.46	5.07	7.60		4%	0%	32%	63%
	Background 1		8/28/2012 10:12			0.49														
	Background 2		8/28/2012 10:12			0.26														
	Background 3		8/28/2012 10:12			0.23														
Background Average						0.33														
Background Standard deviation						0.14														
Oscar 2 Pier																				
Plume Event One	21	3	8/29/2012 9:31	21.34516	-157.96727	59.9	0.00	2.11	0.00	59.7	0.00	0.16	0.00	3.64	3.79		0%	4%	0%	96%
	22	15	8/29/2012 9:32	21.34505	-157.96750	46.1	0.00	1.36	1.22	43.8	0.00	0.53	4.05	12.98	16.92		0%	3%	24%	73%
	23	3	8/29/2012 9:34	21.34495	-157.96813	62.3	1.05	1.36	1.28	58.7	0.08	0.06	0.89	1.61	2.54		3%	2%	35%	60%
	24	15	8/29/2012 9:35	21.34492	-157.96824	60.7	1.58	1.65	0.00	58.2	0.53	0.18	0.00	4.67	5.19		10%	3%	0%	86%
	25	3	8/29/2012 9:37	21.34475	-157.96860	51.8	0.00	1.91	0.00	51.3	0.00	0.33	0.00	6.88	7.13		0%	5%	0%	95%
Plume Event Two	26	15	8/29/2012 9:38	21.34460	-157.96868	40.5	0.11	0.74	0.18	39.5	1.50	0.41	0.81	19.36	21.59		7%	2%	4%	87%
	27	3	8/29/2012 10:34	21.34526	-157.96704	49.9	0.61	1.26	0.93	47.1	18.36	0.33	1.74	11.44	31.23		59%	1%	6%	35%
	28	15	8/29/2012 10:35	21.34512	-157.96745	60.6	1.36	0.00	0.15	59.5	0.38	0.00	4.56	4.67	9.53		4%	0%	48%	48%
	29	3	8/29/2012 10:36	21.34488	-157.96768	60.1	1.37	-0.02	0.35	58.4	0.83	0.00	3.20	6.17	10.02		8%	0%	32%	60%
	30	15	8/29/2012 10:37	21.34466	-157.96786	38.1	0.00	0.91	0.00	38.2	0.00	0.55	0.00	11.79	12.38		0%	4%	0%	96%
Plume Event Three	31	3	8/29/2012 10:41	21.34506	-157.96832	55.6	1.77	0.08	0.73	53.1	0.60	0.01	0.98	5.57	6.90		9%	0%	14%	77%
	32	15	8/29/2012 10:42	21.34513	-157.96831	52.6	0.41	1.20	0.00	51.5	0.27	0.20	0.00	6.80	7.12		4%	3%	0%	93%
	33	15	8/29/2012 11:36	21.34469	-157.96816	55.7	0.61	0.00	0.57	55.6	0.20	0.00	4.56	5.05	9.81		2%	0%	47%	51%
	34	15	8/29/2012 11:37	21.34442	-157.96844	61.1	1.84	0.00	0.00	61.3	0.35	0.00	0.00	2.85	3.21		11%	0%	0%	89%
	35	15	8/29/2012 11:39	21.34441	-157.96863	58.1	0.00	0.05	0.00	60.0	0.00	0.01	0.00	4.60	4.75		0%	0%	0%	100%
	36	15	8/29/2012 11:40	21.34440	-157.96863	52.1	0.23	0.00	0.00	53.2	3.23	0.00	0.00	8.01	11.42		28%	0%	0%	72%
	37	15	8/29/2012 11:41	21.34442	-157.96880	59.1	0.85	-0.01	0.90	57.4	0.61	0.00	2.03	5.85	8.31		7%	0%	24%	68%
	38	15	8/29/2012 11:43	21.34450	-157.96912	55.9	0.93	0.00	1.46	54.0	0.28	0.00	13.12	5.50	18.71		1%	0%	70%	28%
	39	15	8/29/2012 11:54	21.34489	-157.96939	45.9	0.00	2.33	0.00	46.5	0.00	0.77	0.00	9.07	9.97		0%	8%	0%	92%
	40	15	8/29/2012 12:01	21.34475	-157.96978	44.5	1.14	0.00	0.59	43.4	34.15	0.00	0.40	11.84	46.10		74%	0%	1%	25%
	Background 1		8/29/2012 9:09			0.42														
	Background 2		8/29/2012 9:09			0.43														
	Background 3		8/29/2012 9:09			0.35														
Background Average						0.40														
Background Standard deviation						0.040														

Table D-3. Nickel data for Pearl Harbor Field Study, 28–29 August 2012.

Pearl Harbor		Nickel				1	2	3	4	5	6	7	8	9						
	Station	Depth (ft)	Sampling date and time	Latitude	Longitude	TOTAL Filtered solution (µg/L)	SAND Filtered solution (µg/L)	SILT Filtered solution (µg/L)	CLAY Filtered solution (µg/L)	DISSOLVED Filtered solution (µg/L)	Mass of metal in SAND fraction (µg/mg)	Mass of metal in SILT fraction (µg/mg)	Mass of metal in CLAY fraction (µg/mg)	Mass of metal in TOTAL fraction (µg/mg)	TOTAL Summ of fractions (µg/mg)	as Mass of metal in SAND fraction (%)	Mass of metal in SILT fraction (%)	Mass of metal in CLAY fraction (%)	Mass of DISSOLVED metal associated to TOTAL fraction (%)	
						< 2 mm	≥ 60 µm	60 µm to 5 µm	5 µm to 0.4 µm	< 0.4 µm	≥ 60 µm	60 µm to 5 µm	5 µm to 0.4 µm	< 2 mm		≥ 60 µm	60 µm to 5 µm	5 µm to 0.4 µm	< 0.4 µm	
Bravo 22 Pier	Plume	1	3	8/28/2012 10:40	21.35519	-157.94936	71.3	0.4	7.0	0.1	63.7	0.02	0.13	0.01	0.87	0.94	2%	14%	1%	83%
	Event One	2	15	8/28/2012 10:41	21.35519	-157.94936	103.7	0.0	0.9	0.0	105.4	0.00	0.15	0.00	10.14	10.45	0%	1%	0%	99%
		3	3	8/28/2012 10:45	21.35562	-157.94884	66.1	0.0	3.0	0.0	63.4	0.00	0.16	0.00	2.29	2.36	0%	7%	0%	93%
		4	15	8/28/2012 10:46	21.35562	-157.94884	104.5	0.0	3.3	0.0	102.9	0.00	0.29	0.00	5.42	5.63	0%	5%	0%	95%
		5	3	8/28/2012 10:50	21.35559	-157.94874	68.9	1.3	4.1	0.0	65.9	0.09	0.10	0.00	1.16	1.30	7%	8%	0%	85%
		6	15	8/28/2012 10:51	21.35559	-157.94874	66.9	0.0	0.7	0.0	69.7	0.00	0.02	0.00	1.58	1.67	0%	1%	0%	99%
	Event Two	7	3	8/28/2012 11:03	21.35492	-157.94861	64.8	0.3	0.3	1.4	62.7	0.04	0.01	0.59	1.41	2.01	2%	0%	29%	68%
		8	15	8/28/2012 11:04	21.35492	-157.94861	65.5	0.0	2.7	0.0	65.2	0.00	0.07	0.00	1.13	1.20	0%	6%	0%	94%
		9	3	8/28/2012 11:05	21.35542	-157.94893	65.9	1.4	5.4	0.0	64.5	0.04	0.08	0.00	0.57	0.67	5%	12%	0%	83%
		10	15	8/28/2012 11:06	21.35542	-157.94893	65.3	0.0	0.0	2.6	65.3	0.00	0.00	0.33	1.83	2.16	0%	0%	15%	85%
		11	3	8/28/2012 11:07	21.35595	-157.94889	67.6	3.7	0.0	0.0	64.3	0.26	0.00	0.00	1.75	1.92	13%	0%	0%	87%
	Plume Event Three	12	15	8/28/2012 11:08	21.35595	-157.94889	66.8	0.5	3.7	4.1	58.4	0.05	0.10	0.63	1.23	1.85	2%	5%	34%	58%
		13	15	8/28/2012 11:51	21.35512	-157.94920	65.9	0.0	1.5	0.1	65.3	0.00	0.05	0.02	1.57	1.63	0%	3%	1%	96%
		14	15	8/28/2012 11:53	21.35550	-157.94871	67.2	0.0	3.8	0.1	63.7	0.00	0.06	0.01	0.70	0.73	0%	8%	1%	91%
		15	15	8/28/2012 11:55	21.35542	-157.94815	66.2	2.4	3.4	0.9	59.5	0.06	0.04	0.10	0.50	0.65	9%	6%	16%	69%
		16	15	8/28/2012 11:56	21.35554	-157.94820	73.0	8.9	4.5	0.0	62.0	0.24	0.07	0.00	0.68	0.88	27%	7%	0%	65%
		17	15	8/28/2012 0:04	21.35562	-157.94794	68.5	1.0	2.5	1.6	63.4	0.06	0.06	0.55	1.08	1.67	3%	4%	33%	60%
		18	15	8/28/2012 0:11	21.35696	-157.94902	66.4	0.0	4.5	0.3	64.0	0.00	0.16	0.15	1.86	2.10	0%	8%	7%	85%
		19	15	8/28/2012 0:19	21.35694	-157.94997	102.8	0.1	1.6	0.1	101.1	0.00	0.31	0.13	5.94	6.29	0%	5%	2%	93%
		20	15	8/28/2012 0:27	21.35693	-157.95011	63.4	0.0	3.0	2.0	60.1	0.00	0.22	1.14	3.53	4.70	0%	5%	24%	71%
	Background 1		8/28/2012 10:12			0.83														
	Background 2		8/28/2012 10:12			0.75														
	Background 3		8/28/2012 10:12			0.64														
					Background Average	0.74														
					Background Standard deviation	0.093														
Oscar 2 Pier	Plume	21	3	8/29/2012 9:31	21.34516	-157.96727	38.4	0.69	0.00	0.00	38.1	0.31	0.00	0.00	2.34	2.63	12%	0%	0%	88%
	Event One	22	15	8/29/2012 9:32	21.34505	-157.96750	44.2	0.00	0.00	1.22	44.6	0.00	0.00	4.06	12.45	16.62	0%	0%	24%	76%
		23	3	8/29/2012 9:34	21.34495	-157.96813	39.5	3.47	0.49	0.00	37.1	0.25	0.02	0.00	1.02	1.23	20%	2%	0%	78%
		24	15	8/29/2012 9:35	21.34492	-157.96824	42.0	0.75	0.45	0.55	40.2	0.25	0.05	0.69	3.23	4.09	6%	1%	17%	76%
		25	3	8/29/2012 9:37	21.34475	-157.96860	45.3	0.31	0.00	1.96	43.7	0.24	0.00	3.92	6.01	9.96	2%	0%	39%	58%
		Plume Event Two	26	15	8/29/2012 9:38	21.34460	-157.96868	44.4	0.42	0.00	0.14	45.3	5.98	0.00	0.61	21.20	28.25	21%	0%	2%
	27		3	8/29/2012 10:34	21.34526	-157.96704	45.3	1.74	0.00	4.23	41.6	52.34	0.00	7.93	10.37	69.80	75%	0%	11%	14%
	28		15	8/29/2012 10:35	21.34512	-157.96745	38.3	0.02	0.00	0.00	41.9	0.01	0.00	0.00	2.95	3.23	0%	0%	0%	100%
	29		3	8/29/2012 10:36	21.34488	-157.96768	43.1	4.59	0.00	0.00	41.6	2.80	0.00	0.00	4.43	7.07	40%	0%	0%	60%
	30		15	8/29/2012 10:37	21.34466	-157.96786	45.5	0.70	0.77	0.00	45.5	1.16	0.47	0.00	14.09	15.72	7%	3%	0%	90%
	Plume Event Three	31	3	8/29/2012 10:41	21.34506	-157.96832	44.6	0.35	1.51	0.00	44.8	0.12	0.24	0.00	4.46	4.84	2%	5%	0%	93%
		32	15	8/29/2012 10:42	21.34513	-157.96831	44.9	0.23	0.00	0.68	45.7	0.15	0.00	5.13	5.80	11.19	1%	0%	46%	53%
		33	15	8/29/2012 11:36	21.34469	-157.96816	40.2	0.00	3.54	0.00	43.2	0.00	0.46	0.00	3.65	4.38	0%	10%	0%	90%
		34	15	8/29/2012 11:37	21.34442	-157.96844	38.3	0.00	4.11	0.00	37.4	0.00	0.25	0.00	1.78	1.99	0%	13%	0%	87%
		35	15	8/29/2012 11:39	21.34441	-157.96863	37.2	0.00	0.00	0.96	38.0	0.00	0.00	28.82	2.95	31.83	0%	0%	91%	9%
		36	15	8/29/2012 11:40	21.34440	-157.96863	46.3	2.09	0.00	1.13	45.3	29.80	0.00	1.74	7.13	38.51	77%	0%	5%	18%
		37	15	8/29/2012 11:41	21.34442	-157.96880	41.0	0.00	0.00	4.42	40.1	0.00	0.00	9.94	4.06	13.90	0%	0%	71%	29%
		38	15	8/29/2012 11:43	21.34450	-157.96912	48.5	3.50	2.25	0.00	45.5	1.05	0.34	0.00	4.77	5.86	18%	6%	0%	76%
		39	15	8/29/2012 11:54	21.34489	-157.96939	44.5	1.92	0.00	0.16	43.6	57.53	0.00	0.08	8.79	66.22	87%	0%	0%	13%
		40	15	8/29/2012 12:01	21.34475	-157.96978	43.7	0.00	0.00	0.30	46.0	0.00	0.00	0.20	11.64	12.45	0%	0%	2%	98%
	Background 1		8/29/2012 9:09			1.01														
	Background 2		8/29/2012 9:09			0.97														
	Background 3		8/29/2012 9:09			0.83														
					Background Average	0.94														
					Background Standard deviation	0.098														

Table D-4. Copper data for Pearl Harbor Field Study, 28–29 August 2012.

Pearl Harbor		Copper				1	2	3	4	5	6	7	8	9					
	Station	Depth (ft)	Sampling date and time	Latitude	Longitude	TOTAL Filtered solution (µg/L)	SAND Filtered solution (µg/L)	SILT Filtered solution (µg/L)	CLAY Filtered solution (µg/L)	DISSOLVED Filtered solution (µg/L)	Mass of metal in SAND fraction (µg/mg)	Mass of metal in SILT fraction (µg/mg)	Mass of metal in CLAY fraction (µg/mg)	Mass of metal in TOTAL fraction (µg/mg)	TOTAL Summ of fractions (µg/mg)	as Mass of metal in SAND fraction (%)	Mass of metal in SILT fraction (%)	Mass of metal in CLAY fraction (%)	Mass of DISSOLVED metal associated to TOTAL fraction (%)
						< 2 mm	≥ 60 µm	60 µm to 5 µm	5 µm to 0.4 µm	< 0.4 µm	≥ 60 µm	60 µm to 5 µm	5 µm to 0.4 µm	< 2 mm		≥ 60 µm	60 µm to 5 µm	5 µm to 0.4 µm	< 0.4 µm
Bravo 22 Pier																			
Plume Event One	1	3	8/28/2012 10:40	21.35519	-157.94936	29.6	7.2	14.5	2.4	5.6	0.33	0.26	0.48	0.36	1.13	29%	23%	42%	6%
	2	15	8/28/2012 10:41	21.35519	-157.94936	10.8	0.3	0.6	0.0	10.7	0.32	0.09	0.00	1.06	1.46	22%	6%	0%	72%
	3	3	8/28/2012 10:45	21.35562	-157.94884	12.6	1.8	4.5	0.6	5.7	0.31	0.25	0.13	0.44	0.89	35%	28%	15%	22%
	4	15	8/28/2012 10:46	21.35562	-157.94884	12.6	1.5	2.9	0.9	7.4	0.45	0.25	0.19	0.65	1.28	36%	20%	15%	30%
	5	3	8/28/2012 10:50	21.35559	-157.94874	24.9	7.9	11.1	0.9	4.9	0.55	0.28	0.17	0.42	1.09	51%	26%	15%	8%
Plume Event Two	6	15	8/28/2012 10:51	21.35559	-157.94874	17.5	3.6	7.1	1.3	5.6	0.43	0.24	0.31	0.41	1.11	39%	21%	28%	12%
	7	3	8/28/2012 11:03	21.35492	-157.94861	16.2	0.5	8.0	1.4	6.3	0.06	0.22	0.58	0.35	1.01	6%	22%	58%	14%
	8	15	8/28/2012 11:04	21.35492	-157.94861	20.1	3.5	9.8	0.2	6.6	0.27	0.24	0.04	0.35	0.67	40%	37%	6%	17%
	9	3	8/28/2012 11:05	21.35542	-157.94893	32.5	8.6	17.7	0.9	5.3	0.23	0.25	0.12	0.28	0.64	35%	39%	18%	7%
	10	15	8/28/2012 11:06	21.35542	-157.94893	15.2	3.5	5.0	1.1	5.5	1.30	0.20	0.14	0.42	1.79	72%	11%	8%	9%
Plume Event Three	11	3	8/28/2012 11:07	21.35595	-157.94889	17.3	6.9	3.8	0.8	5.6	0.49	0.20	0.17	0.45	1.00	49%	20%	17%	15%
	12	15	8/28/2012 11:08	21.35595	-157.94889	18.8	2.1	10.4	0.0	8.3	0.20	0.28	0.00	0.34	0.63	32%	44%	0%	24%
	13	15	8/28/2012 11:51	21.35512	-157.94920	15.0	0.5	7.6	1.5	5.4	0.07	0.27	0.27	0.36	0.73	9%	37%	37%	18%
	14	15	8/28/2012 11:53	21.35550	-157.94871	24.0	0.9	15.2	2.4	5.6	0.04	0.24	0.27	0.25	0.60	6%	40%	44%	10%
	15	15	8/28/2012 11:55	21.35542	-157.94815	36.0	7.7	21.7	1.2	5.4	0.18	0.27	0.13	0.27	0.62	30%	43%	20%	7%
	16	15	8/28/2012 11:56	21.35554	-157.94820	35.5	20.6	8.0	1.7	5.2	0.56	0.12	0.69	0.33	1.42	40%	8%	49%	3%
	17	15	8/28/2012 12:04	21.35562	-157.94794	27.0	2.8	17.3	1.4	5.5	0.16	0.40	0.51	0.43	1.15	14%	35%	44%	8%
	18	15	8/28/2012 0:11	21.35696	-157.94902	16.2	0.0	9.5	0.9	5.9	0.00	0.35	0.51	0.45	1.02	0%	34%	50%	16%
	19	15	8/28/2012 0:19	21.35694	-157.94997	12.6	1.1	2.2	0.0	9.2	0.10	0.43	0.00	0.73	1.06	9%	41%	0%	50%
	20	15	8/28/2012 0:27	21.35693	-157.95011	12.9	0.9	6.0	0.1	5.9	0.42	0.43	0.05	0.71	1.22	34%	35%	4%	27%
Background 1						3.45													
Background 2						3.30													
Background 3						3.34													
Background Average						3.37													
Background Standard deviation						0.078													
Oscar 2 Pier																			
Plume Event One	21	3	8/29/2012 9:31	21.34516	-157.96727	4.9	1.12	2.75	0.38	0.7	0.51	0.21	0.45	0.30	1.21	42%	17%	37%	3%
	22	15	8/29/2012 9:32	21.34505	-157.96750	2.3	0.14	0.00	0.87	1.7	0.21	0.00	2.89	0.65	3.57	6%	0%	81%	13%
	23	3	8/29/2012 9:34	21.34495	-157.96813	5.2	1.52	2.77	0.73	0.2	0.11	0.12	0.50	0.14	0.74	15%	16%	68%	1%
	24	15	8/29/2012 9:35	21.34492	-157.96824	2.9	1.99	0.00	1.66	0.0	0.67	0.00	2.08	0.22	2.75	24%	0%	76%	0%
	25	3	8/29/2012 9:37	21.34475	-157.96860	3.4	1.62	0.17	0.92	0.7	1.28	0.03	1.84	0.45	3.23	39%	1%	57%	3%
Plume Event Two	26	15	8/29/2012 9:38	21.34460	-157.96868	1.7	0.00	0.00	0.87	1.6	0.00	0.00	3.91	0.82	4.69	0%	0%	83%	17%
	27	3	8/29/2012 10:34	21.34526	-157.96704	1.5	0.33	0.00	0.64	0.9	9.92	0.00	1.19	0.34	11.32	88%	0%	11%	2%
	28	15	8/29/2012 10:35	21.34512	-157.96745	2.6	0.55	0.51	1.54	0.0	0.15	0.05	46.15	0.20	46.35	0%	0%	100%	0%
	29	3	8/29/2012 10:36	21.34488	-157.96768	1.2	0.00	0.00	1.51	0.5	0.00	0.00	13.94	0.12	13.99	0%	0%	100%	0%
	30	15	8/29/2012 10:37	21.34466	-157.96786	0.8	0.00	0.54	0.00	2.0	0.00	0.32	0.00	0.25	0.93	0%	35%	0%	65%
Plume Event Three	31	3	8/29/2012 10:41	21.34506	-157.96832	2.8	2.16	1.08	0.00	0.0	0.73	0.17	0.00	0.28	0.91	81%	19%	0%	0%
	32	15	8/29/2012 10:42	21.34513	-157.96831	2.2	0.00	2.32	0.00	0.4	0.00	0.38	0.00	0.28	0.43	0%	88%	0%	12%
	33	15	8/29/2012 11:36	21.34469	-157.96816	1.3	0.00	1.39	0.91	0.0	0.00	0.18	7.31	0.12	7.49	0%	2%	98%	0%
	34	15	8/29/2012 11:37	21.34442	-157.96844	2.8	0.76	1.10	0.17	0.7	0.15	0.07	1.22	0.13	1.46	10%	5%	83%	2%
	35	15	8/29/2012 11:39	21.34441	-157.96863	1.5	0.40	1.44	0.00	2.3	0.12	0.15	0.00	0.12	0.46	27%	33%	0%	40%
	36	15	8/29/2012 11:40	21.34440	-157.96863	2.9	0.12	1.69	0.00	1.4	1.77	0.29	0.00	0.45	2.28	78%	13%	0%	9%
	37	15	8/29/2012 11:41	21.34442	-157.96880	4.2	1.31	1.49	1.33	0.1	0.93	0.18	3.00	0.42	4.11	23%	4%	73%	0%
	38	15	8/29/2012 11:43	21.34450	-157.96912	3.0	0.00	3.26	0.00	1.0	0.00	0.49	0.00	0.30	0.59	0%	83%	0%	17%
	39	15	8/29/2012 11:54	21.34489	-157.96939	0.5	0.64	0.00	2.19	0.0	19.10	0.00	1.10	0.11	20.20	95%	0%	5%	0%
	40	15	8/29/2012 12:01	21.34475	-157.96978	1.8	0.50	0.00	1.20	2.5	15.13	0.00	0.80	0.48	16.60	91%	0%	5%	4%
Background 1						3.08													
Background 2						3.85													
Background 3						3.16													
Background Average						3.36													
Background Standard deviation						0.422													

Table D-5. Zinc data for Pearl Harbor Field Study, 28–29 August 2012.

Pearl Harbor		Zinc			1	2	3	4	5	6	7	8	9							
	Station	Depth (ft)	Sampling date and time	Latitude	Longitude	TOTAL Filtered solution (µg/L)	SAND Filtered solution (µg/L)	SILT Filtered solution (µg/L)	CLAY Filtered solution (µg/L)	DISSOLVED Filtered solution (µg/L)	Mass of metal in SAND fraction (µg/mg)	Mass of metal in SILT fraction (µg/mg)	Mass of metal in CLAY fraction (µg/mg)	Mass of metal in TOTAL fraction (µg/mg)	TOTAL Summ of fractions (µg/mg)	as Mass of metal in SAND fraction (%)	Mass of metal in SILT fraction (%)	Mass of metal in CLAY fraction (%)	Mass of DISSOLVED metal associated to TOTAL fraction (%)	
						< 2 mm	≥ 60 µm	60 µm to µm	5	5 µm to 0.4 µm	< 0.4 µm	≥ 60 µm	60 µm to 5 µm	5 µm to 0.4 µm	< 2 mm		≥ 60 µm	60 µm to 5 µm	5 µm to 0.4 µm	< 0.4 µm
Bravo 22 Pier																				
Plume Event One	1	3	8/28/2012 10:40	21.35519	-157.94936	32.4	3.6	16.1	1.6	11.1	0.16	0.29	0.31	0.39	0.90	18%	32%	35%	15%	
	2	15	8/28/2012 10:41	21.35519	-157.94936	17.7	1.7	2.1	0.4	13.5	1.76	0.33	0.14	1.73	3.54	50%	9%	4%	37%	
	3	3	8/28/2012 10:45	21.35562	-157.94884	15.3	0.1	4.5	0.7	10.0	0.01	0.25	0.15	0.53	0.75	2%	33%	20%	46%	
	4	15	8/28/2012 10:46	21.35562	-157.94884	17.1	1.1	2.0	0.0	14.2	0.32	0.17	0.00	0.88	1.22	26%	14%	0%	60%	
	5	3	8/28/2012 10:50	21.35559	-157.94874	32.7	9.5	12.9	0.1	10.2	0.66	0.33	0.02	0.55	1.18	56%	28%	2%	15%	
Plume Event Two	6	15	8/28/2012 10:51	21.35559	-157.94874	19.3	2.1	5.6	1.2	10.5	0.25	0.19	0.30	0.46	0.98	25%	19%	30%	25%	
	7	3	8/28/2012 11:03	21.35492	-157.94861	20.9	2.0	6.2	3.0	9.8	0.27	0.17	1.24	0.46	1.89	14%	9%	65%	11%	
	8	15	8/28/2012 11:04	21.35492	-157.94861	25.4	5.1	8.4	1.5	10.4	0.39	0.21	0.32	0.44	1.10	35%	19%	29%	16%	
	9	3	8/28/2012 11:05	21.35542	-157.94893	36.5	4.9	19.0	2.0	10.6	0.13	0.27	0.26	0.32	0.76	17%	36%	35%	12%	
	10	15	8/28/2012 11:06	21.35542	-157.94893	21.3	6.0	4.4	1.0	9.9	2.20	0.18	0.12	0.60	2.78	79%	6%	4%	10%	
Plume Event Three	11	3	8/28/2012 11:07	21.35595	-157.94889	23.9	9.6	2.8	1.4	10.1	0.67	0.14	0.26	0.62	1.34	50%	11%	20%	19%	
	12	15	8/28/2012 11:08	21.35595	-157.94889	24.9	3.6	9.5	0.9	10.9	0.34	0.25	0.13	0.46	0.92	36%	28%	14%	22%	
	13	15	8/28/2012 11:51	21.35512	-157.94920	21.4	2.3	9.1	0.0	10.3	0.28	0.33	0.00	0.51	0.85	33%	38%	0%	29%	
	14	15	8/28/2012 11:53	21.35550	-157.94871	27.5	0.2	14.7	1.6	11.1	0.01	0.23	0.17	0.29	0.53	1%	44%	33%	22%	
	15	15	8/28/2012 11:55	21.35542	-157.94815	43.3	5.0	27.8	0.2	10.2	0.12	0.34	0.02	0.33	0.57	21%	61%	4%	14%	
	16	15	8/28/2012 11:56	21.35554	-157.94820	42.8	24.3	7.7	0.0	11.8	0.66	0.11	0.00	0.40	0.89	75%	13%	0%	12%	
	17	15	8/28/2012 0:04	21.35562	-157.94794	28.8	2.5	15.8	0.0	11.0	0.14	0.37	0.00	0.45	0.68	21%	54%	0%	25%	
	18	15	8/28/2012 0:11	21.35696	-157.94902	18.5	0.1	7.3	0.9	10.2	0.02	0.27	0.49	0.52	1.06	2%	25%	46%	27%	
	19	15	8/28/2012 0:19	21.35694	-157.94997	16.8	0.0	4.0	0.0	13.8	0.00	0.77	0.00	0.97	1.58	0%	49%	0%	51%	
	20	15	8/28/2012 0:27	21.35693	-157.95011	16.6	-0.4	5.5	0.0	11.8	-0.18	0.39	0.00	0.92	1.05			38%	0%	62%
	Background 1	8/28/2012 10:12				2.87														
	Background 2	8/28/2012 10:12				2.75														
	Background 3	8/28/2012 10:12				2.66														
			Background Average			2.76														
			Background Standard deviation			0.106														
Oscar 2 Pier																				
Plume Event One	21	3	8/29/2012 9:31	21.34516	-157.96727	5.0	0.00	2.11	0.85	2.4	0.00	0.16	1.00	0.30	1.31	0%	12%	77%	11%	
	22	15	8/29/2012 9:32	21.34505	-157.96750	2.5	0.00	1.31	0.00	1.8	0.00	0.50	0.00	0.71	1.02	0%	50%	0%	50%	
	23	3	8/29/2012 9:34	21.34495	-157.96813	7.0	1.71	1.96	1.41	2.0	0.12	0.08	0.97	0.18	1.23	10%	7%	79%	4%	
	24	15	8/29/2012 9:35	21.34492	-157.96824	4.8	2.81	0.00	0.00	4.1	0.95	0.00	0.00	0.37	1.26	75%	0%	0%	25%	
	25	3	8/29/2012 9:37	21.34475	-157.96860	4.1	-0.03	1.96	0.00	2.7	-0.02	0.34	0.00	0.54	0.70		48%	0%	52%	
Plume Event Two	26	15	8/29/2012 9:38	21.34460	-157.96868	3.4	2.01	0.00	0.50	1.1	28.72	0.00	2.26	1.61	31.49	91%	0%	7%	2%	
	27	3	8/29/2012 10:34	21.34526	-157.96704	2.9	0.85	0.00	0.00	5.7	25.63	0.00	0.00	0.66	26.94	95%	0%	0%	5%	
	28	15	8/29/2012 10:35	21.34512	-157.96745	3.0	0.00	1.16	0.00	2.3	0.00	0.12	0.00	0.23	0.30	0%	41%	0%	59%	
	29	3	8/29/2012 10:36	21.34488	-157.96768	5.5	1.16	0.00	1.56	2.9	0.70	0.00	14.35	0.56	15.36	5%	0%	93%	2%	
	30	15	8/29/2012 10:37	21.34466	-157.96786	3.4	0.00	1.31	0.00	3.9	0.00	0.79	0.00	1.05	2.01	0%	39%	0%	61%	
Plume Event Three	31	3	8/29/2012 10:41	21.34506	-157.96832	6.3	3.97	0.00	1.66	2.0	1.35	0.00	2.21	0.63	3.76	36%	0%	59%	5%	
	32	15	8/29/2012 10:42	21.34513	-157.96831	3.0	0.00	0.45	0.65	2.6	0.00	0.07	4.90	0.38	5.31	0%	1%	92%	6%	
	33	15	8/29/2012 11:36	21.34469	-157.96816	4.7	1.26	0.00	0.07	3.8	0.40	0.00	0.52	0.43	1.27	32%	0%	41%	27%	
	34	15	8/29/2012 11:37	21.34442	-157.96844	6.3	0.00	2.71	1.21	3.0	0.00	0.17	8.44	0.30	8.75	0%	2%	96%	2%	
	35	15	8/29/2012 11:39	21.34441	-157.96863	5.9	1.21	2.36	0.00	2.8	0.37	0.25	0.00	0.47	0.85	44%	30%	0%	26%	
	36	15	8/29/2012 11:40	21.34440	-157.96863	5.7	0.25	1.16	0.10	4.2	3.59	0.20	0.15	0.88	4.59	78%	4%	3%	14%	
	37	15	8/29/2012 11:41	21.34442	-157.96880	7.5	1.56	0.00	0.70	5.5	1.11	0.00	1.58	0.74	3.23	34%	0%	49%	17%	
	38	15	8/29/2012 11:43	21.34450	-157.96912	6.8	0.00	0.90	0.00	8.6	0.00	0.13	0.00	0.67	0.98	0%	14%	0%	86%	
	39	15	8/29/2012 11:54	21.34489	-157.96939	5.3	0.85	0.00	0.00	6.2	25.63	0.00	0.00	1.05	26.86	95%	0%	0%	5%	
	40	15	8/29/2012 12:01	21.34475	-157.96978	2.5	0.10	0.00	1.41	5.0	3.02	0.00	0.94	0.66	5.28	57%	0%	18%	25%	
	Background 1	8/29/2012 9:09				3.66														
	Background 2	8/29/2012 9:09				3.22														
	Background 3	8/29/2012 9:09				2.27														
			Background Average			3.05														
			Background Standard deviation			0.707														

Table D-6. Arsenic data for Pearl Harbor Field Study, 28–29 August 2012.

Pearl Harbor		Arsenic				1	2	3	4	5	6	7	8	9						
	Station	Depth (ft)	Sampling date and time	Latitude	Longitude	TOTAL Filtered solution (µg/L)	SAND Filtered solution (µg/L)	SILT Filtered solution (µg/L)	CLAY Filtered solution (µg/L)	DISSOLVED Filtered solution (µg/L)	Mass of metal in SAND fraction (µg/mg)	Mass of metal in SILT fraction (µg/mg)	Mass of metal in CLAY fraction (µg/mg)	Mass of metal in TOTAL fraction (µg/mg)	TOTAL Summ of fractions (µg/mg)	as Mass of metal in SAND fraction (%)	Mass of metal in SILT fraction (%)	Mass of metal in CLAY fraction (%)	Mass of DISSOLVED metal associated to TOTAL fraction (%)	
						< 2 mm	≥ 60 µm	60 µm to 5 µm	5 µm to 0.4 µm	< 0.4 µm	≥ 60 µm	60 µm to 5 µm	5 µm to 0.4 µm	< 2 mm		≥ 60 µm	60 µm to 5 µm	5 µm to 0.4 µm	< 0.4 µm	
Bravo 22 Pier																				
Plume	1	3	8/28/2012 10:40	21.35519	-157.94936	10.3	-0.8	0.3	1.3	9.5	-0.04	0.01	0.27	0.13	0.39			1%	69%	30%
Event	2	15	8/28/2012 10:41	21.35519	-157.94936	6.0	-0.9	1.1	-3.1	8.9	-0.91	0.18	-1.08	0.59	1.04			17%	83%	
One	3	3	8/28/2012 10:45	21.35562	-157.94884	9.0	0.6	1.4	1.0	6.0	0.11	0.08	0.21	0.31	0.60	18%	13%	35%	34%	
	4	15	8/28/2012 10:46	21.35562	-157.94884	6.7	-0.3	0.7	0.7	5.6	-0.08	0.06	0.16	0.35	0.51			11%	32%	57%
	5	3	8/28/2012 10:50	21.35559	-157.94874	9.5	3.4	-2.5	0.2	8.4	0.24	-0.06	0.04	0.16	0.42	57%		9%	34%	
	6	15	8/28/2012 10:51	21.35559	-157.94874	9.3	0.6	-1.5	-1.7	11.9	0.07	-0.05	-0.43	0.22	0.36	21%			79%	
Plume	7	3	8/28/2012 11:03	21.35492	-157.94861	7.5	-1.5	-3.1	4.7	7.4	-0.21	-0.09	1.96	0.16	2.12			-4%	92%	8%
Event	8	15	8/28/2012 11:04	21.35492	-157.94861	7.9	-1.7	1.7	-4.3	12.2	-0.13	0.04	-0.94	0.14	0.25			17%	83%	
Two	9	3	8/28/2012 11:05	21.35542	-157.94893	9.5	1.0	2.1	-4.4	10.8	0.03	0.03	-0.58	0.08	0.15	18%	20%		62%	
	10	15	8/28/2012 11:06	21.35542	-157.94893	7.3	-1.7	-2.8	4.5	7.4	-0.63	-0.11	0.56	0.20	0.77			73%	27%	
	11	3	8/28/2012 11:07	21.35595	-157.94889	5.1	-1.9	-2.2	3.6	5.7	-0.14	-0.12	0.70	0.13	0.85			83%	17%	
	12	15	8/28/2012 11:08	21.35595	-157.94889	7.9	-0.2	-0.7	2.7	6.2	-0.02	-0.02	0.40	0.14	0.52			78%	22%	
Plume	13	15	8/28/2012 11:51	21.35512	-157.94920	6.6	-2.4	-0.1	1.2	7.9	-0.29	0.00	0.21	0.16	0.40			54%	47%	
Event	14	15	8/28/2012 11:53	21.35550	-157.94871	9.2	-1.2	-0.4	1.3	9.5	-0.05	-0.01	0.15	0.10	0.25			60%	40%	
Three	15	15	8/28/2012 11:55	21.35542	-157.94815	8.8	2.0	-2.2	1.8	7.2	0.05	-0.03	0.20	0.07	0.30	16%		66%	18%	
	16	15	8/28/2012 11:56	21.35554	-157.94820	12.6	4.5	0.9	0.1	7.1	0.12	0.01	0.04	0.12	0.24	51%	6%	15%	28%	
	17	15	8/28/2012 0:04	21.35562	-157.94794	8.9	-1.0	-1.5	3.3	8.2	-0.06	-0.04	1.18	0.14	1.31			90%	10%	
	18	15	8/28/2012 0:11	21.35696	-157.94902	7.1	-4.3	3.9	0.3	7.1	-0.64	0.14	0.17	0.20	0.52			28%	34%	39%
	19	15	8/28/2012 0:19	21.35694	-157.94997	6.8	2.3	0.4	0.0	4.1	0.20	0.08	0.09	0.39	0.60	33%	14%	14%	39%	
	20	15	8/28/2012 0:27	21.35693	-157.95011	3.7	-3.8	1.6	-0.7	6.6	-1.74	0.11	-0.37	0.21	0.48			23%	77%	
	Background 1		8/28/2012 10:12			0.60														
	Background 2		8/28/2012 10:12			0.42														
	Background 3		8/28/2012 10:12			0.53														
				Background Average		0.52														
				Background Standard deviation		0.094														
Oscar 2 Pier																				
Plume	21	3	8/29/2012 9:31	21.34516	-157.96727	2.4	4.54	-2.59	-0.71	1.2	2.07	-0.19	-0.84	0.15	2.14	97%			3%	
Event	22	15	8/29/2012 9:32	21.34505	-157.96750	12.0	-2.63	1.30	0.79	12.6	-3.96	0.50	2.65	3.38	6.68		8%	40%	53%	
One	23	3	8/29/2012 9:34	21.34495	-157.96813	-0.9	1.29	-0.58	-3.06	1.5	0.09	-0.02	-2.12	-0.02	0.13	71%			29%	
	24	15	8/29/2012 9:35	21.34492	-157.96824	4.3	0.57	-3.06	5.46	1.3	0.19	-0.33	6.82	0.33	7.11	3%		96%	1%	
	25	3	8/29/2012 9:37	21.34475	-157.96860	10.6	2.50	-2.11	1.51	8.7	1.97	-0.37	3.02	1.41	6.15	32%		49%	19%	
	26	15	8/29/2012 9:38	21.34460	-157.96868	11.1	2.85	-6.06	1.98	12.3	40.65	-3.37	8.90	5.30	55.45	73%		16%	11%	
Plume	27	3	8/29/2012 10:34	21.34526	-157.96704	9.2	0.51	-0.97	1.43	8.3	15.19	-0.26	2.69	2.12	19.77	77%		14%	10%	
Event	28	15	8/29/2012 10:35	21.34512	-157.96745	2.4	0.85	-4.58	1.10	5.0	0.24	-0.49	33.14	0.19	33.77	1%		98%	1%	
Two	29	3	8/29/2012 10:36	21.34488	-157.96768	6.0	3.77	-2.80	1.82	3.2	2.30	-0.35	16.77	0.61	19.40	12%		86%	2%	
	30	15	8/29/2012 10:37	21.34466	-157.96786	10.6	-4.20	-0.59	2.73	12.7	-7.00	-0.35	2.80	3.29	6.74			42%	58%	
	31	3	8/29/2012 10:41	21.34506	-157.96832	10.0	4.17	-2.02	0.52	7.3	1.42	-0.32	0.70	1.00	2.85	50%		24%	26%	
	32	15	8/29/2012 10:42	21.34513	-157.96831	8.1	-0.12	-3.11	1.49	9.8	-0.08	-0.51	11.19	1.05	12.46			90%	10%	
	33	15	8/29/2012 11:36	21.34469	-157.96816	3.6	-9.14	6.82	1.08	4.8	-2.94	0.88	8.63	0.33	9.94		9%	87%	4%	
Plume	34	15	8/29/2012 11:37	21.34442	-157.96844	0.5	-0.05	0.31	1.82	-1.6	-0.01	0.02	12.77	0.02	12.79		0%	100%		
Event	35	15	8/29/2012 11:39	21.34441	-157.96863	0.6	-0.34	-0.56	2.36	-0.8	-0.10	-0.06	70.81	0.05	70.75			100%	0%	
Three	36	15	8/29/2012 11:40	21.34440	-157.96863	10.9	1.95	-3.27	0.43	11.8	27.85	-0.57	0.66	1.68	30.32	92%		2%	6%	
	37	15	8/29/2012 11:41	21.34442	-157.96880	0.7	-5.43	-6.88	9.46	3.6	-3.85	-0.83	21.29	0.07	21.64			98%	2%	
	38	15	8/29/2012 11:43	21.34450	-157.96912	15.0	2.28	5.52	-5.31	12.5	0.68	0.82	-47.81	1.47	2.73	25%	30%		45%	
	39	15	8/29/2012 11:54	21.34489	-157.96939	9.7	0.39	-1.52	1.46	9.4	11.58	-0.50	0.73	1.91	14.16	82%		5%	13%	
	40	15	8/29/2012 12:01	21.34475	-157.96978	7.4	-2.83	-6.95	8.97	8.2	-84.93	-3.13	5.98	1.97	8.17			73%	27%	
	Background 1		8/29/2012 9:09			0.11														
	Background 2		8/29/2012 9:09			0.22														
	Background 3		8/29/2012 9:09			0.25														
				Background Average		0.19														
				Background Standard deviation		0.073														

Table D-7. Silver data for Pearl Harbor Field Study, 28–29 August 2012.

Pearl Harbor		Silver				1	2	3	4	5	6	7	8	9					
	Station	Depth (ft)	Sampling date and time	Latitude	Longitude	TOTAL Filtered solution (µg/L)	SAND Filtered solution (µg/L)	SILT Filtered solution (µg/L)	CLAY Filtered solution (µg/L)	DISSOLVED Filtered solution (µg/L)	Mass of metal in SAND fraction (µg/mg)	Mass of metal in SILT fraction (µg/mg)	Mass of metal in CLAY fraction (µg/mg)	Mass of metal in TOTAL fraction (µg/mg)	TOTAL Summ of fractions (µg/mg)	as Mass of metal in SAND fraction (%)	Mass of metal in SILT fraction (%)	Mass of metal in CLAY fraction (%)	Mass of DISSOLVED metal associated to TOTAL fraction (%)
						< 2 mm	≥ 60 µm	60 µm to 5 µm	5 µm to 0.4 µm	< 0.4 µm	≥ 60 µm	60 µm to 5 µm	5 µm to 0.4 µm	< 2 mm		≥ 60 µm	60 µm to 5 µm	5 µm to 0.4 µm	< 0.4 µm
Bravo 22 Pier																			
Plume	1	3	8/28/2012 10:40	21.35519	-157.94936	0.72	0.0	0.1	0.0	0.71	0.00	0.00	-0.01	0.01	0.01	0%	10%	0%	97%
Event	2	15	8/28/2012 10:41	21.35519	-157.94936	0.80	0.0	0.0	0.0	0.79	0.01	-0.01	0.01	0.08	0.10	11%	0%	11%	78%
One	3	3	8/28/2012 10:45	21.35562	-157.94884	0.76	0.0	0.0	0.0	0.78	0.00	0.00	0.00	0.03	0.03	0%	0%	9%	93%
	4	15	8/28/2012 10:46	21.35562	-157.94884	0.79	0.0	0.0	0.0	0.79	0.00	0.00	0.00	0.04	0.04	0%	5%	0%	95%
	5	3	8/28/2012 10:50	21.35559	-157.94874	0.74	0.0	0.0	0.0	0.70	0.00	0.00	0.01	0.01	0.02	6%	0%	35%	61%
	6	15	8/28/2012 10:51	21.35559	-157.94874	0.75	0.0	0.0	0.0	0.74	0.00	0.00	0.00	0.02	0.02	0%	3%	0%	97%
Plume	7	3	8/28/2012 11:03	21.35492	-157.94861	0.74	0.0	0.0	0.0	0.74	0.00	0.00	-0.01	0.02	0.02	7%	2%	0%	91%
Event	8	15	8/28/2012 11:04	21.35492	-157.94861	0.73	0.0	0.0	0.0	0.71	0.00	0.00	0.00	0.01	0.02	10%	0%	11%	81%
Two	9	3	8/28/2012 11:05	21.35542	-157.94893	0.73	0.0	0.0	0.0	0.68	0.00	0.00	0.00	0.01	0.01	15%	2%	0%	89%
	10	15	8/28/2012 11:06	21.35542	-157.94893	0.77	0.0	0.0	0.0	0.77	0.00	0.00	0.00	0.02	0.02	0%	1%	4%	95%
	11	3	8/28/2012 11:07	21.35595	-157.94889	0.80	0.0	0.0	0.0	0.79	0.00	0.00	0.00	0.02	0.02	4%	1%	0%	95%
	12	15	8/28/2012 11:08	21.35595	-157.94889	0.76	0.0	0.0	0.0	0.73	0.00	0.00	0.00	0.01	0.02	13%	2%	0%	85%
Plume	13	15	8/28/2012 11:51	21.35512	-157.94920	0.76	0.0	0.0	0.0	0.72	0.00	0.00	0.01	0.02	0.02	0%	2%	27%	71%
Event	14	15	8/28/2012 11:53	21.35550	-157.94871	0.72	0.0	0.0	0.0	0.71	0.00	0.00	0.00	0.01	0.01	3%	6%	0%	91%
Three	15	15	8/28/2012 11:55	21.35542	-157.94815	0.73	0.0	0.0	0.0	0.70	0.00	0.00	0.00	0.01	0.01	6%	9%	0%	86%
	16	15	8/28/2012 11:56	21.35554	-157.94820	0.73	0.0	0.1	0.0	0.69	0.00	0.00	-0.01	0.01	0.01	6%	10%	0%	84%
	17	15	8/28/2012 0:04	21.35562	-157.94794	0.74	0.0	0.0	0.0	0.71	0.00	0.00	0.00	0.01	0.01	11%	1%	0%	87%
	18	15	8/28/2012 0:11	21.35696	-157.94902	0.77	0.0	0.1	0.0	0.75	-0.01	0.00	0.00	0.02	0.02	0%	8%	5%	87%
	19	15	8/28/2012 0:19	21.35694	-157.94997	0.81	0.0	0.0	0.0	0.82	0.00	0.00	0.01	0.05	0.05	1%	0%	10%	88%
	20	15	8/28/2012 0:27	21.35693	-157.95011	0.78	0.0	0.0	0.0	0.77	0.01	0.00	0.00	0.04	0.05	15%	0%	6%	79%
	Background 1		8/28/2012 10:12			-3.40													
	Background 2		8/28/2012 10:12			-1.91													
	Background 3		8/28/2012 10:12			-3.76													
					Background Average	-3.02													
					Background Standard deviation	0.98													
Oscar 2 Pier																			
Plume	21	3	8/29/2012 9:31	21.34516	-157.96727	0.68	0.03	-0.02	0.01	0.67	0.01	0.00	0.01	0.04	0.06	20%	0%	10%	69%
Event	22	15	8/29/2012 9:32	21.34505	-157.96750	0.67	0.00	-0.02	0.01	0.67	0.01	-0.01	0.03	0.19	0.22	2%	0%	13%	85%
One	23	3	8/29/2012 9:34	21.34495	-157.96813	0.69	0.02	-0.01	-0.02	0.70	0.00	0.00	-0.01	0.02	0.02	9%	0%	0%	94%
	24	15	8/29/2012 9:35	21.34492	-157.96824	0.67	0.00	0.02	0.00	0.65	0.00	0.00	0.00	0.05	0.05	0%	3%	4%	93%
	25	3	8/29/2012 9:37	21.34475	-157.96860	0.66	0.00	0.00	-0.01	0.67	0.00	0.00	-0.01	0.09	0.09	0%	0%	0%	100%
	26	15	8/29/2012 9:38	21.34460	-157.96868	0.66	-0.02	0.00	-0.03	0.70	-0.22	0.00	-0.12	0.31	0.34	0%	1%	0%	99%
Plume	27	3	8/29/2012 10:34	21.34526	-157.96704	0.67	0.01	0.00	-0.01	0.67	0.26	0.00	-0.03	0.15	0.41	63%	0%	0%	37%
Event	28	15	8/29/2012 10:35	21.34512	-157.96745	0.65	-0.03	0.02	0.01	0.66	-0.01	0.00	0.16	0.05	0.21	0%	1%	75%	24%
Two	29	3	8/29/2012 10:36	21.34488	-157.96768	0.68	0.01	0.02	-0.03	0.68	0.01	0.00	-0.27	0.07	0.08	7%	3%	0%	90%
	30	15	8/29/2012 10:37	21.34466	-157.96786	0.69	0.00	-0.01	-0.01	0.72	-0.01	-0.01	-0.01	0.21	0.22	0%	0%	0%	100%
	31	3	8/29/2012 10:41	21.34506	-157.96832	0.67	-0.01	0.00	0.02	0.66	0.00	0.00	0.03	0.07	0.10	0%	0%	31%	69%
	32	15	8/29/2012 10:42	21.34513	-157.96831	0.67	-0.03	0.01	0.02	0.67	-0.02	0.00	0.18	0.09	0.27	0%	1%	68%	32%
Plume	33	15	8/29/2012 11:36	21.34469	-157.96816	0.67	0.01	-0.02	0.01	0.66	0.00	0.00	0.12	0.06	0.18	2%	0%	65%	33%
Event	34	15	8/29/2012 11:37	21.34442	-157.96844	0.69	0.03	-0.02	0.02	0.66	0.01	0.00	0.16	0.03	0.19	3%	0%	81%	16%
Three	35	15	8/29/2012 11:39	21.34441	-157.96863	0.68	0.00	0.02	0.01	0.65	0.00	0.00	0.16	0.05	0.21	0%	1%	74%	25%
	36	15	8/29/2012 11:40	21.34440	-157.96863	0.68	-0.01	0.01	0.02	0.66	-0.15	0.00	0.04	0.10	0.14	0%	1%	27%	72%
	37	15	8/29/2012 11:41	21.34442	-157.96880	0.67	-0.01	0.02	-0.01	0.68	-0.01	0.00	-0.03	0.07	-0.04	19%	0%	81%	-174%
	38	15	8/29/2012 11:43	21.34450	-157.96912	0.66	-0.03	0.02	-0.01	0.68	-0.01	0.00	-0.06	0.06	-0.07	12%	0%	88%	-94%
	39	15	8/29/2012 11:54	21.34489	-157.96939	0.67	-0.02	0.01	-0.01	0.68	-0.47	0.00	0.00	0.13	-0.47	99%	0%	1%	-28%
	40	15	8/29/2012 12:01	21.34475	-157.96978	0.66	-0.01	-0.01	-0.02	0.69	-0.36	0.00	-0.01	0.17	0.18	0%	0%	0%	100%
	Background 1		8/29/2012 9:09			-3.60													
	Background 2		8/29/2012 9:09			-1.51													
	Background 3		8/29/2012 9:09			1.16													
					Background Average	-1.32													
					Background Standard deviation	2.39													

Table D-8. Cadmium data for Pearl Harbor Field Study, 28–29 August 2012.

Pearl Harbor			Cadmium			1	2	3	4	5	6	7	8	9										
Station	Depth (ft)	Sampling date and time	Latitude	Longitude	TOTAL Filtered solution (µg/L)	SAND Filtered solution (µg/L)	SILT Filtered solution (µg/L)	CLAY Filtered solution (µg/L)	DISSOLVED Filtered solution (µg/L)	Mass of metal in SAND fraction (µg/mg)	Mass of metal in SILT fraction (µg/mg)	Mass of metal in CLAY fraction (µg/mg)	Mass of metal in TOTAL fraction (µg/mg)	TOTAL Summ of fractions (µg/mg)	as	Mass of metal in SAND fraction (%)	Mass of metal in SILT fraction (%)	Mass of metal in CLAY fraction (%)	Mass of DISSOLVED metal associated to TOTAL fraction (%)					
					< 2 mm	≥ 60 µm	60 µm to 5 µm	5 µm to 0.4 µm	< 0.4 µm	≥ 60 µm	60 µm to 5 µm	5 µm to 0.4 µm	< 2 mm			≥ 60 µm	60 µm to 5 µm	5 µm to 0.4 µm	< 0.4 µm					
Bravo 22 Pier																								
Plume Event One	1	3	8/28/2012 10:40	21.35519	-157.94936	0.06	-0.1	0.0	0.0	0.10	0.00	0.00	0.01	0.00	0.01	0%	4%	78%	17%					
	2	15	8/28/2012 10:41	21.35519	-157.94936	0.16	0.0	0.0	0.0	0.18	0.04	-0.01	-0.01	0.02	0.06	71%	0%	0%	29%					
	3	3	8/28/2012 10:45	21.35562	-157.94884	0.10	0.0	0.0	-0.1	0.14	0.00	0.00	-0.01	0.00	0.01	28%	0%	0%	72%					
	4	15	8/28/2012 10:46	21.35562	-157.94884	0.14	0.0	0.0	0.0	0.08	-0.01	0.00	0.01	0.01	0.02	0%	19%	56%	26%					
	5	3	8/28/2012 10:50	21.35559	-157.94874	0.13	0.0	0.1	0.0	0.10	0.00	0.00	0.00	0.00	0.00	0%	45%	0%	55%					
Plume Event Two	6	15	8/28/2012 10:51	21.35559	-157.94874	0.15	0.0	0.0	0.0	0.16	0.00	0.00	0.00	0.00	0.01	48%	0%	0%	52%					
	7	3	8/28/2012 11:03	21.35492	-157.94861	0.08	0.0	0.0	0.0	0.12	-0.01	0.00	0.00	0.00	0.01	0%	0%	54%	46%					
	8	15	8/28/2012 11:04	21.35492	-157.94861	0.10	0.0	-0.1	0.0	0.10	0.00	0.00	0.01	0.00	0.01	21%	0%	66%	13%					
	9	3	8/28/2012 11:05	21.35542	-157.94893	0.09	0.0	0.0	0.0	0.11	0.00	0.00	0.00	0.00	0.00	35%	0%	0%	89%					
	10	15	8/28/2012 11:06	21.35542	-157.94893	0.10	0.0	0.0	0.0	0.15	0.01	0.00	0.00	0.00	0.01	56%	0%	0%	44%					
Plume Event Three	11	3	8/28/2012 11:07	21.35595	-157.94889	0.06	0.0	0.0	0.0	0.14	0.00	0.00	0.00	0.00	0.00	0%	0%	0%	100%					
	12	15	8/28/2012 11:08	21.35595	-157.94889	0.09	0.0	0.0	0.1	0.08	0.00	0.00	0.01	0.00	0.01	0%	0%	84%	16%					
	13	15	8/28/2012 11:51	21.35512	-157.94920	0.12	0.0	-0.1	0.1	0.09	0.00	0.00	0.01	0.00	0.02	27%	0%	61%	12%					
	14	15	8/28/2012 11:53	21.35550	-157.94871	0.09	0.0	-0.1	0.0	0.10	0.00	0.00	0.00	0.00	0.00	12%	0%	66%	22%					
	15	15	8/28/2012 11:55	21.35542	-157.94815	0.11	0.0	0.0	0.0	0.12	0.00	0.00	0.00	0.00	0.00	0%	23%	0%	95%					
	16	15	8/28/2012 11:56	21.35554	-157.94820	0.11	0.0	-0.1	0.0	0.13	0.00	0.00	0.01	0.00	0.01	11%	0%	79%	10%					
	17	15	8/28/2012 0:04	21.35562	-157.94794	0.09	0.0	0.0	0.0	0.08	0.00	0.00	0.02	0.00	0.02	0%	0%	93%	7%					
	18	15	8/28/2012 0:11	21.35696	-157.94902	0.14	0.0	0.0	0.0	0.12	0.00	0.00	0.02	0.00	0.03	6%	0%	81%	13%					
	19	15	8/28/2012 0:19	21.35694	-157.94997	0.18	0.1	0.0	0.0	0.13	0.01	-0.01	0.04	0.01	0.05	11%	0%	73%	16%					
	20	15	8/28/2012 0:27	21.35693	-157.95011	0.13	0.0	0.0	0.0	0.13	0.00	0.00	0.00	0.01	0.01	0%	12%	0%	88%					
Background 1			8/28/2012 10:12		0.0062																			
Background 2			8/28/2012 10:12		0.0072																			
Background 3			8/28/2012 10:12		0.0080																			
				Background Average	0.0072																			
				Background Standard deviation	0.0009																			
Oscar 2 Pier																								
Plume Event One	21	3	8/29/2012 9:31	21.34516	-157.96727	0.76	0.03	-0.02	0.02	0.73	0.02	0.00	0.02	0.05	0.08	19%	0%	25%	56%					
	22	15	8/29/2012 9:32	21.34505	-157.96750	0.69	-0.02	-0.03	0.02	0.73	-0.04	-0.01	0.08	0.20	0.29	0%	0%	29%	71%					
	23	3	8/29/2012 9:34	21.34495	-157.96813	0.75	0.01	0.03	-0.04	0.75	0.00	0.00	-0.02	0.02	0.02	3%	6%	0%	91%					
	24	15	8/29/2012 9:35	21.34492	-157.96824	0.73	0.02	-0.01	0.02	0.70	0.01	0.00	0.03	0.06	0.09	8%	0%	31%	61%					
	25	3	8/29/2012 9:37	21.34475	-157.96860	0.71	-0.01	0.02	-0.03	0.73	-0.01	0.00	-0.06	0.09	0.10	0%	4%	0%	96%					
Plume Event Two	26	15	8/29/2012 9:38	21.34460	-157.96868	0.73	0.01	0.01	-0.05	0.76	0.08	0.00	-0.21	0.35	0.45	18%	1%	0%	82%					
	27	3	8/29/2012 10:34	21.34526	-157.96704	0.73	-0.01	0.02	0.00	0.72	-0.33	0.01	0.00	0.17	0.17	0%	4%	0%	96%					
	28	15	8/29/2012 10:35	21.34512	-157.96745	0.72	0.03	-0.05	-0.02	0.76	0.01	0.00	-0.66	0.06	0.07	12%	0%	0%	88%					
	29	3	8/29/2012 10:36	21.34488	-157.96768	0.75	0.04	-0.03	-0.02	0.75	0.03	0.00	-0.15	0.08	0.10	25%	0%	0%	75%					
	30	15	8/29/2012 10:37	21.34466	-157.96786	0.74	-0.03	-0.01	0.02	0.75	-0.04	0.00	0.02	0.23	0.26	0%	0%	9%	91%					
Plume Event Three	31	3	8/29/2012 10:41	21.34506	-157.96832	0.74	0.01	0.04	-0.04	0.73	0.00	0.01	-0.05	0.07	0.08	2%	7%	0%	90%					
	32	15	8/29/2012 10:42	21.34513	-157.96831	0.75	0.02	-0.01	0.01	0.73	0.02	0.00	0.08	0.10	0.19	9%	0%	43%	49%					
	33	15	8/29/2012 11:36	21.34469	-157.96816	0.71	-0.02	0.01	-0.02	0.74	-0.01	0.00	-0.20	0.06	0.07	0%	2%	0%	98%					
	34	15	8/29/2012 11:37	21.34442	-157.96844	0.77	0.03	0.02	0.01	0.71	0.01	0.00	0.06	0.04	0.10	6%	2%	59%	34%					
	35	15	8/29/2012 11:39	21.34441	-157.96863	0.73	0.02	-0.02	-0.01	0.75	0.01	0.00	-0.33	0.06	0.07	9%	0%	0%	91%					
	36	15	8/29/2012 11:40	21.34440	-157.96863	0.75	0.02	0.01	-0.02	0.75	0.27	0.00	-0.04	0.12	0.39	70%	1%	0%	29%					
	37	15	8/29/2012 11:41	21.34442	-157.96880	0.75	0.03	-0.02	0.01	0.73	0.02	0.00	0.03	0.07	0.12	16%	0%	25%	59%					
	38	15	8/29/2012 11:43	21.34450	-157.96912	0.73	0.02	-0.01	0.01	0.71	0.00	0.00	0.12	0.07	0.20	2%	0%	62%	35%					
	39	15	8/29/2012 11:54	21.34489	-157.96939	0.71	-0.01	-0.02	-0.03	0.77	-0.16	-0.01	-0.02	0.14	0.15	0%	0%	0%	100%					
	40	15	8/29/2012 12:01	21.34475	-157.96978	0.74	0.01	-0.05	0.04	0.75	0.33	-0.02	0.02	0.20	0.55	60%	0%	4%	36%					
Background 1			8/29/2012 9:09		0.0074																			
Background 2			8/29/2012 9:09		0.0075																			
Background 3			8/29/2012 9:09		0.0059																			
				Background Average	0.0069																			
				Background Standard deviation	0.0009																			

Table D-9. Lead data for Pearl Harbor Field Study, 28–29 August 2012.

Pearl Harbor		Lead				1	2	3	4	5	6	7	8	9						
	Station	Depth (ft)	Sampling date and time	Latitude	Longitude	TOTAL Filtered solution (µg/L)	SAND Filtered solution (µg/L)	SILT Filtered solution (µg/L)	CLAY Filtered solution (µg/L)	DISSOLVED Filtered solution (µg/L)	Mass of metal in SAND fraction (µg/mg)	Mass of metal in SILT fraction (µg/mg)	Mass of metal in CLAY fraction (µg/mg)	Mass of metal in TOTAL fraction (µg/mg)	TOTAL Summ of fractions (µg/mg)	as	Mass of metal in SAND fraction (%)	Mass of metal in SILT fraction (%)	Mass of metal in CLAY fraction (%)	Mass of DISSOLVED metal associated to TOTAL fraction (%)
						< 2 mm	≥ 60 µm	60 µm to 5 µm	5 µm to 0.4 µm	< 0.4 µm	≥ 60 µm	60 µm to 5 µm	5 µm to 0.4 µm	< 2 mm			≥ 60 µm	60 µm to 5 µm	5 µm to 0.4 µm	< 0.4 µm
Bravo 22 Pier																				
Plume Event One	1	3	8/28/2012 10:40	21.35519	-157.94936	11.1	2.8	7.1	0.6	0.5	0.13	0.13	0.12	0.13	0.39		33%	33%	32%	2%
	2	15	8/28/2012 10:41	21.35519	-157.94936	1.9	0.3	0.7	0.1	0.8	0.30	0.10	0.03	0.19	0.52		58%	20%	6%	16%
	3	3	8/28/2012 10:45	21.35562	-157.94884	3.2	0.2	2.1	0.1	0.7	0.03	0.12	0.03	0.11	0.20		16%	59%	13%	13%
	4	15	8/28/2012 10:46	21.35562	-157.94884	2.9	0.6	1.2	0.1	0.9	0.19	0.11	0.03	0.15	0.38		51%	29%	8%	12%
	5	3	8/28/2012 10:50	21.35559	-157.94874	7.7	2.8	4.0	0.3	0.6	0.20	0.10	0.05	0.13	0.36		54%	28%	15%	3%
Plume Event Two	6	15	8/28/2012 10:51	21.35559	-157.94874	4.8	1.0	3.0	0.2	0.6	0.12	0.10	0.06	0.11	0.29		40%	35%	20%	5%
	7	3	8/28/2012 11:03	21.35492	-157.94861	4.8	0.1	3.9	0.2	0.6	0.02	0.11	0.10	0.11	0.24		8%	45%	41%	5%
	8	15	8/28/2012 11:04	21.35492	-157.94861	6.1	1.1	4.0	0.4	0.6	0.09	0.10	0.08	0.11	0.28		31%	36%	30%	4%
	9	3	8/28/2012 11:05	21.35542	-157.94893	11.4	2.7	7.7	0.4	0.6	0.07	0.11	0.05	0.10	0.24		30%	47%	21%	2%
	10	15	8/28/2012 11:06	21.35542	-157.94893	4.7	2.1	1.9	0.1	0.6	0.76	0.08	0.01	0.13	0.87		88%	9%	2%	2%
Plume Event Three	11	3	8/28/2012 11:07	21.35595	-157.94889	5.9	3.2	1.8	0.2	0.7	0.23	0.09	0.04	0.15	0.38		59%	25%	12%	4%
	12	15	8/28/2012 11:08	21.35595	-157.94889	5.9	0.9	4.1	0.3	0.6	0.08	0.11	0.05	0.11	0.25		32%	44%	20%	4%
	13	15	8/28/2012 11:51	21.35512	-157.94920	4.5	0.6	3.0	0.4	0.6	0.07	0.11	0.07	0.11	0.26		27%	41%	26%	6%
	14	15	8/28/2012 11:53	21.35550	-157.94871	7.6	0.7	5.7	0.6	0.5	0.03	0.09	0.07	0.08	0.19		15%	47%	35%	3%
	15	15	8/28/2012 11:55	21.35542	-157.94815	12.8	3.1	9.0	0.1	0.5	0.08	0.11	0.02	0.10	0.21		37%	54%	7%	2%
	16	15	8/28/2012 11:56	21.35554	-157.94820	12.1	8.1	3.2	0.2	0.6	0.22	0.05	0.07	0.11	0.35		64%	14%	21%	2%
	17	15	8/28/2012 0:04	21.35562	-157.94794	8.4	1.4	6.4	0.1	0.6	0.08	0.15	0.04	0.13	0.27		28%	55%	14%	3%
	18	15	8/28/2012 0:11	21.35696	-157.94902	4.3	-0.1	3.5	0.3	0.6	-0.01	0.13	0.14	0.12	0.29		44%	50%	6%	6%
	19	15	8/28/2012 0:19	21.35694	-157.94997	2.3	0.4	1.0	0.0	0.8	0.04	0.19	0.08	0.13	0.35		10%	53%	23%	14%
	20	15	8/28/2012 0:27	21.35693	-157.95011	2.9	0.0	1.9	0.1	0.9	0.00	0.13	0.07	0.16	0.26		2%	53%	27%	19%
Background																				
	Background 1	8/28/2012 10:12				0.56														
	Background 2	8/28/2012 10:12				0.49														
	Background 3	8/28/2012 10:12				0.78														
	Background Average					0.61														
	Background Standard deviation					0.15														
Oscar 2 Pier																				
Plume Event One	21	3	8/29/2012 9:31	21.34516	-157.96727	1.5	0.06	0.75	0.10	0.6	0.03	0.06	0.12	0.09	0.24		12%	24%	50%	15%
	22	15	8/29/2012 9:32	21.34505	-157.96750	0.8	-0.02	0.22	0.05	0.6	-0.03	0.08	0.16	0.24	0.41		21%	38%	41%	41%
	23	3	8/29/2012 9:34	21.34495	-157.96813	2.5	0.56	1.22	0.07	0.6	0.04	0.05	0.05	0.06	0.16		26%	33%	30%	10%
	24	15	8/29/2012 9:35	21.34492	-157.96824	1.4	0.57	0.21	0.02	0.6	0.19	0.02	0.03	0.11	0.29		66%	8%	10%	16%
	25	3	8/29/2012 9:37	21.34475	-157.96860	1.3	0.14	0.53	0.03	0.6	0.11	0.09	0.07	0.17	0.35		31%	26%	20%	23%
Plume Event Two	26	15	8/29/2012 9:38	21.34460	-157.96868	0.8	0.00	0.15	0.02	0.6	-0.01	0.08	0.11	0.37	0.48		17%	23%	60%	6%
	27	3	8/29/2012 10:34	21.34526	-157.96704	0.9	0.07	0.25	0.03	0.6	2.00	0.06	0.05	0.22	2.25		89%	3%	2%	6%
	28	15	8/29/2012 10:35	21.34512	-157.96745	1.4	0.23	0.48	0.04	0.6	0.06	0.05	1.23	0.10	1.39		5%	4%	88%	3%
	29	3	8/29/2012 10:36	21.34488	-157.96768	1.2	0.31	0.32	0.05	0.6	0.19	0.04	0.48	0.13	0.76		24%	5%	63%	8%
	30	15	8/29/2012 10:37	21.34466	-157.96786	0.9	0.13	0.15	-0.09	0.8	0.22	0.09	-0.09	0.29	0.54		40%	17%	43%	43%
Plume Event Three	31	3	8/29/2012 10:41	21.34506	-157.96832	1.2	0.15	0.33	0.06	0.6	0.05	0.05	0.08	0.12	0.25		21%	21%	33%	24%
	32	15	8/29/2012 10:42	21.34513	-157.96831	2.5	0.03	1.46	0.18	0.9	0.02	0.24	1.34	0.33	1.71		1%	14%	78%	6%
	33	15	8/29/2012 11:36	21.34469	-157.96816	1.2	0.19	0.38	0.04	0.6	0.06	0.05	0.30	0.11	0.47		13%	10%	64%	12%
	34	15	8/29/2012 11:37	21.34442	-157.96844	1.5	0.01	0.87	0.03	0.6	0.00	0.05	0.19	0.07	0.27		0%	20%	70%	10%
	35	15	8/29/2012 11:39	21.34441	-157.96863	1.4	0.18	0.56	0.06	0.6	0.06	0.06	1.76	0.11	1.92		3%	3%	92%	2%
	36	15	8/29/2012 11:40	21.34440	-157.96863	1.4	0.44	0.30	0.09	0.6	6.23	0.05	0.14	0.22	6.51		96%	1%	2%	1%
	37	15	8/29/2012 11:41	21.34442	-157.96880	1.3	0.01	0.63	0.04	0.6	0.01	0.08	0.08	0.13	0.23		4%	34%	36%	27%
	38	15	8/29/2012 11:43	21.34450	-157.96912	5.8	1.14	3.37	0.20	1.1	0.34	0.50	1.78	0.57	2.73		12%	18%	65%	4%
	39	15	8/29/2012 11:54	21.34489	-157.96939	0.8	0.04	0.07	-0.01	0.7	1.17	0.02	-0.01	0.15	1.31		89%	2%	0%	10%
	40	15	8/29/2012 12:01	21.34475	-157.96978	0.8	0.05	-0.01	0.12	0.7	1.58	-0.01	0.08	0.22	1.83		86%	0%	4%	10%
Background																				
	Background 1	8/29/2012 9:09				0.24														
	Background 2	8/29/2012 9:09				0.54														
	Background 3	8/29/2012 9:09				0.26														
	Background Average					0.35														
	Background Standard deviation					0.16														

APPENDIX E

GRAPHIC MAYNORD'S MODEL OUTPUT FILE AND FORMAT

This model was based on a study conducted by Donald F. Hayes et al., published in the Journal of Dredging Engineering (Vol. 12, No. 2, Oct. 2012) entitled “Vessel-induced sediment resuspension”. The goal of this modeling effort was to determine the significance of the impact on a predefined sediment bed caused by propeller-induced fluid turbulence. When propeller-induced fluid velocities produced a shear stress in excess of the critical shear for a given sediment type, sediment was entrained into the water column, and transported via advection.

Below are the quick procedures to run the model and generate model output:

The MATLAB® PropWash GUI will appear in a new window (Figure E-1)

Locate the ‘**User-Defined Parameters**’ window (Figure E-2)

Insert the desired **parameters**

Locate the ‘**Command Panel**’ window

Click ‘**Calculate**’

Locate Export Data

Click ‘EXCEL’ or ‘ASCII’

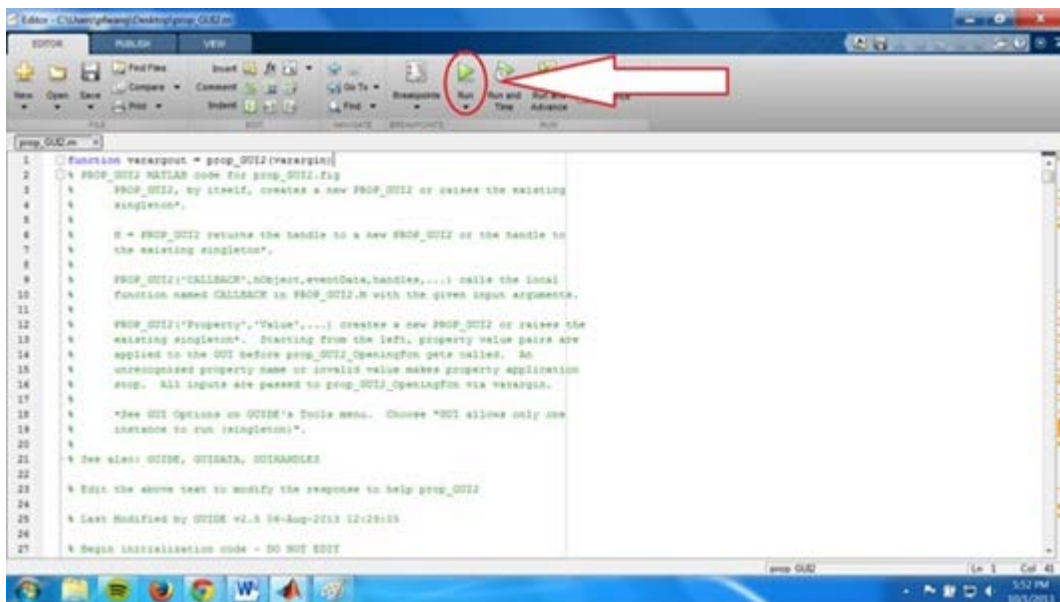


Figure E-1. MATLAB® Model GUI for the Graphic Maynard's Model.

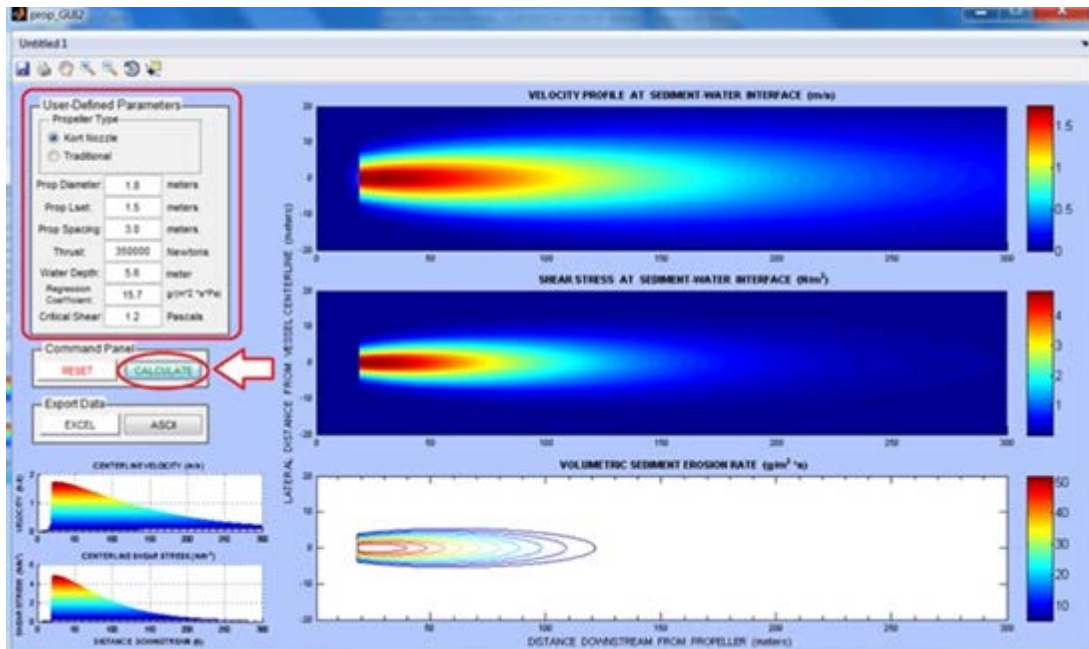


Figure E-2. Graphic interface of model input and output of the Graphic Maynard's Model.

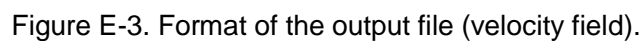
Instructions on data export:

1. Run prop_GUI2_winxx.exe. A splash screen will appear while the prop_GUI application is loading.
2. Enter the desired User-Defined Parameters.
3. Click “Calculate” in the Command Panel. The contour plots on the bottom and right hand side will populate.
4. If the plots are satisfactory, click either “Excel” or “ASCII” to export the data in the desired format. Please wait until one data export process is complete before starting another. Make sure to click “Calculate” after any user-defined parameters are changed to ensure that the data is updated before it is exported. Clicking “Reset” will return the default User-Defined Parameters.
 - a. The ASCII export option will create 4 comma-delimited text files named prop_velocity.txt, prop_shear.txt, prop_erosion.txt, and prop_erosion2.txt in the same folder as prop_GUI2_winxx.exe resides. These text files can be opened later with Microsoft® Excel®.
 - b. The Excel® export option will generate an Excel file named prop_data[*current date and time*].xlsx. This file will have four sheets named, Sheet1, Sheet2, Sheet3, and Sheet4. It will reside in the same directory as prop_GUI2_winxx.exe. The four sheets contain velocity, shear, erosion, and erosion2 data. Please be patient. The Excel data export takes about 5 minutes. Please refrain from executing any other commands in the prop_GUI window during this time. A message box will notify you when the export is complete.

Exporting data directly into Excel® requires a considerable amount of time. It is much faster to export the data as ASCII files and open them in Excel®.

In the Excel® data file, Sheet 1 contains the velocity data. The first column of cells, A4:A84, contain the y data, the third row of cells, B3:WC3, contain the x data. The units of x and y are

Figure E-3 shows the format of the output file for velocity and shear stress near the bottom in the wake of the tugboat propellers.



APPENDIX F

FORMULAS USED TO SPECIFY INPUT CONCENTRATIONS OF METAL BINDING PHASES IN WHAM

Particulate and Colloidal Humic and Fulvic Acid

The generalized formulas describing the conversion from particulate organic carbon (POC) and dissolved organic carbon (DOC) (in units of g OC/L) to particulate humic acid (HA_p) / particulate fulvic acid (FA_p) and dissolved HA (HA_d) / dissolved FA (FA_d) (all in units g HA/L or g FA/L) are:

$$HA_p = \frac{[POC]}{f_{OC,p}} f_{act,p} (1 - f_{FA,p}) \quad (1)$$

$$FA_p = \frac{[POC]}{f_{OC,p}} f_{act,p} f_{FA,p} \quad (2)$$

$$HA_d = \frac{[DOC]}{f_{OC,d}} f_{act,d} (1 - f_{FA,d}) \quad (3)$$

$$FA_d = \frac{[DOC]}{f_{OC,d}} f_{act,d} f_{FA,d} \quad (4)$$

where

$f_{OC,p}$ =	fraction of particulate organic matter (POM) that is POC {g POC / g POM}
$f_{OC,d}$ =	fraction of dissolved organic matter (DOM) that is DOC {g DOC / g DOM}
$f_{act,p}$ =	fraction of POM that is active for proton/metal binding {g POM _{active} / g POM}
$f_{act,d}$ =	fraction of DOM that is active for proton/metal binding {g DOM _{active} / g DOM}
$f_{FA,p}$ =	fraction of active POM that is FA {g FA _p / g POM _{active} }
$f_{FA,d}$ =	fraction of active DOM that is FA {g FA _p / g DOM _{active} }

The WHAM7 simulations for Delaware Bay, San Diego Bay and the look-up table development, the following values were used:

$f_{OC,p}$ =	0.5
$f_{OC,d}$ =	0.5
$f_{act,p}$ =	1
$f_{act,d}$ =	0.68
$f_{FA,p}$ =	0.5
$f_{FA,d}$ =	1

Particulate Hydrous Iron Oxide

To estimate metal binding to HFO, the WHAM model requires specification of the mass concentration (e.g., g/L) of particulate HFO (denoted “FeOx” in WHAM). Typical particulate iron measurements have units of mg Fe/L. To convert the particulate iron concentration in mg Fe/L to particulate HFO in g/L the following equation is used:

$$\text{HFO} = \text{Fe} \times \left(\frac{1 \text{ g}}{1000 \text{ mg}} \right) \times f_{\text{HFO}} \times \left(\frac{1 \text{ mol Fe}}{55.845 \text{ mg Fe}} \right) \times \left(\frac{90 \text{ g HFO}}{1 \text{ mol Fe}} \right) \quad (5)$$

where

Fe is the particulate iron concentration measured in a water sample in mass units (mg/L)

f_{HFO} is the fraction of the total iron in suspended particulate material that is HFO (g/g)

The final conversion from moles of Fe to grams HFO is taken from Dzombak and Morel (1990). Research indicates that approximately 40% of the particulate Fe in suspended particulate material is HFO (HydroQual and Manhattan College, 2010).

Partitioning Relationships

Assuming porosity very close to 1

$$K_D = \frac{r}{C_{dis}} \left\{ \frac{M_{partMe}/M_{solid}}{M_{disMe}/L_{water}^3} \right\} = \left\{ \frac{L_{water}^3}{M_{solid}} \right\}$$

$$C_{part} = r \cdot TSS \left\{ \frac{M_{partCu}}{L_{water}^3} \right\}$$

$$K_D = \frac{C_{part}}{C_{dis} \cdot TSS}$$

$$K_D' = K_D \cdot TSS = \frac{C_{part}}{C_{dis}}$$

$$f_{part} = \frac{C_{part}}{C_{dis} + C_{part}} = \frac{K_D'}{1 + K_D'}$$

Note: "Me" in the above stands for "metal"

Input and Output from Look-Up Table Development

Table F-1. State variable for model input.

STATE VARIABLES FOR MODEL INPUT						
Input Number	Total Cu (mol/L)	pH	POC (mg/L)	DOC (mg/L)	Particulate Iron (mg Fe/L)	Salinity (psu)
1	6.29E-08	7.8	0.04	0.75	0.05	32
2	6.29E-08	7.8	0.04	0.75	0.05	33.5
3	6.29E-08	7.8	0.04	0.75	0.05	35
4	6.29E-08	7.8	0.04	0.75	0.4	32
5	6.29E-08	7.8	0.04	0.75	0.4	33.5
6	6.29E-08	7.8	0.04	0.75	0.4	35
7	6.29E-08	7.8	0.04	0.75	3.25	32
8	6.29E-08	7.8	0.04	0.75	3.25	33.5

STATE VARIABLES FOR MODEL INPUT						
Input Number	Total Cu (mol/L)	pH	POC (mg/L)	DOC (mg/L)	Particulate Iron (mg Fe/L)	Salinity (psu)
9	6.29E-08	7.8	0.04	0.75	3.25	35
10	6.29E-08	7.8	0.04	1.5	0.05	32
11	6.29E-08	7.8	0.04	1.5	0.05	33.5
12	6.29E-08	7.8	0.04	1.5	0.05	35
13	6.29E-08	7.8	0.04	1.5	0.4	32
14	6.29E-08	7.8	0.04	1.5	0.4	33.5
15	6.29E-08	7.8	0.04	1.5	0.4	35
16	6.29E-08	7.8	0.04	1.5	3.25	32
17	6.29E-08	7.8	0.04	1.5	3.25	33.5
18	6.29E-08	7.8	0.04	1.5	3.25	35
19	6.29E-08	7.8	0.04	4	0.05	32
20	6.29E-08	7.8	0.04	4	0.05	33.5
21	6.29E-08	7.8	0.04	4	0.05	35
22	6.29E-08	7.8	0.04	4	0.4	32
23	6.29E-08	7.8	0.04	4	0.4	33.5
24	6.29E-08	7.8	0.04	4	0.4	35
25	6.29E-08	7.8	0.04	4	3.25	32
26	6.29E-08	7.8	0.04	4	3.25	33.5
27	6.29E-08	7.8	0.04	4	3.25	35
28	6.29E-08	7.8	0.25	0.75	0.05	32
29	6.29E-08	7.8	0.25	0.75	0.05	33.5
30	6.29E-08	7.8	0.25	0.75	0.05	35
31	6.29E-08	7.8	0.25	0.75	0.4	32
32	6.29E-08	7.8	0.25	0.75	0.4	33.5
33	6.29E-08	7.8	0.25	0.75	0.4	35
34	6.29E-08	7.8	0.25	0.75	3.25	32
35	6.29E-08	7.8	0.25	0.75	3.25	33.5
36	6.29E-08	7.8	0.25	0.75	3.25	35
37	6.29E-08	7.8	0.25	1.5	0.05	32
38	6.29E-08	7.8	0.25	1.5	0.05	33.5
39	6.29E-08	7.8	0.25	1.5	0.05	35
40	6.29E-08	7.8	0.25	1.5	0.4	32
41	6.29E-08	7.8	0.25	1.5	0.4	33.5
42	6.29E-08	7.8	0.25	1.5	0.4	35
43	6.29E-08	7.8	0.25	1.5	3.25	32
44	6.29E-08	7.8	0.25	1.5	3.25	33.5
45	6.29E-08	7.8	0.25	1.5	3.25	35
46	6.29E-08	7.8	0.25	4	0.05	32
47	6.29E-08	7.8	0.25	4	0.05	33.5
48	6.29E-08	7.8	0.25	4	0.05	35
49	6.29E-08	7.8	0.25	4	0.4	32
50	6.29E-08	7.8	0.25	4	0.4	33.5
51	6.29E-08	7.8	0.25	4	0.4	35
52	6.29E-08	7.8	0.25	4	3.25	32
53	6.29E-08	7.8	0.25	4	3.25	33.5
54	6.29E-08	7.8	0.25	4	3.25	35
55	6.29E-08	7.8	1.6	0.75	0.05	32
56	6.29E-08	7.8	1.6	0.75	0.05	33.5

STATE VARIABLES FOR MODEL INPUT						
Input Number	Total Cu (mol/L)	pH	POC (mg/L)	DOC (mg/L)	Particulate Iron (mg Fe/L)	Salinity (psu)
57	6.29E-08	7.8	1.6	0.75	0.05	35
58	6.29E-08	7.8	1.6	0.75	0.4	32
59	6.29E-08	7.8	1.6	0.75	0.4	33.5
60	6.29E-08	7.8	1.6	0.75	0.4	35
61	6.29E-08	7.8	1.6	0.75	3.25	32
62	6.29E-08	7.8	1.6	0.75	3.25	33.5
63	6.29E-08	7.8	1.6	0.75	3.25	35
64	6.29E-08	7.8	1.6	1.5	0.05	32
65	6.29E-08	7.8	1.6	1.5	0.05	33.5
66	6.29E-08	7.8	1.6	1.5	0.05	35
67	6.29E-08	7.8	1.6	1.5	0.4	32
68	6.29E-08	7.8	1.6	1.5	0.4	33.5
69	6.29E-08	7.8	1.6	1.5	0.4	35
70	6.29E-08	7.8	1.6	1.5	3.25	32
71	6.29E-08	7.8	1.6	1.5	3.25	33.5
72	6.29E-08	7.8	1.6	1.5	3.25	35
73	6.29E-08	7.8	1.6	4	0.05	32
74	6.29E-08	7.8	1.6	4	0.05	33.5
75	6.29E-08	7.8	1.6	4	0.05	35
76	6.29E-08	7.8	1.6	4	0.4	32
77	6.29E-08	7.8	1.6	4	0.4	33.5
78	6.29E-08	7.8	1.6	4	0.4	35
79	6.29E-08	7.8	1.6	4	3.25	32
80	6.29E-08	7.8	1.6	4	3.25	33.5
81	6.29E-08	7.8	1.6	4	3.25	35
82	6.29E-08	8.2	0.04	0.75	0.05	32
83	6.29E-08	8.2	0.04	0.75	0.05	33.5
84	6.29E-08	8.2	0.04	0.75	0.05	35
85	6.29E-08	8.2	0.04	0.75	0.4	32
86	6.29E-08	8.2	0.04	0.75	0.4	33.5
87	6.29E-08	8.2	0.04	0.75	0.4	35
88	6.29E-08	8.2	0.04	0.75	3.25	32
89	6.29E-08	8.2	0.04	0.75	3.25	33.5
90	6.29E-08	8.2	0.04	0.75	3.25	35
91	6.29E-08	8.2	0.04	1.5	0.05	32
92	6.29E-08	8.2	0.04	1.5	0.05	33.5
93	6.29E-08	8.2	0.04	1.5	0.05	35
94	6.29E-08	8.2	0.04	1.5	0.4	32
95	6.29E-08	8.2	0.04	1.5	0.4	33.5
96	6.29E-08	8.2	0.04	1.5	0.4	35
97	6.29E-08	8.2	0.04	1.5	3.25	32
98	6.29E-08	8.2	0.04	1.5	3.25	33.5
99	6.29E-08	8.2	0.04	1.5	3.25	35
100	6.29E-08	8.2	0.04	4	0.05	32
101	6.29E-08	8.2	0.04	4	0.05	33.5
102	6.29E-08	8.2	0.04	4	0.05	35
103	6.29E-08	8.2	0.04	4	0.4	32
104	6.29E-08	8.2	0.04	4	0.4	33.5

STATE VARIABLES FOR MODEL INPUT						
Input Number	Total Cu (mol/L)	pH	POC (mg/L)	DOC (mg/L)	Particulate Iron (mg Fe/L)	Salinity (psu)
105	6.29E-08	8.2	0.04	4	0.4	35
106	6.29E-08	8.2	0.04	4	3.25	32
107	6.29E-08	8.2	0.04	4	3.25	33.5
108	6.29E-08	8.2	0.04	4	3.25	35
109	6.29E-08	8.2	0.25	0.75	0.05	32
110	6.29E-08	8.2	0.25	0.75	0.05	33.5
111	6.29E-08	8.2	0.25	0.75	0.05	35
112	6.29E-08	8.2	0.25	0.75	0.4	32
113	6.29E-08	8.2	0.25	0.75	0.4	33.5
114	6.29E-08	8.2	0.25	0.75	0.4	35
115	6.29E-08	8.2	0.25	0.75	3.25	32
116	6.29E-08	8.2	0.25	0.75	3.25	33.5
117	6.29E-08	8.2	0.25	0.75	3.25	35
118	6.29E-08	8.2	0.25	1.5	0.05	32
119	6.29E-08	8.2	0.25	1.5	0.05	33.5
120	6.29E-08	8.2	0.25	1.5	0.05	35
121	6.29E-08	8.2	0.25	1.5	0.4	32
122	6.29E-08	8.2	0.25	1.5	0.4	33.5
123	6.29E-08	8.2	0.25	1.5	0.4	35
124	6.29E-08	8.2	0.25	1.5	3.25	32
125	6.29E-08	8.2	0.25	1.5	3.25	33.5
126	6.29E-08	8.2	0.25	1.5	3.25	35
127	6.29E-08	8.2	0.25	4	0.05	32
128	6.29E-08	8.2	0.25	4	0.05	33.5
129	6.29E-08	8.2	0.25	4	0.05	35
130	6.29E-08	8.2	0.25	4	0.4	32
131	6.29E-08	8.2	0.25	4	0.4	33.5
132	6.29E-08	8.2	0.25	4	0.4	35
133	6.29E-08	8.2	0.25	4	3.25	32
134	6.29E-08	8.2	0.25	4	3.25	33.5
135	6.29E-08	8.2	0.25	4	3.25	35
136	6.29E-08	8.2	1.6	0.75	0.05	32
137	6.29E-08	8.2	1.6	0.75	0.05	33.5
138	6.29E-08	8.2	1.6	0.75	0.05	35
139	6.29E-08	8.2	1.6	0.75	0.4	32
140	6.29E-08	8.2	1.6	0.75	0.4	33.5
141	6.29E-08	8.2	1.6	0.75	0.4	35
142	6.29E-08	8.2	1.6	0.75	3.25	32
143	6.29E-08	8.2	1.6	0.75	3.25	33.5
144	6.29E-08	8.2	1.6	0.75	3.25	35
145	6.29E-08	8.2	1.6	1.5	0.05	32
146	6.29E-08	8.2	1.6	1.5	0.05	33.5
147	6.29E-08	8.2	1.6	1.5	0.05	35
148	6.29E-08	8.2	1.6	1.5	0.4	32
149	6.29E-08	8.2	1.6	1.5	0.4	33.5
150	6.29E-08	8.2	1.6	1.5	0.4	35
151	6.29E-08	8.2	1.6	1.5	3.25	32
152	6.29E-08	8.2	1.6	1.5	3.25	33.5

STATE VARIABLES FOR MODEL INPUT						
Input Number	Total Cu (mol/L)	pH	POC (mg/L)	DOC (mg/L)	Particulate Iron (mg Fe/L)	Salinity (psu)
153	6.29E-08	8.2	1.6	1.5	3.25	35
154	6.29E-08	8.2	1.6	4	0.05	32
155	6.29E-08	8.2	1.6	4	0.05	33.5
156	6.29E-08	8.2	1.6	4	0.05	35
157	6.29E-08	8.2	1.6	4	0.4	32
158	6.29E-08	8.2	1.6	4	0.4	33.5
159	6.29E-08	8.2	1.6	4	0.4	35
160	6.29E-08	8.2	1.6	4	3.25	32
161	6.29E-08	8.2	1.6	4	3.25	33.5
162	6.29E-08	8.2	1.6	4	3.25	35
163	6.29E-08	8.6	0.04	0.75	0.05	32
164	6.29E-08	8.6	0.04	0.75	0.05	33.5
165	6.29E-08	8.6	0.04	0.75	0.05	35
166	6.29E-08	8.6	0.04	0.75	0.4	32
167	6.29E-08	8.6	0.04	0.75	0.4	33.5
168	6.29E-08	8.6	0.04	0.75	0.4	35
169	6.29E-08	8.6	0.04	0.75	3.25	32
170	6.29E-08	8.6	0.04	0.75	3.25	33.5
171	6.29E-08	8.6	0.04	0.75	3.25	35
172	6.29E-08	8.6	0.04	1.5	0.05	32
173	6.29E-08	8.6	0.04	1.5	0.05	33.5
174	6.29E-08	8.6	0.04	1.5	0.05	35
175	6.29E-08	8.6	0.04	1.5	0.4	32
176	6.29E-08	8.6	0.04	1.5	0.4	33.5
177	6.29E-08	8.6	0.04	1.5	0.4	35
178	6.29E-08	8.6	0.04	1.5	3.25	32
179	6.29E-08	8.6	0.04	1.5	3.25	33.5
180	6.29E-08	8.6	0.04	1.5	3.25	35
181	6.29E-08	8.6	0.04	4	0.05	32
182	6.29E-08	8.6	0.04	4	0.05	33.5
183	6.29E-08	8.6	0.04	4	0.05	35
184	6.29E-08	8.6	0.04	4	0.4	32
185	6.29E-08	8.6	0.04	4	0.4	33.5
186	6.29E-08	8.6	0.04	4	0.4	35
187	6.29E-08	8.6	0.04	4	3.25	32
188	6.29E-08	8.6	0.04	4	3.25	33.5
189	6.29E-08	8.6	0.04	4	3.25	35
190	6.29E-08	8.6	0.25	0.75	0.05	32
191	6.29E-08	8.6	0.25	0.75	0.05	33.5
192	6.29E-08	8.6	0.25	0.75	0.05	35
193	6.29E-08	8.6	0.25	0.75	0.4	32
194	6.29E-08	8.6	0.25	0.75	0.4	33.5
195	6.29E-08	8.6	0.25	0.75	0.4	35
196	6.29E-08	8.6	0.25	0.75	3.25	32
197	6.29E-08	8.6	0.25	0.75	3.25	33.5
198	6.29E-08	8.6	0.25	0.75	3.25	35
199	6.29E-08	8.6	0.25	1.5	0.05	32
200	6.29E-08	8.6	0.25	1.5	0.05	33.5

STATE VARIABLES FOR MODEL INPUT						
Input Number	Total Cu (mol/L)	pH	POC (mg/L)	DOC (mg/L)	Particulate Iron (mg Fe/L)	Salinity (psu)
201	6.29E-08	8.6	0.25	1.5	0.05	35
202	6.29E-08	8.6	0.25	1.5	0.4	32
203	6.29E-08	8.6	0.25	1.5	0.4	33.5
204	6.29E-08	8.6	0.25	1.5	0.4	35
205	6.29E-08	8.6	0.25	1.5	3.25	32
206	6.29E-08	8.6	0.25	1.5	3.25	33.5
207	6.29E-08	8.6	0.25	1.5	3.25	35
208	6.29E-08	8.6	0.25	4	0.05	32
209	6.29E-08	8.6	0.25	4	0.05	33.5
210	6.29E-08	8.6	0.25	4	0.05	35
211	6.29E-08	8.6	0.25	4	0.4	32
212	6.29E-08	8.6	0.25	4	0.4	33.5
213	6.29E-08	8.6	0.25	4	0.4	35
214	6.29E-08	8.6	0.25	4	3.25	32
215	6.29E-08	8.6	0.25	4	3.25	33.5
216	6.29E-08	8.6	0.25	4	3.25	35
217	6.29E-08	8.6	1.6	0.75	0.05	32
218	6.29E-08	8.6	1.6	0.75	0.05	33.5
219	6.29E-08	8.6	1.6	0.75	0.05	35
220	6.29E-08	8.6	1.6	0.75	0.4	32
221	6.29E-08	8.6	1.6	0.75	0.4	33.5
222	6.29E-08	8.6	1.6	0.75	0.4	35
223	6.29E-08	8.6	1.6	0.75	3.25	32
224	6.29E-08	8.6	1.6	0.75	3.25	33.5
225	6.29E-08	8.6	1.6	0.75	3.25	35
226	6.29E-08	8.6	1.6	1.5	0.05	32
227	6.29E-08	8.6	1.6	1.5	0.05	33.5
228	6.29E-08	8.6	1.6	1.5	0.05	35
229	6.29E-08	8.6	1.6	1.5	0.4	32
230	6.29E-08	8.6	1.6	1.5	0.4	33.5
231	6.29E-08	8.6	1.6	1.5	0.4	35
232	6.29E-08	8.6	1.6	1.5	3.25	32
233	6.29E-08	8.6	1.6	1.5	3.25	33.5
234	6.29E-08	8.6	1.6	1.5	3.25	35
235	6.29E-08	8.6	1.6	4	0.05	32
236	6.29E-08	8.6	1.6	4	0.05	33.5
237	6.29E-08	8.6	1.6	4	0.05	35
238	6.29E-08	8.6	1.6	4	0.4	32
239	6.29E-08	8.6	1.6	4	0.4	33.5
240	6.29E-08	8.6	1.6	4	0.4	35
241	6.29E-08	8.6	1.6	4	3.25	32
242	6.29E-08	8.6	1.6	4	3.25	33.5
243	6.29E-08	8.6	1.6	4	3.25	35
244	1.57E-07	7.8	0.04	0.75	0.05	32
245	1.57E-07	7.8	0.04	0.75	0.05	33.5
246	1.57E-07	7.8	0.04	0.75	0.05	35
247	1.57E-07	7.8	0.04	0.75	0.4	32
248	1.57E-07	7.8	0.04	0.75	0.4	33.5

STATE VARIABLES FOR MODEL INPUT						
Input Number	Total Cu (mol/L)	pH	POC (mg/L)	DOC (mg/L)	Particulate Iron (mg Fe/L)	Salinity (psu)
249	1.57E-07	7.8	0.04	0.75	0.4	35
250	1.57E-07	7.8	0.04	0.75	3.25	32
251	1.57E-07	7.8	0.04	0.75	3.25	33.5
252	1.57E-07	7.8	0.04	0.75	3.25	35
253	1.57E-07	7.8	0.04	1.5	0.05	32
254	1.57E-07	7.8	0.04	1.5	0.05	33.5
255	1.57E-07	7.8	0.04	1.5	0.05	35
256	1.57E-07	7.8	0.04	1.5	0.4	32
257	1.57E-07	7.8	0.04	1.5	0.4	33.5
258	1.57E-07	7.8	0.04	1.5	0.4	35
259	1.57E-07	7.8	0.04	1.5	3.25	32
260	1.57E-07	7.8	0.04	1.5	3.25	33.5
261	1.57E-07	7.8	0.04	1.5	3.25	35
262	1.57E-07	7.8	0.04	4	0.05	32
263	1.57E-07	7.8	0.04	4	0.05	33.5
264	1.57E-07	7.8	0.04	4	0.05	35
265	1.57E-07	7.8	0.04	4	0.4	32
266	1.57E-07	7.8	0.04	4	0.4	33.5
267	1.57E-07	7.8	0.04	4	0.4	35
268	1.57E-07	7.8	0.04	4	3.25	32
269	1.57E-07	7.8	0.04	4	3.25	33.5
270	1.57E-07	7.8	0.04	4	3.25	35
271	1.57E-07	7.8	0.25	0.75	0.05	32
272	1.57E-07	7.8	0.25	0.75	0.05	33.5
273	1.57E-07	7.8	0.25	0.75	0.05	35
274	1.57E-07	7.8	0.25	0.75	0.4	32
275	1.57E-07	7.8	0.25	0.75	0.4	33.5
276	1.57E-07	7.8	0.25	0.75	0.4	35
277	1.57E-07	7.8	0.25	0.75	3.25	32
278	1.57E-07	7.8	0.25	0.75	3.25	33.5
279	1.57E-07	7.8	0.25	0.75	3.25	35
280	1.57E-07	7.8	0.25	1.5	0.05	32
281	1.57E-07	7.8	0.25	1.5	0.05	33.5
282	1.57E-07	7.8	0.25	1.5	0.05	35
283	1.57E-07	7.8	0.25	1.5	0.4	32
284	1.57E-07	7.8	0.25	1.5	0.4	33.5
285	1.57E-07	7.8	0.25	1.5	0.4	35
286	1.57E-07	7.8	0.25	1.5	3.25	32
287	1.57E-07	7.8	0.25	1.5	3.25	33.5
288	1.57E-07	7.8	0.25	1.5	3.25	35
289	1.57E-07	7.8	0.25	4	0.05	32
290	1.57E-07	7.8	0.25	4	0.05	33.5
291	1.57E-07	7.8	0.25	4	0.05	35
292	1.57E-07	7.8	0.25	4	0.4	32
293	1.57E-07	7.8	0.25	4	0.4	33.5
294	1.57E-07	7.8	0.25	4	0.4	35
295	1.57E-07	7.8	0.25	4	3.25	32
296	1.57E-07	7.8	0.25	4	3.25	33.5

STATE VARIABLES FOR MODEL INPUT						
Input Number	Total Cu (mol/L)	pH	POC (mg/L)	DOC (mg/L)	Particulate Iron (mg Fe/L)	Salinity (psu)
297	1.57E-07	7.8	0.25	4	3.25	35
298	1.57E-07	7.8	1.6	0.75	0.05	32
299	1.57E-07	7.8	1.6	0.75	0.05	33.5
300	1.57E-07	7.8	1.6	0.75	0.05	35
301	1.57E-07	7.8	1.6	0.75	0.4	32
302	1.57E-07	7.8	1.6	0.75	0.4	33.5
303	1.57E-07	7.8	1.6	0.75	0.4	35
304	1.57E-07	7.8	1.6	0.75	3.25	32
305	1.57E-07	7.8	1.6	0.75	3.25	33.5
306	1.57E-07	7.8	1.6	0.75	3.25	35
307	1.57E-07	7.8	1.6	1.5	0.05	32
308	1.57E-07	7.8	1.6	1.5	0.05	33.5
309	1.57E-07	7.8	1.6	1.5	0.05	35
310	1.57E-07	7.8	1.6	1.5	0.4	32
311	1.57E-07	7.8	1.6	1.5	0.4	33.5
312	1.57E-07	7.8	1.6	1.5	0.4	35
313	1.57E-07	7.8	1.6	1.5	3.25	32
314	1.57E-07	7.8	1.6	1.5	3.25	33.5
315	1.57E-07	7.8	1.6	1.5	3.25	35
316	1.57E-07	7.8	1.6	4	0.05	32
317	1.57E-07	7.8	1.6	4	0.05	33.5
318	1.57E-07	7.8	1.6	4	0.05	35
319	1.57E-07	7.8	1.6	4	0.4	32
320	1.57E-07	7.8	1.6	4	0.4	33.5
321	1.57E-07	7.8	1.6	4	0.4	35
322	1.57E-07	7.8	1.6	4	3.25	32
323	1.57E-07	7.8	1.6	4	3.25	33.5
324	1.57E-07	7.8	1.6	4	3.25	35
325	1.57E-07	8.2	0.04	0.75	0.05	32
326	1.57E-07	8.2	0.04	0.75	0.05	33.5
327	1.57E-07	8.2	0.04	0.75	0.05	35
328	1.57E-07	8.2	0.04	0.75	0.4	32
329	1.57E-07	8.2	0.04	0.75	0.4	33.5
330	1.57E-07	8.2	0.04	0.75	0.4	35
331	1.57E-07	8.2	0.04	0.75	3.25	32
332	1.57E-07	8.2	0.04	0.75	3.25	33.5
333	1.57E-07	8.2	0.04	0.75	3.25	35
334	1.57E-07	8.2	0.04	1.5	0.05	32
335	1.57E-07	8.2	0.04	1.5	0.05	33.5
336	1.57E-07	8.2	0.04	1.5	0.05	35
337	1.57E-07	8.2	0.04	1.5	0.4	32
338	1.57E-07	8.2	0.04	1.5	0.4	33.5
339	1.57E-07	8.2	0.04	1.5	0.4	35
340	1.57E-07	8.2	0.04	1.5	3.25	32
341	1.57E-07	8.2	0.04	1.5	3.25	33.5
342	1.57E-07	8.2	0.04	1.5	3.25	35
343	1.57E-07	8.2	0.04	4	0.05	32
344	1.57E-07	8.2	0.04	4	0.05	33.5

STATE VARIABLES FOR MODEL INPUT						
Input Number	Total Cu (mol/L)	pH	POC (mg/L)	DOC (mg/L)	Particulate Iron (mg Fe/L)	Salinity (psu)
345	1.57E-07	8.2	0.04	4	0.05	35
346	1.57E-07	8.2	0.04	4	0.4	32
347	1.57E-07	8.2	0.04	4	0.4	33.5
348	1.57E-07	8.2	0.04	4	0.4	35
349	1.57E-07	8.2	0.04	4	3.25	32
350	1.57E-07	8.2	0.04	4	3.25	33.5
351	1.57E-07	8.2	0.04	4	3.25	35
352	1.57E-07	8.2	0.25	0.75	0.05	32
353	1.57E-07	8.2	0.25	0.75	0.05	33.5
354	1.57E-07	8.2	0.25	0.75	0.05	35
355	1.57E-07	8.2	0.25	0.75	0.4	32
356	1.57E-07	8.2	0.25	0.75	0.4	33.5
357	1.57E-07	8.2	0.25	0.75	0.4	35
358	1.57E-07	8.2	0.25	0.75	3.25	32
359	1.57E-07	8.2	0.25	0.75	3.25	33.5
360	1.57E-07	8.2	0.25	0.75	3.25	35
361	1.57E-07	8.2	0.25	1.5	0.05	32
362	1.57E-07	8.2	0.25	1.5	0.05	33.5
363	1.57E-07	8.2	0.25	1.5	0.05	35
364	1.57E-07	8.2	0.25	1.5	0.4	32
365	1.57E-07	8.2	0.25	1.5	0.4	33.5
366	1.57E-07	8.2	0.25	1.5	0.4	35
367	1.57E-07	8.2	0.25	1.5	3.25	32
368	1.57E-07	8.2	0.25	1.5	3.25	33.5
369	1.57E-07	8.2	0.25	1.5	3.25	35
370	1.57E-07	8.2	0.25	4	0.05	32
371	1.57E-07	8.2	0.25	4	0.05	33.5
372	1.57E-07	8.2	0.25	4	0.05	35
373	1.57E-07	8.2	0.25	4	0.4	32
374	1.57E-07	8.2	0.25	4	0.4	33.5
375	1.57E-07	8.2	0.25	4	0.4	35
376	1.57E-07	8.2	0.25	4	3.25	32
377	1.57E-07	8.2	0.25	4	3.25	33.5
378	1.57E-07	8.2	0.25	4	3.25	35
379	1.57E-07	8.2	1.6	0.75	0.05	32
380	1.57E-07	8.2	1.6	0.75	0.05	33.5
381	1.57E-07	8.2	1.6	0.75	0.05	35
382	1.57E-07	8.2	1.6	0.75	0.4	32
383	1.57E-07	8.2	1.6	0.75	0.4	33.5
384	1.57E-07	8.2	1.6	0.75	0.4	35
385	1.57E-07	8.2	1.6	0.75	3.25	32
386	1.57E-07	8.2	1.6	0.75	3.25	33.5
387	1.57E-07	8.2	1.6	0.75	3.25	35
388	1.57E-07	8.2	1.6	1.5	0.05	32
389	1.57E-07	8.2	1.6	1.5	0.05	33.5
390	1.57E-07	8.2	1.6	1.5	0.05	35
391	1.57E-07	8.2	1.6	1.5	0.4	32
392	1.57E-07	8.2	1.6	1.5	0.4	33.5

STATE VARIABLES FOR MODEL INPUT						
Input Number	Total Cu (mol/L)	pH	POC (mg/L)	DOC (mg/L)	Particulate Iron (mg Fe/L)	Salinity (psu)
393	1.57E-07	8.2	1.6	1.5	0.4	35
394	1.57E-07	8.2	1.6	1.5	3.25	32
395	1.57E-07	8.2	1.6	1.5	3.25	33.5
396	1.57E-07	8.2	1.6	1.5	3.25	35
397	1.57E-07	8.2	1.6	4	0.05	32
398	1.57E-07	8.2	1.6	4	0.05	33.5
399	1.57E-07	8.2	1.6	4	0.05	35
400	1.57E-07	8.2	1.6	4	0.4	32
401	1.57E-07	8.2	1.6	4	0.4	33.5
402	1.57E-07	8.2	1.6	4	0.4	35
403	1.57E-07	8.2	1.6	4	3.25	32
404	1.57E-07	8.2	1.6	4	3.25	33.5
405	1.57E-07	8.2	1.6	4	3.25	35
406	1.57E-07	8.6	0.04	0.75	0.05	32
407	1.57E-07	8.6	0.04	0.75	0.05	33.5
408	1.57E-07	8.6	0.04	0.75	0.05	35
409	1.57E-07	8.6	0.04	0.75	0.4	32
410	1.57E-07	8.6	0.04	0.75	0.4	33.5
411	1.57E-07	8.6	0.04	0.75	0.4	35
412	1.57E-07	8.6	0.04	0.75	3.25	32
413	1.57E-07	8.6	0.04	0.75	3.25	33.5
414	1.57E-07	8.6	0.04	0.75	3.25	35
415	1.57E-07	8.6	0.04	1.5	0.05	32
416	1.57E-07	8.6	0.04	1.5	0.05	33.5
417	1.57E-07	8.6	0.04	1.5	0.05	35
418	1.57E-07	8.6	0.04	1.5	0.4	32
419	1.57E-07	8.6	0.04	1.5	0.4	33.5
420	1.57E-07	8.6	0.04	1.5	0.4	35
421	1.57E-07	8.6	0.04	1.5	3.25	32
422	1.57E-07	8.6	0.04	1.5	3.25	33.5
423	1.57E-07	8.6	0.04	1.5	3.25	35
424	1.57E-07	8.6	0.04	4	0.05	32
425	1.57E-07	8.6	0.04	4	0.05	33.5
426	1.57E-07	8.6	0.04	4	0.05	35
427	1.57E-07	8.6	0.04	4	0.4	32
428	1.57E-07	8.6	0.04	4	0.4	33.5
429	1.57E-07	8.6	0.04	4	0.4	35
430	1.57E-07	8.6	0.04	4	3.25	32
431	1.57E-07	8.6	0.04	4	3.25	33.5
432	1.57E-07	8.6	0.04	4	3.25	35
433	1.57E-07	8.6	0.25	0.75	0.05	32
434	1.57E-07	8.6	0.25	0.75	0.05	33.5
435	1.57E-07	8.6	0.25	0.75	0.05	35
436	1.57E-07	8.6	0.25	0.75	0.4	32
437	1.57E-07	8.6	0.25	0.75	0.4	33.5
438	1.57E-07	8.6	0.25	0.75	0.4	35
439	1.57E-07	8.6	0.25	0.75	3.25	32
440	1.57E-07	8.6	0.25	0.75	3.25	33.5

STATE VARIABLES FOR MODEL INPUT						
Input Number	Total Cu (mol/L)	pH	POC (mg/L)	DOC (mg/L)	Particulate Iron (mg Fe/L)	Salinity (psu)
441	1.57E-07	8.6	0.25	0.75	3.25	35
442	1.57E-07	8.6	0.25	1.5	0.05	32
443	1.57E-07	8.6	0.25	1.5	0.05	33.5
444	1.57E-07	8.6	0.25	1.5	0.05	35
445	1.57E-07	8.6	0.25	1.5	0.4	32
446	1.57E-07	8.6	0.25	1.5	0.4	33.5
447	1.57E-07	8.6	0.25	1.5	0.4	35
448	1.57E-07	8.6	0.25	1.5	3.25	32
449	1.57E-07	8.6	0.25	1.5	3.25	33.5
450	1.57E-07	8.6	0.25	1.5	3.25	35
451	1.57E-07	8.6	0.25	4	0.05	32
452	1.57E-07	8.6	0.25	4	0.05	33.5
453	1.57E-07	8.6	0.25	4	0.05	35
454	1.57E-07	8.6	0.25	4	0.4	32
455	1.57E-07	8.6	0.25	4	0.4	33.5
456	1.57E-07	8.6	0.25	4	0.4	35
457	1.57E-07	8.6	0.25	4	3.25	32
458	1.57E-07	8.6	0.25	4	3.25	33.5
459	1.57E-07	8.6	0.25	4	3.25	35
460	1.57E-07	8.6	1.6	0.75	0.05	32
461	1.57E-07	8.6	1.6	0.75	0.05	33.5
462	1.57E-07	8.6	1.6	0.75	0.05	35
463	1.57E-07	8.6	1.6	0.75	0.4	32
464	1.57E-07	8.6	1.6	0.75	0.4	33.5
465	1.57E-07	8.6	1.6	0.75	0.4	35
466	1.57E-07	8.6	1.6	0.75	3.25	32
467	1.57E-07	8.6	1.6	0.75	3.25	33.5
468	1.57E-07	8.6	1.6	0.75	3.25	35
469	1.57E-07	8.6	1.6	1.5	0.05	32
470	1.57E-07	8.6	1.6	1.5	0.05	33.5
471	1.57E-07	8.6	1.6	1.5	0.05	35
472	1.57E-07	8.6	1.6	1.5	0.4	32
473	1.57E-07	8.6	1.6	1.5	0.4	33.5
474	1.57E-07	8.6	1.6	1.5	0.4	35
475	1.57E-07	8.6	1.6	1.5	3.25	32
476	1.57E-07	8.6	1.6	1.5	3.25	33.5
477	1.57E-07	8.6	1.6	1.5	3.25	35
478	1.57E-07	8.6	1.6	4	0.05	32
479	1.57E-07	8.6	1.6	4	0.05	33.5
480	1.57E-07	8.6	1.6	4	0.05	35
481	1.57E-07	8.6	1.6	4	0.4	32
482	1.57E-07	8.6	1.6	4	0.4	33.5
483	1.57E-07	8.6	1.6	4	0.4	35
484	1.57E-07	8.6	1.6	4	3.25	32
485	1.57E-07	8.6	1.6	4	3.25	33.5
486	1.57E-07	8.6	1.6	4	3.25	35
487	4.09E-07	7.8	0.04	0.75	0.05	32
488	4.09E-07	7.8	0.04	0.75	0.05	33.5

STATE VARIABLES FOR MODEL INPUT						
Input Number	Total Cu (mol/L)	pH	POC (mg/L)	DOC (mg/L)	Particulate Iron (mg Fe/L)	Salinity (psu)
489	4.09E-07	7.8	0.04	0.75	0.05	35
490	4.09E-07	7.8	0.04	0.75	0.4	32
491	4.09E-07	7.8	0.04	0.75	0.4	33.5
492	4.09E-07	7.8	0.04	0.75	0.4	35
493	4.09E-07	7.8	0.04	0.75	3.25	32
494	4.09E-07	7.8	0.04	0.75	3.25	33.5
495	4.09E-07	7.8	0.04	0.75	3.25	35
496	4.09E-07	7.8	0.04	1.5	0.05	32
497	4.09E-07	7.8	0.04	1.5	0.05	33.5
498	4.09E-07	7.8	0.04	1.5	0.05	35
499	4.09E-07	7.8	0.04	1.5	0.4	32
500	4.09E-07	7.8	0.04	1.5	0.4	33.5
501	4.09E-07	7.8	0.04	1.5	0.4	35
502	4.09E-07	7.8	0.04	1.5	3.25	32
503	4.09E-07	7.8	0.04	1.5	3.25	33.5
504	4.09E-07	7.8	0.04	1.5	3.25	35
505	4.09E-07	7.8	0.04	4	0.05	32
506	4.09E-07	7.8	0.04	4	0.05	33.5
507	4.09E-07	7.8	0.04	4	0.05	35
508	4.09E-07	7.8	0.04	4	0.4	32
509	4.09E-07	7.8	0.04	4	0.4	33.5
510	4.09E-07	7.8	0.04	4	0.4	35
511	4.09E-07	7.8	0.04	4	3.25	32
512	4.09E-07	7.8	0.04	4	3.25	33.5
513	4.09E-07	7.8	0.04	4	3.25	35
514	4.09E-07	7.8	0.25	0.75	0.05	32
515	4.09E-07	7.8	0.25	0.75	0.05	33.5
516	4.09E-07	7.8	0.25	0.75	0.05	35
517	4.09E-07	7.8	0.25	0.75	0.4	32
518	4.09E-07	7.8	0.25	0.75	0.4	33.5
519	4.09E-07	7.8	0.25	0.75	0.4	35
520	4.09E-07	7.8	0.25	0.75	3.25	32
521	4.09E-07	7.8	0.25	0.75	3.25	33.5
522	4.09E-07	7.8	0.25	0.75	3.25	35
523	4.09E-07	7.8	0.25	1.5	0.05	32
524	4.09E-07	7.8	0.25	1.5	0.05	33.5
525	4.09E-07	7.8	0.25	1.5	0.05	35
526	4.09E-07	7.8	0.25	1.5	0.4	32
527	4.09E-07	7.8	0.25	1.5	0.4	33.5
528	4.09E-07	7.8	0.25	1.5	0.4	35
529	4.09E-07	7.8	0.25	1.5	3.25	32
530	4.09E-07	7.8	0.25	1.5	3.25	33.5
531	4.09E-07	7.8	0.25	1.5	3.25	35
532	4.09E-07	7.8	0.25	4	0.05	32
533	4.09E-07	7.8	0.25	4	0.05	33.5
534	4.09E-07	7.8	0.25	4	0.05	35
535	4.09E-07	7.8	0.25	4	0.4	32
536	4.09E-07	7.8	0.25	4	0.4	33.5

STATE VARIABLES FOR MODEL INPUT						
Input Number	Total Cu (mol/L)	pH	POC (mg/L)	DOC (mg/L)	Particulate Iron (mg Fe/L)	Salinity (psu)
537	4.09E-07	7.8	0.25	4	0.4	35
538	4.09E-07	7.8	0.25	4	3.25	32
539	4.09E-07	7.8	0.25	4	3.25	33.5
540	4.09E-07	7.8	0.25	4	3.25	35
541	4.09E-07	7.8	1.6	0.75	0.05	32
542	4.09E-07	7.8	1.6	0.75	0.05	33.5
543	4.09E-07	7.8	1.6	0.75	0.05	35
544	4.09E-07	7.8	1.6	0.75	0.4	32
545	4.09E-07	7.8	1.6	0.75	0.4	33.5
546	4.09E-07	7.8	1.6	0.75	0.4	35
547	4.09E-07	7.8	1.6	0.75	3.25	32
548	4.09E-07	7.8	1.6	0.75	3.25	33.5
549	4.09E-07	7.8	1.6	0.75	3.25	35
550	4.09E-07	7.8	1.6	1.5	0.05	32
551	4.09E-07	7.8	1.6	1.5	0.05	33.5
552	4.09E-07	7.8	1.6	1.5	0.05	35
553	4.09E-07	7.8	1.6	1.5	0.4	32
554	4.09E-07	7.8	1.6	1.5	0.4	33.5
555	4.09E-07	7.8	1.6	1.5	0.4	35
556	4.09E-07	7.8	1.6	1.5	3.25	32
557	4.09E-07	7.8	1.6	1.5	3.25	33.5
558	4.09E-07	7.8	1.6	1.5	3.25	35
559	4.09E-07	7.8	1.6	4	0.05	32
560	4.09E-07	7.8	1.6	4	0.05	33.5
561	4.09E-07	7.8	1.6	4	0.05	35
562	4.09E-07	7.8	1.6	4	0.4	32
563	4.09E-07	7.8	1.6	4	0.4	33.5
564	4.09E-07	7.8	1.6	4	0.4	35
565	4.09E-07	7.8	1.6	4	3.25	32
566	4.09E-07	7.8	1.6	4	3.25	33.5
567	4.09E-07	7.8	1.6	4	3.25	35
568	4.09E-07	8.2	0.04	0.75	0.05	32
569	4.09E-07	8.2	0.04	0.75	0.05	33.5
570	4.09E-07	8.2	0.04	0.75	0.05	35
571	4.09E-07	8.2	0.04	0.75	0.4	32
572	4.09E-07	8.2	0.04	0.75	0.4	33.5
573	4.09E-07	8.2	0.04	0.75	0.4	35
574	4.09E-07	8.2	0.04	0.75	3.25	32
575	4.09E-07	8.2	0.04	0.75	3.25	33.5
576	4.09E-07	8.2	0.04	0.75	3.25	35
577	4.09E-07	8.2	0.04	1.5	0.05	32
578	4.09E-07	8.2	0.04	1.5	0.05	33.5
579	4.09E-07	8.2	0.04	1.5	0.05	35
580	4.09E-07	8.2	0.04	1.5	0.4	32
581	4.09E-07	8.2	0.04	1.5	0.4	33.5
582	4.09E-07	8.2	0.04	1.5	0.4	35
583	4.09E-07	8.2	0.04	1.5	3.25	32
584	4.09E-07	8.2	0.04	1.5	3.25	33.5

STATE VARIABLES FOR MODEL INPUT						
Input Number	Total Cu (mol/L)	pH	POC (mg/L)	DOC (mg/L)	Particulate Iron (mg Fe/L)	Salinity (psu)
585	4.09E-07	8.2	0.04	1.5	3.25	35
586	4.09E-07	8.2	0.04	4	0.05	32
587	4.09E-07	8.2	0.04	4	0.05	33.5
588	4.09E-07	8.2	0.04	4	0.05	35
589	4.09E-07	8.2	0.04	4	0.4	32
590	4.09E-07	8.2	0.04	4	0.4	33.5
591	4.09E-07	8.2	0.04	4	0.4	35
592	4.09E-07	8.2	0.04	4	3.25	32
593	4.09E-07	8.2	0.04	4	3.25	33.5
594	4.09E-07	8.2	0.04	4	3.25	35
595	4.09E-07	8.2	0.25	0.75	0.05	32
596	4.09E-07	8.2	0.25	0.75	0.05	33.5
597	4.09E-07	8.2	0.25	0.75	0.05	35
598	4.09E-07	8.2	0.25	0.75	0.4	32
599	4.09E-07	8.2	0.25	0.75	0.4	33.5
600	4.09E-07	8.2	0.25	0.75	0.4	35
601	4.09E-07	8.2	0.25	0.75	3.25	32
602	4.09E-07	8.2	0.25	0.75	3.25	33.5
603	4.09E-07	8.2	0.25	0.75	3.25	35
604	4.09E-07	8.2	0.25	1.5	0.05	32
605	4.09E-07	8.2	0.25	1.5	0.05	33.5
606	4.09E-07	8.2	0.25	1.5	0.05	35
607	4.09E-07	8.2	0.25	1.5	0.4	32
608	4.09E-07	8.2	0.25	1.5	0.4	33.5
609	4.09E-07	8.2	0.25	1.5	0.4	35
610	4.09E-07	8.2	0.25	1.5	3.25	32
611	4.09E-07	8.2	0.25	1.5	3.25	33.5
612	4.09E-07	8.2	0.25	1.5	3.25	35
613	4.09E-07	8.2	0.25	4	0.05	32
614	4.09E-07	8.2	0.25	4	0.05	33.5
615	4.09E-07	8.2	0.25	4	0.05	35
616	4.09E-07	8.2	0.25	4	0.4	32
617	4.09E-07	8.2	0.25	4	0.4	33.5
618	4.09E-07	8.2	0.25	4	0.4	35
619	4.09E-07	8.2	0.25	4	3.25	32
620	4.09E-07	8.2	0.25	4	3.25	33.5
621	4.09E-07	8.2	0.25	4	3.25	35
622	4.09E-07	8.2	1.6	0.75	0.05	32
623	4.09E-07	8.2	1.6	0.75	0.05	33.5
624	4.09E-07	8.2	1.6	0.75	0.05	35
625	4.09E-07	8.2	1.6	0.75	0.4	32
626	4.09E-07	8.2	1.6	0.75	0.4	33.5
627	4.09E-07	8.2	1.6	0.75	0.4	35
628	4.09E-07	8.2	1.6	0.75	3.25	32
629	4.09E-07	8.2	1.6	0.75	3.25	33.5
630	4.09E-07	8.2	1.6	0.75	3.25	35
631	4.09E-07	8.2	1.6	1.5	0.05	32
632	4.09E-07	8.2	1.6	1.5	0.05	33.5

STATE VARIABLES FOR MODEL INPUT						
Input Number	Total Cu (mol/L)	pH	POC (mg/L)	DOC (mg/L)	Particulate Iron (mg Fe/L)	Salinity (psu)
633	4.09E-07	8.2	1.6	1.5	0.05	35
634	4.09E-07	8.2	1.6	1.5	0.4	32
635	4.09E-07	8.2	1.6	1.5	0.4	33.5
636	4.09E-07	8.2	1.6	1.5	0.4	35
637	4.09E-07	8.2	1.6	1.5	3.25	32
638	4.09E-07	8.2	1.6	1.5	3.25	33.5
639	4.09E-07	8.2	1.6	1.5	3.25	35
640	4.09E-07	8.2	1.6	4	0.05	32
641	4.09E-07	8.2	1.6	4	0.05	33.5
642	4.09E-07	8.2	1.6	4	0.05	35
643	4.09E-07	8.2	1.6	4	0.4	32
644	4.09E-07	8.2	1.6	4	0.4	33.5
645	4.09E-07	8.2	1.6	4	0.4	35
646	4.09E-07	8.2	1.6	4	3.25	32
647	4.09E-07	8.2	1.6	4	3.25	33.5
648	4.09E-07	8.2	1.6	4	3.25	35
649	4.09E-07	8.6	0.04	0.75	0.05	32
650	4.09E-07	8.6	0.04	0.75	0.05	33.5
651	4.09E-07	8.6	0.04	0.75	0.05	35
652	4.09E-07	8.6	0.04	0.75	0.4	32
653	4.09E-07	8.6	0.04	0.75	0.4	33.5
654	4.09E-07	8.6	0.04	0.75	0.4	35
655	4.09E-07	8.6	0.04	0.75	3.25	32
656	4.09E-07	8.6	0.04	0.75	3.25	33.5
657	4.09E-07	8.6	0.04	0.75	3.25	35
658	4.09E-07	8.6	0.04	1.5	0.05	32
659	4.09E-07	8.6	0.04	1.5	0.05	33.5
660	4.09E-07	8.6	0.04	1.5	0.05	35
661	4.09E-07	8.6	0.04	1.5	0.4	32
662	4.09E-07	8.6	0.04	1.5	0.4	33.5
663	4.09E-07	8.6	0.04	1.5	0.4	35
664	4.09E-07	8.6	0.04	1.5	3.25	32
665	4.09E-07	8.6	0.04	1.5	3.25	33.5
666	4.09E-07	8.6	0.04	1.5	3.25	35
667	4.09E-07	8.6	0.04	4	0.05	32
668	4.09E-07	8.6	0.04	4	0.05	33.5
669	4.09E-07	8.6	0.04	4	0.05	35
670	4.09E-07	8.6	0.04	4	0.4	32
671	4.09E-07	8.6	0.04	4	0.4	33.5
672	4.09E-07	8.6	0.04	4	0.4	35
673	4.09E-07	8.6	0.04	4	3.25	32
674	4.09E-07	8.6	0.04	4	3.25	33.5
675	4.09E-07	8.6	0.04	4	3.25	35
676	4.09E-07	8.6	0.25	0.75	0.05	32
677	4.09E-07	8.6	0.25	0.75	0.05	33.5
678	4.09E-07	8.6	0.25	0.75	0.05	35
679	4.09E-07	8.6	0.25	0.75	0.4	32
680	4.09E-07	8.6	0.25	0.75	0.4	33.5

STATE VARIABLES FOR MODEL INPUT						
Input Number	Total Cu (mol/L)	pH	POC (mg/L)	DOC (mg/L)	Particulate Iron (mg Fe/L)	Salinity (psu)
681	4.09E-07	8.6	0.25	0.75	0.4	35
682	4.09E-07	8.6	0.25	0.75	3.25	32
683	4.09E-07	8.6	0.25	0.75	3.25	33.5
684	4.09E-07	8.6	0.25	0.75	3.25	35
685	4.09E-07	8.6	0.25	1.5	0.05	32
686	4.09E-07	8.6	0.25	1.5	0.05	33.5
687	4.09E-07	8.6	0.25	1.5	0.05	35
688	4.09E-07	8.6	0.25	1.5	0.4	32
689	4.09E-07	8.6	0.25	1.5	0.4	33.5
690	4.09E-07	8.6	0.25	1.5	0.4	35
691	4.09E-07	8.6	0.25	1.5	3.25	32
692	4.09E-07	8.6	0.25	1.5	3.25	33.5
693	4.09E-07	8.6	0.25	1.5	3.25	35
694	4.09E-07	8.6	0.25	4	0.05	32
695	4.09E-07	8.6	0.25	4	0.05	33.5
696	4.09E-07	8.6	0.25	4	0.05	35
697	4.09E-07	8.6	0.25	4	0.4	32
698	4.09E-07	8.6	0.25	4	0.4	33.5
699	4.09E-07	8.6	0.25	4	0.4	35
700	4.09E-07	8.6	0.25	4	3.25	32
701	4.09E-07	8.6	0.25	4	3.25	33.5
702	4.09E-07	8.6	0.25	4	3.25	35
703	4.09E-07	8.6	1.6	0.75	0.05	32
704	4.09E-07	8.6	1.6	0.75	0.05	33.5
705	4.09E-07	8.6	1.6	0.75	0.05	35
706	4.09E-07	8.6	1.6	0.75	0.4	32
707	4.09E-07	8.6	1.6	0.75	0.4	33.5
708	4.09E-07	8.6	1.6	0.75	0.4	35
709	4.09E-07	8.6	1.6	0.75	3.25	32
710	4.09E-07	8.6	1.6	0.75	3.25	33.5
711	4.09E-07	8.6	1.6	0.75	3.25	35
712	4.09E-07	8.6	1.6	1.5	0.05	32
713	4.09E-07	8.6	1.6	1.5	0.05	33.5
714	4.09E-07	8.6	1.6	1.5	0.05	35
715	4.09E-07	8.6	1.6	1.5	0.4	32
716	4.09E-07	8.6	1.6	1.5	0.4	33.5
717	4.09E-07	8.6	1.6	1.5	0.4	35
718	4.09E-07	8.6	1.6	1.5	3.25	32
719	4.09E-07	8.6	1.6	1.5	3.25	33.5
720	4.09E-07	8.6	1.6	1.5	3.25	35
721	4.09E-07	8.6	1.6	4	0.05	32
722	4.09E-07	8.6	1.6	4	0.05	33.5
723	4.09E-07	8.6	1.6	4	0.05	35
724	4.09E-07	8.6	1.6	4	0.4	32
725	4.09E-07	8.6	1.6	4	0.4	33.5
726	4.09E-07	8.6	1.6	4	0.4	35
727	4.09E-07	8.6	1.6	4	3.25	32
728	4.09E-07	8.6	1.6	4	3.25	33.5

STATE VARIABLES FOR MODEL INPUT						
Input Number	Total Cu (mol/L)	pH	POC (mg/L)	DOC (mg/L)	Particulate Iron (mg Fe/L)	Salinity (psu)
729	4.09E-07	8.6	1.6	4	3.25	35

Table F-2. WHAM input deck and outputs.

WHAM7 INPUT																				WHAM7 OUTPUT	
Description	SPM (g/L)	Temp (K)	pCO2 (atm)	pH	Part HA (g/L)	Part FA (g/L)	Part FeOx (g/L)	Coll HA (g/L)	Coll FA (g/L)	Na (M)	Mg (M)	{Al3+} (M)	K (M)	Ca (M)	{Fe3+} (M)	Tot Cu (M)	Cl (M)	SO4 (M)	CO3 (M)	log(KD' = log(KD x TSS) (dimensionless))	Fract. Part. (dimensionless)
1	1000	298.15	---	7.8	4.000E-05	4.000E-05	3.223E-05	0.000E+00	1.020E-03	4.279E-01	4.865E-02	1.259E-15	9.328E-03	9.354E-03	3.221E-19	6.295E-08	4.983E-01	2.579E-02	2.250E-03	-1.00	0.091
2	1000	298.15	---	7.8	4.000E-05	4.000E-05	3.223E-05	0.000E+00	1.020E-03	4.480E-01	5.093E-02	1.259E-15	9.764E-03	9.777E-03	3.221E-19	6.295E-08	5.216E-01	2.699E-02	2.315E-03	-1.00	0.091
3	1000	298.15	---	7.8	4.000E-05	4.000E-05	3.223E-05	0.000E+00	1.020E-03	4.680E-01	5.320E-02	1.259E-15	1.020E-02	1.020E-02	3.221E-19	6.295E-08	5.450E-01	2.820E-02	2.380E-03	-1.00	0.090
4	1000	298.15	---	7.8	4.000E-05	4.000E-05	2.579E-04	0.000E+00	1.020E-03	4.279E-01	4.865E-02	1.259E-15	9.328E-03	9.354E-03	3.221E-19	6.295E-08	4.983E-01	2.579E-02	2.250E-03	-0.62	0.193
5	1000	298.15	---	7.8	4.000E-05	4.000E-05	2.579E-04	0.000E+00	1.020E-03	4.480E-01	5.093E-02	1.259E-15	9.764E-03	9.777E-03	3.221E-19	6.295E-08	5.216E-01	2.699E-02	2.315E-03	-0.62	0.193
6	1000	298.15	---	7.8	4.000E-05	4.000E-05	2.579E-04	0.000E+00	1.020E-03	4.680E-01	5.320E-02	1.259E-15	1.020E-02	1.020E-02	3.221E-19	6.295E-08	5.450E-01	2.820E-02	2.380E-03	-0.62	0.193
7	1000	298.15	---	7.8	4.000E-05	4.000E-05	2.095E-03	0.000E+00	1.020E-03	4.279E-01	4.865E-02	1.259E-15	9.328E-03	9.354E-03	3.221E-19	6.295E-08	4.983E-01	2.579E-02	2.250E-03	0.07	0.541
8	1000	298.15	---	7.8	4.000E-05	4.000E-05	2.095E-03	0.000E+00	1.020E-03	4.480E-01	5.093E-02	1.259E-15	9.764E-03	9.777E-03	3.221E-19	6.295E-08	5.216E-01	2.699E-02	2.315E-03	0.07	0.541
9	1000	298.15	---	7.8	4.000E-05	4.000E-05	2.095E-03	0.000E+00	1.020E-03	4.680E-01	5.320E-02	1.259E-15	1.020E-02	1.020E-02	3.221E-19	6.295E-08	5.450E-01	2.820E-02	2.380E-03	0.07	0.540
10	1000	298.15	---	7.8	4.000E-05	4.000E-05	3.223E-05	0.000E+00	2.040E-03	4.279E-01	4.865E-02	1.259E-15	9.328E-03	9.354E-03	3.221E-19	6.295E-08	4.983E-01	2.579E-02	2.250E-03	-1.27	0.050
11	1000	298.15	---	7.8	4.000E-05	4.000E-05	3.223E-05	0.000E+00	2.040E-03	4.480E-01	5.093E-02	1.259E-15	9.764E-03	9.777E-03	3.221E-19	6.295E-08	5.216E-01	2.699E-02	2.315E-03	-1.28	0.050
12	1000	298.15	---	7.8	4.000E-05	4.000E-05	3.223E-05	0.000E+00	2.040E-03	4.680E-01	5.320E-02	1.259E-15	1.020E-02	1.020E-02	3.221E-19	6.295E-08	5.450E-01	2.820E-02	2.380E-03	-1.28	0.050
13	1000	298.15	---	7.8	4.000E-05	4.000E-05	2.579E-04	0.000E+00	2.040E-03	4.279E-01	4.865E-02	1.259E-15	9.328E-03	9.354E-03	3.221E-19	6.295E-08	4.983E-01	2.579E-02	2.250E-03	-0.94	0.103
14	1000	298.15	---	7.8	4.000E-05	4.000E-05	2.579E-04	0.000E+00	2.040E-03	4.480E-01	5.093E-02	1.259E-15	9.764E-03	9.777E-03	3.221E-19	6.295E-08	5.216E-01	2.699E-02	2.315E-03	-0.94	0.103
15	1000	298.15	---	7.8	4.000E-05	4.000E-05	2.579E-04	0.000E+00	2.040E-03	4.680E-01	5.320E-02	1.259E-15	1.020E-02	1.020E-02	3.221E-19	6.295E-08	5.450E-01	2.820E-02	2.380E-03	-0.94	0.103
16	1000	298.15	---	7.8	4.000E-05	4.000E-05	2.095E-03	0.000E+00	2.040E-03	4.279E-01	4.865E-02	1.259E-15	9.328E-03	9.354E-03	3.221E-19	6.295E-08	4.983E-01	2.579E-02	2.250E-03	-0.24	0.365
17	1000	298.15	---	7.8	4.000E-05	4.000E-05	2.095E-03	0.000E+00	2.040E-03	4.480E-01	5.093E-02	1.259E-15	9.764E-03	9.777E-03	3.221E-19	6.295E-08	5.216E-01	2.699E-02	2.315E-03	-0.24	0.365
18	1000	298.15	---	7.8	4.000E-05	4.000E-05	2.095E-03	0.000E+00	2.040E-03	4.680E-01	5.320E-02	1.259E-15	1.020E-02	1.020E-02	3.221E-19	6.295E-08	5.450E-01	2.820E-02	2.380E-03	-0.24	0.365
19	1000	298.15	---	7.8	4.000E-05	4.000E-05	3.223E-05	0.000E+00	5.440E-03	4.279E-01	4.865E-02	1.259E-15	9.328E-03	9.354E-03	3.221E-19	6.295E-08	4.983E-01	2.579E-02	2.250E-03	-1.68	0.020
20	1000	298.15	---	7.8	4.000E-05	4.000E-05	3.223E-05	0.000E+00	5.440E-03	4.480E-01	5.093E-02	1.259E-15	9.764E-03	9.777E-03	3.221E-19	6.295E-08	5.216E-01	2.699E-02	2.315E-03	-1.68	0.020
21	1000	298.15	---	7.8	4.000E-05	4.000E-05	3.223E-05	0.000E+00	5.440E-03	4.680E-01	5.320E-02	1.259E-15	1.020E-02	1.020E-02	3.221E-19	6.295E-08	5.450E-01	2.820E-02	2.380E-03	-1.68	0.020
22	1000	298.15	---	7.8	4.000E-05	4.000E-05	2.579E-04	0.000E+00	5.440E-03	4.279E-01	4.865E-02	1.259E-15	9.328E-03	9.354E-03	3.221E-19	6.295E-08	4.983E-01	2.579E-02	2.250E-03	-1.39	0.039
23	1000	298.15	---	7.8	4.000E-05	4.000E-05	2.579E-04	0.000E+00	5.440E-03	4.480E-01	5.093E-02	1.259E-15	9.764E-03	9.777E-03	3.221E-19	6.295E-08	5.216E-01	2.699E-02	2.315E-03	-1.39	0.039
24	1000	298.15	---	7.8	4.000E-05	4.000E-05	2.579E-04	0.000E+00	5.440E-03	4.680E-01	5.320E-02	1.259E-15	1.020E-02	1.020E-02	3.221E-19	6.295E-08	5.450E-01	2.820E-02	2.380E-03	-1.39	0.039
25	1000	298.15	---	7.8	4.000E-05	4.000E-05	2.095E-03	0.000E+00	5.440E-03	4.279E-01	4.865E-02	1.259E-15	9.328E-03	9.354E-03	3.221E-19	6.295E-08	4.983E-01	2.579E-02	2.250E-03	-0.70	0.167
26	1000	298.15	---	7.8	4.000E-05	4.000E-05	2.095E-03	0.000E+00	5.440E-03	4.480E-01	5.093E-02	1.259E-15	9.764E-03	9.777E-03	3.221E-19	6.295E-08	5.216E-01	2.699E-02	2.315E-03	-0.70	0.167
27	1000	298.15	---	7.8	4.000E-05	4.000E-05	2.095E-03	0.000E+00	5.440E-03	4.680E-01	5.320E-02	1.259E-15	1.020E-02	1.020E-02	3.221E-19	6.295E-08	5.450E-01	2.820E-02	2.380E-03	-0.70	0.167
28	1000	298.15	---	7.8	2.500E-04	2.500E-04	3.223E-05	0.000E+00	1.020E-03	4.279E-01	4.865E-02	1.259E-15	9.328E-03	9.354E-03	3.221E-19	6.295E-08	4.983E-01	2.579E-02	2.250E-03	-0.27	0.347
29	1000	298.15	---	7.8	2.500E-04	2.500E-04	3.223E-05	0.000E+00	1.020E-03	4.480E-01	5.093E-02	1.259E-15	9.764E-03	9.777E-03	3.221E-19	6.295E-08	5.216E-01	2.699E-02	2.315E-03	-0.28	0.346
30	1000	298.15	---	7.8	2.500E-04	2.500E-04	3.223E-05	0.000E+00	1.020E-03	4.680E-01	5.320E-02	1.259E-15	1.020E-02	1.020E-02	3.221E-19	6.295E-08	5.450E-01	2.820E-02	2.380E-03	-0.28	0.346
31	1000	298.15	---	7.8	2.500E-04	2.500E-04	2.579E-04	0.000E+00	1.020E-03	4.279E-01	4.865E-02	1.259E-15	9.328E-03	9.354E-03	3.221E-19	6.295E-08	4.983E-01	2.579E-02	2.250E-03	-0.18	0.398
32	1000	298.15	---	7.8	2.500E-04	2.500E-04	2.579E-04	0.000E+00	1.020E-03	4.480E-01	5.093E-02	1.259E-15	9.764E-03	9.777E-03	3.221E-19	6.295E-08	5.216E-01	2.699E-02	2.315E-03	-0.18	0.398
33	1000	298.15	---	7.8	2.500E-04	2.500E-04	2.579E-04	0.000E+00	1.020E-03	4.680E-01	5.320E-02	1.259E-15	1.020E-02	1.020E-02	3.221E-19	6.295E-08	5.450E-01	2.820E-02	2.380E-03	-0.18	0.397
34	1000	298.15	---	7.8	2.500E-04	2.500E-04	2.095E-03	0.000E+00	1.020E-03	4.279E-01	4.865E-02	1.259E-15	9.328E-03	9.354E-03	3.221E-19	6.295E-08	4.983E-01	2.579E-02	2.250E-03	0.20	0.613
35	1000	298.15	---	7.8	2.500E-04	2.500E-04	2.095E-03	0.000E+00	1.020E-03	4.480E-01	5.093E-02	1.259E-15	9.764E-03	9.777E-03	3.221E-19	6.295E-08	5.216E-01	2.699E-02	2.315E-03	0.20	0.613
36	1000	298.15	---	7.8	2.500E-04	2.500E-04	2.095E-03	0.000E+00	1.020E-03	4.680E-01	5.320E-02	1.259E-15	1.020E-02	1.020E-02	3.221E-19	6.295E-08	5.450E-01	2.820E-02	2.380E-03	0.20	0.613
37	1000	298.15	---	7.8	2.500E-04	2.500E-04	3.223E-05	0.000E+00	2.040E-03	4.279E-01	4.865E-02	1.259E-15	9.328E-03	9.354E-03	3.221E-19	6.295E-08	4.983E-01	2.579E-02	2.250E-03	-0.54	0.224
38	1000	298.15	---	7.8	2.500E-04	2.500E-04	3.223E-05	0.000E+00	2.040E-03	4.480E-01	5.093E-02	1.259E-15	9.764E-03	9.777E-03	3.221E-19	6.295E-08	5.216E-01	2.699E-02	2.315E-03	-0.54	0.223
39	1000	298.15	---	7.8	2.500E-04	2.500E-04	3.223E-05	0.000E+00	2.040E-03	4.680E-01	5.320E-02	1.259E-15	1.020E-02	1.020E-02	3.221E-19	6.295E-08	5.450E-01	2.820E-02	2.380E-03	-0.54	0.223
40	1000	298.15	---	7.8	2.500E-04	2.500E-04	2.579E-04	0.000E+00	2.040E-03	4.279E-01	4.865E-02	1.259E-15	9.328E-03	9.354E-03	3.221E-19	6.295E-08	4.983E-01	2.579E-02	2.250E-03	-0.46	0.258
41	1000	298.15	---	7.8	2.500E-04	2.500E-04	2.579E-04	0.000E+00	2.040E-03	4.480E-01	5.093E-02	1.259E-15	9.764E-03	9.777E-03	3.221E-19	6.295E-08	5.216E-01	2.699E-02	2.315E-03	-0.46	0.258
42	1000	298.15	---	7.8	2.500E-04	2.500E-04	2.579E-04	0.000E+00	2.040E-03	4.680E-01	5.320E-02	1.259E-15	1.020E-02	1.020E-02	3.221E-19	6.295E-08	5.450E-01	2.820E-02	2.380E-03	-0.46	0.257
43	1000	298.15	---	7.8	2.500E-04	2.500E-04	2.095E-03	0.000E+00	2.040E-03	4.279E-01	4.865E-02	1.259E-15	9.328E-03	9.354E-03	3.221E-19	6.295E-08	4.983E-01	2.579E-02	2.250E-03	-0.10	0.445
44	1000	298.15	---	7.8	2.500E-04	2.500E-04	2.095E-03	0.000E+00	2.040E-03	4.480E-01	5.093E-02	1.259E-15	9.764E-03	9.777E-03	3.221E-19	6.295E-08	5.216E-01	2.699E-02	2.315E-03	-0.10	0.445
45	1000	298.15	---	7.8	2.500E-04	2.500E-04	2.095E-03	0.000E+00	2.040E-03	4.680E-01	5.320										

AM7 INPUT																				WHAM7 OUTPUT	
Description	SPM (g/L)	Temp (K)	pCO2 (atm)	pH	Part HA (g/L)	Part FA (g/L)	Part FeOx (g/L)	Coll HA (g/L)	Coll FA (g/L)	Na (M)	Mg (M)	{Al3+} (M)	K (M)	Ca (M)	{Fe3+} (M)	Tot Cu (M)	Cl (M)	SO4 (M)	CO3 (M)	logK ₀ = log(K ₀ x TSS) (dimensionless)	Fract. Part. (dimensionless)
64	1000	298.15	---	7.8	1.600E-03	1.600E-03	3.223E-05	0.000E+00	2.040E-03	4.279E-01	4.865E-02	1.259E-15	9.328E-03	9.354E-03	3.221E-19	6.295E-08	4.983E-01	2.579E-02	2.250E-03	0.28	0.654
65	1000	298.15	---	7.8	1.600E-03	1.600E-03	3.223E-05	0.000E+00	2.040E-03	4.480E-01	5.093E-02	1.259E-15	9.764E-03	9.777E-03	3.221E-19	6.295E-08	5.216E-01	2.699E-02	2.315E-03	0.27	0.653
66	1000	298.15	---	7.8	1.600E-03	1.600E-03	3.223E-05	0.000E+00	2.040E-03	4.680E-01	5.320E-02	1.259E-15	1.020E-02	1.020E-02	3.221E-19	6.295E-08	5.450E-01	2.820E-02	2.380E-03	0.27	0.652
67	1000	298.15	---	7.8	1.600E-03	1.600E-03	2.579E-04	0.000E+00	2.040E-03	4.279E-01	4.865E-02	1.259E-15	9.328E-03	9.354E-03	3.221E-19	6.295E-08	4.983E-01	2.579E-02	2.250E-03	0.29	0.660
68	1000	298.15	---	7.8	1.600E-03	1.600E-03	2.579E-04	0.000E+00	2.040E-03	4.480E-01	5.093E-02	1.259E-15	9.764E-03	9.777E-03	3.221E-19	6.295E-08	5.216E-01	2.699E-02	2.315E-03	0.29	0.659
69	1000	298.15	---	7.8	1.600E-03	1.600E-03	2.579E-04	0.000E+00	2.040E-03	4.680E-01	5.320E-02	1.259E-15	1.020E-02	1.020E-02	3.221E-19	6.295E-08	5.450E-01	2.820E-02	2.380E-03	0.29	0.659
70	1000	298.15	---	7.8	1.600E-03	1.600E-03	2.095E-03	0.000E+00	2.040E-03	4.279E-01	4.865E-02	1.259E-15	9.328E-03	9.354E-03	3.221E-19	6.295E-08	4.983E-01	2.579E-02	2.250E-03	0.37	0.703
71	1000	298.15	---	7.8	1.600E-03	1.600E-03	2.095E-03	0.000E+00	2.040E-03	4.480E-01	5.093E-02	1.259E-15	9.764E-03	9.777E-03	3.221E-19	6.295E-08	5.216E-01	2.699E-02	2.315E-03	0.37	0.703
72	1000	298.15	---	7.8	1.600E-03	1.600E-03	2.095E-03	0.000E+00	2.040E-03	4.680E-01	5.320E-02	1.259E-15	1.020E-02	1.020E-02	3.221E-19	6.295E-08	5.450E-01	2.820E-02	2.380E-03	0.37	0.702
73	1000	298.15	---	7.8	1.600E-03	1.600E-03	3.223E-05	0.000E+00	5.440E-03	4.279E-01	4.865E-02	1.259E-15	9.328E-03	9.354E-03	3.221E-19	6.295E-08	4.983E-01	2.579E-02	2.250E-03	-0.13	0.426
74	1000	298.15	---	7.8	1.600E-03	1.600E-03	3.223E-05	0.000E+00	5.440E-03	4.480E-01	5.093E-02	1.259E-15	9.764E-03	9.777E-03	3.221E-19	6.295E-08	5.216E-01	2.699E-02	2.315E-03	-0.13	0.425
75	1000	298.15	---	7.8	1.600E-03	1.600E-03	3.223E-05	0.000E+00	5.440E-03	4.680E-01	5.320E-02	1.259E-15	1.020E-02	1.020E-02	3.221E-19	6.295E-08	5.450E-01	2.820E-02	2.380E-03	-0.13	0.424
76	1000	298.15	---	7.8	1.600E-03	1.600E-03	2.579E-04	0.000E+00	5.440E-03	4.279E-01	4.865E-02	1.259E-15	9.328E-03	9.354E-03	3.221E-19	6.295E-08	4.983E-01	2.579E-02	2.250E-03	-0.12	0.432
77	1000	298.15	---	7.8	1.600E-03	1.600E-03	2.579E-04	0.000E+00	5.440E-03	4.480E-01	5.093E-02	1.259E-15	9.764E-03	9.777E-03	3.221E-19	6.295E-08	5.216E-01	2.699E-02	2.315E-03	-0.12	0.431
78	1000	298.15	---	7.8	1.600E-03	1.600E-03	2.579E-04	0.000E+00	5.440E-03	4.680E-01	5.320E-02	1.259E-15	1.020E-02	1.020E-02	3.221E-19	6.295E-08	5.450E-01	2.820E-02	2.380E-03	-0.12	0.430
79	1000	298.15	---	7.8	1.600E-03	1.600E-03	2.095E-03	0.000E+00	5.440E-03	4.279E-01	4.865E-02	1.259E-15	9.328E-03	9.354E-03	3.221E-19	6.295E-08	4.983E-01	2.579E-02	2.250E-03	-0.04	0.478
80	1000	298.15	---	7.8	1.600E-03	1.600E-03	2.095E-03	0.000E+00	5.440E-03	4.480E-01	5.093E-02	1.259E-15	9.764E-03	9.777E-03	3.221E-19	6.295E-08	5.216E-01	2.699E-02	2.315E-03	-0.04	0.477
81	1000	298.15	---	7.8	1.600E-03	1.600E-03	2.095E-03	0.000E+00	5.440E-03	4.680E-01	5.320E-02	1.259E-15	1.020E-02	1.020E-02	3.221E-19	6.295E-08	5.450E-01	2.820E-02	2.380E-03	-0.04	0.477
82	1000	298.15	---	8.2	4.000E-05	4.000E-05	3.223E-05	0.000E+00	1.020E-03	4.279E-01	4.865E-02	7.943E-17	9.328E-03	9.354E-03	3.251E-20	6.295E-08	4.983E-01	2.579E-02	2.250E-03	-0.95	0.100
83	1000	298.15	---	8.2	4.000E-05	4.000E-05	3.223E-05	0.000E+00	1.020E-03	4.480E-01	5.093E-02	7.943E-17	9.764E-03	9.777E-03	3.251E-20	6.295E-08	5.216E-01	2.699E-02	2.315E-03	-0.95	0.100
84	1000	298.15	---	8.2	4.000E-05	4.000E-05	3.223E-05	0.000E+00	1.020E-03	4.680E-01	5.320E-02	7.943E-17	1.020E-02	1.020E-02	3.251E-20	6.295E-08	5.450E-01	2.820E-02	2.380E-03	-0.95	0.100
85	1000	298.15	---	8.2	4.000E-05	4.000E-05	2.579E-04	0.000E+00	1.020E-03	4.279E-01	4.865E-02	7.943E-17	9.328E-03	9.354E-03	3.251E-20	6.295E-08	4.983E-01	2.579E-02	2.250E-03	-0.53	0.229
86	1000	298.15	---	8.2	4.000E-05	4.000E-05	2.579E-04	0.000E+00	1.020E-03	4.480E-01	5.093E-02	7.943E-17	9.764E-03	9.777E-03	3.251E-20	6.295E-08	5.216E-01	2.699E-02	2.315E-03	-0.53	0.229
87	1000	298.15	---	8.2	4.000E-05	4.000E-05	2.579E-04	0.000E+00	1.020E-03	4.680E-01	5.320E-02	7.943E-17	1.020E-02	1.020E-02	3.251E-20	6.295E-08	5.450E-01	2.820E-02	2.380E-03	-0.53	0.229
88	1000	298.15	---	8.2	4.000E-05	4.000E-05	2.095E-03	0.000E+00	1.020E-03	4.279E-01	4.865E-02	7.943E-17	9.328E-03	9.354E-03	3.251E-20	6.295E-08	4.983E-01	2.579E-02	2.250E-03	0.16	0.593
89	1000	298.15	---	8.2	4.000E-05	4.000E-05	2.095E-03	0.000E+00	1.020E-03	4.480E-01	5.093E-02	7.943E-17	9.764E-03	9.777E-03	3.251E-20	6.295E-08	5.216E-01	2.699E-02	2.315E-03	0.16	0.593
90	1000	298.15	---	8.2	4.000E-05	4.000E-05	2.095E-03	0.000E+00	1.020E-03	4.680E-01	5.320E-02	7.943E-17	1.020E-02	1.020E-02	3.251E-20	6.295E-08	5.450E-01	2.820E-02	2.380E-03	0.16	0.593
91	1000	298.15	---	8.2	4.000E-05	4.000E-05	3.223E-05	0.000E+00	2.040E-03	4.279E-01	4.865E-02	7.943E-17	9.328E-03	9.354E-03	3.251E-20	6.295E-08	4.983E-01	2.579E-02	2.250E-03	-1.26	0.052
92	1000	298.15	---	8.2	4.000E-05	4.000E-05	3.223E-05	0.000E+00	2.040E-03	4.480E-01	5.093E-02	7.943E-17	9.764E-03	9.777E-03	3.251E-20	6.295E-08	5.216E-01	2.699E-02	2.315E-03	-1.26	0.052
93	1000	298.15	---	8.2	4.000E-05	4.000E-05	3.223E-05	0.000E+00	2.040E-03	4.680E-01	5.320E-02	7.943E-17	1.020E-02	1.020E-02	3.251E-20	6.295E-08	5.450E-01	2.820E-02	2.380E-03	-1.26	0.052
94	1000	298.15	---	8.2	4.000E-05	4.000E-05	2.579E-04	0.000E+00	2.040E-03	4.279E-01	4.865E-02	7.943E-17	9.328E-03	9.354E-03	3.251E-20	6.295E-08	4.983E-01	2.579E-02	2.250E-03	-0.88	0.117
95	1000	298.15	---	8.2	4.000E-05	4.000E-05	2.579E-04	0.000E+00	2.040E-03	4.480E-01	5.093E-02	7.943E-17	9.764E-03	9.777E-03	3.251E-20	6.295E-08	5.216E-01	2.699E-02	2.315E-03	-0.88	0.117
96	1000	298.15	---	8.2	4.000E-05	4.000E-05	2.579E-04	0.000E+00	2.040E-03	4.680E-01	5.320E-02	7.943E-17	1.020E-02	1.020E-02	3.251E-20	6.295E-08	5.450E-01	2.820E-02	2.380E-03	-0.88	0.117
97	1000	298.15	---	8.2	4.000E-05	4.000E-05	2.095E-03	0.000E+00	2.040E-03	4.279E-01	4.865E-02	7.943E-17	9.328E-03	9.354E-03	3.251E-20	6.295E-08	4.983E-01	2.579E-02	2.250E-03	-0.16	0.408
98	1000	298.15	---	8.2	4.000E-05	4.000E-05	2.095E-03	0.000E+00	2.040E-03	4.480E-01	5.093E-02	7.943E-17	9.764E-03	9.777E-03	3.251E-20	6.295E-08	5.216E-01	2.699E-02	2.315E-03	-0.16	0.408
99	1000	298.15	---	8.2	4.000E-05	4.000E-05	2.095E-03	0.000E+00	2.040E-03	4.680E-01	5.320E-02	7.943E-17	1.020E-02	1.020E-02	3.251E-20	6.295E-08	5.450E-01	2.820E-02	2.380E-03	-0.16	0.408
100	1000	298.15	---	8.2	4.000E-05	4.000E-05	3.223E-05	0.000E+00	5.440E-03	4.279E-01	4.865E-02	7.943E-17	9.328E-03	9.354E-03	3.251E-20	6.295E-08	4.983E-01	2.579E-02	2.250E-03	-1.70	0.020
101	1000	298.15	---	8.2	4.000E-05	4.000E-05	3.223E-05	0.000E+00	5.440E-03	4.480E-01	5.093E-02	7.943E-17	9.764E-03	9.777E-03	3.251E-20	6.295E-08	5.216E-01	2.699E-02	2.315E-03	-1.70	0.020
102	1000	298.15	---	8.2	4.000E-05	4.000E-05	3.223E-05	0.000E+00	5.440E-03	4.680E-01	5.320E-02	7.943E-17	1.020E-02	1.020E-02	3.251E-20	6.295E-08	5.450E-01	2.820E-02	2.380E-03	-1.70	0.020
103	1000	298.15	---	8.2	4.000E-05	4.000E-05	2.579E-04	0.000E+00	5.440E-03	4.279E-01	4.865E-02	7.943E-17	9.328E-03	9.354E-03	3.251E-20	6.295E-08	4.983E-01	2.579E-02	2.250E-03	-1.36	0.042
104	1000	298.15	---	8.2	4.000E-05	4.000E-05	2.579E-04	0.000E+00	5.440E-03	4.480E-01	5.093E-02	7.943E-17	9.764E-03	9.777E-03	3.251E-20	6.295E-08	5.216E-01	2.699E-02	2.315E-03	-1.36	0.042
105	1000	298.15	---	8.2	4.000E-05	4.000E-05	2.579E-04	0.000E+00	5.440E-03	4.680E-01	5.320E-02	7.943E-17	1.020E-02	1.020E-02	3.251E-20	6.295E-08	5.450E-01	2.820E-02	2.380E-03	-1.36	0.042
106	1000	298.15	---	8.2	4.000E-05	4.000E-05	2.095E-03	0.000E+00	5.440E-03	4.279E-01	4.865E-02	7.943E-17	9.328E-03	9.354E-03	3.251E-20	6.295E-08	4.983E-01	2.579E-02	2.250E-03	-0.63	0.189
107	1000	298.15	---	8.2	4.000E-05	4.000E-05	2.095E-03	0.000E+00	5.440E-03	4.480E-01	5.093E-02	7.943E-17	9.764E-03	9.777E-03	3.251E-20	6.295E-08	5.216E-01	2.699E-02	2.315E-03	-0.63	0.189
108	1000	298.15	---	8.2	4.000E-05	4.000E-05	2.095E-03	0.000E+00	5.440E												

WHAM7 INPUT																			WHAM7 OUTPUT			
Description	SPM (g/L)	Temp (K)	pCO2 (atm)	pH	Part HA (g/L)	Part FA (g/L)	Part FeOx (g/L)	Coll HA (g/L)	Coll FA (g/L)	Na (M)	Mg (M)	{Al3+} (M)	K (M)	Ca (M)	{Fe3+} (M)	Tot Cu (M)	Cl (M)	SO4 (M)	CO3 (M)	logK0' = log(K0 x TSS) (dimensionless)	Fract. Part. (dimensionless)	
631	1000	298.15	---	8.2	1.600E-03	1.600E-03	3.223E-05	0.000E+00	2.040E-03	4.279E-01	4.865E-02	7.943E-17	9.328E-03	9.354E-03	3.251E-20	4.092E-07	4.983E-01	2.579E-02	2.250E-03	0.23	0.629	
632	1000	298.15	---	8.2	1.600E-03	1.600E-03	3.223E-05	0.000E+00	2.040E-03	4.480E-01	5.093E-02	7.943E-17	9.764E-03	9.777E-03	3.251E-20	4.092E-07	5.216E-01	2.699E-02	2.315E-03	0.23	0.629	
633	1000	298.15	---	8.2	1.600E-03	1.600E-03	3.223E-05	0.000E+00	2.040E-03	4.680E-01	5.320E-02	7.943E-17	1.020E-02	1.020E-02	3.251E-20	4.092E-07	5.450E-01	2.820E-02	2.380E-03	0.23	0.628	
634	1000	298.15	---	8.2	1.600E-03	1.600E-03	2.579E-04	0.000E+00	2.040E-03	4.279E-01	4.865E-02	7.943E-17	9.328E-03	9.354E-03	3.251E-20	4.092E-07	4.983E-01	2.579E-02	2.250E-03	0.26	0.646	
635	1000	298.15	---	8.2	1.600E-03	1.600E-03	2.579E-04	0.000E+00	2.040E-03	4.480E-01	5.093E-02	7.943E-17	9.764E-03	9.777E-03	3.251E-20	4.092E-07	5.216E-01	2.699E-02	2.315E-03	0.26	0.645	
636	1000	298.15	---	8.2	1.600E-03	1.600E-03	2.579E-04	0.000E+00	2.040E-03	4.680E-01	5.320E-02	7.943E-17	1.020E-02	1.020E-02	3.251E-20	4.092E-07	5.450E-01	2.820E-02	2.380E-03	0.26	0.645	
637	1000	298.15	---	8.2	1.600E-03	1.600E-03	2.095E-03	0.000E+00	2.040E-03	4.279E-01	4.865E-02	7.943E-17	9.328E-03	9.354E-03	3.251E-20	4.092E-07	4.983E-01	2.579E-02	2.250E-03	0.43	0.728	
638	1000	298.15	---	8.2	1.600E-03	1.600E-03	2.095E-03	0.000E+00	2.040E-03	4.480E-01	5.093E-02	7.943E-17	9.764E-03	9.777E-03	3.251E-20	4.092E-07	5.216E-01	2.699E-02	2.315E-03	0.43	0.728	
639	1000	298.15	---	8.2	1.600E-03	1.600E-03	2.095E-03	0.000E+00	2.040E-03	4.680E-01	5.320E-02	7.943E-17	1.020E-02	1.020E-02	3.251E-20	4.092E-07	5.450E-01	2.820E-02	2.380E-03	0.43	0.728	
640	1000	298.15	---	8.2	1.600E-03	1.600E-03	3.223E-05	0.000E+00	5.440E-03	4.279E-01	4.865E-02	7.943E-17	9.328E-03	9.354E-03	3.251E-20	4.092E-07	4.983E-01	2.579E-02	2.250E-03	-0.18	0.398	
641	1000	298.15	---	8.2	1.600E-03	1.600E-03	3.223E-05	0.000E+00	5.440E-03	4.480E-01	5.093E-02	7.943E-17	9.764E-03	9.777E-03	3.251E-20	4.092E-07	5.216E-01	2.699E-02	2.315E-03	-0.18	0.398	
642	1000	298.15	---	8.2	1.600E-03	1.600E-03	3.223E-05	0.000E+00	5.440E-03	4.680E-01	5.320E-02	7.943E-17	1.020E-02	1.020E-02	3.251E-20	4.092E-07	5.450E-01	2.820E-02	2.380E-03	-0.18	0.397	
643	1000	298.15	---	8.2	1.600E-03	1.600E-03	2.579E-04	0.000E+00	5.440E-03	4.279E-01	4.865E-02	7.943E-17	9.328E-03	9.354E-03	3.251E-20	4.092E-07	4.983E-01	2.579E-02	2.250E-03	-0.16	0.411	
644	1000	298.15	---	8.2	1.600E-03	1.600E-03	2.579E-04	0.000E+00	5.440E-03	4.480E-01	5.093E-02	7.943E-17	9.764E-03	9.777E-03	3.251E-20	4.092E-07	5.216E-01	2.699E-02	2.315E-03	-0.16	0.411	
645	1000	298.15	---	8.2	1.600E-03	1.600E-03	2.579E-04	0.000E+00	5.440E-03	4.680E-01	5.320E-02	7.943E-17	1.020E-02	1.020E-02	3.251E-20	4.092E-07	5.450E-01	2.820E-02	2.380E-03	-0.16	0.410	
646	1000	298.15	---	8.2	1.600E-03	1.600E-03	2.095E-03	0.000E+00	5.440E-03	4.279E-01	4.865E-02	7.943E-17	9.328E-03	9.354E-03	3.251E-20	4.092E-07	4.983E-01	2.579E-02	2.250E-03	-0.01	0.493	
647	1000	298.15	---	8.2	1.600E-03	1.600E-03	2.095E-03	0.000E+00	5.440E-03	4.480E-01	5.093E-02	7.943E-17	9.764E-03	9.777E-03	3.251E-20	4.092E-07	5.216E-01	2.699E-02	2.315E-03	-0.01	0.493	
648	1000	298.15	---	8.2	1.600E-03	1.600E-03	2.095E-03	0.000E+00	5.440E-03	4.680E-01	5.320E-02	7.943E-17	1.020E-02	1.020E-02	3.251E-20	4.092E-07	5.450E-01	2.820E-02	2.380E-03	-0.01	0.493	
649	1000	298.15	---	8.6	4.000E-05	4.000E-05	3.223E-05	0.000E+00	1.020E-03	4.279E-01	4.865E-02	5.012E-18	9.328E-03	9.354E-03	3.281E-21	4.092E-07	4.983E-01	2.579E-02	2.250E-03	-0.96	0.099	
650	1000	298.15	---	8.6	4.000E-05	4.000E-05	3.223E-05	0.000E+00	1.020E-03	4.480E-01	5.093E-02	5.012E-18	9.764E-03	9.777E-03	3.281E-21	4.092E-07	5.216E-01	2.699E-02	2.315E-03	-0.96	0.099	
651	1000	298.15	---	8.6	4.000E-05	4.000E-05	3.223E-05	0.000E+00	1.020E-03	4.680E-01	5.320E-02	5.012E-18	1.020E-02	1.020E-02	3.281E-21	4.092E-07	5.450E-01	2.820E-02	2.380E-03	-0.96	0.099	
652	1000	298.15	---	8.6	4.000E-05	4.000E-05	2.579E-04	0.000E+00	1.020E-03	4.279E-01	4.865E-02	5.012E-18	9.328E-03	9.354E-03	3.281E-21	4.092E-07	4.983E-01	2.579E-02	2.250E-03	-0.28	0.346	
653	1000	298.15	---	8.6	4.000E-05	4.000E-05	2.579E-04	0.000E+00	1.020E-03	4.480E-01	5.093E-02	5.012E-18	9.764E-03	9.777E-03	3.281E-21	4.092E-07	5.216E-01	2.699E-02	2.315E-03	-0.28	0.346	
654	1000	298.15	---	8.6	4.000E-05	4.000E-05	2.579E-04	0.000E+00	1.020E-03	4.680E-01	5.320E-02	5.012E-18	1.020E-02	1.020E-02	3.281E-21	4.092E-07	5.450E-01	2.820E-02	2.380E-03	-0.28	0.346	
655	1000	298.15	---	8.6	4.000E-05	4.000E-05	2.095E-03	0.000E+00	1.020E-03	4.279E-01	4.865E-02	5.012E-18	9.328E-03	9.354E-03	3.281E-21	4.092E-07	4.983E-01	2.579E-02	2.250E-03	0.51	0.764	
656	1000	298.15	---	8.6	4.000E-05	4.000E-05	2.095E-03	0.000E+00	1.020E-03	4.480E-01	5.093E-02	5.012E-18	9.764E-03	9.777E-03	3.281E-21	4.092E-07	5.216E-01	2.699E-02	2.315E-03	0.51	0.765	
657	1000	298.15	---	8.6	4.000E-05	4.000E-05	2.095E-03	0.000E+00	1.020E-03	4.680E-01	5.320E-02	5.012E-18	1.020E-02	1.020E-02	3.281E-21	4.092E-07	5.450E-01	2.820E-02	2.380E-03	0.51	0.765	
658	1000	298.15	---	8.6	4.000E-05	4.000E-05	3.223E-05	0.000E+00	2.040E-03	4.279E-01	4.865E-02	5.012E-18	9.328E-03	9.354E-03	3.281E-21	4.092E-07	4.983E-01	2.579E-02	2.250E-03	-1.16	0.065	
659	1000	298.15	---	8.6	4.000E-05	4.000E-05	3.223E-05	0.000E+00	2.040E-03	4.480E-01	5.093E-02	5.012E-18	9.764E-03	9.777E-03	3.281E-21	4.092E-07	5.216E-01	2.699E-02	2.315E-03	-1.16	0.065	
660	1000	298.15	---	8.6	4.000E-05	4.000E-05	3.223E-05	0.000E+00	2.040E-03	4.680E-01	5.320E-02	5.012E-18	1.020E-02	1.020E-02	3.281E-21	4.092E-07	5.450E-01	2.820E-02	2.380E-03	-1.16	0.065	
661	1000	298.15	---	8.6	4.000E-05	4.000E-05	2.579E-04	0.000E+00	2.040E-03	4.279E-01	4.865E-02	5.012E-18	9.328E-03	9.354E-03	3.281E-21	4.092E-07	4.983E-01	2.579E-02	2.250E-03	-0.53	0.227	
662	1000	298.15	---	8.6	4.000E-05	4.000E-05	2.579E-04	0.000E+00	2.040E-03	4.480E-01	5.093E-02	5.012E-18	9.764E-03	9.777E-03	3.281E-21	4.092E-07	5.216E-01	2.699E-02	2.315E-03	-0.53	0.228	
663	1000	298.15	---	8.6	4.000E-05	4.000E-05	2.579E-04	0.000E+00	2.040E-03	4.680E-01	5.320E-02	5.012E-18	1.020E-02	1.020E-02	3.281E-21	4.092E-07	5.450E-01	2.820E-02	2.380E-03	-0.53	0.228	
664	1000	298.15	---	8.6	4.000E-05	4.000E-05	2.095E-03	0.000E+00	2.040E-03	4.279E-01	4.865E-02	5.012E-18	9.328E-03	9.354E-03	3.281E-21	4.092E-07	4.983E-01	2.579E-02	2.250E-03	0.19	0.605	
665	1000	298.15	---	8.6	4.000E-05	4.000E-05	2.095E-03	0.000E+00	2.040E-03	4.480E-01	5.093E-02	5.012E-18	9.764E-03	9.777E-03	3.281E-21	4.092E-07	5.216E-01	2.699E-02	2.315E-03	0.19	0.606	
666	1000	298.15	---	8.6	4.000E-05	4.000E-05	2.095E-03	0.000E+00	2.040E-03	4.680E-01	5.320E-02	5.012E-18	1.020E-02	1.020E-02	3.281E-21	4.092E-07	5.450E-01	2.820E-02	2.380E-03	0.19	0.607	
667	1000	298.15	---	8.6	4.000E-05	4.000E-05	3.223E-05	0.000E+00	5.440E-03	4.279E-01	4.865E-02	5.012E-18	9.328E-03	9.354E-03	3.281E-21	4.092E-07	4.983E-01	2.579E-02	2.250E-03	-1.61	0.024	
668	1000	298.15	---	8.6	4.000E-05	4.000E-05	3.223E-05	0.000E+00	5.440E-03	4.480E-01	5.093E-02	5.012E-18	9.764E-03	9.777E-03	3.281E-21	4.092E-07	5.216E-01	2.699E-02	2.315E-03	-1.61	0.024	
669	1000	298.15	---	8.6	4.000E-05	4.000E-05	3.223E-05	0.000E+00	5.440E-03	4.680E-01	5.320E-02	5.012E-18	1.020E-02	1.020E-02	3.281E-21	4.092E-07	5.450E-01	2.820E-02	2.380E-03	-1.61	0.024	
670	1000	298.15	---	8.6	4.000E-05	4.000E-05	2.579E-04	0.000E+00	5.440E-03	4.279E-01	4.865E-02	5.012E-18	9.328E-03	9.354E-03	3.281E-21	4.092E-07	4.983E-01	2.579E-02	2.250E-03	-1.09	0.075	
671	1000	298.15	---	8.6	4.000E-05	4.000E-05	2.579E-04	0.000E+00	5.440E-03	4.480E-01	5.093E-02	5.012E-18	9.764E-03	9.777E-03	3.281E-21	4.092E-07	5.216E-01	2.699E-02	2.315E-03	-1.09	0.075	
672	1000	298.15	---	8.6	4.000E-05	4.000E-05	2.579E-04	0.000E+00	5.440E-03	4.680E-01	5.320E-02	5.012E-18	1.020E-02	1.020E-02	3.281E-21	4.092E-07	5.450E-01	2.820E-02	2.380E-03	-1.09	0.075	
673	1000	298.15	---	8.6	4.000E-05	4.000E-05	2.095E-03	0.000E+00	5.440E-03	4.279E-01	4.865E-02	5.012E-18	9.328E-03	9.354E-03	3.281E-21	4.092E-07	4.983E-01	2.579E-02	2.250E-03	-0.33	0.317	
674	1000	298.15	---	8.6	4.000E-05	4.000E-05	2.095E-03	0.000E+00	5.440E-03	4.480E-01	5.093E-02	5.012E-18	9.764E-03	9.777E-03	3.281E-21	4.092E-07	5.216E-01	2.699E-02	2.315E-03	-0.33	0.318	
675	1000	298.15	---	8.6</																		

APPENDIX G **SEDIMENT PROFILE IMAGE ANALYSIS RESULTS**

Table G-1. Sediment Profile Image Analysis results

STATION	REP	DATE	TIME	Calibration Constant	Penetration Area (sq.cm)	Average Penetration (cm)	Minimum Penetration (cm)	Maximum Penetration (cm)	Sus Sed Area (sq.cm)	Sus Sed (cm)	Area of Water Visible (sq cm)	Water Visible (cm)	COMMENT
Pearl Harb_B22	1	8/30/2012	11:08:51	14.455	305.69	21.15	21.03	-	-	-	4.35	0.30	
Pearl Harb_B22	2	8/30/2012	11:08:54	14.455	305.79	21.15	21.03	-	-	-	4.26	0.29	
Pearl Harb_B22	3	8/30/2012	11:08:57	14.455	305.72	21.15	21.03	-	-	-	4.33	0.30	
Pearl Harb_B22	4	8/30/2012	11:09:00	14.455	305.93	21.16	21.03	-	-	-	4.11	0.28	
Pearl Harb_B22	5	8/30/2012	11:09:03	14.455	305.69	21.15	21.03	-	-	-	4.35	0.30	
Pearl Harb_B22	6	8/30/2012	11:09:06	14.455	305.70	21.15	21.03	-	-	-	4.34	0.30	
Pearl Harb_B22	7	8/30/2012	11:09:09	14.455	305.77	21.15	21.03	-	-	-	4.27	0.30	
Pearl Harb_B22	8	8/30/2012	11:09:12	14.455	305.70	21.15	21.03	-	-	-	4.34	0.30	
Pearl Harb_B22	9	8/30/2012	11:09:15	14.455	305.75	21.15	21.03	-	-	-	4.29	0.30	
Pearl Harb_B22	10	8/30/2012	11:09:18	14.455	305.56	21.14	21.03	-	-	-	4.48	0.31	
Pearl Harb_B22	11	8/30/2012	11:09:21	14.455	305.77	21.15	21.03	-	-	-	4.27	0.30	
Pearl Harb_B22	12	8/30/2012	11:09:24	14.455	305.76	21.15	21.03	-	-	-	4.28	0.30	
Pearl Harb_B22	13	8/30/2012	11:09:27	14.455	305.66	21.15	21.03	-	-	-	4.38	0.30	
Pearl Harb_B22	14	8/30/2012	11:09:30	14.455	305.84	21.16	21.03	-	-	-	4.20	0.29	
Pearl Harb_B22	15	8/30/2012	11:09:33	14.455	305.68	21.15	21.03	-	-	-	4.36	0.30	
Pearl Harb_B22	16	8/30/2012	11:09:36	14.455	305.84	21.16	21.03	-	-	-	4.20	0.29	
Pearl Harb_B22	17	8/30/2012	11:09:39	14.455	305.84	21.16	21.03	-	-	-	4.21	0.29	
Pearl Harb_B22	18	8/30/2012	11:09:42	14.455	305.81	21.16	21.03	-	-	-	4.23	0.29	
Pearl Harb_B22	19	8/30/2012	11:09:45	14.455	305.81	21.16	21.03	-	-	-	4.23	0.29	
Pearl Harb_B22	20	8/30/2012	11:09:48	14.455	305.75	21.15	21.03	-	-	-	4.30	0.30	
Pearl Harb_B22	21	8/30/2012	11:09:51	14.455	305.81	21.16	21.03	-	-	-	4.24	0.29	
Pearl Harb_B22	22	8/30/2012	11:09:54	14.455	305.80	21.16	21.03	-	-	-	4.24	0.29	
Pearl Harb_B22	23	8/30/2012	11:09:57	14.455	305.72	21.15	21.03	-	-	-	4.32	0.30	
Pearl Harb_B22	24	8/30/2012	11:10:00	14.455	305.76	21.15	21.03	-	-	-	4.28	0.30	
Pearl Harb_B22	25	8/30/2012	11:10:03	14.455	305.83	21.16	21.03	-	-	-	4.21	0.29	
Pearl Harb_B22	26	8/30/2012	11:10:06	14.455	305.83	21.16	21.03	-	-	-	4.21	0.29	
Pearl Harb_B22	27	8/30/2012	11:10:09	14.455	305.83	21.16	21.03	-	-	-	4.21	0.29	
Pearl Harb_B22	28	8/30/2012	11:10:12	14.455	305.80	21.16	21.03	-	-	-	4.24	0.29	
Pearl Harb_B22	29	8/30/2012	11:10:15	14.455	305.90	21.16	21.03	-	-	-	4.14	0.29	
Pearl Harb_B22	30	8/30/2012	11:10:18	14.455	305.94	21.16	21.03	-	-	-	4.10	0.28	
Pearl Harb_B22	31	8/30/2012	11:10:21	14.455	305.93	21.16	21.03	-	-	-	4.11	0.28	
Pearl Harb_B22	32	8/30/2012	11:10:24	14.455	305.93	21.16	21.03	-	-	-	4.11	0.28	
Pearl Harb_B22	33	8/30/2012	11:10:27	14.455	305.83	21.16	21.03	-	-	-	4.21	0.29	
Pearl Harb_B22	34	8/30/2012	11:10:30	14.455	305.90	21.16	21.03	-	-	-	4.14	0.29	
Pearl Harb_B22	35	8/30/2012	11:10:33	14.455	305.91	21.16	21.03	-	-	-	4.13	0.29	
Pearl Harb_B22	36	8/30/2012	11:10:36	14.455	305.93	21.16	21.03	-	-	-	4.12	0.28	
Pearl Harb_B22	37	8/30/2012	11:10:39	14.455	305.83	21.16	21.05	-	-	-	4.21	0.29	
Pearl Harb_B22	38	8/30/2012	11:10:42	14.455	305.94	21.17	21.05	-	-	-	4.10	0.28	
Pearl Harb_B22	39	8/30/2012	11:10:45	14.455	305.91	21.16	21.04	-	-	-	4.13	0.29	
Pearl Harb_B22	40	8/30/2012	11:10:48	14.455	306.03	21.17	21.06	-	-	-	4.02	0.28	
Pearl Harb_B22	41	8/30/2012	11:10:51	14.455	306.02	21.17	21.06	-	-	-	4.02	0.28	
Pearl Harb_B22	42	8/30/2012	11:10:54	14.455	305.90	21.16	21.05	-	-	-	4.14	0.29	
Pearl Harb_B22	43	8/30/2012	11:10:57	14.455	305.94	21.16	21.04	-	-	-	4.11	0.28	
Pearl Harb_B22	44	8/30/2012	11:11:00	14.455	305.90	21.16	21.05	-	-	-	4.14	0.29	
Pearl Harb_B22	45	8/30/2012	11:11:03	14.455	306.01	21.17	21.05	-	-	-	4.03	0.28	
Pearl Harb_B22	46	8/30/2012	11:11:06	14.455	305.92	21.16	21.03	-	-	-	4.13	0.29	
Pearl Harb_B22	47	8/30/2012	11:11:09	14.455	305.93	21.16	21.05	-	-	-	4.11	0.28	

STATION	REP	DATE	TIME	Calibration Constant	Penetration Area (sq.cm)	Average Penetration (cm)	Minimum Penetration (cm)	Maximum Penetration (cm)	Sus Sed Area (sq.cm)	Sus Sed (cm)	Area of Water Visible (sq cm)	Water Visible (cm)	COMMENT
Pearl Harb_B22	48	8/30/2012	11:11:12	14.455	305.91	21.16	21.05	-	-	-	4.13	0.29	
Pearl Harb_B22	49	8/30/2012	11:11:15	14.455	305.84	21.16	21.02	-	-	-	4.20	0.29	
Pearl Harb_B22	50	8/30/2012	11:11:18	14.455	305.84	21.16	21.03	-	-	-	4.20	0.29	
Pearl Harb_B22	51	8/30/2012	11:11:21	14.455	305.93	21.16	21.04	-	-	-	4.11	0.28	
Pearl Harb_B22	52	8/30/2012	11:11:24	14.455	305.91	21.16	21.03	-	-	-	4.13	0.29	
Pearl Harb_B22	53	8/30/2012	11:11:27	14.455	305.94	21.16	21.04	-	-	-	4.10	0.28	
Pearl Harb_B22	54	8/30/2012	11:11:30	14.455	305.87	21.16	21.03	-	-	-	4.17	0.29	
Pearl Harb_B22	55	8/30/2012	11:11:33	14.455	305.94	21.16	21.05	-	-	-	4.10	0.28	
Pearl Harb_B22	56	8/30/2012	11:11:36	14.455	305.91	21.16	21.03	-	-	-	4.13	0.29	
Pearl Harb_B22	57	8/30/2012	11:11:39	14.455	306.03	21.17	21.01	-	-	-	4.01	0.28	
Pearl Harb_B22	58	8/30/2012	11:11:42	14.455	303.21	20.98	20.53	-	-	-	6.83	0.47	chunk of sed at right side, eroded; lower avg and min penetration
Pearl Harb_B22	59	8/30/2012	11:11:45	14.455	303.27	20.98	20.53	-	-	-	6.77	0.47	
Pearl Harb_B22	60	8/30/2012	11:11:48	14.455	303.34	20.99	20.53	-	-	-	6.70	0.46	
Pearl Harb_B22	61	8/30/2012	11:11:51	14.455	303.35	20.99	20.53	-	-	-	6.70	0.46	
Pearl Harb_B22	62	8/30/2012	11:11:54	14.455	303.31	20.98	20.54	-	-	-	6.73	0.47	
Pearl Harb_B22	63	8/30/2012	11:11:57	14.455	303.29	20.98	20.55	-	-	-	6.75	0.47	
Pearl Harb_B22	64	8/30/2012	11:12:00	14.455	303.53	21.00	20.54	-	-	-	6.52	0.45	
Pearl Harb_B22	65	8/30/2012	11:12:03	14.455	303.52	21.00	20.54	-	-	-	6.52	0.45	
Pearl Harb_B22	66	8/30/2012	11:12:06	14.455	303.34	20.98	20.54	-	-	-	6.70	0.46	
Pearl Harb_B22	67	8/30/2012	11:12:09	14.455	303.46	20.99	20.55	-	-	-	6.58	0.46	
Pearl Harb_B22	68	8/30/2012	11:12:12	14.455	303.48	20.99	20.54	-	-	-	6.56	0.45	
Pearl Harb_B22	69	8/30/2012	11:12:15	14.455	303.48	21.00	20.54	-	-	-	6.56	0.45	
Pearl Harb_B22	70	8/30/2012	11:12:18	14.455	303.49	21.00	20.55	-	-	-	6.55	0.45	
Pearl Harb_B22	71	8/30/2012	11:12:21	14.455	303.34	20.99	20.54	-	-	-	6.70	0.46	
Pearl Harb_B22	72	8/30/2012	11:12:24	14.455	303.48	20.99	20.55	-	-	-	6.56	0.45	
Pearl Harb_B22	73	8/30/2012	11:12:27	14.455	303.45	20.99	20.54	-	-	-	6.59	0.46	
Pearl Harb_B22	74	8/30/2012	11:12:30	14.455	303.47	20.99	20.54	-	-	-	6.57	0.45	
Pearl Harb_B22	75	8/30/2012	11:12:33	14.455	303.28	20.98	20.54	-	-	-	6.76	0.47	
Pearl Harb_B22	76	8/30/2012	11:12:36	14.455	303.22	20.98	20.55	-	-	-	6.82	0.47	
Pearl Harb_B22	77	8/30/2012	11:12:39	14.455	303.26	20.98	20.54	-	-	-	6.78	0.47	
Pearl Harb_B22	78	8/30/2012	11:12:42	14.455	303.39	20.99	20.54	-	-	-	6.65	0.46	
Pearl Harb_B22	79	8/30/2012	11:12:45	14.455	303.36	20.99	20.54	-	-	-	6.69	0.46	
Pearl Harb_B22	80	8/30/2012	11:12:48	14.455	303.42	20.99	20.54	-	-	-	6.62	0.46	
Pearl Harb_B22	81	8/30/2012	11:12:51	14.455	303.30	20.98	20.54	-	-	-	6.74	0.47	
Pearl Harb_B22	82	8/30/2012	11:12:54	14.455	303.30	20.98	20.54	-	-	-	6.74	0.47	
Pearl Harb_B22	83	8/30/2012	11:12:57	14.455	303.41	20.99	20.55	-	-	-	6.63	0.46	
Pearl Harb_B22	84	8/30/2012	11:13:00	14.455	303.32	20.98	20.54	-	-	-	6.72	0.46	
Pearl Harb_B22	85	8/30/2012	11:13:03	14.455	303.25	20.98	20.54	-	-	-	6.80	0.47	
Pearl Harb_B22	86	8/30/2012	11:13:06	14.455	303.26	20.98	20.54	-	-	-	6.78	0.47	
Pearl Harb_B22	87	8/30/2012	11:13:09	14.455	303.24	20.98	20.54	-	-	-	6.80	0.47	
Pearl Harb_B22	88	8/30/2012	11:13:12	14.455	303.33	20.98	20.54	-	-	-	6.71	0.46	
Pearl Harb_B22	89	8/30/2012	11:13:15	14.455	303.30	20.98	20.55	-	-	-	6.74	0.47	
Pearl Harb_B22	90	8/30/2012	11:13:18	14.455	303.32	20.98	20.55	-	-	-	6.72	0.47	
Pearl Harb_B22	91	8/30/2012	11:13:21	14.455	303.24	20.98	20.55	-	-	-	6.80	0.47	
Pearl Harb_B22	92	8/30/2012	11:13:24	14.455	303.29	20.98	20.54	-	-	-	6.75	0.47	
Pearl Harb_B22	93	8/30/2012	11:13:27	14.455	303.31	20.98	20.55	-	-	-	6.73	0.47	
Pearl Harb_B22	94	8/30/2012	11:13:30	14.455	303.31	20.98	20.54	-	-	-	6.73	0.47	
Pearl Harb_B22	95	8/30/2012	11:13:33	14.455	303.25	20.98	20.55	-	-	-	6.79	0.47	
Pearl Harb_B22	96	8/30/2012	11:13:36	14.455	303.35	20.99	20.55	-	-	-	6.70	0.46	
Pearl Harb_B22	97	8/30/2012	11:13:39	14.455	303.34	20.99	20.56	-	-	-	6.70	0.46	
Pearl Harb_B22	98	8/30/2012	11:13:42	14.455	303.34	20.98	20.55	-	-	-	6.71	0.46	
Pearl Harb_B22	99	8/30/2012	11:13:45	14.455	303.33	20.98	20.55	-	-	-	6.71	0.46	
Pearl Harb_B22	100	8/30/2012	11:13:48	14.455	303.31	20.98	20.55	-	-	-	6.73	0.47	

STATION	REP	DATE	TIME	Calibration Constant	Penetration Area (sq.cm)	Average Penetration (cm)	Minimum Penetration (cm)	Maximum Penetration (cm)	Sus Sed Area (sq.cm)	Sus Sed (cm)	Area of Water Visible (sq cm)	Water Visible (cm)	COMMENT
Pearl Harb_B22	101	8/30/2012	11:13:51	14.455	303.39	20.99	20.56	-	-	-	6.66	0.46	
Pearl Harb_B22	102	8/30/2012	11:13:54	14.455	303.40	20.99	20.55	-	-	-	6.64	0.46	
Pearl Harb_B22	103	8/30/2012	11:13:57	14.455	303.49	21.00	20.55	-	-	-	6.55	0.45	
Pearl Harb_B22	104	8/30/2012	11:14:00	14.455	303.44	20.99	20.55	-	-	-	6.60	0.46	
Pearl Harb_B22	105	8/30/2012	11:14:03	14.455	303.47	20.99	20.56	-	-	-	6.58	0.45	
Pearl Harb_B22	106	8/30/2012	11:14:06	14.455	303.48	20.99	20.59	-	-	-	6.56	0.45	
Pearl Harb_B22	107	8/30/2012	11:14:09	14.455	303.47	20.99	20.58	-	-	-	6.57	0.45	
Pearl Harb_B22	108	8/30/2012	11:14:12	14.455	303.58	21.00	20.59	-	-	-	6.46	0.45	
Pearl Harb_B22	109	8/30/2012	11:14:15	14.455	303.60	21.00	20.59	-	-	-	6.44	0.45	
Pearl Harb_B22	110	8/30/2012	11:14:18	14.455	303.62	21.00	20.59	-	-	-	6.42	0.44	
Pearl Harb_B22	111	8/30/2012	11:14:21	14.455	303.98	21.03	20.68	-	-	-	6.06	0.42	
Pearl Harb_B22	112	8/30/2012	11:14:24	14.455	303.97	21.03	20.65	-	-	-	6.08	0.42	
Pearl Harb_B22	113	8/30/2012	11:14:27	14.455	303.77	21.01	20.62	-	-	-	6.28	0.43	
Pearl Harb_B22	114	8/30/2012	11:14:30	14.455	303.83	21.02	20.63	-	-	-	6.21	0.43	
Pearl Harb_B22	115	8/30/2012	11:14:33	14.455	303.79	21.02	20.63	-	-	-	6.26	0.43	
Pearl Harb_B22	116	8/30/2012	11:14:36	14.455	303.88	21.02	20.62	-	-	-	6.16	0.43	
Pearl Harb_B22	117	8/30/2012	11:14:39	14.455	303.96	21.03	20.63	-	-	-	6.08	0.42	
Pearl Harb_B22	118	8/30/2012	11:14:42	14.455	303.94	21.03	20.64	-	-	-	6.10	0.42	
Pearl Harb_B22	119	8/30/2012	11:14:45	14.455	303.98	21.03	20.63	-	-	-	6.06	0.42	
Pearl Harb_B22	120	8/30/2012	11:14:48	14.455	303.96	21.03	20.64	-	-	-	6.08	0.42	
Pearl Harb_B22	121	8/30/2012	11:14:51	14.455	304.03	21.03	20.65	-	-	-	6.01	0.42	
Pearl Harb_B22	122	8/30/2012	11:14:54	14.455	303.93	21.03	20.65	-	-	-	6.11	0.42	
Pearl Harb_B22	123	8/30/2012	11:14:57	14.455	303.99	21.03	20.64	-	-	-	6.05	0.42	
Pearl Harb_B22	124	8/30/2012	11:15:00	14.455	303.96	21.03	20.64	-	-	-	6.08	0.42	
Pearl Harb_B22	125	8/30/2012	11:15:03	14.455	303.96	21.03	20.64	-	-	-	6.08	0.42	
Pearl Harb_B22	126	8/30/2012	11:15:06	14.455	303.90	21.02	20.63	-	-	-	6.15	0.43	
Pearl Harb_B22	127	8/30/2012	11:15:09	14.455	304.07	21.04	20.62	-	-	-	5.97	0.41	
Pearl Harb_B22	128	8/30/2012	11:15:12	14.455	303.88	21.02	20.63	-	-	-	6.16	0.43	
Pearl Harb_B22	129	8/30/2012	11:15:15	14.455	303.96	21.03	20.63	-	-	-	6.08	0.42	
Pearl Harb_B22	130	8/30/2012	11:15:18	14.455	303.98	21.03	20.64	-	-	-	6.07	0.42	
Pearl Harb_B22	131	8/30/2012	11:15:21	14.455	303.86	21.02	20.62	-	-	-	6.18	0.43	
Pearl Harb_B22	132	8/30/2012	11:15:24	14.455	304.00	21.03	20.64	-	-	-	6.04	0.42	
Pearl Harb_B22	133	8/30/2012	11:15:27	14.455	303.96	21.03	20.63	-	-	-	6.08	0.42	
Pearl Harb_B22	134	8/30/2012	11:15:30	14.455	303.96	21.03	20.64	-	-	-	6.08	0.42	
Pearl Harb_B22	135	8/30/2012	11:15:33	14.455	303.92	21.02	20.63	-	-	-	6.13	0.42	
Pearl Harb_B22	136	8/30/2012	11:15:36	14.455	303.86	21.02	20.63	-	-	-	6.18	0.43	
Pearl Harb_B22	137	8/30/2012	11:15:39	14.455	303.88	21.02	20.63	-	-	-	6.16	0.43	
Pearl Harb_B22	138	8/30/2012	11:15:42	14.455	303.90	21.02	20.63	-	-	-	6.14	0.42	
Pearl Harb_B22	139	8/30/2012	11:15:45	14.455	303.94	21.03	20.63	-	-	-	6.10	0.42	
Pearl Harb_B22	140	8/30/2012	11:15:48	14.455	303.99	21.03	20.63	-	-	-	6.05	0.42	
Pearl Harb_B22	141	8/30/2012	11:15:51	14.455	303.97	21.03	20.63	-	-	-	6.07	0.42	
Pearl Harb_B22	142	8/30/2012	11:15:54	14.455	303.96	21.03	20.63	-	-	-	6.08	0.42	
Pearl Harb_B22	143	8/30/2012	11:15:57	14.455	303.94	21.03	20.62	-	-	-	6.10	0.42	
Pearl Harb_B22	144	8/30/2012	11:16:00	14.455	304.01	21.03	20.63	-	-	-	6.03	0.42	
Pearl Harb_B22	145	8/30/2012	11:16:03	14.455	303.99	21.03	20.62	-	-	-	6.06	0.42	
Pearl Harb_B22	146	8/30/2012	11:16:06	14.455	303.90	21.02	20.63	-	-	-	6.15	0.43	
Pearl Harb_B22	147	8/30/2012	11:16:09	14.455	304.04	21.03	20.62	-	-	-	6.00	0.42	
Pearl Harb_B22	148	8/30/2012	11:16:12	14.455	303.94	21.03	20.62	-	-	-	6.10	0.42	
Pearl Harb_B22	149	8/30/2012	11:16:15	14.455	303.86	21.02	20.62	-	-	-	6.19	0.43	
Pearl Harb_B22	150	8/30/2012	11:16:18	14.455	303.97	21.03	20.62	-	-	-	6.07	0.42	
Pearl Harb_B22	151	8/30/2012	11:16:21	14.455	304.05	21.03	20.62	-	-	-	5.99	0.41	
Pearl Harb_B22	152	8/30/2012	11:16:24	14.455	303.88	21.02	20.62	-	-	-	6.16	0.43	
Pearl Harb_B22	153	8/30/2012	11:16:27	14.455	303.99	21.03	20.62	-	-	-	6.05	0.42	
Pearl Harb_B22	154	8/30/2012	11:16:30	14.455	303.92	21.03	20.62	-	-	-	6.13	0.42	
Pearl Harb_B22	155	8/30/2012	11:16:33	14.455	303.86	21.02	20.62	-	-	-	6.19	0.43	

STATION	REP	DATE	TIME	Calibration Constant	Penetration Area (sq.cm)	Average Penetration (cm)	Minimum Penetration (cm)	Maximum Penetration (cm)	Sus Sed Area (sq.cm)	Sus Sed (cm)	Area of Water Visible (sq cm)	Water Visible (cm)	COMMENT
Pearl Harb_B22	156	8/30/2012	11:16:36	14.455	303.90	21.02	20.62	-	-	-	6.14	0.43	
Pearl Harb_B22	157	8/30/2012	11:16:39	14.455	303.93	21.03	20.62	-	-	-	6.11	0.42	
Pearl Harb_B22	158	8/30/2012	11:16:42	14.455	303.92	21.03	20.62	-	-	-	6.12	0.42	
Pearl Harb_B22	159	8/30/2012	11:16:45	14.455	303.84	21.02	20.62	-	-	-	6.20	0.43	
Pearl Harb_B22	160	8/30/2012	11:16:48	14.455	303.76	21.01	20.62	-	-	-	6.28	0.43	
Pearl Harb_B22	161	8/30/2012	11:16:51	14.455	303.90	21.02	20.62	-	-	-	6.14	0.43	
Pearl Harb_B22	162	8/30/2012	11:16:54	14.455	303.83	21.02	20.61	-	-	-	6.22	0.43	
Pearl Harb_B22	163	8/30/2012	11:16:57	14.455	303.77	21.01	20.59	-	-	-	6.27	0.43	
Pearl Harb_B22	164	8/30/2012	11:17:00	14.455	303.90	21.02	20.61	-	-	-	6.15	0.43	
Pearl Harb_B22	165	8/30/2012	11:17:03	14.455	303.85	21.02	20.60	-	-	-	6.19	0.43	
Pearl Harb_B22	166	8/30/2012	11:17:06	14.455	303.82	21.02	20.59	-	-	-	6.22	0.43	
Pearl Harb_B22	167	8/30/2012	11:17:09	14.455	303.87	21.02	20.60	-	-	-	6.17	0.43	
Pearl Harb_B22	168	8/30/2012	11:17:12	14.455	303.81	21.02	20.60	-	-	-	6.23	0.43	
Pearl Harb_B22	169	8/30/2012	11:17:15	14.455	303.82	21.02	20.60	-	-	-	6.22	0.43	
Pearl Harb_B22	170	8/30/2012	11:17:18	14.455	303.80	21.02	20.60	-	-	-	6.24	0.43	
Pearl Harb_B22	171	8/30/2012	11:17:21	14.455	303.63	21.01	20.60	-	-	-	6.41	0.44	
Pearl Harb_B22	172	8/30/2012	11:17:24	14.455	303.65	21.01	20.59	-	-	-	6.39	0.44	
Pearl Harb_B22	173	8/30/2012	11:17:27	14.455	303.81	21.02	20.59	-	-	-	6.23	0.43	
Pearl Harb_B22	174	8/30/2012	11:17:30	14.455	303.66	21.01	20.60	-	-	-	6.38	0.44	
Pearl Harb_B22	175	8/30/2012	11:17:33	14.455	303.86	21.02	20.60	-	-	-	6.19	0.43	
Pearl Harb_B22	176	8/30/2012	11:17:36	14.455	303.76	21.01	20.60	-	-	-	6.28	0.43	
Pearl Harb_B22	177	8/30/2012	11:17:39	14.455	303.72	21.01	20.60	-	-	-	6.32	0.44	
Pearl Harb_B22	178	8/30/2012	11:17:42	14.455	303.76	21.01	20.60	-	-	-	6.28	0.43	
Pearl Harb_B22	179	8/30/2012	11:17:45	14.455	303.71	21.01	20.60	-	-	-	6.33	0.44	
Pearl Harb_B22	180	8/30/2012	11:17:48	14.455	303.78	21.02	20.59	-	-	-	6.26	0.43	
Pearl Harb_B22	181	8/30/2012	11:17:51	14.455	303.75	21.01	20.59	-	-	-	6.29	0.44	
Pearl Harb_B22	184	8/30/2012	11:18:00	14.455	303.78	21.02	20.59	-	-	-	6.26	0.43	
Pearl Harb_B22	234	8/30/2012	11:20:30	14.455	303.57	21.00	20.57	-	-	-	6.47	0.45	
Pearl Harb_B22	284	8/30/2012	11:23:00	14.455	303.45	20.99	20.54	-	-	-	6.59	0.46	
Pearl Harb_B22	287	8/30/2012	11:23:09	14.455	303.28	20.98	20.54	-	-	-	6.76	0.47	
Pearl Harb_B22	290	8/30/2012	11:23:18	14.455	303.35	20.99	20.54	-	-	-	6.69	0.46	
Pearl Harb_B22	293	8/30/2012	11:23:27	14.455	303.36	20.99	20.54	-	-	-	6.68	0.46	
Pearl Harb_B22	296	8/30/2012	11:23:36	14.455	303.29	20.98	20.54	-	-	-	6.75	0.47	
Pearl Harb_B22	299	8/30/2012	11:23:45	14.455	303.33	20.98	20.53	-	-	-	6.71	0.46	
Pearl Harb_B22	302	8/30/2012	11:23:54	14.455	303.17	20.97	20.53	-	-	-	6.87	0.48	
Pearl Harb_B22	305	8/30/2012	11:24:03	14.455	303.24	20.98	20.53	-	-	-	6.80	0.47	
Pearl Harb_B22	308	8/30/2012	11:24:12	14.455	303.25	20.98	20.53	-	-	-	6.80	0.47	
Pearl Harb_B22	311	8/30/2012	11:24:21	14.455	303.23	20.98	20.53	-	-	-	6.81	0.47	
Pearl Harb_B22	314	8/30/2012	11:24:30	14.455	303.29	20.98	20.53	-	-	-	6.75	0.47	
Pearl Harb_B22	317	8/30/2012	11:24:39	14.455	303.13	20.97	20.53	-	-	-	6.91	0.48	
Pearl Harb_B22	320	8/30/2012	11:24:48	14.455	303.31	20.98	20.53	-	-	-	6.73	0.47	
Pearl Harb_B22	323	8/30/2012	11:24:57	14.455	303.17	20.97	20.53	-	-	-	6.87	0.48	
Pearl Harb_B22	326	8/30/2012	11:25:06	14.455	303.12	20.97	20.52	-	-	-	6.92	0.48	
Pearl Harb_B22	329	8/30/2012	11:25:15	14.455	303.19	20.97	20.52	-	-	-	6.85	0.47	
Pearl Harb_B22	332	8/30/2012	11:25:24	14.455	303.18	20.97	20.52	-	-	-	6.86	0.47	
Pearl Harb_B22	335	8/30/2012	11:25:33	14.455	303.22	20.98	20.52	-	-	-	6.82	0.47	
Pearl Harb_B22	338	8/30/2012	11:25:42	14.455	303.20	20.98	20.52	-	-	-	6.85	0.47	
Pearl Harb_B22	341	8/30/2012	11:25:51	14.455	303.21	20.98	20.52	-	-	-	6.84	0.47	
Pearl Harb_B22	344	8/30/2012	11:26:00	14.455	303.18	20.97	20.52	-	-	-	6.86	0.47	
Pearl Harb_B22	347	8/30/2012	11:26:09	14.455	303.21	20.98	20.52	-	-	-	6.84	0.47	
Pearl Harb_B22	350	8/30/2012	11:26:18	14.455	303.16	20.97	20.52	-	-	-	6.88	0.48	
Pearl Harb_B22	353	8/30/2012	11:26:27	14.455	303.14	20.97	20.52	-	-	-	6.90	0.48	
Pearl Harb_B22	356	8/30/2012	11:26:36	14.455	303.17	20.97	20.52	-	-	-	6.88	0.48	
Pearl Harb_B22	359	8/30/2012	11:26:45	14.455	303.25	20.98	20.52	-	-	-	6.79	0.47	

STATION	REP	DATE	TIME	Calibration Constant	Penetration Area (sq.cm)	Average Penetration (cm)	Minimum Penetration (cm)	Maximum Penetration (cm)	Sus Sed Area (sq.cm)	Sus Sed (cm)	Area of Water Visible (sq cm)	Water Visible (cm)	COMMENT
Pearl Harb_B22	362	8/30/2012	11:26:54	14.455	303.09	20.97	20.52	-	-	-	6.95	0.48	
Pearl Harb_B22	365	8/30/2012	11:27:03	14.455	303.01	20.96	20.51	-	-	-	7.03	0.49	
Pearl Harb_B22	368	8/30/2012	11:27:12	14.455	303.13	20.97	20.61	-	-	-	6.91	0.48	
Pearl Harb_B22	371	8/30/2012	11:27:21	14.455	303.13	20.97	20.59	-	-	-	6.91	0.48	
Pearl Harb_B22	374	8/30/2012	11:27:30	14.455	302.49	20.93	20.52	-	-	-	7.55	0.52	a little more of SWI visible on left
Pearl Harb_B22	377	8/30/2012	11:27:39	14.455	300.87	20.81	20.42	-	-	-	9.17	0.63	even more of SWI visible on left
Pearl Harb_B22	380	8/30/2012	11:27:48	14.455	297.63	20.59	20.27	-	-	-	12.41	0.86	even more of SWI visible on left; almost all visible
Pearl Harb_B22	383	8/30/2012	11:27:57	14.455	298.83	20.67	20.31	-	-	-	11.22	0.78	
Pearl Harb_B22	386	8/30/2012	11:28:06	14.455	299.25	20.70	20.34	-	-	-	10.80	0.75	
Pearl Harb_B22	389	8/30/2012	11:28:15	14.455	299.75	20.74	20.39	-	-	-	10.29	0.71	
Pearl Harb_B22	392	8/30/2012	11:28:24	14.455	300.04	20.76	20.39	-	-	-	10.01	0.69	
Pearl Harb_B22	395	8/30/2012	11:28:33	14.455	300.07	20.76	20.38	-	-	-	9.97	0.69	
Pearl Harb_B22	398	8/30/2012	11:28:42	14.455	301.12	20.83	20.50	-	-	-	8.93	0.62	a little more of SWI visible on left
Pearl Harb_B22	401	8/30/2012	11:28:51	14.455	301.32	20.85	20.47	-	-	-	8.72	0.60	
Pearl Harb_B22	404	8/30/2012	11:29:00	14.455	304.24	21.05	20.84	-	-	-	5.81	0.40	a clump of sediment that was resuspended at 401, has settled back onto the surface (on right); looking ahead (434), this clump persists and is erodes, so I have measured it as part of the penetration depth
Pearl Harb_B22	407	8/30/2012	11:29:09	14.455	303.99	21.03	20.84	-	-	-	6.05	0.42	
Pearl Harb_B22	410	8/30/2012	11:29:18	14.455	304.11	21.04	20.84	-	-	-	5.93	0.41	a little less of SWI visible on left
Pearl Harb_B22	413	8/30/2012	11:29:27	14.455	304.00	21.03	20.85	-	-	-	6.05	0.42	
Pearl Harb_B22	416	8/30/2012	11:29:36	14.455	303.97	21.03	20.85	-	-	-	6.08	0.42	
Pearl Harb_B22	419	8/30/2012	11:29:45	14.455	304.14	21.04	20.85	-	-	-	5.91	0.41	
Pearl Harb_B22	422	8/30/2012	11:29:54	14.455	304.33	21.05	20.87	-	-	-	5.72	0.40	
Pearl Harb_B22	425	8/30/2012	11:30:03	14.455	304.23	21.05	20.84	-	-	-	5.81	0.40	
Pearl Harb_B22	428	8/30/2012	11:30:12	14.455	304.51	21.07	20.85	-	-	-	5.53	0.38	
Pearl Harb_B22	431	8/30/2012	11:30:21	14.455	304.16	21.04	20.77	-	-	-	5.88	0.41	min penetration is from different point now
Pearl Harb_B22	434	8/30/2012	11:30:30	14.455	304.38	21.06	20.80	-	-	-	5.67	0.39	
Pearl Harb_B22	437	8/30/2012	11:30:39	14.455	304.32	21.05	20.78	-	-	-	5.72	0.40	
Pearl Harb_B22	440	8/30/2012	11:30:48	14.455	303.94	21.03	20.76	-	-	-	6.10	0.42	
Pearl Harb_B22	443	8/30/2012	11:30:57	14.455	303.85	21.02	20.74	-	-	-	6.19	0.43	
Pearl Harb_B22	446	8/30/2012	11:31:06	14.455	303.88	21.02	20.75	-	-	-	6.16	0.43	
Pearl Harb_B22	449	8/30/2012	11:31:15	14.455	303.52	21.00	20.74	-	-	-	6.52	0.45	orangish clump in center (no sign of it before), gone by 461; not measured in penetration depth
Pearl Harb_B22	452	8/30/2012	11:31:24	14.455	303.56	21.00	20.69	-	-	-	6.48	0.45	
Pearl Harb_B22	455	8/30/2012	11:31:33	14.455	303.36	20.99	20.70	-	-	-	6.68	0.46	a little more of SWI visible on left
Pearl Harb_B22	458	8/30/2012	11:31:42	14.455	303.60	21.00	20.73	-	-	-	6.44	0.45	
Pearl Harb_B22	461	8/30/2012	11:31:51	14.455	304.01	21.03	20.76	-	-	-	6.03	0.42	a little less of SWI visible on left
Pearl Harb_B22	464	8/30/2012	11:32:00	14.455	303.71	21.01	20.69	-	-	-	6.34	0.44	
Pearl Harb_B22	467	8/30/2012	11:32:09	14.455	303.97	21.03	20.61	-	-	-	6.07	0.42	
Pearl Harb_B22	470	8/30/2012	11:32:18	14.455	303.25	20.98	20.49	-	-	-	6.79	0.47	
Pearl Harb_B22	473	8/30/2012	11:32:27	14.455	302.84	20.95	20.46	-	-	-	7.20	0.50	
Pearl Harb_B22	476	8/30/2012	11:32:36	14.455	302.65	20.94	20.44	-	-	-	7.39	0.51	
Pearl Harb_B22	479	8/30/2012	11:32:45	14.455	302.65	20.94	20.46	-	-	-	7.40	0.51	
Pearl Harb_B22	482	8/30/2012	11:32:54	14.455	302.82	20.95	20.47	-	-	-	7.22	0.50	
Pearl Harb_B22	485	8/30/2012	11:33:03	14.455	302.65	20.94	20.42	-	-	-	7.39	0.51	
Pearl Harb_B22	486	8/30/2012	11:33:06	14.455	302.85	20.95	20.45	-	-	-	7.19	0.50	
Pearl Harb_B22	489	8/30/2012	11:33:15	14.455	302.78	20.95	20.44	-	-	-	7.27	0.50	
Pearl Harb_B22	492	8/30/2012	11:33:24	14.455	302.83	20.95	20.44	-	-	-	7.22	0.50	
Pearl Harb_B22	495	8/30/2012	11:33:33	14.455	302.83	20.95	20.44	-	-	-	7.21	0.50	a little less of SWI visible on left
Pearl Harb_B22	498	8/30/2012	11:33:42	14.455	302.86	20.95	20.47	-	-	-	7.19	0.50	
Pearl Harb_B22	501	8/30/2012	11:33:51	14.455	302.81	20.95	20.46	-	-	-	7.23	0.50	
Pearl Harb_B22	504	8/30/2012	11:34:00	14.455	301.72	20.87	20.33	-	-	-	8.32	0.58	a little more of SWI visible on left
Pearl Harb_B22	507	8/30/2012	11:34:09	14.455	301.99	20.89	20.34	-	-	-	8.06	0.56	a little more of SWI visible on left

STATION	REP	DATE	TIME	Calibration Constant	Penetration Area (sq.cm)	Average Penetration (cm)	Minimum Penetration (cm)	Maximum Penetration (cm)	Sus Sed Area (sq.cm)	Sus Sed (cm)	Area of Water Visible (sq cm)	Water Visible (cm)	COMMENT
Pearl Harb_B22	510	8/30/2012	11:34:18	14.455	302.83	20.95	20.35	-	-	-	7.21	0.50	clump of sed blew from right over skipped images, settled to right of center, measured in pen
Pearl Harb_B22	513	8/30/2012	11:34:27	14.455	302.13	20.90	20.31	-	-	-	7.91	0.55	
Pearl Harb_B22	516	8/30/2012	11:34:36	14.455	301.73	20.87	20.24	-	-	-	8.31	0.57	
Pearl Harb_B22	519	8/30/2012	11:34:45	14.455	299.66	20.73	20.19	-	-	-	10.38	0.72	more of SWI visible on left; previous clump of sed blown out
Pearl Harb_B22	522	8/30/2012	11:34:54	14.455	293.17	20.28	19.88	21.21	-	-	16.88	1.17	first image with full SWI visible
Pearl Harb_B22	523	8/30/2012	11:34:57	14.455	292.31	20.22	19.73	21.16	1.26	0.09	17.74	1.23	
Pearl Harb_B22	524	8/30/2012	11:35:00	14.455	292.03	20.20	19.78	21.13	4.22	0.29	18.02	1.25	
Pearl Harb_B22	525	8/30/2012	11:35:03	14.455	292.08	20.21	19.73	21.24	0.92	0.06	17.96	1.24	
Pearl Harb_B22	526	8/30/2012	11:35:06	14.455	292.39	20.23	19.80	21.19	3.17	0.22	17.65	1.22	
Pearl Harb_B22	527	8/30/2012	11:35:09	14.455	292.51	20.24	19.78	21.27	3.04	0.21	17.54	1.21	
Pearl Harb_B22	528	8/30/2012	11:35:12	14.455	292.24	20.22	19.80	21.32	2.99	0.21	17.80	1.23	
Pearl Harb_B22	529	8/30/2012	11:35:15	14.455	292.24	20.22	19.78	21.29	1.27	0.09	17.80	1.23	
Pearl Harb_B22	530	8/30/2012	11:35:18	14.455	292.24	20.22	19.78	21.29	0.17	0.01	17.80	1.23	
Pearl Harb_B22	531	8/30/2012	11:35:21	14.455	292.69	20.25	19.78	21.27	0.91	0.06	17.35	1.20	
Pearl Harb_B22	534	8/30/2012	11:35:30	14.455	292.08	20.21	19.74	21.23	0.86	0.06	17.96	1.24	
Pearl Harb_B22	537	8/30/2012	11:35:39	14.455	292.19	20.21	19.74	21.21	0.25	0.02	17.85	1.23	
Pearl Harb_B22	540	8/30/2012	11:35:48	14.455	292.30	20.22	19.73	21.21	0.52	0.04	17.74	1.23	
Pearl Harb_B22	543	8/30/2012	11:35:57	14.455	291.64	20.18	19.69	21.21	0.84	0.06	18.41	1.27	
Pearl Harb_B22	546	8/30/2012	11:36:06	14.455	291.20	20.15	19.59	21.21	0.32	0.02	18.84	1.30	
Pearl Harb_B22	549	8/30/2012	11:36:15	14.455	289.77	20.05	19.62	21.12	1.03	0.07	20.27	1.40	
Pearl Harb_B22	552	8/30/2012	11:36:24	14.455	287.14	19.86	19.61	20.92	9.07	0.63	22.90	1.58	lots of suspended sed- almost entire SWI
Pearl Harb_B22	555	8/30/2012	11:36:33	14.455	283.73	19.63	19.27	20.77	3.79	0.26	26.31	1.82	
Pearl Harb_B22	558	8/30/2012	11:36:42	14.455	283.41	19.61	19.29	20.68	1.63	0.11	26.63	1.84	
Pearl Harb_B22	561	8/30/2012	11:36:51	14.455	283.12	19.59	19.17	20.67	3.46	0.24	26.92	1.86	
Pearl Harb_B22	564	8/30/2012	11:37:00	14.455	283.32	19.60	19.22	20.67	5.11	0.35	26.72	1.85	
Pearl Harb_B22	567	8/30/2012	11:37:09	14.455	281.65	19.48	19.16	20.55	2.62	0.18	28.39	1.96	
Pearl Harb_B22	570	8/30/2012	11:37:18	14.455	279.15	19.31	18.54	20.48	2.78	0.19	30.89	2.14	
Pearl Harb_B22	573	8/30/2012	11:37:27	14.455	280.06	19.37	18.56	20.59	2.71	0.19	29.99	2.07	
Pearl Harb_B22	576	8/30/2012	11:37:36	14.455	278.62	19.27	18.36	20.54	2.12	0.15	31.42	2.17	
Pearl Harb_B22	579	8/30/2012	11:37:45	14.455	277.81	19.22	18.25	20.50	0.97	0.07	32.23	2.23	
Pearl Harb_B22	582	8/30/2012	11:37:54	14.455	279.43	19.33	18.46	20.60	1.55	0.11	30.62	2.12	
Pearl Harb_B22	585	8/30/2012	11:38:03	14.455	279.08	19.31	18.42	20.60	0.85	0.06	30.96	2.14	
Pearl Harb_B22	588	8/30/2012	11:38:12	14.455	278.17	19.24	18.32	20.48	0.50	0.03	31.88	2.21	
Pearl Harb_B22	591	8/30/2012	11:38:21	14.455	277.86	19.22	18.33	20.50	2.35	0.16	32.18	2.23	
Pearl Harb_B22	594	8/30/2012	11:38:30	14.455	277.94	19.23	18.52	20.34	5.27	0.36	32.11	2.22	lots of suspended sed- esp on right
Pearl Harb_B22	597	8/30/2012	11:38:39	14.455	274.97	19.02	18.64	20.37	14.07	0.97	35.07	2.43	
Pearl Harb_B22	600	8/30/2012	11:38:48	14.455	277.61	19.21	18.44	20.37	1.40	0.10	32.43	2.24	
Pearl Harb_B22	603	8/30/2012	11:38:57	14.455	274.68	19.00	18.56	20.30	8.43	0.58	35.37	2.45	lots of suspended sed- including larger clumps
Pearl Harb_B22	606	8/30/2012	11:39:06	14.455	265.28	18.35	18.00	18.60	13.09	0.91	44.76	3.10	top of left side blown up, maximum pen point now in middle
Pearl Harb_B22	609	8/30/2012	11:39:15	14.455	265.35	18.36	17.94	18.52	5.30	0.37	44.69	3.09	
Pearl Harb_B22	612	8/30/2012	11:39:24	14.455	261.10	18.06	17.94	18.45	21.20	1.47	48.94	3.39	lots of suspended sed
Pearl Harb_B22	615	8/30/2012	11:39:33	14.455	252.45	17.46	17.15	18.07	26.71	1.85	57.60	3.98	lots of suspended sed
Pearl Harb_B22	618	8/30/2012	11:39:42	14.455	248.60	17.20	16.42	17.75	12.48	0.86	61.44	4.25	
Pearl Harb_B22	621	8/30/2012	11:39:51	14.455	245.98	17.02	16.35	17.71	6.80	0.47	64.06	4.43	
Pearl Harb_B22	624	8/30/2012	11:40:00	14.455	240.13	16.61	15.86	17.57	24.75	1.71	69.91	4.84	min penetration is from different point now
Pearl Harb_B22	627	8/30/2012	11:40:09	14.455	243.02	16.81	16.23	17.59	13.88	0.96	67.03	4.64	
Pearl Harb_B22	630	8/30/2012	11:40:18	14.455	242.75	16.79	16.23	17.53	11.29	0.78	67.29	4.66	
Pearl Harb_B22	633	8/30/2012	11:40:27	14.455	243.89	16.87	16.43	17.61	11.06	0.76	66.15	4.58	
Pearl Harb_B22	636	8/30/2012	11:40:36	14.455	243.21	16.83	16.27	17.56	5.33	0.37	66.83	4.62	
Pearl Harb_B22	639	8/30/2012	11:40:45	14.455	242.34	16.77	15.95	17.51	1.95	0.14	67.70	4.68	
Pearl Harb_B22	642	8/30/2012	11:40:54	14.455	242.63	16.79	15.96	17.66	14.01	0.97	67.41	4.66	
Pearl Harb_B22	645	8/30/2012	11:41:03	14.455	239.66	16.58	15.85	17.54	13.45	0.93	70.38	4.87	
Pearl Harb_B22	648	8/30/2012	11:41:12	14.455	240.63	16.65	15.94	17.56	7.04	0.49	69.42	4.80	

STATION	REP	DATE	TIME	Calibration Constant	Penetration Area (sq.cm)	Average Penetration (cm)	Minimum Penetration (cm)	Maximum Penetration (cm)	Sus Sed Area (sq.cm)	Sus Sed (cm)	Area of Water Visible (sq cm)	Water Visible (cm)	COMMENT
Pearl Harb_B22	651	8/30/2012	11:41:21	14.455	240.74	16.65	15.90	17.56	7.65	0.53	69.30	4.79	
Pearl Harb_B22	654	8/30/2012	11:41:30	14.455	239.92	16.60	15.97	17.51	9.01	0.62	70.12	4.85	
Pearl Harb_B22	657	8/30/2012	11:41:39	14.455	239.53	16.57	15.85	17.50	19.66	1.36	70.52	4.88	
Pearl Harb_B22	660	8/30/2012	11:41:48	14.455	238.21	16.48	15.61	17.63	50.24	3.48	71.83	4.97	lots of suspended sed- almost entire SWI
Pearl Harb_B22	663	8/30/2012	11:41:57	14.455	238.10	16.47	15.70	17.38	20.94	1.45	71.95	4.98	
Pearl Harb_B22	666	8/30/2012	11:42:06	14.455	237.54	16.43	15.59	17.61	26.25	1.82	72.50	5.02	min pen is now back at the right edge
Pearl Harb_B22	669	8/30/2012	11:42:15	14.455	238.28	16.48	15.74	17.61	15.86	1.10	71.76	4.96	
Pearl Harb_B22	672	8/30/2012	11:42:24	14.455	237.80	16.45	15.57	17.59	11.66	0.81	72.25	5.00	
Pearl Harb_B22	675	8/30/2012	11:42:33	14.455	237.62	16.44	15.55	17.63	17.17	1.19	72.42	5.01	
Pearl Harb_B22	678	8/30/2012	11:42:42	14.455	238.43	16.49	15.58	17.65	11.37	0.79	71.61	4.95	
Pearl Harb_B22	681	8/30/2012	11:42:51	14.455	237.73	16.45	15.55	17.59	8.13	0.56	72.31	5.00	
Pearl Harb_B22	684	8/30/2012	11:43:00	14.455	238.82	16.52	15.51	17.52	13.44	0.93	71.22	4.93	
Pearl Harb_B22	687	8/30/2012	11:43:09	14.455	238.23	16.48	15.48	17.52	22.73	1.57	71.81	4.97	
Pearl Harb_B22	690	8/30/2012	11:43:18	14.455	237.14	16.41	15.46	17.49	18.89	1.31	72.90	5.04	
Pearl Harb_B22	693	8/30/2012	11:43:27	14.455	238.17	16.48	15.56	17.60	12.29	0.85	71.87	4.97	
Pearl Harb_B22	696	8/30/2012	11:43:36	14.455	238.30	16.49	15.52	17.56	3.46	0.24	71.74	4.96	
Pearl Harb_B22	699	8/30/2012	11:43:45	14.455	238.37	16.49	15.52	17.56	4.34	0.30	71.67	4.96	
Pearl Harb_B22	702	8/30/2012	11:43:54	14.455	238.44	16.50	15.51	17.56	13.15	0.91	71.61	4.95	
Pearl Harb_B22	705	8/30/2012	11:44:03	14.455	238.14	16.47	15.49	17.54	27.90	1.93	71.90	4.97	
Pearl Harb_B22	708	8/30/2012	11:44:12	14.455	236.64	16.37	15.43	17.39	29.67	2.05	73.40	5.08	
Pearl Harb_B22	711	8/30/2012	11:44:21	14.455	233.62	16.16	14.16	17.35	29.33	2.03	76.42	5.29	
Pearl Harb_B22	714	8/30/2012	11:44:30	14.455	234.01	16.19	14.16	17.35	29.01	2.01	76.03	5.26	
Pearl Harb_B22	717	8/30/2012	11:44:39	14.455	233.92	16.18	14.53	17.34	19.43	1.34	76.13	5.27	
Pearl Harb_B22	720	8/30/2012	11:44:48	14.455	233.86	16.18	14.51	17.34	5.46	0.38	76.18	5.27	
Pearl Harb_B22	723	8/30/2012	11:44:57	14.455	232.91	16.11	14.34	17.30	4.65	0.32	77.13	5.34	
Pearl Harb_B22	726	8/30/2012	11:45:06	14.455	232.75	16.10	14.16	17.31	5.43	0.38	77.29	5.35	
Pearl Harb_B22	729	8/30/2012	11:45:15	14.455	231.95	16.05	14.10	17.24	11.16	0.77	78.10	5.40	
Pearl Harb_B22	732	8/30/2012	11:45:24	14.455	232.03	16.05	14.07	17.22	14.78	1.02	78.02	5.40	
Pearl Harb_B22	735	8/30/2012	11:45:33	14.455	231.83	16.04	14.09	17.28	10.67	0.74	78.21	5.41	
Pearl Harb_B22	738	8/30/2012	11:45:42	14.455	230.66	15.96	14.07	17.21	20.95	1.45	79.38	5.49	
Pearl Harb_B22	741	8/30/2012	11:45:51	14.455	228.84	15.83	13.58	17.31	45.34	3.14	81.20	5.62	lots of suspended sed- including larger clumps
Pearl Harb_B22	744	8/30/2012	11:46:00	14.455	228.78	15.83	13.60	17.29	46.86	3.24	81.26	5.62	lots of suspended sed- including larger clumps
Pearl Harb_B22	747	8/30/2012	11:46:09	14.455	229.45	15.87	13.61	17.29	8.50	0.59	80.59	5.58	
Pearl Harb_B22	750	8/30/2012	11:46:18	14.455	228.09	15.78	13.53	17.29	5.91	0.41	81.95	5.67	
Pearl Harb_B22	753	8/30/2012	11:46:27	14.455	227.39	15.73	13.51	17.22	20.67	1.43	82.65	5.72	
Pearl Harb_B22	756	8/30/2012	11:46:36	14.455	226.66	15.68	13.48	17.22	19.36	1.34	83.38	5.77	
Pearl Harb_B22	759	8/30/2012	11:46:45	14.455	224.93	15.56	13.47	17.26	35.15	2.43	85.11	5.89	
Pearl Harb_B22	762	8/30/2012	11:46:54	14.455	225.39	15.59	13.39	17.06	14.10	0.98	84.65	5.86	
Pearl Harb_B22	765	8/30/2012	11:47:03	14.455	225.49	15.60	13.49	17.06	21.60	1.49	84.56	5.85	
Pearl Harb_B22	768	8/30/2012	11:47:12	14.455	226.51	15.67	13.58	17.17	23.41	1.62	83.53	5.78	
Pearl Harb_B22	771	8/30/2012	11:47:21	14.455	227.61	15.75	13.57	17.17	28.65	1.98	82.43	5.70	
Pearl Harb_B22	774	8/30/2012	11:47:30	14.455	227.01	15.70	13.54	17.12	18.36	1.27	83.03	5.74	
Pearl Harb_B22	777	8/30/2012	11:47:39	14.455	226.57	15.67	13.53	17.16	28.66	1.98	83.48	5.77	
Pearl Harb_B22	780	8/30/2012	11:47:48	14.455	226.68	15.68	13.50	17.11	29.92	2.07	83.36	5.77	
Pearl Harb_B22	783	8/30/2012	11:47:57	14.455	226.20	15.65	13.50	17.11	19.25	1.33	83.84	5.80	
Pearl Harb_B22	786	8/30/2012	11:48:06	14.455	226.67	15.68	13.53	17.14	4.18	0.29	83.37	5.77	
Pearl Harb_B22	789	8/30/2012	11:48:15	14.455	226.61	15.68	13.53	17.14	8.34	0.58	83.44	5.77	
Pearl Harb_B22	792	8/30/2012	11:48:24	14.455	226.58	15.67	13.52	17.14	11.19	0.77	83.46	5.77	
Pearl Harb_B22	795	8/30/2012	11:48:33	14.455	226.34	15.66	13.50	17.14	4.80	0.33	83.70	5.79	
Pearl Harb_B22	798	8/30/2012	11:48:42	14.455	226.24	15.65	13.50	17.12	6.40	0.44	83.80	5.80	
Pearl Harb_B22	801	8/30/2012	11:48:51	14.455	225.85	15.62	13.47	17.11	6.97	0.48	84.19	5.82	
Pearl Harb_B22	804	8/30/2012	11:49:00	14.455	225.25	15.58	13.45	17.08	7.77	0.54	84.79	5.87	
Pearl Harb_B22	807	8/30/2012	11:49:09	14.455	225.21	15.58	13.44	17.02	4.68	0.32	84.83	5.87	
Pearl Harb_B22	810	8/30/2012	11:49:18	14.455	224.83	15.55	13.44	16.84	6.01	0.42	85.21	5.89	

STATION	REP	DATE	TIME	Calibration Constant	Penetration Area (sq.cm)	Average Penetration (cm)	Minimum Penetration (cm)	Maximum Penetration (cm)	Sus Sed Area (sq.cm)	Sus Sed (cm)	Area of Water Visible (sq cm)	Water Visible (cm)	COMMENT
Pearl Harb_B22	813	8/30/2012	11:49:27	14.455	225.70	15.61	13.49	16.90	5.98	0.41	84.34	5.83	
Pearl Harb_B22	816	8/30/2012	11:49:36	14.455	225.67	15.61	13.50	16.89	14.67	1.01	84.37	5.84	
Pearl Harb_B22	819	8/30/2012	11:49:45	14.455	225.92	15.63	13.49	16.89	11.36	0.79	84.12	5.82	
Pearl Harb_B22	822	8/30/2012	11:49:54	14.455	225.85	15.62	13.49	16.89	19.30	1.33	84.19	5.82	
Pearl Harb_B22	825	8/30/2012	11:50:03	14.455	225.74	15.62	13.49	16.89	14.69	1.02	84.30	5.83	
Pearl Harb_B22	828	8/30/2012	11:50:12	14.455	225.94	15.63	13.49	16.90	17.14	1.19	84.11	5.82	
Pearl Harb_B22	831	8/30/2012	11:50:21	14.455	225.85	15.62	13.51	16.90	19.10	1.32	84.19	5.82	
Pearl Harb_B22	834	8/30/2012	11:50:30	14.455	226.14	15.64	13.56	16.89	30.26	2.09	83.90	5.80	
Pearl Harb_B22	837	8/30/2012	11:50:39	14.455	225.80	15.62	13.50	16.89	34.85	2.41	84.24	5.83	
Pearl Harb_B22	840	8/30/2012	11:50:48	14.455	223.97	15.49	13.43	16.86	18.73	1.30	86.08	5.95	
Pearl Harb_B22	843	8/30/2012	11:50:57	14.455	225.13	15.57	13.55	16.90	32.48	2.25	84.91	5.87	
Pearl Harb_B22	844	8/30/2012	11:51:00	14.455	224.41	15.52	13.55	16.92	27.90	1.93	85.64	5.92	
Pearl Harb_B22	846	8/30/2012	11:51:06	14.455	223.88	15.49	13.55	16.87	14.66	1.01	86.16	5.96	
Pearl Harb_B22	848	8/30/2012	11:51:12	14.455	224.10	15.50	13.52	16.83	27.23	1.88	85.94	5.95	
Pearl Harb_B22	850	8/30/2012	11:51:18	14.455	223.79	15.48	13.52	16.86	28.26	1.96	86.26	5.97	
Pearl Harb_B22	852	8/30/2012	11:51:24	14.455	223.34	15.45	13.48	16.82	35.93	2.49	86.70	6.00	
Pearl Harb_B22	854	8/30/2012	11:51:30	14.455	223.48	15.46	13.50	16.85	16.93	1.17	86.56	5.99	
Pearl Harb_B22	856	8/30/2012	11:51:36	14.455	223.46	15.46	13.50	16.86	18.60	1.29	86.58	5.99	
Pearl Harb_B22	858	8/30/2012	11:51:42	14.455	223.49	15.46	13.48	16.84	12.10	0.84	86.55	5.99	
Pearl Harb_B22	860	8/30/2012	11:51:48	14.455	222.76	15.41	13.44	16.84	27.19	1.88	87.28	6.04	several chunks of sed in sus sed
Pearl Harb_B22	862	8/30/2012	11:51:54	14.455	223.51	15.46	13.45	16.85	10.68	0.74	86.53	5.99	
Pearl Harb_B22	864	8/30/2012	11:52:00	14.455	223.65	15.47	13.45	16.85	10.34	0.72	86.40	5.98	
Pearl Harb_B22	866	8/30/2012	11:52:06	14.455	223.08	15.43	13.44	16.82	5.06	0.35	86.96	6.02	
Pearl Harb_B22	868	8/30/2012	11:52:12	14.455	222.70	15.41	13.43	16.82	1.30	0.09	87.34	6.04	
Pearl Harb_B22	870	8/30/2012	11:52:18	14.455	221.69	15.34	13.42	16.76	9.41	0.65	88.35	6.11	
Pearl Harb_B22	872	8/30/2012	11:52:24	14.455	221.33	15.31	13.40	16.73	21.20	1.47	88.71	6.14	
Pearl Harb_B22	874	8/30/2012	11:52:30	14.455	218.79	15.14	13.21	16.66	13.26	0.92	91.26	6.31	
Pearl Harb_B22	876	8/30/2012	11:52:36	14.455	217.30	15.03	13.21	16.25	13.94	0.96	92.74	6.42	
Pearl Harb_B22	878	8/30/2012	11:52:42	14.455	218.25	15.10	13.25	16.25	33.90	2.35	91.79	6.35	
Pearl Harb_B22	880	8/30/2012	11:52:48	14.455	219.59	15.19	13.27	16.34	22.90	1.58	90.45	6.26	
Pearl Harb_B22	882	8/30/2012	11:52:54	14.455	219.52	15.19	13.28	16.34	20.94	1.45	90.52	6.26	
Pearl Harb_B22	884	8/30/2012	11:53:00	14.455	220.28	15.24	13.35	16.40	13.81	0.96	89.76	6.21	
Pearl Harb_B22	886	8/30/2012	11:53:06	14.455	220.52	15.26	13.39	16.42	21.23	1.47	89.52	6.19	
Pearl Harb_B22	888	8/30/2012	11:53:12	14.455	220.02	15.22	13.31	16.42	27.75	1.92	90.02	6.23	
Pearl Harb_B22	890	8/30/2012	11:53:18	14.455	219.19	15.16	13.33	16.38	11.45	0.79	90.85	6.29	
Pearl Harb_B22	892	8/30/2012	11:53:24	14.455	221.13	15.30	13.53	16.47	31.65	2.19	88.91	6.15	
Pearl Harb_B22	894	8/30/2012	11:53:30	14.455	221.27	15.31	13.52	16.47	17.82	1.23	88.77	6.14	
Pearl Harb_B22	896	8/30/2012	11:53:36	14.455	221.22	15.30	13.51	16.46	6.04	0.42	88.82	6.14	
Pearl Harb_B22	898	8/30/2012	11:53:42	14.455	220.88	15.28	13.40	16.45	12.52	0.87	89.16	6.17	
Pearl Harb_B22	900	8/30/2012	11:53:48	14.455	221.35	15.31	13.39	16.50	30.09	2.08	88.69	6.14	
Pearl Harb_B22	902	8/30/2012	11:53:54	14.455	221.46	15.32	13.41	16.49	33.22	2.30	88.58	6.13	
Pearl Harb_B22	904	8/30/2012	11:54:00	14.455	221.45	15.32	13.42	16.48	13.93	0.96	88.60	6.13	
Pearl Harb_B22	906	8/30/2012	11:54:06	14.455	221.31	15.31	13.42	16.48	22.20	1.54	88.73	6.14	
Pearl Harb_B22	908	8/30/2012	11:54:12	14.455	221.60	15.33	13.27	16.52	29.69	2.05	88.44	6.12	
Pearl Harb_B22	910	8/30/2012	11:54:18	14.455	222.19	15.37	13.28	16.55	20.17	1.40	87.85	6.08	
Pearl Harb_B22	912	8/30/2012	11:54:24	14.455	222.22	15.37	13.32	16.59	14.88	1.03	87.83	6.08	
Pearl Harb_B22	914	8/30/2012	11:54:30	14.455	222.34	15.38	13.48	16.58	30.11	2.08	87.71	6.07	
Pearl Harb_B22	916	8/30/2012	11:54:36	14.455	221.90	15.35	13.43	16.55	21.82	1.51	88.14	6.10	
Pearl Harb_B22	918	8/30/2012	11:54:42	14.455	221.79	15.34	13.29	16.55	31.72	2.19	88.25	6.10	
Pearl Harb_B22	920	8/30/2012	11:54:48	14.455	221.59	15.33	13.29	16.53	16.75	1.16	88.45	6.12	
Pearl Harb_B22	922	8/30/2012	11:54:54	14.455	221.33	15.31	13.27	16.51	19.74	1.37	88.71	6.14	
Pearl Harb_B22	924	8/30/2012	11:55:00	14.455	221.09	15.30	13.27	16.51	14.66	1.01	88.95	6.15	
Pearl Harb_B22	926	8/30/2012	11:55:06	14.455	221.03	15.29	13.27	16.51	11.24	0.78	89.01	6.16	
Pearl Harb_B22	928	8/30/2012	11:55:12	14.455	221.67	15.34	13.40	16.54	10.50	0.73	88.37	6.11	

STATION	REP	DATE	TIME	Calibration Constant	Penetration Area (sq.cm)	Average Penetration (cm)	Minimum Penetration (cm)	Maximum Penetration (cm)	Sus Sed Area (sq.cm)	Sus Sed (cm)	Area of Water Visible (sq cm)	Water Visible (cm)	COMMENT
Pearl Harb_B22	930	8/30/2012	11:55:18	14.455	221.70	15.34	13.44	16.54	12.27	0.85	88.34	6.11	
Pearl Harb_B22	932	8/30/2012	11:55:24	14.455	221.90	15.35	13.49	16.54	13.21	0.91	88.14	6.10	
Pearl Harb_B22	934	8/30/2012	11:55:30	14.455	221.89	15.35	13.46	16.54	15.77	1.09	88.16	6.10	
Pearl Harb_B22	936	8/30/2012	11:55:36	14.455	222.13	15.37	13.49	16.51	11.47	0.79	87.92	6.08	
Pearl Harb_B22	938	8/30/2012	11:55:42	14.455	221.47	15.32	13.45	16.51	15.56	1.08	88.57	6.13	
Pearl Harb_B22	940	8/30/2012	11:55:48	14.455	221.83	15.35	13.32	16.55	22.05	1.53	88.21	6.10	
Pearl Harb_B22	942	8/30/2012	11:55:54	14.455	222.62	15.40	13.32	16.58	18.73	1.30	87.42	6.05	
Pearl Harb_B22	944	8/30/2012	11:56:00	14.455	222.52	15.39	13.33	16.59	14.01	0.97	87.52	6.05	
Pearl Harb_B22	946	8/30/2012	11:56:06	14.455	222.56	15.40	13.29	16.59	22.43	1.55	87.48	6.05	
Pearl Harb_B22	948	8/30/2012	11:56:12	14.455	221.66	15.33	13.32	16.55	11.90	0.82	88.38	6.11	
Pearl Harb_B22	950	8/30/2012	11:56:18	14.455	221.13	15.30	13.28	16.52	15.35	1.06	88.92	6.15	
Pearl Harb_B22	952	8/30/2012	11:56:24	14.455	220.84	15.28	13.27	16.51	19.48	1.35	89.20	6.17	
Pearl Harb_B22	954	8/30/2012	11:56:30	14.455	220.16	15.23	13.21	16.46	11.53	0.80	89.88	6.22	
Pearl Harb_B22	956	8/30/2012	11:56:36	14.455	217.14	15.02	13.07	16.32	38.58	2.67	92.90	6.43	
Pearl Harb_B22	958	8/30/2012	11:56:42	14.455	219.18	15.16	13.33	16.43	31.11	2.15	90.86	6.29	
Pearl Harb_B22	960	8/30/2012	11:56:48	14.455	218.87	15.14	13.33	16.41	31.59	2.19	91.17	6.31	
Pearl Harb_B22	962	8/30/2012	11:56:54	14.455	218.88	15.14	13.14	16.41	26.72	1.85	91.16	6.31	
Pearl Harb_B22	964	8/30/2012	11:57:00	14.455	219.21	15.17	13.19	16.44	18.49	1.28	90.83	6.28	
Pearl Harb_B22	966	8/30/2012	11:57:06	14.455	219.29	15.17	13.19	16.44	29.34	2.03	90.75	6.28	
Pearl Harb_B22	968	8/30/2012	11:57:12	14.455	219.46	15.18	13.20	16.45	19.36	1.34	90.58	6.27	
Pearl Harb_B22	970	8/30/2012	11:57:18	14.455	219.94	15.22	13.22	16.47	13.75	0.95	90.10	6.23	
Pearl Harb_B22	972	8/30/2012	11:57:24	14.455	219.67	15.20	13.39	16.46	26.86	1.86	90.37	6.25	
Pearl Harb_B22	974	8/30/2012	11:57:30	14.455	218.28	15.10	13.15	16.51	41.10	2.84	91.76	6.35	lots of sus sed- also chunk blown out at right
Pearl Harb_B22	976	8/30/2012	11:57:36	14.455	216.99	15.01	13.07	16.45	25.90	1.79	93.05	6.44	
Pearl Harb_B22	978	8/30/2012	11:57:42	14.455	216.35	14.97	13.09	16.45	32.76	2.27	93.69	6.48	
Pearl Harb_B22	980	8/30/2012	11:57:48	14.455	217.26	15.03	13.14	16.47	35.35	2.45	92.78	6.42	
Pearl Harb_B22	982	8/30/2012	11:57:54	14.455	217.57	15.05	13.15	16.49	15.93	1.10	92.48	6.40	
Pearl Harb_B22	984	8/30/2012	11:58:00	14.455	217.29	15.03	13.15	16.47	16.36	1.13	92.75	6.42	
Pearl Harb_B22	986	8/30/2012	11:58:06	14.455	216.89	15.00	13.14	16.46	16.83	1.16	93.15	6.44	
Pearl Harb_B22	988	8/30/2012	11:58:12	14.455	216.98	15.01	13.17	16.44	22.20	1.54	93.07	6.44	
Pearl Harb_B22	990	8/30/2012	11:58:18	14.455	216.98	15.01	13.14	16.47	19.50	1.35	93.06	6.44	
Pearl Harb_B22	992	8/30/2012	11:58:24	14.455	217.14	15.02	13.12	16.47	34.21	2.37	92.90	6.43	
Pearl Harb_B22	994	8/30/2012	11:58:30	14.455	216.55	14.98	13.13	16.48	21.36	1.48	93.50	6.47	
Pearl Harb_B22	996	8/30/2012	11:58:36	14.455	216.96	15.01	13.14	16.51	24.12	1.67	93.08	6.44	
Pearl Harb_B22	998	8/30/2012	11:58:42	14.455	216.86	15.00	13.10	16.48	27.88	1.93	93.18	6.45	
Pearl Harb_B22	1000	8/30/2012	11:58:48	14.455	217.10	15.02	13.17	16.50	11.27	0.78	92.94	6.43	
Pearl Harb_B22	1002	8/30/2012	11:58:54	14.455	217.03	15.01	13.13	16.47	22.65	1.57	93.02	6.43	
Pearl Harb_B22	1004	8/30/2012	11:59:00	14.455	217.11	15.02	13.13	16.50	12.13	0.84	92.94	6.43	
Pearl Harb_B22	1006	8/30/2012	11:59:06	14.455	216.96	15.01	13.13	16.50	16.06	1.11	93.08	6.44	
Pearl Harb_B22	1008	8/30/2012	11:59:12	14.455	217.00	15.01	13.13	16.48	17.46	1.21	93.05	6.44	
Pearl Harb_B22	1010	8/30/2012	11:59:18	14.455	216.99	15.01	13.13	16.48	17.40	1.20	93.05	6.44	
Pearl Harb_B22	1012	8/30/2012	11:59:24	14.455	216.52	14.98	13.13	16.48	20.95	1.45	93.53	6.47	
Pearl Harb_B22	1014	8/30/2012	11:59:30	14.455	216.38	14.97	13.13	16.45	30.03	2.08	93.67	6.48	
Pearl Harb_B22	1016	8/30/2012	11:59:36	14.455	214.32	14.83	13.08	16.43	47.24	3.27	95.72	6.62	lots of suspended sed- almost entire SWI
Pearl Harb_B22	1018	8/30/2012	11:59:42	14.455	211.59	14.64	13.06	16.49	50.58	3.50	98.45	6.81	
Pearl Harb_B22	1020	8/30/2012	11:59:48	14.455	208.89	14.45	12.97	16.04	26.11	1.81	101.16	7.00	
Pearl Harb_B22	1022	8/30/2012	11:59:54	14.455	210.40	14.56	13.07	16.13	18.72	1.30	99.64	6.89	
Pearl Harb_B22	1024	8/30/2012	12:00:00	14.455	209.79	14.51	13.01	16.12	26.41	1.83	100.25	6.94	
Pearl Harb_B22	1026	8/30/2012	12:00:06	14.455	209.48	14.49	13.00	16.10	20.22	1.40	100.56	6.96	
Pearl Harb_B22	1028	8/30/2012	12:00:12	14.455	210.27	14.55	13.05	16.15	22.14	1.53	99.77	6.90	
Pearl Harb_B22	1030	8/30/2012	12:00:18	14.455	210.59	14.57	13.10	16.17	17.17	1.19	99.45	6.88	
Pearl Harb_B22	1032	8/30/2012	12:00:24	14.455	210.69	14.58	13.12	16.19	36.64	2.53	99.36	6.87	
Pearl Harb_B22	1034	8/30/2012	12:00:30	14.455	210.68	14.58	13.10	16.18	39.11	2.71	99.36	6.87	
Pearl Harb_B22	1036	8/30/2012	12:00:36	14.455	209.48	14.49	13.05	16.13	35.05	2.43	100.56	6.96	

STATION	REP	DATE	TIME	Calibration Constant	Penetration Area (sq.cm)	Average Penetration (cm)	Minimum Penetration (cm)	Maximum Penetration (cm)	Sus Sed Area (sq.cm)	Sus Sed (cm)	Area of Water Visible (sq cm)	Water Visible (cm)	COMMENT
Pearl Harb_B22	1038	8/30/2012	12:00:42	14.455	207.24	14.34	12.98	16.10	24.58	1.70	102.80	7.11	small chunk on less blown up
Pearl Harb_B22	1040	8/30/2012	12:00:48	14.455	208.41	14.42	13.06	16.20	73.70	5.10	101.63	7.03	lots of suspended sed- almost entire SWI
Pearl Harb_B22	1042	8/30/2012	12:00:54	14.455	208.21	14.40	12.84	16.09	28.79	1.99	101.83	7.04	large chunks on left side of SWI
Pearl Harb_B22	1044	8/30/2012	12:01:00	14.455	210.39	14.55	12.89	16.22	34.08	2.36	99.66	6.89	large chunks on left side of SWI
Pearl Harb_B22	1046	8/30/2012	12:01:06	14.455	207.78	14.37	12.64	15.98	39.47	2.73	102.26	7.07	cont'd
Pearl Harb_B22	1048	8/30/2012	12:01:12	14.455	208.44	14.42	12.68	15.89	34.04	2.35	101.60	7.03	cont'd
Pearl Harb_B22	1050	8/30/2012	12:01:18	14.455	208.58	14.43	12.71	16.01	19.87	1.37	101.46	7.02	cont'd
Pearl Harb_B22	1052	8/30/2012	12:01:24	14.455	208.72	14.44	12.73	15.89	35.69	2.47	101.32	7.01	cont'd
Pearl Harb_B22	1054	8/30/2012	12:01:30	14.455	208.62	14.43	12.75	15.90	46.50	3.22	101.42	7.02	cont'd
Pearl Harb_B22	1056	8/30/2012	12:01:36	14.455	208.94	14.45	12.70	15.88	30.36	2.10	101.10	6.99	cont'd
Pearl Harb_B22	1058	8/30/2012	12:01:42	14.455	207.35	14.34	11.65	15.85	43.66	3.02	102.70	7.10	lots of sus sed- several med-lrg chunks in suspension
Pearl Harb_B22	1060	8/30/2012	12:01:48	14.455	205.10	14.19	11.55	15.80	22.05	1.53	104.94	7.26	cont'd-large chunks on left side of SWI
Pearl Harb_B22	1062	8/30/2012	12:01:54	14.455	204.65	14.16	11.03	15.80	28.37	1.96	105.39	7.29	cont'd-large chunks on left side of SWI
Pearl Harb_B22	1064	8/30/2012	12:02:00	14.455	204.49	14.15	11.06	16.23	10.14	0.70	105.55	7.30	cont'd-large chunks on left side of SWI
Pearl Harb_B22	1066	8/30/2012	12:02:06	14.455	204.72	14.16	11.06	15.81	18.70	1.29	105.32	7.29	cont'd-large chunks on left side of SWI
Pearl Harb_B22	1068	8/30/2012	12:02:12	14.455	204.88	14.17	11.06	15.81	30.19	2.09	105.17	7.28	cont'd-large chunks on left side of SWI
Pearl Harb_B22	1070	8/30/2012	12:02:18	14.455	204.50	14.15	11.06	15.58	24.90	1.72	105.54	7.30	cont'd-large chunks on left side of SWI
Pearl Harb_B22	1072	8/30/2012	12:02:24	14.455	206.16	14.26	11.23	15.67	3.09	0.21	103.88	7.19	cont'd-large chunks on left side of SWI
Pearl Harb_B22	1074	8/30/2012	12:02:30	14.455	206.55	14.29	11.24	15.69	11.06	0.76	103.49	7.16	cont'd-large chunks on left side of SWI
Pearl Harb_B22	1076	8/30/2012	12:02:36	14.455	206.57	14.29	11.27	15.70	15.11	1.05	103.47	7.16	cont'd-large chunks on left side of SWI
Pearl Harb_B22	1078	8/30/2012	12:02:42	14.455	206.33	14.27	11.26	15.69	14.04	0.97	103.71	7.18	cont'd-large chunks on left side of SWI
Pearl Harb_B22	1080	8/30/2012	12:02:48	14.455	206.29	14.27	11.25	15.69	15.95	1.10	103.75	7.18	cont'd-large chunks on left side of SWI
Pearl Harb_B22	1082	8/30/2012	12:02:54	14.455	206.38	14.28	11.25	15.70	11.60	0.80	103.66	7.17	cont'd-large chunks on left side of SWI
Pearl Harb_B22	1084	8/30/2012	12:03:00	14.455	205.30	14.20	11.54	15.64	17.23	1.19	104.74	7.25	cont'd-large chunks on left side of SWI
Pearl Harb_B22	1086	8/30/2012	12:03:06	14.455	203.29	14.06	11.25	15.46	12.16	0.84	106.76	7.39	cont'd-large chunks on left side of SWI
Pearl Harb_B22	1088	8/30/2012	12:03:12	14.455	194.76	13.47	10.41	14.73	31.29	2.16	115.28	7.97	large chunks on left gone
Pearl Harb_B22	1090	8/30/2012	12:03:18	14.455	196.02	13.56	10.52	14.89	23.27	1.61	114.03	7.89	
Pearl Harb_B22	1092	8/30/2012	12:03:24	14.455	196.96	13.63	10.45	15.04	34.19	2.37	113.09	7.82	
Pearl Harb_B22	1094	8/30/2012	12:03:30	14.455	196.16	13.57	10.46	14.96	52.74	3.65	113.88	7.88	
Pearl Harb_B22	1096	8/30/2012	12:03:36	14.455	200.20	13.85	10.97	15.22	34.65	2.40	109.85	7.60	
Pearl Harb_B22	1098	8/30/2012	12:03:42	14.455	201.35	13.93	11.01	15.30	33.08	2.29	108.70	7.52	
Pearl Harb_B22	1100	8/30/2012	12:03:48	14.455	203.21	14.06	11.07	15.44	44.11	3.05	106.84	7.39	
Pearl Harb_B22	1102	8/30/2012	12:03:54	14.455	203.39	14.07	11.08	15.46	25.96	1.80	106.65	7.38	
Pearl Harb_B22	1104	8/30/2012	12:04:00	14.455	202.70	14.02	11.04	15.30	29.85	2.06	107.34	7.43	
Pearl Harb_B22	1106	8/30/2012	12:04:06	14.455	201.45	13.94	10.98	15.21	11.04	0.76	108.59	7.51	
Pearl Harb_B22	1108	8/30/2012	12:04:12	14.455	201.14	13.91	11.01	15.19	30.35	2.10	108.90	7.53	
Pearl Harb_B22	1110	8/30/2012	12:04:18	14.455	202.40	14.00	11.04	15.23	13.92	0.96	107.64	7.45	
Pearl Harb_B22	1112	8/30/2012	12:04:24	14.455	201.05	13.91	10.77	15.20	51.68	3.58	108.99	7.54	
Pearl Harb_B22	1114	8/30/2012	12:04:30	14.455	201.82	13.96	10.85	15.21	44.91	3.11	108.22	7.49	
Pearl Harb_B22	1116	8/30/2012	12:04:36	14.455	203.88	14.10	10.95	15.35	25.85	1.79	106.16	7.34	
Pearl Harb_B22	1118	8/30/2012	12:04:42	14.455	204.05	14.12	10.97	15.35	38.46	2.66	105.99	7.33	
Pearl Harb_B22	1120	8/30/2012	12:04:48	14.455	205.01	14.18	11.14	15.37	33.78	2.34	105.03	7.27	
Pearl Harb_B22	1122	8/30/2012	12:04:54	14.455	205.17	14.19	11.26	15.39	29.56	2.04	104.87	7.26	
Pearl Harb_B22	1124	8/30/2012	12:05:00	14.455	203.80	14.10	10.92	15.31	11.97	0.83	106.24	7.35	
Pearl Harb_B22	1126	8/30/2012	12:05:06	14.455	203.12	14.05	11.05	15.30	34.72	2.40	106.92	7.40	
Pearl Harb_B22	1128	8/30/2012	12:05:12	14.455	202.89	14.04	11.38	15.27	35.23	2.44	107.16	7.41	
Pearl Harb_B22	1130	8/30/2012	12:05:18	14.455	201.85	13.96	11.04	15.22	21.85	1.51	108.19	7.48	
Pearl Harb_B22	1132	8/30/2012	12:05:24	14.455	202.85	14.03	11.38	15.25	36.73	2.54	107.19	7.42	
Pearl Harb_B22	1134	8/30/2012	12:05:30	14.455	202.59	14.02	11.32	15.25	36.25	2.51	107.45	7.43	large chunk of sed rolling down slope on right
Pearl Harb_B22	1136	8/30/2012	12:05:36	14.455	203.02	14.04	11.66	15.25	24.45	1.69	107.02	7.40	

STATION	REP	DATE	TIME	Calibration Constant	Penetration Area (sq.cm)	Average Penetration (cm)	Minimum Penetration (cm)	Maximum Penetration (cm)	Sus Sed Area (sq.cm)	Sus Sed (cm)	Area of Water Visible (sq cm)	Water Visible (cm)	COMMENT
Pearl Harb_B22	1138	8/30/2012	12:05:42	14.455	202.79	14.03	11.65	15.25	27.47	1.90	107.26	7.42	
Pearl Harb_B22	1140	8/30/2012	12:05:48	14.455	203.21	14.06	11.53	15.29	20.92	1.45	106.83	7.39	
Pearl Harb_B22	1142	8/30/2012	12:05:54	14.455	203.56	14.08	11.16	15.31	2.28	0.16	106.48	7.37	
Pearl Harb_B22	1144	8/30/2012	12:06:00	14.455	203.63	14.09	11.13	15.32	14.19	0.98	106.41	7.36	
Pearl Harb_B22	1145	8/30/2012	12:06:03	14.455	204.14	14.12	11.49	15.34	29.94	2.07	105.91	7.33	
Pearl Harb_B22	1146	8/30/2012	12:06:06	14.455	203.60	14.09	11.16	15.31	23.76	1.64	106.44	7.36	
Pearl Harb_B22	1147	8/30/2012	12:06:09	14.455	203.61	14.09	11.49	15.33	32.71	2.26	106.43	7.36	
Pearl Harb_B22	1148	8/30/2012	12:06:12	14.455	203.54	14.08	11.47	15.30	20.76	1.44	106.51	7.37	one sed chunk in suspension on right
Pearl Harb_B22	1149	8/30/2012	12:06:15	14.455	203.72	14.09	11.52	15.33	25.95	1.80	106.32	7.36	
Pearl Harb_B22	1150	8/30/2012	12:06:18	14.455	203.88	14.10	11.54	15.33	26.52	1.83	106.16	7.34	
Pearl Harb_B22	1151	8/30/2012	12:06:21	14.455	204.00	14.11	11.50	15.34	6.06	0.42	106.04	7.34	
Pearl Harb_B22	1152	8/30/2012	12:06:24	14.455	203.97	14.11	11.50	15.34	32.67	2.26	106.07	7.34	
Pearl Harb_B22	1153	8/30/2012	12:06:27	14.455	204.52	14.15	11.53	15.36	21.63	1.50	105.52	7.30	
Pearl Harb_B22	1154	8/30/2012	12:06:30	14.455	204.49	14.15	11.59	15.35	33.72	2.33	105.55	7.30	
Pearl Harb_B22	1155	8/30/2012	12:06:33	14.455	204.68	14.16	11.58	15.35	35.38	2.45	105.36	7.29	
Pearl Harb_B22	1156	8/30/2012	12:06:36	14.455	204.25	14.13	11.59	15.35	23.26	1.61	105.79	7.32	
Pearl Harb_B22	1157	8/30/2012	12:06:39	14.455	204.17	14.12	11.66	15.34	34.58	2.39	105.87	7.32	
Pearl Harb_B22	1158	8/30/2012	12:06:42	14.455	203.64	14.09	11.66	15.31	26.91	1.86	106.40	7.36	
Pearl Harb_B22	1159	8/30/2012	12:06:45	14.455	203.64	14.09	11.59	15.30	25.35	1.75	106.40	7.36	
Pearl Harb_B22	1160	8/30/2012	12:06:48	14.455	203.42	14.07	11.52	15.31	23.81	1.65	106.63	7.38	
Pearl Harb_B22	1161	8/30/2012	12:06:51	14.455	203.51	14.08	11.57	15.31	19.78	1.37	106.53	7.37	
Pearl Harb_B22	1162	8/30/2012	12:06:54	14.455	203.38	14.07	11.47	15.31	18.02	1.25	106.66	7.38	
Pearl Harb_B22	1163	8/30/2012	12:06:57	14.455	203.71	14.09	11.48	15.33	26.19	1.81	106.34	7.36	
Pearl Harb_B22	1164	8/30/2012	12:07:00	14.455	203.77	14.10	11.47	15.32	26.05	1.80	106.28	7.35	
Pearl Harb_B22	1165	8/30/2012	12:07:03	14.455	203.50	14.08	11.46	15.32	35.72	2.47	106.54	7.37	
Pearl Harb_B22	1166	8/30/2012	12:07:06	14.455	203.67	14.09	11.48	15.31	28.52	1.97	106.37	7.36	
Pearl Harb_B22	1167	8/30/2012	12:07:09	14.455	203.49	14.08	11.48	15.31	8.98	0.62	106.56	7.37	
Pearl Harb_B22	1168	8/30/2012	12:07:12	14.455	203.41	14.07	11.45	15.31	28.60	1.98	106.63	7.38	
Pearl Harb_B22	1169	8/30/2012	12:07:15	14.455	203.33	14.07	11.51	15.31	11.11	0.77	106.71	7.38	
Pearl Harb_B22	1170	8/30/2012	12:07:18	14.455	203.52	14.08	11.50	15.31	19.95	1.38	106.52	7.37	
Pearl Harb_B22	1171	8/30/2012	12:07:21	14.455	203.62	14.09	11.51	15.31	26.22	1.81	106.42	7.36	
Pearl Harb_B22	1172	8/30/2012	12:07:24	14.455	203.52	14.08	11.53	15.32	15.39	1.06	106.53	7.37	
Pearl Harb_B22	1173	8/30/2012	12:07:27	14.455	203.54	14.08	11.66	15.32	15.12	1.05	106.50	7.37	
Pearl Harb_B22	1174	8/30/2012	12:07:30	14.455	203.39	14.07	11.59	15.31	27.67	1.91	106.66	7.38	
Pearl Harb_B22	1175	8/30/2012	12:07:33	14.455	203.29	14.06	11.50	15.30	13.34	0.92	106.76	7.39	
Pearl Harb_B22	1176	8/30/2012	12:07:36	14.455	203.25	14.06	11.47	15.31	25.31	1.75	106.80	7.39	
Pearl Harb_B22	1177	8/30/2012	12:07:39	14.455	203.03	14.05	11.20	15.31	27.66	1.91	107.01	7.40	
Pearl Harb_B22	1178	8/30/2012	12:07:42	14.455	203.28	14.06	11.22	15.31	13.66	0.94	106.76	7.39	
Pearl Harb_B22	1179	8/30/2012	12:07:45	14.455	203.42	14.07	11.16	15.32	5.99	0.41	106.62	7.38	
Pearl Harb_B22	1180	8/30/2012	12:07:48	14.455	203.44	14.07	11.16	15.31	9.60	0.66	106.60	7.37	
Pearl Harb_B22	1181	8/30/2012	12:07:51	14.455	203.21	14.06	11.14	15.32	16.46	1.14	106.84	7.39	
Pearl Harb_B22	1182	8/30/2012	12:07:54	14.455	203.29	14.06	11.18	15.31	16.31	1.13	106.76	7.39	
Pearl Harb_B22	1183	8/30/2012	12:07:57	14.455	203.16	14.05	11.09	15.31	28.75	1.99	106.88	7.39	some chunks in suspension
Pearl Harb_B22	1184	8/30/2012	12:08:00	14.455	203.07	14.05	11.09	15.30	38.80	2.68	106.98	7.40	
Pearl Harb_B22	1185	8/30/2012	12:08:03	14.455	202.66	14.02	11.47	15.28	13.11	0.91	107.38	7.43	
Pearl Harb_B22	1186	8/30/2012	12:08:06	14.455	202.40	14.00	11.46	15.23	18.28	1.26	107.64	7.45	
Pearl Harb_B22	1187	8/30/2012	12:08:09	14.455	202.57	14.01	11.47	15.26	26.15	1.81	107.47	7.44	
Pearl Harb_B22	1188	8/30/2012	12:08:12	14.455	202.16	13.99	11.47	15.23	23.53	1.63	107.88	7.46	
Pearl Harb_B22	1189	8/30/2012	12:08:15	14.455	202.57	14.01	11.48	15.25	23.94	1.66	107.47	7.43	
Pearl Harb_B22	1190	8/30/2012	12:08:18	14.455	203.51	14.08	11.60	15.31	15.44	1.07	106.53	7.37	
Pearl Harb_B22	1191	8/30/2012	12:08:21	14.455	203.82	14.10	11.57	15.32	42.52	2.94	106.22	7.35	
Pearl Harb_B22	1192	8/30/2012	12:08:24	14.455	203.70	14.09	11.55	15.33	28.74	1.99	106.34	7.36	
Pearl Harb_B22	1193	8/30/2012	12:08:27	14.455	204.34	14.14	11.59	15.36	43.73	3.03	105.70	7.31	
Pearl Harb_B22	1194	8/30/2012	12:08:30	14.455	204.29	14.13	11.63	15.33	41.50	2.87	105.75	7.32	

STATION	REP	DATE	TIME	Calibration Constant	Penetration Area (sq.cm)	Average Penetration (cm)	Minimum Penetration (cm)	Maximum Penetration (cm)	Sus Sed Area (sq.cm)	Sus Sed (cm)	Area of Water Visible (sq cm)	Water Visible (cm)	COMMENT
Pearl Harb_B22	1195	8/30/2012	12:08:33	14.455	203.95	14.11	11.56	15.33	27.91	1.93	106.09	7.34	
Pearl Harb_B22	1196	8/30/2012	12:08:36	14.455	203.86	14.10	11.59	15.39	33.83	2.34	106.19	7.35	
Pearl Harb_B22	1197	8/30/2012	12:08:39	14.455	204.09	14.12	11.61	15.39	37.07	2.56	105.95	7.33	
Pearl Harb_B22	1198	8/30/2012	12:08:42	14.455	204.19	14.13	11.53	15.39	25.05	1.73	105.85	7.32	
Pearl Harb_B22	1199	8/30/2012	12:08:45	14.455	204.25	14.13	11.45	15.39	34.82	2.41	105.79	7.32	
Pearl Harb_B22	1200	8/30/2012	12:08:48	14.455	205.43	14.21	11.83	15.43	33.43	2.31	104.61	7.24	
Pearl Harb_B22	1201	8/30/2012	12:08:51	14.455	203.17	14.06	11.67	15.25	69.58	4.81	106.88	7.39	thick cloud of sus sed, few large chunks in suspension as well
Pearl Harb_B22	1202	8/30/2012	12:08:54	14.455	200.65	13.88	11.29	15.16	65.64	4.54	109.40	7.57	lots of sus sed; few chunks in suspension as well
Pearl Harb_B22	1203	8/30/2012	12:08:57	14.455	200.83	13.89	11.21	15.19	53.97	3.73	109.21	7.56	
Pearl Harb_B22	1204	8/30/2012	12:09:00	14.455	201.17	13.92	11.44	15.19	44.23	3.06	108.87	7.53	
Pearl Harb_B22	1205	8/30/2012	12:09:03	14.455	200.65	13.88	11.43	15.16	38.47	2.66	109.39	7.57	
Pearl Harb_B22	1206	8/30/2012	12:09:06	14.455	199.87	13.83	11.43	15.15	40.24	2.78	110.17	7.62	
Pearl Harb_B22	1207	8/30/2012	12:09:09	14.455	199.79	13.82	11.43	15.16	47.94	3.32	110.25	7.63	
Pearl Harb_B22	1208	8/30/2012	12:09:12	14.455	199.28	13.79	11.19	15.13	55.99	3.87	110.76	7.66	
Pearl Harb_B22	1209	8/30/2012	12:09:15	14.455	198.53	13.73	11.15	15.05	32.35	2.24	111.51	7.71	
Pearl Harb_B22	1210	8/30/2012	12:09:18	14.455	199.00	13.77	11.22	15.07	29.62	2.05	111.04	7.68	left edge seems to have been shifted over to right; indent of chunk is reference point
Pearl Harb_B22	1211	8/30/2012	12:09:21	14.455	199.02	13.77	11.28	15.06	43.25	2.99	111.02	7.68	
Pearl Harb_B22	1212	8/30/2012	12:09:24	14.455	195.91	13.55	10.90	14.90	55.33	3.83	114.13	7.90	
Pearl Harb_B22	1213	8/30/2012	12:09:27	14.455	193.83	13.41	10.90	14.85	49.76	3.44	116.21	8.04	
Pearl Harb_B22	1214	8/30/2012	12:09:30	14.455	193.57	13.39	10.90	14.84	54.59	3.78	116.47	8.06	mound on left is now almost entirely out of view on the left side- just top of it
Pearl Harb_B22	1215	8/30/2012	12:09:33	14.455	194.27	13.44	10.88	14.91	43.00	2.97	115.77	8.01	
Pearl Harb_B22	1216	8/30/2012	12:09:36	14.455	193.49	13.39	10.91	14.88	51.21	3.54	116.55	8.06	mound on left is now completely out of view and thick sus sed on left
Pearl Harb_B22	1217	8/30/2012	12:09:39	14.455	193.69	13.40	10.94	14.87	39.90	2.76	116.35	8.05	
Pearl Harb_B22	1218	8/30/2012	12:09:42	14.455	192.41	13.31	10.58	14.79	54.97	3.80	117.63	8.14	
Pearl Harb_B22	1219	8/30/2012	12:09:45	14.455	192.61	13.32	10.90	14.79	39.11	2.71	117.43	8.12	
Pearl Harb_B22	1220	8/30/2012	12:09:48	14.455	193.83	13.41	10.64	14.88	49.37	3.42	116.22	8.04	
Pearl Harb_B22	1221	8/30/2012	12:09:51	14.455	194.74	13.47	10.77	14.95	45.15	3.12	115.30	7.98	
Pearl Harb_B22	1222	8/30/2012	12:09:54	14.455	195.43	13.52	11.08	15.00	31.51	2.18	114.62	7.93	
Pearl Harb_B22	1223	8/30/2012	12:09:57	14.455	195.05	13.49	11.08	14.99	34.81	2.41	115.00	7.96	
Pearl Harb_B22	1224	8/30/2012	12:10:00	14.455	195.09	13.50	11.08	14.97	35.26	2.44	114.95	7.95	
Pearl Harb_B22	1225	8/30/2012	12:10:03	14.455	195.28	13.51	11.11	14.98	32.68	2.26	114.76	7.94	
Pearl Harb_B22	1226	8/30/2012	12:10:06	14.455	195.38	13.52	10.73	14.98	39.70	2.75	114.66	7.93	
Pearl Harb_B22	1227	8/30/2012	12:10:09	14.455	195.33	13.51	10.55	14.98	29.50	2.04	114.71	7.94	
Pearl Harb_B22	1228	8/30/2012	12:10:12	14.455	195.60	13.53	10.58	14.99	34.81	2.41	114.44	7.92	
Pearl Harb_B22	1229	8/30/2012	12:10:15	14.455	198.32	13.72	10.99	15.18	35.89	2.48	111.72	7.73	
Pearl Harb_B22	1230	8/30/2012	12:10:18	14.455	198.78	13.75	11.08	15.21	30.59	2.12	111.26	7.70	
Pearl Harb_B22	1231	8/30/2012	12:10:21	14.455	199.21	13.78	11.40	15.22	35.55	2.46	110.83	7.67	
Pearl Harb_B22	1232	8/30/2012	12:10:24	14.455	199.10	13.77	11.01	15.23	31.60	2.19	110.94	7.68	
Pearl Harb_B22	1233	8/30/2012	12:10:27	14.455	198.89	13.76	10.79	15.22	25.06	1.73	111.15	7.69	
Pearl Harb_B22	1234	8/30/2012	12:10:30	14.455	198.93	13.76	11.03	15.22	28.76	1.99	111.12	7.69	
Pearl Harb_B22	1235	8/30/2012	12:10:33	14.455	199.25	13.78	11.02	15.23	24.71	1.71	110.79	7.66	
Pearl Harb_B22	1236	8/30/2012	12:10:36	14.455	199.32	13.79	11.16	15.23	29.18	2.02	110.72	7.66	
Pearl Harb_B22	1237	8/30/2012	12:10:39	14.455	200.07	13.84	11.53	15.28	29.54	2.04	109.98	7.61	
Pearl Harb_B22	1238	8/30/2012	12:10:42	14.455	200.13	13.85	11.46	15.27	59.97	4.15	109.91	7.60	
Pearl Harb_B22	1239	8/30/2012	12:10:45	14.455	200.27	13.85	11.47	15.27	60.31	4.17	109.77	7.59	
Pearl Harb_B22	1240	8/30/2012	12:10:48	14.455	200.14	13.85	11.43	15.27	43.25	2.99	109.90	7.60	
Pearl Harb_B22	1241	8/30/2012	12:10:51	14.455	200.20	13.85	11.43	15.27	47.44	3.28	109.85	7.60	
Pearl Harb_B22	1242	8/30/2012	12:10:54	14.455	200.47	13.87	11.47	15.27	51.45	3.56	109.57	7.58	
Pearl Harb_B22	1243	8/30/2012	12:10:57	14.455	200.86	13.90	11.39	15.30	60.87	4.21	109.18	7.55	
Pearl Harb_B22	1244	8/30/2012	12:11:00	14.455	201.69	13.95	11.64	15.33	75.63	5.23	108.36	7.50	lots of sus sed; few small chunks in suspension as well
Pearl Harb_B22	1245	8/30/2012	12:11:03	14.455	202.51	14.01	11.85	15.40	61.33	4.24	107.54	7.44	image seems to have shifted up in last 10-15 images

STATION	REP	DATE	TIME	Calibration Constant	Penetration Area (sq.cm)	Average Penetration (cm)	Minimum Penetration (cm)	Maximum Penetration (cm)	Sus Sed Area (sq.cm)	Sus Sed (cm)	Area of Water Visible (sq cm)	Water Visible (cm)	COMMENT
Pearl Harb_B22	1246	8/30/2012	12:11:06	14.455	201.49	13.94	12.14	15.35	80.80	5.59	108.55	7.51	thick cloud of sus sed
Pearl Harb_B22	1247	8/30/2012	12:11:09	14.455	202.16	13.99	12.15	15.38	82.21	5.69	107.89	7.46	thick cloud of sus sed; lots of small chunks of sed on surface, esp to left
Pearl Harb_B22	1248	8/30/2012	12:11:12	14.455	201.63	13.95	12.08	15.34	73.49	5.08	108.41	7.50	lots of small chunks of sed on surface, esp to left
Pearl Harb_B22	1249	8/30/2012	12:11:15	14.455	200.92	13.90	12.05	15.32	67.66	4.68	109.12	7.55	
Pearl Harb_B22	1250	8/30/2012	12:11:18	14.455	201.25	13.92	12.10	15.29	61.80	4.28	108.80	7.53	
Pearl Harb_B22	1251	8/30/2012	12:11:21	14.455	201.52	13.94	12.03	15.28	41.17	2.85	108.53	7.51	
Pearl Harb_B22	1252	8/30/2012	12:11:24	14.455	201.54	13.94	12.03	15.30	51.02	3.53	108.50	7.51	
Pearl Harb_B22	1253	8/30/2012	12:11:27	14.455	201.87	13.97	12.04	15.31	48.41	3.35	108.18	7.48	
Pearl Harb_B22	1254	8/30/2012	12:11:30	14.455	202.41	14.00	12.25	15.33	51.09	3.53	107.64	7.45	
Pearl Harb_B22	1255	8/30/2012	12:11:33	14.455	202.61	14.02	11.90	15.33	55.25	3.82	107.43	7.43	
Pearl Harb_B22	1256	8/30/2012	12:11:36	14.455	202.32	14.00	11.89	15.33	47.91	3.31	107.73	7.45	
Pearl Harb_B22	1257	8/30/2012	12:11:39	14.455	201.20	13.92	11.72	15.26	50.35	3.48	108.84	7.53	
Pearl Harb_B22	1258	8/30/2012	12:11:42	14.455	200.43	13.87	11.67	15.20	43.26	2.99	109.61	7.58	
Pearl Harb_B22	1259	8/30/2012	12:11:45	14.455	200.03	13.84	11.67	15.19	53.76	3.72	110.01	7.61	
Pearl Harb_B22	1260	8/30/2012	12:11:48	14.455	200.28	13.86	11.67	15.21	51.02	3.53	109.77	7.59	
Pearl Harb_B22	1261	8/30/2012	12:11:51	14.455	200.59	13.88	11.70	15.20	37.03	2.56	109.45	7.57	split appears in sediment on right, appearing like a crack, gap seen farther down on right side too several cm below SWI at prism edge
Pearl Harb_B22	1262	8/30/2012	12:11:54	14.455	199.79	13.82	11.74	15.21	45.13	3.12	110.26	7.63	"slump"on right
Pearl Harb_B22	1263	8/30/2012	12:11:57	14.455	199.44	13.80	11.78	15.21	64.34	4.45	110.60	7.65	
Pearl Harb_B22	1264	8/30/2012	12:12:00	14.455	199.70	13.82	11.74	15.21	59.51	4.12	110.34	7.63	
Pearl Harb_B22	1265	8/30/2012	12:12:03	14.455	200.13	13.84	11.77	15.22	60.92	4.21	109.92	7.60	
Pearl Harb_B22	1266	8/30/2012	12:12:06	14.455	201.15	13.92	11.79	15.23	46.90	3.24	108.90	7.53	pieces of sed that had been on surface at left are now incorporated into the SWI- begin measuring as part of penetration depth
Pearl Harb_B22	1267	8/30/2012	12:12:09	14.455	201.58	13.95	11.81	15.24	44.50	3.08	108.46	7.50	
Pearl Harb_B22	1268	8/30/2012	12:12:12	14.455	201.34	13.93	12.17	15.22	47.78	3.31	108.70	7.52	small bit of sediment has settled on top of shelf at right created by slump, now part of penetration depth
Pearl Harb_B22	1269	8/30/2012	12:12:15	14.455	197.26	13.65	11.82	14.93	52.93	3.66	112.79	7.80	
Pearl Harb_B22	1270	8/30/2012	12:12:18	14.455	196.99	13.63	11.80	14.91	47.99	3.32	113.06	7.82	
Pearl Harb_B22	1271	8/30/2012	12:12:21	14.455	197.18	13.64	11.80	14.91	43.52	3.01	112.86	7.81	
Pearl Harb_B22	1272	8/30/2012	12:12:24	14.455	197.29	13.65	11.80	14.91	36.30	2.51	112.76	7.80	
Pearl Harb_B22	1273	8/30/2012	12:12:27	14.455	197.06	13.63	11.80	14.91	40.92	2.83	112.99	7.82	
Pearl Harb_B22	1274	8/30/2012	12:12:30	14.455	196.95	13.62	11.82	14.91	35.07	2.43	113.10	7.82	
Pearl Harb_B22	1275	8/30/2012	12:12:33	14.455	197.19	13.64	11.84	14.92	37.69	2.61	112.85	7.81	
Pearl Harb_B22	1276	8/30/2012	12:12:36	14.455	197.12	13.64	11.84	14.92	33.11	2.29	112.93	7.81	large chunk on left
Pearl Harb_B22	1277	8/30/2012	12:12:39	14.455	196.90	13.62	11.47	14.93	19.93	1.38	113.14	7.83	
Pearl Harb_B22	1278	8/30/2012	12:12:42	14.455	196.80	13.61	11.48	14.93	23.69	1.64	113.25	7.83	
Pearl Harb_B22	1279	8/30/2012	12:12:45	14.455	196.68	13.61	11.47	14.93	21.09	1.46	113.37	7.84	
Pearl Harb_B22	1280	8/30/2012	12:12:48	14.455	196.73	13.61	11.47	14.93	32.07	2.22	113.31	7.84	pieces of sed that had been on surface at left are loosening- begin measuring as part of penetration depth
Pearl Harb_B22	1281	8/30/2012	12:12:51	14.455	196.31	13.58	11.49	14.93	29.38	2.03	113.73	7.87	
Pearl Harb_B22	1282	8/30/2012	12:12:54	14.455	196.15	13.57	11.46	14.92	25.31	1.75	113.90	7.88	
Pearl Harb_B22	1283	8/30/2012	12:12:57	14.455	196.01	13.56	11.47	14.92	33.06	2.29	114.03	7.89	
Pearl Harb_B22	1284	8/30/2012	12:13:00	14.455	195.79	13.54	11.46	14.90	32.59	2.25	114.25	7.90	
Pearl Harb_B22	1285	8/30/2012	12:13:03	14.455	195.01	13.49	11.78	14.88	26.69	1.85	115.03	7.96	
Pearl Harb_B22	1286	8/30/2012	12:13:06	14.455	195.29	13.51	11.79	14.86	32.32	2.24	114.75	7.94	
Pearl Harb_B22	1287	8/30/2012	12:13:09	14.455	195.29	13.51	11.43	14.87	31.65	2.19	114.75	7.94	
Pearl Harb_B22	1288	8/30/2012	12:13:12	14.455	195.32	13.51	11.45	14.88	28.07	1.94	114.72	7.94	
Pearl Harb_B22	1289	8/30/2012	12:13:15	14.455	195.66	13.54	11.81	14.88	22.78	1.58	114.38	7.91	
Pearl Harb_B22	1290	8/30/2012	12:13:18	14.455	194.93	13.49	11.71	14.84	27.66	1.91	115.11	7.96	
Pearl Harb_B22	1291	8/30/2012	12:13:21	14.455	195.02	13.49	11.75	14.83	25.61	1.77	115.02	7.96	
Pearl Harb_B22	1292	8/30/2012	12:13:24	14.455	194.60	13.46	11.33	14.81	54.12	3.74	115.45	7.99	

STATION	REP	DATE	TIME	Calibration Constant	Penetration Area (sq.cm)	Average Penetration (cm)	Minimum Penetration (cm)	Maximum Penetration (cm)	Sus Sed Area (sq.cm)	Sus Sed (cm)	Area of Water Visible (sq cm)	Water Visible (cm)	COMMENT
Pearl Harb_B22	1293	8/30/2012	12:13:27	14.455	187.92	13.00	10.28	14.52	91.45	6.33	122.12	8.45	lots of sus sed, thick, large chunk in suspension, looks like some of surface blown into suspension
Pearl Harb_B22	1294	8/30/2012	12:13:30	14.455	188.69	13.05	10.52	14.46	83.79	5.80	121.35	8.40	small and med chunks in suspension
Pearl Harb_B22	1295	8/30/2012	12:13:33	14.455	187.27	12.96	10.60	14.27	77.21	5.34	122.77	8.49	
Pearl Harb_B22	1296	8/30/2012	12:13:36	14.455	188.60	13.05	10.77	14.34	59.03	4.08	121.45	8.40	
Pearl Harb_B22	1297	8/30/2012	12:13:39	14.455	189.11	13.08	10.74	14.35	57.77	4.00	120.93	8.37	
Pearl Harb_B22	1298	8/30/2012	12:13:42	14.455	189.13	13.08	10.44	14.38	59.86	4.14	120.91	8.36	
Pearl Harb_B22	1299	8/30/2012	12:13:45	14.455	190.22	13.16	10.41	14.46	51.12	3.54	119.82	8.29	gap in sed on right clearly visible few cm below SWI
Pearl Harb_B22	1300	8/30/2012	12:13:48	14.455	195.50	13.52	10.77	14.80	54.44	3.77	114.54	7.92	
Pearl Harb_B22	1301	8/30/2012	12:13:51	14.455	196.74	13.61	11.01	14.88	57.29	3.96	113.30	7.84	
Pearl Harb_B22	1302	8/30/2012	12:13:54	14.455	195.66	13.54	11.03	14.81	45.75	3.16	114.39	7.91	small chunk resting on SWI at right edge
Pearl Harb_B22	1303	8/30/2012	12:13:57	14.455	194.07	13.43	10.88	14.73	63.14	4.37	115.98	8.02	
Pearl Harb_B22	1304	8/30/2012	12:14:00	14.455	193.24	13.37	10.74	14.69	56.88	3.93	116.80	8.08	
Pearl Harb_B22	1305	8/30/2012	12:14:03	14.455	193.22	13.37	10.74	14.67	59.31	4.10	116.83	8.08	
Pearl Harb_B22	1306	8/30/2012	12:14:06	14.455	193.79	13.41	10.74	14.69	44.23	3.06	116.26	8.04	
Pearl Harb_B22	1307	8/30/2012	12:14:09	14.455	193.86	13.41	10.73	14.70	34.15	2.36	116.18	8.04	
Pearl Harb_B22	1308	8/30/2012	12:14:12	14.455	194.00	13.42	10.74	14.71	44.96	3.11	116.04	8.03	
Pearl Harb_B22	1309	8/30/2012	12:14:15	14.455	194.03	13.42	10.70	14.70	49.67	3.44	116.01	8.03	
Pearl Harb_B22	1310	8/30/2012	12:14:18	14.455	193.54	13.39	10.68	14.70	45.26	3.13	116.50	8.06	
Pearl Harb_B22	1311	8/30/2012	12:14:21	14.455	193.40	13.38	10.66	14.70	48.75	3.37	116.64	8.07	
Pearl Harb_B22	1312	8/30/2012	12:14:24	14.455	192.19	13.30	10.61	14.65	54.14	3.75	117.85	8.15	
Pearl Harb_B22	1313	8/30/2012	12:14:27	14.455	192.27	13.30	10.55	14.65	51.03	3.53	117.77	8.15	
Pearl Harb_B22	1314	8/30/2012	12:14:30	14.455	192.59	13.32	10.59	14.66	69.30	4.79	117.45	8.13	
Pearl Harb_B22	1315	8/30/2012	12:14:33	14.455	192.53	13.32	10.53	14.65	58.88	4.07	117.51	8.13	
Pearl Harb_B22	1316	8/30/2012	12:14:36	14.455	191.13	13.22	10.39	14.59	53.44	3.70	118.91	8.23	several chunks in suspension
Pearl Harb_B22	1317	8/30/2012	12:14:39	14.455	189.61	13.12	10.23	14.50	54.79	3.79	120.43	8.33	
Pearl Harb_B22	1318	8/30/2012	12:14:42	14.455	186.07	12.87	10.10	14.34	71.16	4.92	123.98	8.58	
Pearl Harb_B22	1319	8/30/2012	12:14:45	14.455	184.56	12.77	10.13	14.33	84.86	5.87	125.49	8.68	area on left surface blown out, top "peeling back" a bit; crack more fully opening from top mound from the right down and to the left- several cm long
Pearl Harb_B22	1320	8/30/2012	12:14:48	14.455	182.47	12.62	10.11	14.14	79.60	5.51	127.58	8.83	left side gap now closed
Pearl Harb_B22	1321	8/30/2012	12:14:51	14.455	182.36	12.62	10.11	14.23	51.85	3.59	127.69	8.83	long crack is narrower now, three vertical cracks opening up on right, in area that was a "slump" that has widened
Pearl Harb_B22	1322	8/30/2012	12:14:54	14.455	181.00	12.52	10.09	13.98	75.49	5.22	129.04	8.93	
Pearl Harb_B22	1323	8/30/2012	12:14:57	14.455	181.41	12.55	10.07	14.02	67.68	4.68	128.63	8.90	
Pearl Harb_B22	1324	8/30/2012	12:15:00	14.455	182.21	12.61	9.27	14.10	83.79	5.80	127.84	8.84	
Pearl Harb_B22	1325	8/30/2012	12:15:03	14.455	183.29	12.68	9.41	14.16	73.84	5.11	126.76	8.77	
Pearl Harb_B22	1326	8/30/2012	12:15:06	14.455	183.68	12.71	9.23	14.18	69.54	4.81	126.36	8.74	
Pearl Harb_B22	1327	8/30/2012	12:15:09	14.455	183.40	12.69	9.26	14.18	55.41	3.83	126.64	8.76	
Pearl Harb_B22	1328	8/30/2012	12:15:12	14.455	184.53	12.77	9.33	14.27	72.42	5.01	125.51	8.68	
Pearl Harb_B22	1329	8/30/2012	12:15:15	14.455	184.84	12.79	9.40	14.27	61.34	4.24	125.20	8.66	
Pearl Harb_B22	1330	8/30/2012	12:15:18	14.455	184.37	12.75	9.44	14.27	57.25	3.96	125.67	8.69	area on left of center mound has fallen off toward the back, no longer measured as part of SWI
Pearl Harb_B22	1331	8/30/2012	12:15:21	14.455	184.77	12.78	9.44	14.27	48.49	3.35	125.28	8.67	
Pearl Harb_B22	1332	8/30/2012	12:15:24	14.455	184.07	12.73	9.07	14.35	62.64	4.33	125.97	8.71	right edge- connection from surface to gap below almost completely visible
Pearl Harb_B22	1333	8/30/2012	12:15:27	14.455	184.72	12.78	9.20	14.30	68.20	4.72	125.32	8.67	
Pearl Harb_B22	1334	8/30/2012	12:15:30	14.455	184.98	12.80	9.47	14.32	69.86	4.83	125.06	8.65	
Pearl Harb_B22	1335	8/30/2012	12:15:33	14.455	184.89	12.79	9.45	14.32	60.44	4.18	125.15	8.66	
Pearl Harb_B22	1336	8/30/2012	12:15:36	14.455	184.73	12.78	9.39	14.32	34.67	2.40	125.32	8.67	
Pearl Harb_B22	1337	8/30/2012	12:15:39	14.455	183.81	12.72	9.31	14.28	36.85	2.55	126.23	8.73	
Pearl Harb_B22	1338	8/30/2012	12:15:42	14.455	182.33	12.61	9.12	14.18	62.78	4.34	127.71	8.84	
Pearl Harb_B22	1339	8/30/2012	12:15:45	14.455	181.53	12.56	9.37	14.10	46.11	3.19	128.51	8.89	

STATION	REP	DATE	TIME	Calibration Constant	Penetration Area (sq.cm)	Average Penetration (cm)	Minimum Penetration (cm)	Maximum Penetration (cm)	Sus Sed Area (sq.cm)	Sus Sed (cm)	Area of Water Visible (sq cm)	Water Visible (cm)	COMMENT
Pearl Harb_B22	1340	8/30/2012	12:15:48	14.455	173.77	12.02	9.23	13.52	76.11	5.26	136.27	9.43	
Pearl Harb_B22	1341	8/30/2012	12:15:51	14.455	169.72	11.74	9.26	13.31	64.25	4.44	140.32	9.71	small "cave-in" on middle of mound at the center of right
Pearl Harb_B22	1342	8/30/2012	12:15:54	14.455	175.62	12.15	9.30	13.68	65.22	4.51	134.42	9.30	
Pearl Harb_B22	1343	8/30/2012	12:15:57	14.455	176.17	12.19	8.95	13.69	64.82	4.48	133.87	9.26	
Pearl Harb_B22	1344	8/30/2012	12:16:00	14.455	176.22	12.19	8.91	13.70	59.56	4.12	133.82	9.26	
Pearl Harb_B22	1345	8/30/2012	12:16:03	14.455	177.66	12.29	8.92	13.83	65.14	4.51	132.38	9.16	
Pearl Harb_B22	1346	8/30/2012	12:16:06	14.455	178.03	12.32	9.03	13.87	57.28	3.96	132.01	9.13	
Pearl Harb_B22	1347	8/30/2012	12:16:09	14.455	178.39	12.34	8.97	13.87	54.77	3.79	131.65	9.11	
Pearl Harb_B22	1348	8/30/2012	12:16:12	14.455	178.71	12.36	9.13	13.90	59.83	4.14	131.34	9.09	
Pearl Harb_B22	1349	8/30/2012	12:16:15	14.455	181.13	12.53	9.35	14.04	64.36	4.45	128.92	8.92	
Pearl Harb_B22	1350	8/30/2012	12:16:18	14.455	180.92	12.52	9.25	14.09	63.19	4.37	129.12	8.93	
Pearl Harb_B22	1351	8/30/2012	12:16:21	14.455	180.74	12.50	9.25	14.07	51.83	3.59	129.30	8.95	
Pearl Harb_B22	1352	8/30/2012	12:16:24	14.455	181.71	12.57	9.59	14.11	49.03	3.39	128.34	8.88	center of main mound starting to "crack" apart
Pearl Harb_B22	1353	8/30/2012	12:16:27	14.455	181.58	12.56	9.34	14.11	57.95	4.01	128.46	8.89	
Pearl Harb_B22	1354	8/30/2012	12:16:30	14.455	180.69	12.50	9.25	14.14	80.44	5.57	129.36	8.95	think sus sed on right; likely obscuring part of sediment on right near min pen
Pearl Harb_B22	1355	8/30/2012	12:16:33	14.455	180.82	12.51	9.35	14.11	65.65	4.54	129.22	8.94	
Pearl Harb_B22	1356	8/30/2012	12:16:36	14.455	180.30	12.47	9.35	14.04	61.99	4.29	129.75	8.98	
Pearl Harb_B22	1357	8/30/2012	12:16:39	14.455	178.56	12.35	9.39	14.06	59.53	4.12	131.49	9.10	center of main mound has collapsed
Pearl Harb_B22	1358	8/30/2012	12:16:42	14.455	178.08	12.32	9.31	14.10	63.17	4.37	131.96	9.13	
Pearl Harb_B22	1359	8/30/2012	12:16:45	14.455	175.28	12.13	8.94	14.15	98.75	6.83	134.76	9.32	lots of sus sed, more sed dislodged- one chunk on left; more of right cut away, can almost see the connection to gap below SWI
Pearl Harb_B22	1360	8/30/2012	12:16:48	14.455	168.93	11.69	4.92	13.21	97.11	6.72	141.11	9.76	much sus sed, more sed dislodged; right cut away area connected from SWI to lower down now
Pearl Harb_B22	1361	8/30/2012	12:16:51	14.455	168.15	11.63	4.94	13.15	86.98	6.02	141.89	9.82	less sus sed, less chunks in suspension; one chunk resting on left edge
Pearl Harb_B22	1362	8/30/2012	12:16:54	14.455	166.91	11.55	4.72	13.33	83.73	5.79	143.13	9.90	
Pearl Harb_B22	1363	8/30/2012	12:16:57	14.455	167.47	11.59	4.34	13.45	96.58	6.68	142.57	9.86	lots of sus sed, medium chunks in sus; horizontal cracks throughout the upper couple cm
Pearl Harb_B22	1364	8/30/2012	12:17:00	14.455	148.65	10.28	4.38	12.07	111.59	7.72	161.39	11.17	thick sus sed on left; large chunk in sus on right; entire center/right mound blown off; high point is now to left
Pearl Harb_B22	1365	8/30/2012	12:17:03	14.455	146.99	10.17	4.38	12.03	94.83	6.56	163.05	11.28	
Pearl Harb_B22	1366	8/30/2012	12:17:06	14.455	147.61	10.21	4.51	12.01	85.63	5.92	162.44	11.24	more of middle section eroded
Pearl Harb_B22	1367	8/30/2012	12:17:09	14.455	150.35	10.40	4.44	11.97	89.94	6.22	159.70	11.05	
Pearl Harb_B22	1368	8/30/2012	12:17:12	14.455	147.12	10.18	4.54	12.04	101.46	7.02	162.93	11.27	more of middle eroded
Pearl Harb_B22	1369	8/30/2012	12:17:15	14.455	147.95	10.24	4.53	12.04	96.41	6.67	162.09	11.21	
Pearl Harb_B22	1370	8/30/2012	12:17:18	14.455	148.86	10.30	4.50	12.09	87.00	6.02	161.19	11.15	
Pearl Harb_B22	1371	8/30/2012	12:17:21	14.455	148.79	10.29	4.52	12.16	91.56	6.33	161.25	11.16	
Pearl Harb_B22	1372	8/30/2012	12:17:24	14.455	147.76	10.22	4.52	12.18	95.69	6.62	162.29	11.23	
Pearl Harb_B22	1373	8/30/2012	12:17:27	14.455	148.20	10.25	4.57	12.20	98.59	6.82	161.84	11.20	
Pearl Harb_B22	1374	8/30/2012	12:17:30	14.455	148.06	10.24	4.57	12.19	99.59	6.89	161.99	11.21	
Pearl Harb_B22	1375	8/30/2012	12:17:33	14.455	148.41	10.27	4.57	12.19	94.22	6.52	161.63	11.18	
Pearl Harb_B22	1376	8/30/2012	12:17:36	14.455	148.24	10.26	4.57	12.17	79.38	5.49	161.80	11.19	
Pearl Harb_B22	1377	8/30/2012	12:17:39	14.455	147.83	10.23	4.54	12.15	96.19	6.65	162.21	11.22	
Pearl Harb_B22	1378	8/30/2012	12:17:42	14.455	147.77	10.22	4.54	12.15	84.14	5.82	162.27	11.23	
Pearl Harb_B22	1379	8/30/2012	12:17:45	14.455	148.33	10.26	4.58	12.20	81.28	5.62	161.71	11.19	
Pearl Harb_B22	1380	8/30/2012	12:17:48	14.455	141.97	9.82	4.56	12.32	95.18	6.58	168.07	11.63	more sed dislodged, esp from left side
Pearl Harb_B22	1381	8/30/2012	12:17:51	14.455	138.82	9.60	4.54	10.80	95.82	6.63	171.22	11.85	more sed dislodged, esp from left side
Pearl Harb_B22	1382	8/30/2012	12:17:54	14.455	136.38	9.43	4.49	10.62	78.62	5.44	173.66	12.01	chunk of sed rolling 'downhill' on right
Pearl Harb_B22	1383	8/30/2012	12:17:57	14.455	135.37	9.36	4.46	10.57	92.52	6.40	174.68	12.08	very large chunk on surface at center
Pearl Harb_B22	1384	8/30/2012	12:18:00	14.455	132.68	9.18	4.48	10.54	116.42	8.05	177.36	12.27	chunk on right near bottom partly gone and obscured too
Pearl Harb_B22	1385	8/30/2012	12:18:03	14.455	133.51	9.24	4.56	10.51	108.11	7.48	176.54	12.21	
Pearl Harb_B22	1386	8/30/2012	12:18:06	14.455	134.31	9.29	4.62	10.66	83.57	5.78	175.73	12.16	more erosion on right edge
Pearl Harb_B22	1387	8/30/2012	12:18:09	14.455	134.65	9.32	4.54	10.70	100.15	6.93	175.39	12.13	

STATION	REP	DATE	TIME	Calibration Constant	Penetration Area (sq.cm)	Average Penetration (cm)	Minimum Penetration (cm)	Maximum Penetration (cm)	Sus Sed Area (sq.cm)	Sus Sed (cm)	Area of Water Visible (sq cm)	Water Visible (cm)	COMMENT
Pearl Harb_B22	1388	8/30/2012	12:18:12	14.455	134.27	9.29	4.54	10.66	94.23	6.52	175.77	12.16	
Pearl Harb_B22	1389	8/30/2012	12:18:15	14.455	127.39	8.81	4.39	10.11	97.79	6.76	182.65	12.64	part of right lower area "bucking" in toward faceplate
Pearl Harb_B22	1390	8/30/2012	12:18:18	14.455	78.06	5.40	1.31	9.54	186.66	12.91	231.99	16.05	**estimate at best; whole area is blown out, SWI mostly obscured
Pearl Harb_B22	1391	8/30/2012	12:18:21	14.455	74.94	5.18	1.31	9.36	157.42	10.89	235.10	16.26	**SWI still obscured in middle
Pearl Harb_B22	1392	8/30/2012	12:18:24	14.455	99.56	6.89	1.42	9.41	148.36	10.26	210.48	14.56	SWI is more visible, still lots of sus sed and chunks of sed in suspension
Pearl Harb_B22	1393	8/30/2012	12:18:27	14.455	97.91	6.77	0.76	9.46	154.05	10.66	212.13	14.68	
Pearl Harb_B22	1394	8/30/2012	12:18:30	14.455	97.57	6.75	1.00	9.71	135.76	9.39	212.48	14.70	part of faceplate side is somewhat sloughing toward the faceplate; very messy
Pearl Harb_B22	1395	8/30/2012	12:18:33	14.455	115.03	7.96	2.05	9.66	102.85	7.12	195.02	13.49	all of SWI now visible, some against faceplate, some more in background; measure forward part as much as possible
Pearl Harb_B22	1396	8/30/2012	12:18:36	14.455	116.90	8.09	2.05	9.66	118.42	8.19	193.15	13.36	
Pearl Harb_B22	1397	8/30/2012	12:18:39	14.455	111.04	7.68	2.04	9.60	129.00	8.92	199.00	13.77	
Pearl Harb_B22	1398	8/30/2012	12:18:42	14.455	111.42	7.71	2.02	9.63	135.28	9.36	198.62	13.74	
Pearl Harb_B22	1399	8/30/2012	12:18:45	14.455	112.54	7.79	2.06	9.69	119.99	8.30	197.50	13.66	
Pearl Harb_B22	1400	8/30/2012	12:18:48	14.455	113.01	7.82	2.06	9.72	142.46	9.86	197.03	13.63	
Pearl Harb_B22	1401	8/30/2012	12:18:51	14.455	114.60	7.93	2.14	9.76	132.55	9.17	195.44	13.52	
Pearl Harb_B22	1402	8/30/2012	12:18:54	14.455	112.68	7.80	1.99	9.74	131.61	9.10	197.36	13.65	crack opening up to right of center near base
Pearl Harb_B22	1403	8/30/2012	12:18:57	14.455	106.84	7.39	2.13	9.69	125.75	8.70	203.20	14.06	many pieces dislodged, some against faceplate, right SWI obscured
Pearl Harb_B22	1404	8/30/2012	12:19:00	14.455	109.60	7.58	1.98	9.95	133.52	9.24	200.45	13.87	
Pearl Harb_B22	1405	8/30/2012	12:19:03	14.455	111.00	7.68	2.30	10.08	112.41	7.78	199.04	13.77	still very messy; some sed slumping a bit on left few cm down; dislodged chunks pressed against faceplate on right
Pearl Harb_B22	1406	8/30/2012	12:19:06	14.455	124.63	8.62	3.62	10.22	113.50	7.85	185.41	12.83	areas that were eroded previously are getting filled in with resettled sed
Pearl Harb_B22	1407	8/30/2012	12:19:09	14.455	124.14	8.59	3.69	10.17	110.12	7.62	185.90	12.86	
Pearl Harb_B22	1408	8/30/2012	12:19:12	14.455	119.47	8.27	3.27	9.94	131.46	9.09	190.57	13.18	more sed chunks accumulated at center
Pearl Harb_B22	1409	8/30/2012	12:19:15	14.455	118.35	8.19	2.72	9.91	122.92	8.50	191.69	13.26	
Pearl Harb_B22	1410	8/30/2012	12:19:18	14.455	118.24	8.18	3.10	9.88	115.72	8.01	191.80	13.27	
Pearl Harb_B22	1411	8/30/2012	12:19:21	14.455	112.52	7.78	2.39	9.93	133.60	9.24	197.52	13.66	some sed at center now eroded or in suspension; SWI obscured on right
Pearl Harb_B22	1412	8/30/2012	12:19:24	14.455	116.46	8.06	2.44	9.96	126.67	8.76	193.58	13.39	center right blowing up a bit- part at surface lifting and separating some; chunks in suspension
Pearl Harb_B22	1413	8/30/2012	12:19:27	14.455	108.55	7.51	2.40	9.87	141.75	9.81	201.50	13.94	much of right side blown up, lots of chunks in suspension
Pearl Harb_B22	1414	8/30/2012	12:19:30	14.455	110.59	7.65	2.34	9.84	124.08	8.58	199.45	13.80	
Pearl Harb_B22	1415	8/30/2012	12:19:33	14.455	102.82	7.11	1.47	9.37	123.99	8.58	207.23	14.34	
Pearl Harb_B22	1416	8/30/2012	12:19:36	14.455	63.47	4.39	0.12	9.63	202.96	14.04	246.57	17.06	thick cloud of sus sed, chunks in sus; SWI on left visible, but not to right of center
Pearl Harb_B22	1417	8/30/2012	12:19:39	14.455	74.31	5.14	0.12	9.33	205.32	14.20	235.73	16.31	thick cloud of sus sed; left SWI blown up, steep slope visible on right side
Pearl Harb_B22	1418	8/30/2012	12:19:42	14.455	65.70	4.55	0.04	7.69	190.96	13.21	244.34	16.90	thick cloud of sus sed; SWI mostly visible
Pearl Harb_B22	1419	8/30/2012	12:19:45	14.455	66.31	4.59	0.03	7.67	204.45	14.14	243.73	16.86	thick cloud of sus sed
Pearl Harb_B22	1420	8/30/2012	12:19:48	14.455	73.75	5.10	0.03	7.71	185.83	12.86	236.29	16.35	
Pearl Harb_B22	1421	8/30/2012	12:19:51	14.455	70.48	4.88	0.03	7.68	179.46	12.41	239.56	16.57	parts of center blown up; chunk on right dislodged, poised to 'roll'
Pearl Harb_B22	1422	8/30/2012	12:19:54	14.455	67.79	4.69	0.03	7.72	177.75	12.30	242.25	16.76	
Pearl Harb_B22	1423	8/30/2012	12:19:57	14.455	67.64	4.68	0.03	7.76	200.04	13.84	242.40	16.77	
Pearl Harb_B22	1424	8/30/2012	12:20:00	14.455	67.21	4.65	0.03	7.71	190.52	13.18	242.83	16.80	
Pearl Harb_B22	1425	8/30/2012	12:20:03	14.455	66.01	4.57	0.03	7.66	204.95	14.18	244.04	16.88	
Pearl Harb_B22	1426	8/30/2012	12:20:06	14.455	69.69	4.82	0.03	7.84	184.51	12.76	240.35	16.63	
Pearl Harb_B22	1427	8/30/2012	12:20:09	14.455	69.95	4.84	0.03	7.80	153.16	10.60	240.09	16.61	
Pearl Harb_B22	1428	8/30/2012	12:20:12	14.455	70.75	4.89	0.03	7.87	179.87	12.44	239.29	16.55	
Pearl Harb_B22	1429	8/30/2012	12:20:15	14.455	69.25	4.79	0.03	7.83	181.92	12.59	240.79	16.66	
Pearl Harb_B22	1430	8/30/2012	12:20:18	14.455	69.71	4.82	0.03	7.85	152.62	10.56	240.34	16.63	
Pearl Harb_B22	1431	8/30/2012	12:20:21	14.455	70.14	4.85	0.03	7.85	83.82	5.80	239.90	16.60	
Pearl Harb_B22	1432	8/30/2012	12:20:24	14.455	70.09	4.85	0.03	7.82	83.99	5.81	239.95	16.60	

STATION	REP	DATE	TIME	Calibration Constant	Penetration Area (sq.cm)	Average Penetration (cm)	Minimum Penetration (cm)	Maximum Penetration (cm)	Sus Sed Area (sq.cm)	Sus Sed (cm)	Area of Water Visible (sq cm)	Water Visible (cm)	COMMENT
Pearl Harb_B22	1433	8/30/2012	12:20:27	14.455	68.51	4.74	0.03	7.92	99.67	6.90	241.53	16.71	
Pearl Harb_B22	1434	8/30/2012	12:20:30	14.455	68.58	4.74	0.03	7.85	94.48	6.54	241.46	16.70	
Pearl Harb_B22	1435	8/30/2012	12:20:33	14.455	69.36	4.80	0.03	7.83	85.77	5.93	240.68	16.65	
Pearl Harb_B22	1436	8/30/2012	12:20:36	14.455	69.20	4.79	0.03	7.85	100.12	6.93	240.84	16.66	
Pearl Harb_B22	1437	8/30/2012	12:20:39	14.455	69.08	4.78	0.03	7.82	63.30	4.38	240.96	16.67	
Pearl Harb_B22	1438	8/30/2012	12:20:42	14.455	69.14	4.78	0.03	7.81	96.60	6.68	240.91	16.67	
Pearl Harb_B22	1439	8/30/2012	12:20:45	14.455	69.11	4.78	0.03	7.80	66.84	4.62	240.94	16.67	
Pearl Harb_B22	1440	8/30/2012	12:20:48	14.455	69.18	4.79	0.03	7.82	115.37	7.98	240.86	16.66	
Pearl Harb_B22	1441	8/30/2012	12:20:51	14.455	68.60	4.75	0.03	7.85	173.28	11.99	241.44	16.70	thick sus sed
Pearl Harb_B22	1442	8/30/2012	12:20:54	14.455	68.77	4.76	0.03	7.79	158.61	10.97	241.27	16.69	thick sus sed; more sed sloughing toward faceplate to left of center
Pearl Harb_B22	1443	8/30/2012	12:20:57	14.455	69.07	4.78	0.03	7.79	148.01	10.24	240.97	16.67	
Pearl Harb_B22	1444	8/30/2012	12:21:00	14.455	69.20	4.79	0.03	7.81	115.00	7.96	240.84	16.66	
Pearl Harb_B22	1445	8/30/2012	12:21:03	14.455	69.18	4.79	0.03	7.81	130.87	9.05	240.86	16.66	
Pearl Harb_B22	1446	8/30/2012	12:21:06	14.455	68.74	4.76	0.03	7.77	125.49	8.68	241.31	16.69	
Pearl Harb_B22	1447	8/30/2012	12:21:09	14.455	68.98	4.77	0.03	7.82	124.29	8.60	241.06	16.68	
Pearl Harb_B22	1448	8/30/2012	12:21:12	14.455	69.02	4.77	0.03	7.79	121.63	8.41	241.02	16.67	
Pearl Harb_B22	1449	8/30/2012	12:21:15	14.455	68.59	4.75	0.03	7.75	119.46	8.26	241.45	16.70	
Pearl Harb_B22	1450	8/30/2012	12:21:18	14.455	66.48	4.60	0.03	7.61	125.13	8.66	243.56	16.85	
Pearl Harb_B22	1451	8/30/2012	12:21:21	14.455	62.13	4.30	0.03	7.59	184.21	12.74	247.92	17.15	thick cloud of sus sed; eroded section middle left
Pearl Harb_B22	1452	8/30/2012	12:21:24	14.455	66.34	4.59	0.03	7.67	208.46	14.42	243.71	16.86	thick cloud of sus sed
Pearl Harb_B22	1453	8/30/2012	12:21:27	14.455	68.58	4.74	0.03	7.77	150.46	10.41	241.46	16.70	two very large chunks on surface on left
Pearl Harb_B22	1454	8/30/2012	12:21:30	14.455	69.17	4.78	0.03	7.80	162.92	11.27	240.88	16.66	small chunk on left surface; sed still sloughing toward faceplate
Pearl Harb_B22	1455	8/30/2012	12:21:33	14.455	69.67	4.82	0.03	7.93	153.74	10.64	240.37	16.63	
Pearl Harb_B22	1456	8/30/2012	12:21:36	14.455	70.89	4.90	0.03	7.92	168.46	11.65	239.16	16.54	
Pearl Harb_B22	1457	8/30/2012	12:21:39	14.455	71.11	4.92	0.03	7.91	152.74	10.57	238.93	16.53	
Pearl Harb_B22	1458	8/30/2012	12:21:42	14.455	70.68	4.89	0.03	7.92	137.62	9.52	239.36	16.56	
Pearl Harb_B22	1459	8/30/2012	12:21:45	14.455	70.62	4.89	0.03	7.91	109.76	7.59	239.42	16.56	
Pearl Harb_B22	1460	8/30/2012	12:21:48	14.455	70.48	4.88	0.03	7.94	116.90	8.09	239.56	16.57	
Pearl Harb_B22	1461	8/30/2012	12:21:51	14.455	70.81	4.90	0.03	7.98	67.48	4.67	239.24	16.55	
Pearl Harb_B22	1462	8/30/2012	12:21:54	14.455	71.41	4.94	0.03	7.96	64.99	4.50	238.64	16.51	
Pearl Harb_B22	1463	8/30/2012	12:21:57	14.455	71.48	4.95	0.03	7.96	84.84	5.87	238.56	16.50	little bit of sed has resettled on surface, so pen depth has gone up a little bit
Pearl Harb_B22	1464	8/30/2012	12:22:00	14.455	71.45	4.94	0.03	7.89	76.25	5.27	238.60	16.51	
Pearl Harb_B22	1465	8/30/2012	12:22:03	14.455	71.45	4.94	0.03	7.94	75.87	5.25	238.60	16.51	
Pearl Harb_B22	1466	8/30/2012	12:22:06	14.455	71.49	4.95	0.03	7.96	103.14	7.14	238.55	16.50	
Pearl Harb_B22	1467	8/30/2012	12:22:09	14.455	72.20	4.99	0.03	7.96	107.59	7.44	237.84	16.45	
Pearl Harb_B22	1468	8/30/2012	12:22:12	14.455	71.99	4.98	0.03	7.95	117.42	8.12	238.05	16.47	
Pearl Harb_B22	1469	8/30/2012	12:22:15	14.455	72.26	5.00	0.03	8.00	134.77	9.32	237.78	16.45	
Pearl Harb_B22	1470	8/30/2012	12:22:18	14.455	71.94	4.98	0.03	7.97	124.81	8.63	238.11	16.47	
Pearl Harb_B22	1471	8/30/2012	12:22:21	14.455	71.93	4.98	0.03	7.99	86.85	6.01	238.11	16.47	
Pearl Harb_B22	1472	8/30/2012	12:22:24	14.455	71.47	4.94	0.03	7.93	84.71	5.86	238.57	16.50	
Pearl Harb_B22	1473	8/30/2012	12:22:27	14.455	71.38	4.94	0.03	8.00	111.07	7.68	238.66	16.51	
Pearl Harb_B22	1474	8/30/2012	12:22:30	14.455	74.63	5.16	0.03	8.08	103.74	7.18	235.41	16.29	
Pearl Harb_B22	1475	8/30/2012	12:22:33	14.455	72.89	5.04	0.03	8.02	156.59	10.83	237.15	16.41	part of middle blown up- chunks on surface and large ones in suspension
Pearl Harb_B22	1476	8/30/2012	12:22:36	14.455	70.95	4.91	0.03	7.80	184.94	12.79	239.09	16.54	thick cloud of sus sed; chunks in suspension
Pearl Harb_B22	1477	8/30/2012	12:22:39	14.455	70.60	4.88	0.03	7.84	169.33	11.71	239.44	16.56	
Pearl Harb_B22	1478	8/30/2012	12:22:42	14.455	71.77	4.97	0.03	7.97	160.18	11.08	238.27	16.48	
Pearl Harb_B22	1479	8/30/2012	12:22:45	14.455	70.22	4.86	0.03	7.96	131.86	9.12	239.82	16.59	
Pearl Harb_B22	1480	8/30/2012	12:22:48	14.455	66.31	4.59	0.03	8.02	167.87	11.61	243.73	16.86	
Pearl Harb_B22	1481	8/30/2012	12:22:51	14.455	65.53	4.53	0.03	8.00	145.81	10.09	244.51	16.92	
Pearl Harb_B22	1482	8/30/2012	12:22:54	14.455	66.58	4.61	0.03	8.06	115.51	7.99	243.46	16.84	
Pearl Harb_B22	1483	8/30/2012	12:22:57	14.455	66.56	4.60	0.03	8.08	140.00	9.69	243.49	16.84	
Pearl Harb_B22	1484	8/30/2012	12:23:00	14.455	66.80	4.62	0.03	8.08	134.00	9.27	243.24	16.83	

STATION	REP	DATE	TIME	Calibration Constant	Penetration Area (sq.cm)	Average Penetration (cm)	Minimum Penetration (cm)	Maximum Penetration (cm)	Sus Sed Area (sq.cm)	Sus Sed (cm)	Area of Water Visible (sq cm)	Water Visible (cm)	COMMENT
Pearl Harb_B22	1485	8/30/2012	12:23:03	14.455	66.64	4.61	0.03	8.11	108.28	7.49	243.41	16.84	
Pearl Harb_B22	1486	8/30/2012	12:23:06	14.455	67.00	4.63	0.03	8.13	75.19	5.20	243.05	16.81	
Pearl Harb_B22	1487	8/30/2012	12:23:09	14.455	67.07	4.64	0.03	8.10	108.35	7.50	242.97	16.81	
Pearl Harb_B22	1488	8/30/2012	12:23:12	14.455	67.46	4.67	0.03	8.11	77.32	5.35	242.59	16.78	
Pearl Harb_B22	1489	8/30/2012	12:23:15	14.455	68.89	4.77	0.03	8.20	77.47	5.36	241.16	16.68	
Pearl Harb_B22	1490	8/30/2012	12:23:18	14.455	70.31	4.86	0.03	8.24	74.89	5.18	239.73	16.58	
Pearl Harb_B22	1491	8/30/2012	12:23:21	14.455	70.26	4.86	0.03	8.29	79.37	5.49	239.78	16.59	
Pearl Harb_B22	1492	8/30/2012	12:23:24	14.455	70.38	4.87	0.03	8.24	65.71	4.55	239.66	16.58	
Pearl Harb_B22	1493	8/30/2012	12:23:27	14.455	70.35	4.87	0.03	8.24	67.12	4.64	239.69	16.58	
Pearl Harb_B22	1494	8/30/2012	12:23:30	14.455	70.40	4.87	0.03	8.24	57.00	3.94	239.64	16.58	
Pearl Harb_B22	1495	8/30/2012	12:23:33	14.455	70.67	4.89	0.03	8.25	30.07	2.08	239.37	16.56	
Pearl Harb_B22	1496	8/30/2012	12:23:36	14.455	70.59	4.88	0.03	8.25	39.57	2.74	239.45	16.57	
Pearl Harb_B22	1497	8/30/2012	12:23:39	14.455	70.58	4.88	0.03	8.28	44.75	3.10	239.46	16.57	
Pearl Harb_B22	1498	8/30/2012	12:23:42	14.455	70.76	4.90	0.03	8.30	31.92	2.21	239.28	16.55	crustacean- some kind of shrimp- on surface at far left
Pearl Harb_B22	1499	8/30/2012	12:23:45	14.455	70.73	4.89	0.03	8.26	36.52	2.53	239.32	16.56	shrimp walking on surface twd center
Pearl Harb_B22	1500	8/30/2012	12:23:48	14.455	71.29	4.93	0.03	8.33	35.18	2.43	238.76	16.52	shrimp now at center

STATION	REP	DATE	TIME	Penetration Area (sq.cm)	Average Penetration (cm)	Minimum Penetration (cm)	Maximum Penetration (cm)	Sus Sed Area (sq.cm)	Sus Sed (cm)	Area of Water Visible (sq cm)	Water Visible (cm)	COMMENT
Pearl Harb_O2	137	8/30/2012	14:04:00	241.81	16.73	14.96	18.48	5.65	0.39	68.23	4.72	
Pearl Harb_O2	237	8/30/2012	14:09:00	241.49	16.71	14.93	18.44	3.95	0.27	68.55	4.74	rope in view on left
Pearl Harb_O2	337	8/30/2012	14:14:00	241.30	16.69	14.96	18.44	1.69	0.12	68.74	4.76	
Pearl Harb_O2	340	8/30/2012	14:14:09	241.36	16.70	14.93	18.45	1.43	0.10	68.68	4.75	
Pearl Harb_O2	343	8/30/2012	14:14:18	241.32	16.69	14.96	18.41	1.18	0.08	68.72	4.75	
Pearl Harb_O2	346	8/30/2012	14:14:27	241.31	16.69	14.95	18.45	1.75	0.12	68.73	4.75	
Pearl Harb_O2	349	8/30/2012	14:14:36	241.28	16.69	14.96	18.45	1.26	0.09	68.76	4.76	
Pearl Harb_O2	352	8/30/2012	14:14:45	241.25	16.69	14.96	18.45	1.08	0.08	68.79	4.76	
Pearl Harb_O2	355	8/30/2012	14:14:54	241.19	16.69	14.96	18.43	1.01	0.07	68.85	4.76	
Pearl Harb_O2	358	8/30/2012	14:15:03	241.17	16.68	14.95	18.43	1.06	0.07	68.87	4.76	
Pearl Harb_O2	361	8/30/2012	14:15:12	241.20	16.69	14.96	18.43	1.20	0.08	68.85	4.76	rope is now out of view; progressively moved out of view over last images
Pearl Harb_O2	364	8/30/2012	14:15:21	241.15	16.68	14.95	18.43	1.17	0.08	68.89	4.77	
Pearl Harb_O2	367	8/30/2012	14:15:30	241.22	16.69	14.96	18.43	0.88	0.06	68.83	4.76	
Pearl Harb_O2	370	8/30/2012	14:15:39	241.22	16.69	14.96	18.43	0.49	0.03	68.82	4.76	
Pearl Harb_O2	373	8/30/2012	14:15:48	241.14	16.68	14.95	18.43	0.54	0.04	68.90	4.77	
Pearl Harb_O2	376	8/30/2012	14:15:57	241.20	16.69	14.95	18.43	0.55	0.04	68.84	4.76	
Pearl Harb_O2	379	8/30/2012	14:16:06	241.21	16.69	14.94	18.43	0.77	0.05	68.83	4.76	
Pearl Harb_O2	382	8/30/2012	14:16:15	241.19	16.69	14.93	18.43	0.82	0.06	68.85	4.76	
Pearl Harb_O2	385	8/30/2012	14:16:24	241.15	16.68	14.93	18.43	1.08	0.07	68.89	4.77	
Pearl Harb_O2	388	8/30/2012	14:16:33	240.96	16.67	14.89	18.43	4.96	0.34	69.08	4.78	
Pearl Harb_O2	391	8/30/2012	14:16:42	240.82	16.66	14.88	18.42	11.56	0.80	69.22	4.79	
Pearl Harb_O2	394	8/30/2012	14:16:51	240.50	16.64	14.85	18.39	25.90	1.79	69.54	4.81	
Pearl Harb_O2	397	8/30/2012	14:17:00	240.28	16.62	14.84	18.38	17.41	1.20	69.76	4.83	
Pearl Harb_O2	400	8/30/2012	14:17:09	240.19	16.62	14.82	18.37	4.11	0.28	69.85	4.83	
Pearl Harb_O2	403	8/30/2012	14:17:18	240.15	16.61	14.81	18.37	3.37	0.23	69.89	4.84	
Pearl Harb_O2	406	8/30/2012	14:17:27	240.12	16.61	14.83	18.37	0.82	0.06	69.92	4.84	
Pearl Harb_O2	409	8/30/2012	14:17:36	240.06	16.61	14.82	18.37	1.37	0.09	69.98	4.84	
Pearl Harb_O2	412	8/30/2012	14:17:45	239.48	16.57	14.71	18.33	9.79	0.68	70.56	4.88	
Pearl Harb_O2	415	8/30/2012	14:17:54	239.17	16.55	14.75	18.29	25.26	1.75	70.87	4.90	
Pearl Harb_O2	418	8/30/2012	14:18:03	239.28	16.55	14.76	18.29	30.98	2.14	70.77	4.90	

STATION	REP	DATE	TIME	Penetration Area (sq.cm)	Average Penetration (cm)	Minimum Penetration (cm)	Maximum Penetration (cm)	Sus Sed Area (sq.cm)	Sus Sed (cm)	Area of Water Visible (sq cm)	Water Visible (cm)	COMMENT
Pearl Harb_O2	421	8/30/2012	14:18:12	239.27	16.55	14.76	18.27	8.52	0.59	70.77	4.90	
Pearl Harb_O2	424	8/30/2012	14:18:21	239.26	16.55	14.80	18.27	3.16	0.22	70.79	4.90	
Pearl Harb_O2	427	8/30/2012	14:18:30	239.19	16.55	14.80	18.26	5.97	0.41	70.85	4.90	
Pearl Harb_O2	430	8/30/2012	14:18:39	239.17	16.55	14.80	18.27	3.34	0.23	70.87	4.90	
Pearl Harb_O2	433	8/30/2012	14:18:48	239.14	16.54	14.76	18.28	3.62	0.25	70.90	4.90	
Pearl Harb_O2	436	8/30/2012	14:18:57	239.04	16.54	14.76	18.25	4.12	0.29	71.01	4.91	
Pearl Harb_O2	439	8/30/2012	14:19:06	239.07	16.54	14.76	18.25	2.36	0.16	70.97	4.91	
Pearl Harb_O2	442	8/30/2012	14:19:15	239.04	16.54	14.76	18.25	2.17	0.15	71.01	4.91	
Pearl Harb_O2	445	8/30/2012	14:19:24	239.01	16.54	14.76	18.24	2.81	0.19	71.03	4.91	
Pearl Harb_O2	448	8/30/2012	14:19:33	238.83	16.52	14.73	18.22	2.34	0.16	71.21	4.93	
Pearl Harb_O2	451	8/30/2012	14:19:42	238.25	16.48	14.70	18.18	2.16	0.15	71.79	4.97	
Pearl Harb_O2	454	8/30/2012	14:19:51	238.04	16.47	14.71	18.19	2.32	0.16	72.00	4.98	
Pearl Harb_O2	457	8/30/2012	14:20:00	237.85	16.45	14.69	18.16	2.03	0.14	72.20	4.99	
Pearl Harb_O2	460	8/30/2012	14:20:09	237.54	16.43	14.65	18.15	2.75	0.19	72.51	5.02	
Pearl Harb_O2	463	8/30/2012	14:20:18	237.33	16.42	14.63	18.14	4.00	0.28	72.71	5.03	
Pearl Harb_O2	466	8/30/2012	14:20:27	237.36	16.42	14.65	18.14	2.91	0.20	72.68	5.03	
Pearl Harb_O2	469	8/30/2012	14:20:36	237.48	16.43	14.67	18.14	3.44	0.24	72.56	5.02	
Pearl Harb_O2	472	8/30/2012	14:20:45	237.67	16.44	14.69	18.16	2.78	0.19	72.38	5.01	
Pearl Harb_O2	475	8/30/2012	14:20:54	237.56	16.43	14.67	18.16	1.56	0.11	72.48	5.01	
Pearl Harb_O2	478	8/30/2012	14:21:03	237.52	16.43	14.67	18.15	3.16	0.22	72.52	5.02	
Pearl Harb_O2	481	8/30/2012	14:21:12	237.56	16.43	14.67	18.17	1.67	0.12	72.48	5.01	
Pearl Harb_O2	484	8/30/2012	14:21:21	237.68	16.44	14.67	18.17	1.82	0.13	72.36	5.01	
Pearl Harb_O2	487	8/30/2012	14:21:30	237.70	16.44	14.67	18.16	1.14	0.08	72.34	5.00	
Pearl Harb_O2	490	8/30/2012	14:21:39	237.76	16.45	14.68	18.16	1.59	0.11	72.28	5.00	
Pearl Harb_O2	493	8/30/2012	14:21:48	237.71	16.44	14.69	18.17	2.01	0.14	72.33	5.00	
Pearl Harb_O2	496	8/30/2012	14:21:57	237.65	16.44	14.67	18.17	3.79	0.26	72.39	5.01	
Pearl Harb_O2	499	8/30/2012	14:22:06	237.58	16.44	14.67	18.16	3.39	0.23	72.46	5.01	
Pearl Harb_O2	502	8/30/2012	14:22:15	237.54	16.43	14.68	18.17	3.51	0.24	72.50	5.02	
Pearl Harb_O2	505	8/30/2012	14:22:24	237.62	16.44	14.68	18.17	3.80	0.26	72.43	5.01	
Pearl Harb_O2	508	8/30/2012	14:22:33	237.49	16.43	14.68	18.16	3.52	0.24	72.56	5.02	
Pearl Harb_O2	511	8/30/2012	14:22:42	237.45	16.43	14.66	18.16	3.61	0.25	72.59	5.02	
Pearl Harb_O2	514	8/30/2012	14:22:51	237.48	16.43	14.65	18.16	4.70	0.32	72.56	5.02	
Pearl Harb_O2	517	8/30/2012	14:23:00	237.55	16.43	14.65	18.16	6.32	0.44	72.49	5.01	
Pearl Harb_O2	520	8/30/2012	14:23:09	237.53	16.43	14.66	18.16	3.08	0.21	72.51	5.02	
Pearl Harb_O2	523	8/30/2012	14:23:18	237.57	16.43	14.66	18.17	4.25	0.29	72.48	5.01	
Pearl Harb_O2	526	8/30/2012	14:23:27	237.63	16.44	14.65	18.18	2.41	0.17	72.41	5.01	
Pearl Harb_O2	529	8/30/2012	14:23:36	237.67	16.44	14.68	18.17	2.47	0.17	72.37	5.01	
Pearl Harb_O2	532	8/30/2012	14:23:45	237.65	16.44	14.66	18.16	2.76	0.19	72.39	5.01	
Pearl Harb_O2	535	8/30/2012	14:23:54	237.68	16.44	14.66	18.16	2.37	0.16	72.36	5.01	
Pearl Harb_O2	538	8/30/2012	14:24:03	237.73	16.45	14.67	18.17	3.05	0.21	72.31	5.00	
Pearl Harb_O2	541	8/30/2012	14:24:12	237.69	16.44	14.66	18.17	2.72	0.19	72.35	5.01	
Pearl Harb_O2	544	8/30/2012	14:24:21	237.69	16.44	14.67	18.17	3.68	0.25	72.35	5.01	
Pearl Harb_O2	547	8/30/2012	14:24:30	237.74	16.45	14.66	18.17	3.09	0.21	72.30	5.00	
Pearl Harb_O2	550	8/30/2012	14:24:39	237.76	16.45	14.67	18.17	2.12	0.15	72.28	5.00	
Pearl Harb_O2	553	8/30/2012	14:24:48	237.86	16.46	14.68	18.17	3.39	0.23	72.18	4.99	
Pearl Harb_O2	556	8/30/2012	14:24:57	237.90	16.46	14.67	18.17	1.20	0.08	72.14	4.99	
Pearl Harb_O2	559	8/30/2012	14:25:06	237.89	16.46	14.67	18.17	2.50	0.17	72.15	4.99	
Pearl Harb_O2	562	8/30/2012	14:25:15	237.84	16.45	14.66	18.16	1.81	0.12	72.20	5.00	
Pearl Harb_O2	565	8/30/2012	14:25:24	237.85	16.45	14.67	18.17	2.41	0.17	72.19	4.99	
Pearl Harb_O2	568	8/30/2012	14:25:33	237.96	16.46	14.67	18.17	1.84	0.13	72.08	4.99	
Pearl Harb_O2	571	8/30/2012	14:25:42	237.89	16.46	14.66	18.17	2.48	0.17	72.16	4.99	
Pearl Harb_O2	574	8/30/2012	14:25:51	237.92	16.46	14.65	18.17	3.34	0.23	72.12	4.99	
Pearl Harb_O2	577	8/30/2012	14:26:00	237.88	16.46	14.65	18.17	3.30	0.23	72.16	4.99	
Pearl Harb_O2	580	8/30/2012	14:26:09	237.86	16.46	14.65	18.18	3.16	0.22	72.18	4.99	

STATION	REP	DATE	TIME	Penetration Area (sq.cm)	Average Penetration (cm)	Minimum Penetration (cm)	Maximum Penetration (cm)	Sus Sed Area (sq.cm)	Sus Sed (cm)	Area of Water Visible (sq cm)	Water Visible (cm)	COMMENT
Pearl Harb_O2	583	8/30/2012	14:26:18	237.77	16.45	14.65	18.17	7.71	0.53	72.28	5.00	
Pearl Harb_O2	586	8/30/2012	14:26:27	237.78	16.45	14.65	18.16	3.66	0.25	72.26	5.00	
Pearl Harb_O2	589	8/30/2012	14:26:36	237.78	16.45	14.66	18.17	4.03	0.28	72.26	5.00	
Pearl Harb_O2	592	8/30/2012	14:26:45	237.79	16.45	14.67	18.17	6.78	0.47	72.26	5.00	
Pearl Harb_O2	595	8/30/2012	14:26:54	237.80	16.45	14.67	18.16	3.14	0.22	72.24	5.00	
Pearl Harb_O2	598	8/30/2012	14:27:03	237.88	16.46	14.69	18.17	2.49	0.17	72.16	4.99	
Pearl Harb_O2	601	8/30/2012	14:27:12	237.93	16.46	14.69	18.18	2.66	0.18	72.11	4.99	
Pearl Harb_O2	604	8/30/2012	14:27:21	237.92	16.46	14.68	18.17	1.92	0.13	72.13	4.99	
Pearl Harb_O2	607	8/30/2012	14:27:30	237.89	16.46	14.67	18.17	2.56	0.18	72.15	4.99	
Pearl Harb_O2	610	8/30/2012	14:27:39	237.86	16.46	14.68	18.18	1.39	0.10	72.18	4.99	
Pearl Harb_O2	613	8/30/2012	14:27:48	237.88	16.46	14.67	18.18	2.49	0.17	72.17	4.99	
Pearl Harb_O2	616	8/30/2012	14:27:57	237.74	16.45	14.68	18.18	2.13	0.15	72.31	5.00	
Pearl Harb_O2	619	8/30/2012	14:28:06	237.56	16.43	14.69	18.18	2.41	0.17	72.48	5.01	
Pearl Harb_O2	622	8/30/2012	14:28:15	237.57	16.43	14.67	18.16	1.48	0.10	72.48	5.01	
Pearl Harb_O2	625	8/30/2012	14:28:24	237.53	16.43	14.67	18.17	3.48	0.24	72.52	5.02	
Pearl Harb_O2	628	8/30/2012	14:28:33	237.57	16.44	14.68	18.17	2.50	0.17	72.47	5.01	
Pearl Harb_O2	631	8/30/2012	14:28:42	237.53	16.43	14.67	18.17	0.56	0.04	72.51	5.02	
Pearl Harb_O2	634	8/30/2012	14:28:51	237.68	16.44	14.68	18.17	0.97	0.07	72.36	5.01	
Pearl Harb_O2	637	8/30/2012	14:29:00	237.66	16.44	14.68	18.18	1.41	0.10	72.38	5.01	
Pearl Harb_O2	640	8/30/2012	14:29:09	237.44	16.43	14.67	18.16	0.85	0.06	72.61	5.02	
Pearl Harb_O2	643	8/30/2012	14:29:18	237.51	16.43	14.67	18.17	1.03	0.07	72.53	5.02	
Pearl Harb_O2	646	8/30/2012	14:29:27	237.47	16.43	14.67	18.16	1.32	0.09	72.58	5.02	
Pearl Harb_O2	649	8/30/2012	14:29:36	237.43	16.43	14.67	18.16	2.51	0.17	72.61	5.02	
Pearl Harb_O2	652	8/30/2012	14:29:45	237.47	16.43	14.67	18.17	1.84	0.13	72.57	5.02	
Pearl Harb_O2	655	8/30/2012	14:29:54	237.41	16.42	14.67	18.18	1.10	0.08	72.63	5.02	
Pearl Harb_O2	658	8/30/2012	14:30:03	237.38	16.42	14.67	18.18	1.67	0.12	72.67	5.03	
Pearl Harb_O2	661	8/30/2012	14:30:12	237.34	16.42	14.65	18.18	2.55	0.18	72.70	5.03	
Pearl Harb_O2	664	8/30/2012	14:30:21	237.40	16.42	14.66	18.18	2.00	0.14	72.64	5.03	
Pearl Harb_O2	667	8/30/2012	14:30:30	237.40	16.42	14.67	18.18	1.89	0.13	72.64	5.03	
Pearl Harb_O2	670	8/30/2012	14:30:39	237.75	16.45	14.67	18.18	1.32	0.09	72.29	5.00	
Pearl Harb_O2	673	8/30/2012	14:30:48	237.79	16.45	14.68	18.20	1.81	0.13	72.25	5.00	
Pearl Harb_O2	676	8/30/2012	14:30:57	237.76	16.45	14.69	18.20	2.32	0.16	72.28	5.00	
Pearl Harb_O2	679	8/30/2012	14:31:06	237.65	16.44	14.68	18.18	1.12	0.08	72.39	5.01	
Pearl Harb_O2	682	8/30/2012	14:31:15	237.56	16.43	14.68	18.18	1.19	0.08	72.48	5.01	
Pearl Harb_O2	685	8/30/2012	14:31:24	237.56	16.43	14.67	18.19	2.21	0.15	72.48	5.01	
Pearl Harb_O2	688	8/30/2012	14:31:33	237.45	16.43	14.67	18.17	1.73	0.12	72.59	5.02	
Pearl Harb_O2	691	8/30/2012	14:31:42	237.46	16.43	14.66	18.17	0.76	0.05	72.59	5.02	
Pearl Harb_O2	694	8/30/2012	14:31:51	237.29	16.42	14.65	18.15	1.79	0.12	72.75	5.03	
Pearl Harb_O2	697	8/30/2012	14:32:00	237.24	16.41	14.64	18.16	0.62	0.04	72.81	5.04	
Pearl Harb_O2	700	8/30/2012	14:32:09	236.98	16.39	14.63	18.14	0.85	0.06	73.06	5.05	
Pearl Harb_O2	703	8/30/2012	14:32:18	236.80	16.38	14.63	18.13	1.76	0.12	73.24	5.07	
Pearl Harb_O2	706	8/30/2012	14:32:27	236.90	16.39	14.64	18.14	1.28	0.09	73.14	5.06	
Pearl Harb_O2	709	8/30/2012	14:32:36	236.63	16.37	14.62	18.12	1.64	0.11	73.41	5.08	
Pearl Harb_O2	712	8/30/2012	14:32:45	236.50	16.36	14.62	18.12	2.23	0.15	73.54	5.09	
Pearl Harb_O2	715	8/30/2012	14:32:54	236.38	16.35	14.61	18.11	2.61	0.18	73.66	5.10	
Pearl Harb_O2	718	8/30/2012	14:33:03	236.35	16.35	14.60	18.10	1.34	0.09	73.69	5.10	
Pearl Harb_O2	721	8/30/2012	14:33:12	236.25	16.34	14.59	18.10	0.80	0.06	73.80	5.11	
Pearl Harb_O2	724	8/30/2012	14:33:21	236.23	16.34	14.58	18.10	0.81	0.06	73.81	5.11	
Pearl Harb_O2	727	8/30/2012	14:33:30	236.36	16.35	14.61	18.12	1.05	0.07	73.68	5.10	
Pearl Harb_O2	730	8/30/2012	14:33:39	236.58	16.37	14.62	18.12	1.41	0.10	73.46	5.08	
Pearl Harb_O2	733	8/30/2012	14:33:48	236.57	16.37	14.61	18.11	1.23	0.09	73.47	5.08	
Pearl Harb_O2	736	8/30/2012	14:33:57	236.47	16.36	14.61	18.10	1.83	0.13	73.57	5.09	
Pearl Harb_O2	739	8/30/2012	14:34:06	236.53	16.36	14.62	18.11	1.54	0.11	73.51	5.09	
Pearl Harb_O2	742	8/30/2012	14:34:15	236.50	16.36	14.60	18.11	1.30	0.09	73.54	5.09	

STATION	REP	DATE	TIME	Penetration Area (sq.cm)	Average Penetration (cm)	Minimum Penetration (cm)	Maximum Penetration (cm)	Sus Sed Area (sq.cm)	Sus Sed (cm)	Area of Water Visible (sq cm)	Water Visible (cm)	COMMENT
Pearl Harb_O2	745	8/30/2012	14:34:24	236.48	16.36	14.61	18.11	0.97	0.07	73.56	5.09	
Pearl Harb_O2	748	8/30/2012	14:34:33	236.48	16.36	14.61	18.10	1.81	0.13	73.56	5.09	
Pearl Harb_O2	751	8/30/2012	14:34:42	236.40	16.35	14.60	18.10	1.56	0.11	73.65	5.09	
Pearl Harb_O2	754	8/30/2012	14:34:51	236.46	16.36	14.60	18.11	1.38	0.10	73.59	5.09	
Pearl Harb_O2	757	8/30/2012	14:35:00	236.46	16.36	14.61	18.11	2.80	0.19	73.58	5.09	
Pearl Harb_O2	760	8/30/2012	14:35:09	236.43	16.36	14.60	18.12	1.87	0.13	73.61	5.09	
Pearl Harb_O2	763	8/30/2012	14:35:18	236.44	16.36	14.61	18.12	2.08	0.14	73.60	5.09	
Pearl Harb_O2	766	8/30/2012	14:35:27	236.44	16.36	14.61	18.12	2.81	0.19	73.60	5.09	
Pearl Harb_O2	769	8/30/2012	14:35:36	236.64	16.37	14.64	18.10	2.95	0.20	73.40	5.08	
Pearl Harb_O2	772	8/30/2012	14:35:45	236.65	16.37	14.62	18.11	1.98	0.14	73.39	5.08	
Pearl Harb_O2	775	8/30/2012	14:35:54	236.42	16.36	14.61	18.11	3.53	0.24	73.62	5.09	
Pearl Harb_O2	778	8/30/2012	14:36:03	236.29	16.35	14.61	18.09	17.02	1.18	73.76	5.10	
Pearl Harb_O2	781	8/30/2012	14:36:12	236.22	16.34	14.59	18.12	10.69	0.74	73.82	5.11	
Pearl Harb_O2	784	8/30/2012	14:36:21	236.15	16.34	14.58	18.12	1.84	0.13	73.89	5.11	
Pearl Harb_O2	787	8/30/2012	14:36:30	236.12	16.33	14.58	18.10	2.10	0.15	73.92	5.11	
Pearl Harb_O2	790	8/30/2012	14:36:39	236.11	16.33	14.58	18.10	2.99	0.21	73.93	5.11	
Pearl Harb_O2	793	8/30/2012	14:36:48	235.77	16.31	14.61	18.06	2.84	0.20	74.27	5.14	
Pearl Harb_O2	796	8/30/2012	14:36:57	235.79	16.31	14.61	18.03	21.94	1.52	74.25	5.14	
Pearl Harb_O2	799	8/30/2012	14:37:06	236.12	16.33	14.64	18.09	15.12	1.05	73.92	5.11	
Pearl Harb_O2	802	8/30/2012	14:37:15	236.34	16.35	14.62	18.12	14.70	1.02	73.70	5.10	
Pearl Harb_O2	805	8/30/2012	14:37:24	236.29	16.35	14.62	18.12	8.40	0.58	73.75	5.10	
Pearl Harb_O2	808	8/30/2012	14:37:33	236.27	16.34	14.65	18.11	18.17	1.26	73.78	5.10	
Pearl Harb_O2	811	8/30/2012	14:37:42	236.45	16.36	14.65	18.12	3.83	0.27	73.59	5.09	
Pearl Harb_O2	814	8/30/2012	14:37:51	236.29	16.35	14.68	18.06	12.74	0.88	73.76	5.10	
Pearl Harb_O2	817	8/30/2012	14:38:00	236.45	16.36	14.69	18.11	10.41	0.72	73.59	5.09	
Pearl Harb_O2	820	8/30/2012	14:38:09	236.46	16.36	14.70	18.13	6.69	0.46	73.58	5.09	hint of red on the left (later proves to be large crab)
Pearl Harb_O2	823	8/30/2012	14:38:18	236.42	16.36	14.69	18.13	24.16	1.67	73.62	5.09	
Pearl Harb_O2	826	8/30/2012	14:38:27	236.21	16.34	14.69	18.13	19.61	1.36	73.83	5.11	
Pearl Harb_O2	829	8/30/2012	14:38:36	235.94	16.32	14.67	18.10	2.62	0.18	74.10	5.13	
Pearl Harb_O2	832	8/30/2012	14:38:45	235.64	16.30	14.66	17.99	1.84	0.13	74.40	5.15	
Pearl Harb_O2	835	8/30/2012	14:38:54	235.68	16.30	14.67	18.03	3.76	0.26	74.37	5.14	
Pearl Harb_O2	838	8/30/2012	14:39:03	236.09	16.33	14.67	18.05	2.08	0.14	73.95	5.12	opening claw on left facing SPI faceplate, other part of crab visible in background
Pearl Harb_O2	841	8/30/2012	14:39:12	235.85	16.32	14.69	18.02	2.74	0.19	74.20	5.13	left side of a crab visible on the left
Pearl Harb_O2	844	8/30/2012	14:39:21	235.90	16.32	14.89	18.00	6.28	0.43	74.14	5.13	most of crab claw on left
Pearl Harb_O2	847	8/30/2012	14:39:30	236.14	16.34	14.90	18.00	3.08	0.21	73.91	5.11	most of crab claw on left
Pearl Harb_O2	850	8/30/2012	14:39:39	236.11	16.33	14.89	18.00	2.23	0.15	73.93	5.11	most of crab claw on left
Pearl Harb_O2	853	8/30/2012	14:39:48	235.72	16.31	14.81	17.99	9.06	0.63	74.32	5.14	
Pearl Harb_O2	856	8/30/2012	14:39:57	235.27	16.28	14.74	17.98	6.03	0.42	74.77	5.17	
Pearl Harb_O2	859	8/30/2012	14:40:06	235.23	16.27	14.81	17.97	11.65	0.81	74.82	5.18	crab on surface, taking up all but far right of SWI
Pearl Harb_O2	862	8/30/2012	14:40:15	235.57	16.30	14.87	17.99	7.17	0.50	74.48	5.15	crab on surface, covering the whole SWI, disturbing sed
Pearl Harb_O2	865	8/30/2012	14:40:24	238.11	16.47	14.91	17.99	0.76	0.05	71.93	4.98	crab at rest on surface, covering whole SWI
Pearl Harb_O2	868	8/30/2012	14:40:33	238.10	16.47	14.88	17.99	1.47	0.10	71.94	4.98	crab at rest on surface, covering whole SWI
Pearl Harb_O2	871	8/30/2012	14:40:42	237.97	16.46	14.92	17.98	0.67	0.05	72.07	4.99	crab at rest on surface, covering whole SWI
Pearl Harb_O2	874	8/30/2012	14:40:51	237.79	16.45	14.92	17.97	0.83	0.06	72.25	5.00	crab at rest on surface, covering whole SWI
Pearl Harb_O2	877	8/30/2012	14:41:00	237.62	16.44	14.89	17.96	0.52	0.04	72.42	5.01	crab at rest on surface, covering whole SWI
Pearl Harb_O2	880	8/30/2012	14:41:09	237.80	16.45	14.94	17.97	0.12	0.01	72.25	5.00	crab at rest on surface, covering whole SWI
Pearl Harb_O2	883	8/30/2012	14:41:18	237.71	16.45	14.94	17.96	0.55	0.04	72.33	5.00	crab at rest on surface, covering whole SWI
Pearl Harb_O2	886	8/30/2012	14:41:27	237.34	16.42	14.90	17.93	0.25	0.02	72.70	5.03	crab at rest on surface, covering whole SWI
Pearl Harb_O2	889	8/30/2012	14:41:36	237.16	16.41	14.88	17.90	0.81	0.06	72.88	5.04	crab at rest on surface, covering whole SWI
Pearl Harb_O2	892	8/30/2012	14:41:45	237.08	16.40	14.91	17.91	0.23	0.02	72.96	5.05	crab at rest on surface, covering whole SWI
Pearl Harb_O2	895	8/30/2012	14:41:54	237.08	16.40	14.94	17.91	0.14	0.01	72.97	5.05	crab at rest on surface, covering whole SWI
Pearl Harb_O2	898	8/30/2012	14:42:03	237.09	16.40	14.93	17.91	0.24	0.02	72.95	5.05	crab at rest on surface, covering whole SWI
Pearl Harb_O2	901	8/30/2012	14:42:12	235.09	16.26	14.86	17.89	6.33	0.44	74.95	5.19	crab up on its hind legs, most of underside visible, sediment disturbed

STATION	REP	DATE	TIME	Penetration Area (sq.cm)	Average Penetration (cm)	Minimum Penetration (cm)	Maximum Penetration (cm)	Sus Sed Area (sq.cm)	Sus Sed (cm)	Area of Water Visible (sq cm)	Water Visible (cm)	COMMENT
Pearl Harb_O2	904	8/30/2012	14:42:21	234.81	16.24	14.83	17.90	3.28	0.23	75.23	5.20	
Pearl Harb_O2	907	8/30/2012	14:42:30	234.69	16.24	14.81	17.87	1.08	0.07	75.35	5.21	
Pearl Harb_O2	910	8/30/2012	14:42:39	234.62	16.23	14.83	17.89	0.58	0.04	75.42	5.22	
Pearl Harb_O2	913	8/30/2012	14:42:48	234.74	16.24	14.82	17.89	0.31	0.02	75.30	5.21	
Pearl Harb_O2	916	8/30/2012	14:42:57	234.60	16.23	14.82	17.85	1.09	0.08	75.45	5.22	
Pearl Harb_O2	919	8/30/2012	14:43:06	233.69	16.17	14.80	17.78	1.19	0.08	76.35	5.28	
Pearl Harb_O2	922	8/30/2012	14:43:15	233.09	16.13	14.76	17.77	0.64	0.04	76.95	5.32	
Pearl Harb_O2	925	8/30/2012	14:43:24	233.13	16.13	14.74	17.77	0.24	0.02	76.91	5.32	
Pearl Harb_O2	928	8/30/2012	14:43:33	233.22	16.13	14.76	17.79	0.36	0.02	76.82	5.31	
Pearl Harb_O2	931	8/30/2012	14:43:42	233.12	16.13	14.75	17.79	1.19	0.08	76.92	5.32	
Pearl Harb_O2	934	8/30/2012	14:43:51	233.22	16.13	14.76	17.79	0.69	0.05	76.82	5.31	
Pearl Harb_O2	937	8/30/2012	14:44:00	233.21	16.13	14.76	17.81	2.76	0.19	76.83	5.32	
Pearl Harb_O2	940	8/30/2012	14:44:09	233.05	16.12	14.74	17.79	1.83	0.13	76.99	5.33	
Pearl Harb_O2	943	8/30/2012	14:44:18	233.18	16.13	14.75	17.79	7.94	0.55	76.87	5.32	
Pearl Harb_O2	946	8/30/2012	14:44:27	233.44	16.15	14.78	17.80	7.30	0.51	76.60	5.30	
Pearl Harb_O2	949	8/30/2012	14:44:36	233.23	16.14	14.74	17.79	4.22	0.29	76.81	5.31	
Pearl Harb_O2	952	8/30/2012	14:44:45	233.11	16.13	14.74	17.80	1.54	0.11	76.93	5.32	
Pearl Harb_O2	955	8/30/2012	14:44:54	233.16	16.13	14.75	17.79	1.91	0.13	76.89	5.32	
Pearl Harb_O2	958	8/30/2012	14:45:03	233.05	16.12	14.73	17.76	1.93	0.13	76.99	5.33	
Pearl Harb_O2	961	8/30/2012	14:45:12	233.03	16.12	14.73	17.77	3.30	0.23	77.02	5.33	
Pearl Harb_O2	964	8/30/2012	14:45:21	232.96	16.12	14.72	17.80	3.21	0.22	77.08	5.33	
Pearl Harb_O2	967	8/30/2012	14:45:30	233.02	16.12	14.73	17.79	1.89	0.13	77.02	5.33	
Pearl Harb_O2	970	8/30/2012	14:45:39	233.05	16.12	14.73	17.79	2.09	0.14	77.00	5.33	
Pearl Harb_O2	973	8/30/2012	14:45:48	233.05	16.12	14.73	17.79	2.16	0.15	77.00	5.33	
Pearl Harb_O2	976	8/30/2012	14:45:57	233.17	16.13	14.73	17.79	1.12	0.08	76.87	5.32	
Pearl Harb_O2	979	8/30/2012	14:46:06	233.03	16.12	14.73	17.77	1.98	0.14	77.02	5.33	
Pearl Harb_O2	982	8/30/2012	14:46:15	233.46	16.15	14.77	17.76	2.79	0.19	76.59	5.30	
Pearl Harb_O2	985	8/30/2012	14:46:24	233.64	16.16	14.79	17.79	1.30	0.09	76.40	5.29	
Pearl Harb_O2	988	8/30/2012	14:46:33	233.52	16.15	14.79	17.76	3.12	0.22	76.53	5.29	
Pearl Harb_O2	991	8/30/2012	14:46:42	233.29	16.14	14.77	17.75	1.77	0.12	76.75	5.31	small egg sac or invert floating just about SWI on left
Pearl Harb_O2	994	8/30/2012	14:46:51	233.23	16.14	14.76	17.75	1.96	0.14	76.81	5.31	
Pearl Harb_O2	997	8/30/2012	14:47:00	233.03	16.12	14.76	17.76	1.23	0.09	77.01	5.33	
Pearl Harb_O2	1000	8/30/2012	14:47:09	232.81	16.11	14.73	17.74	1.00	0.07	77.23	5.34	
Pearl Harb_O2	1003	8/30/2012	14:47:18	232.77	16.10	14.73	17.74	1.03	0.07	77.28	5.35	
Pearl Harb_O2	1006	8/30/2012	14:47:27	232.19	16.06	14.70	17.72	0.60	0.04	77.86	5.39	
Pearl Harb_O2	1009	8/30/2012	14:47:36	231.65	16.03	14.66	17.72	0.95	0.07	78.39	5.42	
Pearl Harb_O2	1012	8/30/2012	14:47:45	231.60	16.02	14.65	17.71	1.23	0.08	78.44	5.43	
Pearl Harb_O2	1015	8/30/2012	14:47:54	231.11	15.99	14.63	17.71	0.98	0.07	78.93	5.46	
Pearl Harb_O2	1018	8/30/2012	14:48:03	231.22	16.00	14.63	17.69	1.20	0.08	78.82	5.45	
Pearl Harb_O2	1021	8/30/2012	14:48:12	231.10	15.99	14.63	17.69	0.67	0.05	78.94	5.46	
Pearl Harb_O2	1024	8/30/2012	14:48:21	230.61	15.95	14.59	17.69	0.39	0.03	79.44	5.50	
Pearl Harb_O2	1027	8/30/2012	14:48:30	230.40	15.94	14.55	17.69	1.51	0.10	79.64	5.51	
Pearl Harb_O2	1030	8/30/2012	14:48:39	230.96	15.98	14.59	17.73	1.76	0.12	79.08	5.47	
Pearl Harb_O2	1033	8/30/2012	14:48:48	231.29	16.00	14.61	17.74	1.08	0.08	78.75	5.45	
Pearl Harb_O2	1036	8/30/2012	14:48:57	231.28	16.00	14.60	17.71	1.26	0.09	78.76	5.45	
Pearl Harb_O2	1039	8/30/2012	14:49:06	231.25	16.00	14.60	17.73	2.36	0.16	78.79	5.45	
Pearl Harb_O2	1042	8/30/2012	14:49:15	231.23	16.00	14.60	17.74	1.96	0.14	78.81	5.45	
Pearl Harb_O2	1045	8/30/2012	14:49:24	231.38	16.01	14.59	17.77	1.80	0.12	78.67	5.44	
Pearl Harb_O2	1048	8/30/2012	14:49:33	231.24	16.00	14.58	17.74	3.25	0.22	78.80	5.45	
Pearl Harb_O2	1051	8/30/2012	14:49:42	231.22	16.00	14.57	17.74	4.27	0.30	78.82	5.45	
Pearl Harb_O2	1054	8/30/2012	14:49:51	231.11	15.99	14.57	17.73	3.40	0.24	78.94	5.46	
Pearl Harb_O2	1057	8/30/2012	14:50:00	230.93	15.98	14.57	17.71	10.92	0.76	79.11	5.47	
Pearl Harb_O2	1060	8/30/2012	14:50:09	230.48	15.94	14.55	17.69	4.51	0.31	79.56	5.50	
Pearl Harb_O2	1063	8/30/2012	14:50:19	229.91	15.91	14.55	17.68	3.37	0.23	80.13	5.54	

STATION	REP	DATE	TIME	Penetration Area (sq.cm)	Average Penetration (cm)	Minimum Penetration (cm)	Maximum Penetration (cm)	Sus Sed Area (sq.cm)	Sus Sed (cm)	Area of Water Visible (sq cm)	Water Visible (cm)	COMMENT
Pearl Harb_O2	1066	8/30/2012	14:50:28	228.18	15.79	14.40	17.59	1.46	0.10	81.86	5.66	
Pearl Harb_O2	1069	8/30/2012	14:50:36	227.20	15.72	14.32	17.57	1.89	0.13	82.84	5.73	
Pearl Harb_O2	1072	8/30/2012	14:50:45	226.29	15.66	14.32	17.48	52.40	3.63	83.75	5.79	lots of sus sed; filling most of SWI
Pearl Harb_O2	1075	8/30/2012	14:50:55	224.15	15.51	14.22	17.32	10.70	0.74	85.90	5.94	
Pearl Harb_O2	1078	8/30/2012	14:51:04	223.04	15.43	14.10	17.19	54.23	3.75	87.00	6.02	lots of sus sed; filling most of SWI
Pearl Harb_O2	1081	8/30/2012	14:51:13	222.85	15.42	14.03	17.21	43.64	3.02	87.19	6.03	
Pearl Harb_O2	1084	8/30/2012	14:51:21	222.65	15.40	14.07	17.23	24.62	1.70	87.39	6.05	
Pearl Harb_O2	1087	8/30/2012	14:51:30	222.20	15.37	14.02	17.22	14.23	0.98	87.85	6.08	
Pearl Harb_O2	1090	8/30/2012	14:51:40	222.18	15.37	13.99	17.21	17.68	1.22	87.86	6.08	
Pearl Harb_O2	1093	8/30/2012	14:51:49	222.22	15.37	14.01	17.18	5.88	0.41	87.82	6.08	
Pearl Harb_O2	1096	8/30/2012	14:51:57	222.73	15.41	14.00	17.19	23.81	1.65	87.32	6.04	
Pearl Harb_O2	1099	8/30/2012	14:52:06	222.61	15.40	14.01	17.13	20.07	1.39	87.43	6.05	
Pearl Harb_O2	1102	8/30/2012	14:52:16	222.54	15.40	14.01	17.17	9.43	0.65	87.50	6.05	
Pearl Harb_O2	1105	8/30/2012	14:52:25	222.31	15.38	14.03	17.15	2.47	0.17	87.73	6.07	
Pearl Harb_O2	1108	8/30/2012	14:52:33	216.61	14.99	13.61	17.04	9.37	0.65	93.43	6.46	
Pearl Harb_O2	1111	8/30/2012	14:52:42	217.16	15.02	13.60	17.04	14.92	1.03	92.89	6.43	
Pearl Harb_O2	1114	8/30/2012	14:52:52	219.43	15.18	13.65	17.11	7.57	0.52	90.61	6.27	
Pearl Harb_O2	1117	8/30/2012	14:53:01	220.72	15.27	13.73	17.11	0.96	0.07	89.33	6.18	
Pearl Harb_O2	1120	8/30/2012	14:53:09	222.07	15.36	13.80	17.17	0.98	0.07	87.97	6.09	
Pearl Harb_O2	1123	8/30/2012	14:53:18	222.28	15.38	13.81	17.18	1.66	0.11	87.76	6.07	
Pearl Harb_O2	1126	8/30/2012	14:53:28	221.88	15.35	13.80	17.15	0.72	0.05	88.16	6.10	
Pearl Harb_O2	1129	8/30/2012	14:53:37	222.74	15.41	13.87	17.18	3.16	0.22	87.31	6.04	
Pearl Harb_O2	1132	8/30/2012	14:53:45	223.23	15.44	13.90	17.19	1.77	0.12	86.81	6.01	
Pearl Harb_O2	1135	8/30/2012	14:53:54	223.04	15.43	13.88	17.17	1.27	0.09	87.01	6.02	
Pearl Harb_O2	1138	8/30/2012	14:54:04	223.15	15.44	13.89	17.19	0.62	0.04	86.90	6.01	
Pearl Harb_O2	1141	8/30/2012	14:54:13	223.11	15.44	13.88	17.20	1.58	0.11	86.93	6.01	
Pearl Harb_O2	1144	8/30/2012	14:54:21	223.11	15.43	13.88	17.19	0.84	0.06	86.93	6.01	
Pearl Harb_O2	1147	8/30/2012	14:54:30	223.05	15.43	13.88	17.18	0.89	0.06	86.99	6.02	
Pearl Harb_O2	1150	8/30/2012	14:54:40	223.12	15.44	13.89	17.20	0.57	0.04	86.92	6.01	
Pearl Harb_O2	1153	8/30/2012	14:54:49	223.04	15.43	13.88	17.19	0.61	0.04	87.00	6.02	
Pearl Harb_O2	1156	8/30/2012	14:54:57	223.13	15.44	13.88	17.18	0.88	0.06	86.91	6.01	
Pearl Harb_O2	1159	8/30/2012	14:55:06	223.28	15.45	13.88	17.18	1.04	0.07	86.76	6.00	
Pearl Harb_O2	1162	8/30/2012	14:55:16	223.53	15.46	13.93	17.17	0.54	0.04	86.51	5.98	
Pearl Harb_O2	1165	8/30/2012	14:55:25	223.30	15.45	13.93	17.16	4.11	0.28	86.74	6.00	
Pearl Harb_O2	1168	8/30/2012	14:55:34	223.03	15.43	13.93	17.13	1.20	0.08	87.02	6.02	
Pearl Harb_O2	1171	8/30/2012	14:55:42	222.83	15.42	13.90	17.11	1.68	0.12	87.22	6.03	
Pearl Harb_O2	1174	8/30/2012	14:55:52	223.02	15.43	13.91	17.16	1.78	0.12	87.02	6.02	
Pearl Harb_O2	1177	8/30/2012	14:56:01	222.25	15.38	13.84	17.12	3.57	0.25	87.79	6.07	
Pearl Harb_O2	1180	8/30/2012	14:56:10	221.94	15.35	13.81	17.11	0.78	0.05	88.10	6.09	
Pearl Harb_O2	1183	8/30/2012	14:56:18	221.41	15.32	13.80	17.09	0.78	0.05	88.63	6.13	
Pearl Harb_O2	1186	8/30/2012	14:56:28	221.34	15.31	13.78	17.10	0.95	0.07	88.70	6.14	
Pearl Harb_O2	1189	8/30/2012	14:56:37	222.02	15.36	13.80	17.13	0.34	0.02	88.02	6.09	
Pearl Harb_O2	1192	8/30/2012	14:56:46	222.71	15.41	13.94	17.10	1.90	0.13	87.34	6.04	
Pearl Harb_O2	1195	8/30/2012	14:56:54	222.78	15.41	13.98	17.10	0.43	0.03	87.27	6.04	
Pearl Harb_O2	1198	8/30/2012	14:57:04	222.21	15.37	13.93	17.08	0.45	0.03	87.84	6.08	
Pearl Harb_O2	1201	8/30/2012	14:57:13	221.89	15.35	13.89	17.07	1.22	0.08	88.15	6.10	
Pearl Harb_O2	1204	8/30/2012	14:57:22	221.73	15.34	13.87	17.08	3.50	0.24	88.31	6.11	
Pearl Harb_O2	1207	8/30/2012	14:57:30	220.53	15.26	13.75	17.04	34.03	2.35	89.51	6.19	
Pearl Harb_O2	1210	8/30/2012	14:57:40	219.07	15.16	13.71	17.02	35.58	2.46	90.97	6.29	
Pearl Harb_O2	1213	8/30/2012	14:57:49	219.17	15.16	13.68	17.03	12.11	0.84	90.87	6.29	
Pearl Harb_O2	1216	8/30/2012	14:57:58	219.44	15.18	13.67	17.04	7.07	0.49	90.60	6.27	
Pearl Harb_O2	1219	8/30/2012	14:58:06	220.77	15.27	13.72	17.11	1.21	0.08	89.27	6.18	
Pearl Harb_O2	1222	8/30/2012	14:58:16	220.98	15.29	13.74	17.11	2.01	0.14	89.06	6.16	
Pearl Harb_O2	1225	8/30/2012	14:58:25	220.96	15.29	13.75	17.11	2.74	0.19	89.08	6.16	

STATION	REP	DATE	TIME	Penetration Area (sq.cm)	Average Penetration (cm)	Minimum Penetration (cm)	Maximum Penetration (cm)	Sus Sed Area (sq.cm)	Sus Sed (cm)	Area of Water Visible (sq cm)	Water Visible (cm)	COMMENT
Pearl Harb_O2	1228	8/30/2012	14:58:34	220.20	15.23	13.68	17.08	2.10	0.15	89.84	6.21	
Pearl Harb_O2	1231	8/30/2012	14:58:42	220.48	15.25	13.72	17.07	1.49	0.10	89.56	6.20	
Pearl Harb_O2	1234	8/30/2012	14:58:52	220.67	15.27	13.71	17.07	2.99	0.21	89.38	6.18	
Pearl Harb_O2	1237	8/30/2012	14:59:01	220.61	15.26	13.71	17.07	1.17	0.08	89.43	6.19	
Pearl Harb_O2	1240	8/30/2012	14:59:10	220.70	15.27	13.71	17.07	1.93	0.13	89.34	6.18	
Pearl Harb_O2	1243	8/30/2012	14:59:18	220.85	15.28	13.70	17.08	0.66	0.05	89.19	6.17	
Pearl Harb_O2	1246	8/30/2012	14:59:28	220.88	15.28	13.71	17.08	0.45	0.03	89.16	6.17	
Pearl Harb_O2	1249	8/30/2012	14:59:37	220.92	15.28	13.72	17.08	0.50	0.03	89.12	6.17	
Pearl Harb_O2	1252	8/30/2012	14:59:46	220.93	15.28	13.74	17.07	0.97	0.07	89.11	6.16	
Pearl Harb_O2	1255	8/30/2012	14:59:55	221.10	15.30	13.75	17.09	1.47	0.10	88.94	6.15	
Pearl Harb_O2	1258	8/30/2012	15:00:04	221.22	15.30	13.76	17.09	1.17	0.08	88.82	6.14	
Pearl Harb_O2	1259	8/30/2012	15:00:07	220.69	15.27	13.72	17.07	1.11	0.08	89.35	6.18	
Pearl Harb_O2	1260	8/30/2012	15:00:10	220.77	15.27	13.74	17.06	0.99	0.07	89.28	6.18	
Pearl Harb_O2	1261	8/30/2012	15:00:13	220.83	15.28	13.74	17.08	1.64	0.11	89.21	6.17	
Pearl Harb_O2	1262	8/30/2012	15:00:16	220.70	15.27	13.74	17.05	0.98	0.07	89.34	6.18	
Pearl Harb_O2	1263	8/30/2012	15:00:19	220.65	15.26	13.72	17.06	0.91	0.06	89.39	6.18	
Pearl Harb_O2	1264	8/30/2012	15:00:22	221.24	15.31	13.74	17.09	1.17	0.08	88.80	6.14	
Pearl Harb_O2	1265	8/30/2012	15:00:25	221.24	15.31	13.77	17.09	1.02	0.07	88.80	6.14	
Pearl Harb_O2	1266	8/30/2012	15:00:28	221.77	15.34	13.81	17.08	1.39	0.10	88.27	6.11	
Pearl Harb_O2	1267	8/30/2012	15:00:31	221.69	15.34	13.83	17.07	2.28	0.16	88.35	6.11	
Pearl Harb_O2	1268	8/30/2012	15:00:34	221.39	15.32	13.83	17.03	1.78	0.12	88.66	6.13	
Pearl Harb_O2	1269	8/30/2012	15:00:37	221.28	15.31	13.83	17.04	1.69	0.12	88.76	6.14	
Pearl Harb_O2	1270	8/30/2012	15:00:40	220.89	15.28	13.80	17.04	2.04	0.14	89.15	6.17	
Pearl Harb_O2	1271	8/30/2012	15:00:43	220.88	15.28	13.79	17.03	1.15	0.08	89.16	6.17	
Pearl Harb_O2	1272	8/30/2012	15:00:46	220.91	15.28	13.81	17.05	1.93	0.13	89.13	6.17	
Pearl Harb_O2	1273	8/30/2012	15:00:49	220.43	15.25	13.78	17.02	1.28	0.09	89.61	6.20	
Pearl Harb_O2	1274	8/30/2012	15:00:52	220.21	15.23	13.74	17.02	0.88	0.06	89.83	6.21	
Pearl Harb_O2	1275	8/30/2012	15:00:55	219.56	15.19	13.67	17.01	1.12	0.08	90.48	6.26	
Pearl Harb_O2	1276	8/30/2012	15:00:58	219.38	15.18	13.64	17.01	0.92	0.06	90.66	6.27	
Pearl Harb_O2	1277	8/30/2012	15:01:01	219.27	15.17	13.64	17.00	1.16	0.08	90.77	6.28	
Pearl Harb_O2	1278	8/30/2012	15:01:04	219.46	15.18	13.64	17.01	1.16	0.08	90.58	6.27	
Pearl Harb_O2	1279	8/30/2012	15:01:07	219.58	15.19	13.67	17.02	1.23	0.08	90.46	6.26	
Pearl Harb_O2	1280	8/30/2012	15:01:10	219.49	15.18	13.65	17.01	2.36	0.16	90.55	6.26	
Pearl Harb_O2	1281	8/30/2012	15:01:13	219.40	15.18	13.64	17.02	1.74	0.12	90.64	6.27	
Pearl Harb_O2	1282	8/30/2012	15:01:16	219.40	15.18	13.64	17.01	1.11	0.08	90.64	6.27	
Pearl Harb_O2	1283	8/30/2012	15:01:19	219.45	15.18	13.64	17.01	1.27	0.09	90.59	6.27	
Pearl Harb_O2	1284	8/30/2012	15:01:22	219.38	15.18	13.64	17.01	1.10	0.08	90.66	6.27	
Pearl Harb_O2	1285	8/30/2012	15:01:25	219.35	15.17	13.66	17.02	0.64	0.04	90.69	6.27	
Pearl Harb_O2	1286	8/30/2012	15:01:28	219.55	15.19	13.68	17.02	1.10	0.08	90.49	6.26	
Pearl Harb_O2	1287	8/30/2012	15:01:31	219.68	15.20	13.67	17.02	1.33	0.09	90.37	6.25	
Pearl Harb_O2	1288	8/30/2012	15:01:34	219.84	15.21	13.68	17.02	0.83	0.06	90.21	6.24	
Pearl Harb_O2	1289	8/30/2012	15:01:37	219.99	15.22	13.67	17.03	0.60	0.04	90.05	6.23	
Pearl Harb_O2	1290	8/30/2012	15:01:40	219.82	15.21	13.67	17.03	0.93	0.06	90.22	6.24	
Pearl Harb_O2	1291	8/30/2012	15:01:43	219.41	15.18	13.64	17.03	1.75	0.12	90.64	6.27	
Pearl Harb_O2	1292	8/30/2012	15:01:46	219.41	15.18	13.64	17.01	1.69	0.12	90.63	6.27	
Pearl Harb_O2	1293	8/30/2012	15:01:49	219.52	15.19	13.65	17.01	0.91	0.06	90.52	6.26	
Pearl Harb_O2	1294	8/30/2012	15:01:52	219.55	15.19	13.65	17.01	0.94	0.07	90.49	6.26	
Pearl Harb_O2	1295	8/30/2012	15:01:55	219.21	15.17	13.64	17.01	0.76	0.05	90.83	6.28	
Pearl Harb_O2	1296	8/30/2012	15:01:58	219.14	15.16	13.63	17.01	0.81	0.06	90.91	6.29	
Pearl Harb_O2	1297	8/30/2012	15:02:01	218.17	15.09	13.60	16.95	1.31	0.09	91.88	6.36	
Pearl Harb_O2	1298	8/30/2012	15:02:04	217.75	15.06	13.59	16.94	1.08	0.07	92.29	6.38	
Pearl Harb_O2	1299	8/30/2012	15:02:07	217.48	15.05	13.55	16.92	1.43	0.10	92.56	6.40	
Pearl Harb_O2	1300	8/30/2012	15:02:10	216.35	14.97	13.45	16.91	0.88	0.06	93.70	6.48	
Pearl Harb_O2	1301	8/30/2012	15:02:13	216.45	14.97	13.45	16.91	1.23	0.09	93.59	6.47	

STATION	REP	DATE	TIME	Penetration Area (sq.cm)	Average Penetration (cm)	Minimum Penetration (cm)	Maximum Penetration (cm)	Sus Sed Area (sq.cm)	Sus Sed (cm)	Area of Water Visible (sq cm)	Water Visible (cm)	COMMENT
Pearl Harb_O2	1302	8/30/2012	15:02:16	216.50	14.98	13.45	16.93	0.84	0.06	93.54	6.47	
Pearl Harb_O2	1303	8/30/2012	15:02:19	216.49	14.98	13.44	16.91	1.04	0.07	93.55	6.47	
Pearl Harb_O2	1304	8/30/2012	15:02:22	216.50	14.98	13.45	16.91	2.94	0.20	93.55	6.47	
Pearl Harb_O2	1305	8/30/2012	15:02:25	216.09	14.95	13.43	16.91	1.61	0.11	93.95	6.50	edge of crab claw on left side
Pearl Harb_O2	1306	8/30/2012	15:02:28	216.00	14.94	13.37	16.91	1.63	0.11	94.04	6.51	two points of crab visible on left
Pearl Harb_O2	1307	8/30/2012	15:02:31	216.04	14.95	13.34	16.91	1.63	0.11	94.01	6.50	partial view of two legs and one claw of crab on left
Pearl Harb_O2	1308	8/30/2012	15:02:34	215.84	14.93	13.35	16.91	0.75	0.05	94.20	6.52	half of crab at rest on left
Pearl Harb_O2	1309	8/30/2012	15:02:37	215.47	14.91	13.33	16.90	1.59	0.11	94.57	6.54	half of crab standing a bit on left
Pearl Harb_O2	1310	8/30/2012	15:02:40	215.36	14.90	13.32	16.90	0.87	0.06	94.69	6.55	half of crab standing a bit on left
Pearl Harb_O2	1311	8/30/2012	15:02:43	215.68	14.92	13.35	16.90	0.73	0.05	94.37	6.53	claw and one leg of crab visible on left
Pearl Harb_O2	1312	8/30/2012	15:02:46	216.01	14.94	13.41	16.90	0.76	0.05	94.03	6.51	crab claw and three legs visible on left
Pearl Harb_O2	1313	8/30/2012	15:02:49	216.14	14.95	13.61	16.92	1.27	0.09	93.90	6.50	half of crab at rest on left
Pearl Harb_O2	1314	8/30/2012	15:02:52	215.84	14.93	13.53	16.90	2.74	0.19	94.20	6.52	slightly more than half of crab visible on left, standing, belly exposed; minimum pen depth affected by crab
Pearl Harb_O2	1315	8/30/2012	15:02:55	215.48	14.91	13.49	16.90	0.92	0.06	94.56	6.54	almost whole crab visible in crouch, on left side of frame
Pearl Harb_O2	1316	8/30/2012	15:02:58	215.21	14.89	13.45	16.90	9.94	0.69	94.83	6.56	almost whole crab visible in crouch, now on right side of frame
Pearl Harb_O2	1317	8/30/2012	15:03:01	215.24	14.89	13.46	16.90	17.38	1.20	94.80	6.56	
Pearl Harb_O2	1318	8/30/2012	15:03:04	215.26	14.89	13.46	16.90	12.65	0.88	94.78	6.56	
Pearl Harb_O2	1319	8/30/2012	15:03:07	215.33	14.90	13.45	16.90	6.49	0.45	94.71	6.55	
Pearl Harb_O2	1320	8/30/2012	15:03:10	215.74	14.92	13.51	16.90	23.67	1.64	94.30	6.52	
Pearl Harb_O2	1321	8/30/2012	15:03:13	216.90	15.00	13.56	16.92	39.80	2.75	93.15	6.44	cloud of sus sed
Pearl Harb_O2	1322	8/30/2012	15:03:16	218.34	15.10	13.70	16.93	41.95	2.90	91.70	6.34	cloud of sus sed
Pearl Harb_O2	1323	8/30/2012	15:03:19	217.87	15.07	13.66	16.92	47.90	3.31	92.17	6.38	cloud of sus sed on left mostly
Pearl Harb_O2	1324	8/30/2012	15:03:22	217.17	15.02	13.62	16.92	55.57	3.84	92.87	6.42	cloud of sus sed
Pearl Harb_O2	1325	8/30/2012	15:03:25	216.63	14.99	13.58	16.87	44.76	3.10	93.41	6.46	cloud of sus sed
Pearl Harb_O2	1326	8/30/2012	15:03:28	216.27	14.96	13.59	16.87	41.46	2.87	93.77	6.49	cloud of sus sed
Pearl Harb_O2	1327	8/30/2012	15:03:31	215.60	14.92	13.51	16.72	63.47	4.39	94.44	6.53	cloud of sus sed
Pearl Harb_O2	1328	8/30/2012	15:03:34	215.60	14.92	13.56	16.74	54.10	3.74	94.44	6.53	cloud of sus sed
Pearl Harb_O2	1329	8/30/2012	15:03:37	215.36	14.90	13.51	16.76	40.52	2.80	94.68	6.55	cloud of sus sed
Pearl Harb_O2	1330	8/30/2012	15:03:40	215.31	14.90	13.46	16.73	45.87	3.17	94.73	6.55	cloud of sus sed
Pearl Harb_O2	1331	8/30/2012	15:03:43	215.11	14.88	13.42	16.73	28.15	1.95	94.93	6.57	cloud of sus sed
Pearl Harb_O2	1332	8/30/2012	15:03:46	214.85	14.86	13.40	16.70	44.21	3.06	95.19	6.59	cloud of sus sed
Pearl Harb_O2	1333	8/30/2012	15:03:49	212.60	14.71	13.22	16.68	60.10	4.16	97.44	6.74	cloud of sus sed; med chunk of sed on surface at left
Pearl Harb_O2	1334	8/30/2012	15:03:52	210.67	14.57	13.04	16.56	42.84	2.96	99.38	6.87	cloud of sus sed; med chunk of sed on surface at left
Pearl Harb_O2	1335	8/30/2012	15:03:55	209.01	14.46	12.92	16.46	51.80	3.58	101.03	6.99	cloud of sus sed; med chunk of sed on surface at left
Pearl Harb_O2	1336	8/30/2012	15:03:58	208.99	14.46	12.91	16.42	47.45	3.28	101.05	6.99	cloud of sus sed; med chunk of sed on surface at left
Pearl Harb_O2	1337	8/30/2012	15:04:01	208.76	14.44	12.91	16.39	50.14	3.47	101.29	7.01	cloud of sus sed; med chunk of sed on surface at left
Pearl Harb_O2	1338	8/30/2012	15:04:04	208.66	14.44	12.90	16.35	42.86	2.96	101.38	7.01	cloud of sus sed
Pearl Harb_O2	1339	8/30/2012	15:04:07	208.68	14.44	12.88	16.36	35.37	2.45	101.36	7.01	cloud of sus sed
Pearl Harb_O2	1340	8/30/2012	15:04:10	208.60	14.43	12.89	16.37	43.98	3.04	101.44	7.02	cloud of sus sed
Pearl Harb_O2	1341	8/30/2012	15:04:13	208.45	14.42	12.88	16.34	37.36	2.58	101.59	7.03	cloud of sus sed
Pearl Harb_O2	1342	8/30/2012	15:04:16	207.86	14.38	12.85	16.32	27.37	1.89	102.18	7.07	cloud of sus sed
Pearl Harb_O2	1343	8/30/2012	15:04:19	204.34	14.14	12.55	16.18	50.44	3.49	105.70	7.31	cloud of sus sed
Pearl Harb_O2	1344	8/30/2012	15:04:22	204.83	14.17	12.65	16.20	53.04	3.67	105.21	7.28	cloud of sus sed
Pearl Harb_O2	1345	8/30/2012	15:04:25	204.96	14.18	12.67	16.20	39.41	2.73	105.08	7.27	cloud of sus sed
Pearl Harb_O2	1346	8/30/2012	15:04:28	205.01	14.18	12.66	16.20	17.92	1.24	105.03	7.27	
Pearl Harb_O2	1347	8/30/2012	15:04:31	205.48	14.21	12.72	16.23	8.05	0.56	104.56	7.23	
Pearl Harb_O2	1348	8/30/2012	15:04:34	206.35	14.28	12.75	16.24	3.23	0.22	103.69	7.17	
Pearl Harb_O2	1349	8/30/2012	15:04:37	206.55	14.29	12.73	16.24	9.65	0.67	103.50	7.16	
Pearl Harb_O2	1350	8/30/2012	15:04:40	206.80	14.31	12.77	16.26	7.09	0.49	103.24	7.14	
Pearl Harb_O2	1351	8/30/2012	15:04:43	207.13	14.33	12.79	16.25	7.81	0.54	102.91	7.12	
Pearl Harb_O2	1352	8/30/2012	15:04:46	207.21	14.33	12.83	16.28	9.42	0.65	102.83	7.11	
Pearl Harb_O2	1353	8/30/2012	15:04:49	207.24	14.34	12.75	16.26	8.52	0.59	102.80	7.11	
Pearl Harb_O2	1354	8/30/2012	15:04:52	207.29	14.34	12.80	16.24	26.50	1.83	102.75	7.11	

STATION	REP	DATE	TIME	Penetration Area (sq.cm)	Average Penetration (cm)	Minimum Penetration (cm)	Maximum Penetration (cm)	Sus Sed Area (sq.cm)	Sus Sed (cm)	Area of Water Visible (sq cm)	Water Visible (cm)	COMMENT
Pearl Harb_O2	1355	8/30/2012	15:04:55	207.39	14.35	12.85	16.25	40.25	2.78	102.65	7.10	cloud of sus sed
Pearl Harb_O2	1356	8/30/2012	15:04:58	207.71	14.37	12.87	16.30	47.86	3.31	102.33	7.08	cloud of sus sed
Pearl Harb_O2	1357	8/30/2012	15:05:01	208.22	14.40	12.87	16.26	41.15	2.85	101.83	7.04	cloud of sus sed
Pearl Harb_O2	1358	8/30/2012	15:05:04	208.52	14.43	12.91	16.25	31.34	2.17	101.52	7.02	cloud of sus sed
Pearl Harb_O2	1359	8/30/2012	15:05:07	208.71	14.44	12.90	16.28	58.85	4.07	101.33	7.01	cloud of sus sed
Pearl Harb_O2	1360	8/30/2012	15:05:10	208.93	14.45	12.96	16.28	51.65	3.57	101.11	7.00	cloud of sus sed
Pearl Harb_O2	1361	8/30/2012	15:05:13	209.00	14.46	12.94	16.26	32.31	2.24	101.04	6.99	cloud of sus sed
Pearl Harb_O2	1362	8/30/2012	15:05:16	209.17	14.47	12.97	16.26	27.10	1.87	100.87	6.98	
Pearl Harb_O2	1363	8/30/2012	15:05:19	209.04	14.46	12.95	16.26	23.13	1.60	101.01	6.99	
Pearl Harb_O2	1364	8/30/2012	15:05:22	209.06	14.46	12.94	16.26	18.72	1.29	100.98	6.99	
Pearl Harb_O2	1365	8/30/2012	15:05:25	209.08	14.46	12.95	16.26	11.91	0.82	100.96	6.98	
Pearl Harb_O2	1366	8/30/2012	15:05:28	209.02	14.46	12.96	16.26	12.33	0.85	101.03	6.99	
Pearl Harb_O2	1367	8/30/2012	15:05:31	209.03	14.46	12.94	16.25	11.09	0.77	101.01	6.99	
Pearl Harb_O2	1368	8/30/2012	15:05:34	208.95	14.46	12.92	16.26	3.86	0.27	101.09	6.99	
Pearl Harb_O2	1369	8/30/2012	15:05:37	208.88	14.45	12.92	16.22	3.05	0.21	101.16	7.00	
Pearl Harb_O2	1370	8/30/2012	15:05:40	208.90	14.45	12.90	16.25	3.97	0.27	101.14	7.00	
Pearl Harb_O2	1371	8/30/2012	15:05:43	208.89	14.45	12.94	16.24	5.20	0.36	101.15	7.00	
Pearl Harb_O2	1372	8/30/2012	15:05:46	208.82	14.45	12.96	16.24	4.32	0.30	101.23	7.00	
Pearl Harb_O2	1373	8/30/2012	15:05:49	207.22	14.34	12.77	16.21	4.81	0.33	102.83	7.11	
Pearl Harb_O2	1374	8/30/2012	15:05:52	207.23	14.34	12.78	16.22	3.48	0.24	102.82	7.11	
Pearl Harb_O2	1375	8/30/2012	15:05:55	207.03	14.32	12.76	16.22	3.69	0.26	103.01	7.13	
Pearl Harb_O2	1376	8/30/2012	15:05:58	206.52	14.29	12.71	16.19	10.96	0.76	103.52	7.16	
Pearl Harb_O2	1377	8/30/2012	15:06:01	205.40	14.21	12.62	16.19	19.94	1.38	104.65	7.24	
Pearl Harb_O2	1378	8/30/2012	15:06:04	205.47	14.21	12.64	16.20	22.58	1.56	104.57	7.23	
Pearl Harb_O2	1379	8/30/2012	15:06:07	206.32	14.27	12.68	16.16	22.80	1.58	103.72	7.18	cloud of sus sed
Pearl Harb_O2	1380	8/30/2012	15:06:10	206.52	14.29	12.71	16.15	31.29	2.16	103.52	7.16	cloud of sus sed
Pearl Harb_O2	1381	8/30/2012	15:06:13	206.59	14.29	12.71	16.15	27.73	1.92	103.45	7.16	
Pearl Harb_O2	1382	8/30/2012	15:06:16	206.85	14.31	12.75	16.15	16.75	1.16	103.19	7.14	
Pearl Harb_O2	1383	8/30/2012	15:06:19	207.21	14.34	12.81	16.16	19.51	1.35	102.83	7.11	small cloud of sus sed
Pearl Harb_O2	1384	8/30/2012	15:06:22	207.42	14.35	12.80	16.17	29.80	2.06	102.62	7.10	cloud of sus sed
Pearl Harb_O2	1385	8/30/2012	15:06:25	207.55	14.36	12.80	16.17	33.58	2.32	102.49	7.09	cloud of sus sed
Pearl Harb_O2	1386	8/30/2012	15:06:28	207.26	14.34	12.84	16.14	50.83	3.52	102.78	7.11	cloud of sus sed
Pearl Harb_O2	1387	8/30/2012	15:06:31	205.90	14.24	12.94	15.67	64.37	4.45	104.14	7.20	cloud of sus sed; top of right side of SWI blown off; max point different now
Pearl Harb_O2	1388	8/30/2012	15:06:34	206.32	14.27	12.86	15.54	44.10	3.05	103.72	7.18	cloud of sus sed; med/large sediment chunks on surface in back on right
Pearl Harb_O2	1389	8/30/2012	15:06:37	206.71	14.30	12.90	15.81	51.53	3.57	103.34	7.15	cloud of sus sed; med/large sediment chunks on surface in back on right
Pearl Harb_O2	1390	8/30/2012	15:06:40	207.02	14.32	12.92	15.78	50.16	3.47	103.02	7.13	cloud of sus sed; med/large sediment chunks on surface in back on right
Pearl Harb_O2	1391	8/30/2012	15:06:43	207.42	14.35	12.98	15.75	34.19	2.37	102.62	7.10	small cloud of sus sed; med/large sediment chunks on surface in back on right
Pearl Harb_O2	1392	8/30/2012	15:06:46	207.98	14.39	13.01	15.74	25.95	1.80	102.06	7.06	small cloud of sus sed; med/large sediment chunks on surface in back on right
Pearl Harb_O2	1393	8/30/2012	15:06:49	208.18	14.40	13.06	15.77	24.57	1.70	101.86	7.05	small cloud of sus sed; med/large sediment chunks on surface in back on right
Pearl Harb_O2	1394	8/30/2012	15:06:52	208.18	14.40	13.02	15.65	24.56	1.70	101.87	7.05	small cloud of sus sed; med/large sediment chunks on surface in back on right
Pearl Harb_O2	1395	8/30/2012	15:06:55	207.83	14.38	12.98	15.71	42.16	2.92	102.21	7.07	cloud of sus sed; med/large sediment chunks on surface in back on right
Pearl Harb_O2	1396	8/30/2012	15:06:58	207.49	14.35	13.04	15.64	33.84	2.34	102.55	7.09	cloud of sus sed; sml sediment chunk on surface and med rolling? out to right in back on right
Pearl Harb_O2	1397	8/30/2012	15:07:01	207.73	14.37	12.99	15.54	16.45	1.14	102.31	7.08	sml chunk of sed on right
Pearl Harb_O2	1398	8/30/2012	15:07:04	207.83	14.38	13.07	15.53	12.74	0.88	102.21	7.07	sml chunk of sed on right
Pearl Harb_O2	1399	8/30/2012	15:07:07	207.94	14.39	13.06	15.54	17.27	1.19	102.11	7.06	sml chunk of sed on right
Pearl Harb_O2	1400	8/30/2012	15:07:10	207.70	14.37	13.08	15.51	13.06	0.90	102.34	7.08	sml chunk of sed on right
Pearl Harb_O2	1401	8/30/2012	15:07:13	207.59	14.36	13.06	15.50	11.15	0.77	102.45	7.09	sml chunk of sed on right
Pearl Harb_O2	1402	8/30/2012	15:07:16	207.44	14.35	13.04	15.50	16.72	1.16	102.61	7.10	sml chunk of sed on right
Pearl Harb_O2	1403	8/30/2012	15:07:19	207.21	14.33	13.02	15.49	15.71	1.09	102.83	7.11	sml chunk of sed on right

STATION	REP	DATE	TIME	Penetration Area (sq.cm)	Average Penetration (cm)	Minimum Penetration (cm)	Maximum Penetration (cm)	Sus Sed Area (sq.cm)	Sus Sed (cm)	Area of Water Visible (sq cm)	Water Visible (cm)	COMMENT
Pearl Harb_O2	1404	8/30/2012	15:07:22	207.04	14.32	12.99	15.47	13.38	0.93	103.00	7.13	sml chunk of sed on right
Pearl Harb_O2	1405	8/30/2012	15:07:25	206.93	14.32	12.99	15.47	22.46	1.55	103.12	7.13	sml chunk of sed on right
Pearl Harb_O2	1406	8/30/2012	15:07:28	206.95	14.32	12.99	15.45	29.06	2.01	103.10	7.13	sml chunk of sed on right
Pearl Harb_O2	1407	8/30/2012	15:07:31	206.89	14.31	13.01	15.45	10.92	0.76	103.15	7.14	sml chunk of sed on right
Pearl Harb_O2	1408	8/30/2012	15:07:34	206.92	14.31	13.01	15.45	14.00	0.97	103.13	7.13	sml chunk of sed on right
Pearl Harb_O2	1409	8/30/2012	15:07:37	207.24	14.34	13.01	15.49	14.25	0.99	102.80	7.11	sml chunk of sed on right
Pearl Harb_O2	1410	8/30/2012	15:07:40	207.55	14.36	13.06	15.52	27.32	1.89	102.49	7.09	small cloud of sus sed; sml chunk of sed on right
Pearl Harb_O2	1411	8/30/2012	15:07:43	207.63	14.36	13.07	15.52	37.68	2.61	102.41	7.08	cloud of sus sed; sml chunk of sed on right
Pearl Harb_O2	1412	8/30/2012	15:07:46	207.51	14.36	13.05	15.51	38.93	2.69	102.53	7.09	cloud of sus sed; sml chunk of sed on right
Pearl Harb_O2	1413	8/30/2012	15:07:49	207.27	14.34	13.05	15.47	34.29	2.37	102.77	7.11	small cloud of sus sed
Pearl Harb_O2	1414	8/30/2012	15:07:52	207.35	14.34	13.09	15.45	20.49	1.42	102.69	7.10	
Pearl Harb_O2	1415	8/30/2012	15:07:55	207.35	14.34	13.08	15.45	20.15	1.39	102.69	7.10	
Pearl Harb_O2	1416	8/30/2012	15:07:58	208.15	14.40	13.14	15.48	8.84	0.61	101.89	7.05	
Pearl Harb_O2	1417	8/30/2012	15:08:01	208.50	14.42	13.13	15.52	10.73	0.74	101.55	7.03	
Pearl Harb_O2	1418	8/30/2012	15:08:04	208.81	14.45	13.19	15.53	14.77	1.02	101.23	7.00	
Pearl Harb_O2	1419	8/30/2012	15:08:07	208.95	14.45	13.17	15.53	12.61	0.87	101.10	6.99	
Pearl Harb_O2	1420	8/30/2012	15:08:10	208.92	14.45	13.18	15.55	12.27	0.85	101.12	7.00	
Pearl Harb_O2	1421	8/30/2012	15:08:13	208.99	14.46	13.17	15.55	8.40	0.58	101.05	6.99	
Pearl Harb_O2	1422	8/30/2012	15:08:16	209.03	14.46	13.18	15.55	9.08	0.63	101.01	6.99	
Pearl Harb_O2	1423	8/30/2012	15:08:19	208.94	14.45	13.18	15.54	8.69	0.60	101.10	6.99	
Pearl Harb_O2	1424	8/30/2012	15:08:22	208.96	14.46	13.16	15.55	6.17	0.43	101.08	6.99	
Pearl Harb_O2	1425	8/30/2012	15:08:25	208.93	14.45	13.16	15.56	7.93	0.55	101.11	6.99	
Pearl Harb_O2	1426	8/30/2012	15:08:28	208.93	14.45	13.16	15.54	11.18	0.77	101.11	6.99	
Pearl Harb_O2	1427	8/30/2012	15:08:31	208.96	14.46	13.15	15.55	9.91	0.69	101.08	6.99	
Pearl Harb_O2	1428	8/30/2012	15:08:34	208.97	14.46	13.15	15.55	9.61	0.66	101.07	6.99	
Pearl Harb_O2	1429	8/30/2012	15:08:37	208.43	14.42	13.15	15.50	11.50	0.80	101.61	7.03	
Pearl Harb_O2	1430	8/30/2012	15:08:40	208.53	14.43	13.11	15.51	15.86	1.10	101.51	7.02	
Pearl Harb_O2	1431	8/30/2012	15:08:43	208.57	14.43	13.13	15.53	12.36	0.85	101.48	7.02	
Pearl Harb_O2	1432	8/30/2012	15:08:46	208.56	14.43	13.13	15.51	13.00	0.90	101.48	7.02	
Pearl Harb_O2	1433	8/30/2012	15:08:49	206.17	14.26	12.91	15.38	10.95	0.76	103.87	7.19	
Pearl Harb_O2	1434	8/30/2012	15:08:52	206.33	14.27	12.97	15.39	9.53	0.66	103.71	7.17	
Pearl Harb_O2	1435	8/30/2012	15:08:55	209.09	14.46	13.17	15.57	6.86	0.47	100.95	6.98	
Pearl Harb_O2	1436	8/30/2012	15:08:58	209.75	14.51	13.19	15.62	12.81	0.89	100.30	6.94	
Pearl Harb_O2	1437	8/30/2012	15:09:01	209.78	14.51	13.18	15.59	13.20	0.91	100.27	6.94	
Pearl Harb_O2	1438	8/30/2012	15:09:04	209.87	14.52	13.21	15.60	10.49	0.73	100.17	6.93	
Pearl Harb_O2	1439	8/30/2012	15:09:07	210.02	14.53	13.21	15.62	8.90	0.62	100.02	6.92	
Pearl Harb_O2	1440	8/30/2012	15:09:10	210.03	14.53	13.21	15.61	13.73	0.95	100.01	6.92	
Pearl Harb_O2	1441	8/30/2012	15:09:13	210.18	14.54	13.25	15.63	8.28	0.57	99.86	6.91	
Pearl Harb_O2	1442	8/30/2012	15:09:16	210.78	14.58	13.30	15.64	12.37	0.86	99.26	6.87	
Pearl Harb_O2	1443	8/30/2012	15:09:19	210.91	14.59	13.32	15.65	11.80	0.82	99.13	6.86	
Pearl Harb_O2	1444	8/30/2012	15:09:22	210.50	14.56	13.29	15.61	18.03	1.25	99.55	6.89	small cloud of sus sed
Pearl Harb_O2	1445	8/30/2012	15:09:25	209.87	14.52	13.23	15.61	11.67	0.81	100.17	6.93	
Pearl Harb_O2	1446	8/30/2012	15:09:28	208.29	14.41	13.05	15.56	11.11	0.77	101.75	7.04	
Pearl Harb_O2	1447	8/30/2012	15:09:31	207.81	14.38	13.03	15.52	10.50	0.73	102.24	7.07	
Pearl Harb_O2	1448	8/30/2012	15:09:34	207.49	14.35	12.97	15.51	12.75	0.88	102.55	7.09	
Pearl Harb_O2	1449	8/30/2012	15:09:37	207.51	14.36	12.98	15.53	9.48	0.66	102.54	7.09	
Pearl Harb_O2	1450	8/30/2012	15:09:40	207.63	14.36	12.97	15.53	7.51	0.52	102.42	7.09	
Pearl Harb_O2	1451	8/30/2012	15:09:43	207.78	14.37	13.00	15.56	7.14	0.49	102.26	7.07	
Pearl Harb_O2	1452	8/30/2012	15:09:46	207.98	14.39	12.99	15.55	9.01	0.62	102.06	7.06	
Pearl Harb_O2	1453	8/30/2012	15:09:49	208.16	14.40	13.02	15.57	9.00	0.62	101.88	7.05	
Pearl Harb_O2	1454	8/30/2012	15:09:52	208.52	14.43	13.02	15.61	9.16	0.63	101.53	7.02	
Pearl Harb_O2	1455	8/30/2012	15:09:55	208.74	14.44	13.06	15.62	11.62	0.80	101.31	7.01	
Pearl Harb_O2	1456	8/30/2012	15:09:58	208.89	14.45	13.06	15.62	8.06	0.56	101.15	7.00	
Pearl Harb_O2	1457	8/30/2012	15:10:01	208.94	14.45	13.07	15.64	10.99	0.76	101.10	6.99	

STATION	REP	DATE	TIME	Penetration Area (sq.cm)	Average Penetration (cm)	Minimum Penetration (cm)	Maximum Penetration (cm)	Sus Sed Area (sq.cm)	Sus Sed (cm)	Area of Water Visible (sq cm)	Water Visible (cm)	COMMENT
Pearl Harb_O2	1458	8/30/2012	15:10:04	209.03	14.46	13.07	15.64	11.77	0.81	101.02	6.99	
Pearl Harb_O2	1459	8/30/2012	15:10:07	209.08	14.46	13.08	15.64	11.40	0.79	100.96	6.98	
Pearl Harb_O2	1460	8/30/2012	15:10:10	209.17	14.47	13.07	15.64	3.77	0.26	100.88	6.98	
Pearl Harb_O2	1461	8/30/2012	15:10:13	209.21	14.47	13.10	15.64	4.50	0.31	100.83	6.98	
Pearl Harb_O2	1462	8/30/2012	15:10:16	209.18	14.47	13.09	15.66	8.96	0.62	100.87	6.98	
Pearl Harb_O2	1463	8/30/2012	15:10:19	209.18	14.47	13.07	15.66	3.37	0.23	100.86	6.98	
Pearl Harb_O2	1464	8/30/2012	15:10:22	209.27	14.48	13.11	15.66	3.57	0.25	100.77	6.97	
Pearl Harb_O2	1465	8/30/2012	15:10:25	209.28	14.48	13.11	15.66	5.64	0.39	100.76	6.97	
Pearl Harb_O2	1466	8/30/2012	15:10:28	209.36	14.48	13.11	15.64	2.02	0.14	100.69	6.97	
Pearl Harb_O2	1467	8/30/2012	15:10:31	209.30	14.48	13.11	15.66	3.72	0.26	100.74	6.97	
Pearl Harb_O2	1468	8/30/2012	15:10:34	209.31	14.48	13.11	15.66	4.72	0.33	100.74	6.97	
Pearl Harb_O2	1469	8/30/2012	15:10:37	209.85	14.52	13.18	15.66	3.33	0.23	100.19	6.93	
Pearl Harb_O2	1470	8/30/2012	15:10:40	209.89	14.52	13.19	15.66	3.68	0.25	100.16	6.93	
Pearl Harb_O2	1471	8/30/2012	15:10:43	209.88	14.52	13.18	15.66	1.01	0.07	100.16	6.93	
Pearl Harb_O2	1472	8/30/2012	15:10:46	209.83	14.52	13.17	15.66	5.46	0.38	100.21	6.93	
Pearl Harb_O2	1473	8/30/2012	15:10:49	209.75	14.51	13.16	15.65	3.41	0.24	100.29	6.94	
Pearl Harb_O2	1474	8/30/2012	15:10:52	209.66	14.50	13.15	15.65	4.67	0.32	100.38	6.94	
Pearl Harb_O2	1475	8/30/2012	15:10:55	209.72	14.51	13.14	15.66	7.36	0.51	100.33	6.94	
Pearl Harb_O2	1476	8/30/2012	15:10:58	209.73	14.51	13.14	15.64	3.89	0.27	100.31	6.94	
Pearl Harb_O2	1477	8/30/2012	15:11:01	209.78	14.51	13.16	15.64	4.81	0.33	100.26	6.94	
Pearl Harb_O2	1478	8/30/2012	15:11:04	209.77	14.51	13.19	15.65	2.13	0.15	100.27	6.94	
Pearl Harb_O2	1479	8/30/2012	15:11:07	209.52	14.49	13.18	15.62	6.17	0.43	100.52	6.95	
Pearl Harb_O2	1480	8/30/2012	15:11:10	209.50	14.49	13.17	15.61	16.52	1.14	100.54	6.96	
Pearl Harb_O2	1481	8/30/2012	15:11:13	209.47	14.49	13.18	15.59	28.99	2.01	100.57	6.96	small cloud of sus sed
Pearl Harb_O2	1482	8/30/2012	15:11:16	209.50	14.49	13.18	15.60	28.26	1.96	100.54	6.96	
Pearl Harb_O2	1483	8/30/2012	15:11:19	209.41	14.49	13.14	15.59	18.87	1.31	100.63	6.96	
Pearl Harb_O2	1484	8/30/2012	15:11:22	209.49	14.49	13.17	15.58	10.46	0.72	100.56	6.96	
Pearl Harb_O2	1485	8/30/2012	15:11:25	209.52	14.49	13.17	15.58	4.29	0.30	100.53	6.95	
Pearl Harb_O2	1486	8/30/2012	15:11:28	209.50	14.49	13.21	15.60	3.61	0.25	100.54	6.96	
Pearl Harb_O2	1487	8/30/2012	15:11:31	209.47	14.49	13.21	15.60	3.05	0.21	100.57	6.96	
Pearl Harb_O2	1488	8/30/2012	15:11:34	209.09	14.46	13.20	15.56	6.54	0.45	100.95	6.98	
Pearl Harb_O2	1489	8/30/2012	15:11:37	207.82	14.38	13.10	15.48	30.42	2.10	102.22	7.07	small cloud of sus sed
Pearl Harb_O2	1490	8/30/2012	15:11:40	206.84	14.31	13.05	15.42	26.70	1.85	103.20	7.14	small cloud of sus sed
Pearl Harb_O2	1491	8/30/2012	15:11:43	206.61	14.29	13.05	15.41	18.64	1.29	103.43	7.16	
Pearl Harb_O2	1492	8/30/2012	15:11:46	206.54	14.29	13.02	15.40	5.70	0.39	103.50	7.16	
Pearl Harb_O2	1493	8/30/2012	15:11:49	205.04	14.18	12.91	15.35	5.47	0.38	105.01	7.26	
Pearl Harb_O2	1494	8/30/2012	15:11:52	203.46	14.08	12.82	15.27	8.95	0.62	106.58	7.37	
Pearl Harb_O2	1495	8/30/2012	15:11:55	204.19	14.13	12.86	15.32	15.55	1.08	105.86	7.32	
Pearl Harb_O2	1496	8/30/2012	15:11:58	205.26	14.20	12.94	15.36	17.22	1.19	104.78	7.25	
Pearl Harb_O2	1497	8/30/2012	15:12:01	205.74	14.23	12.99	15.39	8.84	0.61	104.30	7.22	
Pearl Harb_O2	1498	8/30/2012	15:12:04	205.91	14.24	13.01	15.38	4.97	0.34	104.13	7.20	
Pearl Harb_O2	1499	8/30/2012	15:12:07	206.25	14.27	13.06	15.41	6.71	0.46	103.79	7.18	
Pearl Harb_O2	1500	8/30/2012	15:12:10	206.44	14.28	13.08	15.42	4.62	0.32	103.60	7.17	

APPENDIX H
DATA FOR SEDIMENT TRAP STUDY IN PIER 7
SINCLAIR INLET, WA

Table H-1. Particle and metal deposition rates (g/m² d) for Event 1.

Sediment Trap No.	SAMPLE ID by SIZE FRACTION	Deploy time (days)	Total Dry Particle Deposition Rate (g/m ² d)	Copper Deposition Rate (g/m ² d)	Chromium Deposition Rate (g/m ² d)	Nickel Deposition Rate (g/m ² d)	Zinc Deposition Rate (g/m ² d)	Arsenic Deposition Rate (g/m ² d)	Silver Deposition Rate (g/m ² d)	Cadmium Deposition Rate (g/m ² d)	Lead Deposition Rate (g/m ² d)	Mercury Deposition Rate (g/m ² d)
1	PSNS-1 9Apr14 2mm to 60µm	76	20.84	0.002709	0.000904	0.000658	0.006249	0.000313	0.000048	0.000054	0.001188	5.226E-08
2	PSNS-2 9Apr14 2mm to 60µm	76	8.26	0.001719	0.000264	0.000410	0.002976	0.000096	0.000018	0.000015	0.000351	4.163E-08
3	PSNS-3 9Apr14 2mm to 60µm	76	7.17	0.001862	0.000368	0.000376	0.003185	0.000184	0.000019	0.000017	0.000544	4.163E-08
4	PSNS-4 9Apr14 2mm to 60µm	76	8.98	0.001495	0.000398	0.000319	0.002868	0.000179	0.000020	0.000016	0.000617	5.175E-08
5	PSNS-5 9Apr14 2mm to 60µm	76	8.84	0.002600	0.000492	0.000366	0.003819	0.000169	0.000020	0.000022	0.000822	3.180E-09
6	PSNS-6 9Apr14 2mm to 60µm	76	10.02	0.002820	0.000519	0.000440	0.004003	0.000222	0.000022	0.000023	0.000795	5.135E-08
7	PSNS-7 9Apr14 2mm to 60µm	76	9.06	0.002458	0.000430	0.000350	0.004078	0.000190	0.000019	0.000023	0.000803	3.271E-08
8	PSNS-8 9Apr14 2mm to 60µm	76	9.95	0.002770	0.000522	0.000449	0.003726	0.000229	0.000027	0.000022	0.000933	4.335E-08
9	PSNS-9 19Apr14 2mm to 60µm	76	8.03	0.002048	0.000528	0.000530	0.003295	0.000162	0.000021	0.000028	0.000699	4.537E-08
1	PSNS-1 9Apr14 60µm to 5µm	76	14.24	0.002278	0.000693	0.000550	0.003204	0.000287	0.000035	0.000019	0.000815	4.359E-08
2	PSNS-2 9Apr14 60µm to 5µm	76	26.68	0.003290	0.000960	0.000786	0.004303	0.000392	0.000054	0.000026	0.001115	1.129E-07
3	PSNS-3 9Apr14 60µm to 5µm	76	34.95	0.004367	0.001334	0.001138	0.006949	0.000557	0.000088	0.000045	0.001680	1.017E-07
4	PSNS-4 9Apr14 60µm to 5µm	76	38.90	0.004571	0.001669	0.001359	0.007683	0.000544	0.000094	0.000047	0.001944	1.285E-07
5	PSNS-5 9Apr14 60µm to 5µm	76	33.04	0.004601	0.001334	0.001121	0.006603	0.000472	0.000062	0.000038	0.001704	8.680E-08

Sediment Trap No.	SAMPLE ID by SIZE FRACTION	Deploy time (days)	Total Dry Particle Deposition Rate (g/m ² d)	Copper Deposition Rate (g/m ² d)	Chromium Deposition Rate (g/m ² d)	Nickel Deposition Rate (g/m ² d)	Zinc Deposition Rate (g/m ² d)	Arsenic Deposition Rate (g/m ² d)	Silver Deposition Rate (g/m ² d)	Cadmium Deposition Rate (g/m ² d)	Lead Deposition Rate (g/m ² d)	Mercury Deposition Rate (g/m ² d)
6	PSNS-6 9Apr14 60µm to 5µm	76	44.84	0.005588	0.001995	0.001652	0.008686	0.000706	0.000105	0.000058	0.002422	1.505E-07
7	PSNS-7 9Apr14 60µm to 5µm	76	63.74	0.008678	0.002799	0.002275	0.013078	0.000995	0.000122	0.000074	0.003792	2.068E-08
8	PSNS-8 9Apr14 60µm to 5µm	76	43.63	0.006570	0.001704	0.001446	0.007824	0.000651	0.000098	0.000052	0.002320	1.181E-07
9	PSNS-9 9Apr14 60µm to 5µm	76	35.26	0.005095	0.001537	0.001302	0.007255	0.000546	0.000079	0.000055	0.001964	1.214E-07
1	PSNS-1 9Apr14 5 µm to 0.45µm	76	-0.002	0.000002	0.000001	0.000003	0.000005	0.000004	-1.892E-06	3.207E-08	9.241E-07	9.874E-14
2	PSNS-2 9Apr14 5 µm to 0.45µm	76	0.005	0.000007	0.000001	0.000002	0.000004	0.000018	-1.546E-06	2.949E-08	1.228E-06	7.109E-14
3	PSNS-3 9Apr14 5 µm to 0.45µm	76	-0.001	0.000027	0.000002	0.000005	0.000018	0.000012	-1.640E-06	9.052E-08	4.491E-07	2.567E-13
4	PSNS-4 9Apr14 5 µm to 0.45µm	76	0.006	0.000001	0.000013	0.000005	0.000006	0.000206	-1.251E-06	1.570E-08	9.625E-08	2.528E-13
5	PSNS-5 9Apr14 5 µm to 0.45µm	76	0.012	0.000008	0.000005	0.000006	0.000021	0.000016	-2.324E-06	8.432E-08	9.190E-07	3.555E-13
6	PSNS-6 9Apr14 5 µm to 0.45µm	76	0.008	0.000003	0.000003	0.000003	0.000023	0.000105	-6.309E-07	1.273E-07	2.900E-07	9.874E-14
7	PSNS-7 9Apr14 5 µm to 0.45µm	76	0.006	0.000004	0.000002	0.000002	0.000010	0.000030	-7.175E-07	3.943E-08	2.426E-07	4.581E-13
8	PSNS-8 9Apr14 5 µm to 0.45µm	76	-0.003	0.000006	0.000002	0.000006	0.000009	0.000008	-2.145E-06	4.374E-07	5.462E-08	5.213E-13
9	PSNS-9 9Apr14 5 µm to 0.45µm	76	0.005	0.000004	0.000011	0.000005	0.000005	0.000353	-2.335E-06	1.352E-08	3.999E-07	2.962E-13
1	PSNS-1 9Apr14 < 0.45µm	76		0.000007	0.000002	0.000009	0.000033	0.000074	-0.000002	3.336E-08	9.513E-06	
2	PSNS-2 9Apr14 < 0.45µm	76		0.000005	0.000005	0.000005	0.000007	0.000041	-0.000002	2.917E-08	1.239E-06	
3	PSNS-3 9Apr14 < 0.45µm	76		0.000003	0.000001	0.000005	0.000014	0.000017	-0.000002	6.571E-08	3.585E-07	
4	PSNS-4 9Apr14 < 0.45µm	76		0.000001	0.000001	0.000004	0.000000	0.000004	-0.000002	-2.212E-08	-1.777E-07	
5	PSNS-5 9Apr14 < 0.45µm	76		0.000001	0.000002	0.000006	0.000016	0.000026	-0.000002	5.920E-08	3.028E-07	

Sediment Trap No.	SAMPLE ID by SIZE FRACTION	Deploy time (days)	Total Dry Particle Deposition Rate (g/m ² d)	Copper Deposition Rate (g/m ² d)	Chromium Deposition Rate (g/m ² d)	Nickel Deposition Rate (g/m ² d)	Zinc Deposition Rate (g/m ² d)	Arsenic Deposition Rate (g/m ² d)	Silver Deposition Rate (g/m ² d)	Cadmium Deposition Rate (g/m ² d)	Lead Deposition Rate (g/m ² d)	Mercury Deposition Rate (g/m ² d)
6	PSNS-6 9Apr14 < 0.45µm	76		0.000004	0.000000	0.000004	0.000003	0.000024	-0.000003	5.857E-08	8.235E-07	
7	PSNS-7 9Apr14 < 0.45µm	76		0.000004	0.000001	0.000008	0.000016	0.000016	-0.000001	9.040E-08	6.373E-07	
8	PSNS-8 9Apr14 < 0.45µm	76		0.000000	-0.000001	0.000001	-0.000008	0.000002	-0.000003	1.048E-07	-2.629E-07	
9	PSNS-9 9Apr14 < 0.45µm	76		0.000009	0.000005	0.000005	0.000004	0.000015	-0.000002	-1.979E-08	3.018E-09	

Table H-1. Particle and Metal Deposition Rates (g/m² d) for the Second Event.

Sediment Trap No.	SAMPLE ID by SIZE FRACTION	Deploy time (days)	Total Dry Particle Deposition Rate (g/m ² d)	Copper Deposition Rate (g/m ² d)	Chromium Deposition Rate (g/m ² d)	Nickel Deposition Rate (g/m ² d)	Zinc Deposition Rate (g/m ² d)	Arsenic Deposition Rate (g/m ² d)	Silver Deposition Rate (g/m ² d)	Cadmium Deposition Rate (g/m ² d)	Lead Deposition Rate (g/m ² d)	Mercury Deposition Rate (g/m ² d)
1	PSNS-1 14May14 2mm to 60µm	33	12.35	0.001371	0.000485	0.000333	0.003107	0.000164	0.000029	0.000026	0.000581	
2	PSNS-2 14May14 2mm to 60µm	33	23.68	0.002923	0.000919	0.000654	0.007738	0.000334	0.000060	0.000053	0.001213	
3	PSNS-3 14May14 2mm to 60µm	33	14.79	0.002018	0.000549	0.000435	0.003964	0.000172	0.000032	0.000029	0.000786	
4	PSNS-4 14May14 2mm to 60µm	33	31.95	0.002915	0.001045	0.000851	0.005622	0.000354	0.000062	0.000051	0.001288	
5	PSNS-5 14May14 2mm to 60µm	33	15.49	0.001998	0.000877	0.000418	0.004244	0.000210	0.000039	0.000037	0.000873	
6	PSNS-6 14May14 2mm to 60µm	33	30.67	0.003655	0.001189	0.000895	0.008420	0.000448	0.000082	0.000079	0.001911	
7	PSNS-7 14May14 2mm to 60µm	33	18.92	0.003814	0.000878	0.000651	0.006467	0.000321	0.000051	0.000053	0.001329	
8	PSNS-8 14May14 2mm to 60µm	33	73.34	0.009069	0.002664	0.002092	0.015588	0.001025	0.000189	0.000149	0.003559	
9	PSNS-9 14May14 2mm to 60µm	33	46.88	0.006213	0.001915	0.001359	0.012347	0.000684	0.000120	0.000115	0.002573	
1	PSNS-1 14May14 60µm to 5µm	33	28.75	0.002705	0.000956	0.000802	0.005359	0.000358	0.000069	0.000043	0.001211	
2	PSNS-2 14May14 60µm to 5µm	33	47.16	0.004109	0.001230	0.001105	0.007594	0.000413	0.000092	0.000066	0.001551	
3	PSNS-3 14May14 60µm to 5µm	33	30.75	0.002885	0.000921	0.000736	0.004990	0.000336	0.000076	0.000048	0.001118	
4	PSNS-4 14May14 60µm to 5µm	33	17.51	0.001527	0.000553	0.000462	0.002788	0.000228	0.000042	0.000030	0.000658	
5	PSNS-5 14May14 60µm to 5µm	33	43.18	0.004315	0.001577	0.001165	0.008319	0.000565	0.000110	0.000080	0.001780	
6	PSNS-6 14May14 60µm to 5µm	33	46.59	0.004487	0.001661	0.001394	0.008924	0.000584	0.000109	0.000095	0.002155	
7	PSNS-7 14May14 60µm to 5µm	33	29.60	0.002999	0.001109	0.000828	0.005802	0.000377	0.000074	0.000055	0.001256	

8	PSNS-8 14May14 60µm to 5µm	33	34.53	0.004112	0.001180	0.001030	0.005903	0.000412	0.000083	0.000063	0.001596	
9	PSNS-9 14May14 60µm to 5µm	33	29.20	0.003215	0.000974	0.000827	0.005430	0.000363	0.000072	0.000053	0.001281	
1	PSNS-1 14May14 5 µm to 0.45µm	33	0.001	0.000006	0.000017	0.000007	0.000007	0.000043	-0.000003	1.511E-08	2.734E-07	
2	PSNS-2 14May14 5 µm to 0.45µm	33	0.013	0.000002	0.000011	0.000022	0.000013	0.000015	-0.000004	1.661E-07	2.968E-07	
3	PSNS-3 14May14 5 µm to 0.45µm	33	0.014	0.000002	0.000023	0.000010	0.000010	0.000064	-0.000003	4.036E-08	3.032E-07	
4	PSNS-4 14May14 5 µm to 0.45µm	33	0.045	0.000013	0.000003	0.000013	0.000011	0.000009	-0.000002	7.955E-08	6.486E-07	
5	PSNS-5 14May14 5 µm to 0.45µm	33	0.033	0.000001	0.000001	0.000010	-0.000001	0.000005	-0.000003	3.756E-08	1.466E-07	
6	PSNS-6 14May14 5 µm to 0.45µm	33	0.007	0.000017	0.000005	0.000015	0.000019	0.000012	-0.000004	7.523E-08	5.558E-07	
7	PSNS-7 14May14 5 µm to 0.45µm	33	0.035	0.000003	0.000002	0.000011	0.000008	0.000010	-0.000003	5.087E-08	3.025E-07	
8	PSNS-8 14May14 5 µm to 0.45µm	33	0.019	0.000010	0.000011	0.000004	0.000008	0.000016	-0.000003	9.257E-08	7.770E-07	
9	PSNS-9 14May14 5 µm to 0.45µm	33	0.013	0.000004	0.000004	0.000008	0.000010	0.000004	-0.000002	7.227E-08	5.993E-07	
1	PSNS-1 14May14 < 0.45µm	33		0.000003	0.000010	0.000005	0.000004	0.000006	-0.000003	-1.910E-08	-8.345E-08	
2	PSNS-2 14May14 < 0.45µm	33		0.000005	0.000005	0.000017	0.000005	0.000014	-0.000003	7.433E-08	2.571E-08	
3	PSNS-3 14May14 < 0.45µm	33		0.000005	0.000007	0.000010	0.000011	0.000010	-0.000002	2.985E-08	-7.348E-08	
4	PSNS-4 14May14 < 0.45µm	33		0.000005	0.000000	0.000009	0.000009	0.000008	-0.000002	7.304E-08	-1.053E-07	
5	PSNS-5 14May14 < 0.45µm	33		0.000001	-0.000001	0.000008	0.000011	0.000009	-0.000002	6.520E-08	4.169E-09	
6	PSNS-6 14May14 < 0.45µm	33		0.000016	0.000003	0.000016	0.000017	0.000016	0.000000	1.123E-07	-2.007E-08	
7	PSNS-7 14May14 < 0.45µm	33		0.000002	0.000002	0.000013	0.000008	0.000012	-0.000002	4.682E-08	-4.913E-08	
8	PSNS-8 14May14 < 0.45µm	33		0.000018	0.000002	0.000005	0.000006	0.000007	-0.000002	8.364E-08	1.472E-08	
9	PSNS-9 14May14 < 0.45µm	33		0.000004	0.000001	0.000008	0.000006	0.000005	-0.000002	7.205E-08	-7.968E-09	

Table H-2. Particle and Metal Deposition Rates (g/m² d) for the Third Event.

Sediment Trap No.	SAMPLE ID by SIZE FRACTION	Deploy time (days)	Total Dry Particle Deposition Rate (g/m ² d)	Copper Deposition Rate (g/m ² d)	Chromium Deposition Rate (g/m ² d)	Nickel Deposition Rate (g/m ² d)	Zinc Deposition Rate (g/m ² d)	Arsenic Deposition Rate (g/m ² d)	Silver Deposition Rate (g/m ² d)	Cadmium Deposition Rate (g/m ² d)	Lead Deposition Rate (g/m ² d)	Mercury Deposition Rate (g/m ² d)
1	PSNS-1 24Jun14 2mm to 60µm	40	44.26	0.005836	0.001907	0.001549	0.010001	0.000691	0.000120	0.000109	0.002504	
2	PSNS-2 24Jun14 2mm to 60µm	40	19.71	0.001832	0.000768	0.000549	0.004159	0.000221	0.000043	0.000040	0.000879	
3	PSNS-3 24Jun14 2mm to 60µm	40	8.24	0.000672	0.000258	0.000200	0.001871	0.000087	0.000016	0.000015	0.000344	
4	PSNS-4 24Jun14 2mm to 60µm	40	4.02	0.000435	0.000167	0.000129	0.001030	0.000061	0.000011	0.000011	0.000195	
5	PSNS-5 24Jun14 2mm to 60µm	40	12.34	0.001860	0.000530	0.000398	0.004445	0.000188	0.000031	0.000043	0.000932	
6	PSNS-6 24Jun14 2mm to 60µm	40	15.14	0.001822	0.000616	0.000488	0.003507	0.000195	0.000035	0.000038	0.000822	
7	PSNS-7 24Jun14 2mm to 60µm	40	8.09	0.001294	0.000425	0.000283	0.002694	0.000155	0.000023	0.000025	0.000574	
8	PSNS-8 24Jun14 2mm to 60µm	40	35.69	0.004719	0.001463	0.001174	0.009547	0.000518	0.000098	0.000092	0.002014	
9	PSNS-9 24Jun14 2mm to 60µm	40	8.10	0.001129	0.000392	0.000282	0.002410	0.000129	0.000023	0.000025	0.000501	
1	PSNS-1 24Jun14 60µm to 5µm	40	21.20	0.002282	0.000731	0.000594	0.003538	0.000264	0.000054	0.000044	0.001014	
2	PSNS-2 24Jun14 60µm to 5µm	40	35.41	0.003613	0.001206	0.000997	0.005772	0.000489	0.000096	0.000076	0.001592	
3	PSNS-3 24Jun14 60µm to 5µm	40	14.33	0.001197	0.000434	0.000339	0.002225	0.000175	0.000041	0.000027	0.000545	
4	PSNS-4 24Jun14 60µm to 5µm	40	5.76	0.000445	0.000167	0.000139	0.000929	0.000067	0.000013	0.000010	0.000218	
5	PSNS-5 24Jun14 60µm to 5µm	40	19.68	0.002137	0.000760	0.000597	0.004016	0.000282	0.000053	0.000046	0.000950	
6	PSNS-6 24Jun14 60µm to 5µm	40	20.56	0.002161	0.000773	0.000612	0.003629	0.000270	0.000048	0.000045	0.000968	
7	PSNS-7 24Jun14 60µm to 5µm	40	22.99	0.002520	0.000859	0.000684	0.004146	0.000300	0.000060	0.000047	0.001036	
8	PSNS-8 24Jun14 60µm to 5µm	40	15.51	0.001879	0.000600	0.000510	0.003204	0.000254	0.000042	0.000036	0.000758	

9	PSNS-9 24Jun14 60µm to 5µm	40	13.45	0.001271	0.000457	0.000384	0.002420	0.000158	0.000031	0.000026	0.000555	
1	PSNS-1 24Jun14 5 µm to 0.45µm	40	0.204	0.000006	0.000004	0.000007	0.000012	0.000007	-0.000003	1.008E-07	5.114E-07	
2	PSNS-2 24Jun14 5 µm to 0.45µm	40	0.108	0.000030	0.000002	0.000332	0.000008	0.000070	-0.000002	6.559E-08	3.526E-07	
3	PSNS-3 24Jun14 5 µm to 0.45µm	40	0.027	0.000005	0.000001	0.000006	0.000035	0.000003	-0.000001	3.615E-07	0.000009	
4	PSNS-4 24Jun14 5 µm to 0.45µm	40	-0.010	0.000001	0.000001	0.000003	-0.000002	0.000010	-0.000003	5.507E-08	3.527E-07	
5	PSNS-5 24Jun14 5 µm to 0.45µm	40	-0.015	0.000003	0.000000	0.000010	0.000014	0.000005	-0.000002	9.030E-08	3.066E-07	
6	PSNS-6 24Jun14 5 µm to 0.45µm	40	-0.016	0.000003	0.000004	0.000015	0.000134	0.000008	-0.000002	1.418E-06	0.000018	
7	PSNS-7 24Jun14 5 µm to 0.45µm	40	-0.039	0.000008	0.000002	0.000018	0.000008	0.000014	-0.000004	9.589E-08	6.373E-07	
8	PSNS-8 24Jun14 5 µm to 0.45µm	40	-0.001	0.000006	0.000004	0.000008	0.000015	0.000008	-0.000003	1.380E-07	5.373E-07	
9	PSNS-9 24Jun14 5 µm to 0.45µm	40	-0.007	0.000001	0.000002	0.000005	0.000007	0.000006	-0.000003	5.033E-08	1.228E-06	
1	PSNS-1 24Jun14 < 0.45µm	40		0.000006	1.986E-06	0.000009	0.000015	0.000005	-0.000003	1.222E-07	5.002E-08	
2	PSNS-2 24Jun14 < 0.45µm	40		0.000005	4.777E-07	0.000249	0.000002	0.000067	-0.000002	3.572E-08	-1.077E-07	
3	PSNS-3 24Jun14 < 0.45µm	40		0.000001	-3.939E-07	0.000005	0.000024	0.000003	0.000000	3.558E-07	2.755E-06	
4	PSNS-4 24Jun14 < 0.45µm	40		0.000001	9.204E-07	0.000006	0.000003	0.000006	-0.000002	1.848E-07	6.554E-08	
5	PSNS-5 24Jun14 < 0.45µm	40		0.000021	3.817E-07	0.000006	0.000004	0.000027	-0.000001	2.124E-07	9.527E-09	
6	PSNS-6 24Jun14 < 0.45µm	40		0.000006	-6.877E-07	0.000012	0.000051	0.000014	-0.000003	8.891E-06	4.492E-06	
7	PSNS-7 24Jun14 < 0.45µm	40		0.000002	-1.398E-07	0.000019	0.000012	0.000011	0.000000	1.204E-07	-5.695E-08	
8	PSNS-8 24Jun14 < 0.45µm	40		0.000003	1.759E-06	0.000009	0.000009	0.000009	0.000000	8.399E-08	2.487E-07	
9	PSNS-9 24Jun14 < 0.45µm	40		0.000001	9.565E-07	0.000006	0.000004	0.000005	-0.000001	1.517E-08	2.770E-07	

Table H-3. Particle Load (g/m²) and Net (background corrected) Metal Load (g/m² d) for the First Event.

Sediment Trap No.	SAMPLE ID by SIZE FRACTION	Deploy time (days)	Particle Load (g/m ²)	Copper Background corrected Load (g/m ²)	Chromium Background corrected Load (g/m ²)	Nickel Background corrected Load (g/m ²)	Zinc Background corrected Load (g/m ²)	Arsenic Background corrected Load (g/m ²)	Silver Background corrected Load (g/m ²)	Cadmium Background corrected Load (g/m ²)	Lead Background corrected Load (g/m ²)	Mercury Background corrected Load (g/m ²)
1	PSNS-1 9Apr14 2mm to 60µm	0	1584	0.0751	0.0136	0.0073	0.1400	0.0048	0.0003	0.0008	0.0163	3.972E-06
2	PSNS-2 9Apr14 2mm to 60µm	76	628	-0.0001	-0.0351	-0.0115	-0.1088	-0.0117	-0.0020	-0.0022	-0.0473	3.164E-06
3	PSNS-3 9Apr14 2mm to 60µm	76	545	0.0108	-0.0271	-0.0141	-0.0929	-0.0050	-0.0019	-0.0021	-0.0327	3.164E-06
4	PSNS-4 9Apr14 2mm to 60µm	76	682	-0.0171	-0.0249	-0.0184	-0.1170	-0.0054	-0.0019	-0.0021	-0.0271	3.933E-06
5	PSNS-5 9Apr14 2mm to 60µm	76	672	0.0668	-0.0177	-0.0149	-0.0447	-0.0061	-0.0018	-0.0017	-0.0115	2.417E-07
6	PSNS-6 9Apr14 2mm to 60µm	76	761	0.0836	-0.0156	-0.0092	-0.0307	-0.0021	-0.0017	-0.0016	-0.0136	3.903E-06
7	PSNS-7 9Apr14 2mm to 60µm	76	689	0.0561	-0.0224	-0.0160	-0.0250	-0.0046	-0.0019	-0.0016	-0.0130	2.486E-06
8	PSNS-8 9Apr14 2mm to 60µm	76	756	0.0798	-0.0154	-0.0085	-0.0518	-0.0015	-0.0013	-0.0017	-0.0031	3.294E-06
9	PSNS-9 19Apr14 2mm to 60µm	76	610	0.0249	-0.0150	-0.0024	-0.0845	-0.0066	-0.0018	-0.0012	-0.0209	3.448E-06
1	PSNS-1 9Apr14 60µm to 5µm	76	1082	0.0253	0.0021	0.0008	-0.0088	0.0028	-0.0011	-0.0016	-0.0026	3.313E-06
2	PSNS-2 9Apr14 60µm to 5µm	76	2028	0.1023	0.0224	0.0187	0.0747	0.0107	0.0004	-0.0011	0.0203	8.579E-06
3	PSNS-3 9Apr14 60µm to 5µm	76	2656	0.1841	0.0508	0.0455	0.2758	0.0232	0.0030	0.0004	0.0632	7.729E-06
4	PSNS-4 9Apr14 60µm to 5µm	76	2956	0.1996	0.0763	0.0623	0.3316	0.0223	0.0035	0.0006	0.0832	9.768E-06
5	PSNS-5 9Apr14 60µm to 5µm	76	2511	0.2019	0.0508	0.0442	0.2495	0.0168	0.0010	-0.0001	0.0650	6.597E-06
6	PSNS-6 9Apr14 60µm to 5µm	76	3408	0.2769	0.1011	0.0846	0.4078	0.0346	0.0043	0.0014	0.1196	1.144E-05
7	PSNS-7 9Apr14 60µm to 5µm	76	4845	0.5117	0.1622	0.1319	0.7416	0.0565	0.0056	0.0026	0.2237	1.571E-06
8	PSNS-8 9Apr14 60µm to 5µm	76	3316	0.3515	0.0789	0.0689	0.3423	0.0304	0.0038	0.0010	0.1118	8.975E-06

9	PSNS-9 9Apr14 60µm to 5µm	76	2680	0.2394	0.0662	0.0580	0.2991	0.0224	0.0023	0.0012	0.0848	9.230E-06
1	PSNS-1 9Apr14 5 µm to 0.45µm	76	-0.16	-0.000417	-0.000120	-0.003176	-0.001553	-0.000786	0.000057	-0.000018	-0.000191	7.504E-12
2	PSNS-2 9Apr14 5 µm to 0.45µm	76	0.36	-0.000014	-0.000127	-0.003243	-0.001627	0.000278	0.000084	-0.000018	-0.000168	5.403E-12
3	PSNS-3 9Apr14 5 µm to 0.45µm	76	-0.10	0.001507	-0.000025	-0.003028	-0.000583	-0.000169	0.000076	-0.000013	-0.000227	1.951E-11
4	PSNS-4 9Apr14 5 µm to 0.45µm	76	0.48	-0.000469	0.000834	-0.003074	-0.001518	0.014511	0.000106	-0.000019	-0.000254	1.921E-11
5	PSNS-5 9Apr14 5 µm to 0.45µm	76	0.89	0.000042	0.000246	-0.002977	-0.000374	0.000107	0.000024	-0.000014	-0.000191	2.701E-11
6	PSNS-6 9Apr14 5 µm to 0.45µm	76	0.60	-0.000336	0.000064	-0.003156	-0.000178	0.006865	0.000153	-0.000010	-0.000239	7.504E-12
7	PSNS-7 9Apr14 5 µm to 0.45µm	76	0.47	-0.000263	0.000003	-0.003253	-0.001156	0.001145	0.000146	-0.000017	-0.000242	3.482E-11
8	PSNS-8 9Apr14 5 µm to 0.45µm	76	-0.20	-0.000091	0.000004	-0.002986	-0.001217	-0.000534	0.000038	0.000013	-0.000257	3.962E-11
9	PSNS-9 9Apr14 5 µm to 0.45µm	76	0.36	-0.000234	0.000688	-0.003041	-0.001546	0.025743	0.000024	-0.000019	-0.000230	2.251E-11
1	PSNS-1 9Apr14 < 0.45µm	76		0.000175	0.000104	-0.002051	0.001466	0.004350	-0.000058	-0.000082	0.000658	
2	PSNS-2 9Apr14 < 0.45µm	76		-0.000015	0.000328	-0.002290	-0.000502	0.001906	-0.000045	-0.000082	0.000029	
3	PSNS-3 9Apr14 < 0.45µm	76		-0.000167	0.000029	-0.002322	0.000045	0.000033	-0.000039	-0.000080	-0.000038	
4	PSNS-4 9Apr14 < 0.45µm	76		-0.000331	0.000010	-0.002433	-0.001026	-0.000954	-0.000052	-0.000086	-0.000079	
5	PSNS-5 9Apr14 < 0.45µm	76		-0.000330	0.000143	-0.002228	0.000178	0.000703	-0.000060	-0.000080	-0.000042	
6	PSNS-6 9Apr14 < 0.45µm	76		-0.000101	-0.000038	-0.002422	-0.000843	0.000556	-0.000111	-0.000080	-0.000003	
7	PSNS-7 9Apr14 < 0.45µm	76		-0.000118	0.000055	-0.002082	0.000143	-0.000044	0.000052	-0.000078	-0.000017	
8	PSNS-8 9Apr14 < 0.45µm	76		-0.000349	-0.000091	-0.002602	-0.001619	-0.001079	-0.000113	-0.000077	-0.000085	
9	PSNS-9 9Apr14 < 0.45µm	76		0.000307	0.000303	-0.002359	-0.000755	-0.000065	-0.000079	-0.000086	-0.000065	

Table H-4. Particle Load (g/m²) and Net (background corrected) Metal Load (g/m² d) for the Second Event.

Sediment Trap No.	SAMPLE ID by SIZE FRACTION	Deploy time (days)	Particle Load (g/m ²)	Copper Background corrected Load (g/m ²)	Chromium Background corrected Load (g/m ²)	Nickel Background corrected Load (g/m ²)	Zinc Background corrected Load (g/m ²)	Arsenic Background corrected Load (g/m ²)	Silver Background corrected Load (g/m ²)	Cadmium Background corrected Load (g/m ²)	Lead Background corrected Load (g/m ²)	Mercury Background corrected Load (g/m ²)
1	PSNS-1 14May14 2mm to 60µm	0	408	-0.0115	-0.0079	-0.0075	-0.0429	-0.0028	-0.0005	-0.0006	-0.0130	
2	PSNS-2 14May14 2mm to 60µm	33	781	0.0397	0.0064	0.0031	0.1099	0.0028	0.0005	0.0003	0.0079	
3	PSNS-3 14May14 2mm to 60µm	33	488	0.0098	-0.0058	-0.0042	-0.0146	-0.0026	-0.0004	-0.0005	-0.0062	
4	PSNS-4 14May14 2mm to 60µm	33	1054	0.0394	0.0106	0.0095	0.0401	0.0034	0.0006	0.0002	0.0104	
5	PSNS-5 14May14 2mm to 60µm	33	511	0.0092	0.0050	-0.0047	-0.0054	-0.0013	-0.0002	-0.0002	-0.0033	
6	PSNS-6 14May14 2mm to 60µm	33	1012	0.0638	0.0153	0.0110	0.1324	0.0066	0.0012	0.0011	0.0309	
7	PSNS-7 14May14 2mm to 60µm	33	624	0.0691	0.0051	0.0030	0.0680	0.0024	0.0002	0.0003	0.0117	
8	PSNS-8 14May14 2mm to 60µm	33	2420	0.2425	0.0640	0.0505	0.3690	0.0256	0.0048	0.0035	0.0853	
9	PSNS-9 14May14 2mm to 60µm	33	1547	0.1483	0.0393	0.0263	0.2620	0.0143	0.0025	0.0024	0.0528	
1	PSNS-1 14May14 60µm to 5µm	33	949	0.0251	0.0096	0.0086	0.0673	0.0035	0.0007	0.0001	0.0120	
2	PSNS-2 14May14 60µm to 5µm	33	1556	0.0714	0.0186	0.0187	0.1411	0.0054	0.0014	0.0009	0.0232	
3	PSNS-3 14May14 60µm to 5µm	33	1015	0.0310	0.0084	0.0065	0.0551	0.0028	0.0009	0.0003	0.0089	
4	PSNS-4 14May14 60µm to 5µm	33	578	-0.0138	-0.0037	-0.0026	-0.0175	-0.0008	-0.0002	-0.0003	-0.0063	
5	PSNS-5 14May14 60µm to 5µm	33	1425	0.0782	0.0301	0.0207	0.1650	0.0104	0.0020	0.0013	0.0307	
6	PSNS-6 14May14 60µm to 5µm	33	1537	0.0839	0.0329	0.0282	0.1849	0.0110	0.0020	0.0018	0.0431	
7	PSNS-7 14May14 60µm to 5µm	33	977	0.0348	0.0147	0.0095	0.0819	0.0042	0.0008	0.0005	0.0134	
8	PSNS-8 14May14 60µm to 5µm	33	1140	0.0715	0.0170	0.0162	0.0852	0.0053	0.0011	0.0008	0.0247	

9	PSNS-9 14May14 60µm to 5µm	33	964	0.0419	0.0102	0.0095	0.0696	0.0037	0.0008	0.0004	0.0143	
1	PSNS-1 14May14 5 µm to 0.45µm	33	0.02	-0.000043	0.000473	-0.001268	-0.000623	0.000924	0.000002	-0.000008	-0.000104	
2	PSNS-2 14May14 5 µm to 0.45µm	33	0.41	-0.000178	0.000286	-0.000770	-0.000401	0.000013	-0.000058	-0.000003	-0.000103	
3	PSNS-3 14May14 5 µm to 0.45µm	33	0.45	-0.000175	0.000674	-0.001171	-0.000511	0.001628	-0.000018	-0.000007	-0.000103	
4	PSNS-4 14May14 5 µm to 0.45µm	33	1.48	0.000190	0.000027	-0.001072	-0.000480	-0.000174	0.000027	-0.000006	-0.000092	
5	PSNS-5 14May14 5 µm to 0.45µm	33	1.08	-0.000217	-0.000050	-0.001158	-0.000867	-0.000322	-0.000013	-0.000007	-0.000108	
6	PSNS-6 14May14 5 µm to 0.45µm	33	0.24	0.000324	0.000099	-0.000983	-0.000220	-0.000080	-0.000040	-0.000006	-0.000095	
7	PSNS-7 14May14 5 µm to 0.45µm	33	1.15	-0.000119	0.000005	-0.001126	-0.000592	-0.000151	-0.000005	-0.000007	-0.000103	
8	PSNS-8 14May14 5 µm to 0.45µm	33	0.62	0.000090	0.000274	-0.001357	-0.000583	0.000031	-0.000016	-0.000006	-0.000088	
9	PSNS-9 14May14 5 µm to 0.45µm	33	0.43	-0.000087	0.000053	-0.001233	-0.000513	-0.000341	0.000030	-0.000006	-0.000093	
1	PSNS-1 14May14 < 0.45µm	33		-0.000075	0.000296	-0.001004	-0.000335	-0.000335	-0.000054	-0.000037	-0.000031	
2	PSNS-2 14May14 < 0.45µm	33		-0.000014	0.000133	-0.000601	-0.000294	-0.000080	-0.000064	-0.000034	-0.000028	
3	PSNS-3 14May14 < 0.45µm	33		0.000002	0.000223	-0.000848	-0.000084	-0.000208	-0.000026	-0.000036	-0.000031	
4	PSNS-4 14May14 < 0.45µm	33		-0.000011	-0.000012	-0.000886	-0.000170	-0.000273	-0.000027	-0.000034	-0.000032	
5	PSNS-5 14May14 < 0.45µm	33		-0.000129	-0.000039	-0.000913	-0.000093	-0.000240	-0.000027	-0.000035	-0.000028	
6	PSNS-6 14May14 < 0.45µm	33		0.000353	0.000073	-0.000635	0.000112	-0.000006	0.000046	-0.000033	-0.000029	
7	PSNS-7 14May14 < 0.45µm	33		-0.000093	0.000059	-0.000761	-0.000189	-0.000135	-0.000007	-0.000035	-0.000030	
8	PSNS-8 14May14 < 0.45µm	33		0.000423	0.000034	-0.001023	-0.000252	-0.000295	-0.000022	-0.000034	-0.000028	
9	PSNS-9 14May14 < 0.45µm	33		-0.000042	0.000020	-0.000901	-0.000240	-0.000389	-0.000018	-0.000034	-0.000029	

Table H-5. Particle Load (g/m²) and Net (background corrected) Metal Load (g/m² d) for the Third Event.

Sediment Trap No.	SAMPLE ID by SIZE FRACTION	Deploy time (days)	Particle Load (g/m ²)	Copper Background corrected Load (g/m ²)	Chromium Background corrected Load (g/m ²)	Nickel Background corrected Load (g/m ²)	Zinc Background corrected Load (g/m ²)	Arsenic Background corrected Load (g/m ²)	Silver Background corrected Load (g/m ²)	Cadmium Background corrected Load (g/m ²)	Lead Background corrected Load (g/m ²)	Mercury Background corrected Load (g/m ²)
1	PSNS-1 24Jun14 2mm to 60µm	0	1.1	0.1646	0.0473	0.0395	0.2238	0.0176	0.0030	0.0026	0.0612	
2	PSNS-2 24Jun14 2mm to 60µm	40	0.5	0.0045	0.0017	-0.0005	-0.0099	-0.0011	-0.0001	-0.0002	-0.0038	
3	PSNS-3 24Jun14 2mm to 60µm	40	0.2	-0.0419	-0.0187	-0.0145	-0.1014	-0.0065	-0.0011	-0.0012	-0.0252	
4	PSNS-4 24Jun14 2mm to 60µm	40	0.1	-0.0514	-0.0223	-0.0173	-0.1351	-0.0075	-0.0013	-0.0013	-0.0311	
5	PSNS-5 24Jun14 2mm to 60µm	40	0.3	0.0056	-0.0078	-0.0065	0.0015	-0.0025	-0.0005	0.0000	-0.0017	
6	PSNS-6 24Jun14 2mm to 60µm	40	0.4	0.0041	-0.0044	-0.0029	-0.0360	-0.0022	-0.0004	-0.0002	-0.0061	
7	PSNS-7 24Jun14 2mm to 60µm	40	0.2	-0.0171	-0.0120	-0.0111	-0.0685	-0.0038	-0.0008	-0.0008	-0.0160	
8	PSNS-8 24Jun14 2mm to 60µm	40	0.9	0.1199	0.0295	0.0245	0.2056	0.0107	0.0021	0.0019	0.0416	
9	PSNS-9 24Jun14 2mm to 60µm	40	0.2	-0.0237	-0.0133	-0.0112	-0.0799	-0.0048	-0.0009	-0.0008	-0.0189	
1	PSNS-1 24Jun14 60µm to 5µm	40	0.5	0.0135	0.0026	0.0022	0.0087	0.0005	0.0002	0.0002	0.0066	
2	PSNS-2 24Jun14 60µm to 5µm	40	0.9	0.0667	0.0216	0.0183	0.0981	0.0095	0.0019	0.0015	0.0297	
3	PSNS-3 24Jun14 60µm to 5µm	40	0.4	-0.0299	-0.0093	-0.0080	-0.0438	-0.0030	-0.0003	-0.0005	-0.0121	
4	PSNS-4 24Jun14 60µm to 5µm	40	0.1	-0.0600	-0.0199	-0.0160	-0.0956	-0.0074	-0.0014	-0.0012	-0.0252	
5	PSNS-5 24Jun14 60µm to 5µm	40	0.5	0.0077	0.0038	0.0023	0.0278	0.0012	0.0002	0.0002	0.0041	
6	PSNS-6 24Jun14 60µm to 5µm	40	0.5	0.0086	0.0043	0.0029	0.0124	0.0008	0.0000	0.0002	0.0048	
7	PSNS-7 24Jun14 60µm to 5µm	40	0.6	0.0230	0.0077	0.0058	0.0330	0.0019	0.0005	0.0003	0.0075	
8	PSNS-8 24Jun14 60µm to 5µm	40	0.4	-0.0026	-0.0026	-0.0012	-0.0046	0.0001	-0.0003	-0.0002	-0.0036	

9	PSNS-9 24Jun14 60µm to 5µm	40	0.3	-0.0270	-0.0083	-0.0062	-0.0360	-0.0037	-0.0007	-0.0006	-0.0117	
1	PSNS-1 24Jun14 5 µm to 0.45µm	40	0.01	-0.000039	0.000082	-0.001520	-0.000560	-0.000287	-0.000030	-0.000007	-0.000117	
2	PSNS-2 24Jun14 5 µm to 0.45µm	40	0.00	0.000934	0.000006	0.011463	-0.000685	0.002214	0.000010	-0.000008	-0.000123	
3	PSNS-3 24Jun14 5 µm to 0.45µm	40	0.00	-0.000072	-0.000052	-0.001543	0.000390	-0.000471	0.000046	0.000004	0.000204	
4	PSNS-4 24Jun14 5 µm to 0.45µm	40	0.00	-0.000239	-0.000044	-0.001673	-0.001110	-0.000177	-0.000016	-0.000008	-0.000123	
5	PSNS-5 24Jun14 5 µm to 0.45µm	40	0.00	-0.000148	-0.000070	-0.001419	-0.000479	-0.000366	0.000019	-0.000007	-0.000125	
6	PSNS-6 24Jun14 5 µm to 0.45µm	40	0.00	-0.000170	0.000067	-0.001193	0.004321	-0.000271	0.000022	0.000046	0.000600	
7	PSNS-7 24Jun14 5 µm to 0.45µm	40	0.00	0.000031	-0.000027	-0.001064	-0.000719	-0.000025	-0.000035	-0.000007	-0.000112	
8	PSNS-8 24Jun14 5 µm to 0.45µm	40	0.00	-0.000055	0.000056	-0.001461	-0.000436	-0.000274	0.000003	-0.000005	-0.000116	
9	PSNS-9 24Jun14 5 µm to 0.45µm	40	0.00	-0.000244	-0.000019	-0.001591	-0.000723	-0.000343	-0.000020	-0.000009	-0.000088	
1	PSNS-1 24Jun14 < 0.45µm	40		0.000024	0.000056	-0.001065	0.000064	-0.000463	-0.000073	-0.000040	-0.000032	
2	PSNS-2 24Jun14 < 0.45µm	40		0.000013	-0.000004	0.008536	-0.000467	0.002042	-0.000021	-0.000043	-0.000039	
3	PSNS-3 24Jun14 < 0.45µm	40		-0.000161	-0.000039	-0.001234	0.000405	-0.000549	0.000050	-0.000030	0.000076	
4	PSNS-4 24Jun14 < 0.45µm	40		-0.000164	0.000013	-0.001194	-0.000438	-0.000414	-0.000035	-0.000037	-0.000032	
5	PSNS-5 24Jun14 < 0.45µm	40		0.000618	-0.000008	-0.001171	-0.000392	0.000432	0.000009	-0.000036	-0.000034	
6	PSNS-6 24Jun14 < 0.45µm	40		0.000054	-0.000051	-0.000944	0.001505	-0.000109	-0.000047	0.000311	0.000145	
7	PSNS-7 24Jun14 < 0.45µm	40		-0.000124	-0.000029	-0.000670	-0.000087	-0.000200	0.000068	-0.000040	-0.000037	
8	PSNS-8 24Jun14 < 0.45µm	40		-0.000077	0.000047	-0.001073	-0.000206	-0.000295	0.000042	-0.000041	-0.000024	
9	PSNS-9 24Jun14 < 0.45µm	40		-0.000182	0.000015	-0.001184	-0.000384	-0.000445	0.000007	-0.000044	-0.000023	

REPORT DOCUMENTATION PAGE				<i>Form Approved</i> OMB No. 0704-01-0188	
<p>The public reporting burden for this collection of information is estimated to average 1 hour per response, including the time for reviewing instructions, searching existing data sources, gathering and maintaining the data needed, and completing and reviewing the collection of information. Send comments regarding this burden estimate or any other aspect of this collection of information, including suggestions for reducing the burden to Department of Defense, Washington Headquarters Services Directorate for Information Operations and Reports (0704-0188), 1215 Jefferson Davis Highway, Suite 1204, Arlington VA 22202-4302. Respondents should be aware that notwithstanding any other provision of law, no person shall be subject to any penalty for failing to comply with a collection of information if it does not display a currently valid OMB control number.</p> <p>PLEASE DO NOT RETURN YOUR FORM TO THE ABOVE ADDRESS.</p>					
1. REPORT DATE (DD-MM-YYYY) September 2016		2. REPORT TYPE Final		3. DATES COVERED (From - To)	
4. TITLE AND SUBTITLE Evaluation of Resuspension from Propeller Wash in DoD Harbors				5a. CONTRACT NUMBER	
				5b. GRANT NUMBER	
				5c. PROGRAM ELEMENT NUMBER	
6. AUTHORS Pei-Fang Wang Ignacio Rivera-Duarte Ken Richter SSC Pacific				5d. PROJECT NUMBER	
				5e. TASK NUMBER	
				5f. WORK UNIT NUMBER	
7. PERFORMING ORGANIZATION NAME(S) AND ADDRESS(ES) SSC Pacific 53560 Hull Street San Diego, CA 92152-5001				8. PERFORMING ORGANIZATION REPORT NUMBER TR 3049	
9. SPONSORING/MONITORING AGENCY NAME(S) AND ADDRESS(ES) SERDP and ESTCP Office 4800 Mark Center Drive, Suite 17D08 Alexandria, VA 22350-3605				10. SPONSOR/MONITOR'S ACRONYM(S)	
				11. SPONSOR/MONITOR'S REPORT NUMBER(S) ESTCP	
12. DISTRIBUTION/AVAILABILITY STATEMENT Approved for public release.					
13. SUPPLEMENTARY NOTES This is a work of the United States Government and therefore is not copyrighted. This work may be copied and disseminated without restriction.					
14. ABSTRACT A study was conducted to evaluate impacts of resuspension from propeller wash in Department of Defense (DoD) harbors. This study included both field data measurement and calibration of numerical models. The study included three linked, yet separate studies, including resuspension potential by tug wash, fate and transport, and remigration, redeposition and recontamination potential of the sediment plumes from tug wash. Model-data comparisons were conducted for both the erosion potential model (Graphic Maynard's model) and the fate and transport model (CH3D) for San Diego Bay, CA. The calibrated models were then used to evaluate propeller wash impact in Pearl Harbor, HI, and Sinclair Inlet, WA. Study results demonstrated that, despite the complexities associated with the transport and dynamics of propeller-wash induced sediment resuspension, study tools, including both key field data and adequately calibrated models, were effectively developed and applied to describe and predict key processes and impacts associated with propeller wash in DoD harbors.					
15. SUBJECT TERMS propeller wash; contaminated sediment; tugboat, models; fate and transport; CH3D, Maynard's Model; FANS; metal partitioning					
16. SECURITY CLASSIFICATION OF:			17. LIMITATION OF ABSTRACT	18. NUMBER OF PAGES	19a. NAME OF RESPONSIBLE PERSON
a. REPORT	b. ABSTRACT	c. THIS PAGE			Pei-Fang Wang
U	U	U	U	325	19b. TELEPHONE NUMBER (Include area code) (619) 553-9192

INITIAL DISTRIBUTION

84300	Library	(1)
85300	Archive/Stock	(1)
71750	P.-F. Wang	(1)
71750	I. Rivera-Duarte	(1)
71760	K. Richter	(1)
Defense Technical Information Center		
Fort Belvoir, VA 22060–6218		(1)

Approved for public release.



SSC Pacific
San Diego, CA 92152-5001